UNIVERSITÉ DE STRASBOURG

UMR7156, Dynamique et Plasticité des synthétases (DyPS)

THÈSE présentée par :

Nathaniel Yakobov

soutenue le : **29 Octobre 2020**

pour obtenir le grade de :

DOCTEUR DE L'UNIVERSITÉ DE STRASBOURG

Discipline : **Sciences du Vivant**

Spécialité : **Aspects Moléculaires et Cellulaires de la Biologie**

Découverte de l'aminoacylation ARNt-dépendante de l'ergostérol chez les champignons

THÈSE dirigée par :

    Dr. SENGER Bruno   PhD, (UMR7156), IPCB, Université de Strasbourg, France
    Pr. BECKER Hubert   Professeur des Universités, (UMR7156) IPCB, Université de Strasbourg, France

RAPPORTEURS EXTERNES:

    Pr. DEL POETA Maurizio   MD, Group leader, Université Stony Brook, New York, USA
    Dr. BLAISE Mickael   Directeur de recherches, IRIM, (CNRS/UM, UMR9004), Montpellier, France

EXAMINATEURS :

    Dr. FRUGIER Magali   Directrice de recherches, Université de Strasbourg, France   *Présidente du jury*
    Pr. STATHOPOULOS Constantinos Professeur, departement de biochemie, Université de Patras, Grèce

THESIS presented by:

Nathaniel YAKOBOV

defended on **October 29th, 2020**

to obtain the degree of:

DOCTOR OF THE UNIVERSITY OF STRASBOURG

Discipline: **Life Sciences**

Option: **Molecular and Cellular Biology**

Discovery of tRNA-dependent ergosterol aminoacylation in fungi

THESIS supervisors:

    Dr. SENGER Bruno   PhD, (UMR7156), IPCB University of Strasbourg, France

    Pr. BECKER Hubert   Professor, (UMR7156) IPCB, University of Strasbourg, France

EXTERNAL REFEREES:

    Pr. DEL POETA Maurizio   MD, Group leader, Stony Brook University, New York, USA

    Dr. BLAISE Mickael   Directeur de recherches, IRIM, (CNRS/UM, UMR9004), Montpellier, France

EXAMINERS:

    Dr. FRUGIER Magali   Directrice de recherches, University of Strasbourg, France   *President of the Jury*

    Pr. STATHOPOULOS Constantinos Professor, Dept. of Biochemistry, University of Patras, Greece

Remerciements / acknowledgements

The following acknowledgements will be in French but at first, I would like to greatly thank the jury members, namely Prof. Maurizio Del Poeta (USA), Prof. Constantinos Stathopoulos, Dr. Michael Blaise and Dr. Magali Frugier who accepted to evaluate my thesis work. It is an honor, a privilege, and a gratification for me to be reviewed by such a jury.

A ce jour je suis sur le point de devenir docteur diplômé de l'Université de Strasbourg et si j'en suis arrivé là c'est grâce aux nombreuses personnes qui m'ont entourées aussi bien dans et en dehors du laboratoire.

Tout d'abord je voudrais remercier mon directeur de laboratoire, le professeur **Hubert Becker** qui est aussi mon co-directeur de thèse. Hubert, la liste des raisons pour lesquelles je dois te remercier est longue et il m'est difficile de te remercier comme il se doit en quelques lignes. En effet, avant même d'envisager une thèse dans le domaine de la biologie j'ai eu le privilège de bénéficier de ton enseignement ce qui a éveillé en moi une passion pour la biologie moléculaire et de manière plus générale pour la recherche. Puis, en m'accueillant dans ton équipe en tant que stagiaire dans le cadre de mon master, tu m'as offert une opportunité unique. Cette expérience m'a fait prendre conscience que je voulais réellement intégrer la recherche scientifique, ce milieu qui éveille en nous une curiosité insatiable que nous essayons tant bien que mal d'apaiser en répondant à quelques-unes des innombrables problématiques que la science nous impose. Tu as été pour moi un directeur de laboratoire exceptionnel en m'encourageant sans cesse à m'améliorer, à repousser mes limites et à avoir un niveau d'exigence toujours plus élevé, dans le but d'atteindre le plus haut niveau d'expertise. Tu as toujours été présent à mes côtés en répondant à mes sollicitations et en m'aidant à solutionner les obstacles auxquels je pouvais être confronté tout en me laissant une réelle liberté de manœuvre afin de m'encourager à développer mon autonomie. Au-delà de tes fonctions de directeur de laboratoire, tu t'es toujours montré compréhensif et arrangeant par rapport à ma vie privée et à mon caractère quelque peu exubérant. Pour toutes ces raisons mais aussi pour avoir cru en moi et pour m'avoir fait confiance je te remercie du fond du cœur.

Je voudrais tout particulièrement remercier mon directeur de thèse, le docteur **Bruno Senger**, à qu'il a été incombé les lourde tâches de me faire découvrir le monde de la recherche à

mon arrivée dans le laboratoire lors de mon master. Bruno, tu m'as formé aux pratiques de laboratoire tu m'as appris comment affronter des problématiques scientifiques et comment mener un projet de recherche de manière autonome. Ce que tu m'as transmis (dont l'incontournable théorème de la pointe de spatule) restera à jamais le socle de mes compétences de chercheur. Malgré mes difficultés, mes erreurs et mes interruptions sans cesse tu t'es toujours montré disponible, patient et généreux. Je te remercie de m'avoir dirigé et conseillé avec passion et enthousiasme tout au long de ma thèse mais aussi pour ton dévouement et ton indéfectible soutien. Il me semble aussi indispensable d'ajouter un merci pour ton travail pendant la rédaction du présent manuscrit. En dehors du fait que tu as été extrêmement efficace je te suis reconnaissant d'avoir pris de ton temps pour répondre à mes questions et corriger mes proses alors que tu étais en congés. Merci aussi d'avoir été un ami en plus d'un exceptionnel directeur de thèse et sois-en sûr je serai toujours dans le coin pour piéger ta souris, scotcher ta chaise ou te débrancher tes câbles.

Fred, sans toi le projet des protéines à domaines DUF2156 eucaryotes n'aurait sûrement pas encore vu le jour et notre pauvre mère science n'aurait pas révélé l'existence de lipides aminoacylés chez les eucaryotes… pauvres de nous… Tu es le vrai moteur du projet et dès ton arrivée au labo j'ai été très enthousiasmé de former un duo de choc que rien ne pouvait arrêter et qui a rapidement porté ses fruits. Même si officiellement tu n'étais pas mon directeur de thèse, tu as été une pièce maîtresse de manière générale sur le projet mais aussi pour mon travail de thèse et je t'en suis extrêmement reconnaissant. Bien que tu avais une charge de travail importante entre l'enseignement et la recherche, tu n'as jamais ménagé tes efforts pour m'emmener là où je suis aujourd'hui. Je te remercie pour cela mais aussi pour avoir continuellement nourri mes connaissances. Merci d'avoir été mon mentor, mon complice…et mon ami.

Nassira, depuis ton arrivée dans le laboratoire tu as apporté ton expérience, ton savoir-faire et tant d'autres compétences essentielles au projet DUF2156. Je te remercie de m'avoir donné une autre perspective de la recherche ainsi que pour ton investissement dans le projet, ton aide précieuse et tes conseils judicieux. Je reste convaincu que ta motivation, ta rigueur et ton regard critique te mèneront à réaliser de grandes choses, et j'espère que tu seras celle qui très bientôt

m'appelleras pour me dire que tu as découvert la fonction physiologique des stérols aminonoacylés chez les champignons. Merci pour ta franchise, ton authenticité et ton amitié.

Enfin mon cher **Guillaume**, tu as commencé ta thèse depuis un peu plus d'un an mais tu es déjà impliqué dans quasiment tous les projets du labo. Mr. Multifonction, toujours prêt à te lancer dans des expériences rocambolesques, tu n'as pas peur de la difficulté ou de la montagne de travail toujours grandissante que l'on t'impose et les défis (que tu t'imposes souvent tout seul !!!!) sont ton moteur. Tu le sais sûrement, je suis un peu déçu d'abandonner le projet DUF2156 qui me tient tant à cœur, mais le fait de savoir que tu le reprendras (au moins en partie) me console un peu. Bien évidemment toi et moi resterons liés à jamais par les liens de notre carburant, le coca !!!

Comment ne pas évoquer notre chère technicienne dans cette partie de remerciements ? Ma chère Laurence (**Lolo**), si j'ai pu fournir le présent travail c'est aussi grâce à l'énorme quantité de travail dont tu m'as déchargé. Tu étais toujours là à me proposer ton aide et dès que j'avais besoin de quelque chose je pouvais compter sur ta rapidité, ton efficacité et ta bonne volonté. Même si je te demandais de faire150 minipreps, de rester pendant 1h devant une colonne à regarder des gouttes qui coulent ou encore de me préparer des milieux en dernière minute tu t'efforçais de faire de ton mieux pour que je puisse avancer sur autre chose de mon côté. Tout simplement… Merci Lolo !

Je voudrais aussi remercier nos nombreux collaborateurs, notamment **Dr. Hervé Roy** (University of Central Florida, USA), **Dr. Tetsuo Kushiro** (Meiji University, Japan) et **Pr. Osamu Nureki** (University of Tokyo, Japan) avec qui j'ai travaillé en lien étroit. Hervé, les expériences de spectrométrie de masse ont nécessité un nombre considérable de mises au point et je suis conscient que ça t'a demandé beaucoup de temps et beaucoup d'énergie. Malgré cela tu n'as jamais abandonné et grâce ta persévérance et ton expertise tu as finalement réussi à identifier les composés en question. Merci Hervé pour l'énorme travail que tu as fourni qui sans aucun doute a considérablement augmenté la valeur de mon travail de thèse.

Merci aussi à toi **Johan** de m'avoir supporté et pour tes nombreux conseils. Bien que tu aies quitté le labo de Hubert pour rejoindre d'autres horizons c'est toujours un véritable plaisir d'échanger avec toi.

Et puis il y a tous mes compagnons de galère qui ont toujours été là quand j'avais besoin d'aide ou de conseils. En particulier **Gaëtan**, je te remercie d'avoir passé des heures à me préparer pour mes présentations et de t'être toujours manifesté pour me donner un petit coup de main par ci par là. Tu as été bien plus qu'un simple collègue de travail… ensemble on a inculqué au labo les valeurs de la musique, la vrai… Maitre Gims, Soprano ou encore magic system, pour le plus grand bonheur de Johan. Je suis heureux que malgré ton départ du labo, nous sommes restés proches car tu es un ami qui m'est très cher. J'en profite aussi pour te féliciter pour la naissance ton petit Hugo !!!

Merci aux autres doctorants avec qui j'ai eu le plaisir de partager pendant un certain temps les joies et les galères de la thèse. Merci **Marine,** notamment pour tes nombreuses relectures, les nombreux services que tu m'as rendus mais surtout pour nos nombreuses discussions en bas de l'IPCB et de l'institut de botanique. Je remercie **Sylvain**, Monsieur ENS Cachan (pour ne pas utiliser d'autres surnoms que je me suis permis de t'attribuer) et enfin **Marion**.

Je te remercie particulièrement **Benoit** (Masquida) pour tes nombreux conseils et ton aide précieuse tout au long de ma thèse. En particulier, ton expertise dans le domaine des ARN catalytiques a été atout majeur et m'a permis d'atteindre mes objectifs en un temps record.

Merci aussi à toute l'équipe de Sylvie Friant (**Bruno** Rinaldi, **Séverine** Bär, mon ami **Abdel** !!!...) avec laquelle j'ai eu le plaisir d'interagir quotidiennement pendant ma thèse. J'en profite pour te remercier personnellement **Sylvie** d'avoir pris le temps d'évaluer mon travail de recherche lors des mi-parcours, mais aussi pour tes nombreux conseils sur mon sujet de recherche et bien sur pour ton amitié.

Je tiens à remercier le Dr. **Ivan Tarassov** de m'avoir accueilli au sein de l'UMR7156 et les responsables de l'école doctorale ED414 sans qui cette thèse n'aurait pas eu lieu.

Merci aux responsables pédagogiques de l'UE de biochimie qui m'ont donné l'opportunité de gouter à l'enseignement. Je suis tout particulièrement reconnaissant à **Joern** (Puetz) qui m'a guidé avec beaucoup d'enthousiasme pendant les 3 années de monitorat en TP de L2 que j'ai réalisé.

J'en profite aussi pour remercier le Dr. **Pierre Antony** qui a fait partie mes comités de suivi de thèse (CST) et qui a évalué mon travail de recherche tout au long de ces 4 dernières années. Merci pour vos appréciations et vos précieux conseils.

J'ai gardé pour la fin ceux qui me sont chers, ma famille et mes amis qui m'ont toujours accompagné, soutenus et encouragés. Merci **maman**, merci **papa** pour tout ce que vous avez fait pour moi et de vous être démenés à chaque fois que j'en avais besoin. Parmi vos récents exploits je vous remercie d'avoir gardé Sam cet été pendant deux semaines pour que je puisse continuer à travailler ma thèse.

Merci à mes amis qui m'ont soutenu tout au long de mon cursus et accueilli depuis mon arrivée à Strasbourg. Je pense notamment à **Henri & Sandrine, Albert et Ava, Netanel & Sarah, Manou & Myriam, Yoel & Debo, Yaakov & Dvora, Noemie** pour n'en citer que quelques-uns. Je vous remercie d'avoir été là pour me rendre heureux et prendre soin de moi, notamment dans les moments difficiles.

Et pour finir à toi **Kika**, ma chère et tendre épouse, ces quelques lignes ne peuvent évidemment pas représenter l'importance que tu as à mes yeux. Je te remercie Kika pour l'amour que tu me portes et ton soutien inconditionnel, en particulier ces derniers mois au cours desquels tu t'es démenée pour me permettre de rédiger ma thèse dans les meilleures conditions. Enfin à mon fils **Sam** je voudrais dire merci de m'avoir tenu compagnie toutes ces nuits. Je suis convaincu qu'a de maintes reprises tu as essayé de me dire que je faisais fausse route et peut-être qu'un jour, sait-on jamais, tu consulteras ce manuscrit de thèse.

List of abbreviations

A, T, G, C, U: nucleic acid bases Adenine, Thymine, Guanine, Cytosine, Uracil

aa: amino acid

aa-AMP: aminoacyl-adenylate

aa-tRNA: aminoacyl-tRNA

aaCL: aminoacyl-cardiolipin

aaCLS: aminoacyl-cardiolipin synthase

aaL: aminoacyl-lipid

aaPG: aminoacyl-phosphatidylglycerol

aaLS: aminoacyl-lipid synthase

aaLH: aminoacyl-lipid hydrolase

aaPGS: aminoacyl-phosphatidylglycerol

aaPGS: aminoacyl-phosphatidylglycerol synthase

aaRS: aminoacyl-tRNA synthetase

Afm: *Aspergillus fumigatus*

Aor: *Aspergillus oryzae*

AMP: adenosine monophosphate

Amp: Ampicillin

AS: aminoacyl-sterol

ASS: aminoacyl-sterol synthase

ASH: aminoacyl-sterol hydrolase

ATP: adenosine triphosphate

ATT: aminoacyl-tRNA transferase

Bba: *Beauveria bassiana*

CAMP: cationic antimicrobial peptide

CDP: Cytidine diphosphate

CHCl₃: chloroform

Cho: cholesterol

DAG: diacylglycerol

DNA: Deoxyribonucleic acid

DUF2156: domain of unknown function 2156

EMSA: Electrophoretic mobility shift assays

Erg: ergosterol

Erg-aa: ergosteryl-amino acid

Erg-Asp: Ergosteryl3-β-O-L-aspartate

ErdS: Erg-Asp synthase

ErdH: Erg-Asp hydrolase

Erg-Gly: Ergosteryl3-β-O-glycine

ErgS: Erg-Gly synthase

EtOH: Ethanol

fDUF2156: freestanding DUF2156

FT: flow through

fwd, rv: forward-, reverse-primer

g, L, h, min, s: gram, liter, hour, minute, second

GDP: guanosine diphosphate

GF: Gel filtration

GFP: Green Fluorescent Protein

GlcNAc: N-acetyl glucosamine

GNAT: GCN5-related N-acetyltransferase

GST: Glutathione S-transferase

GTP: guanosine triphosphate

HPLC: High-performance liquid chromatography

IB: Immuno Blot

KAN: kanamycin

kb: kilo base pairs

kDa: kilodalton

M: Molar

MBP: Maltose binding protein

MeOH: Methanol

MIC: minimal inhibitory concentration

MprF: Multiple peptide resistance Factor

mRNA: messenger RNA

MS: Mass Spectrometry

MSC: MultiSynthetase Complex

MurNAc: N-actyl muramic acid

MW: molecular weight

N-ter/Nt: N-terminal

ncRNA: non-coding RNA

ND: Non-Discriminant

nt: nucleotide

O/N: Overnight

OB: oligonucleotide/oligosaccharide-binding

OD: Optical Density

PAGE: PolyAcrylamide Gel Electrophoresis

PCR: Polymerase Chain Reaction

PG: phosphatidylglycerol

PPi: pyrophosphate

Pyl: Pyrrolysine

PA: phosphatidic acid

PS: phosphatidylserine

PE: phosphatidylethanolamine

PM: plasma membrane

RNA: Ribonucleic acid

rRNA: ribosomal RNA

Sec: selenocysteine

Sce: *S. cerevisiae*

SC: Synthetic Complete

SDS: Sodium DodecylSulfate

TCA: trichloroacetic acid

TEV: Tobacco Etch Virus protease

TevCS: TEV specific cleavage site

TLC: thin layer chromatography

TMH: transmembrane helix

tRNA: transfer RNA

U/: enzymatic units/

UDP: Uridine diphosphate

w/v: weight/volume

WB: Western Blot

WT/wt: Wild Type

v : v: volume : volume

Yli: *Yarrowia lipolytica*

μ-, n-, m-: micro-, nano-, milli-

Nomenclature of amino acids and aminoacyl-tRNA synthetases

amino acids				aminoacyl-tRNA synthetase	
Name	3 letters	1 letter		Name	abbreviation
Alanine	Ala	A		Alanyl-tRNA synthetase	AlaRS
Arginine	Arg	R		Arginyl-tRNA synthetase	ArgRS
Asparagine	Asn	N		Asparaginyl-tRNA synthetase	AsnRS
Aspartate	Asp	D		Aspartate-tRNA synthetase	AspRS
Cysteine	Cys	C		Cysteinyl-tRNA synthetase	CysRS
Glutamate	Glu	E		Glutamyl-tRNA synthetase	GluRS
Glutamine	Gln	Q		Glutaminyl-tRNA synthetase	GlnRS
Glycine	Gly	G		Glycyl-tRNA synthetase	GlyRS
Histidine	His	H		Histidyl-tRNA synthetase	HisRS
Isoleucine	Ile	I		Isoleucyl-tRNA synthetase	IleRS
Leucine	Leu	L		Leucyl-tRNA synthetase	LeuRS
Lysine	Lys	K		Lysyl-tRNA synthetase	LysRS
Methionine	Met	M		Methionyl-tRNA synthetase	MetRS
Phenylalanine	Phe	F		Phenylalanyl-tRNA synthetase	PheRS
Proline	Pro	P		Prolyl-tRNA synthetase	ProRS
Serine	Ser	S		Seryl-tRNA synthetase	SerRS
Threonine	Thr	T		Threonyl-tRNA synthetase	ThrRS
Tryptophan	Trp	W		Tryptophanyl-tRNA synthetase	TrpRS
Tyrosine	Tyr	Y		Tyrosyl-tRNA synthetase	TyrRS
Valine	Val	V		Valyl-tRNA synthetase	ValRS

Table of contents

PREAMBLE

Figure A-1: aa-tRNA synthesis and their use as substrates for protein biosynthesis and for other pathways beyond translation. Protein biosynthesis requires a large diversity of macromolecules including various classes of RNA molecules. The messenger RNA serves as template during protein biosynthesis and is translated by the ribosome composed of large (LSU; red) and small (SSU; orange) sub-units both containing ribosomal RNAs (rRNA) and proteins. Through their primary function, aminoacyl-tRNA synthetases (aaRSs) provide a full set of cognate aa-tRNAs which are used to decode and translate the mRNA. However, beyond translation, aaRSs were shown to be involved in a wide range of so called non-canonical functions and aa-tRNAs can be highjacked by so-called aa-tRNA-utilizing enzymes (mainly aminoacyl-tRNA transferases (ATT) that transfer the aa onto a wide range of macromolecules in a tRNA dependent way). The examples illustrated here represent aa-tRNA dependent lipid or peptidoglycan-precursor (Lipid II) modification pathways achieved by ATTs in bacteria.

Genes are informational units encoded in the form of DNA in all living cells. How we define genes is not that simple, as it has continually been refined, especially over the past decades with the discovery of several phenomena (Portin and Wilkins 2017). A gene can be defined as any discrete region, *i.e.* a locus, which contains — or encodes the information of — a heritable trait (Pearson 2006; Pennisi 2007). A more specific definition is the following, in which a gene is a nucleotide (nt) sequence, flanked by its *cis*-regulatory elements, *i. e.* promoter and the terminator, whose expression product is responsible for one or various cellular functions.

However, the genetic information contained within DNA — the "gene" — is probably the most stable and inert information that the cell contains. Consequently, cellular machineries must "realize" it into a "usable" form and interpret or convert encoded messages into active components capable of sustaining life or at least of performing molecular functions. Francis Crick proposed as early as 1970, that the first molecular process that initiates expression of the genetic information from DNA should be transcription of genes — the inert information — into a ribonucleic acid (RNA) molecule, that can either be a coding RNA or a noncoding RNA (Crick 1970) (**Figure A-1**). Noncoding RNAs (ncRNA) are transcribed from so-called RNA-genes that will never be translated into proteins but some of them (ribosomal RNAs (rRNA) and transfer RNAs (tRNA)) ultimately serve for the translation of coding/messenger RNAs (**Figure A-1**) and the flow of genetic information stops at this step. Resulting ncRNAs can adopt a myriad of secondary and functional tertiary structures and can also be subjected to posttranscriptional modification(s). These structural considerations are essential, as the tertiary structure of ncRNAs are crucial for their functions, that range from transporting "usable" forms of amino acids to the translation machinery (tRNA), regulating transcription or translation (riboswitches, etc.) to catalyzing chemical reactions (transpeptidation by rRNA or mRNA maturation in the case of self-splicing introns) (Serganov and Nudler 2013; Saad *et al.*, 2013; Zhang *et al.*, 2019). Noncoding RNAs that catalyze biochemical reactions are termed ribozymes and are ubiquitous throughout the tree of life (Doherty and Doudna 2000).

In contrast, coding RNAs are those that contain a kind of genetic information that must be further converted into other types of macromolecules in a second major process termed translation (Dever *et al.*, 2016). In this case, coding RNAs are referred to as messenger RNAs (mRNA) because they carry an information that must be translated into another language. The translational

machinery uses "coding" RNAs and translates the genetic information that they contain into functional molecules called proteins (**Figure A-1**). A ribonucleoprotein complex, the ribosome, is at the center of this process (Ramakrishnan 2002; Myasnikov *et al.,* 2009). Even though the ribosome cannot achieve protein synthesis on its own, it can be compared to a factory or a platform onto which all the partners necessary for protein synthesis are recruited. During translation, the ribosome "reads" mRNA from its 5'- to 3'-end. Precisely, the ribosome specifically "reads" and "translates" the open reading frame (ORF) of a mRNA, that can therefore be compared to a sentence in which words are represented by a succession of three consecutive nt called codons.

This crypted sentence must then be faithfully decoded and translated into the effector-language using a decoding key: the universal genetic code, that is sometimes also referred to as "the genetic Rosetta stone" (**Figure A-2**) (Nirenberg *et al.,* 1966). This code encrypts 20 (extended to 22 in some cases) proteinogenic amino acids (aa). Following the amino acid – codons correspondence rules, the ribosome sequentially links up amino acids into polypeptides — proteins — following the order imposed by codons along the mRNA (the ORF). The genetic code is composed of 4 nt x 4 nt x 4 nt = 64 different codons, of which 61 are amino acid-coding units, e. g. they can be translated to one of the 20 proteogenic amino acids found in the standard code (Nirenberg *et al.,* 1966). The representation of the genetic code proposed by Nirenberg is particularly convenient for its comprehension but more importantly it highlights the ingenuity of this code (**Figure A-2**). First, this table representation points out all the 64 possible triplet combinations (codons) found in mRNA and their corresponding aa. Second, its reading takes in consideration the order of the 3 nt composing the codon; the first letter is represented at the left edge of the table, the second at the upper and the third at the right. Note that the four nt possibilities for each letter of the codon are organized invariably as U, C, A and G *i. e.* both pyrimidines are followed by both purines. Thus, the first and the last codons correspond to UUU encoding Phe (upper left) and to GGG encoding Gly (lower right). Third, the four codons containing the same letters at positions 1 and 2 are regrouped in the same box which highlights the degenerate nature of the codon – aa assignments. This degeneracy is central to keep the integrity of the genetic information despite codon mutations. Indeed, due to the degenerate character of the genetic code, aa encoded by 4 codons are not affected by the mutation of their 3rd codon nt (called wobble position) since these mutations

Figure A-2: The standard genetic code. In this representation, the meaning of a codon (indicated at the left of each column) in its aa «language» (in bold) is given by intersecting the first, the second and the third letter of the given triplet. Each aa box is indicated with a different color which reveals that most of them are encoded by 2 or 4 codons but Ser, Arg and Leu are encoded by as much as 6 codons. In the standard code, only 1 codon is assigned to each, Met or Trp, while Ile is the sole aa encoded by 3 codons. Stop codons are indicated in white boxes. Note that codons reassignments were described in bacterial, eukaryotic and organellar genomes. For more details on deviations from the standard genetic code, refer to Ambrogelly *et al*, 2007; Sengupta and Higgs, 2015; Mukai *et al*, 2017.

generate a "synonym" codon. Similarly, aa encoded by two codons are only affected by transversion (*i. e.* pyrimidine to purine and vice versa) but not by transition (purine to another purine or pyrimidine to another pyrimidine) mutations at this position. Furthermore, in some cases, missense mutation of the wobble position changes the aa identity but not its nature as it is the case for codons encoding Asp (GAU, GAC) and Glu (GAA, GAG). Similarly, XUX codon correspond all to hydrophobic aa. However, mutation of the first or second nt leads in almost all cases to missense mutation and more dramatically to non-sense mutation (mutation to a stop-codon). Thus, as mentioned above, decoding of the mRNA and aa incorporation into polypeptides during translation must be done with high fidelity to ensure that the information stored in the form of DNA and expressed as mRNA be eventually faithfully translated into proteins. Finally, some expansions of the code —with respect to the "standard" genetic code— exist in restricted taxonomic groups, as for example in some archaea and bacteria where the UAG Stop-codon encodes pyrrolysine (Pyl), while the UGA Stop-codon encodes selenocysteine (Sec) in all kingdoms of life (detailed in **chapter A § IV** of the present introduction).

However, despite the fact that genetic code support some peculiarities, it is considered that in a canonical context, each ORF starts with the initiator AUG codon translated to methionine (Thach *et al.*, 1966; Adams and Capecchi 1966), whereas the three remaining non proteogenic codons (UAA, UAG and UGA) are called Stop-codons since their occurrence leads to the dissociation of translational machinery (**Figure A-2**). Consequently, the ribosome translates the mRNA sequentially codon after codon, with respect to the genetic code —using the "rules" of correspondences between codons and amino acids—, thereby producing a polypeptide in which the order of aa condensation is determined by the mRNA sequence.

But how can the ribosome, mechanistically speaking, translate a given codon into the cognate aa? As postulated early by Crick in his adaptor hypothesis (Crick 1956), each one of the twenty aa used for protein synthesis is paired with its cognate "adaptor", capable of recognizing — interacting and "reading"— its own codon through sequence-specific non-covalent interactions (the decoding mechanism will be shortly described in **chapter A § I**). This adaptor corresponds to the transfer RNA (tRNA; detailed in **chapter A § I** of the present introduction). Aminoacyl-tRNA (aa-tRNAs) are produced by a family of enzymes called aminoacyl-tRNA synthetases (aaRS; detailed in

chapter A § III of the present introduction) that each catalyze the specific attachment —
"**aminoacylation**" (detailed in **chapter A § II**) — of one aa onto its cognate tRNA (**Figure A-1**). This
means that 20 aaRSs are required to recognize the 20 proteinogenic aa to attach them onto the 20
cognate tRNA families required to yield the full set of 20 aa-tRNAs necessary to ribosomal protein
synthesis. For this process, high fidelity is crucial to avoid mis-incorporation of aa into proteins
that would otherwise lead to altered proteomes, which is generally prejudicial to cells.

AaRSs are modular proteins that always contain a catalytic core responsible for tRNA
aminoacylation — aa activation and tRNA aminoacylation — and, most often, a tRNA anticodon-
binding domain that helps the enzyme associate to its cognate tRNA. Apart from the core catalytic
domain, they are also often fused to additional domains that are required for accurate recognition
of the cognate tRNA and more importantly to ensure high fidelity during tRNA aminoacylation (Ling
et al., 2009). One particularity of eukaryotic cells is the formation of Multi-Synthetase Complexes
(MSC) that aggregates and anchors a sub-group of aaRS and auxiliary proteins in the cytoplasm
[reviewed in (Laporte *et al.,* 2014; Mirande 2017)]. The minimal MSC complex from the yeast *S.
cerevisiae* is, for example, composed of methionyl-tRNA-synthetase (MetRS) and glutaminyl-tRNA
synthetase both bound to the auxiliary assembly factor Arc1 (Frechin *et al.,* 2010), while the human
MARS complex contains 9 aaRSs, organized around 3 auxiliary factors, termed AIMPs (for
Aminoacyl-tRNA Synthetase Interacting Multifunctional Proteins). Assembling aaRSs into MSCs has
been suggested to be important to modulate the translational activities of aaRSs, but also to
regulate the non-translational functions that these enzymes can additionally perform beyond tRNA
aminoacylation (Mirande 2017). In fact, the participation of MSC-bound and "freestanding" aaRS in
a **plethora of additional noncanonical functions beyond tRNA aminoacylation**, ranging from
regulation of transcription to the modulation of angiogenesis, is often correlated to their ability to
relocate to unsuspected cellular compartments and to their propensity to have **additional
functional domains** besides the catalytic core and the anticodon-binding domain [reviewed in (Guo
and Schimmel 2013; Yakobov *et al.,* 2018). The latter review, to which I participated as a first author
is found at the end of the present manuscript].

Strikingly, early after it was established that (aa-)tRNA primary function is to define and to
translate the genetic code for protein biosynthesis, an unexpected concept emerged and

postulated that (aa-)tRNA also participate to other processes; as early as in 1965, M. Matsuhashi and colleagues demonstrated the tRNA dependent transfer of aa onto other macromolecules such as peptidoglycan (Matsuhashi *et al.*, 1965). Later, the involvement of tRNAs and aa-tRNAs (canonically synthesized by aaRSs) in numerous pathways beyond protein biosynthesis was extensively established (Katz *et al.*, 2016; Schimmel 2018) and several aa-tRNA-utilizing enzymes/pathways have been subsequently described (Moutiez *et al.*, 2017; Hemmerle *et al.*, 2020). Among them, **aminoacyl-tRNA transferases** (**ATT**; briefly introduced in **chapter B** of the present introduction and extensively reviewed in our recent review to which I participated (Hemmerle *et al.*, 2020)) highjack aa-tRNA species from their primary destination (i. e. the ribosome) and transfer the aa moiety onto a wide range of final acceptor substrates (Dare and Ibba 2012; Moutiez *et al.*, 2017; Hemmerle *et al.*, 2020) (**Figure A-1**). Notably, **aminoacyl-lipid synthases** (**aaLS**; extensively detailed in **chapter C** of the present introduction) achieve their ATT activity by transferring aa from given aa-tRNAs onto membranous glycerolipids from the inner leaflet of the plasma membrane (PM) (**Figure A-1**) (Roy 2009). The cytoplasmic ATT domain of aaLSs is fused to a membranous domain which at least in some cases achieves flippase activity by translocating **aminoacylated lipids** (**aaL**) to the outer leaflet of the PM (Slavetinsky *et al.*, 2017) (**Figure A-1**). Those lipid-modifying factors were so far only described in bacteria and are of particular interest for the purpose of my thesis. Of note, while most aaLSs are implemented by aa-tRNAs that are synthesized by freestanding aaRSs, species belonging to actinobacteria have inherited aaRS-fused aaLSs that synthesize aa-tRNA assumed to be directly channeled to the ATT domain for lipid aminoacylation (Maloney *et al.*, 2009).

My PhD aimed to study a tRNA-dependent lipid aminoacylation mechanism that came out to be even more unique than those that were described when I started my project. However, in order to comprehensively present the objectives of my work, it seemed to me essential to first introduce the way aa-tRNA are synthetized and the state of art concerning lipid aminoacylation before I present the results I obtained in the course of my PhD.

INTRODUCTION

A. aa-tRNA synthesis and their utilization for protein synthesis

I. Transfer RNA (tRNA)

In the late 50's it was suggested that a particular class of "soluble RNA" (sRNA) was involved in the translation process of genetic information (Hoagland *et al.,* 1958). Soluble RNAs were soon renamed tRNA for "transfer" RNA from the deciphering of their function as being the physical interpreters between the nucleotide language of mRNA and the peptide/protein language. Each tRNA contains internal informations called "determinants" that dedicates it to be charged with a given proteogenic aa. For example, determinants of tRNA^{Ala} from *Sce*, dedicates it to be charged specifically with Ala. Each living cell necessarily encodes and transcribes a minimal set of 20 tRNA families that are subsequently charged with one of the twenty proteogenic amino acids by aaRS.

The 2D "cloverleaf" model of tRNAs (**Figure I-1**) was initially proposed by RW. Holley and colleagues in 1965 as they achieved for the first time the complete sequencing of an tRNA namely tRNA^{Ala} from *S. cerevisiae* (Holley *et al.,* 1965). tRNA^{Ser}, tRNA^{Tyr}, and tRNA^{phe} sequences from *Sce* were obtained in the next two years and from then on to 1974 at least 60 tRNA sequences were resolved. In addition, important structure probing analysis through RNase treatment, argued for a common structure shared throughout all tRNA (RajBhandary and Chang 1968; Kim *et al.,* 1974). Finally, the first 3D structure of tRNA was resolved in 1973 through analysis of X-ray diffraction data (Kim *et al.,* 1973).

Even though the cloverleaf representation of tRNA does not correspond to the physiological and functional 3D "L-shaped" structure, it allowed to understand how tRNAs act as an intermediate. According to the established nomenclature, each tRNA nt are designated by a fixed number ranging from 1 to 76 (Sprinzl *et al.,* 1998). Thus, in tRNAs containing more than 76 nt, inserted positions are designated by the number of the preceding canonical position followed by an alphabetic letter. For example, an insertion between positions 17 and 18 will be named 17A. Concomitantly, the four final unpaired positions corresponding to the discriminator base followed by the invariable 3'-CCA are named 73, 74, 75 and 76 respectively even in tRNA composed of less than 76 nt (**Figure I-1**).

In their secondary structure, the first 7 bases (from 5') and the 7 bases preceding the discriminator base of the tRNA are paired through canonical WC and Wobble base pairing (Wobble pairing; see below). The resulting helix together with the four unpaired bases at the 3' end is called the **acceptor-stem** as its extremity is crucial to accept the cognate aa during the aminoacylation reaction. When reading the tRNA sequence from 5' to 3', the first 7 bases are followed by two unpaired nt and the **D-stem-loop** (a 4 base-pairs helix followed by a 8-11 bases loop) whose name is due to the presence of a modified base called dihydrouridine (D) in the loop. A single nt separates the D-stem-loop from the next secondary structure composed of 5 base-pairs and a 7 nt-long loop, forming the **anticodon stem-loop**. As it will be detailed later, nt 34, 35 and 36 constitute the **anticodon**, which is the main feature required to decode the codons on the mRNA during protein synthesis. Following the anticodon stem comes a structure which is variable in its size and length called **V-loop**. tRNAs with few nt in this region belong to class I tRNA whereas tRNA containing more nt belong to class II tRNA. $tRNA^{Ser}$, $tRNA^{Leu}$, $tRNA^{Tyr}$ and $tRNA^{Sec}$ are members of class II and can consequently form a **Variable-stem-loop (or variable arm)**. Finally, the **T-stem-loop** harbors a 5 base-pairs helix and a 7 nt loop with two conserved nt modifications namely T_{54} and pseudouridine (Ψ_{55}). Even though the cloverleaf structure is shared by all tRNA, it is worth noting that in addition to the mentioned variations in the V-loop and the D-loop, numerous variations occur among tRNA. For example, the acceptor stems of $tRNA^{Sec}$ and $tRNA^{His}$ contain 8 base-pairs while mitochondrial tRNAs in nematodes can be missing either the D- or T-stem-loop or even both.
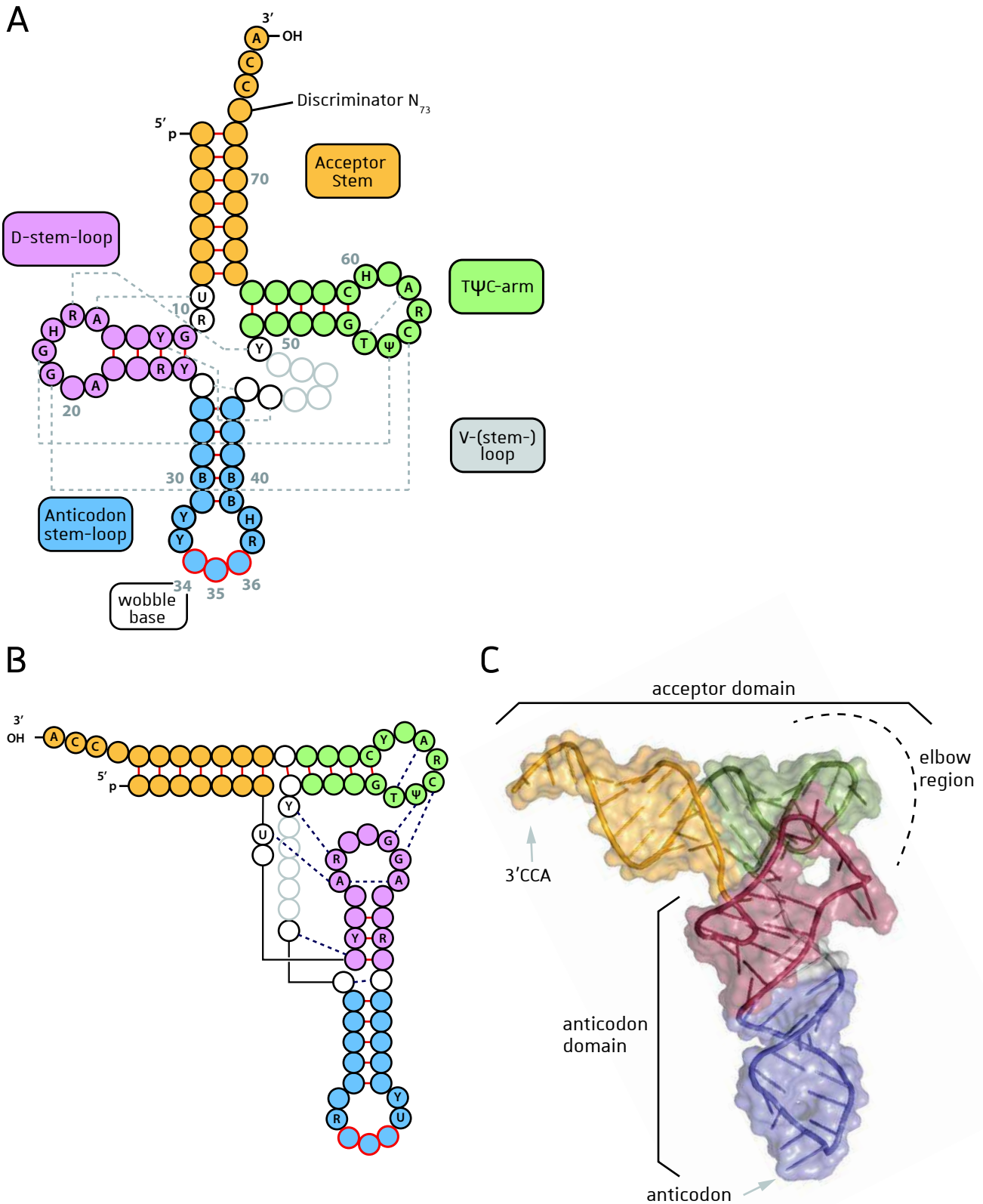
Figure I-1: tRNA structure (modified from Debard, 2019 with permission). (A) The cloverleaf structure of tRNAs and consensus residues in Sce according to Marck et al, 2002. **(B)** Planar representation of the consensus L-shaped tRNAs. **(C)** 3D structure of the tRNA^{Asp} from Sce (pdb: 1VTQ). A, adenosine; U, uridine; T, thymidine; G, guanosine; C, cytidine; R, purine; Y, pyrimidine; H, correspond to A, C or U; B indicate C, G or U; red sticks and circles indicate WC interactions (including Wobble pairing) and dash lines indicate non-WC interactions.

The herein cloverleaf representation of tRNA results from important works done since the late 60's (RajBhandary and Chang 1968; Kim *et al.,* 1973; Kim *et al.,* 1974) and its conservation throughout the three kingdoms of life was confirmed in the following decades (Marck and Grosjean 2002; Sprinzl and Vassilenko 2005). However, the 3D physiological "L-shape" of tRNA in living cells implies that the different secondary structure elements of the cloverleaf interact together by establishing *trans* bases-pairing. Therefore, single-stranded nt from loops and bulges can base-pair together or even with already established base-pairs. To render this possible, the implicated nucleotides generate so-called non-canonical base-pairing by interacting notably through their Hoogsteen edge rather than their Watson-Crick (WC) edge. Consequently, nt involved in both, WC- and Hoogsteen-edge interaction, form base triples. Based on the resolved structure of tRNA^{phe}, SH Kim proposed a planar representation of the folded tRNA L-shape depicted on **Figure I-1**. (Kim 1978; Kim *et al.,* 1973; Kim *et al.,* 1974). In this conformation, the T-stem-loop stacks together with the acceptor stem forming an unique 12 bp loop-minihelix while the "dumbbell" formed by the D- and the anticodon-stem-loops encloses an 9 bp minihelix flanked by two loops. One extremity of the resulting L-shape corresponds to the **amino-acid acceptor 3'CCA** whereas the **anticodon** is found at the other extremity. In addition to these considerations, numerous specific nt posttranscriptional modifications (PtrM) involved in maintaining the tRNA "L-shape", modulating the codon-decoding capacity and regulating several physiological function(s) (Vare *et al.,* 2017; Koh and Sarin 2018; Sokolowski *et al.,* 2018).

The **decoding mechanism achieved during translation** relies on Watson-Crick interaction between a given **codon** of the mRNA and the **anticodon** of the corresponding tRNA (**Figure I-2**). Whereas nt positions N_{35} and N_{36} of the tRNA anticodon interacts respectively with N_2 and N_1 of the cognate codon only through canonical Watson-Crick pairing, N_{34} interaction with N_3 implicates Wobble pairing (also called extended Watson-Crick pairing) (Crick 1966). Hence, the Wobble base-pairing stipulates that at this position, G can face to U whereas I_{34} of the tRNA potentially decodes codon positions A_3, U_3 or C_3. Therefore, position N_{34} of the tRNA is called the Wobble position.

As evidenced by the genetic code, beside Met and Trp, all aa are encoded by more than one codon which confers to the genetic code its degenerated character and introduces the notion of codon usage bias. Consequently, a given aa can be loaded on "isoacceptors" tRNAs containing
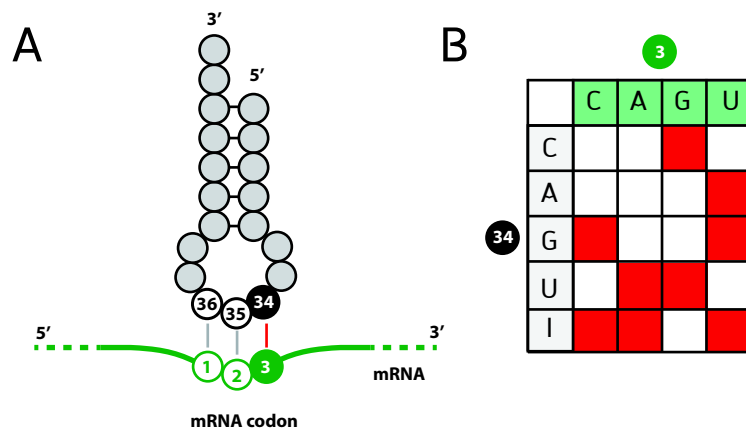
Figure I-2: Decoding mRNA during translation by codon-anticodon pairing. (A) Illustration of the interaction between the anticodon of a given tRNA and its cognate codon in the mRNA. While N_1-N_{36} and N_2-N_{35} interact only through canonical WC base pairing, N_3-N_{34} involves Wobble pairing. Interactions occurring at N_3-N_{34} are summarized in **(B)** (indicated by red squares). A, adenosine; U, uridine; G, guanosine; C, cytidine; I, inosine.

different anticodons. Finally, "isodecoders" corresponds to tRNAs that share the same anticodon, and obviously the same identity determinants but other nucleotide positions vary.

II. Aminoacylation of tRNA

As mentioned, tRNAs are the physical bridge between a specific mRNA codon and the corresponding aa to be incorporated in the nascent protein. A full sub-set of (at least) 20 faithfully synthetized aa-tRNAs has to be synthesized in all living cells. This is done by a family of enzymes called aminoacyl-tRNA synthetases (aaRS). Each aaRS must select a specific L-aa (and reject its D-conformation) in order to transfer it onto its cognate tRNA. AaRSs stated to be characterized in the 50's. At this time scientists discovered that prior to their incorporation into proteins, the aa must be activated in an enzymatic-dependent manner (Hoagland 1955; Zamecnik *et al.,* 1958). These studies showed that only L-aa are competent to undergo this activation mechanism. The discovery of in 1958 lead finally to the establishment that aaRS are enzymes that transfer a specific aa onto its cognate tRNA by catalyzing two successive reactions.

During the first reaction of aminoacylation, an aa and ATP are recruited into the active site of the corresponding aaRS (in the presence of Mg^{2+}). The α carboxyl group of the aa attacks the α-phosphate group of ATP (nucleophilic attack) which produces *i)* an inorganic pyrophosphate (PPi) released from the active site and *ii)* an aa-adenylate (aa-AMP) that remains in the active site. In a second step, the 2' or 3' hydroxyl group of the terminal adenine from the tRNA attacks the carbon of the α-COOH from the aa which results in the esterification of the aa onto its cognate tRNA (**Figure I-3**). Note that for the aa activation reaction, the tRNA is generally not required except for glutaminyl-tRNA Synthetase (GlnRS), glutamyl-tRNA Synthetase (GluRS) (Ravel *et al.,* 1965), arginyl-tRNA Synthetase (ArgRS) (Mitra and Mehler 1967) and class I lysyl-tRNA Synthetase (LysRS) (Ibba *et al.,* 1999). As illustrated by these few examples, the nomenclature of aaRS is closely related to their activity. However, their abbreviation using the three-letter code of the aa followed by "RS" is more convenient and will be preferred in this manuscript.
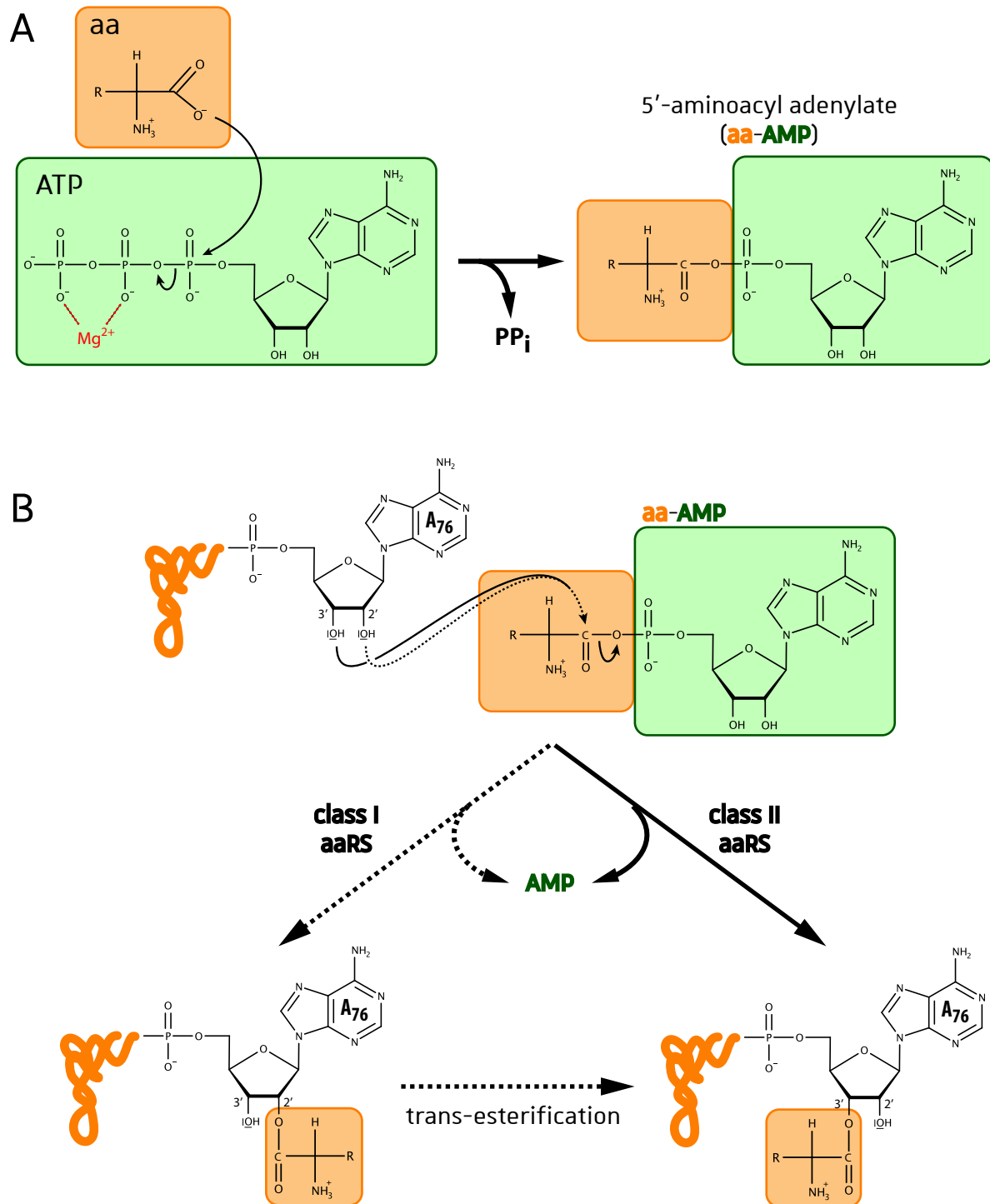
Figure I-3: Aminoacylation reaction catalyzed by aaRSs. (A) The first step leads to the formation of an aminoacyl-adenylate (aa-AMP) in the presence of an ATP molecule (stabilized with Mg2+ in the active site of the aaRS) and an aa. **(B)** The second step corresponds to the transfer of the activated aa onto a hydroxyl group of the terminal tRNA nt (*i. e.* A_{76}) and leads to the synthesis of a cognate aa-tRNA. However, events from this step differ somewhat according to aaRS classes since the aa is transferred onto the 2'OH or the 3'OH of A_{76} by class I (dashed lines) or class II aaRSs (solid lines), respectively. Aa charged by class I aaRS are then rapidly transesterified onto the 3'OH.

III. Class I and class II aaRSs

All aaRS are modular enzymes composed of a catalytic domain and an anticodon-binding domain (ABD) but often other domains were recruited during evolution (Guo and Yang 2014). However, there are structural and functional differences that lead to their segregation into two so-called classes of aaRSs (Eriani *et al.,* 1990) (**Figure I-3, Figure I-4** and **Table I-1**). Concerning their evolutionary history, all members of each class of aaRSs are believed to result from multiple duplication events originating from initially a unique "minimal enzyme" called urzyme followed by domain rearrangement and acquisition of new aa and tRNA specificities (Rodin and Ohno 1995; Carter and Duax 2002; Rodin *et al.,* 2009; Pham *et al.,* 2010; Rubio Gomez and Ibba 2020). A relatively simple example, GlnRS is only present in eukaryotes and γ-proteobacteria comes from a duplication of the GluRS gene that happened in the eukaryote ancestor (Lamour *et al.,* 1994). Similarly, AsnRS, absent in half of the archaea and bacteria, originates from a duplication of an archaeal AspRS gene (Roy *et al.,* 2003).

III.1. The catalytic domain, the major discriminator of class I and II

It is believed that aaRS appeared early during evolution and that the last universal common ancestor (LUCA) contained already an almost complete set of aaRS (Rubio Gomez and Ibba 2020). To date 22 different tRNA aminoacylation activities, ensured by 23 different aaRSs each belonging to class I or to class II, were described. LysRS is a singular case since it can be of both classes according to the species (Ibba *et al.,* 1997). Most species contain the class II LysRS and only a few species encode class I LysRS or both forms (Polycarpo *et al.,* 2003). The two latest characterized members of the aaRS family (22 and 23) are SepRS and PylRS (both belonging to class II aaRSs) which are involved in cysteinyl-tRNA^{Cys} or selenocysteinyl-tRNA^{Sec} and pyrrolysyl-tRNA^{Pyl} formation, respectively. The structural and functional characteristics that divided aaRSs into two classes are listed in **Table I-1**. The catalytic domain of Class I aaRS contain a Rossman fold (Rossmann *et al.,* 1974) composed of five parallel β-strands flanked by α-helices (**Figure I-4**). In class I aaRS where it is generally located at their N-terminus, the Rossman fold is split in two domains separated by a connective peptide 1 (CP1) (Starzyk *et al.,* 1987). Each domain encloses one of both class I aaRS signature sequences namely HIGH and KMSKS (according to their aa composition using the 1 letter
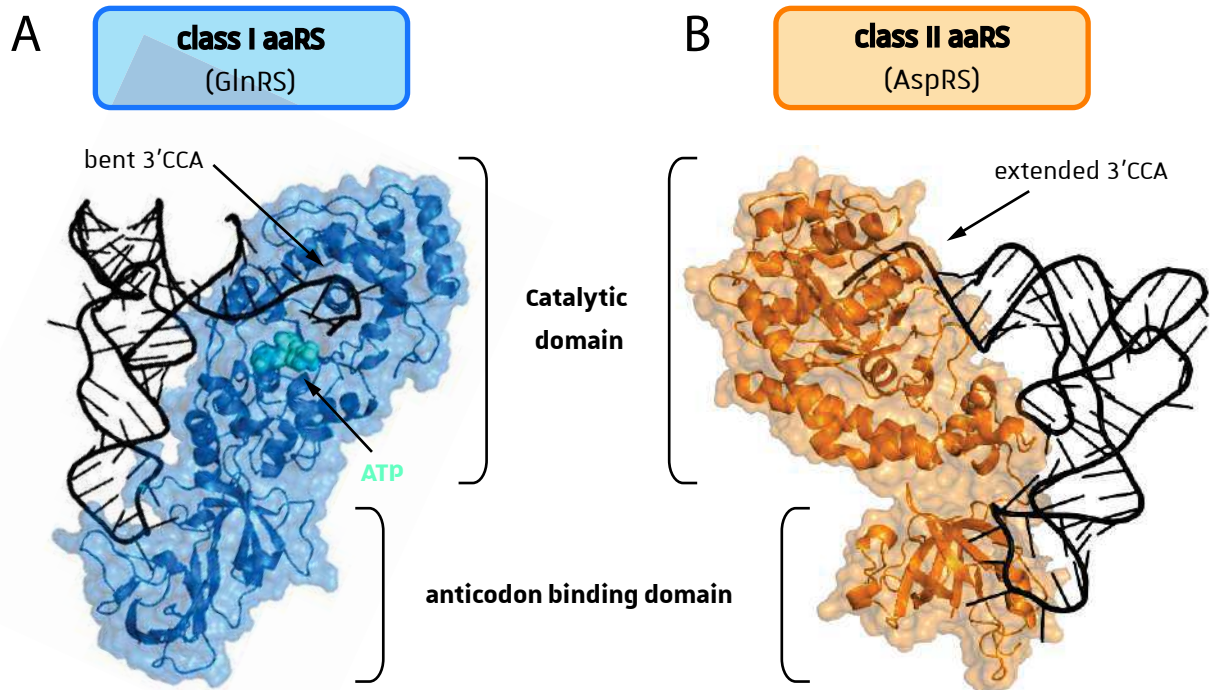
Figure I-4: 3D structures of aaRSs and their interaction with the tRNA. (A) The catalytic domain of Class I aaRSs, exemplified by *E. coli* GlnRS (pdb: 1GTR) corresponds to a modified Rossman fold and recognizes the bent 3'CCA extremity through the minor groove of the tRNA acceptor-stem. **(B)** In contrast the catalytic domain of class II aaRS, exemplified by *S. cerevisiae* AspRS (pdb: 1ASY), is characterized by 7 β-strands and contains characteristic motifs 1, 2 and 3. Class II aaRSs bind the extended 3'CCA extremity through the major groove of the tRNA acceptor stem. Most aaRSs (excluding SerRS) contain an anticodon binding domain but their structural organization differs between aaRS subclasses. Inspired from Debard, 2019.

code) which are essential motifs of the catalytic site (Eriani *et al.,* 1990). Importantly, CP1 recognizes the single stranded 3'-end of the tRNA but in the cases of ValRS, LeuRS and IleRS the inserted domain is implicated in aa-tRNA editing (Ling *et al.,* 2009). Note that there are sub-classes within each Class of aaRSs (**Table I-1**).

The active site organization of class II aaRS is strikingly different since it is composed of 7 anti-parallel β-strands forming a β-sheet flanked by two α-helices (**Figure I-4**). Consensus sequences are less conserved than in class I aaRS and consist of three degenerated motifs (Eriani *et al.,* 1990). The Φ-X-X-X-+-Gly-Φ-X-X-ΦX-X-Pro-Φ-Φ sequence corresponds to motif 1 where X correspond to non-conserved aa residues whereas + and Φ indicate a basic or a hydrophobic residue, respectively. Motif 2 corresponds to +-Φ-Φ-X-Φ-X-X-X-(Phe/His/Tyr)-Arg-X-(Glu/Asp)-X-4-12-(Arg/His)-ΦX-Phe-X-X-X-Φ-X-Φ-Φ and motif 3 to λ-X-Φ-Gly-Φ-Gly-Φ-Gly-Φ-Glu-Arg-Φ-Φ-Φ-Φ-Φ-X7-12- Φ-Pro where λ indicates an aa that harbor a long lateral chain (**Table I-1**). Motif one is mostly implicated in class II aaRS dimerization whereas motif 2 and 3 constitute the catalytic site. Beside the herein described consensus sequences, aaRS harbor idiosyncratic signature sequence as for example the Gln-Ser-Pro-Gln (QSPQ) AspRS motif which is involved in Asp recognition (Eriani *et al.,* 1993; Cavarelli *et al.,* 1994).

III.2.   aaRS oligomerisation

Another important characteristic of aaRS is their oligomerization state. Class I aaRSs are in general active as monomers (α) except for TyrRS and TrpRS that homodimerize (α2) through their CP1 domain. Class II aaRSs are generally homodimers (α_2) and less often homotetramers (α4) or heterotetramers ($\alpha_2\beta_2$). Usually, the oligomeric nature of an aaRS is conserved across species (e.g. AspRS is an α_2 homodimer in all studied species). However, GlyRS (class II aaRS) oligomerization varies and was described in eukaryotes and archaea to be α_2 and in most bacteria to be $\alpha_2\beta_2$. Both are structurally class II aaRS but the α_2 form belongs to the IIa sub-class whereas $\alpha_2\beta_2$ GlyRS is sub-classified as IIc aaRS (O'Donoghue and Luthey-Schulten 2003) (Perona and Hadd 2012). Variations related to the oligomerization were described for other aaRS too (Rubio Gomez and Ibba 2020) (**Table I-1**).

	Class I			Class II		
	aaRS	**Oligomerization**	**Editing**	**aaRS**	**Oligomerization**	**Editing**
Subaclass a	MetRS	α α_2	Yes	SerRS	α_2	Yes
	ValRS	α	Yes	ThrRS	α_2	Yes
	IleRS	α	Yes	AlaRS	α_2	Yes
	LeuRS	α	Yes	GlyRS	α_2 $(\alpha\beta)_2$	
	CysRS	α α_2		ProRS	α_2	Yes
	ArgRS	α		HisRS	α_2	
Subclass b	**GluRS**	α		AspRS	α_2	
	GlnRS	α		AsnRS	α_2	
	LysRS	α		LysRS	α_2	Yes
Subclass C	TyrRS	α α_2		PheRS	α $(\alpha\beta)_2$	Yes
	TrpRS	α_2		SepRS	α_4	
				PylRS	α_2	
Features of the Catalytic domain	Rossman fold: 5 parallel b-strands connected by a-helices			7 antiparallel b-strands flanked by a-helices		
	HIGH & KMSKS in the active site			Motif 1: ΦXXX+GΦXXXXP$\Phi\Phi$ Motif 2: +$\Phi\Phi$XΦXXX(F/H/Y)RX(E/D)(4-12X)(R/H)ΦXF XXXΦX$\Phi\Phi$ Motif 3: λXΦGΦGΦGΦER$\Phi\Phi\Phi\Phi$(7-12X)ΦP		
Mechanistic features	Approach the **minor** groove of the tRNA			Approach the **major** groove of the tRNA		
	Transfer the aa onto the **2'OH** of A76			Transfer the aa onto the **3'OH** of A76 (except PheRS)		
	Bind ATP in an **extended** conf.			Bind ATP in a **bent** conformation		
	Terminal 3'CCA of the tRNA in a **bent (hairpin)** conformation			Terminal 3'CCA of the tRNA in an **extended** conformation		
	aa-tRNA release is generally the rate-limiting step			**aa activation** is generally the rate-limiting step		

Table I-1: Standard classification of and features of aaRSs. Based on data from Ribas de Pouplana and Schimmel, 2001; Perona and Hadd, 2012 and Rubio and Ibba, 2020. aaRSs for which editing processes were documented are specified. **Figure I-7B** shows aa being edited by those aaRSs. AaRSs in bold require the presence of the tRNA for aa-activation. Aa are noted in their 1 letter code; X, any aa; +, basic aa; Φ, hydrophobic aa; λ, small aa.

III.3.   aaRS sub-classification

Indeed, beside their well-established classification into two classes, aaRSs can be further divided in subclasses (**Table I-1**). Many studies attempted to propose such subgroups of aaRS based on evolution (Wolf *et al.*, 1999; Woese *et al.*, 2000; O'Donoghue and Luthey-Schulten 2003), sequence, structural domain organization (Perona and Hadd 2012) and docking analyses (Ribas de Pouplana and Schimmel 2001). Whereas the different investigations approve generally to divide class II aaRSs in 3 subclasses (not always for the same reasons), the situation of class I is often confused and generally divided either in 3 (Cusack 1995; Ribas de Pouplana and Schimmel 2001) or in 5 subclasses (Perona and Hadd 2012). The ABD is more variable in terms of structure but participate to the sub-classification of aaRS. The C-terminal ABD of ArgRS, LeuRS, IleRS, ValRS, MetRS (Wolf *et al.*, 1999) and probably CysRS (Hou and Perona 2005) is an α-helical rich domain (DALR/Add2) that classifies them as sub-class Ia aaRSs which is also characterized by the fact that those aaRS recognize mainly aliphatic and thiolated amino acids. GluRS, GlnRS and LysRS I belong to sub-class Ib aaRSs and harbor either an OB-fold at their C-terminus or an α-helix-cage to recognize the anticodon. Finally, TyrRS and TrpRS, forming the sub-class Ic, recognize aromatic residues and were thought to be the only class I aaRSs as α2 oligomers (Beikirch *et al.*, 1972; Hossain and Kallenbach 1974). Class II aaRSs can also be divided into 3 subclasses according to their ABD. Sub-class IIa aaRSs (except SerRS in which tRNA recognition does not involve the anticodon) were considered to recognize the anticodon through a C-terminal module composed of a 7 stranded β-sheet flanked by two α-helices, whereas Sub-class IIb contain an N-terminal OB-fold composed by a 5 stranded β-sheet splited by an α-helix between strand 3 and 4. Note that class IIa activates hydrophobic and small polar residues whereas both sub-classes Ib and IIb activate aa that are large and charged (Glu, Gln, Lys and Asp, Asn, Lys respectively). Another characteristic specific to sub-class IIb is that the second base of their cognate tRNA (i. e. tRNA^{Asp}, tRNA^{Asn} and tRNA^{Lys}) corresponds to U_{35}. Finally, PheRS and the non-canonical SepRS and PylRS constitute the sub-class IIc.

As mentioned above, this "relaxed" sub-classification of aaRS takes in consideration the ABD but this feature alone is not sufficient to discriminate them fully. Therefore, other criteria are included and as mentioned above other classification systems were proposed.

III.4. Mechanistic features differentiating both aaRS classes

Due to conformational constraints that have evolved among aaRS, additional features distinguish both classes. To catalyze aminoacylation, the ATP and the terminal 3'-CCA of the tRNA must fit into the aaRS active site. Class I aaRSs bind the ATP in its straight conformation and the terminal 3'-CCA in its bent conformation site (exceptions: TrpRS (Shen *et al.,* 2006) and TyrRS (Yaremchuk *et al.,* 2002), belonging to class I, recognize tRNAs with extended 3'-CCA) in contrast to class II aaRSs where the bent ATP and the extended tRNA end are required to fit into the active (exception: PheRS (Goldgur *et al.,* 1997)) (Rubio Gomez and Ibba 2020) (**Table I-1**; **Figure I-4**). Furthermore, class I aaRS transfer the aa onto the terminal 2' hydroxyl group of the tRNA terminal adenosine and bind the tRNA through the minor groove of the acceptor stem helix while class II aaRS aminoacylate the terminal 3'OH group of the tRNA terminal adenosine and bind the tRNA *via* the major groove of the acceptor stem (Sprinzl and Cramer 1975; Rubio Gomez and Ibba 2020) (**Table I-1**; **Figure I-3**). However, because only 3'-OH charged aa-tRNAs are channeled to the ribosome (*via* EF-Tu or eEF1A), 2'-OH charged residues are rapidly trans-esterified onto the 3'-OH charged ones. Finally, the rate limiting step during class I aaRS aminoacylation is thought to be the release of the final aa-tRNA which is not the case in class II aaRS where the rate limiting step is either the aa activation or the transfer reaction (Rubio Gomez and Ibba 2020).

IV. Alternate and so-called indirect aminoacylation pathways

Many prokaryotes are missing either GlnRS or AsnRS or CysRS and sometimes even two or three of these aaRSs (*e. g.Methanococcus jannaschii* lacking AsnRS, GlnRS and CysRS (Bult *et al.,* 1996)). In these organisms, the missing aaRS is compensated by a so-called indirect tRNA aminoacylation pathway. In these pathways the orphan tRNA will first be charged with a non-cognate aa by a nondiscriminating aaRS and then the mischarged aa will be tRNA-dependently (while attached to the tRNA) converted into the cognate aa by a second enzyme (Hemmerle *et al.,* 2020).

IV.1.   Cys-tRNA^{Cys} formation in methanogenic archaea lacking CyRS

To complement the missing CysRS activity, archaea have developed a pathway that requires the non-canonical class II o-phosphseryl-tRNA synthetase (SepRS) to mischarge tRNA^{Cys} with o-phosphoserine. Cys-tRNA synthase (SepCysS) transforms the non-proteinogenic Sep while attached to tRNA^{Cys} into Cys in the presence of a sulfur donor (Sauerwald *et al.,* 2005; Mukai *et al.,* 2017) (**Figure I-5A**).

IV.2.   Gln-tRNA^{Gln} and Asn-tRNA^{Asn} in bacteria, archaea and eukaryotic organelles lacking GlnRS and/or AsnRS

GlnRS is missing in all archaea and in the majority of bacteria and eukaryotic organelles and AsnRS in half of bacteria and archaea. These organisms synthetize Gln-tRNA^{Gln} and Asn-tRNA^{Asn} by the same indirect pathway called the transamidation pathway. First, a non-discriminating GluRS (ND-GluRS) or -AspRS (ND-AspRS) mischarges respectively Glu onto tRNA^{Gln} (Lapointe *et al.,* 1986) (**Figure I-5B**) or an Asp onto tRNA^{Asp} and tRNA^{Asn}(Becker *et al.,* 1997) (**Figure I-5C**). The resulting non-cognate Asp-tRNA^{Asn} and Glu-tRNA^{Gln} become substrates for tRNA dependent amidotransferases (AdT) that amidates the non-cognate Glu or Asp by transferring a -NH2 from an aa donor, either Gln or Asn to obtain the cognate Gln-tRNA^{Gln} and Asn-tRNA^{Asn} (Curnow *et al.,* 1997) (Becker and Kern 1998). Various AdTs were described depending on the considered species or organelles. The trimeric GatCAB AdT is composed of the amidohydrolase GatA subunit, the catalytic and tRNA-binding GatB subunit and the scaffolding and chaperone GatC subunit. It is responsible for Gln-tRNA^{Gln} synthesis (Glu-AdT) in bacteria and organelles and for Asn-tRNA^{Asn} synthesis (Asp-AdT) in bacteria and archaea (Curnow *et al.,* 1997; Sheppard *et al.,* 2008). Note that some bacteria deprived of both GlnRS and AsnRS use a single Asp/Glu-AdT to generate both Gln-tRNA^{Gln} and Asn-tRNA^{Asn} (Raczniak *et al.,* 2001). However, all archaea also possess a dimeric and restricted Glu-AdT called GatDE composed of a L-asparaginase paralog (GatD) and a catalytic and tRNA-binding GatB paralog (GatE) (Tumbula *et al.,* 2000). Thus, archaea missing GlnRS and AsnRS require GatCAB as an Asp-AdT and GatDE as a Glu-AdT. A more sporadic dimeric GatAB was described in the human parasite *Plasmodium falciparum* where GatC is missing (Mailu *et al.,* 2015). Finally, for mitochondrial synthesis of Gln-tRNA^{Gln} in the yeast *Saccharomyces cerevisiae*, the mis-charging
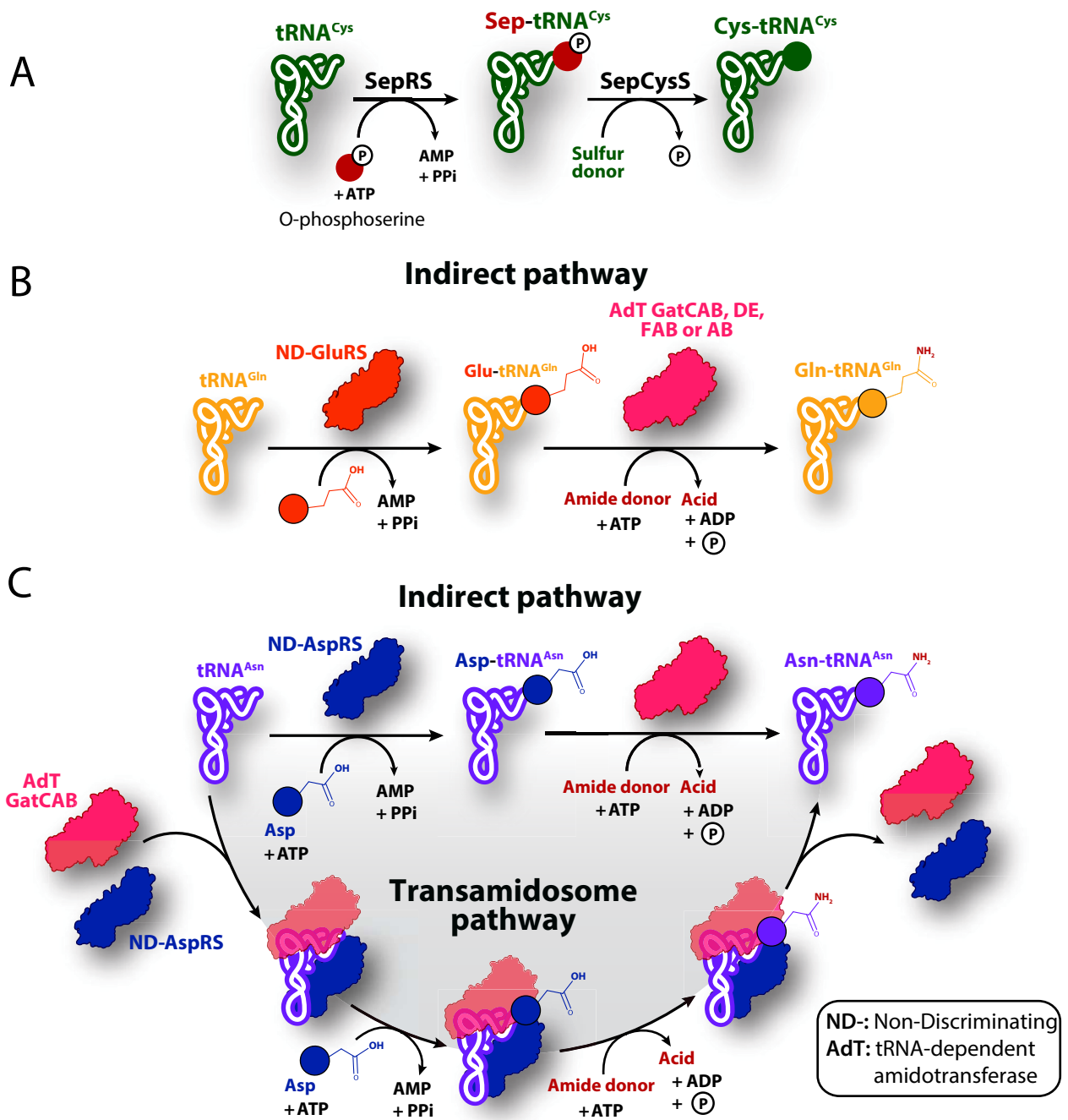
Figure I-5: Indirect aminoacylation pathways. [Figure and legend extracted from our recent review (Hemmerle *et al.* 2020) with minor modifications]. **(A)**: Two-step biosynthesis of Cys-tRNA^{Cys} in archaea lacking CysRS. **(B)** Two-step transamidation pathway of Gln-tRNA^{Gln} synthesis used by bacteria, archaea, mitochondria and chloroplasts. GatCAB AdT: Glu-tRNA^{Gln} amidotransferase used by bacteria, most eukaryotic organelles; GatDE: Glu-tRNA^{Gln} amidotransferase used by archaea; GatFAB AdT: Glu-tRNA^{Gln} amidotransferase of yeast mitochondria; GatAB: Glutamyl-tRNA^{Gln} amidotransferase used by apicoplast. **(C)** Two-step transamidation pathway or transamidosome-mediated route of Asn-tRNA^{Asn} synthesis used by bacteria, archaea deprived of AsnRS or of asparagine synthetase. The amide donor is either Gln or Asn and is deaminated to form Glu or Asp (acid) during transamidation, respectively.

step is carried out through the import of the cytoplasmic GluRS which behaves as an ND-GluRS in this bacteria-like organelle and a GatFAB AdT amidates subsequently Glu-tRNA^{Gln} to Gln-tRNA^{Gln} (Frechin *et al.,* 2009). Importantly, the herein described pathways raise the critical issue of incorrect incorporation of Asp-tRNA^{Asn} and Glu-tRNA^{Gln} during protein biosynthesis. However, EF-Tu has been shown to have the capacity to discriminate the mischarged Glu-tRNA^{Gln} and Asp-tRNA^{Asn} (Stanzel *et al.,* 1994) (Roy *et al.,* 2007) avoiding misincorporation at Gln and Asn codons. Alternatively, the ND-aaRSs, the AdT and the tRNA can also form a complex called transamidosome **(Figure I-5C)** in which the non-cognate aa-tRNA is directly channeled from one enzyme to the other (Bailly *et al.,* 2007; Rathnayake *et al.,* 2017) preventing Asp-tRNA^{Asn} and Glu-tRNA^{Gln} of reaching the ribosome. (Debard 2019)

V. Incorporating non-standard aa into proteins

In addition to the 20 aa used universally for protein biosynthesis, two non-standard aa can incorporated during protein biosynthesis. Selenocysteine (Sec) was the first one discovered and appeared to be present in bacteria, archaea and eukaryotes (Cone *et al.,* 1976; Chambers *et al.,* 1986; Zinoni *et al.,* 1986). Structurally, Sec is very similar to cysteine since the sole difference is that the sulfur (S) atom is replaced by selenium (Se), preferred in the active site of some oxidoreductases (Johansson *et al.,* 2004; Reich and Hondal 2016). The second non-standard amino acid regarding protein biosynthesis is pyrrolysine (Pyl) which is incorporated into methyltransferases and was described since 2002 in some genera of methanogenic archaea (e. g. *Methanosarcinaceae*) and in few bacteria (Srinivasan *et al.,* 2002; Zhang and Gladyshev 2007). However, because 61 out of 64 codons encode selectively for one of the 20 "classical" aa, the introduction of an additional aa-tRNA must occur by reprogramming at least one codon of the genetic code. More precisely, one out of the 3 remaining Stop codons is reprogrammed to decode the additional aa instead.

V.1. Pyl-tRNA^{Pyl} synthesis and incorporation

Pyrrolysyl-tRNA synthetase (PylRS) ressembles a calssical class II aaRS and belongs to this class (Blight *et al.,* 2004). However, tRNA^{Pyl} displays particularities since its V-loop is composed of only 3 nt, its anticodon binding stem is extended to six base-pairs instead of five, its D-loop harbors

only 5 nt, its T-loop lacks the canonical TΨC motif and finally its junction between the D-stem-loop and the acceptor stem is ensured only by one base (Srinivasan et al., 2002). Furthermore, tRNA^{Pyl} is an amber suppressor tRNA that specifically decodes UAG stop codon in a context-dependent manner. This means that a UAG can either be a stop codon or a "Pyl" codon depending if it is followed by a mRNA secondary structure called PYLIS (the context) that facilitate Pyl incorporation (Theobald-Dietrich et al., 2005). However, the PYLIS element was found not to be essential for Pyl incorporation. Finally, upon release from PylRS, Pyl-tRNA^{Pyl} is efficiently channeled to the ribosome by the regular elongation factor-Tu (EF-Tu) or -1A (EF-1A) (Krzycki 2004).

V.2.   Sec-tRNA^{Sec} synthesis

In contrast to the case of Pyl-tRNA^{Pyl}, no SecRS has been found so far, which implies that Sec-tRNA^{Sec} must be synthetized through an alternate pathway (**Figure I-6**). The first step of this pathway is in all cases catalyzed by SerRS which mischarges tRNA^{Sec} with Ser while the following events are carried out by two different mechanisms according to the organism's origin. In bacteria, selenocysteine synthase (SelA) replaces, tRNA-dependently, the -SH group of the charged Ser by -SeH using seleno-phosphate as donor resulting into the synthesis of Sec-tRNA^{Sec} (Leinfelder et al., 1988). In eukaryotes and archaea, Ser-tRNA^{Sec} is phosphorylated by O-phosphoseryl-tRNA kinase (PSTK) to obtain O-phosphoseryl-tRNA^{Sec} subsequently transformed to Sec by SepSecP (Yuan et al., 2006). Like tRNA^{Pyl}, tRNA^{Sec} has some particularities, namely an extended V-loop (which qualifies it as class II tRNA), an acceptor stem having of 8 bp instead of classically 7 bp, a longer D-stem and a shorter T-stem (Hubert et al., 1998). As EF-Tu only recognizes aa-tRNAs in which the tRNA acceptor stem has 7 bp, Sec-tRNA^{Sec} cannot be channeled by EF-Tu and must be brought to the ribosome by a specific elongation factor called SelB in bacteria (Rasubala et al., 2005) and eEF-Sec in eukaryotes and archaea (Tujebajeva et al., 2000). Furthermore, tRNA^{Sec} is an opal suppressor tRNA that decodes the UGA stop codon in a context-dependent manner, since recognition of UGA Sec codons requires the presence of a so called SECIS element (a stem-loop) located either near the UGA codon (bacteria) (Liu et al., 1998) or in the 3'UTR (eukaryotes and archaea) of selenoprotein mRNAs (Zinoni et al., 1990; Berry et al., 1993).
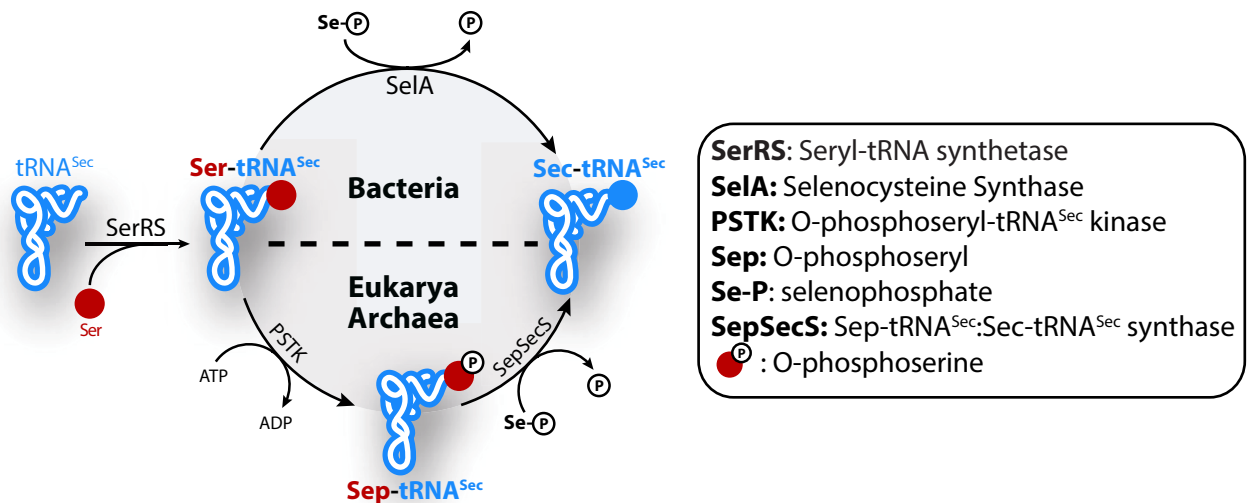
Figure I-6: Incorporation of the non-canonical aa Sec through indirect aminoacylation pathway. [Figure and legend extracted from our recent review (Hemmerle *et al.*, 2020) with minor modifications]. Biosynthesis of Sec-tRNA^{Sec} by a two-step pathway in bacteria (upper panel) and a three-step pathway in eukaryotes and archaea (lower panel). Adapted from Yuan *et al.*, 2006.

VI. aaRS substrates specificity

Because aminoacylation is crucial to ensure faithful correspondence between a given codon and the aa incorporated at a precise position of the growing peptide, life has evolved various checkpoints and mechanisms to avoid mis-aminoacylation and mis-incorporation. Obviously, accurate synthesis of aa-tRNAs is one of these checkpoints and is mediated by aaRS substrate specificities. However, aaRS sometimes generate non-cognate aa-tRNA species that must be avoided from the translational machinery through the action of so called pre- and/or post-transfer editing mechanisms that, as their name indicate, occur prior and/or after to transfer of the activated aa onto the cognate tRNA. I will not go into details, but the reader can refer to following excellent reviews (Ling *et al.,* 2009; Rubio Gomez and Ibba 2020) and to **Figure I-7** to have a very succinct and schematic overview of editing check-points. Furthermore, EF-Tu and EF-1A carrying the aa-tRNA to the ribosome as well as the ribosome itself significantly participate to avoid aa misincorporation (LaRiviere *et al.,* 2001). Nevertheless, translation remains the most error prone step during the entire process of transfer of genetic information: (10^{-4}) for translation compared to (10^{-5}) for transcription and (10^{-8}) for DNA replication (Rosenberger and Hilton 1983; Kunkel and Bebenek 2000). This is coherent since incorporated mutations into DNA are maintained until cell death whereas errors occurring during transcription and translation are ephemeral and are not conserved for the next expression cycle (Rosenberger and Hilton 1983; Kunkel and Bebenek 2000). However, accumulation of mis-translational events and thus of truncated or mis-folded proteins is harmful for the cell as illustrated by the important evolutionary pressure to ensure accurate aminoacylation.

VI.1. tRNA identity elements

aaRS recognize first the tRNA by its L-shaped structure yielding non-specific interactions that result majorly from the fact that the RNA backbone is ubiquitously composed of ribose and phosphate that interacts through electrostatic interaction with positively charged residues of aaRS. tRNA are further inspected by aaRS through semi-specific interactions that depends on their structure, base stacking, and charge distribution (Beuning and Musier-Forsyth 1999; Tworowski *et al.,* 2005; Perona and Hou 2007). This step allows aaRS to recognize the global shape of the tRNA in

A

Pre-transfer editing

non-cognate aa

cognate aa

ATP

non-cognate aa
activation

aa-adenylate
release

aaRS

larger aa
repulsion

spontaneous
hydrolysis

+

AMP

active-site (&
editing site)
editing

transfer of the
non-cognate aa
to the tRNA

Post-transfer editing

TRANS editing

CIS editing
(editing site)

hydrolysis

+
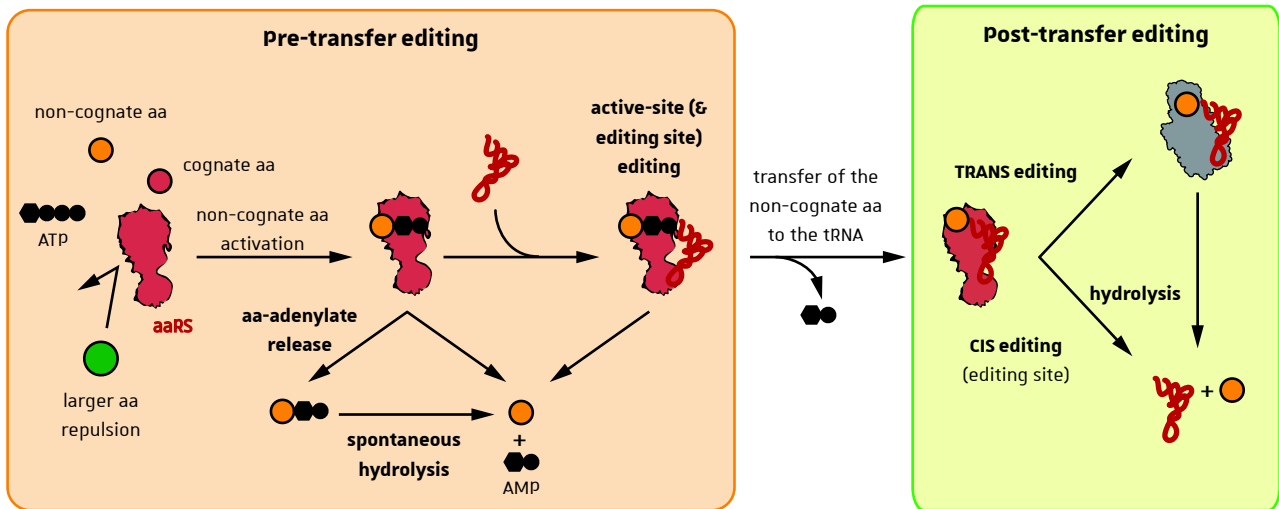
B

Pre-transfer editing aaRSs
MetRS: *Hcy*, *Nle*
SerRS: Thr, Cys, *SerHX*
LysRS: Met, Leu, Cys, H*cy*,
Hse, *Orn*, *Nle*, *Nva*

Pre & Post transfer editing aaRSs
LeuRS: Met, Val, Ile, *Nva*, *Hcy*, *Nle*
IleRS: Val, Cys, Thr, Leu, *Hcy*, *Nle*, *Abu*
ValRS: Thr, Cys, Ala, *Abu*, *Hcy*, *Nle*
ThrRS: Ser
PheRS: Tyr, Ile
ProRS: Ala, Cys, *4hPro*
AlaRS: Gly, Ser

Trans-editing factors
YbaK: Cys-tRNA^{Pro}
ProX: Ala-tRNA^{Pro}
ProXp-ST1/ST2: non-cognate
Ser-tRNAs and Thr-tRNAs
AlaX: Ser-tRNA^{Ala}, Gly-tRNA^{Ala}
DTD: D-aa-tRNA and Gly-tRNA^{Ala}

Figure I-7: Simplified overview of aaRS editing mechanisms. (A) Editing pathways are divided in pre- (orange background) and post-transfer editing (green background) and are indicated in bold. In addition to the active site, the catalytic domain of some aaRSs, contains an editing site that proofreads the mischarged tRNA. Non-cognate aa-adenylate can be released from the active site and hydrolyzed or edited within the catalytic domain of the aaRS. After the second step of aminoacylation (transfer), the resulting aa-tRNA can be edited by the editing site of the aaRS or by trans-editing factors. **(B)** The editing aaRSs with their corresponding edited aa are listed in the lower panel, as well as trans-editing factors with their associated edited aa-tRNA(s). Non-proteinogenic aa are in italic. Hcy, homocysteine; Nva, norvaline; Hse, homoserine; Orn, ornithine; SerHX, serine hydroxamate; 4hPro 4-hydroxyproline; Abu, α-aminobuty-rate; Nle, norleucine; DTD, d-aminoacyl-tRNA deacylase. Data compiled from Ling, Reynolds and Ibba, 2009; Rubio and Ibba, 2020 and Debard, 2019. Figure inspired from Rubio and Ibba, 2020.

order to discriminate it from other RNAs and macromolecules. The "initial" interactions also participate to the discrimination of class II tRNA due to their large V-(stem-)loop for example (Asahara *et al.,* 1993; Park and Schimmel 1988; Dock-Bregeon *et al.,* 1990). Specific interactions occur then between the aaRS and specific nt of the tRNA called determinants that were defined as nt that increase significantly the aaRS-tRNA interaction and the tRNA aminoacylation rate. On another hand, anti-determinants correspond to nt that prevent recognition and/or charging of a non-cognate tRNA. Determinants and anti-determinants represent therefore identity elements and are mostly located in the acceptor-stem and the anticodon-stem-loop highly prone to sequence variation in contrast to the well conserved D- and T-stem-loop (Giege *et al.,* 1998; Vasil'eva and Moor 2007). Positions 35, 36 and in a lesser extend the wobble position 34 forming the tRNA anticodon specific for each aa are important determinants but other nt such as the discriminator base at position 73 (just before the CCA acceptor end) are also often crucial identity elements. For example, yeast tRNA[Asp] identity (isoacceptors and isodocoders) is composed of the anticodon triplet (G34, U35, C36), the G38 nt, the wobble base pair G10-U25 located in the D-stem-loop and the discriminator base G73 whereas methylated m^1G_{37} is an anti-determinant to prevent mis-aminoacylation by ArgRS (**Figure I-8**) (Putz *et al.,* 1991; Putz *et al.,* 1994). Thus, as mentioned in the corresponding section, nt modifications participate also to accurate tRNA selection. Furthermore, even if the set of of the major identity elements is usually conserved across species minor identity element may varies among species. For example, in *E. coli,* tRNA[Asp] identity elements are the same as for yeast except that G2-C71 is an additional determinant and G10-U25 wobble pair is not (Moulinier *et al.,* 2001). Finally, tRNA[Ala] G3-U70 is a good example of a highly conserved and robust identity element considered as determinant and anti-determinant (against ThrRS) regardless of the species considered (Giege *et al.,* 1998).

VI.2.   Aa recognition

Studies showed that aaRS select the cognate aa through various mechanism. This selection is very challenging for the cell since beside the important pool of non-proteogenic aa present in the cell, the differences between proteogenic aa are sometimes subtle as for example Gly and Ala or Ser and Thr differ only by a methyl group. Discrimination of Phe from Tyr is dependent on an Ala residue located in the active site of cytoplasmic PheRS whereas GlyRS discriminate the smallest
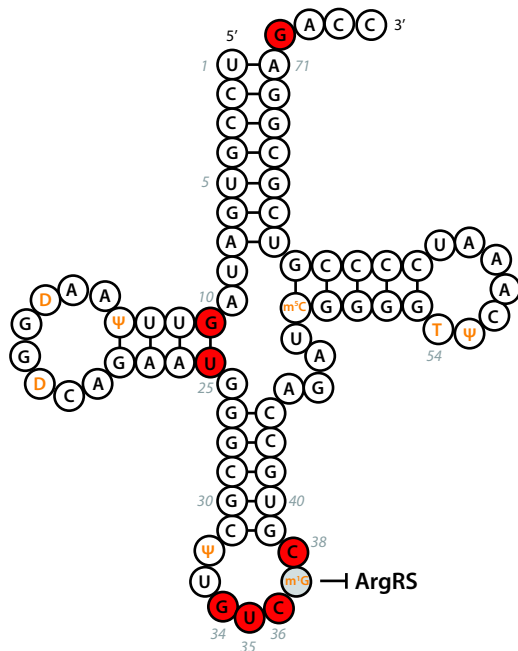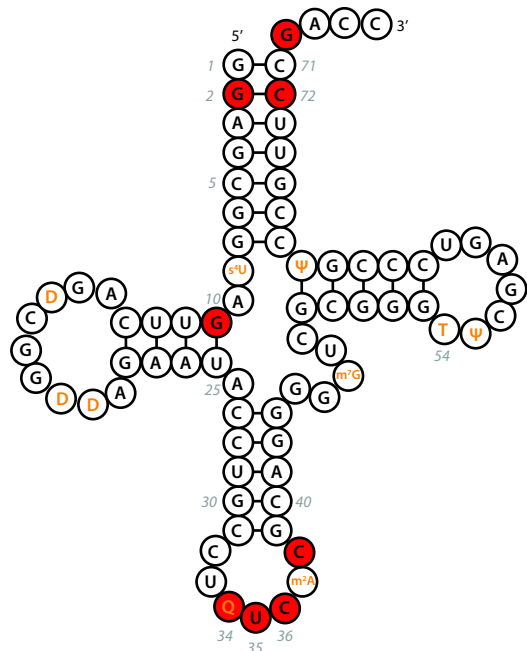
Figure I-8: Cloverleaf structures of tRNA^{Asp} from *S. cerevisiae* (A) and from *E. coli* (B) and comparison of their identity elements. nt are determinants that are shared between *S. cerevisiae* and *E. coli* are indicated in red. Modified bases (T, thymidine; D, dihydrouridine; Q, quosine; Ψ, pseudouridine; s^4U, 4-thiouridine, m^1G, 1-methylguanosine; m^2A, 2-methyladenosine) are in orange. Among them, the gray-shaded m^1G_{37} is an anti-determinant which prevents mischarging of *S. cerevisiae* tRNA^{Asp} by ArgRS.

proteogenic aa from all others, either through a Ser (eukaryotes) residue or two Thr residues (bacteria) in its catalytic site (Valencia-Sanchez *et al.*, 2016). Other aaRS use a mechanism involving a metal atom that is coordinated by residues within the aaRS active site. Through binding of the cognate aa the coordination state undergoes a conformational change which is not induced by the non-homologous aa and consequently hinders its mis-activation. In this way SerRS from methanogenic archaea, CysRS and ThrRS discriminate their cognate aa from Thr, Ser and Val respectively (Bilokapic *et al.*, 2008; Zhang *et al.*, 2003; Sankaranarayanan *et al.*, 2000). It was also shown that the active site configuration of at least, TyrRS, CysRS, some SerRS, AspRS and ArgRS are highly selective for their aa whereas MetRS, IleRS, LeuRS, ValRS, AlaRS, LysRS, ProRS, PheRS, and ThrRS can activate and/or aminoacylate non-cognate aa (Jakubowski and Goldman 1992; Jakubowski 2011). However, even though the aaRS cited here are "highly selective" for their aa, some of them as for example TyrRS have large aa binding pockets and thus discriminate hardly L- and D-enantiomers. In contrast, aaRS charging small aa, have smaller aa binding pockets, avoid D- aa mainly through steric exclusion or inappropriate positioning with respect to catalysis. For this reason, evolutionary pressure has led to the inheritance of proofreading domains responsible for editing of mischarged aa-tRNA.

VII. Final remarks

Each living cell contain a set of aaRSs that can vary from one species to another, but they must unequivocally provide at least 20 aa-tRNA substrates brought the ribosome by EF-Tu (or EF-1a). To ensure accurate aminoacylation and translation, the aaRS substrates must be produced in sufficient amount and specificity. This overall process includes several tRNA maturation that I haven't described in details but that are essential too (Vare *et al.*, 2017; Hopper 2013; Hopper and Nostramo 2019). In addition, accurate tRNA aminoacylation is challenging for aaRS and thus evolution put a considerable pressure to develop various quality control mechanisms. aaRS pre- and post-editing mechanisms occurring through cis- and trans acting elements are important checkpoints to ensure accurate aminoacylation (Rubio Gomez and Ibba 2020; Ling *et al.*, 2009). However quality control steps occur also during the transfer of the set of aa-tRNAs mediated by EF-Tu which is not described into details but also very important (Kuncha *et al.*, 2019). Synthetic studies using flexizymes investigated the rate of D-aa incorporation into growing peptides and

showed that some D-aa are more prone to be incorporated into the growing peptide and can reach up to 40 % of elongation efficiencies (Fujino *et al.,* 2013). However, in physiological systems, the ribosome was shown to hinder the peptide bond formation between the D-aa-tRNA located in the A-site and the peptidyl-tRNA in the P-site. Thus, all along the process starting from the selection of the cognate aa and tRNA pairs by aaRSs until the transfer of the aa onto the growing peptide, numerous checkpoints ensure the accurate synthesis and usage of aa-tRNA to avoid mis-incorporations. Despite this numerous checkpoints, mis-incorporation of aa occurs during translation and are in most cases detrimental for cells. However, recent studies highlighted that under certain environmental conditions, these events induce selective advantages (Pan 2013) as for example mis-methionylation of protein under oxidative stress is a mean for cells to "absorb" reactive oxygen species (Ribas de Pouplana *et al.,* 2014; Wiltrout *et al.,* 2012).

As described above aaRS are modular enzymes organized around the catalytic domain and eventually the tRNA binding domain, required to achieve tRNA aminoacylation. In addition, they have inherited additional domains (mostly in eukaryotes) [reviewed in (Guo and Yang 2014)] that resulted in *1)* the capacity to form Multi-Synthetase Complexes (MSC) seen as cytoplasmic reservoirs for relocating multifunctional aaRSs [reviewed in (Laporte *et al.,* 2014; Mirande 2017)] and *2)* the participation of those aaRS in a plethora of additional functions that range from transcription regulation to the modulation of angiogenesis [reviewed in (Guo and Schimmel 2013)]. These two consequences are intimately related since relocation of MSC-bound aaRSs but also of "freestanding" aaRSs usually is a prerequisite to achieve non-canonical functions, including essential processes that can link aaRS to diseases [reviewed in (Park *et al.,* 2008; Yao and Fox 2013)]. During my thesis I participated as a first author to the publication of an article in which we reviewed all aaRS relocations and their associated canonical and non-canonical functions [please refer to (Yakobov *et al.,* 2018) at the end of the manuscript].

B. Deviating aa-tRNA from protein biosynthesis by dupli-GNAT aa-tRNA transferases.

As detailed in the previous chapter, the fundamental role of tRNAs is to define and translate the genetic code. However, the tRNA can be hijacked to achieve several functions beyond protein biosynthesis (Katz *et al.,* 2016). When aminoacylated, tRNAs, whose primary function is to participate to protein synthesis, can also be rerouted from the translational machinery – either by a distinct enzyme or, more rarely, by an aaRS fused domain - and serve as substrate for other mechanisms (**Figure A-1).** Those aa-tRNA utilizing enzymes were extensively reviewed elsewhere (Moutiez *et al.,* 2017) and in our recent review where we presented those aspects too [please refer to (Hemmerle *et al.,* 2020) at the end of the manuscript].

Among them, aminoacyl-tRNA transferases (ATT) are enzymes that hijack aa-tRNAs and transfer the aa onto a wide range of substrates. For example, Cyclodipeptide Synthases (CDPS), sequentially use two aa-tRNAs and catalyze the formation of cyclodipeptides. Among them, AlbC from *Streptomyces noursei* synthetizes cyclo-(L-Phe-L-Leu), by utilizing Phe-tRNA^{Phe} and Leu-tRNA^{Leu} (Lautru *et al.,* 2002; Gondry *et al.,* 2009). Thereafter, CDPS synthetized products are modified by numerous cyclodipeptides-tailoring enzymes which enables the formation of several diketopiperazines (Giessen and Marahiel 2012; Jacques *et al.,* 2015). Those aa-tRNA-dependent synthases are structurally characterized by the presence of a Rossman fold which resembles those found in class Ic aaRSs (*i. e.* TyrRS and TrpRS) (Sauguet *et al.,* 2011).

Class I lanthipeptide (Chatterjee *et al.,* 2005) (e. g. the lantibiotic nisin) and thiopeptides (Bagley *et al.,* 2005) are subfamilies of ribosomally synthesized and post-translationally modified peptides (RiPP). Both subfamilies members contain unconventional didehydroalanine (Dha) and/or

didehydroaminobutyric acid (Dhb) aa in their peptide sequences that result from Glu-tRNA^{Glu} dependent dehydration of Ser and Thr residues by LanB enzymes, respectively. These enzymes belong also to ATT because during the enzymatic reaction Glu is transferred from its tRNA onto the lateral hydroxyl group of the target residue. The subsequent elimination of Glu results in dehydrated Ser or Thr. Structurally, LanB or LanB-like enzymes contain a N-terminal lanthipeptide dehydratase domain and a small C-terminal SpaB_C domain (Moutiez *et al.,* 2017).

To better replace the topic of my thesis among aa-tRNA utilizing enzymes, I will focus here on a structurally unrelated ATT family regarding those mentioned in the previous paragraphs. Enzymes from this class catalyze the transfer of an aa from their cognate tRNA onto a broad range of second substrates and importantly, they are structurally characterized by the presence of **GCN5-related N-acetyltransferase (GNAT)** folds. GNAT folds are found in numerous proteins (beyond ATTs) among prokaryotes, eukaryotes and archaea and all catalyze the transfer of an acyl group from an acyl-donor onto an acyl-acceptor. According to the Protein FAMily database (Pfam; https://pfam.xfam.org/) (El-Gebali *et al.,* 2019), 44 protein families harboring at least one GNAT domain form together Clan 0257. Despite very low sequence identities (typically < 30 %) or even low similarities between GNAT proteins, their overall secondary and tertiary structures are well-conserved and consists of 6 or 7 β-strands and 4 α-helices (**Figure I-9**) (Favrot *et al.,* 2016). Most of standalone GNAT proteins are acetyltransferases that use acetyl-coenzyme A (Ac-CoA) as a donor and transfer the "acetyl" moiety onto an acceptor molecule. Among them Aminoglycosides N-Acetyltransferases (AAC) (**Figure I-10A**) acetylate amino groups of aminoglycosides (*e. g.* streptomycin) while GCN5 histone acetyl transferases found in yeast *Sce* acetylate Lys residues of histones (Brownell *et al.,* 1996; Favrot *et al.,* 2016).

In addition to single-GNAT containing enzymes, there are other transferases that contain GNAT subdomains in tandem (Dupli-GNAT). However, according to the enzyme, both GNAT domains can be linked in two different ways. In acetyl- or acyl- CoA dependent transferases, both GNAT domains are attached by a flexible loop. For example, MshD (which is a transferase but not an ATT) acetylates 1-D-myo-inosityl-2-L-cysteinylamino-2-deoxy-α-D-glucopyranoside (Cys-GlcN-Ins) during the last step of Mycothiol (MSH) synthesis found in actinobacteria (Koledin *et al.,* 2002). The
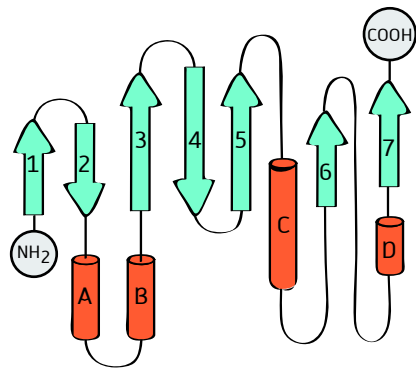
Figure I-9: Topology of the consensus GNAT domain according to Favrot *et al.*, 2016. β-strands are numbered from 1 to 7 and are colored in blue. α-helixes (A-D) are in orange.

A

aminoglycoside acetyltransferase (AAC)
Salmonella enterica
2PRB

B

GNAT1

flexible loop

GNAT2

Mycothiol Synthase (MsHD)
M. tuberculosis
2C27

C

peptidyl-RNA conjugate

α$^{(+)}$ helix

GNAT1

GNAT2

peptidoglycan precursor

Fem X
Weissella viridescens
4II9

D

GNAT1

α$^{(+)}$ helix

coiled-coil

GNAT2

Fem A
S. aureus
4II9
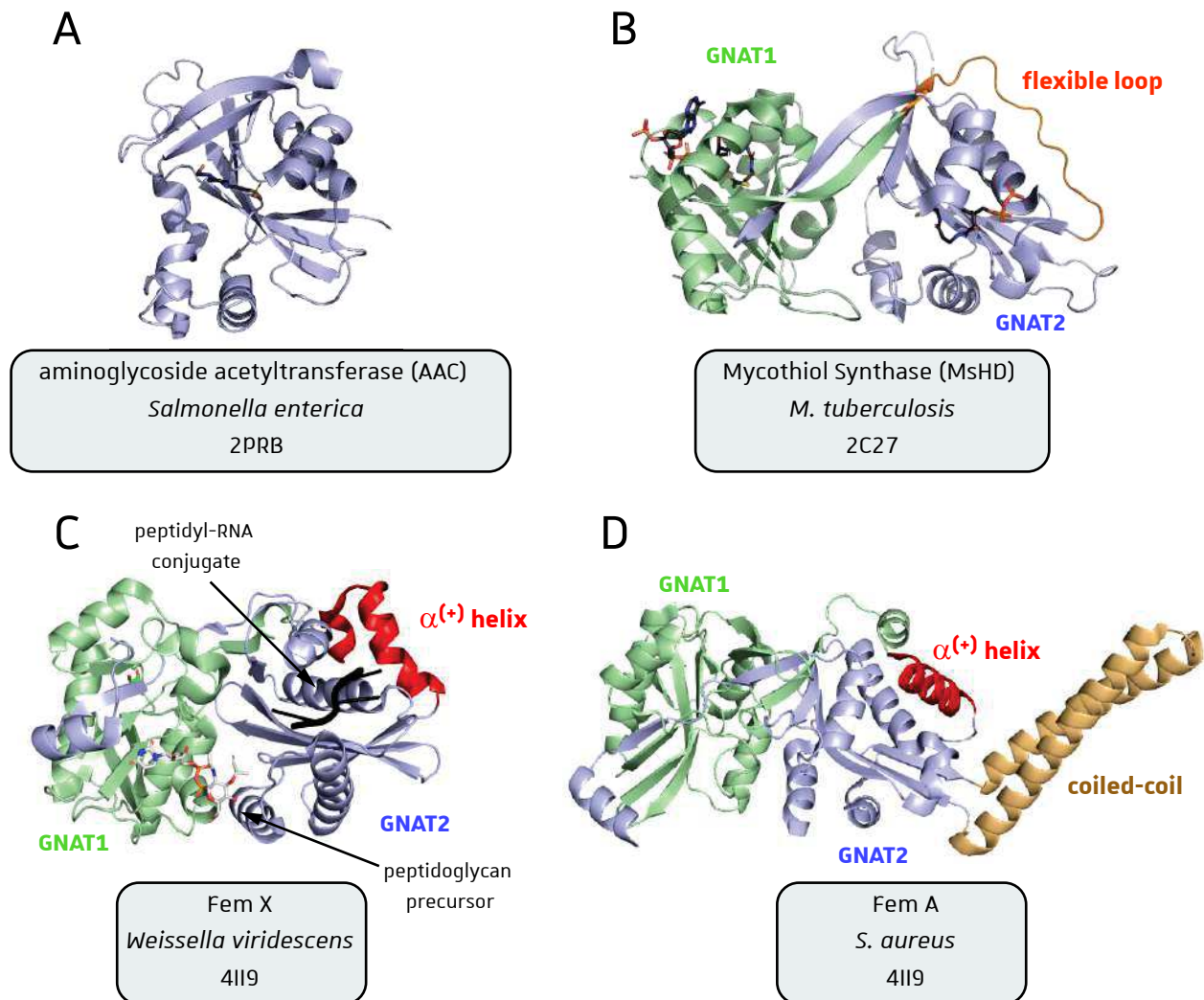
Figure I-10: Structural diversity of GNAT containing transferases. (A) Structure of the aminoglycoside acetyltransferase from *S. enterica* as an example of single GNAT containing protein in contrast to other factors, such as the Mycothiol Synthase **(B)** from actinobacteria, that contain GNAT folds in tandem, separated by a flexible loop (in orange). Both mentioned proteins are not ATTs. **(C)** and **(D)**. In contrast, Fem ligases achieve tRNA dependent ATT activities and also contain a Dupli-GNAT organization but importantly both GNAT domains are separated by the "hallmark" of Dupli-GNAT/ATTs, namely the positively charged α-helix (red). Note the coiled coil inserted in GNAT domain 2 of *S. aureus* Fem A, in comparison to Fem X from *W. viridescens*. GNAT domain 1 and 2 are colored in green pale and light blue, respectively. PDB references are indicated for each structure.

3D structure of MshD from *M. tuberculosis* revealed that GNAT1 and GNAT2 domains are linked by a flexible loop (Vetting *et al.,* 2003; Vetting *et al.,* 2006) (**Figure I-10B**).

In contrast, several dupli-GNAT containing ATTs (aminoacyl-tRNA transferases) were described and shown to link both GNAT domains by a **positively charged (Lys- and Arg-containing) alpha helix** (Moutiez *et al.,* 2017). In the lab, we noticed that this so-called $\alpha^{(+)}$ helix seems to be the hallmark of ATTs of the dupli-GNAT family, since it is always absent in acetyl- or acyl- CoA dependent transferases, but present in ATTs of the same fold, such as the Fem-ligases (**Figure I-10C & D**) involved in the modification of peptidoglycan in Gram-positive bacteria, Leu/Phe-tRNA protein transferases (LFT) and Arg-tRNA protein transferases (RTT) involved in the N-end rule pathway (Hemmerle *et al.,* 2020).

Fem ligases participate in the formation of the peptidoglycan sacculus surrounding bacteria cells. The peptidoglycan sub-unit corresponds to the extensively studied Lipid II, composed of a disaccharide (N-acetyl glucosamine (GlcNAc) linked to N-actyl muramic acid (MurNAc) decorated with a pentapeptide called stem-peptide (**Figure I-11**). Once synthetized, lipid II is further modified by the tRNA dependent addition of a peptide-bridge directly linked onto the stem peptide. This Lipid II modification mechanism is achieved by ATT activities of Fem ligases but the number of aa constituting the peptide bridge vary from one species to another. After translocation to the periplasm, peptidoglycan subunits are incorporated into the growing sacculus, notably though a transpeptidation mechanism between the free extremity of the peptide-bridge and the stem-peptide of an adjacent lipid II (Hemmerle *et al.,* 2020).

The crystal structure of *Weisellia viridescens* FemX (Fonvielle *et al.,* 2013) and *S. aureus* FemA (Benson *et al.,* 2002) involved in the modification of peptidoglycan have been obtained and showed that, indeed, both ATTs share similar dupli-GNAT folds (**Figure I-10C & D**). *S. Aureus* FemA possesses an additional coiled coil structure, absent in FemX, that was proposed to participate in Gly-tRNA[Gly] binding. This coiled-coil domain has a strong structural homology with the N-terminal and tRNA-binding domain of bacterial seryl-tRNA synthetases (SerRS) (Benson *et al.,* 2002; Belrhali *et al.,* 1994). Both GNAT domains face to each other so that the extended cleft formed between them can accommodate and bring the two substrates (*i. e.* lipid II and the aa-tRNA) close together. Importantly, in FemX, the UDP-MurNAc-stem-peptide (precursor of the peptidoglycan subunit, that
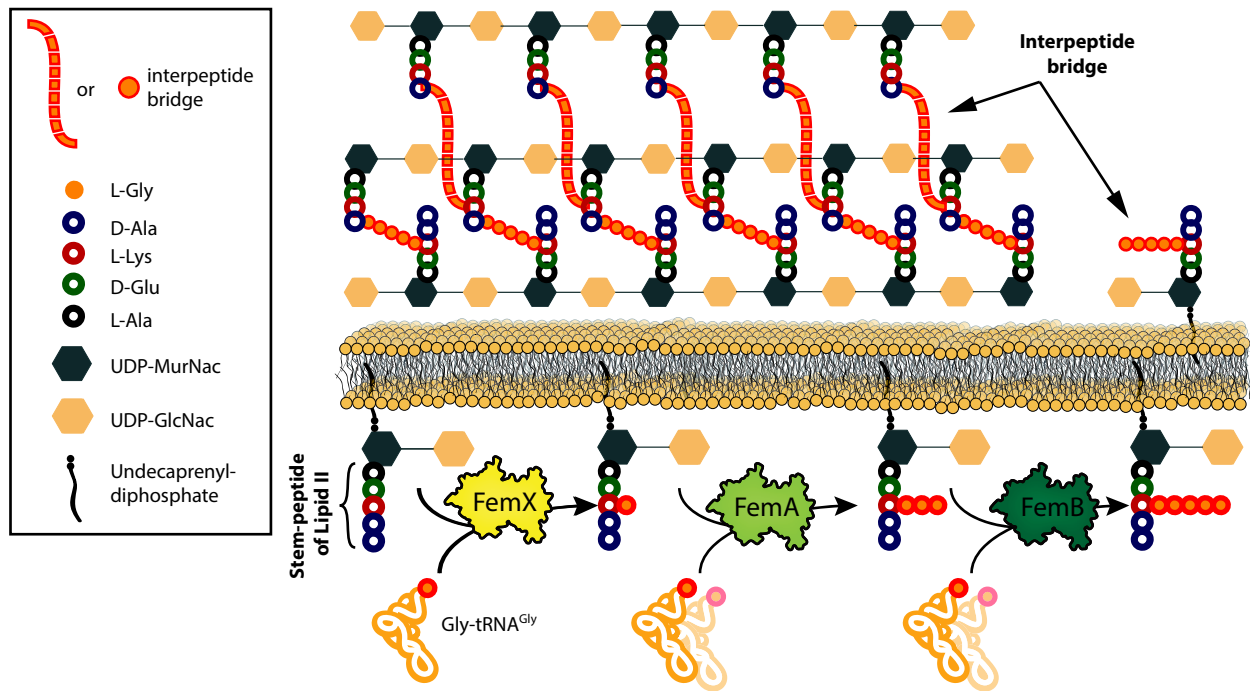
Figure I-11: Aminoacyl-tRNA-dependent cell wall remodeling in prokaryotes. [Figure and legend extracted from our recent review (Hemmerle *et al.*, 2020) with minor modifications]. **(A)** In *S. aureus*, the stem peptide composed of L-Ala1-D-Glu2-Lys3-D-Ala4-D-Ala5 is added onto Lipid I to form the well-characterized Lipid II. Aminoacyl-tRNA transferases (ATT) belonging to the Fem ligases family then successively add a variable number of aa to form the interpeptide bridge. For example, in *S. aureus* FemX adds a single glycine, FemA adds Gly_2 and Gly_3 and finally, FemB adds Gly_4 and Gly_5 onto the L-Lys of the stem-peptide. The resulting peptidoglycan subunit is then flipped out to the outer cytoplasmic-membrane leaflet, and the link to the growing peptidoglycan saccule is made by PBP transpeptidases. MurNac: N-Acetylmuramic acid, GlcNac: N-Acetylglucosamine.

is the "acceptor" substrate of the enzyme, onto which the aa moiety shall be transferred) is mainly recognized by the GNAT1 subdomain, while the acceptor stem of the aa-tRNA donor is accommodated by the GNAT2 subdomain (Fonvielle *et al.*, 2013). Recognition of the aa-tRNA moiety by the GNAT2 domain seems to be a common feature of dupli-GNAT ATTs, which explains that recognition and binding modes of aa-tRNA are conserved among these proteins (Moutiez *et al.*, 2017).

We noticed that the GNAT2 domain is more often conserved in terms of sequence, despite the fact that those enzymes have to accommodate different aa-tRNA substrates suggesting that the presence of key residues within the GNAT2 structure. However, the "acceptor" substrate (that becomes aminoacylated) strongly differs between ATT types and is generally achieved by GNAT1, whose features are idiosyncratic at least to each substrate class. Transferases involved in tRNA-dependent synthesis of antibiotics constitute another example of enzymes containing a dupli-GNAT domain. For example, VlmA, DhpHK, PacB and Orf11 utilize Ser-tRNA^{Ser}, Gly-tRNA^{Gly}, Leu-tRNA^{Leu}, Ala-tRNA^{Ala} and Val-tRNA^{Val} (Moutiez *et al.*, 2017). Even if the structures of those enzymes have not been determined yet, sequence analyses and structure prediction confirm that the two GNAT domains are always separated by a *bona fide* $\alpha^{(+)}$ helix that would help bind the aa-tRNA substrate (F. Fischer, personal communication). The role of the $\alpha^{(+)}$ helix in tRNA binding seems to be confirmed by the orientation of the tRNA CCA mimic used in the crystal structure of FemX (Fonvielle *et al.*, 2013).

Finally, one dupli-GNAT ATT family essential for the understanding of my work was not mentioned in this part namely aminoacyl-lipid synthases (aaLS) that aminoacylate lipids using aa-tRNAs as aa donor. The description of this class of enzymes is the aim of the coming chapter.
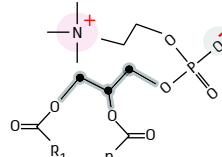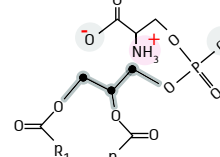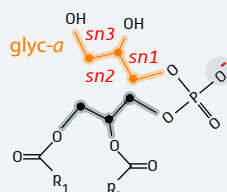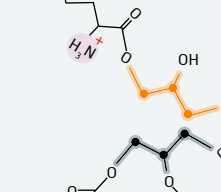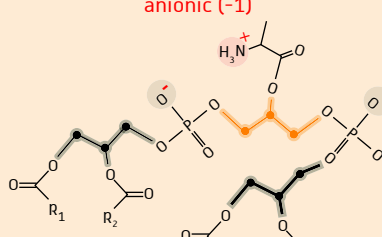
Figure I-12: Structure of main glycerolipids (black box) of cell membranes and of bacterial O-esterified aminoacylated lipids (aaLs; red box). The central glyc-C_n glycerol of glycerolipids, indicated in black bold lines is acylated with fatty acids that can vary through their unsaturation rates, length, and presence of branched groups. The acylation rate indicates if the lipid is a mono-, di- or tri-glyceride. PG, CL and their aminoacylated derivatives harbor an additional glycerol (glyc-C_a in orange bold lines) linked to glyc-C_n by a phosphodiester bond. Stereospecific *sn1-3* positions of both involved glycerols are indicated (see DAG and PG). R_n corresponds to fatty acid chains that are acylated at snn positions of glyc-C_n. Non-acylated sn positions of glyc-C_a from PG and CL can be esterified with Lys, Ala, Arg or Orn, while the sole non-acylated *sn*-position of DAG can be subjected to alanylation or lysinylation in some species. Charges brought by polar headgroups of those constituents (including the phosphate group and aa) are indicated and determine the global charge of the lipid (indicated in red between brackets). PG and its aminoacylated derivates (aaPGs) are highlighted by the gray background while CL and it derivates (aaCLs) are indicated by a light orange background. Note that CL species contains two distinct glyc-C_n that are not distinguished here, one for each of both PG "subunits". The *sn2* carbon of glyc-C_n and the C_α of aa are asymmetric. However, these aspects were not taken in consideration in the present illustration.
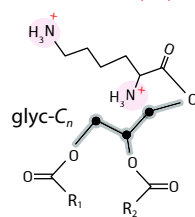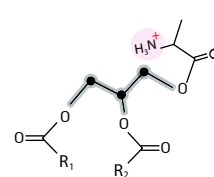
C. Aa-tRNA-dependent lipid aminoacylation in bacteria

I. Introduction and description of O-aminoacylated-lipids

Glycerides or glycerolipids are a large class of lipids that share a glycerol backbone with three stereo-specifically numbered positions called *sn1*, *sn2* and *sn3* relative to the three carbons of glycerol. Glycerol can be esterified with one, two or three acyl chains (*i. e.* fatty acid composed of a carboxylic acid with long hydrocarbon chains), which forms mono-, di- or triacylglycerols (Alvarez and Steinbuchel 2002). Diacylglycerol (DAG) (**Figure I-12**) and its cytidine-diphosphate activated version (CDP-DAG) are crucial metabolites precursors for the synthesis of phospholipids in both prokaryotes and eukaryotes (Sohlenkamp and Geiger 2016).

Phospholipids are the most represented lipid class in the cytoplasmic membrane across all living species (Sohlenkamp and Geiger 2016; Vance 2018) and contain either a sphingosine backbone (sphingophospholipids) or more commonly the above-described glycerolipid backbone (glycerophospholipids) (**Figure I-12**). Sphingosine-based phospholipids are rare in bacteria and will not be considered here, whereas glycerophospholipids are in general the main lipids in prokaryotes. As a common characteristic of membranous lipids, phospholipids are amphiphilic (i.e. bipolar molecules); the fatty acids (*i. e.* carboxyl-containing long aliphatic hydrocarbon chains) confer hydrophobicity, whereas the polar moiety is brought by with a variable hydrophilic headgroup (**Figure I-12**). In terms of structure, DAG represents a common feature of glycerophospholipids as, for example, phosphatidylglycerol (PG), that corresponds to DAG esterified on its glycerol *sn3* position with glycerol-phosphate (**Figure I-12**).

The minimal glycerophospholipid unit is the well-known phosphatidic acid (PA) composed of glycerol esterified on position *sn1* and *sn2* with two fatty acid chains and on *sn3* with a phosphate group (**Figure I-12**). However, PA is rarely found in the bacterial cytoplasmic membrane, rather acting as a lipid precursor (comparable to CDP-DAG). In bacteria, major glycerophospholipids found in the cytoplasmic membrane are PG, cardiolipin (CL, *di-phosphatidylglycerol*) and phosphatidylethanolamine (PE), while phosphatidylcholine (PC; zwitterionic) and phosphatidylserine (PS; anionic), if present, are mainly used as precursors or intermediates during glyerolipid biosynthesis (Geiger *et al.*, 2010; Sohlenkamp and Geiger 2016). However few exceptions exist such as in *Bacillus megaterium*, where the amount of PS reaches 5-10 % of total lipids (Langley *et al.*, 1979). Structures of those lipids are depicted in **Figure I-12**.

A particularly interesting feature in the bacterial cytoplasmic membrane is the ratio between anionic and zwitterionic lipids. The amounts of PE, PG and CL vary significantly between Gram-negative and Gram-positive bacteria. In Gram-negatives, such as *E. coli*, *Pseudomonas aeruginosa* or *Proteus mirabilis* (γ-proteobacteria) the zwitterionic PE represents 60-80 % of total lipids and PG 10-21 %. In contrast, Gram-positive bacteria have generally very low amounts of zwitterionic lipids in comparison to anionic-lipids (Epand *et al.*, 2007). For example, in *Staphylococcus aureus* (Firmicute) the phospholipid content is of 58 % PG and 42 % CL (anionic) (Beining *et al.*, 1975), which resembles the 50-50 % PG-CL repartition of *Streptococcus pneumonia* (Firmicute) (Trombe *et al.*, 1979).

However, exceptions to those tendencies exist. For instance, the Gram-negative *Caulobacter crescentus* has increased amounts of the anionic PG (at least 40 %) (Jones and Smith 1979; Contreras *et al.*, 1978; De Siervo and Homola 1980), while the Gram-positive *Bacillus subtilis* has unusually high amount of PE (60 %) (Clejan *et al.*, 1986) [reviewed in (Epand *et al.*, 2007)]. Furthermore, this lipid repartition must be considered carefully and put into perspective, since important variations occur with and/or upon environmental changes. For example, under acidic pH conditions, PG amounts vary in *S. aureus* (Haest *et al.*, 1972) and another study demonstrated increased CL (5 up to 30 %) and decreased PG (76 down to 38 %) following shift from exponential to stationary growth phase (Short and White 1971). More recently, (Gidden *et al.*, 2009) provided a comparative study of the lipid contents in *E. coli* and *B. subtilis* throughout growth phases.

Importantly, membrane lipids, especially glycerolipids, contribute to the global negative charge observed in bacterial cytoplasmic membranes. Gram-positive bacteria contain higher PG/PE ratios than Gram-negative cells, explaining that the global negative charge is higher than Gram-negative cytoplasmic membranes (Epand *et al.,* 2007; Atila and Luo 2016). The high level of anionic components in the cytoplasmic membrane was often related to the higher susceptibility of Gram-positive bacteria to cationic antimicrobial peptides (CAMPs) and ceragenins (*i. e.* cationic steroid antimicrobials corresponding to bile acid derivates decorated by amines) in comparison to Gram-negatives (Epand *et al.,* 2007). In contrast, high PE levels in the cytoplasmic membrane were shown to confer high susceptibility to other antimicrobials such as certain α/β-peptides (Epand *et al.,* 2006).

Taken together, the lipids mentioned above are major phospholipids found in all species (prokaryotes and eukaryotes), either as part of the cytoplasmic membrane or as important lipid precursors. However, in terms of diversity, there are innumerable other lipid components of very different classes found across bacteria (Sohlenkamp and Geiger 2016), including phosphoinositides, sterols, hopanoids, plasmalogens, sphingolipids and others. In addition, there is another class of lipids that was not mentioned before namely, amino-acid-containing lipids.

I.1. The distinct classes of amino-acid-containing lipids

Beside the ubiquitous and well-known glycerolipids described above, cell membranes also contain lipids that can be decorated with aa's. Many studies already suggested during the late 50's the presence of lipoamino-acids such as *Penicillium* spp. (Gaby *et al.,* 1959), *Pseudomonas spp.* etc but also in *Drosophila melanogaster* (Westley *et al.,* 1957) and animal tissues as for example in hen-oviduct (Hendler 1959) and rabbit tissues (Gaby and Silberman 1960; Hunter and Goodsall 1961). However, the lack of chemical compositions and consequently the difficulties to distinguish unequivocally those lipids from other metabolites that contain amino-acids as well as the presence of artefacts, led to strong doubt concerning their very existence (Hunter and Goodsall 1961; Macfarlane 1964). Finally, the study of MacFarlane in 1962 (Macfarlane 1962) marked a fundamental breakthrough and in the following decades the number of described amino-acid-containing lipids greatly increased. Importantly, those lipoamino acids belong to different classes

that can be divided according to the chemical link between the amino-acid moiety and the other part of the molecule. In fact, attachment of the aa moiety can occur via;

i. the lateral chain of the aa, as it is the case for the above-mentioned PS. In the case of PS, serine is attached to the glycerophospholipid through a phosphoester bond (**Figure I-12**). PS is the only lipid for which the attachment between the aa and the phospholipid is catalyzed by an alcohol phosphotransferase (Sohlenkamp *et al.*, 2004; Geiger *et al.*, 2010).

ii. the α-NH$_2$ group of the aa, as in *N*-amino-acylated lipids; for example, Ornithine Lipids (OL) that are widely found in bacteria, especially within the Gram-negative outer membranes, but are not found in eukaryotes (Vences-Guzman *et al.*, 2012). Other bacterial lipids belonging to this group are glutamine lipids, cerilipins, *N*-acyl-leucine, *N*-acyl-D-asparagine, *N*-acyl-serine, among others (Geiger *et al.*, 2010). *N*-aminoacylated lipids are also found in eukaryotes (Hanus *et al.*, 2014) and more complex components such as proteolipids and lipopeptides where largely described throughout all kingdoms.

iii. the α-COOH group of the aa, making *O*-amino-acylated lipids. To this class belong *O*-amino-acid esters of glycerolipids that will be further developed in the following sections. For the sake of clarity, in this manuscript, **"aminoacylated lipids" (aaL) shall be considered hydroxyl-containing lipids to which a _single_ aa is linked through its $\underline{\alpha}$-carboxyl group.**

I.2. The discovery of *O*-amino-acyl esters of glycerolipids since the early 60's

Marjorie G. MacFarlane was the first to provide strong evidence for the existence of *O*-amino-acyl esters of phospholipids. In 1962, she extracted total lipids from *Clostridium welchii* (now known as *C. perfringens*) and fractionated them using silicic acid and magnesium trisilicate column chromatography. Five fractions of interest were analyzed (*A-E*). *A* and *B* contained phosphatidylglycerols, fatty acid and glycolipids, whereas fraction *C* and *D* retained particular attention since they contained phospholipids that were ninhydrin-stained (amino-group positive). From fraction *C* MacFarlane isolated and fully characterized the structure of alanyl-phosphatidylglycerol (AlaPG) but this study also evidenced lysyl-phosphatidylglycerol (LysPG) (**Figure I-12**) that was also confirmed in 1965 to be present in large amounts (60 % of total

phospholipids) in *S. aureus* (Macfarlane 1962; Macfarlane 1964; Houtsmuller and van Deenen 1965). Despite the fact that Macfarlane could detect other aa (Asp, Glu, Arg, His) in fraction *D*, further studies in the 60's showed that only Lys (*S. aureus*), Ala (*C. perfringens*) and ornithine (*Bacillus cereus*) (Houtsmuller and van 1963) were *O*-amino-acyl esters of PG. Finally, in 1970, JM. Dos Santos Mota described arginyl-phosphatidylglycerol (ArgPG) (**Figure I-12**) and dilysyl-PG in *Streptococcus faecalis* ATCC9790 (now known as *Enterococcus faecalis*) (dos Santos Mota *et al.,* 1970).

Furthermore, beside PG, another major bacterial phospholipid was found to be *O*-aminoacylated, namely CL (also called di-phosphatidylglycerol) (**Figure I-12**). However, such *O*-amino-acylated CL are restricted to a few species as lysyl-cardiolipin (LysCL; **Figure I-12**) was only described in *Listeria* spp. (Fischer and Leopold 1999), *Anoxybacillus rupiensis* (Rezanka *et al.,* 2012), *Vagococcus fluvialis* (Peter-Katalinic and Fischer 1998) and probably in *E. faecalis*, while alanyl-Cardiolipin (AlaCL; **Figure I-12**) was only detected in *A. rupiensis* (Rezanka *et al.,* 2012) and *V. fluvialis* (Fischer and Arneth-Seifert 1998).

Finally, DAG was also found to be *O*-amino acylated. In *Mycobacterium phlei*, lysyl-diacylglycerol (LysDAG; **Figure I-12**) was described (Lerouge *et al.,* 1988) and more recently, Smith and colleagues described alanyl-diacylglycerol (AlaDAG; **Figure I-12**) in *Corynebacterium glutamicum* (Smith *et al.,* 2015). Consequently, AlaDAG and LysDAG are up to date the only known cases for which the lipid moiety of *O*-aminoacylated lipids are glycerolipids but not phosphoglycerolipids.

This historical overview nicely shows that since the early 60's, efforts were made to enrich our knowledge about *O*-amino acylated lipids. Taken together, eight lipids varying in their aa and/or lipid moieties were described: AlaPG and LysPG are widespread across bacteria, whereas OrnPG, ArgPG, LysCL, AlaCL, AlaDAG and LysDAG are found, to date, in few species. An interesting final remark to this part is that MG MacFarlane noticed, already in 1964, that *O*-amino-acyl glycerolipids are not present in mammalian tissues and this observation will be largely discussed in further sections.

I.3. Structure of O-amino-acid esters of glycerolipids and their consequence on ionic characteristics.

Beside exceptions of AlaDAG and LysDAG, all other *O*-amino-acylated lipids (aaL) described so far, result from the esterification between the α-carboxyl group of an aa and one of the hydroxyl groups of the glycerol moiety from PG or CL. However, PG and CL harbor two and three glycerol units respectively that must be distinguished. Therefore, ***C_n*-glycerol** shall describe the fatty acid-substituted glycerol, whereas the other glycerol that is attached to the aa moiety, will be called ***C_a*-glycerol** (**Figure I-12**). With this nomenclature, two acyl chains are esterified on C_n-glycerol on positions *sn1* and *sn2*, whereas *a*-glycerol is attached to the remaining phosphate-substituted *sn3* position of C_n-glycerol through a phosphodiester bond. Therefore, the three *sn* positions of PG's C_n-glycerol are substituted, while *sn2* and *sn3* positions of *a*-glycerol remain free and susceptible to additional esterifications (**Figure I-12**). In contrast, CL results from the condensation of CDP-DAG and PG and structurally corresponds to two PA (each containing C_n-glycerol) esterified (two phosphodiester bonds) to the *a*-glycerol of the precursor PG. Consequently, only the *a*-glycerol *sn2* position of CL remains free to be esterified with the aa (**Figure I-12**).

However, an important feature that must be considered is the consequence of such lipid aminoacylation on the charge of the resulting aaL. In fact, the presence of a phosphate group engaged in a phosphodiester bond confers a negative charge to PG (-1). The *O*-esterification of Lys implies that its α-COO$^-$ —engaged in an ester bond — does not contribute anymore to the overall charge of the aaL; however, Lys carries 2 positive charges due to its α-NH$_3^+$ and its lateral-chain δ-NH$_3^+$. Therefore, the resulting LysPG inverts the initial negative charge of PG to a cationic lipid (+1). Similarly, *O*-esterification of Orn or Arg brings a common α-NH$_3^+$ and an additional (+1) from their lateral chain (δ- NH$_3^+$) onto the anionic PG (-1), which yields cationic OrnPG (+1) and ArgPG (+1), respectively (**Figure I-12**). In contrast, CL harbors two phosphate groups bearing each an anionic charge. Consequently, *O*-esterification of Lys (+2), neutralizes the global (-2) charge of CL and results in a zwitterionic LysCL. Following the same logic, *O*-esterified Ala (+1 from the α-NH$_3^+$) makes PG (-1) or on CL (-2) zwitterionic AlaPG (0) and anionic AlaCL (-1) respectively. However, despite the fact that AlaCL remains anionic, this mechanism lowers the negativity of the final lipid.

Finally, O-esterification of Lys or Ala onto the sole hydroxyl group of DAG's glycerol, leads to cationic LysDAG (+2) and AlaDAG (+1) (**Figure I-12**). Furthermore, the effect that such ionic changes induce must be considered regarding the biological cytoplasmic membrane context.

I.4. *O*-aminoacylated lipids levels in bacterial cytoplasmic membranes.

After *O*-amino-acid esters of phospholipids had been described, many studies attempted to measure levels of those lipids (**Table I-2**) as well as their abundances with respect to growth phase and environmental cues. OrnPG was detected in *B. megaterium* and in *M. tuberculosis* (11-13 % of total phospholipids) but only in the presence of glucose (Houtsmuller and Van 1964; Khuller and Subrahmanyam 1970), whereas the ratio between LysPG and PG in *S. aureus* and in *E. faecalis* significantly increased under the same conditions. However, these observations were finally attributed to pH variations as a direct consequence of glucose fermentation. When pH is stabilized at 7.4 in the absence of glucose, LysPG amount was very low (<8 %) whereas acidic conditions (pH = 4,8) induced 75 % of total LysPG production. Finally, when cells were cultivated under classical conditions (presence of glucose, starting pH = 7.4 without pH stabilization, 16 h at 37°C) the pH decreased to 4.8 and the rate of LysPG reached 40 % (stationary phase) (Houtsmuller and Van 1964; Houtsmuller and van Deenen 1965). These results were in agreement with *1)* the increased amount of incorporated lysine into the lipid fraction observed by Gale and Folkes (Gale and Folkes 1965), *2)* the fact that LysPG amount remains constant as long as pH is stabilized around 7.2 (Short and White 1971) and finally *3)* the similar rate of LysPG obtained by Haest and colleagues in acidic conditions (80 % of total lipids) (Haest *et al.,* 1972). Whereas LysPG becomes the most abundant lipid under certain conditions, AlaPG in contrast was estimated to shift from 1% to only 6% in *P. aeruginosa* under acidification (Klein *et al.,* 2009). As an exception, *Streptococcus mutans* raises its AlaPG content up to 20 % during stationary phase (Custer *et al.,* 2014). Finally, the percentage of LysCL is assumed to vary among *Listeria* spp. from 12 % to 47.3 % during stationary phase (Fischer and Leopold 1999) whereas D-AlaCL was estimated to 11 % during the exponential phase and 26 % during the stationary phase in *Vagococcus fluvialis* (Fischer and Arneth-Seifert 1998).

This example of aaL amount variations arises the complexity to estimate the amount of lipids that varies according multiple parameters. However, many studies determined these

Species	LysPG	AlaPG	ArgPG	OrnPG	LysCL	AlaCL	LysDAG	AlaDAG	aaLS (specificity)
Agrobacterium tumefaciens	+	–	–	–	–	–	–	–	LpiA (LysPG)
Anoxybacillus rupiensis	+	+	–	–	+	+	–	–	
Bacillus anthracis	10%	–	–	–	–	–	–	–	BAS1375 (LysPG)
Bacillus cereus	+	–	–	+	–	–	–	–	
Bacillus licheniformis	3%	–	–	–	–	–	–	–	YfiX (LysPG)
Bacillus megaterium	+	–	–	+	–	–	–	–	
Bacillus siamensis	+	–	–	–	–	–	–	–	
Bacillus subtilis	L-and N-succinyl-LysPG (17%exp-15%stat)	L- & D-AlaPG	–	–	–	–	–	–	MprF (LysPG/AlaPG)
Bacillus. thuringiensis	10%	–	–	–	–	–	–	–	Bthur0008_13400 (LysPG)
Bifidobacterium spp.	–	+	–	–	–	–	–	–	
Brucella melitensis	+	–	–	–	–	–	–	–	
Burkholderia phymatum	–	0,5% (2)	–	–	–	–	–	–	Bphy_4019 (AlaPG)
Caulobacter crescentus	10,4-11,4%	–	–	–	–	–	–	–	CC_2047 (LysPG)
Clostridium perfringens	+	+	–	–	–	–	–	–	*Cpr* MprF1 (AlaPG) *Cpr* MprF2 (LysPG)
Cohnella spp.	+	–	–	–	–	–	–	–	
Corynebacterium glutamicum	–	+	–	–	–	–	–	+	Cg1103 (AlaDAG)
Enterococcus faecalis	+	+	+	–	+	–	–	–	
Enterococcus faecium	+	+	+	–	– (1)	–	–	–	RakPGS (LysPG, AlaPG, ArgPG)
Halobacillus halophilus	–	+	–	–	–	–	–	–	
Kineococcus radiotolerans	–	0,5 % (2)	–	–	–	–	–	–	Krad_4555 (AlaPG)
Lactobacillus spp.	+	–	–	–	–	–	–	–	
Listeria innocua	8,6%stat	–	–	–	12%stat	–	–	–	
Listeria monocytogenes	30-70%stat; 5,4-25exp	–	–	–	3-12,3%stat	–	–	–	Lmo1695 (LysPG, LysCL)
Listeria seeligeri	2,9%stat	–	–	–	37,4%stat	–	–	–	
Listeria welshimeri	10,8%stat	–	–	–	47,3%stat	–	–	–	
Methanosarcina barkeri	–	+ (2)	–	–	–	–	–	–	Mbar_A2435 (AlaPG)
Micrococcus luteus B-P26	+	–	–	–	–	–	–	–	
Mycobacterium phlei	–	–	–	–	–	–	+	–	
Mycobacterium smegmatis	+	–	–	–	–	–	–	–	LysX (LysPG)
Mycobacterium tuberculosis	+	–	–	+	–	–	–	–	LysX (LysPG)
Mycoplasma laidlawii	–	L- & D-AlaPG	–	–	–	–	–	–	
Paenibacillus polymyxa	–	4% (2)	–	–	–	–	–	–	A-PGS (AlaPG)
Pseudomonas aeruginosa PAO1	–	1-6%exp	–	–	–	–	–	–	PA0920 (AlaPG)
P. aeruginosa NCTC6750	+	– (1)	–	–	–	–	–	–	
P. aeruginosa UCBPP-PA14	–	0,5-4%	–	–	–	–	–	–	PA14_52350 (AlaPG)
Pseudomonas putida	–	0,5-5% (2)	–	–	–	–	–	–	PP_1202 (AlaPG)
Rhizobium tropici	0,6-1,2%	–	–	–	–	–	–	–	LpiA (LysPG)
Staphylococcus aureus	20-40%	–	–	–	–	–	–	–	MprF (LysPG)
Staphylococcus xylosus	+	–	–	–	–	–	–	–	
Streptococcus agalactiae	+	–	–	–	–	–	–	–	
Streptococcus mutans	–	1,7-2,9%exp 13,2-20%stat	–	–	–	–	–	–	
Streptococcus thermophilus	10% (2)	–	–	–	–	–	–	–	stu1256 (LysPG)
Vagococcus fluvialis	+	D-AlaPG	–	–	D-AlaCL (11-26%)	–	–	–	

Table I-2: Documented aminoacylated lipid occurrence and characterized aaLS activities. Inspired from Slavetinsky *et al.* 2017. Data were compiled from Slavetinsky *et al.* 2017 and from Arendt *et al.* 2012. +, presence of the lipid; –, absence of the lipid regarding the currently available data; (1), not proven but very likely; (2), detected through heterologous expression of the aaLS; exp, exponential growth phase; stat, stationary growth phase; %, percentage of total phospholipids. AaLSs described in the literature are listed in the last column and their specificity is indicated between brackets.

characteristics for different aaL as reviewed by (Slavetinsky *et al.,* 2017) and taken together, it seems that acidification of the growth environment and growth phase are the major parameter to induce aaL amount variation.

I.5. Distribution of O-amino-acylated lipids throughout prokaryotes

Beside the relative amounts of aaL that varies from one bacterial species to another, it is also interesting to investigate the phylogenetic distribution of such membranous components. In fact, it was long assumed that aaLs are restricted to Gram positive bacteria including most of Firmicutes and many Actinobacteria. However, it became clear that aaLs are also present in Gram negative bacteria, not only as exceptions, but their occurrence is more limited and the aaL amount is generally lower (Sohlenkamp and Geiger 2016; Slavetinsky *et al.,* 2017). Especially LysPG, thought to be restricted to Gram positive bacteria was found in α-proteobacteria *Caulobacter crescentus* (Jones and Smith 1979) (around 10 %), *Agrobacterium tumefaciens* (Roy and Ibba 2009), *Rhizobium tropici* (Sohlenkamp *et al.,* 2007), *Brucella melitensis* and in γ-proteobacteria *P. aeruginosa* NCTC 6750 (Kenward *et al.,* 1979) (**Table I-2**). In *Sphingomonas sp.* (α-proteobacteria) (Rowe *et al.,* 2000; Zhang *et al.,* 2005), β-proteobacteria *Ralstonia solanacearum* (Yabuuchi *et al.,* 1995), γ-proteobacteria *Xanthomonas campestris* (Moser *et al.,* 2014) and δ-proteobacteria *Stigmatella aurantiaca*, significant amounts of an amino-phospholipid were detected but their identities are not clear. Furthermore, in many other species, homologs of factors responsible for aaL synthesis (aminoacyl-Lipid synthase detailed in **Chapter C, § II**) were detected and this argues for their potential ability to synthetize aaL even if the lipid was not detected so far (Smith *et al.,* 2015). Whereas LysPG and in a lesser extent AlaPG were widely found in bacteria, the other above described O-aminoacylated lipids were reported in limited number. OrnPG was described in *M. tuberculosis*, *B. cereus*, *B. megatherium* (Houtsmuller and Van 1964; Khuller and Subrahmanyam 1970) (**Table I-2**) and was suggested to be present in *Vibrio cholerae* (Blass 1956) and *Brucella melitensis* whereas ArgPG was only detected in *E. faecalis* and *E. faecium* (dos Santos Mota *et al.,* 1970). Concerning O-amino-acid esters of CL, AlaCL and LysCL were characterized in two Gram positive species (*Anoxybacillus rupiensis* and *Vagococcus fluvialis*) in addition to *Listeria sp.* and *E. faecalis* that also contain LysCL (**Table I-2**). Finally, AlaDAG and LysDAG were only described in *C. glutamicum* and *M. phlei* so far (Smith *et al.,* 2015; Lerouge *et al.,* 1988) (**Table I-2**).

Surprisingly, some aaLs are probably also present in Archaea since AlaPG was synthetized through heterologous expression of the archaeon alanyl-phosphatidylglycerol synthase (the factor that synthetizes AlaPG; see in further sections) from *Methanosarcina barkeri* (**Table I-2**). Finally, it is extremely important to note that as MG Macfarlane noticed already in 1964, O-amino-acid esters of lipids were never described so far eukaryote species.

It is also worth mentioning that, according to the present data, some bacterial species contain a single "class" of aaL whereas other harbor a combination of aaLs. *Staphylococcus sp.* and *Streptococcus agalactiae* cytoplasmic membrane have only LysPG whereas AlaPG is the sole aaL described in *Streptococcus mutans, Pseudomonas aeruginosa* and *Mycoplasma laidlawii* (**Table I-2**). In the latter case however, both D-Ala and L-Ala isomers were found to be esterified to PG (Koostra and Smith 1969). In contrast, *B. subtilis* synthetizes D-AlaPG and L-AlaPG (minor) in addition to L-LysPG and N-succinyl-LysPG (Atila *et al.,* 2016; Atila and Luo 2016) (**Table I-2**). Other species such as *C. perfringens* enclose only both major PG derivate (AlaPG and LysPG). In contrast the Gram negative *Anoxybacillus rupiensis* possess LysPG, LysCL, AlaPG and AlaCL (Rezanka *et al.,* 2012) (**Table I-2**). Interestingly, in *Vagococcus fluvialis*, no L-Ala derivate aaL was found but instead two D-Ala containing aaLs were described (D-AlaPG and D-AlaCL) in addition to LysCL (Fischer and Arneth-Seifert 1998; Peter-Katalinic and Fischer 1998). Similarly, 4 different aaLs were described in *E. faecalis* but in contrast to *A. rupiensis*, AlaCL is replaced by the rare ArgPG. In *B. cereus, B. megatherium* and *M. tuberculosis,* OrnPG is associated to LysPG (Houtsmuller and Van 1964) (**Table I-2**).

Finally, *Listeria sp.* contain LysPG and LysCL but interestingly during the stationary phase in *Listeria monocytogenes* the amount of LysPG decreases and LysCL increases concomitantly (Fischer and Leopold 1999) (**Table I-2**). At a first look, the case of *L. monocytogenes* seems contradictory regarding the behavior of LysPG during growth phase described above. However, one can hypothesize that for an unknown reason this organism developed a balance between LysPG and LysCL as a response to cellular stresses. Since L-Lys is an essential aa for protein biosynthesis, it is possible that during the stationary phase *L. monocytogenes* must provide sufficient L-Lys for protein biosynthesis and for lipid aminoacylation. Thus, one can speculate that it is more "energy saving" for bacteria to transfer Lys onto CL instead of PG since CL results from

the condensation of two PG. Another possibility is that since LysPG is cationic and that LysCL is zwitterionic, bacteria could use this mechanism to modulate its global cytoplasmic membrane charge.

Despite the effort to give an overview on the knowledge about O-aminoacylated lipids, the herein description is not exhaustive. The aim of this part of my introduction was to highlight the repertoire of O-aminoacylated lipids and to give a general overview on the main insights that have to be considered when dealing with those membranous components. On another hand, different recent reviews present a more complete overview about the topic (Sohlenkamp and Geiger 2016; Slavetinsky *et al.*, 2017) and (Geiger *et al.*, 2010). Despite the importance of these descriptions, they must be considered with much hindsight since further studies will undoubtedly bring further knowledges that will have to be taken in consideration.

II. Aminoacyl-Lipid synthases (aaLSs)

In the previous section of the present manuscript, I gave an overview of the variety of aminoacylated lipids (aaL), that have been described since the early 60's. As illustrated, the aa-moieties implicated are mostly Lys and Ala while PG, CL and DAG are aa-acceptors. However, important structural variations such as aa-isomers and fatty acid composition as well as the substituted glycerol positions enrich the repertoire of bacterial *O*-aminoacylated lipids. I also discussed some important aspects of tRNAs and tRNA aminoacylation by aaRS, in the context of protein biosynthesis. Finally, I introduced the change of paradigm that rapidly emerged when aa-tRNAs were shown to be used as aa donors in numerous other pathways.

Early studies during the 60's, achieved by WJ. Lennarz and his collaborators, set up appropriate *in vitro* transfer assays and demonstrated that aaLs synthesis is tRNA dependent. This was notably demonstrated by the abolition of the lipid modification activity in assays treated with the RNase (Lennarz *et al.*, 1966). The aa transfer activity to lipids was attributed to enzymes belonging to aminoacyl-tRNA transferases (ATT) — *i.e.* enzymes that use aa-tRNAs to transfer the aa moiety that they carry onto acceptor molecules (**Chapter B** and (Hemmerle *et al.*, 2020)). Another important observation was that inhibitors targeting the ribosome did not affect ATT activities. These investigations additionally revealed that despite common functional features,

lipid- and peptidoglycan aminoacylations differ in molecular details: the chemical bond between the aa and the acceptor is not the same in the case of aaLs and modified peptidoglycan: *O*-ester-bonds are the rule in aaLs, whereas peptide (amide) bonds are found between aa and the peptidoglycan.

Studies demonstrated that the aa moiety of charged Lys-tRNA^{Lys} (*O*-esterified Lys) is transferred onto PG in the presence of cellular extracts prepared from *S. aureus* (Lennarz *et al.*, 1966). RM Gould and WJ Lennarz further tested the ability of various bacterial cell-extracts to use aa-tRNAs as aa-donors in the synthesis of aaLs. Interestingly, *B. megaterium*, *B. cereus* and *S. aureus* preparations catalyzed only LysPG synthesis, while *C. welchii* extracts contained LysPG and AlaPG synthase activities, while *S. faecalis* (*E. faecium*) could synthetize at least LysPG, AlaPG and ArgPG. As expected, cellular extracts of species that do not contain aminoacylated PG derivatives (i. e. *Sarcina lutea*, *E. coli* and *M. lysodeiticus*) could not catalyze aaL synthesis (Gould and Lennarz 1967). These early observations suggested that some species might either contain enzymes with broader specificities or encode more than one enzyme to yield different aaLs.

In all cases, those pioneer studies showed that synthesis of aaLs occurred in two steps. The aa-tRNA is first synthetized by the cognate aaRS and serves as an aa-donor for a particular enzyme that, in a second step, transfers the aa moiety onto the final acceptor substrate, namely PG (in this case). In addition, they suggested that the corresponding enzymes should specifically recognize the aa-tRNA donor as well as the lipid acceptor. However, despite these early efforts to characterize the tRNA-dependent lipid modification pathway, none of the abovementioned seminal studies succeeded in isolating the ATT enzymatic factor thought to be responsible for aaLs synthesis.

Finally, the important development of technologies enabled, much later, the identification of the enzymes that were termed **a**mino**a**cyl-**p**hosphatidyl**g**lycerol **s**ynthases (**aaPGS**). However, because recent studies showed that **ATT can aminoacylate lipids other than PG, implying that aaPGSs form a subclass of a more general class of enzymes**: **a**mino**a**cyl-**L**ipid **S**ynthases (**aaLS**).

II.1. Aminoacyl-Phosphatidylglycerol synthases (aaPGS)

II.1.1. LysPG synthesis catalyzed by MprF from *S. aureus*

II.1.1.1. Discovery of the first aaPGS and establishment of its physiologic functions

In 2001, A. Peschel and colleagues conducted a genetic screen that aimed to identify *Staphylococcus* spp. mutants with increased antimicrobial peptides (AMP) sensitivity. Insertion of a transposon in the *mprF* gene increased *S. xyolsus* sensitivity to the lantibiotic gallidermin. In accordance, deletion of the *mprF* gene in *S. aureus* strains (Δ*mprF*) correlated with increased sensitivity to lantibiotics such as gallidermin and nisin, but also to other AMPs including human defensins HNP1-3, protegrins 3/5, tachyplesin I and magainin II (**Table I-3**). While the minimal inhibitory concentrations (MIC) decreased up to 38-fold for some of those positively charged AMP (CAMPs or CAMPs-like), no significant changes in sensitivity were observed when assaying *S. aureus* wt and Δ*mprF* strains with neutral peptides (Peschel *et al.,* 2001). Thereafter, several studies related *mprF* from *S. aureus* to the resistance against numerous additional cationic molecules [reviewed in (Kuhn *et al.,* 2015)], including aminoglycosides, β-lactamines, glycopeptides and even to the mammalian group IIA phospholipase A2, which harbors cationic properties (Koprivnjak *et al.,* 2002; Komatsuzawa *et al.,* 2001; Nishi *et al.,* 2004) (**Table I-3**). Therefore, the encoded protein was classified as the "**Multiple peptide resistance Factor**" (**MprF**) of *S. aureus*.

The initial study also investigated the capacity of animal immune cells to kill *S. aureus*. In fact, animals developed specific phagocytes, called neutrophils, that achieve pathogen clearance either by releasing the content of their CAMP enriched granules (*i.e.* degranulation) or by generating toxic reactive oxygen species (Mayadas *et al.,* 2014) (**Table I-3**). While phagocytosis of *S. aureus* was by itself not changed for WT or Δ*mprF* strains *of S. aureus*, neutrophils were able to clear Δ*mprF* much faster than wt strains (Peschel *et al.,* 2001). Another study from the same team investigated this aspect into more details and notably showed that the increased susceptibility to clearance of the deletant strain was mediated by the defensin-killing rather than the oxygen-dependent pathway (Kristian *et al.,* 2003). Finally, other phenotypes including decreased virulence

Species	aaL	Phenotypes associated with inactivation of respective aaLS		
		Impact on basic cellular processes or tolerance to environmental challenges	Increased susceptibility to antimicrobial agents	*In vivo* effect during host infection
Bacillus anthracis	LysPG	N.D.	HNP-1; LL-37; protamine sulfate	N.D.
Bacillus subtilis	(L- and D-AlaPG), LysPG (1)	Increased swarming motility; decreased spore germination, spore wet heat resistance and increased spore resistance; decrease in conjugation efficiency, especially under changing ionic conditions	Azlocillin; cefsulodin; daptomycin; nisin	N.D.
Enterococcus faecalis	AlaPG, ArgPG, LysPG	Increased biofilm formation and eDNA level	Colistin; HBD-3; nisin; polymyxin B	Increased resistance to opsonophagocytic killing by PMNs in serum containing complement factors and antibodies against LTA
Listeria monocytogene	LysPG, LysCL	Reduced survival in the presence of osmotic stress; maintenance of flagellum motility	(HNP-1)(2); HNP-2; gallidermin	Reduced invasion of epithelial cells and macrophages; attenuated virulence in infection of mice
Mycobacterium tuberculosis	LysPG, (OrnPG) (3)	Altered membrane potential	HNP-1; lysozyme; polymyxin B; vancomycin	Reduced survival in macrophages and growth defects in mouse and guinea pig lung infections
Myxococcus xanthus	Unknown	Increased swarming motility; defective perception or response to OME (outer membrane exchange)	N.D.	N.D.
Pseudomonas aeruginosa	AlaPG	Reduced tolerance to CrCl3 or sodium lactate; production of AlaPG primarily occurs under acid conditions		N.D.
Staphylococcus aureus	LysPG	Distinct changes in the membrane proteome and membrane-sensory regulators (e.g. reduced amounts of SaeSR and MsrR)	CAP18; cefoxitin; daptomycin; gallidermin; gentamicin; group IIA phospholipase A2; HBD-3; HNP1-3; imipenem; indolicidin; LL-37; magainin;melittin; methicillin; nisin; oxacillin; protegrins; platelet microbicidal proteins; tPMP-1; tachiplesin; vancomycin	Reduced survival in neutrophils; attenuated virulence in infection of miceand rabbits
Rhizobium tropici	LysPG	Reduced resistance to acidic conditions	Polymyxin B (phenotype especially manifests under acidic conditions)	Reduced nodulation competitiveness in bean roots
Corynebacterium glutamicum	AlaDAG, AlaPG	decreased fitness (μmax) to lactic acid and CAMPs i. e. protamine sulfate and polymyxin B whithout MIC changes		

Table I-3: Impact of aminoacylated lipids on bacterial cellular processes and pathogenicity. Reproduced from Slavetinsky *et al.*, 2017 with minor modifications. (1), traces of L- and D-AlaPG have recently been detected, while its phenotypic relevance has not yet been elucidated (Atila *et al.*, 2016); (2), Increased susceptibility to HNP-1 was found by Thedieck *et al.*, 2009 but disproved by Dare *et al.*, 2014; (3) OrnPG has not been detected in the study of an MprF homolog in *M. tuberculosis* Maloney *et al.*, 2009.

in various animal models (rabbit endocarditis model (Weidenmaier *et al.,* 2005); mouse sepsis and septic arthritis models (Peschel *et al.,* 2001)) where attributed to Δ*mprF* strains (**Table I-3**).

Total lipid analysis by thin layer chromatography (TLC) combined to mass spectrometry (MS) experiments revealed for the first time that the newly evidenced factor (MprF) is responsible for the synthesis of LysPG. In correlation with early studies, various forms of LysPG, mainly differing according to their fatty acyl chain compositions but probably also their esterified position on C_a-glycerol (the major *sn3-* vs. the minor *sn2*-Lys), were identified. As a reminder, lysylation of PG reverses the negative charge of the phosphate- containing lipids. This was an additional argument that, besides Lipopolysaccharide (LPS) modifications and Teichoic acids D-alanylation, MprF provides an additional resistance mechanism towards CAMPs, likely using charge repulsion (Peschel 2002). Accordingly, Δ*mprF* strains bind positively charged compounds, such as cytochrome c, tachyplesin I and gallidermin more efficiently in comparison to the *S. aureus* wt strain (Peschel *et al.,* 2001; Ernst *et al.,* 2009). This result suggested that LysPG would lay in the outer leaflet of the PM and strongly supported the postulated "charge repulsion" mechanism. However, since aa-tRNA-dependent PG aminoacylation was thought to occur in the cytoplasm — where tRNAs and aaRSs are found along with ATP and aa —, a LysPG translocation pathway was postulated to be necessary. This issue will be discussed later.

Because aaPGs had been previously described in many bacteria species, it was not surprising that MprF homologs were rapidly detected in numerous Gram-positive and Gram-negative species, suggesting the lipid aminoacylation pathway to be a common resistance mechanism across bacteria (Smith *et al.,* 2015; Weidenmaier *et al.,* 2003).

Regulation of PG aminoacylation

Various studies showed that antimicrobials targeting the cell-envelope such as methicillin, vancomycin, penicillin-G, D-cycloserine, and bacitracin enhance the cellular content of LysPG, while antibiotics inhibiting the translational machinery had no such effect (Hebeler *et al.,* 1973; Rozgonyi *et al.,* 1980; Rozgonyi *et al.,* 1981). The GraS protein contains an anionic extracellular loop that is able to interact with various CAMPs. CAMP-sensing is achieved through GraX-mediated interaction of GraS with VraFG. This sensing complex was shown to activate the transcription factor

GraR, which in turn activates the expression of *vraFG*, *dltABCD* operon and *mprF* in *S. aureus* [detailed in (Fields and Roy 2018) and the herein references].

Effects on membrane proteins

S. Sievers and colleagues aimed to verify if the deletion of *mprF* in *S. aureus* significantly affects the membrane proteome (Sievers *et al.,* 2010). Using gel-free proteomics technology described elsewhere (Speers and Wu 2007) they quantified 840 integral membrane proteins but could not detect drastic differences between the wt and the Δ*mprF* strains. However, distinctive up-regulation were noticed for 13 proteins, while 31 membrane proteins, showed significant down-regulation. Notably, proteins involved in sensing (the two-component sensing system SaeSR and MsrR), and in glycolipid or cell-wall metabolism were down regulated (Sievers *et al.,* 2010). Proteome changes were also checked in *L. monocytogenes* and *B. subtillis* but no significant changes have been reported (Dare *et al.,* 2014). Therefore, it was suggested that membrane associated protein composition might be idiosyncratic to each species or at least to each phylum.

II.1.1.2. MprF consists of two separate functional domains achieving LysPG synthesis and translocation.

Biochemical characterizations aimed to rapidly decipher the pathway of LysPG synthesis and showed that Lys-tRNA^{Lys}, synthetized by the cytoplasmic LysRS, is indeed used by the membrane-associated MprF as a substrate to transfer the aa-moiety onto PG. These experiments were performed *in vitro* by assaying the lipid modification activities of membranes fractions prepared either from *S. aureus*, encoding MprF, or from *E. coli* heterologously expressing MprF. Similar to the observation made by Lennarz, removal of tRNAs by RNase treatment or appropriate inhibition of LysRS (cadaverin) completely abolished LysPG synthesis (Oku *et al.,* 2004; Staubitz *et al.,* 2004). Importantly, all aaPGSs described to date (see below and **Table I-2**) share a common structural organization, consisting of a C-terminal cytoplasmic domain, anchored into the PM through an N-terminally fused integral membrane domain which notably varies from an aaPGS to another through the number of its transmembrane helices (TMH) (Smith *et al.,* 2015). While the activity of the aa-tRNA transferase domain was determined for numerous aaLSs, very little is known about the function of the N-terminal domain. In fact, it is assumed that they are required

to anchor the protein at the membrane, thereby favoring the lipid remodeling mechanism, but the high number of TMHs in many aaLS suggests that another activity might be associated to this proteins. The team of A. Peschel put a particular effort towards the characterization of the N-terminal hydrophobic domain and showed that the MprF protein of *S. aureus* consists of two functionally distinct domains (Ernst *et al.*, 2009) (**Figure I-13**).

II.1.1.2.1.   The synthase domain of *S. aureus* MprF consists of 6 TMHs fused to the cytoplasmic domain

To determine experimentally the topology of the transmembrane N-terminal domain of LysPGS from *S. aureus* (i. e. MprF), authors fused various truncated versions of the N-terminal domain either to the cytoplasmic β-galactosidase (LacZ) or to the periplasmic phosphatase PhoA (only active within the cytoplasm), as previously used to overcome similar issues (Haardt and Bremer 1996). Measuring the relative activities of both proteins led finally to establish that in contrast to the initial 14 predicted TMHs, only 12 helices are embedded within the PM, and separated by a large central intra-cellular loop, between TMHs 6 and 7, that consists probably of two membrane-associated helices (**Figure I-13**). Functional tests designed to monitor the LysPGS activity showed that the cytoplasmic C-terminal domain together with the 6 last TMHs form the LysPG synthase domain are necessary and sufficient for full LysPG synthesis activity (Ernst *et al.*, 2009; Ernst *et al.*, 2015). Interestingly, the number of TMHs required for aaPG synthesis may vary from an aaPGS to another since deletion of the entire N-terminal domain (all TMHs) from *B. subtillis* LysPGS or of *C. perfringens* AlaPGS (CpMprF1), among others, did not affect Lys- or AlaPG synthesis *in vitro* (Roy and Ibba 2009).

II.1.1.2.2.   N-termini TMHs of the hydrophobic domain enable LysPG translocation.

Sequential deletions of 2, 4, 6 or 8 N-terminal TMHs severely reduced CAMPs resistance of *S. aureus*, including to the CAMP-like daptomycin. As expected, expression of a truncated MprF version containing only the 8 N-terminal TMHs did not restore the CAMP resistance of a *S. aureus* Δ*mprF* strain. Furthermore, CM. Ernst and colleagues determined the ratio of LysPG content in the inner and the outer leaflet of the PM by measuring the ability of the membrane-impermeable
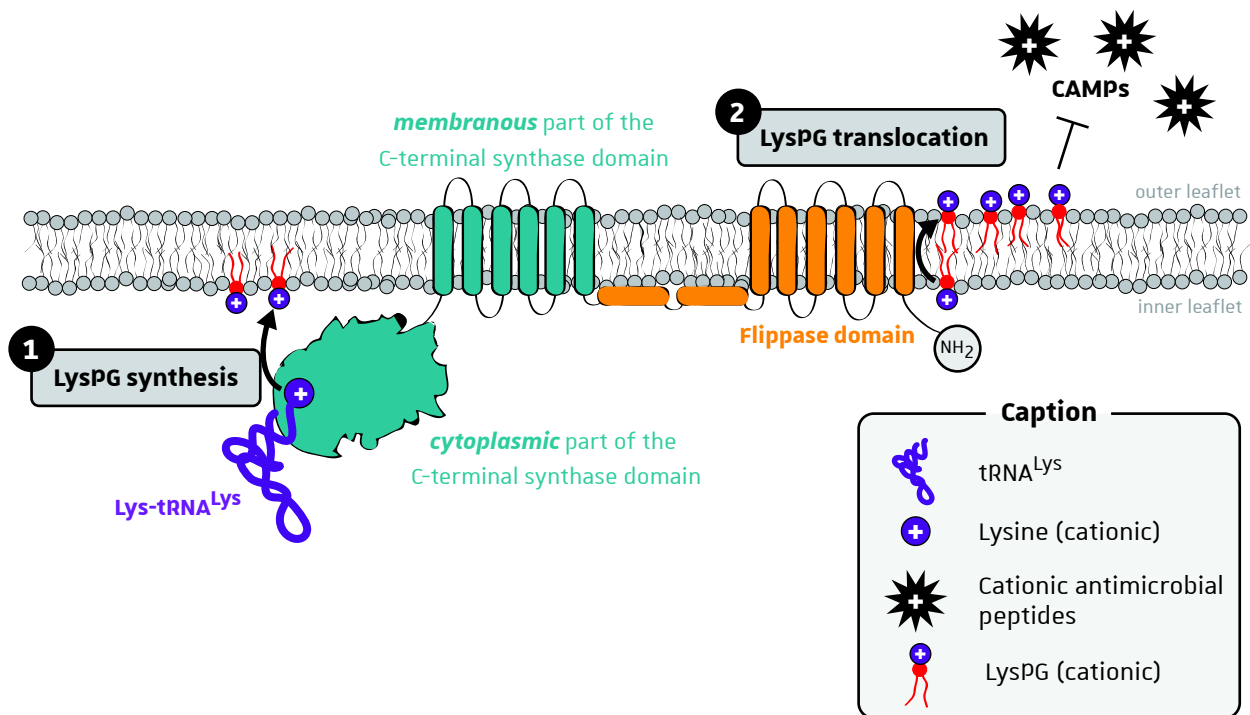
Figure I-13: *S. aureus* MprF has two separate functional domains. The synthase domain is composed of 6 TMHs fused to the C-terminal cytoplasmic domain (blue) and achieves tRNA dependent PG lysylation at the cytoplasmic edge of the PM (*i. e.* ATT activity). Cationic LysPGs are then flipped out by the flippase domain (orange), consisting of the 6 N-terminal TMHs and both membrane-associated helixes that form a large intracellular loop. This lipid remodeling pathway increases *S. aureus* resistance to positively charge antibiotics, mainly to CAMPs, through charge repulsion. (+) specify charged molecules (Lysine, LysPG and CAMPs) and NH_2 indicate the N-terminal extremity of the protein. Based on data from Ernst *et al.* 2015 and figure inspired from Slavetinsky *et al.* 2017.

fluorescent dye fluorescamine to react with LysPG. Accordingly, only expression of both domains, even in *trans*, led to an important increase of LysPG on the outer leaflet, while the strain expressing the synthase (ATT) domain alone had enriched amounts of LysPG only in the inner leaflet. In accordance, the positively charged cytochrome *c* was more efficiently retained by the cell surface of *S. aureus* expressing either the N-terminal or the C-terminal domain alone, while expression of both, restored the repulsion capacity observed in the wt (Ernst *et al.,* 2009; Ernst *et al.,* 2015). Taken together these results strongly suggest that N-terminal TMHs of MprF form a flippase domain which is responsible to translocate LysPG (synthetized by the C-terminal synthase domain) from the inner to the outer leaflet of the plasma membrane (**Figure I-13**).

Multiple sequence alignment revealed conserved residues in the N-terminal flippase and the C-terminal synthase domains that were shown to be essential for LysPG synthesis and subsequent translocation. In particular, Glu206, found in the center of the fifth TMH was suggested to participate to the accommodation of the positively charged Lys moiety of LysPG during translocation. Finally, experiments showed that the flippase and the synthase domains homo-oligomerize and interact with each other. Accordingly, authors demonstrated that MprF oligomerize through intermolecular interactions (Ernst *et al.,* 2009; Ernst *et al.,* 2015).

II.1.1.2.3. Gain-of-function mutations in the flippase domain lead to increased daptomycin resistances

Daptomycin is a lipopeptide that harbors a net negative charge but that is thought to behave as a CAMPs upon binding to Ca^{2+}. The full mode of action was not elucidated to date but daptomycin was shown to interact with phospholipids that form fluid lipids microdomains, thereby preventing the association of essential membrane proteins and leading to cell death (Muller *et al.,* 2016). This powerful antibiotic is used to treat methicillin-resistant *S. aureus* strains (MRSA), but in recent years daptomycin-resistant strains (DAP-R) emerged. Daptomycin resistance has been correlated to point mutations in various regions of MprF (Bayer *et al.,* 2013; Ernst *et al.,* 2015; Ernst *et al.,* 2009). In their recent study, CM Ernst and colleagues focused on the effect of Thr345 and Val351 gain-of-function mutations, two residues located at the junction between the flippase and synthase domains, and demonstrated that they specifically increase daptomycin resistance as well as resistance to the closely related friulimicin B. Interestingly, Thr345Ala mutation did not

alter LysPG production or translocation, and the overall cell surface charge remained unchanged. In contrast, this mutation reduced intramolecular interactions between the flippase domain and the LysPG synthase domain (Ernst *et al.*, 2018). Finally, it was suggested that the relaxed intramolecular interaction induced by Thr345Ala enables MprF to accommodate daptomycin and to remove it from fluid microdomains, but no experimental evidences were provided for the moment to support this hypothesis (Ernst and Peschel 2019).

II.1.1.2.4. Dual specificity of the flippase domain allows AlaPG and LysPG translocation

As mentioned above, many other aaPGS contain N-terminal domains with 12-14 TMHs that are probably also required to expose aaPGS at the surface of cells (flippase domains) (Smith *et al.*, 2015). However, questions are raised in the case of putative aaPGSs that contain shorter N-terminal domains (< 12 TMHs), since according to the investigations conducted by A. Peschel's team, a complete set of 12 TMHs are required for the aaPG flippase activity (at least in *S. aureus*). This issue was partially investigated with the two MprF paralogs from *C. perfringens*, that contain 12-14 TMHs (LysPGS, CpMprF2) and 6 TMHs (AlaPGS, CpMprF1) (detailed in **§ II.1.3.**). Heterologous expression of CpMprF1 or CpMprF2 into *S. aureus ΔmprF* leads to the synthesis of AlaPG or LysPG, respectively, in comparable amounts to LysPG found in *S. aureus* wt strains. However, CpMprF1 alone failed to confer efficient resistance to CAMPs, while its expression together with functional N-terminal domains of either MprF from *S. aureus* or CpMprF2 from *C. perfringens* restored *S. aureus* resistance. These results strongly suggest (if not demonstrate) that AlaPG and LysPG are both translocated by the same flippase in *C. perfringens* (i. e. the N-terminal hydrophobic domain of CpMprF2), and that AlaPG-dependent resistance is mediated through its translocation, as detailed above for LysPG (Slavetinsky *et al.*, 2012). This broad specificity of the flippase domain might be present in other species that contain various paralogs of aaPGS and conveniently explains the presence of two paralogs in some cases: indeed, one of the paralogs harbours the flippase activity and compensates the absence of this activity in the other paralogue (with N-ter domains < 12 TMHs). In contrast, species encoding only aaPGS with short N-terminal domain may probably use a trans-acting flippase to achieve aaPGs exposure. In *Myxococcus xanthus*, a genetic screen led to the discovery of a "split *mprF* gene", with one gene encoding the flippase domain, while the

second encodes the aa-tRNA transferase domain. This illustrates cases in which standalone aa-tRNA transferase MprF-like domains, incapable of catalyzing aaPG translocation, are aided by a separate flippase protein (Dey and Wall 2014). One particularly interesting case is rakPGS of *E. faecium*, for which the flippase domain presumably has broad range aaPG specificity.

Remarkably, even if it is assumed that flippases are implicated in the asymmetric distribution of aaLs in the PM, the MprF flippase domain is the first phospholipid flippase characterized in bacteria. However, its molecular mechanism is far from being elucidated and several points, such as its energy-dependency for example, must be clarified.

II.1.2. AlaPG synthase is encoded by *PA0920* in *P. aeruginisa*

In contrast to LysPG found in *S. aureus* and several other species (**Table I-2**), S. Klein and colleagues noticed in *P. aerugionsa* (Gram-negative) an increasing amount of AlaPG under acidic growth conditions and identified the *PA0920* gene to encode the corresponding AlaPGS. Heterologous expression of AlaPGS from *P. aeruginosa* in *E. coli*, followed by separate analysis of the inner (IM) and the outer membrane (OM), showed that the 14 TMH containing (bioinformatic prediction) enzyme was located into the IM, whereas AlaPG was found to be equally distributed between both types of membranes. Furthermore, partial purification of AlaPGS and *in vitro* amino acid transfer assays confirmed the Ala-tRNA^{Ala} dependency for PG alanylation (Klein *et al.,* 2009).

It is noteworthy that, in comparison to LysPG that can reach 40 % of total lipids during exponential growth phase in *S. aureus* and *L. monocytogenes* respectively, AlaPG was found to vary from 0.5 % at neutral pH to maximal 6% under acidic conditions (**Table I-2**). Accordingly, at pH 5.3 and to a lesser extent 6.3, the P_{PA0920} promoter activity increased significantly.

However, despite these considerations, the *ΔPA0920* strain was more susceptible to the CAMP protamine sulfate, the β-lactam antibiotic cefsulodin, the nucleic acid damaging heavy metal Cr^{3+}, and the osmolyte sodium lactate (**Table I-3**), but interestingly these four stressors failed to increase cellular levels of AlaPG, which suggested that the low level (0.5-1 %) of the modified lipid is sufficient to influence resistance to antimicrobials (Klein *et al.,* 2009). Another study from the same team showed that increased susceptibility of *P. aeruginosa ΔPA0920* strains to the tested β-lactams (ampicillin, oxacillin and cefsulodin), glycolipid (daptomycin, nevertheless considered

also as a CAMP-like) and CAMPs (protamine sulfate, poly-L-Lysine, polymyxin E) (**Table I-3**) was not complemented by heterologous expression of LysPGS from *S. aureus* or *B. subtilis* despite the presence of important levels of LysPG (120 % in comparison to AlaPG level in *P. aeruginosa* wt strain). Furthermore, reintroducing the endogenous AlaPGS (PA0290) in the *P. aeruginosa* ΔPA0920 strain, led to a 2-fold increased amount of AlaPG. Surprisingly, this complemented strain was only able to restitute the wt MICs for ampicillin and oxacillin. Taken together, these results were striking arguments against antimicrobial resistance through a "simple" charge repulsion-only mechanism. In addition, a broader examination of the transcriptional activities of *PA0920* showed that depending on the pH conditions some antimicrobials differentially modulate the promotor P$_{PA0920}$. Therefore, it was proposed that the fine-tuning of AlaPG content in *P. aeruginosa* may regulate the overall permeability of the PM, but other uncharacterized elements might also be implicated. For example, AlaPG found in the OM may modulate β-lactams efflux by regulating the activity of some porins or efflux pumps (Klein *et al.,* 2009; Arendt *et al.,* 2012).

Taken together these studies suggested that AlaPG synthesis may be a central mechanism to the adaptation of *P. aeruginosa* under acidic conditions and because AlaPG is zwitterionic the authors further excluded a simple CAMP resistance mechanism through charge repulsion (Klein *et al.,* 2009). Interestingly, acidic growth conditions seem to be important environmental inducers of lipid aminoacylation since increasing LysPG levels under low pH was also shown to occur in *B. subtilis* (den Kamp *et al.,* 1969; van Iterson and den Kamp 1969), *B. megaterium* (den Kamp *et al.,* 1965), *S. aureus* (Houtsmuller and Van 1964; Houtsmuller and van Deenen 1965; Gould and Lennarz 1970) and in bacterial symbionts *R. tropici* and *Sinorhizobium medicae*.

In addition, 9 substrate specificities of aaPGSs orthologues were evidenced by W. Arendt and colleagues, which increased the number of characterized lipid O-aminoacylation factors to 22 just a bit more than a decade after A. Peschel identified the first MprF (Arendt *et al.,* 2012). Note that since then only one additional aaLS was characterized (**Table I-2**).

II.1.3. Synthesis of distinct aaPG in the same species: displaying a single aaPGS with broad substrate specificity or encoding distinct homologs.

P. aeruginosa and *S. aureus* are thought to encode only one aaPGSs homolog (MprF), that in both cases has restricted specificity towards lipids and aa-Trna substrates to synthetize either AlaPG or LysPG, respectively. In *Clostridium perfringens* (*Cpr*) that produces both AlaPG and LysPG, two distinct aaPGS are encoded, notably *Cpr*MprF1, that uses Ala-tRNA[Ala], and *Cpr*MprF2 that uses Lys-tRNA[Lys], both enzymes modifying PG. Thus, *C. perfringens* was the first organism in which two aaPGS homologs have been functionally characterized (Roy and Ibba 2008b).

In contrast to the previously described aaPGSs that are each specific to a single aa-tRNA substrate, one of the MprF paralogs of *E. faecium*, referred to as the "RakPGS" or MprF2, displayed broad-range specificity for its aa-tRNA substrates, since it could use Arg-, Ala- and Lys-tRNAs to produce ArgPG, AlaPG and LysPG *in vitro* and *in vivo* upon heterologous expression in *E. coli* (Roy and Ibba 2009). In addition to RakPGS (MprF2), *E. faecium* contains another homolog referred to as MprF1. Deletion of the RakPGS completely abolished aaPG synthesis, while no changes in the lipid pattern were noticed in the Δ*mprF1* strains. As expected, *E. faecium* Δ*mprF2* strain exhibited increased susceptibility to CAMPs (nisin, colistin, polymyxin B and HBD-3) but also increased propency to form biofilms, as well as increased resistance to opsonic killing, while virulence in mice remained unchanged in comparison to the wt strain (**Table I-3**). Accordingly, none of the mentioned phenotypes were observed in the Δ*mprF1*, which strongly suggest that only MprF2 is implicated in lipid aminoacylation (Bao *et al.,* 2012).

II.1.4. LysPG, D-AlaPG and succinylated LysPG in *B. subtilis*

Another extensively studied aaPGS is the *B. subtilis* MprF, which was early shown to synthetize LysPG (Staubitz and Peschel 2002). H. Roy and M. Ibba put an effort to characterize the molecular mechanism achieved by this aaPGS. By doing so they set up and optimized an *in vitro* lipid aminoacylation assay (LAA), mimicking the 2-step formation of aaPG, and provided important tools to quantitatively monitor the activities of aaPGSs containing membranes *in vitro*. Notably, this study showed that the specific activity of LysPG synthesis of *B. subtillis* MprF varies *in vitro* according to pre-incubation times of the reactional media, to PG concentrations and to the

presence of detergents (Roy and Ibba 2008a). In addition to LysPG, *B. subtilis* also synthetizes AlaPG (Atila and Luo 2016). Initially, both aaPGS activities were thought to be catalyzed by the same aaPGS, since when the author examined its activity through heterologous expression in *E. coli* and by *in vitro* assays, MprF had dual specificity for Ala-tRNA^{Ala} and Lys-tRNA^{Lys} (Roy and Ibba 2009). However, MS analysis revealed the presence of only LysPG in *B. subtilis* membranes (Gidden *et al.*, 2009), while later structural investigations conducted by M. Atila and Yu Luo detected in the same organism LysPG and D-AlaPG but not L-AlaPG (Atila and Luo 2016).

D-isomers of aa are implicated in numerous cellular mechanisms raising from signaling pathways in eukaryotes to the above-described cell wall synthesis in bacteria [reviewed in (Kuncha *et al.*, 2019)]. Intracellular concentration of L- and D-aa varies generally from nanomolar to micromolar levels and prevalence of one of both enantiomers can lead to cell toxicity. Noteworthy, D-aa can reach millimolar concentrations in some prokaryotes (Schieber *et al.*, 1999; Kirschner and Green 2009). In particular, D-Ala, which is used in bacteria in the synthesis of peptidoglycan, TA, and apparently for PG aminoacylation, was found in higher concentration than its L-isomer (Radkov and Moe 2014). However, because D-aa-tRNAs are harmful when incorporated during protein biosynthesis, several chiral-checkpoints and editing mechanisms are used to avoid them (Kuncha *et al.*, 2019). This includes D- to L-isomers racemization and D-aminoacyl-tRNA deacylase which is a trans-editing factor hydrolyzing specifically D-aa-tRNA (e. g. D-Tyr-tRNA^{Tyr}) but interestingly not D-Ala-tRNA^{Ala}. In *Thermus thermophilus* the latter was shown to be hydrolyzed directly by the editing domain of AlaRS (Rybak *et al.*, 2019). However, such mechanisms were not reported in bacteria and tRNA dependent D-AlaPG synthesis would be very surprising. In addition to this, deletion of MprF in *B. subtillis* abolished LysPG synthesis but importantly not D-AlaPG synthesis. Finally, it was suggested that D-AlaPG could be an intermediate for Teichoic acid d-alanylation by the *dltABCD* operon (Atila and Luo 2016).

Beside LysPG and D-AlaPG, *B. subtillis* is also capable of LysPG N-succinylation by an unknown mechanism and its biologic significance will be discussed later (Atila *et al.*, 2016).

Intriguingly, the LysPGS encoded by *B. subtillis* and *E. faecium* were both localized at their septa (*i. e.* the structure that separates two dividing daughter cells) which suggests that MprF-type lipid modifying factors could specifically generate aaPG microdomains in this region. A recent

study suggested that β-defensins, such as hBD2 and hBD3, target SecYEG translocases and SrtA sortases which are also found near the septum. Therefore, it was proposed that LysPG microdomains, located at the septum together with cell-wall biosynthesis and cell-division machineries, could protect this region through CAMP repulsion (Nishibori *et al.*, 2005; Kandaswamy *et al.*, 2013). This hypothesis is further supported by the important LysPG accumulation during the exponential phase in several species. Finally, the *B. subtilis ΔmprF* deletion strain exhibits defects in sporulation and spore properties (Griffiths and Setlow 2009), in motility and conjugation efficiency (Johnson and Grossman 2016), in addition to increased antimicrobial susceptibility (Salzberg and Helmann 2008; Dare *et al.*, 2014; Hachmann *et al.*, 2009) (**Table I-3**).

II.1.5. LysX from *Mycobacterium tuberculosis*

In contrast to the classical aaPGS domain organization consisting of an N-terminal hydrophobic domain fused N-terminally to the cytoplasmic aaPG synthase domain, a sub-group of actinobacteria encode aaPGS homologs directly fused to a C-terminal LysRS. In *M. tuberculosis*, the C-terminal LysRS domain is essential to LysPG synthesis, which suggests a mechanism in which Lys-tRNA^{Lys} is directly channeled from the LysRS domain to the LysPGS domain. Interestingly, while LysPG generally constitute an important proportion of total phospholipids, ranging from 10 to 75 % in Firmicutes (den Kamp *et al.*, 1965; Haest *et al.*, 1972; Fischer and Leopold 1999) (Thedieck *et al.*, 2006; Dare *et al.*, 2014), only it represents 0.3 % in *M. tuberculosis* (**Table I-2**). Despite low levels, LysPG enhances CAMP resistance and virulence, enables survival of bacteria within phagocytes and maintains the membrane potential (Maloney *et al.*, 2009; Maloney *et al.*, 2011; Fol *et al.*, 2013). These results further support that other mechanisms beyond charge repulsion, that include modulation of the membrane fluidity and permeability, and/or probably also more complex indirect pathways, are associated with aaLs aminoacylation.

II.1.6. Succinct and simplified description of lipid aminoacylation pathways mediated by aaPGSs

In previous sections I illustrated the functional variety of aaLS, including the MprF of *S. aureus* which characterization is probably the most advanced. Taken together the reported works allowed to propose a general functional pathway in which aa-tRNAs, synthesized by their cognate

cytoplasmic aaRSs, are highjacked by the cytoplasmic C-terminal synthase domain of aaPGSs in order to transfer the aa moiety onto PG from the inner leaflet of the PM. Then, aaPGs are translocated and exposed to the outer membrane leaflet either by a fused flippase or by a trans-acting flippase (**Figure I-14A**). As detailed later, bioinformatic studies predicted aaLSs homologs to be present in several species (Arendt *et al.*, 2012; Smith *et al.*, 2015). Even if important aspects related to aaLSs will only be described in coming sections, it is convenient to already notice that the pathway descried here is thought to be the general mechanism for membrane remodeling, at least by PG aminoacylation factors (*i. e*. aaPGS). This is supported by several evidences. First, experimental procedures and bioinformatic predictions showed that all aaLSs contain TMHs assumed to anchor the protein to the PM, as expected for membrane remodeling factors (Roy and Ibba 2009; Slavetinsky *et al.*, 2012; Ernst *et al.*, 2015; Smith *et al.*, 2015). The membranous behavior of those factors was also demonstrated by that the transferase activity is enclosed in membrane preparations (Oku *et al.*, 2004; Staubitz *et al.*, 2004; Klein *et al.*, 2009). Second, the tRNA dependency of the pathway was clearly established for several aaLSs and since the aa-donor (*i. e.* the aa-tRNA) is synthesized in the cytoplasmic compartment, it is assumed that the transferase activity occurs at the cytoplasmic edge of the PM. Third, concerning aaL translocation, studies showed that aaLs are exposed to the exterior of the cell (Slavetinsky *et al.*, 2017), in addition to that aaL hydrolases (**§ III**) are located at the outer space of the cell where aaLs might be exposed (Arendt *et al.*, 2013; Groenewold *et al.*, 2019). Obviously, beside the general mechanism presented here there are MprF homologs that differ in their lipid aminoacylation pathway, such as LysX from *M. tuberculosis* (**§ II.1.5.** and **Figure I-14B**) in which the "MprF-module" (i. e. the synthase domain and the membranous domain) is directly fused to the cognate LysRS. This leads to the distinction between "freestanding MprFs/aaPGSs" and aaRS-fused aaPGSs (**Figure I-14**).

II.2.　　Beyond PG aminoacylation

II.2.1. LysCLS in *Listeria* spp.

The above-described lipid aminoacylation pathways are all specific to PG. As described in previous sections of this introduction, other glycerolipids can also be modified. However, to date
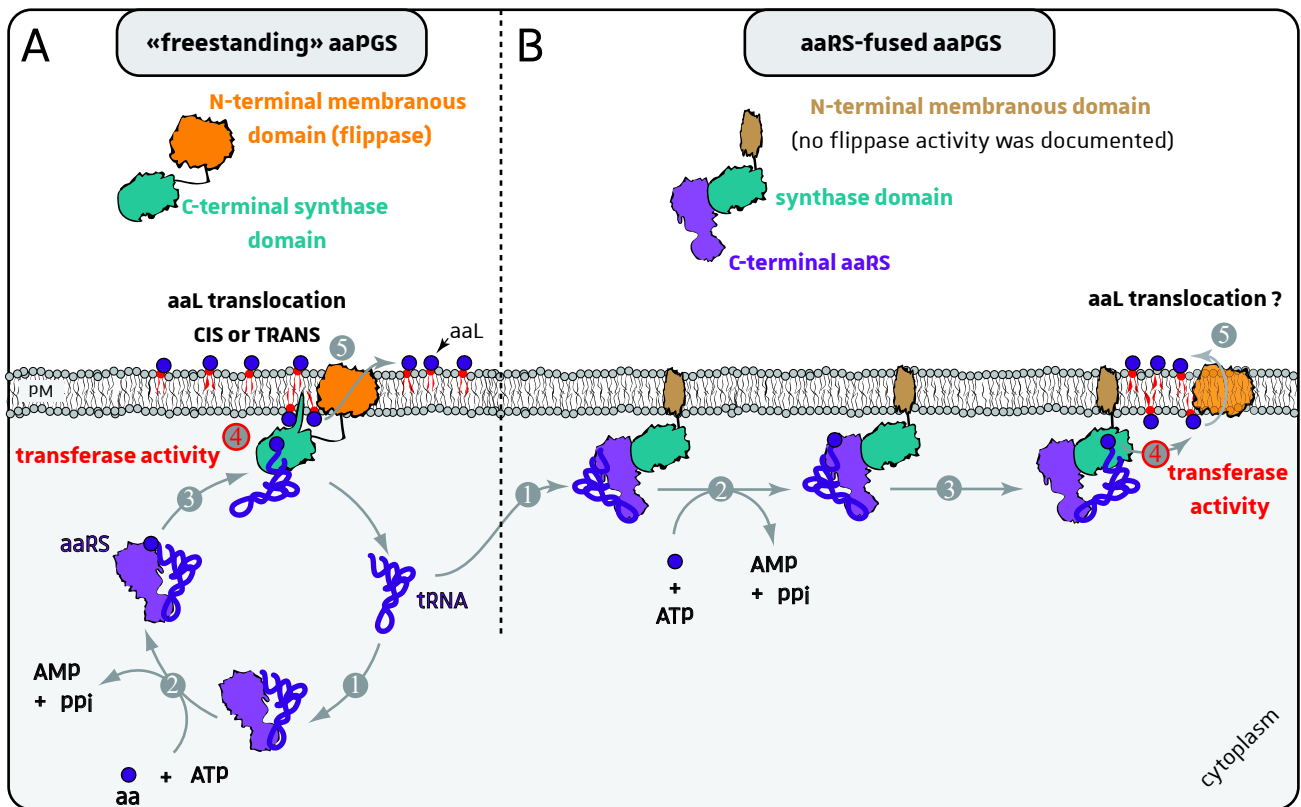
Figure I-14: Proposed lipid aminoacylation pathways achieved by bacteria aaPGSs. (A) Most documented lipid aminoacylation factors are not fused to any aaRS and regarding this are considered as **freestanding aaPGSs**. **(B) aaRS-fused aaPGSs** are rare and are restricted to few actinobacteria species including *M. tuberculosis*. The structural organization of both aaPGSs forms is depicted at the top of each panel and their associated pathway is detailed below.

Steps 1 and **2**, corresponding to the recruitment of the cognate tRNA followed by its aminoacylation, are similar in both cases with the notable difference that the aa-tRNA is synthesized by a cytoplasmic aaRS in (A) and by the aaPGS-fused aaRS in (B). The resulting aa-tRNA is then (**step 3**) **hijacked** by the synthase domain (A) or **channeled** from the aaRS to the synthase domain of aaPGS (B). The latter transfers the aa-moiety from the aa-tRNA onto PGs that are located at the inner leaflet of the PM (**transferase activity; step 4**), which results in aaLs synthesis . Finally, aaLs are translocated to the outer leaflet of the PM either by the fused membranous domain or by a trans-acting flippase (**step 5**). The translocation mechanism associated to aaRS-fused aaPGSs (if exists) is not known and might probably be achieved by a trans-acting flippase.

Please note that the lipid aminoacylation activity of MprF from *S. aureus* was shown to require a portion of the N-terminal membranous domain (refer to the text and **Figure I-13**). However, other studies showed that the C-terminal domain alone is sufficient for the transferase activity. To simplify the present illustration, these aspects were therefore not taken in consideration.

only two cases were experimentally related to MprF-like mechanisms. *L. monocytogenes* is an intracellular gastrointestinal pathogen that causes food poisoning and listeriosis. As described before this bacterium contains LysPG and LysCL. The *Lmo1695* gene encodes a protein that has sequence and domain similarities with the MprF of *S. aureus*, i. e. a C-terminal domain predicted to by cytoplasmic anchored within membranes by a hydrophobic (integral membrane) N-terminal domain predicted to contain 13 TMHs. Note that, initially, the N-terminal domain of *S. aureus* was also predicted to contain 13 TMHs but later experiments demonstrated that it contains 14 helices. Therefore, it is presumable that in *Listeria* spp. the hydrophobic domain also contains a paired number of helices; see below). Deleting *lmo1695* in *L. monocytogenes* resulted in the complete loss of both LysPG and LysCL (Thedieck *et al.,* 2006). However, it was not established if the Lmo1695 protein has PG and CL specificities or if LysCL results from the condensation of a LysPG and an unmodified PG, as one could expect from the CL synthesis pathway in which CDP-DAG (cytidine diphospate-diacylglycerol) is condensed to PG (or, putatively, LysPG). Furthermore, no clear evidences were brought about concerning the tRNA-dependency of LysPG or LysCL synthesis, although it could reasonably infer from other bacteria.

The phenotypic "pattern" of the Δ*lmo1695* strain — i.e. distinguishing it from the wt strain— was initially shown to be similar to those described in *S. aureus* and other LysPGS encoding species, i. e. reduced resistance to antimicrobials (including CAMPs ant the lanthionine- containing gallidermin), reduced invasion capacity of human epithelial cells and mouse macrophages as well as reduced virulence, as shown by following infection kinetics in the mouse model (**Table I-3**). All those phenotypes were recovered upon complementation of the Δ*lmo1695* mutation by re-introducing a wt *lmo1695* genomic copy. In contrast, cell-to-cell spreading as well as the capacity of the deleted strain to grow inside the "poorly" infected cells remained unchanged with regard to the wt strain. Despite its clear implication in virulence, *lmo1695* is surprisingly not regulated by the virulence regulator PrfA (Thedieck *et al.,* 2006). Another study extensively reinvestigated the biologic relevance of LysPG and LysCL biosynthesis and showed, notably, that their relative amounts vary importantly throughout growth phases and with temperature. Confirming early observations reported in a previous chapter, LysPG reached near to 55 % and 75 % of total phospholipids during the exponential phase at 30 °C and 37 °C respectively. LysCL was also found to be a major component of the PM with amounts of 25 to 39 % during the stationary growth

phase at the tested temperature. This work also showed that absence of lysylated lipids (LysPG and LysCL) rendered *L. monocytogenes* susceptible to osmolytic stress but, interestingly, that it retained flagella-mediated motility. Taken together these observations showed that lipid aminoacylation, at least in *L. monocytogenes*, has broader function than previously expected (Dare et al., 2014).

II.2.2. The alanyl-diacylglycerol synthase of *Corynebacterium glutamicum*

In contrast to phospholipids that were early described to be esterified with aa, the first case of a phosphate-free aaL was described only recently. M. Smith and colleagues performed an important phylogenic analysis that focused on the C-terminal domain of aaPGSs and proposed that their homologs are distributed within seven distinct phylogenetic types (discussed later) (Smith et al., 2015). This study focused on type VII aaPGS homologs, exclusively found in Actinobacteria, and aimed to characterize the case of *Corynebacterium glutamicum*. The corresponding "MprF-like" gene is *Cg1103*. *In vitro* assays testing either membrane fractions extracted from *C. glutamicum* or the purified C-terminal domain of the Cg1103 protein (TMH-deleted MprF version) confirmed tRNA-dependent lipid modification in the presence of radiolabeled Ala. Surprisingly, this MprF-like protein was not able to modify PG, which correlated to the fact that the Cg1103-modified lipid had a migration pattern that differed from AlaPG on thin layer chromatography. The modified lipid was purified by column chromatography and identified by LC-MS/MS as being DAG, making Cg1103 an alanyl-diacylglycerol synthase (AlaDAGS). Though MS analysis, authors noticed, however, that in addition to AlaDAG, the membrane fraction of *C. glutamicum* also contained AlaPG. Surprisingly, the synthesis of the latter depended on the presence of a periplasmic esterase called pesT, whose gene is frequently found next to the *alaDAGS* gene in Actinobacteria. Because pesT-dependent AlaPG synthesis requires the presence of AlaDAG, it was suggested that the aa-moiety is likely transferred from DAG onto PG either through an esterase or transferase activity. Taken together, this work provided the first example of the aminoacylation of a phosphate-lacking lipid and of an original pathway through which bacteria can finely modulate their lipid composition. Interestingly, deletion of *cg1103* but not of *pesT* decreased the fitness of *C. glutamicum* in the presence lactic acid (as in *P. aeruginosa* (Klein et al., 2009; Arendt et al., 2012)) and CAMPs (protamine sulfate and

polymyxin B), as shown by the determination of maximal growth rates (µmax) of bacteria. The corresponding MICs, however, remained unchanged (**Table I.3**).

III. aaL homeostasis

The amount of aaLs was proposed to be finely regulated since in some species, artificial upregulation of those lipids resulted in phenotypes similar to those observed upon deletion of the MprF encoding gene. Investigating the genomic contexts of 605 aaLS loci from 493 bacterial species, revealed the frequent occurrence of at least one putative hydrolase factor adjacent to the lipid modifying gene. Three structurally unrelated and semi-conserved hydrolase families were implicated. VirJ (Pfam: PF06057) proteins are found adjacent to aaPGS from Gram-negative — mainly Proteobacteria and Bacteroidetes— but are excluded from Gram-positive bacteria. AaPGS-associated α/β hydrolases such as AhyD (PF12697) are widely distributed in Gram-positive genera, δ-proteo- and cyanobacteria, while putative esterases from the PF00756 family are found in actino- and cyanobacteria in an operon with aaPGSs (Smith *et al.,* 2013; Smith *et al.,* 2015). One representative of each class was at least partially characterized and shown to finely regulate aaL's levels (**Figure I-15**).

III.1. The VirJ-family hydrolase

III.1.1. The AlaPG hydrolase (AlaPGH) PA0919 in *P. aeruginosa*

The importance of aaPG homeostasis was early evidenced in *P. aeruginosa*, since over-production of AlaPG did not fully restore resistance to various tested compounds (Arendt *et al.,* 2012). Recently a hydrolase belonging to the VirJ-like family was shown to confer an AlaPG hydrolase (AlaPGH) activity to *P. aeruginosa*. Topological and sequence analyses predicted the PM-anchored AlaPGH to face the periplasm, thereby enabling exposed AlaPG to be hydrolyzed. Importantly, the corresponding *PA0919* gene is located adjacent to the AlaPGS encoding gene (*PA0920*) and its expression is also upregulated under acidic growth conditions. As expected, abolishing the AlaPG hydrolytic activity, resulted in higher amounts of AlaPG levels but was correlated to significantly increased susceptibilities towards several antimicrobials. Furthermore, $\Delta PA0919$ mutants exhibit reduced growth phenotype under acidic conditions. Taken together the
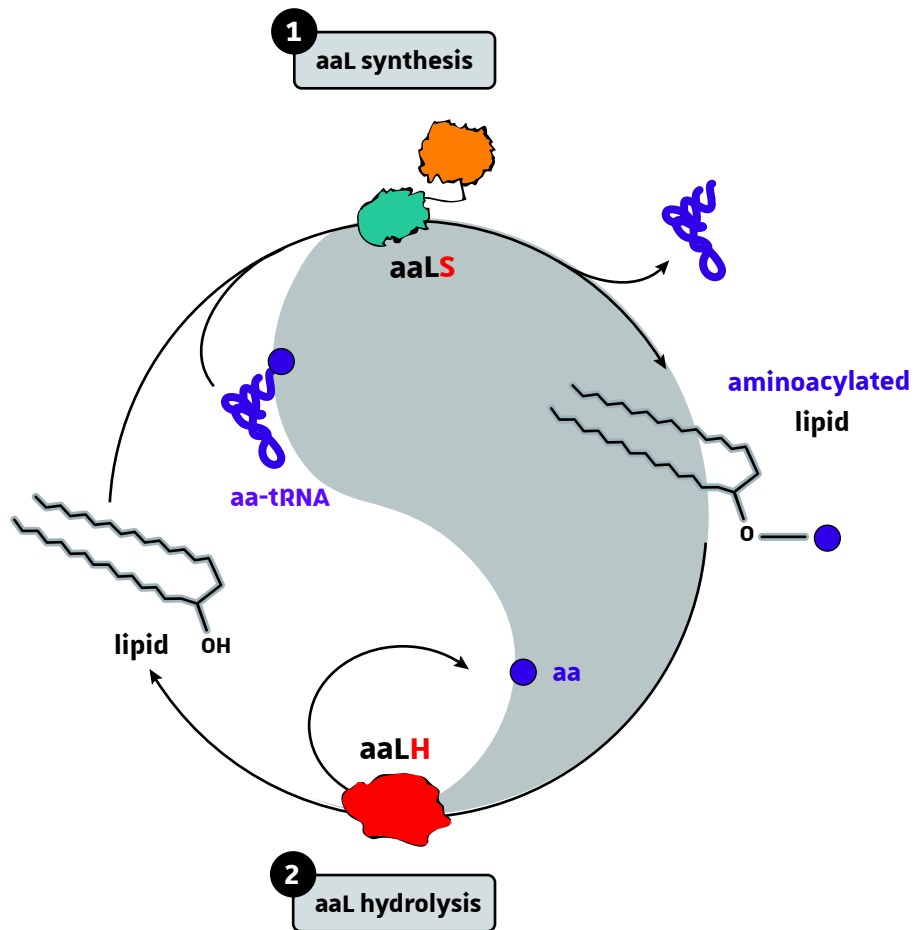
Figure I-15: Schematic representation of aaL homeostasis ~~maintenance~~ in bacteria. AaLs are synthesized by aaLSs and hydrolyzed by aaLHs that have esterase activities. Genes encoding aaLS and aaLH are often clustered at the same locus (Smith *et al.*, 2015), but their regulation is not well understood.

antagonist activities of AlaPGS and AlaPGH share several regulation and phenotypic aspects, which prompted the authors to propose that the fine-tuning of AlaPG levels is required for optimal growth and resistance. Finally, the study brought evidence that Ser240, Ser307 and His401 form a catalytic triad in which Ser307 achieves nucleophilic attack onto the Cα of the esterified Ala moiety. It is worth noting that the *virJ*-encoded AlaPGH could also hydrolyze the aa-moiety of artificial substrates harboring Gly, Ala and Lys (Arendt *et al.,* 2013) *in vitro*.

III.1.2. The LysPG hydrolase (LysPGH) of in *A. tumefaciens*

The LysPG synthesis activity of the protein encoded by the *lpiA/mprF* gene in *A. tumefaciens* was first demonstrated through heterologous expression in *E. coli* (Roy and Ibba 2009). Recently J. Moser's team aimed to investigate the regulatory mechanism of LysPG homeostasis in *A. tumefaciens* and confirmed the MprF/LpiA-dependent synthesis of aminoacylated lipids (Groenewold *et al.,* 2019). However, LysPG levels were barely detectable in neutral pH growth conditions, whereas they tended to increase when the pH of the growth media was acidified. Analysis of the *A. tumefaciens* genome revealed that, similar to the situation in *P. aeruginosa* (Arendt *et al.,* 2013), in which the *PA0919/PA0920* genes encode MprF and a aaPG hydrolase (aaPGH), a putative hydrolase belonging to the VirJ family (Pfam: PF06057) was found to be encoded by the *acvB* gene located in the same operon as *lpiA/mprF*. The AcvB protein harbors, at its N-terminal extremity, a signal peptide that was shown to be responsible for AcvB secretion to the periplasm. In contrast to LysPGH (PA0919) described in *P. aeruginosa*, AcvB is a soluble protein in the periplasm and it does not remain anchored to the inner membrane. More importantly, a ten-fold increase of LysPG levels was observed in a *ΔacvB* mutant of *A. tumefasciens* and *in vitro* experiments confirmed that AcvB is a genuine esterase, responsible for the LysPGH activity (Groenewold *et al.,* 2019). Then, authors investigated the physiological relevance of LysPG homeostasis and showed that *ΔacvB* strains presented more severe growth defects under acidic growth conditions, whereas it was not the case for the *ΔlpiA/mprF* strain, highlighting the detrimental effect of the accumulation of LysPG. *A. tumefaciens* is a plant pathogen that transfers oncogenic T-DNA to dicotolyc plant species *via* a type IV secretion system (T4SS). Once transferred, the linear T-DNA becomes integrated into the plant genome and induces tumor formations. Strikingly, increased levels of LysPG, either found in the *ΔacvB* strain or induced

through *lpiA/mprF* overexpression, impaired tumor formation and T-DNA transfer, while levels of key components of the T4SS were not or only slightly reduced (Groenewold *et al.,* 2019). Taken together, results clearly highlight the relation between virulence of *A. tumefaciens* and proper homeostasis of LysPG, further evidencing and extending the relevance of regulating aaL homeostasis.

III.2. AhyD in *E. faecium*

Similarly, the α/β hydrolase-family AhyD protein, whose gene *ahyD*, located immediately adjacent to the *rakPGS* in *E. faecium*, has broad-range aaLs specificity and can hydrolyze at least AlaPG and LysPG. The aaPG levels in *E. faecium* were not correlated to significant tolerance to acidic conditions but similar to what happened in *P. aeruginosa*, unbalancing aaPG levels and homeostasis induced susceptibility to lactic acid (Smith *et al.,* 2013). Since the latter is a toxic osmolyte known to diffuse passively into the cell (Rubin *et al.,* 1982), it was suggested that aaPG synthesis and hydrolysis regulates resistance of *E. faecium* to molecules produced at low pH rather than directly protecting from acidic conditions.

III.3. The PesT putative esterase in *C. glutamicum*

The PesT protein encoded by the *pest* gene in *C. glutamicum* belongs to the Pfam PF00756 esterase family and was proposed to hydrolyze the Ala moiety of AlaDAG and to enable AlaPG synthesis at the same time (see above). However, the clear function of this third class of aaPG hydrolases was not established for the moment (Smith *et al.,* 2015).

III.4. Concluding remarks

The pathways presented herein regarding aaLs homeostasis involve mainly genes encoding a hydrolase in the same operon as that of the aaLS gene. However, it is assumable that this synteny might not be conserved in several species and that aaL hydrolases could also be encoded at independent loci or belong to other structural types. Such independent genes will be more difficult to identify, since for the moment no sequence signature specific to aaL hydrolases has been established. In addition to that, hydrolases especially from the esterase and α/β hydrolase families are quite common, with sometimes very different activities in addition to be widely distributed.

Numerous representatives of each family are found in a given species. Besides, their broad-range specificities (functional promiscuity) make that they are involved in the hydrolysis of numerous distinct esterified molecules, despite sequence conservation.

In addition to aaPG hydrolases, another mechanism regulating the cell surface's charge was proposed. In their recent study, M. Atila and colleagues showed that LysPG from *B. subtillis* can itself be over-modified through the addition of a succinyl group on one of both amines of Lys (α-NH3 or ε-NH3). Such a modification neutralizes the positive charge brought about by the ε-NH$_3^+$ group of the lateral chain of LysPG: this amino group becomes trapped in an amide bond with one of the carboxyles of the succinyl modifier, the second one remaining free to add a negative charge (COO$^-$). This confers to the resulting lipid a single anionic charge, as it is the case for unmodified PG. The biological function of succinylated LysPG was not established but it was suggested that it could be an alternative for the regulation of the cell surface charge distribution in species lacking an aaPG hydrolase (Atila *et al.,* 2016).

IV. Phylogenic distribution of aaLS throughout bacteria

IV.1. Classification of aaLS homologs into 7 phylogenetically related types (Smith *et al.,* 2015)

As mentioned before, several phylogenic studies aimed to investigate the distribution of aaPGSs throughout bacteria. Interestingly, none of those study could establish a convincing link between the substrate specificities and the phylogenic distribution of aaLS, since aaLS with distinct substrate specificities did not cluster inside delimited clades. Based on the alignment of a 160-residue sequence from 253 aaLSs, Smith and colleagues reconstructed the phylogeny of this enzyme family. From this phylogenetic reconstruction, they proposed lipid aminoacylation factors to be distributed into 7 sequence types (clades) (Smith *et al.,* 2015). Types I and V belong mostly to proteobacteria, while types II transferases are exclusively found in firmicutes. Almost all 23 aaLSs that had been experimentally characterized, including LysPGSs, AlaPGSs and the broad range specific rakPGS from *E. faecium*, belong to types I and II. Type IV is restricted to actinobacteria and includes the cluster containing all aaPGSs fused C-terminally to a LysRS, while type VII transferases, also restricted to actinobacteria, encloses the only AlaDAGS characterized so far. Finally, type VI

transferases gathers only freestanding transferases with no predicted TMH domains but the sole experimentally characterized factor of this type corresponds to VlmA (containing a Dupli-GNAT fold with an $\alpha^{(+)}$ helix), that catalyzes Ser-tRNA^{Ser}-dependent serylation of an antibiotic precursor in valinimycin biosynthesis (Garg *et al.,* 2008; Hemmerle *et al.,* 2020), which prompted the authors to suggest that members of this group are not implicated in lipid aminoacylation. Note that 3 of them are encoded by fungal species (eukaryotes).

IV.2.   TMHs variations throughout the different transferase types

AM. Smith and colleagues also investigated the correlation between the different aaLS types and the TMHs number found in the N-terminal domain. Most of type I, II and VII transferases contain 12-14 TMHs and those that effectively have aaLS activities might therefore be able to translocate (flip) synthetized aaLs, as demonstrated for LysPGS from *S. aureus* and *C. perfringens*. On the contrary, putative aaPGS that have less TMHs, especially those which have 2-6 TMHs would be defective for aaLs translocation. Moreover, some aaPGS seem to require *at least* 6 TMH for their intrinsic lipid aminoacylation activity (*S. aureus* MprF), while other require only the cytoplasmic C-terminal aaL synthase domain (AlaPGS from *C. perfringens* (6 N-terminal TMHs), *P. aeruginosa* (12-14 N-terminal TMHs), LysPGS from *B. subtilis* (12-14 N-terminal TMHs) and *B. licheniformis* (12-14 N-terminal TMHs) (Hebecker *et al.,* 2015; Roy and Ibba 2009; Ernst *et al.,* 2009)) in addition to at least 6 supplementary TMHs for the flipase activity. One might speculate that those aaPGSs (especially type IV transferases) that are defective in aaL translocation activities can combine with another flippase, including those of other paralogous aaPGSs. It is the case for CpMprF1 (AlaPGS), that exposes AlaPG using the flipase of CpMprF2 (LysPGS) in *C. perfringens* (Slavetinsky *et al.,* 2012). In fact, several species encode numerous aaPGS homologs either from the same type or from different types. For example, *Kineococcus radiotolerans* contains one free-standing type I LysPGS domain, a closely related type I homolog containing 12-14 TMHs and a type IV homolog containing 6-8 TMHs. (Smith *et al.,* 2015).

IV.3. Occurrence of the 3 aaLs hydrolases families adjacent to the aaLS gene

Finally, investigating the genomic context of *aaPGSs* genes and the adjacent hydrolases indicated that VirJ proteins (Pfam: PF06057) are exclusively found in Gram-negative bacteria, adjacent to type I transferases. α/β-hydrolases from the Pfam family PF12697 are present in both Gram-positive and Gram-negative bacteria and include the broad range AhyD hydrolase characterized in *E. faecium* (AlaPG and LysPG hydrolase). Finally, PesT belonging to the putative esterase family (Pfam: PF00756) is present adjacent to several type VII but also in some type IV transferases and is mostly restricted to actinobacteria.

For more extensive discussions on aaPGS phylogeny refer to (Roy and Ibba 2008b; Ernst and Peschel 2011; Arendt *et al.,* 2012; Smith *et al.,* 2015).

V. Structure of aaPGSs and substrate specificity

V.1. Establishing of the substrate specificity of aaPGS for aa-tRNA

Experiments were conducted very early to assess the specificity of the PG modification pathway (Lennarz *et al.,* 1967). Concomitantly, two other studies investigated the specificity of the so-called "particulate enzyme" (i. e. aaPGS), in order to determine the aa-tRNA substrate, in other words, to specify its tRNA and aa moieties. Nesbitt and colleagues used the capacity of the LysRS from *E. coli* to mischarge 2-β-aminoethylcystein onto tRNA^{Lys} (Stern and Mehler 1965) and showed that cell extracts from *S. aureus* synthetize 2-β-aminoathylcysteinyl-PG from 2-β-aminoathylcysteinyl-tRNA^{Lys} but not from 2-β-aminoathylcysteinyl-tRNA^{Cys} (Nesbitt and Lennarz 1968). At the same time, the same team showed that cell-extracts prepared from *C. perfringens* (formerly known as *C. welchii*) could not transfer the acylated moieties of lactyl- and N-acetylalanyl-tRNA^{Ala} (derivate of Ala-tRNA^{Ala}) onto PG. Moreover, the non-cognate Ala-tRNA^{Cys}—that had successfully been used to test the specificity of translation of a poly-UG RNA by the translational machinery— proved unsuitable to achieve AlaPG synthesis (Gould *et al.,* 1968). Taken together these early results suggested that aaPGS may specifically recognize both moieties of the aa-tRNA and the lipidic substrate.

V.2. The identity determinants for tRNA recognition by aaPGS are located in the acceptor stem

Over the two past decades, some studies tried to further decipher the molecular mechanism of lipid aminoacylation by re-investigating the specificities of aaPGS for their substrates and by resolving the structure of those proteins. H. Roy and M. Ibba used a tRNA^{Ala} minihelix, corresponding to an acceptor-T-stem-loop (Francklyn and Schimmel 1989), and showed that the anticodon-stem-loop, the D-stem-loops and consequently the overall tRNA L-shape are dispensable for PG alanylation by the AlaPGS from *C. perfringens*. Note that this is the only work that investigated the possible competition between the translational machinery and the lipid modification pathway regarding their common aa-tRNA substrate. Their results show that both EF-Tu (elongation factor Tu) and MprF have similar affinities for the aa-tRNA substrate (Roy and Ibba 2008b), suggesting that the aa-tRNA ligand should partition equally between both pathways.

S. Hebecker and colleagues further investigated the tRNA specificity of MprFs and showed that alanylated microhelices, consisting of a 7 base-pair stem-loop that mimics the acceptor terminal part of tRNAs, are used by the purified C-terminal (i. e. the aaPG synthase domain) domain of *P. aeruginosa* AlaPGS (residues 543 to 881; AlaPGS$_{543-881}$) and that the enzyme retains similar lipid aminoacylation activities when compared to wt (full-length) tRNA^{Ala}. Consequently, several site directed mutations inside this tRNA microhelix revealed that the terminal 5 base-pairs (together with the discriminator A73 and the 3'CCA) must contain all essential determinants required for the recognition of Ala-tRNA^{Ala} (from other aa-tRNAs) and the transfer of Ala onto PG by AlaPGS. Notably, the C5-G68 pair seems to be a key player in the lipid aminoacylation step, while as a reminder, G3-U70 and the discriminator A73 are strong determinant for tRNA^{Ala} alanylation by AlaRS (Hebecker *et al.*, 2011).

V.3. Discrimination of Ala-tRNA^{Ala} from Lys-tRNA^{Lys}

The cytoplasmic domains of *P. aeruginosa* AlaPGS and *B. licheniformis* LysPGS (AlaPGS$_{543-881}$and LysPGS$_{519-850}$) showed high substrate specificity for their respective Ala-tRNA^{Ala} and Lys-tRNA^{Lys} substrates. The acceptor stems of both tRNAs share the discriminator base A73, base pairs G1-C72, G2-C71, U7-A66 and the critical C5-G68. In contrast G4-C69, C6-G67 and G3-U70 of tRNA^{Ala}

are replaced by U4-A69, G6-C67 and G3-C70 in the tRNA^{Lys} (**Figure I-16**). G3-U70 in tRNA^{Ala} and G3-C70 in tRNA^{Lys} are identity determinant for accurate recognition by their corresponding aaRS (AlaRS and LysRS). Accordingly, mutated tRNA^{Lys} U70C is not aminoacylated by LysRS but instead used by AlaRS to synthetize Ala-tRNA^{Lys} U70C. More importantly, the latter was accepted by *P. aeruginosa* AlaPGS, but not by *B. licheniformis* LysPGS, to produce AlaPG. From these considerations, it was concluded that position N70 of the tRNA might be an essential element to discriminate Ala-tRNA^{Ala} and Lys-tRNA^{Lys} for accurate substrate recognition by aaPGSs of restricted specificities (Hebecker *et al.,* 2011; Hebecker *et al.,* 2015).

V.4. Structures of aaPGSs and accommodation of the lipid substrate

As mentioned before, the C-terminal domain of most aaPGSs retains full lipid aminoacylation activity *in vivo* and *in vitro* when the N-terminal integral membrane (and flippase) domain is removed (note that *S. aureus* MprF can be considered an exception since, so far, it is the only one aaPGS for which the last 6 TMH, out of 14, have been shown to be required for lipid lysylation). Therefore, to facilitate molecular, biochemical, and biophysical characterizations, several authors used recombinant versions of aaPGSs in which the hydrophobic N-terminal domain was completely removed. Notably, the team of J. Moser successfully purified recombinant versions of two C-terminal domains (AlaPGS$_{543-881}$ from *P. aeruginosa* and LysPGS$_{519-850}$ from *B. licheniformis*), which enabled determining the crystal structures of both modules and shed light onto important aspects of the molecular/enzymatic mechanisms of aaPGSs (Hebecker *et al.,* 2015).

Both domains that have been crystallized correspond to the aa-tRNA transferase domains (AlaPGS$_{543-881}$ from *P. aeruginosa* and LysPGS$_{519-850}$ from *B. licheniformis*) of MprFs/aaPGSs. They share a common fold, referred to as the **DUF2156 domain, that is constituted of two GCN5- N-acetyltransferase (GNAT)-like subdomains in tandem (Dupli-GNAT).**

The structures of *P. aeruginosa* AlaPGS$_{543-881}$ and *B. licheniformis* LysPGS$_{519-850}$ share important features with dupli-GNATs and accordingly, the strongest structural homolog was *W.viridescens* FemX (Fonvielle *et al.,* 2013). A quick overview of this dupli-GNAT structure reveals that, in comparison to the conserved secondary structure of the reference standalone GNAT fold (**Chapter B**), GNAT1 of aaPGSs lacks the most N-terminally β-strands, GNAT2 has two additional α-

Figure I-16: Comparing substrate recognition of aaPGSs toward aa-tRNAs. In their study, Hebecker and colleagues synthesized Ala-tRNA^{Ala}, Lys-tRNA^{Lys}, and a misacylated Ala-tRNA^{Lys}C70U (the mutated position indicated by * is required for tRNA^{Lys} mis-alanylation by AlaRS) and tested their ability to be used by *B. licheniformis* LysPGS and by *P. aeruginosa* AlaPGS (Hebecker *et al.*, 2015). Identity elements of respective tRNA acceptor-stems are in red shaded circles (Giege *et al.*, 1998) and nt differences between Ala-tRNA^{Ala}, Lys-tRNA^{Lys} are indicated by blue circles. The red box highlights the C5-G68 base pair shown to be essential for AlaPG synthesis by AlaPGS (Hebecker *et al.*, 2011) which is also found in tRNA^{Lys}. Ala-tRNA^{Ala} and Lys-tRNA^{Lys} are specifically used by AlaPGS and LysPGS, respectively, while the artificial Ala-tRNA^{Lys}C70U was substrate of AlaPGS, but not of LysPGS. **Figure modified from Hebecker *et al.*, 2015**.

helices (8a and 9) and finally both GNATs share two common β-strands (K,E) (**Figure I-17A**). Analysis of the structures showed that aaPGSs contain two opposite cavities connected to each other by a "bottleneck" (**Figure I-17B & C**). One cavity (CAV$_{CCA-aa}$) is delineated by numerous secondary structures belonging to GNAT2 and contains several conserved residues. Mutagenesis of those residues combined to structure superimposition with the Fem X co-crystallized CCA-aa analogue, and manual substrate docking, strongly suggest that the charged CCA of tRNA enters this cavity and interacts with Phe839 and Lys840 of *P. aeruginosa* AlaPGS. These residues are essential and conserved in the homologous *B. licheniformis* LysPGS and in *W. viridescens* FemX. Furthermore, as expected for this type of ATT, **the essential $\alpha^{(+)}$ helix is present adjacent to CAV$_{CCA-aa}$.** Point mutations of basic residues (i. e. Lys and Arg) to Glu reverses the local electrostatic charge, thereby abolishing aaPG synthesis, likely because negatively charged Glu residues now "repel" the aa-tRNA substrate, that possesses a negatively charged phosphate-sugar backbone, which prevents substrate recognition and activity. In conformity with the distance between the $\alpha^{(+)}$ helix and CAV$_{CCA-aa}$, authors proposed that those positively charged residues interact with the tRNA acceptor stem (Hebecker *et al.*, 2015).

In the PFAM database, the ATT domain of aaPGSs is recognized to belong to the *Domain of Unknown Function 2156* (DUF2156) family in the PFAM database. This fold is, in reality, a dupli-GNAT fold in which the two GNAT subdomains are attached by an $\alpha^{(+)}$ helix, as demonstrated by the determination of the structure of *P. aeruginosa* and *B. licheniformis* aaPGSs structures. Therefore, in the following, "DUF2156 domain" will refer to a "dupli-GNAT fold domain in which GNAT 1 and 2 are separated by an $\alpha^{(+)}$ helix". In other words, **GNAT1-$\alpha^{(+)}$-GNAT2 –type proteins will be termed "DUF2156" proteins**.

Surprisingly, despite their substrate specificities, no relevant structural or residue determinants have between found in the AlaPGS and LysPGS that could explain how Ala is discriminated from the bulkier Lys and vice versa. Concerning the catalytic mechanism, solid evidences argues for direct transesterification rather than a covalent attachment of the aa onto the protein achieved for example by acyl-carrier proteins. In their structural work, S. Hebecker and colleagues showed that the Cα of the co-crystallized L-Lys analogue points toward the bottleneck of the tunnel and is surrounded by a conserved aa network. LysPGS Tyr705 and Asp739

A — GNAT domain 1, GNAT domain 2, INS 6-7, Positively charged helix ($\alpha^{(+)}$)

B

C — 180°C, E658, Q836
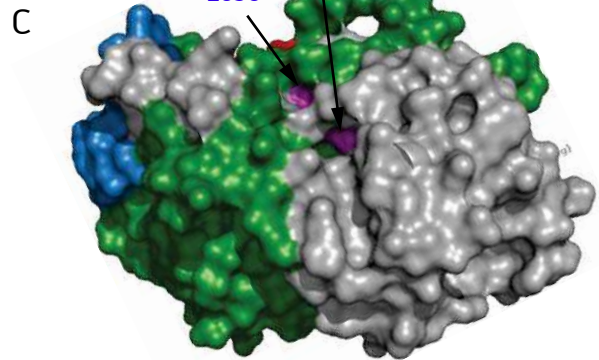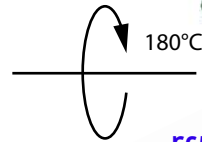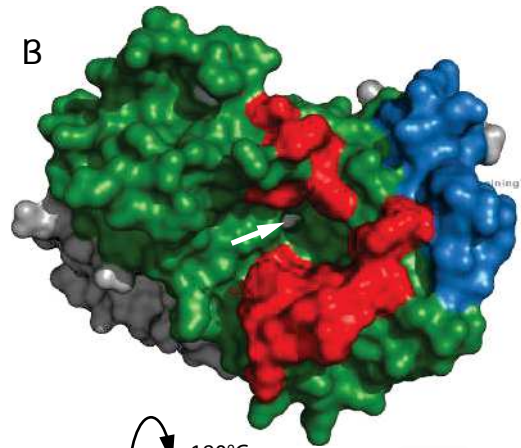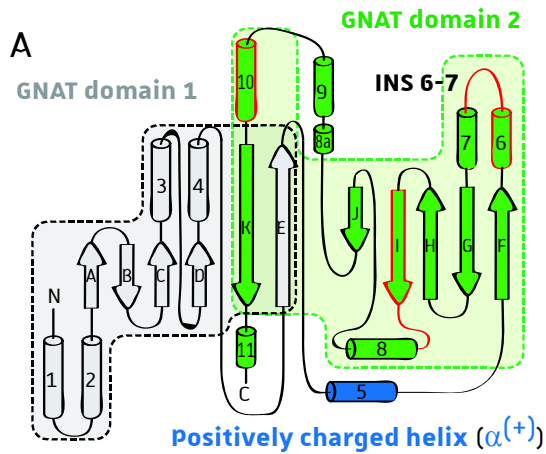
Figure I-17: Structural organization of AlaPGS.
(A) Topology of the Dupli-GNAT fold of AlaPGS from *P. auruginosa*. GNAT domain 1 and GNAT domain 2 are in gray and green respectively, while the positively charged α-helix is colored in blue. Secondary structures from GNAT domain 2 in red delimitate the CAV_{CAA-aa} and contain conserved residues. Both GNAT domains share β-strands K and E. **(B)** The AlaPGS structure is presented as a Van der Waals surface therby showing the cavity supposed to accommodate the 3'CCA-aa of the aa-tRNA (CAV_{CAA-aa}). From this edge, the mentioned bottleneck is appreciable (white arrow). **(C)** The same structure after 180° rotation reveals the cavity accommodating the lipidic substrate (CAV_{Lip}) by a backdoor entrance mechanism. Residues in purple are conserved within the CAV_{Lip}. Note that both GNAT domains were delineated by the positively charged α-helix and that the same color code was used in A, B and C. Residues from the inserted INS 6-7 loop were suggested to contribute to the delimitation of CAV_{CAA-aa} and of CAV_{Lip}, thereby probably forming the aa-tRNA/lipid interface.

(Tyr732 and Asp765 from AlaPGS) participate to the interaction with the α-NH2 of the aa, while Glu693 and Ser684 (Glu720 and Ser709 from AlaPGS) are essential to optimally position Arg742 (Arg768 from AlaPG). With regard to transesterification, interaction of this Arg with the a-carboxyl group of the aa-substrate and its activation, may facilitate the nucleophilic attack mediated by the 3'-hydroxyl group of PG leading to the formation of an ester linked aaPG (Hebecker et al., 2015).

In contrast to the aa-tRNA that enters the above described cavity, PG was proposed to enter through the opposite cavity (CAV_{Lip}) (**Figure I-17C**). The bottleneck between them enables the catalytic interaction between both substrates. It is noteworthy that FemX proteins accommodate a polar aa-acceptor substrate into a water accessible "open" cleft, while aaPGS must deal with an amphipathic second substrate that contains large hydrophobic fatty acid chains. A closer look at the aaPGS structure reveals the presence of a large inserted loop between helices 6 and 7 (INS_{6-7}), an extension at the GNAT2 C-terminal extremity, and an overall reclined GNAT1 in comparison to FemX. These structural rearrangements lead to the formation of a restricted hydrophobic space, comparable to a tight tunnel which is protected from the water-soluble environment, thereby favorizing the accommodation of the lipidic substrate.

Molecular docking predicts the polar headgroup of PG to partially traverse the bottleneck and thus to access the aminoacyl-binding site, while the fatty acid chains appeared to have high degree of flexibility inside the hydrophobic CAV_{Lip} (Hebecker et al., 2015). These theorical consideration are supported by in vitro tests assaying aaPGS activities in the presence of several PG derivates. The results showed indeed that fourfold methylation of the acyl chains, variations of their length or their saturation and even suppressing one of both acyl chains retained substantial activities. In contrast AlaPGS could not retain any detectable activity when the polar head group of PG was affected by replacing the terminal glycerol by ethylene glycol (Hebecker et al., 2011).

In conclusion, the two major studies conducted by S. Hebecker and colleagues shed in light several mechanistic aspects of lipid aminoacylation and proposed an original model for the aaPGS activity at the water-soluble interface. Despite many points were only theoretically postulated it is important to point out that almost each hypothesis was supported by biochemical experiments. Taken together, the team of J. Moser showed that dupli-GNAT containing aaPGSs folds so that two cavities interact through a bottleneck. Based on their extensive biochemical data authors proposed

that one cavity accommodates the terminal CCA-aa of the aa-tRNA with high substrate specificity while the hydrophobic lipid enters the opposite tunnel. At the bottleneck, the glycerol of PG is supposed to traverse the aa-tRNA binding site and may interact with the Cα of the aa to enable transesterification. Finally, the description these structures further argues for the conserved aa-tRNA recognition mode by the GNAT2 domain throughout ATT. This includes several residues delineating CAV$_{CCA-aa}$ and obviously the positively charged α-helix that interacts with the acceptor stem. On the other hand, the recognition mode of the aa-acceptor varies importantly according to the nature of the molecule that must be taken in charge. This latter aspect is mainly enabled by the fact that GNAT1-fold adapted during evolution.

D. Purpose of my thesis work

When I started my master and then my PhD, only prokaryotic aminoacyl-tRNA transferases (ATT) of the dupli-GNAT-$\alpha^{(+)}$ fold were known: the Fem-ligases that use aa-tRNAs to modify the peptidoglycan, mostly in monoderms (Gram positive bacteria), Fem homologs that participate in the tRNA-dependent biosynthesis of antibiotics, the Leu/Phe-tRNA::protein transferases (LFT) that participate in the N-end rule pathway and the aminoacyl-glycerolipid synthases (MprFs). In eukaryotes, only the Arg-tRNA transferase (RTT) that mediates the N-end rule pathway was known. They all possess a dupli-GNAT-$\alpha^{(+)}$ fold, but only the $\alpha^{(+)}$ helix and GNAT II subdomains share partial sequence motifs that make them members of the N-acetyltransferase superfamily (NAT-SF), while the GNAT I subdomain, that recognizes a variety of "acceptor" substrates (peptidoglycan precursors in the case of Fem ligases, glycerolipids in the case of MprF, various proteins for LFT and RTT, multiple classes of small metabolites for Fem-like proteins that participate in the synthesis of antibiotics) presents strong sequence divergences. This leads to multiple classes of dupli-GNAT-$\alpha^{(+)}$ fold proteins: **FemAB** (PFAM: PF02388, Fem-ligases), , **Leu_Phe_trans** (PF03588,like LFTs), **ATE_N** and **ATE_C** (N- and C-ter parts of RTT, PF04376 and PF04377, respectively) and **DUF2156** (PF09924). The latter, DUF2156, is the dupli-GNAT-$\alpha^{(+)}$ fold that is found in prokaryotic MprFs. Among these 5 families, protein members are exclusively found in prokaryotes (bacteria and archaea) and none (or very rare) instances are detected in eukaryotes, which supported claims on the prokaryotic-specific distribution of ATTs, especially in the case of MprFs.

In addition, from the discovery of MprFs and over the past decades, tRNA-dependent lipid aminoacylation pathways had never been described in eukaryotes, nor DUF2156 proteins detected, explaining why MprF or MprF-like proteins were through to be absent in eukaryotes, *i.e.* to be

restricted to prokaryotes (Smith *et al.*, 2015; Fields and Roy 2018). However, Dr. Frédéric Fischer performed a preliminary and large-scale bioinformatic study on DUF2156/MprF-like proteins and unexpectedly detected several potential **DUF2156 proteins, homologous to bacterial MprFs, in most "higher" fungi (Dikarya)** (*i. e.* ascomycota and basidiomycota). According to structure predictions and sequence analyses, those proteins shared the dupli-GNAT-$\alpha^{(+)}$ fold (two GNAT subdomains separated by a positively charged helix) of bacterial MprFs, which suggested that eukaryotes, in particular fungi, might use bacterial-like ATTs to achieve aa-tRNA-dependent transferase activities. Sequence analyses further revealed that **two distinct DUF2156 protein families** coexisted in "higher" fungi, including human, plant and insect pathogens. One of both proteins, termed **freestanding DUF2156 (fDUF2156)** is composed of a regular DUF2156 domain (dupli-GNAT-$\alpha^{(+)}$) fused to an N-terminal extension of variable size for which no homology to other proteins was predicted. The second protein is composed of an aspartyl-tRNA synthetase (AspRS) paralog fused at its C-terminus to the DUF2156 domain. This predicted fusion protein was termed **AspRS-DUF2156**. The presence of the AspRS domain, that contained all sequence features of functional AspRSs, strongly advocated for a role of the appended DUF2156 in a aa-tRNA-dependent process, making the enzyme a probable ATT involved in the aminoacylation of an unknown acceptor molecule. In both cases (fDUF2156 and AspRS-DUF2156), sequence homology with bacterial DUF2156 domains of MprFs suggested that these fungal proteins might be lipid modification enzymes.

When taking a closer look to the phylogenomic distribution of fungal DUF2156 proteins, F. Fischer evidenced that both types of fungal DUF2156 proteins co-occur only in ascomycota, while basidiomycota generally encode only the AspRS-DUF2156 form. Species encoding only the fDUF2156 version are very rare. Intriguingly, **no DUF2156 proteins were detected in Taphrinomycotina and Saccharomycotina**, including *Saccharomyces cervisiae* (*Sce*) and *Candida* spp. Fungal DUF2156 proteins therefore seemed to be restricted to **Pezizomycotina**, that comprise **filamentous fungi**. However, one notable exception is found in *Y. lipolytica* (*Yli*) since this yeast species that belongs to Saccharomycetes encodes the fDUF2156 protein. Previously, a bioinformatic study, that aimed to detect unique and novel domains in aaRS from human fungal pathogens detected the AspRS-DUF2156 proteins in one species (*A. niger*) (Datt and Sharma 2014) and during their phylogenetic study AM. Smith and colleagues detected freestanding DUF2156

proteins in three fungal species: *Metarhizium acridum* (pathogen specific to grasshoppers), *Nectria haematococca* (human and plants pathogen) and *Fusarium oxysporum* (plant pathogen) (Smith *et al.,* 2015). However, none of these studies aimed to characterize or even postulated the activity of fungal DUF2156 proteins, making **fungal DUF2156 proteins functionally uncharacterized.**

F. Fischer further investigated fungal DUF2156 proteins and combining sequence alignments, phylogeny, and structure predictions showed that DUF2156 domains from filamentous fungi are phylogenetically and structurally related to bacterial MprF homologs (i. e. aaLSs). F. Fischer was therefore convinced that fungal DUF2156 proteins might be implicated in remodeling of membranous lipids and proposed Pr. H. Becker's team to start the "fungal DUF2156 project", for which I was recruited. In order to study those proteins, we chose *A. fumigatus* (*Afm*) because 1) both proteins, AspRS-DUF2156 and fDUF2156, are encoded in its genome, and 2) this filamentous fungus is an important opportunistic human pathogen that causes several diseases in immunocompromised but also in immunocompetent patients and, more importantly, for which genetic tools do exist (Latge and Chamilos 2019). Our lab had expertise in yeast (*S. cerevisiae*) genetics, so part of my project was to characterize fungal DUF2156 proteins using the heterologous yeast model before we could use *A. fumigatus* and other filamentous models.

I. Biological questions and working hypotheses

When I entered the laboratory, my objectives were to functionally characterize AspRS-DUF2156 and fDUF2156 proteins; the project was therefore to determine whether they were regular ATTs and, of course, what aa-tRNAs and acceptor substrates they used. To this aim, I addressed the following questions.

I.1. Does the fungal AspRS-DUF2156 has an aspartyl-tRNA synthetase activity?

Because AspRS-DUF2156 proteins possess an AspRS domain and a DUF2156/ATT-like domain, the most parsimonious hypothesis was that the AspRS domain could synthesize Asp-

tRNA^{Asp} from Asp, ATP and tRNA^{Asp} — like a regular AspRS — and that the appended DUF2156 domain would use this Asp-tRNA^{Asp} to transfer the Asp moiety onto an acceptor molecule. This contrasted with the fDUF2156 version, for which no sequence motif or protein domain could be used to infer the aa-tRNA substrate. We therefore chose the AspRS-DUF2156 version at first. Importantly, all filamentous fungi encoding AspRS-DUF2156 also encode a cytoplasmic "freestanding" (canonical) AspRS, assumed to provide Asp-tRNA^{Asp} for protein biosynthesis. This observation supported the hypothesis that AspRS-DUF2156 might participate in non-canonical functions, like other aaRS paralogs (Guo and Schimmel 2013; Yakobov *et al.,* 2018). Sequence and phylogenetic analyses suggested that the AspRS domain of AspRS-DUF2156 is a paralog of the cytoplasmic AspRS from eukaryotes, which possesses all structural (catalytic core, anticodon-binding domain) and sequence (3 class II aaRS motifs, a QSPQ aa motif within the active site) features typical of functional AspRSs (Yakobov *et al.,* 2020). This strongly suggested that the AspRS domain was indeed a *bona fide* AspRS. Thus, the first step was to determine if the AspRS moiety of AspRS-DUF2156 achieves Asp-tRNA^{Asp} synthesis before trying to determine the Asp-acceptor substrate. Taken together our working hypothesis was that the AspRS domain of AspRS-DUF2156 aspartylates its cognate tRNA^{Asp} and channels the resulting Asp-tRNA^{Asp} to the DUF2156 domain, which then transfers Asp onto an unknown lipid. For fDUF2156, the sory was more complex since even though the general lipid modification pathway remains the same, both substrates (i. e. the aa-tRNA and the lipid) remained to be determined, because no appended aaRS domain or sequence motifs predicting its activity could be found.

I.2. Do fungal DUF2156 proteins really modify membrane lipids?

Answering this question was even more challenging due to the fact that DUF2156 domains are present in ATTs targeting a variety of acceptor substrates, including, in the case of MprFs, lipids. In fact, DUF2156 domains share very low sequence conservation and often have very different acceptor substrates (Favrot *et al.,* 2016; Moutiez *et al.,* 2017; Hemmerle *et al.,* 2020). VlmA, which is a bacterial ATT found in *Streptomyces* spp., for example, is phylogenetically close to MprFs (Smith *et al.,* 2015), uses an aa-tRNA, but transfers the aa moiety onto a small metabolite (hydroxylamine), a substrate that strongly differs from glycerolipids (Hemmerle *et al.,* 2020). Therefore, it was not possible to predict with certainty and without experimental procedures that

fungal DUF2156 proteins are implicated in the modification of lipids rather than of another macromolecules or small molecules, especially given that fungi are known to produce a vast variety of secondary metabolites, including amino acids-derived molecules (Macheleidt *et al.*, 2016). However, structure predictions using the Phyre2 software (Kelley *et al.*, 2015) showed that the closest homologs are AlaPGS from *P. aeruginosa*, LysPGS from *B. licheniformis* (as also evidenced by phylogenetic analyses performed by F. Fischer) and FemX from *W. viridescens*. Therefore, we needed procedures and experimental setups to determine and prove that fungal DUF2156 could modify lipids. This was a substantial part of my work: building up and optimizing methods to visualize, extract and identify products of fungal DUF2156 to obtain information on their aa-tRNA and acceptor substrates, as well as enzymatic methods to confirm their activities.

I.3. What is the aa-tRNA substrate of fungal DUF2156/ATTs?

Due to its fusion to the AspRS, it was quite evident that if AspRS-DUF2156 aminoacylates a lipid it would transfer Asp from tRNA^{Asp} onto an acceptor molecule, likely a lipid. In contrast, fDUF2156 is not fused to an aaRS and therefore it was not possible to predict what aa-tRNA would be rerouted to achieve the aminoacylation of an acceptor substrate (also likely a lipid). However, using methods first developed to study AspRS-DUF2156 proteins, we investigated the activity of fDUF2156 proteins to determine the aa-tRNA and acceptor substrates of the protein in several organisms.

I.4. What is the lipid substrate of fungal DUF2156/ATTs?

As described in the general introduction of the present manuscript, all bacterial aaLSs, (*i. e.* MprF homologs) that had been characterized before this work had been shown to aminoacylate glycerolipids (PG, CL, DAG). The sequence and predicted structural features of fungal DUF2156 proteins (fDUF2156 and AspRS-DUF2156), as well as their phylogenetical relationships with MprFs, were compatible with a function in lipid aminoacylation as well, although other possibilities could not, at that time, be excluded. Therefore, it was reasonable to hypothesize that fungal DUF2156 would modify a phospholipid. However, the variety of lipid species in eukaryotes that can be aminoacylated — on a hydroxyl or possibly on an amine function — is much more important, which increased the likelihood for fungal DUF2156 proteins to recognize and modify other types of lipid

species. We therefore needed a pipeline of techniques to uncover the identity of the putative substrate lipid, as well as the amino acid moiety attached by the proteins to eventually demonstrate that fungal DUF2156 proteins are genuine ATTs that add amino acids to lipids.

I.5. How are modified lipid levels regulated?

The importance of finely regulating aaL levels was demonstrated in bacteria, in which dedicated hydrolases exist to remove the aa moiety from the lipid part. If we considered that fungal DUF2156 proteins could modify one or several lipids, the question of the aa's removal was pending. Therefore, once the enzymatic function of fungal DUF2156 was deciphered, we wondered whether dedicated hydrolases, functionally equivalent to those found in bacteria, could exist.

I.6. What is the biological function of aaLs in fungi?

In bacteria, aaLS-dependent lipid aminoacylation decreases the global negative charge of the PM, thereby promoting resistance to positively charged antimicrobials (i. e. CAMPs) and increasing immune escape and virulence in pathogens. In contrast to bacteria, the PM of eukaryotic cells is enriched in neutral lipids and contains low levels of anionic lipids. By analogy, we speculated that fungal aaLs could potentially be involved in similar processes, but also in a plethora of other pathways typical of eukaryotes, including signaling, trafficking, virulence, autophagy etc. We expected that deciphering the enzymatic function of fDUF2156 and AspRS-DUF2156, the substrates that they use (aa-tRNAs, lipids) and the product that they synthesize (aminoacylated lipids) could provide hints into their putative function, a subject that will be discussed.

II. Working strategies

At the beginning, we focused our research on the AspRS-DUF2156 and fDUF2156 proteins encoded by the human opportunistic pathogen *A. fumigatus* (*Afm)* but later during my PhD, we included additional homologs to have a more "global" view on the function of fungal DUF2156

proteins. In order to address the above listed problematics, I used during my thesis mainly two strategies.

II.1. Functional characterization of fungal DUF2156 proteins from *Afm* through heterologous expression in the yeast *Sce*.

At the very start of the project, our laboratory had no expertise with filamentous fungi and the technical support required to manipulate such organisms was also lacking. Furthermore, obtaining deletion strains in filamentous fungi and in general experimentation on filamentous fungi can rapidly become challenging and are time consuming. Because the whole fungal DUF2156 project was based on bioinformatic predications, there was an important risk to take the wrong research direction and therefore the aim was to adopt a strategy that would rapidly provide experimental evidences supporting at least partially our hypothesis. Accordingly, our laboratory has a strong background in employing the yeast *Sce* as a model organism. Yeast is a eukaryotic microorganism which has many advantages as an experimental model, including its ease of genetic manipulation in the haploid and diploid forms, its rapid growth, its similarities with several eukaryotic cells in many biological processes etc. More importantly, metabolomic pathways of lipid biosynthesis are highly conserved between *Sce* and other eukaryotic cells and even more with filamentous fungi, thereby rendering it a very advantageous model organism for studying lipid homeostasis and functions (Santos and Riezman 2012). The similarities between biosynthesis pathways of *Sce* and filamentous fungi are evidenced when using for example the KEGG pathway database and several studies investigated the lipid compositions of those species (Birch *et al.*, 1998; Ejsing *et al.*, 2009; Feofilova *et al.*, 2015). Finally, several findings related to the cell-wall of filamentous fungi were first reported in *Sce* (Levin 2011) and sequence analysis revealed highly conserved enzymes and pathways throughout fungal species (Horn *et al.*, 2012; Valiante *et al.*, 2015). The latter observation further demonstrates the high degree of similarities between the yeast and filamentous fungi. But what made from the yeast a nearly perfect model to initiate the present topic is that *1)* it contains no DUF2156 proteins, *2)* a deletion library of lipid biosynthesis enzymes is available in our laboratory and *3)* specific *Sce* strains can be used to test the ability of the AspRS-DUF2156 to complement the loss of the endogenous, cytoplasmic, and essential AspRS gene by performing plasmid shuffling experiments.

Advocated by all these reasons, the choice of the organism model in the present case was evident and during my thesis I studied AspRS-DUF2156 and fDUF2156 proteins through heterologous expression in the yeast *Sce*.

II.2.   Molecular characterization of the lipid modification pathway

This strategy was used to unwind the molecular mechanism of the lipid modification pathway. To this end I overexpressed recombinant version of fungal DUF2156 proteins in *E. coli* strains and I purified them. Adequate in vitro assays were set up and allowed us to assay both, the tRNA aminoacylation activities of AspRS-DUF2156 and the aa-tRNA transferases activities (i. e. the lipid aminoacylation activities) of both fungal DUF2156 proteins. These experiments allowed us also to determine the substrate dependencies. During my thesis I also designed and purified transcript tRNAs that are suitable for *in vitro* assays and will be important to establish the substrate specificities and the tRNA determinants required for lipid modification.

Later during my thesis, we obtained filamentous fungal strains, we equipped our laboratory to study them and we acquired the competences and the knowledges to manipulate them. Beside both strategies mentioned here, we thus also used a third major strategy, namely *in vivo* characterization using filamentous fungi encoding naturally DUF2156 proteins, but experiments belonging to this third axe were mainly performed by Dr. Frederic Fischer and Dr. Nassira Mahmoudi-Kaidi. However, I also actively participated to these approaches by cloning several cassettes that were used to construct deletion/complementation strains and by performing lipid and protein analysis.

Results & Discussions

PART I: Discovery and characterization of an Ergosteryl-3-β-O-L-Aspartate synthesis pathway involving AspRS-DUF2156 in fungi

I. Publication: RNA-dependent sterol aspartylation in fungi. Yakobov *et al.*, 2020. PNAS

Summary of the main results

Rerouting aminoacyl-tRNAs from protein synthesis to aminoacylate cell wall constituents, is a well-known process used by a wide range of bacteria. By tRNA-dependently adding amino acids to peptidoglycan or glycerolipids, bacteria change the properties of their cell surface which intensifies their resistance to antimicrobial drugs, their pathogenicity and virulence. This process is carried out by a widespread family of enzymes called MprF in bacteria and archaea. No equivalent aminoacylated lipids have been uncovered in any eukaryotic species thus far, suggesting that tRNA-dependent lipid remodelling is a process restricted to prokaryotes.

This manuscript details a discovery that constitutes a change of paradigm for researcher working on sterols' biology and more broadly on lipids but also for those working in the tRNA and aminoacyl-tRNA synthetase field. Indeed, besides the fact that we prove that eukaryotes can remodel their lipids in a tRNA-dependent manner, the use of aspartic acid (Asp) as a lipid modifier and the fact it is conjugated to a sterol (and not a glycerolipid) has, to our knowledge, never been described.

Into more details, our manuscript reports the discovery of ergosteryl-3-β-O-L-aspartate (Erg-Asp), a novel conjugated sterol that is produced by tRNA-dependent aminoacylation of ergosterol by a new type of bi-functional enzyme that we termed ergosteryl-3-β-O-L-aspartate synthase (ErdS). ErdS corresponds to a unique fusion of an aspartyl-tRNA synthetase (AspRS) – that produces Asp-tRNA^{Asp} – and of a Domain of Unknown Function 2156 (DUF2156) that transfers Asp from Asp-tRNA^{Asp} onto the 3 -OH group of ergosterol (Erg). We also uncovered that removal of the Asp modifier from Erg-Asp is catalysed by a second enzyme, ErdH that is a genuine Erg-Asp hydrolase participating in the turnover of conjugated sterol in vivo. Finally, we show that Erg-Asp remained unnoticed in most fungi, including species of biotechnological interest (*Neurospora crassa, Aspergillus oryzae*) and, importantly, human opportunistic pathogens (*Aspergillus fumigatus, Cryptococcus neoformans*).

Sterol modifications influence multiple central biological processes, in particular membrane trafficking, antimicrobial resistance and autophagy as well as pathogenicity in various fungi. Because sterols are the main target of currently used antifungals, we are convinced that our results could be of broad interest to the scientific community working on the relationships between antifungal resistance and sterol metabolism and homeostasis, especially when one considers the broad distribution of the ErdS/ErdH enzymatic system and Erg-Asp across fungi.

RNA-dependent sterol aspartylation in fungi

Nathaniel Yakobov[a,1] , Frédéric Fischer[a,1,2] , Nassira Mahmoudi[a,3], Yusuke Saga[b,3] , Christopher D. Grube[c], Hervé Roy[c], Bruno Senger[a] , Guillaume Grob[a] , Shunsuke Tatematsu[b], Daisuke Yokokawa[b], Isabelle Mouyna[d], Jean-Paul Latgé[d], Harushi Nakajima[b], Tetsuo Kushiro[b], and Hubert D. Becker[a,2]

[a]Université de Strasbourg, CNRS, Génétique Moléculaire, Génomique, Microbiologie, UMR 7156, 67084 Strasbourg Cedex, France; [b]School of Agriculture, Meiji University, Kawasaki 214-8571, Japan; [c]Burnett School of Biomedical Sciences, College of Medicine, University of Central Florida, Orlando, FL 32826; and [d]Unité des Aspergillus, Département de Mycologie, Institut Pasteur, 75724 Paris Cedex 15, France

Diverting aminoacyl-transfer RNAs (tRNAs) from protein synthesis is a well-known process used by a wide range of bacteria to aminoacylate membrane constituents. By tRNA-dependently adding amino acids to glycerolipids, bacteria change their cell surface properties, which intensifies antimicrobial drug resistance, pathogenicity, and virulence. No equivalent aminoacylated lipids have been uncovered in any eukaryotic species thus far, suggesting that tRNA-dependent lipid remodeling is a process restricted to prokaryotes. We report here the discovery of ergosteryl-3β-*O*-L-aspartate (Erg-Asp), a conjugated sterol that is produced by the tRNA-dependent addition of aspartate to the 3β-OH group of ergosterol, the major sterol found in fungal membranes. In fact, Erg-Asp exists in the majority of "higher" fungi, including species of biotechnological interest, and, more importantly, in human pathogens like *Aspergillus fumigatus*. We show that a bifunctional enzyme, ergosteryl-3β-*O*-L-aspartate synthase (ErdS), is responsible for Erg-Asp synthesis. ErdS corresponds to a unique fusion of an aspartyl-tRNA synthetase—that produces aspartyl-tRNA^Asp (Asp-tRNA^Asp)—and of a *Domain of Unknown Function 2156*, which actually transfers aspartate from Asp-tRNA^Asp onto ergosterol. We also uncovered that removal of the Asp modifier from Erg-Asp is catalyzed by a second enzyme, ErdH, that is a genuine Erg-Asp hydrolase participating in the turnover of the conjugated sterol in vivo. Phylogenomics highlights that the entire Erg-Asp synthesis/degradation pathway is conserved across "higher" fungi. Given the central roles of sterols and conjugated sterols in fungi, we propose that this tRNA-dependent ergosterol modification and homeostasis system might have broader implications in membrane remodeling, trafficking, antimicrobial resistance, or pathogenicity.

aminoacyl-tRNA | ergosterol | fungi | DUF2156 | lipid aminoacylation

Remodeling of membranes and lipid modifications are processes used by living cells to interact with and adapt to their environment. They are notably critical for host/pathogens interactions, antimicrobial resistance, and virulence in both bacteria (1, 2) and fungi (3). MprFs are bacterial virulence factors that transfer amino acids (aa) onto membrane glycerolipids in a so-called aminoacylation reaction (4). This process requires aminoacyl-transfer RNAs (aa-tRNA) that are first synthesized by aminoacyl-tRNA synthetases (aaRS) (5), prior transfer of the aa moiety onto a lipid acceptor substrate, that is, phosphatidylglycerol, cardiolipin, or diacylglycerol (4). The aminoacyl-tRNA transferase (AAT) module, that catalyzes the transfer, belongs to the DUF2156 family and recognizes both the aa-tRNA and the lipid substrates (6). Glycerolipid aminoacylation modifies the overall charge, fluidity, and permeability of bacterial membranes, which enhances antimicrobial resistance, explaining why these enzymes have been termed multiple peptides resistance factors (MprF) (4). Glycerolipid aminoacylations also affect host/pathogen interactions and have been shown to potentiate immune escape and to increase virulence of pathogens (7). In *Pseudomonas aeruginosa* (8), *Enterococcus faecium* (9), and *Agrobacterium tumefaciens* (10), extracytoplasmic esterases of the VirJ or α/β-hydrolase family participate in the homeostasis of aminoacylated lipids and hydrolyze the modifying aa from lipids.

So far, only glycerolipids have been shown to be aminoacylated and only by MprFs in prokaryotes. In the present study, we show that eukaryotes aminoacylate sterols in a tRNA-dependent modification pathway that mimics those described in bacteria. In higher fungi, we functionally characterized a novel enzyme, the ergosteryl-3β-*O*-L-aspartate synthase (ErdS), composed of a DUF2156/AAT domain fused to an aspartyl-tRNA synthetase (AspRS) paralog. We show that ErdS synthesizes ergosteryl-3β-*O*-L-aspartate (Erg-Asp), a previously undetected conjugated sterol. Moreover, most of higher fungi (Dikarya), including opportunistic human pathogens such as *Aspergillus fumigatus* (*Afm*), encode this ErdS and produce Erg-Asp, suggesting that the system is widespread in "higher" fungi. We also evidenced that these species express a dedicated Erg-Asp hydrolase (ErdH) that deacylates Erg-Asp and whose gene is almost always located in a two-gene cluster next to the *erdS* gene. In conclusion, our data unravel an evolutionary conserved sterol—aa conjugation pathway. We discuss the potential implications of this pathway in the context of lipid homeostasis and antimicrobial resistance.

Significance

Bacteria are known to add amino acids (aa) to membrane lipids to resist antimicrobials and escape immune responses. This surface lipid aminoacylation process requires diverting aminoacyl-tRNAs from protein synthesis. While widespread in bacteria, no analogous lipid remodeling system had thus far been evidenced in eukaryotes. We uncovered that most fungi tRNA-dependently add aspartate onto ergosterol (ergosteryl-3β-*O*-L-aspartate [Erg-Asp]), the major sterol found in fungal membranes. Asp addition is catalyzed by an ergosteryl-3β-*O*-L-aspartate synthase (ErdS) and its removal by a dedicated hydrolase (ErdH). This pathway is conserved across "higher" fungi, including pathogens. Given the central roles of sterols and derivatives in fungi, we propose that the Erg-Asp homeostasis system might impact membrane remodeling, trafficking, antimicrobial resistance, or pathogenicity.

Results

DUF2156 Proteins Are Present in Fungi. Although DUF2156 domains were thought to be absent or rare outside prokaryotes (11), we identified, in most higher fungi, DUF2156-containing proteins fused to the C terminus of an aaRS-like domain (Fig. 1*A* and *SI Appendix*, Fig. S1*A*), that we named ErdS for reasons that will be presented below. This protein architecture, previously detected in two fungi (12), is actually widespread across fungi, including the well-characterized *Afm*, *Aspergillus oryzae* (*Aor*), or *Neurospora crassa* (*Ncr*) (Fig. 1*A*). Firstly, sequence analyses and structure predictions of the detected DUF2156 domains suggested that they all adopt the characteristic double Gcn5-like *N*-acetyltransferase (GNAT) fold observed in bacterial MprFs (6). In fungal DUF2156 domains, the GNAT I (recognition of the acceptor substrate) and II (transferase activity) subdomains of the double GNAT fold are separated, like in bacteria, by a positively charged $\alpha^{(+)}$ helix involved (Fig. 1 *A* and *B*) in the binding of aa-tRNAs (6), suggesting that 1) they could indeed be aa-tRNA–utilizing modules and 2) they might transfer the aa moiety of aa-tRNAs onto lipids. Second, the aaRS domains contain bona fide AspRS signature sequences including the known residues (13) involved in tRNA^{Asp}, Asp, and adenosine 5′-triphosphate (ATP) binding ubiquitously found in functional AspRSs (*SI Appendix*, Fig. S1*B*). These considerations prompted us to propose the following working hypothesis: The AspRS domain of ErdS would generate Asp-tRNA^{Asp} from ATP, L-Asp, and tRNA^{Asp}, which would then be transferred to the DUF2156 module, thought to carry the AAT activity, to transfer the Asp residue onto a yet-to-be identified lipid (Fig. 1*C*).

ErdS Is Essential for the Synthesis of a Lipid in Filamentous Fungi. In order to test our hypothesis on the function of ErdSs, we deleted the corresponding *erdS* genes in two fungi (Fig. 2*A* and *SI Appendix*, Fig. S2), namely, the human opportunistic pathogen *Afm* and the species of biotechnological and industrial interest *Aor*. Both Δ*erdS* mutants grew normally on solid media (*SI Appendix*, Fig. S3), demonstrating that the genes are not essential under standard growth conditions. To visualize whether ErdSs are involved in lipid aminoacylation, we analyzed total lipids from mycelia of the wild-type (WT) and Δ*erdS* strains by thin-layer chromatography (TLC), and results revealed, in both fungi, the presence of an additional ErdS-dependent lipid (hereafter, lipid X or LX) with a distinctive brownish staining that migrates between phosphatidylethanolamine (PE) and phosphatidylcholine (PC) (Fig. 2 *B* and *C*).

To verify the ErdS dependency of LX synthesis, we constructed an *Afm* Δ*erdS*::P$_{xyl}$-*erdS* strain, in which we reintroduced the WT *erdS* gene under the control of a xylose (Xyl)-inducible promoter (P$_{xyl}$-*erdS*) at the Δ*erdS* locus (Fig. 2*A* and *SI Appendix*, Fig. S2). Under noninduced conditions (in the presence of glucose), LX was barely undetectable in the Δ*erdS*::P$_{xyl}$-*erdS* strain compared to the WT, while, under induction conditions (in the presence of Xyl), strong accumulation of LX occurred (Fig. 2*B*). In *Aor*, complementation of the Δ*erdS* mutation with the WT *erdS* copy (Fig. 2*A*) at an ectopic locus under the control of its own promoter again restored LX synthesis (Fig. 2*C*), which proved that LX synthesis is dependent on ErdS expression. Interestingly, only the full-length ErdS could sustain efficient LX synthesis in *Aor*, while an ErdS mutant in which the AspRS domain was deleted (Fig. 2*C*, Δ*erdS*+*erdS-ΔaspRS*) could not, at least not at detectable levels.

Fungal ErdS Catalyzes tRNA-Dependent Aspartylation of a Lipid. To dissect the mechanism of LX synthesis, we transferred the synthesis of LX, hypothesized to rely on the sole ErdS enzyme, to the budding yeast *Saccharomyces cerevisiae* (*Sce*), in which we overexpressed *Afm* ErdS. Switching to a heterologous yeast system was dictated for three main reasons: 1) Genetic engineering is far more time consuming in *Afm* than in *Sce*; 2) no DUF2156-containing proteins were detected in *Sce* (*SI Appendix*, Fig. S1*A*); and 3) the lipid synthesis pathways are conserved across ascomycetes (amigo.geneontology.org/amigo/term/GO:0006629), and thus the lipid contents of these species belonging to the same phylum are likely to be very similar (14). To start with and test whether the AspRS moiety was functional, *Afm* ErdS or ErdS-ΔDUF, that is an ErdS form that comprises only the AspRS domain, was expressed in the *Sce* Δ*dps1* strain (15) (*DPS1* encodes the essential AspRS), and complementation of the Δ*dps1* mutation lethality was tested by plasmid shuffling (Fig. 3*A* and *SI Appendix*, Fig. S4*A*). Results show that both ErdS and ErdS-ΔDUF functionally replaced *Sce* AspRS in vivo. This was not observed with a catalytic null mutant (ErdS$_{AAPA}$) of the AspRS domain (Fig. 3*A* and *SI Appendix*, Fig. S4*A*), in which the QSPQ signature motif (16) was mutated to AAPA. In addition, in vitro aminoacylation assays with purified recombinant *Afm* ErdS and *Sce* tRNA^{Asp} confirmed ErdS's capacity to generate Asp-tRNA^{Asp} (*SI Appendix*, Fig. S4*B*). Interestingly, full-length ErdS displays a lower complementation efficiency of the *Sce* Δ*dps1* strain compared to ErdS-ΔDUF (*SI Appendix*, Fig. S4*A*). We interpreted that, in the full-length ErdS, the DUF2156 domain likely transfers
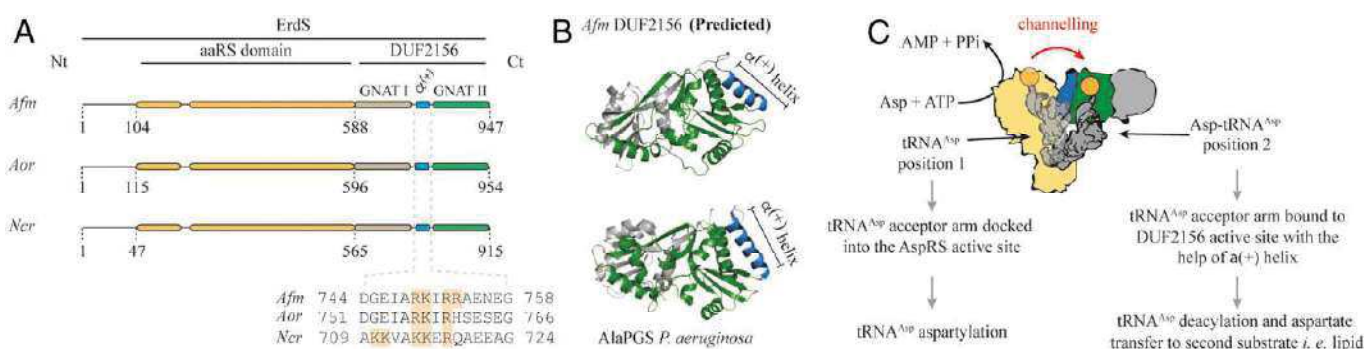
Fig. 1. Filamentous fungi AspRS-DUF2156, proteins termed ErdSs, are potential lipid aminoacylation factors. (*A*) *In silico* analyses predicted *Afm*, *Aor*, or *Ncr erdS* genes to encode proteins composed of an AspRS domain N-terminally fused to a DUF2156 domain. Protein domains were delimited by confronting data obtained from Protein Families database (PFAM) and from multiple alignments as described in *SI Appendix, Supplementary Materials and Methods*. Critical positively charged residues in the alpha helix ($\alpha^{(+)}$) separating both GNAT folds are indicated (orange). (*B*) Comparison of the DUF2156 structure of AlaPGS (alanyl-phosphatidylglycerol synthase, MprF) from *P. aeruginosa* to the Phyre2 prediction of *Afm* DUF2156. GNAT I and II subdomains are highlighted in gray and green, respectively, with the positively charged $\alpha^{(+)}$ helix in blue. (*C*) Schematic representation of the hypothetical ErdS reaction mechanism during which tRNA^{Asp} shift from the AspRS catalytic site (position 1: tRNA^{Asp} aspartylation) to the DUF2156 active site (position 2: Asp transfer from Asp-tRNA^{Asp} onto a lipid substrate). The $\alpha^{(+)}$ helix is indicated in blue, and the active site is indicated in green. Aspartate is represented in orange.

BIOCHEMISTRY
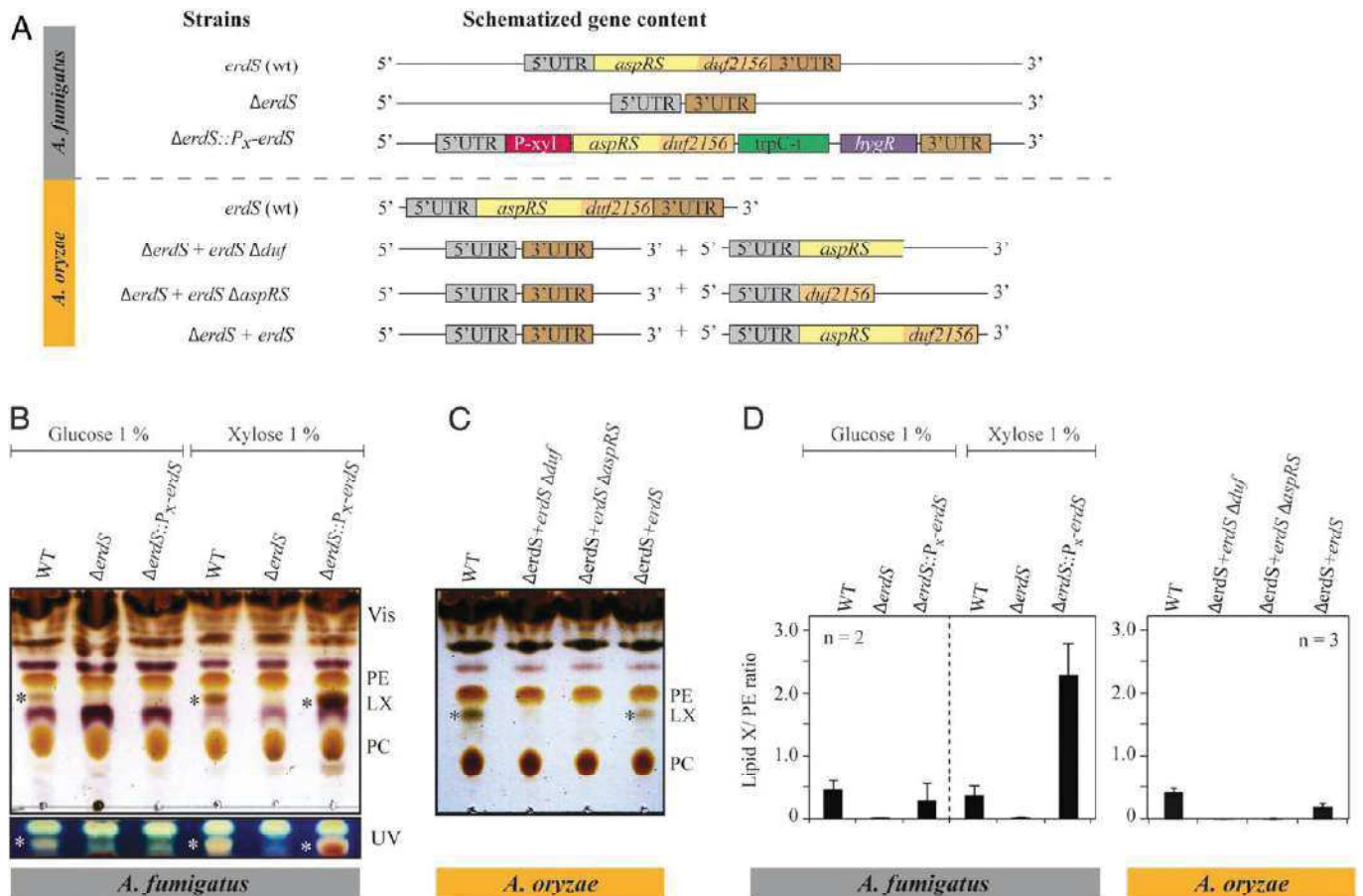
Fig. 2. Identification of an *Aspergillus* lipid species, whose synthesis requires ErdS. (*A*) Deletions of *erdS* from *Afm* and from *Aor* were performed by homologous recombination (see *SI Appendix* for details). The genotypes of the strains are indicated. For *Afm*, the *ΔerdS* strain shown corresponds to the strain after excision of the deletion cassette, whereas, for the complemented *ΔerdS::P_X-erdS* strain, the selection marker is still present. For *Aor*, the ORF of *erdS* was replaced by a *pyrG*-containing module and subsequently excised by selection on 5-FOA medium. Complementation was operated by ectopic expression of *erdS-ΔDUF*, *erdS-ΔAspRS*, or *erdS*. (*B* and *C*) Total lipids extracted from the different strains described in *A* were analyzed by TLC and stained with a sulfuric acid/MnCl$_2$ solution. TLC plates were observed either under white light or under UV light. Cultures were done in glucose or xylose containing media; * indicates the LX. (*D*) Quantification of the TLCs shown in *B* and *C*. LX signal (number of pixels) was normalized to that of PE (phosphatidylethanolamine) (LX/PE ratio). All TLCs are representative of at least two independent experiments (*n* = 2).

Asp from Asp-tRNA^{Asp} onto an accepting lipid, thereby decreasing the amount of Asp-tRNA^{Asp} available for protein synthesis and impacting growth.

To determine whether the DUF2156 module of ErdS transfers Asp from Asp-tRNA^{Asp} onto lipids in vivo, as suggested from the results obtained in *Aspergillus* spp. (Fig. 2 *B* and *C*), we analyzed the total lipid composition of a WT *Sce* strain bearing plasmids that express *Afm* or *Aor* full-length or truncated ErdSs (Fig. 3*A*). Expression of proteins was confirmed by Western blot with anti-ErdS antibodies that recognize both *Afm* and *Aor* ErdS (Fig. 3*B*), and analyses of total lipids by TLC revealed the presence of an additional brownish lipid, absent in WT *Sce* strains, when *Afm* and *Aor* ErdS were expressed. This lipid presents the same migration profile as the LX detected in *Afm* and *Aor* (*SI Appendix*, Fig. S4*C*), strongly suggesting that heterologous expression of *Afm* or *Aor* ErdS in *Sce* allows complete and correct synthesis of LX. Positive staining of LX with ninhydrin (detection of primary amine) and bromocresol green (detection of carboxyl) further suggested that it contained an aa moiety, likely L-Asp ester- or amide-linked through its α-carboxyl the lipid moiety, with free α-NH$_3^+$ and β-COO$^-$ groups (*SI Appendix*, Fig. S4*D*).

To investigate whether ErdS transfers Asp from Asp-tRNA^{Asp} onto a lipid in a DUF2156-dependent manner, we analyzed the total lipids produced by ErdS-ΔDUF, ErdS-ΔAspRS, and

ErdS$_{AAPA}$ expressed in *Sce* (Fig. 3*B*). Expression of the different constructs was confirmed by anti-ErdS Western blot (Fig. 3*B*). The ErdS-ΔDUF could not be detected, because our antibodies were raised against the DUF2156 domain; however, complementation of the lethal *Δdps1* mutation in *Sce* by ErdS-ΔDUF confirmed that the AspRS moiety was expressed and functional (*SI Appendix*, Fig. S4*A*). LX spots were quantified and normalized to those of PE (LX/PE ratio, presented in Fig. 3*B*). Of note is that, in the absence of LX, PG becomes visible at the same position in *Sce*, a reason for which the PG/PE ratio was used as a "background" signal (Fig. 3*B*, gray background). LX was not observed in *Sce* upon removal of the DUF2156 domain from ErdS (LX/PE ratio similar to the PG/PX ratio of the WT strain), and expression of the DUF2156 domain *in trans* in the *Sce*+ErdS-ΔDUF strain restored LX synthesis (Fig. 3*B*, *Sce*+ΔA+ΔD), although at lower levels, with an LX/PE ratio close to that of the PG/PE ratio of the WT strain. Only the specific brown staining of LX confirmed its low-level production. These data demonstrate that synthesis of LX is DUF2156 dependent. The reduced level of LX in the *Sce*+ErdS-ΔAspRS strain, despite proper expression of the enzyme, shows that the lipid synthesis activity of the standalone DUF2156 domain is weaker than when fused to its AspRS moiety (low LX/PE ratio), which recalls results obtained in *Aor* (Fig. 2*C*). Similarly, in the
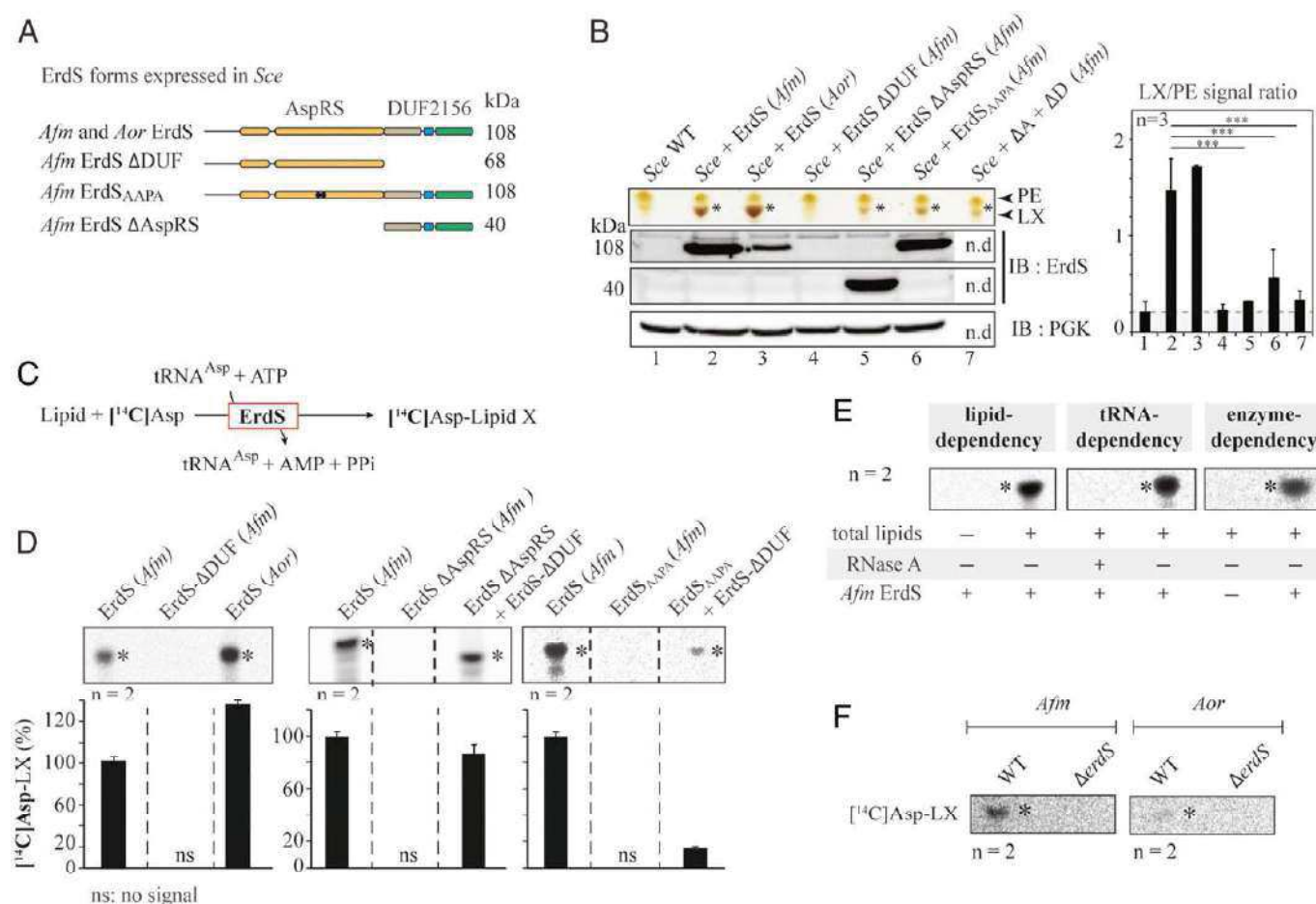
Fig. 3. Dissecting ErdS lipid modification mechanism. (*A*) Schematized modular organization of full-length ErdS (108 kDa, *Afm* and *Aor*) and of its variants (*Afm*) that were expressed in the *Sce* heterologous model. ErdS-ΔDUF: AspRS standalone domain; ErdS-ΔAspRS: DUF2156 standalone domain (40 kDa); ErdS$_{AAPA}$: catalytic null of the AspRS moiety (108 kDa). (*B*) TLC-based analysis of total lipids from *Sce* expressing ErdS variants described in *A* and *Sce* + (ΔD + ΔA) corresponds to the double expression of ErdS-ΔDUF + ErdS-ΔAspRS in *Sce*. The TLC plate stained with sulfuric acid/MnCl$_2$ was cropped to the area of interest. LX signal (number of pixels) was normalized to that of PE in each case, and the LX/PE ratio is represented in a graph (*Right*). In the absence of LX, PG (phosphatidylglycerol) becomes visible; thus the PG/LX ratio obtained was considered "background signal" (gray background). However, the brown staining of LX (yellow for PG) made it possible to visually assess the presence of LX even for low LX/PE values. The Student's *t* test was used to assess the significance of the means of the data; ***$P < 0.005$. ErdS variants expression was analyzed by Western blot with an anti-*Afm* DUF2156 polyclonal antibodies (IB:ErdS), and loading control was performed with anti-PGK antibodies (IB:PGK). (*C*) Schematized reaction of the LA assay, described in *Materials and Methods*. (*D*) LX synthesis by the purified recombinant full-length and mutant ErdSs was measured using the LA assay. When mixed, proteins were in equimolar ratios. The [^{14}C]-Asp lipid levels (percent) are provided below each TLC. (*E*) Verification of tRNA, lipid, and ErdS dependency of LX synthesis using LA assay; +: presence; −: absence. (*F*) Measurements of lipid X synthesis (ErdS activity) by WT and Δ*erdS Aspergillus* spp. crude extracts using LA assay; *: LX. The [^{14}C]Asp lipids were revealed using phosphorimaging (*D–F*). TLCs and immunoblots are representative of two to three independent experiments, and the number of replicates (*n*) is indicated.

Sce strain that expresses ErdS with a catalytically null AspRS moiety (*Sce*+ErdS$_{AAPA}$), LX levels mirrored those of the *Sce*+ErdS-ΔAspRS and *Sce*+ΔA+ΔD strains (Fig. 3*B*). These experiments show, in addition, that the DUF2156 domain of ErdS can efficiently utilize *Sce* Asp-tRNA^{Asp}, regardless of whether it was generated by the *Afm* AspRS moiety of ErdS or by the endogenous *Sce* AspRS.

To better characterize the ErdS catalytic mechanism, we developed an in vitro lipid aminoacylation assay (LA assay), using purified *Afm* or *Aor* recombinant ErdS incubated with purified *Sce* tRNA^{Asp}, ATP, and [^{14}C]-Asp in the presence of *Sce* total lipids (Fig. 3*C*). Reaction products from the LA assay were analyzed by TLC (Fig. 3 *D* and *E*). Results confirmed that *Afm* or *Aor* recombinant ErdSs catalyzed the formation of a [^{14}C]-labeled lipid (Fig. 3*D*). Adding RNase or removing lipids from the LA assay abolished synthesis of [^{14}C]-lipid, thereby proving the tRNA and lipid dependency of LX synthesis by *Afm* ErdS

(Fig. 3*E*). When the recombinant *Afm* ErdS-ΔDUF protein was used, synthesis of the [^{14}C]-lipid was abolished, proving that the reaction is, indeed, DUF2156 dependent (Fig. 3*D*). Likewise, when ErdS-ΔAspRS or ErdS$_{AAPA}$ were used in the LA assay, synthesis of the [^{14}C]-lipid was abolished (Fig. 3*D*), but fully restored upon addition of the AspRS domain of ErdS in trans. These data confirm results obtained in *Sce* but also that the DUF2156 is capable of capturing Asp-tRNA^{Asp} formed by an AspRS expressed in trans (Fig. 3*D*).

Finally, crude extracts from WT *Afm* or *Aor* mycelia also catalyzed a [^{14}C]-Asp-tRNA^{Asp}–dependent [^{14}C]-lipid synthesis in vitro, whereas crude extracts from Δ*erdS* mutant strains did not (Fig. 3*F*). However, for reasons that will be discussed below, the ErdS activity was hardly detectable in crude extracts, especially for *Aor*, when compared to recombinant ErdS.

Altogether, these results show that ErdS produces Asp-tRNA^{Asp} from ATP, L-Asp, and tRNA^{Asp} in its AspRS domain,

and that the Asp-tRNA^{Asp} product likely shifts from the AspRS active site to the DUF2156 module, that transfers the Asp acylating tRNA^{Asp} onto a lipid, which mirrors the activity of bacterial DUF2156 proteins (4).

Liquid chromatography-MS/MS Reveals that ErdS Aspartylates Ergosterol.

To identify the substrate lipid of ErdS, we fractionated total lipids from an ErdS overexpressing *Sce* strain by column chromatography and isolated LX at ~80% purity (*SI Appendix*, Fig. S5A). Fractions were submitted to mass spectrometry (MS) analyses and compared to equivalent fractions obtained from total lipids of a WT yeast strain. Strikingly, MS electrospray ionization quadrupole time-of-flight (MS-ESI-QTOF) spectra revealed two peaks, absent in WT fractions, with *m/z* of 379.3380 and 534.3565 that were submitted to a second round of MS/MS collision-induced dissociation QTOF (MS/MS-CID-QTOF) (Fig. 4A). Contrary to bacterial MprF-aminoacylated lipids, results were not compatible with LX being a glycerolipid derivative. Fragmentation pattern of the first peak was rather consistent with a dehydrated ergosterol (Erg) (*m/z* 379.3355), which was supported by the presence of characteristic additional Erg fragmentation products (Fig. 4A) (17). The

second peak gave similar fragmentation products together with that of Asp (*m/z* of 156.0265, [C$_4$H$_7$NO$_4$Na]$^+$) and of an aspartylated form of Erg (534.3547, [M~aspartyl+Na]$^+$). Results were consistent with an Erg moiety esterified with Asp on the β-OH group in position 3 of the A ring, making this species an Erg-Asp (Fig. 4B). Finally, liquid chromatography (LC)-ESI-MS/MS analyses of total lipids extracted directly from *Afm* confirmed that Erg-Asp was indeed present (*SI Appendix*, Fig. S5B). In parallel, we chemically synthesized Erg-Asp that we compared, on TLC, to Erg-Asp present in total lipids of *Afm*, *Aor*, or *Sce* expressing *Afm* ErdS and confirmed that, as expected, it shared the exact same migration properties (*SI Appendix*, Fig. S6).

To confirm that Erg is the substrate of ErdS, we performed LA assays using either [^{3}H]-Erg and cold Asp or cold Erg and [^{14}C]-Asp. Analyses of reaction products by TLC revealed that ErdS indeed produced [^{3}H]-Erg-Asp (Fig. 4C) or [^{14}C]-Erg-Asp (Fig. 4D) in a tRNA-dependent manner, and that it requires L-Asp, ATP, and tRNA^{Asp} for activity. Interestingly, in the presence of cholesterol (Cho), the animal equivalent of Erg and [^{14}C]-Asp, ErdS also produced cholesteryl-aspartate (Cho-Asp) (Fig. 4D), indicating that it likely has a relaxed specificity toward
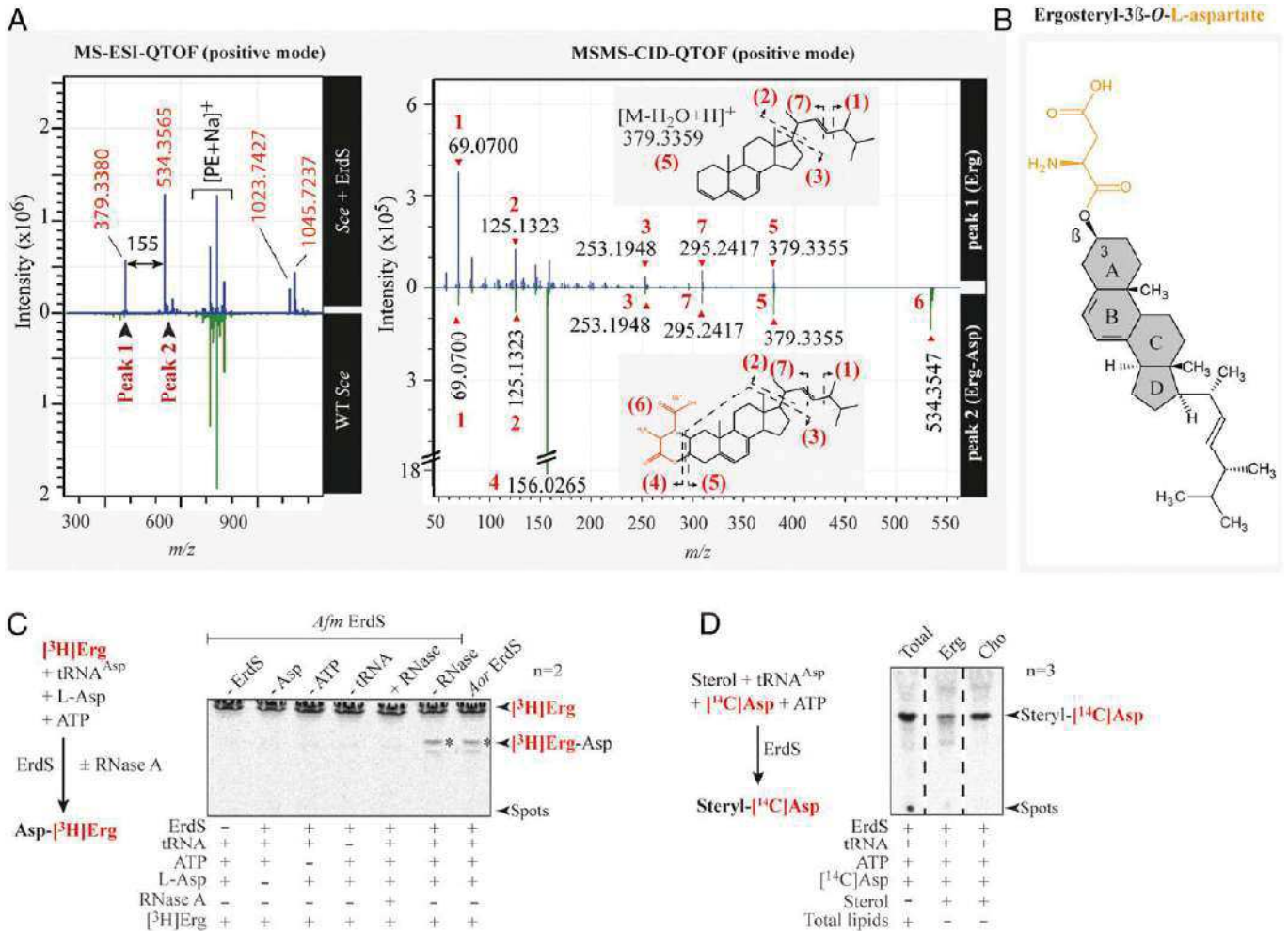
Fig. 4. Identification of the ergosteryl-3β-*O*-L-aspartate produced by ErdS in vivo and in vitro. (*A*) MS-ESI-QTOF spectrum (positive mode) of a lipid fraction containing LX extracted and purified from an *Sce* WT strain expressing *Afm* ErdS (upper spectrum, blue) or not (bottom spectrum, green). Peaks 1 and 2 have been analyzed by MS/MS collision-induced dissociation (CID) QTOF analysis in the positive mode. (*B*) Chemical structure of ergosteryl-3β-*O*-L-aspartate (Erg-Ap) corresponding to LX deduced from MS spectra shown in *A*. (*C*) The [^{3}H]Erg-Asp synthesis was measured by LA assay in the presence of purified *Afm* ErdS, pure *Sce* tRNA^{Asp}, radiolabeled [^{3}H]Erg, and cold Asp in the presence (+) or absence (−) of the enzyme or of the indicated substrates. Tests included addition (+) or not (−) of RNase A. [^{3}H]Erg-Asp is indicated with an asterisk. (*D*) Erg-[^{14}C]Asp synthesis measured by LA assay using purified *Afm* ErdS, pure *Sce* tRNA^{Asp}, radiolabeled [^{14}C] Asp, and indicated sterols. LA assay using total lipids from WT *Sce* was used as a migration control. The adapted LA assay reactions are displayed (simplified) next to the corresponding TLCs. Radiolabeled compounds are highlighted in red, and the number of independent experiments (*n*) is indicated.

its sterol substrate. Overall, our results demonstrate that ErdSs represent a novel type of bifunctional AspRS/ergosteryl-aspartate synthases that we named ergosteryl-3β-*O*-ʟ-aspartate synthases or ErdS, with "Er" standing for "ergosteryl," "d" for Asp, and "S" for synthase.

Fungi Having ErdS also Encode a Dedicated Erg-Asp Hydrolase Involved in Erg-Asp Turnover. Bacteria that possess MprFs are also equipped with dedicated hydrolases that remove aa modifiers from lipids, and whose gene usually lays next to *mprF* genes (8, 9). In *Afm*, *Aor*, and *Ncr*, we observed that the *erdS* gene (*AFUA_1g02570* in *Afm* Af293, *AO090005000838* in *Aor* RIB40, and *NCU007082* in *Ncr* OR74A) is found close to a gene encoding a protein belonging to the α/β-hydrolase family (PFAM: PF07859) (*AFUA_1g02580*, *AO090005000837*, and *NCU007081*, respectively) (Fig. 5*A*). These α/β-hydrolases all contain three conserved residues, Ser153, Asp277, and His307 (numbering of *Afm*), that are typical of the catalytic triad of esterases/lipases, a finding supported by structure predictions (Fig. 5*A*).

To determine whether these esterases were involved in the Erg-Asp metabolic pathway, we used *Ncr* because, in this fungus, despite the presence of an *erdS* gene (Fig. 5*A* and *SI Appendix*, Fig. S1*A*), we could not observe Erg-Asp in total lipids, although an ErdS activity could be detected using the LA assay in crude protein extracts (*SI Appendix*, Fig. S7). The WT, Δ*erdS*, and Δ*esterase* deletion mutants of *Ncr* were obtained from the Fungal Genetic Stock Center (FGSC) (18, 19). We compared total lipids profiles of *Ncr* WT, Δ*erdS*, and Δ*esterase* mutants by TLC (Fig. 5*B*). As stated, Erg-Asp was undetectable in the WT or Δ*erdS* strains of *Ncr* but accumulated at high levels in the Δ*esterase* strain (Fig. 5*B*), suggesting that the enzyme was most likely responsible for the absence of detectable Erg-Asp in WT *Ncr*. This esterase, seemingly involved in Erg-Asp degradation, was therefore named ErdH, for Erg-Asp hydrolase, and the Δ*esterase* strain was renamed Δ*erdH* (Fig. 5 *A* and *B*). Additionally, we monitored the Erg-[^{14}C]-Asp synthesis activity by LA assay in protein extracts from WT *Ncr*, Δ*erdS*, and Δ*erdH* strains. Our data show that, while almost undetectable under the conditions tested in the WT and Δ*erdS* strains, Erg-[^{14}C]-Asp levels were much higher (>23-fold) in the Δ*erdH* strain (Fig. 5*C*). This is again in agreement with ErdH being involved in Erg-Asp deacylation, which most likely masked the Erg-Asp synthesis activity of ErdS in the WT *Ncr* strain. Similarly, Erg-Asp synthesis was hardly monitored in vitro using total protein extracts of *Afm* and *Aor* (Fig. 3*F*), suggesting either low expression levels of ErdS or that ErdH hydrolyzed the Erg-Asp product.

In order to confirm that ErdH was indeed an Erg-Asp hydrolase, we used an in vitro Erg-Asp deacylation assay. Erg-[^{14}C]-Asp incubated for 30 min with purified recombinant *Afm* ErdH was almost entirely hydrolyzed (88 ± 2%), while, in the same reaction performed without ErdH, Erg-[^{14}C]-Asp levels remained stable (Fig. 5*D*). In addition, purified ErdH mutants of the catalytic triad (S153A, D277A, or H307A) did not hydrolyze Erg-[^{14}C]-Asp in vitro (Fig. 5*D*). All these results demonstrate the presence of two enzymes in fungi that regulate the synthesis and degradation of Erg-Asp, namely ErdS and ErdH.

An Evolutionary Conserved Synteny between *erdS* and *erdH*. ErdS and ErdH are present in *Afm*, *Aor*, and *Ncr*, with their respective genes found at the same locus and encoded as divergent expression units. In order to analyze whether ErdS and ErdH are more generally found in fungi and/or other eukaryotes, we performed bioinformatics searches (*SI Appendix*, *Supplemental Materials and Methods*). We first searched ErdS sequences among eukaryotes using the basic local alignment search tool (BLAST) with the *Afm* ErdS sequence as a probe and found 7,584 protein sequences (only those with lengths 200 to 2,000 residues), that corresponded to ErdS, standalone DUF2156 domains, canonical AspRSs, and homologous aaRSs such as asparaginyl- and lysyl-tRNA synthetases. Among them, 1,006 (13.3%) were bona fide DUF2156-containing
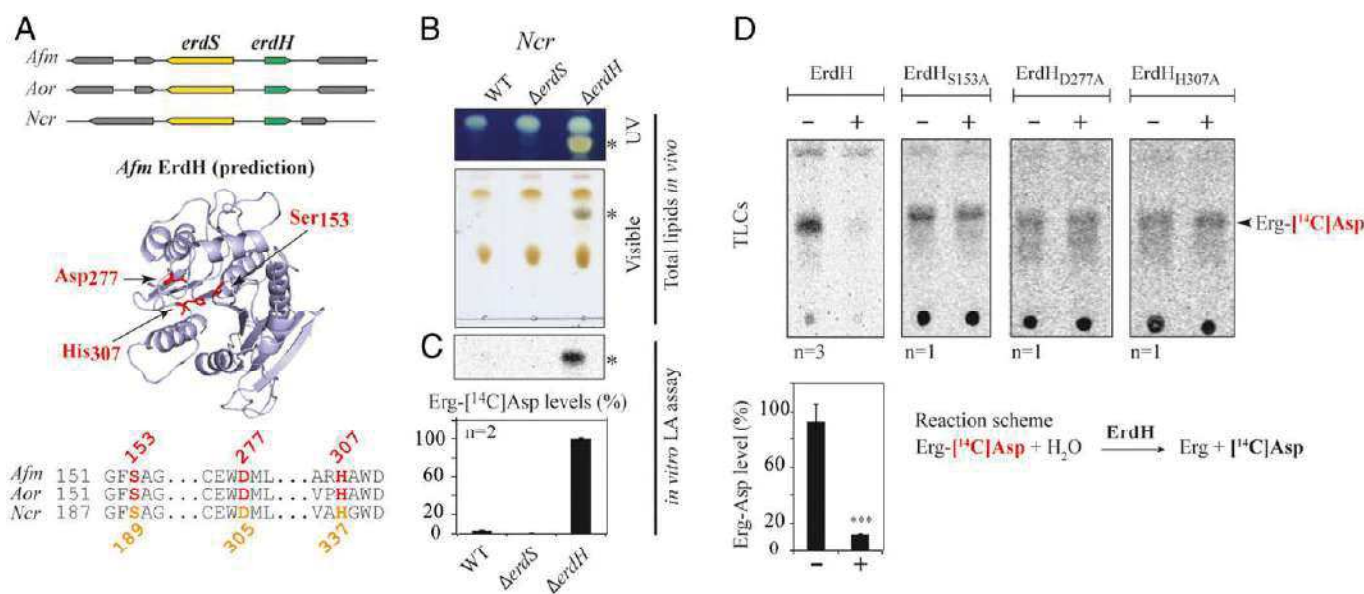
Fig. 5. Detection and characterization of ErdH in fungi carrying ErdS. (*A*) Schematic representation of the genomic context of the *erdS* (yellow) and *erdH* (for Erg-Asp hydrolase, in green) genes locus from *Afm*, *Aor*, and *Ncr* that highlights that *erdS* and *erdH* are found in a divergent orientation. Phyre2-based α/β-hydrolase–like predicted structure of *Afm* ErdH and active site alignments of *Afm*, *Aor*, and *Ncr* ErdHs. Ser-Asp-His catalytic triads of α/β-hydrolases/lipases (S153, D277, and H307 in *Afm* ErdH) are displayed and highlighted on the structure prediction and the alignment. (*B*) Total lipids from WT, Δ*erdS*, and Δ*erdH* *Ncr* strains were separated by TLC and stained with sulfuric acid/MnCl₂ and observed under UV or visible light (*n* = 3); * indicates Erg-Asp. (*C*) In vitro measurements of Erg-[^{14}C]Asp synthesis by LA assay using protein extracts from the WT, Δ*erdS*, and Δ*erdH* *Ncr* strain protein extracts, using pure *Sce* tRNA^{Asp} as a substrate (*n* = 2). (*D*) In vitro measurement of the Erg-[^{14}C]Asp hydrolase activities of purified recombinant WT (*n* = 3) or catalytic mutant *Ncr* ErdHs (*n* = 1). (*C* and *D*) The Student's *t* test was used to determine significance of the means of the data; ***P < 0.005.

proteins, with 780 (77%) being ErdS with a minimal length of ~800 aa (no N- or C-terminal extensions) and a maximal length of 1,417 aa (with long N- and/or C-terminal appendages). "Standalone" DUF2156 domains (23%) were also detected and often accounted for ErdS forms with either the AspRS or the DUF2156 domain truncated. A closer look at the phylogenomic distribution of complete ErdS (AspRS-DUF2156 fusions) highlighted that they are present only in "higher" fungi (Dikarya, both Ascomycota and Basidiomycota), and specifically among 9 out of the 13 fungal lineages analyzed (Fig. 6A), with the notable exception of Saccharomycotina (including Sce), Lecanoromycetes, and Pezizomycetes. ErdS is present in prominent human pathogens such as Afm (20), Histoplasma capsulatum, or Cryptococcus neoformans (Cne), plant pathogens such as Fusarium oxysporum, Magnaporthe oryzae, or Ustilago maydis, insect pathogens like Beauveria bassiana or Metarhizium spp., and also fungi of biotechnological interest like Aor or Ncr. We then visualized the synteny of the erdS gene in various fungi and observed that, in most of the cases, the erdH gene was almost always present next to erdS with the same divergent orientation in numerous species, showing that the linkage between the two genes is conserved. In fungi lacking erdS, the erdH genes were also absent,

as judged from the absence of proteins with significant sequence homology to ErdH (Fig. 6A). Overall, the whole ErdS/ErdH enzymatic pathway seemed conserved across "higher" fungi.

Finally, in order to confirm that Erg-Asp is synthesized in several representative ErdS/ErdH-containing fungi, we extracted and analyzed, by TLC, total lipids from a collection of 15 fungal species (13 Ascomycota and 2 Basidiomycota). As expected from the absence of an erdS gene, Erg-Asp was absent in the four tested Saccharomycotina. However, it was detected in eight Ascomycota and one Basidiomycota species tested (Fig. 6B). The only exceptions were Ncr (Ascomycota), as already explained above, and Cne (Basidiomycota), for which the erdS gene regulation and/or the activity of ErdH could also account for the absence of Erg-Asp. Taken together, our results confirm that Erg-Asp is likely widely distributed and conserved across fungi.

Discussion

A wide range of bacteria possess membrane proteins with an AAT activity, namely MprFs, that reroute aa-tRNAs from protein synthesis to cell surface remodeling, thereby intensifying antimicrobial resistance, pathogenicity, and/or virulence (4, 7,
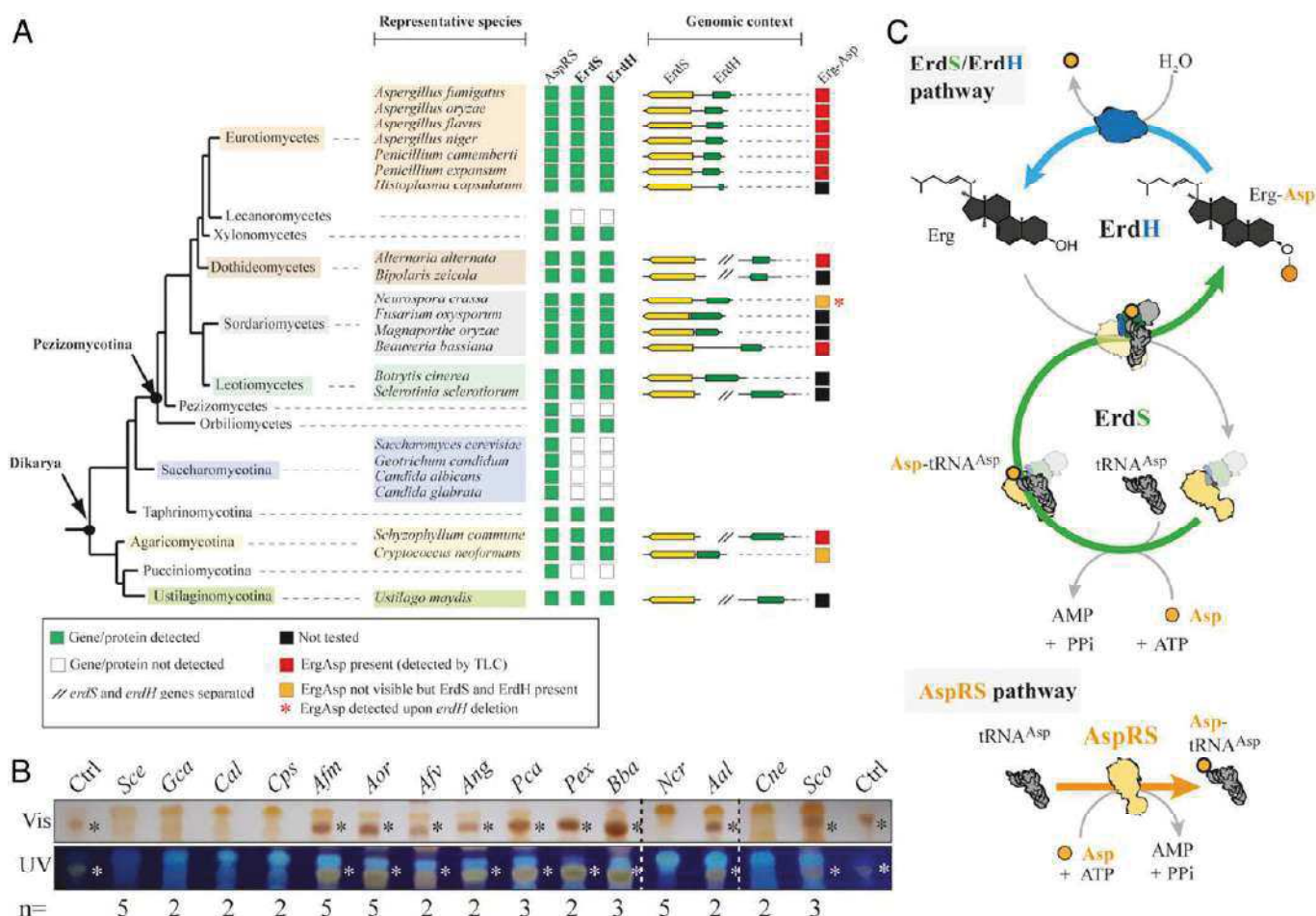
Fig. 6. The Erg-Asp lipid metabolic enzymes ErdS and ErdH are conserved across "higher" fungi. (A) The presence (green square) or absence (white squares) of a regular AspRS, ErdS (yellow), or ErdH (green) genes across fungal species is indicated, and the organization of the locus is shown; // indicates that erdS and erdH genes are interspaced. (B) TLC-based analysis of total lipids extracted from 15 species among the representative ones displayed in A. The TLC plates (number of replicates indicated for each strain) stained with sulfuric acid/MnCl$_2$ solution and observed under white (Vis) or UV light were cropped to the area of interest; * indicates Erg-Asp synthesis (red squares in A) as revealed by the detection of a dark brown band with mobility equivalent to control Erg-Asp. Gca: Geotrichum candidum; Cal: Candida albicans; Cps: Candida parapsilosis; Afv: Aspergillus flavus; Ang: Aspergillus niger; Pca: Penicillium camemberti; Pex: Penicillium expansum; Bba: Beauveria bassiana; Aal: Alternaria alternata; Sco: Schizophyllum commune. (C) A schematic model representing the turnover between Erg-Asp synthesis, and hydrolysis. The green arrow shows ErdS activities (Asp-tRNA^{Asp} production and Asp modification of Erg), and the blue arrow indicates the ErdH-dependent hydrolysis of Erg-Asp. All ErdS-containing fungi always possess a canonical AspRS to ensure Asp-tRNA^{Asp} production for protein synthesis (AspRS pathway).

11). Our work reveals that most of the fungal species found within the Dikarya subkingdom possess bifunctional enzymes, ErdS, that use ATP, L-Asp, and tRNA^{Asp} to produce Asp-tRNA^{Asp} in the AspRS domain, this latter product being used in a second step by the appended DUF2156/Asp-tRNA transferase module to transfer Asp from its tRNA^{Asp} onto the 3β-OH group of Erg, yielding a novel form of conjugated sterol, Erg-Asp (Fig. 6C). Erg-Asp synthesis constitutes a change of paradigm for three main reasons: 1) this is a tRNA-dependent lipid modification process in eukaryotes; 2) the use of Asp as a lipid modifier, that has no equivalent in bacteria, and 3) the modification of Erg (instead of glycerolipids) with an aa that had, to our knowledge, never been described, despite the widespread distribution of Erg-Asp synthesis in fungi (Fig. 6B). Moreover, we found no evidence in the literature or databases of any 3β-O-aminoacylated sterols. Erg-Asp likely escaped previous detection because, as an ester, most of alkaline extraction procedures used for sterols extraction promote its hydrolysis. Erg-Asp is therefore a novel type of sterol conjugate, specific to fungi, that is performed by ErdSs enzymes, through a tRNA-dependent process. It is worth noting that the fusion of the AspRS and the transferase (DUF2156) domain is required for full activity, since the standalone DUF2156 domain was poorly active in the Sce heterologous model (Fig. 3B) or inactive in Aor (Fig. 2C). Channeling of Asp-tRNA^{Asp} from the AspRS to the appended DUF2156 is the most plausible explanation. It would explain the better capacity of the AspRS domain alone, that releases Asp-tRNA^{Asp}, to complement the Sce Δdps1 strain over the full-length ErdS (SI Appendix, Fig. S4A), that transfers Asp-tRNA^{Asp} directly to the transferase domain for sterol aspartylation, likely without releasing it frequently. Of note is that all fungal species that encode ErdS also possess a regular cytoplasmic AspRS (Fig. 6A and SI Appendix, Fig. S1A), suggesting that the Asp-tRNA^{Asp} generated by the AspRS moiety of ErdS is probably entirely dedicated to lipid modification, thereby necessitating a second AspRS to produce the Asp-tRNA^{Asp} used for translation, as observed in all inspected fungi (Fig. 6 A and C and SI Appendix, Fig. S1A).

Characterization of ErdH, that hydrolyzes Erg-Asp in fungi, revealed that, like in bacteria, ErdS-containing fungi possess a homeostasis system that enables the tRNA-dependent aminoacylation of a lipid (ErdS) and its deacylation through hydrolysis (ErdH), suggesting that Erg-Asp levels might be tightly controlled. This provides an explanation for the apparent absence of Erg-Asp in total lipids from Ncr or Cne (Figs. 5B and 6B) under the growth conditions used. Of note is that this turnover cycle recalls that of the acyl-CoA transferase-dependent fatty acylation and lipase-dependent deacylation systems involved in sterols storage, turnover, and trafficking in eukaryotes, including fungi (21). The erdS and erdH genes tend to cluster as divergently expressed units within the same genomic locus, which resembles the cluster organization of genes with metabolically related functions found in many fungi (22). This suggests that erdS and erdH may be coregulated at the transcriptional level, likely to control the balance between Erg and Erg-Asp, a tempting hypothesis that remains to be analyzed. Erg-Asp levels could also depend on the turnover (expression and degradation) and regulation (posttranslational modifications, etc.) of ErdS and ErdH and/or on the relative subcellular localization of both enzymes. Such potential species-specific spatiotemporal regulations of Erg-Asp homeostasis could account for the different steady-state levels of Erg-Asp that we observed between the various fungal species, especially between Aspergillus spp. and Ncr. We have not been able, so far, to identify the subcellular localization of either ErdS or ErdH. Bioinformatics predictions (Wolf PSort, MitoProt II software), however, suggest that ErdH might be mitochondrial in Aspergillus spp., while ErdS is predicted to be cytoplasmic and/or nucleocytoplasmic, a fact that is not unusual for aaRSs (23). Also, no plausible membrane-spanning or membrane-anchoring helices could be predicted in ErdS or ErdH, which differs from bacterial homologs: MprFs have N-terminal membrane-spanning domains, and aminoacyl-glycerolipid hydrolases have N-terminal secretion signals to ensure correct periplasmic or extracellular localization (4). Very preliminary subcellular fractionation experiments suggest that, in Afm or in the heterologous model Sce, ErdS is not soluble but is associated with membranes, but the nature of those membranes remains unknown. Of note, in any case, is that membrane association of ErdS—to recognize Erg—requires that the enzyme be exposed to the cytoplasmic space, where its tRNA^{Asp}, Asp, and ATP substrates are present (SI Appendix, Fig. S8).

Erg is the major sterol found in fungal plasma membranes (24). Its function is analogous to that of Cho in mammals, which includes modulating permeability and fluidity of the lipid bilayer (25, 26) and regulating the activity of membrane proteins, such as G protein-coupled receptors (27) or V-ATPases (28). Erg, together with sphingolipids, regulates membrane trafficking, which is illustrated in filamentous species, such as Aspergillus spp., by a constant supply of Erg at the tip of mycelia to form lipid microdomains that are crucial to polarized cell growth (29). Erg also plays multiple roles in pathogenicity and in antifungal resistance (24, 30, 31). Incidentally, because Erg biosynthesis pathway differs from that found in humans for Cho, it is one of the main targets of current antifungal drugs (32).

Although we deciphered the function of ErdS and ErdH, the role of Erg-Asp in the biology of fungi now remains to be discovered, and this will be the focus of our future work. The viability of the ΔerdS strains of Afm, Aor, and Ncr shows that neither ErdS nor ErdH are essential under standard growth conditions. However, as discussed below, this fact does not exclude functions that could become essential or contribute to the overall fitness of fungi under challenging conditions, such as in the presence of membrane-targeting antifungals or antimicrobial peptides, which may explain the evolutionary conservation of the enzymatic system across Dikarya. As a first hypothesis, aspartylation of Erg by ErdS might play a role similar to aminoacylated glycerolipids in bacteria, regarding antimicrobial resistance (4, 7, 11, 32). Indeed, addition of L-Asp on the neutral and highly hydrophobic Erg leads to a novel zwitterionic sterol, which may significantly change Erg physicochemical properties within membranes, by influencing its phase behavior, its lateral diffusion, and/or its interaction with other lipids. Local Erg-Asp synthesis might, in turn, influence membranes' overall properties such as interface hydration, membrane proteins composition, permeability, and/or fluidity, or the activity and/or localization of membrane proteins. Therefore, Erg-Asp could participate in membrane remodeling processes that might have an impact on antifungal resistance, notably, in the case of polyenes, known to directly interact with Erg to form pores, since aspartylation of the 3β-OH could change their interactions with Erg (33), a hypothesis that we will explore. Erg-Asp levels (7 to 20% of free Erg in Aor; SI Appendix, Fig. S9) upon growth in rich medium seem incompatible with an overall surface remodeling; however, nothing is currently known on the regulation of Erg-Asp synthesis and the amount of modification that can occur under challenging conditions. As an illustration, in Sce, an Erg acetylation/deacylation cycle, that functionally resembles our ErdS/ErdH enzymatic system, involves the Atf2 acetyltransferase and the Say1 esterase. This nonessential enzymatic system protects cells from the accumulation of toxic Erg intermediates within membranes, and from the effect of membrane-disrupting agents such as the antifungal agent eugenol (34), suggesting that the ErdS/ErdH system and Erg aspartylation might be of importance in resistance when Erg biosynthesis inhibitors, such as azole derivatives, that trigger accumulation of toxic Erg intermediates, are used against fungi. This could be tested by determining the susceptibility of WT (Erg-Asp-containing), ΔerdS (Erg-Asp-deficient), ΔerdH (Erg-Asp-accumulating),

BIOCHEMISTRY

or overexpressing (Erg-Asp-overproducing) strains in the presence of azole derivatives.

While lipid modifications are usually involved in cells' surface remodeling and antimicrobial resistance in bacteria (7, 35), they also often participate in membrane trafficking and lipid-derived signaling in eukaryotes (3), like, for example, in the case of phosphoinositides or sphingolipids (36). Erg-Asp is produced at levels (7 to 20% of free Erg in *Aor*; *SI Appendix*, Fig. S9) that could be compatible with such cellular functions. Ergosteryl-3β-*O*-glucoside (Erg-Glc), another sterol conjugate, produced by Erg glycosylation, is nonessential, but known to actively participate in the regulation of autophagy in several yeasts and in *Aor* (37, 38), likely through the recruitment of protein partners on membrane structures (39). It is therefore possible that Erg aspartylation could intervene in the recruitment of protein factors on membranes (Erg-containing microdomains, etc.) and influence regulatory or trafficking pathways. Finally, bacterial esterases that remove aa modifications from glycerolipids also influence virulence in *A. tumefaciens* (10). Those observations in various bacterial lipid aminoacylation systems or fungal sterol modification pathways raise the question of the contribution of Erg aspartylation and deacylation to those processes in fungi. Given the conservation of the ErdS/ErdH enzymatic system across Dikarya, these aspects will now have to be addressed experimentally to decipher the function of Erg-Asp.

Materials and Methods

Materials, Strains, and Growth Condition. The *erdS* codon-optimized synthetic gene was purchased from the Genscript Corporation. The anti-DUF2156 polyclonal antibody production was performed by Covalab (R&D in Biotechnology). Some of the fungal strains were ordered from the Fungal Genetics Stock Center. The CEA17 Δ*akuB*KU80 strain of *Afm* (40) and the RIB40 strain of *Aor* (41) have been used as parental strain for this study. The routine growth and maintenance of *Afm* and *Aor* are described in *SI Appendix, Supplementary Materials and Methods*. The strains (bacterial and fungi) used in this study are listed in *SI Appendix*, Table S1.

Total Lipid Extraction from *Sce* and from Filamentous Fungi. Lipid extraction protocols for *Sce* and filamentous fungi were adapted from the Bligh and Dyer procedure (42). Briefly, *Sce* strains were grown in synthetic complete (SC) medium without leucine (SC-LEU) (MP Biomedicals) until optical density 600 nm (OD$_{600 nm}$) reached 1.0. An equivalent of 150 OD$_{600 nm}$ of *Sce* cells were centrifuged at 4,000 × *g* for 15 min at 4 °C. The cell pellet was resuspended in 1 mL of Na-acetate 120 mM pH 4.5. Mechanical cell disruption was performed in a FastPrep-24 apparatus (MP Biomedicals, serial no. 10020698) in the presence of 400 μL of glass beads (ø 0.25 mm to 0.5 mm, Roth) at 6 m/s, for 1 min repeated 6 times, with cooling on ice between each step; 3.75 vol of MeOH:CHCl$_3$ 2:1 (v:v) were added, and the mixture was incubated on a rotating wheel at 4 °C for 3 h. Then, 1.25 vol of CHCl$_3$ and Na-acetate 120 mM pH 4.5 were successively added and mixed by vortexing. The mixture was then centrifuged at 4,000 × *g*, 4 °C for 10 min to obtain two phases. The lower organic phase, containing the lipids, was transferred into a new tube, dried under vacuum, and stored at −20 °C until use or resuspended in 50 μL to 200 μL of MeOH:CHCl$_3$ 1:1 (vol/vol) for analysis by TLC.

For filamentous fungi, the same protocol was applied on 2 g of mycelia that were ground in a mortar with a pestle in liquid nitrogen to obtain a fine powder. Furthermore, the incubation on the rotating wheel was performed overnight at 4 °C.

Lipid X Purification. LX was purified from adaptation of the flash chromatography procedure used for bacterial aminoacylated lipids (11). Total lipids extracted from 500 OD$_{600 nm}$ of *Sce* cells were solubilized in 200 μL of chloroform and loaded on a 1.5-mL silica gel (Sigma-Aldrich, pore size 60) glass column preequilibrated with CHCl$_3$. After absorption of lipids on the column, nonpolar lipids and glycolipids were eluted with 10 mL of chloroform followed by 10 mL of acetone, respectively. To elute polar lipids, various ratios of CHCl$_3$:MeOH from 9:1 to 6:4 (vol/vol) (20 mL each) were used, and elution fractions were collected in 2-mL samples in glass tubes. Fractions were dried under vacuum, resolubilized in 35 μL of MeOH:CHCl$_3$ (1:1, vol/vol), and visualized by TLC.

TLC Analyses. Dried lipid samples were resuspended in MeOH:CHCl$_3$ (1:1, vol/vol) and spotted onto 10 × 20 cm silica gel on TLC Al foils (Sigma-Aldrich). TLC was developed with a CHCl$_3$:MeOH:H$_2$O (130:50:8 vol/vol/vol) mobile phase (10 min at room temperature [RT]), and plates were stained with either MnCl$_2$/sulphuric acid or ninhydrin or bromocresol green. MnCl$_2$/sulphuric acid, a universal staining (43), was prepared with 0.8 g of MnCl$_2$ tetrahydrate dissolved in 240 mL of 50% (vol/vol) MeOH supplemented with 9 mL of concentrated sulphuric acid. To detect primary amines (pink color), ninhydrin 0.4% (wt/vol) (Sigma-Aldrich) was used. To reveal carboxylate-containing compounds (blue color) with a pK$_a$ below 5.0 (44), bromocresol green (0.04 g) (Sigma-Aldrich) dissolved in absolute ethanol and NaOH 0.1 M was used. In the case of MnCl$_2$/sulphuric acid and ninhydrin stains, plates were heated at 100 °C until coloration developed, while direct ultraviolet (UV) (254 or 315 nm) visualization was performed with bromocresol green. Quantification of LX (Erg-Asp), PE, or PG spots was performed using the ImageJ software. Lipid spots signals (number of pixels, *N*) were normalized to that of PE (N_{LX}/N_{PE}). In the absence of LX (Erg-Asp), PG becomes visible at the same position; the PG/PE signal thus represents the background signal in the absence of LX.

MS Analyses. Analyses of total purified lipid extracts were performed on a liquid chromatograph Surveyor Plus with an autosampler and coupled with an LTQ-XL ion trapanalyzer (Thermo Finnigan). Ten microliters of filtered lipid extracts were injected on a Cogent Diamond Hydride (250 × 4.6 mm, 4 μm, Microsolv) at a temperature of 40 °C as described in ref. 45 with minor modifications. Briefly, elution was performed at a flow rate of 1 mL/min in hydrophilic interaction liquid chromatography (HILIC) conditions with a binary gradient running from 99.7:0.3 (A:B) to 75:25 in 40 min, where A was acetonitrile and B was 40 mM aqueous ammonium formate. Both solutions contained 5.5 mM formic acid. The instrument was tuned by direct infusion of cholesterol (Avanti) in positive mode. Drying gas flow rate was 20 units, and temperature of the ESI was 380 °C. Full-scan spectra were collected in the 110 to 2,000 *m/z* range, and data-dependent Zoom and MS2 spectra were acquired on the 15 most intense peaks. Data were analyzed with XcaliburQual Browser.

In Vitro LA Assay. Prior to lipid aminoacylation, the in vitro tRNA^{Asp} aspartylation was performed as described in *SI Appendix, Supplementary Materials and Methods*. Lipid or sterols aspartylation assays were adapted from lipid aminoacylation protocols used for bacterial MprFs (42). Briefly, reactions were performed in the following aminoacylation mix: Na-Hepes 100 mM pH 7.2 buffer containing KCl 30 mM, MgCl$_2$ 12 mM, ATP 10 mM, bovine serum albumin 0.1 mg/mL, pure yeast tRNA^{Asp} (10 μM) (46), [U-^{14}C]-Asp (280 cpm/pmol, Perkin-Elmer, NEC268E050UC) in a final volume of 50 μL. To test the transfer of [^{14}C]-Asp onto lipids, total lipids were added to a final concentration of 2 mg/mL, and commercial pure sterols (Erg and Cho) were added to a final concentration of 0.5 mg/mL. When [^{3}H]-Erg (10 Ci/mmol, Hartmann Analytic) was used, 20,000 cpm were added to the reaction mix. The resulting suspension was sonicated for 30 s in a sonicator bath at RT, and the enzyme (0.1 to 0.5 μg) or crude extracts of *Afm*, *Aor*, or *Ncr* (20 μg total proteins) were added to initiate the reaction before a 40-min-long incubation at 30 °C (1 h for crude extracts). To test the tRNA dependency of the reaction, 1 μg of RNase A from bovine pancreas was added 10 min before initiation of the reaction.

After incubation, reactions were stopped with addition of 500 μL of CHCl$_3$:MeOH:Na-acetate 120 mM pH 4.5 (130:50:8, vol/vol/v) and vortexing. Then, 130 μL of CHCl$_3$ and 130 μL of Na-acetate 120 mM pH 4.5 were successively added, and the mixture was vortexed and centrifuged for 1 min at 5,000 × *g* (RT). The lower organic phase was recovered and dried under vacuum. Reaction products were dissolved in a CHCl$_3$:MeOH (1:1, v:v) mixture, spotted on TLC plates, and separated with the CHCl$_3$:MeOH:H$_2$O mobile phase. TLC plates were exposed onto an imaging plate (Fuji Imaging plate) for at least 2 h. Radioactivity was detected using a Typhoon TRIO variable Mode Imager (GE Healthcare). Quantification of LX (Erg-Asp) radioactive spots was performed using the ImageJ software (number of pixels).

In Vitro Lipid Deacylation Assay. To generate Erg-[^{14}C]-Asp, we used the protocol described above for LA assay. RNase A was added and incubated for 20 min at 30 °C to hydrolyze tRNA^{Asp} and stop the tRNA-dependent aspartylation catalyzed by ErdS. Then, 0.1 μM of purified recombinant ErdH or ErdH variants were added, and the reaction mixture was incubated for 30 min at 30 °C. Lipids were extracted with the Bligh and Dyer procedure as described above, dried, resuspended in CHCl$_3$:MeOH (1:1, vol/vol), and analyzed on TLC with the CHCl$_3$:MeOH:H$_2$O (130:50:8, v:v:v) solvent, and results were analyzed by phosphorimaging as described above.

Yakobov et al.

1. O. Bohuszewicz, J. Liu, H. H. Low, Membrane remodelling in bacteria. *J. Struct. Biol.* **196**, 3–14 (2016).
2. E. M. Fozo, E. A. Rucks, The making and taking of lipids: The role of bacterial lipid synthesis and the harnessing of host lipids in bacterial pathogenesis. *Adv. Microb. Physiol.* **69**, 51–155 (2016).
3. A. Singh, M. Del Poeta, Lipid signalling in pathogenic fungi. *Cell. Microbiol.* **13**, 177–185 (2011).
4. R. N. Fields, H. Roy, Deciphering the tRNA-dependent lipid aminoacylation systems in bacteria: Novel components and structural advances. *RNA Biol.* **15**, 480–491 (2018).
5. M. Ibba, D. Soll, Aminoacyl-tRNA synthesis. *Annu. Rev. Biochem.* **69**, 617–650 (2000).
6. S. Hebecker *et al.*, Structures of two bacterial resistance factors mediating tRNA-dependent aminoacylation of phosphatidylglycerol with lysine or alanine. *Proc. Natl. Acad. Sci. U.S.A.* **112**, 10691–10696 (2015).
7. C. Slavetinsky, S. Kuhn, A. Peschel, Bacterial aminoacyl phospholipids–Biosynthesis and role in basic cellular processes and pathogenicity. *Biochim. Biophys. Acta Mol. Cell Biol. Lipids* **1862**, 1310–1318 (2017).
8. W. Arendt, M. K. Groenewold, S. Hebecker, J. S. Dickschat, J. Moser, Identification and characterization of a periplasmic aminoacyl-phosphatidylglycerol hydrolase responsible for *Pseudomonas aeruginosa* lipid homeostasis. *J. Biol. Chem.* **288**, 24717–24730 (2013).
9. A. M. Smith, J. S. Harrison, K. M. Sprague, H. Roy, A conserved hydrolase responsible for the cleavage of aminoacylphosphatidylglycerol in the membrane of *Enterococcus faecium*. *J. Biol. Chem.* **288**, 22768–22776 (2013).
10. M. K. Groenewold *et al.*, Virulence of *Agrobacterium tumefaciens* requires lipid homeostasis mediated by the lysyl-phosphatidylglycerol hydrolase AcvB. *Mol. Microbiol.* **111**, 269–286 (2019).
11. A. M. Smith *et al.*, tRNA-dependent alanylation of diacylglycerol and phosphatidylglycerol in *Corynebacterium glutamicum*. *Mol. Microbiol.* **98**, 681–693 (2015).
12. M. Datt, A. Sharma, Novel and unique domains in aminoacyl-tRNA synthetases from human fungal pathogens *Aspergillus niger*, *Candida albicans* and *Cryptococcus neoformans*. *BMC Genomics* **15**, 1069 (2014).
13. M. Ruff *et al.*, Class II aminoacyl transfer RNA synthetases: Crystal structure of yeast aspartyl-tRNA synthetase complexed with tRNA(Asp). *Science* **252**, 1682–1689 (1991).
14. L. Klug, G. Daum, Yeast lipid metabolism at a glance. *FEMS Yeast Res.* **14**, 369–388 (2014).
15. L. Ador *et al.*, Active site mapping of yeast aspartyl-tRNA synthetase by in vivo selection of enzyme mutations lethal for cell growth. *J. Mol. Biol.* **288**, 231–242 (1999).
16. J. Cavarelli *et al.*, The active site of yeast aspartyl-tRNA synthetase: Structural and functional aspects of the aminoacylation reaction. *EMBO J.* **13**, 327–337 (1994).
17. J. V. Headley, K. M. Peru, B. Verma, R. D. Robarts, Mass spectrometric determination of ergosterol in a prairie natural wetland. *J. Chromatogr. A* **958**, 149–156 (2002).
18. H. V. Colot *et al.*, A high-throughput gene knockout procedure for *Neurospora* reveals functions for multiple transcription factors. *Proc. Natl. Acad. Sci. U.S.A.* **103**, 10352–10357 (2006).
19. K. McCluskey, A. Wiest, M. Plamann, The fungal genetics Stock center: A repository for 50 years of fungal genetics research. *J. Biosci.* **35**, 119–126 (2010).
20. A. Abad *et al.*, What makes *Aspergillus fumigatus* a successful pathogen? Genes and molecules involved in invasive aspergillosis. *Rev. Iberoam. Micol.* **27**, 155–182 (2010).
21. N. Jacquier, R. Schneiter, Mechanisms of sterol uptake and transport in yeast. *J. Steroid Biochem. Mol. Biol.* **129**, 70–78 (2012).
22. H. W. Nützmann, C. Scazzocchio, A. Osbourn, Metabolic gene clusters in eukaryotes. *Annu. Rev. Genet.* **52**, 159–183 (2018).
23. S. Debard *et al.*, Nonconventional localizations of cytosolic aminoacyl-tRNA synthetases in yeast and human cells. *Methods* **113**, 91–104 (2017).
24. M. L. Rodrigues, The multifunctional fungal ergosterol. *MBio* **9**, e01755-18 (2018).
25. L. M. Douglas, J. B. Konopka, Fungal membrane organization: The eisosome concept. *Annu. Rev. Microbiol.* **68**, 377–393 (2014).
26. M. Kodedová, H. Sychrová, Changes in the sterol composition of the plasma membrane affect membrane potential, salt tolerance and the activity of multidrug resistance pumps in *Saccharomyces cerevisiae*. *PLoS One* **10**, e0139306 (2015).
27. S. Morioka *et al.*, Effect of sterol composition on the activity of the yeast G-protein-coupled receptor Ste2. *Appl. Microbiol. Biotechnol.* **97**, 4013–4020 (2013).
28. Y. Q. Zhang *et al.*, Requirement for ergosterol in V-ATPase function underlies antifungal activity of azole drugs. *PLoS Pathog.* **6**, e1000939 (2010).
29. R. Fischer, N. Zekert, N. Takeshita, Polarized growth in fungi—Interplay between the cytoskeleton, positional markers and membrane domains. *Mol. Microbiol.* **68**, 813–826 (2008).
30. L. Alcazar-Fuoli, E. Mellado, Ergosterol biosynthesis in *Aspergillus fumigatus*: Its relevance as an antifungal target and role in antifungal drug resistance. *Front. Microbiol.* **3**, 439 (2013).
31. K. Koselny *et al.*, A genome-wide screen of deletion mutants in the filamentous Saccharomyces cerevisiae background identifies ergosterol as a direct trigger of macrophage pyroptosis. *MBio* **9**, e01204-18 (2018).
32. T. K. Mazu, B. A. Bricker, H. Flores-Rozas, S. Y. Ablordeppey, The mechanistic targets of antifungal agents: An overview. *Mini Rev. Med. Chem.* **16**, 555–578 (2016).
33. D. M. Kaminski, Recent progress in the study of the interactions of amphotericin B with cholesterol and ergosterol in lipid environments. *Eur. Biophys. J.* **43**, 453–467 (2014).
34. R. Tiwari, R. Köffel, R. Schneiter, An acetylation/deacetylation cycle controls the export of sterols and steroids from S. cerevisiae. *EMBO J.* **26**, 5109–5119 (2007).
35. R. Nuri, T. Shprung, Y. Shai, Defensive remodeling: How bacterial surface properties and biofilm formation promote resistance to antimicrobial peptides. *Biochim. Biophys. Acta* **1848**, 3089–3100 (2015).
36. J. O. De Craene, D. L. Bertazzi, S. Bär, S. Friant, Phosphoinositides, major actors in membrane trafficking and lipid signaling pathways. *Int. J. Mol. Sci.* **18**, 634 (2017).
37. S. Grille, A. Zaslawski, S. Thiele, J. Plat, D. Warnecke, The functions of steryl glycosides come to those who wait: Recent advances in plants, fungi, bacteria and animals. *Prog. Lipid Res.* **49**, 262–288 (2010).
38. T. Kikuma, T. Tadokoro, J. I. Maruyama, K. Kitamoto, AoAtg26, a putative sterol glucosyltransferase, is required for autophagic degradation of peroxisomes, mitochondria, and nuclei in the filamentous fungus *Aspergillus oryzae*. *Biosci. Biotechnol. Biochem.* **81**, 384–395 (2017).
39. S. Yamashita, M. Oku, Y. Sakai, Functions of PI4P and sterol glucoside are necessary for the synthesis of a nascent membrane structure during pexophagy. *Autophagy* **3**, 35–37 (2007).
40. M. E. da Silva Ferreira *et al.*, The akuB(KU80) mutant deficient for nonhomologous end joining is a powerful tool for analyzing pathogenicity in *Aspergillus fumigatus*. *Eukaryot. Cell* **5**, 207–211 (2006).
41. M. Machida *et al.*, Genome sequencing and analysis of *Aspergillus oryzae*. *Nature* **438**, 1157–1161 (2005).
42. H. Roy, M. Ibba, Monitoring Lys-tRNA(Lys) phosphatidylglycerol transferase activity. *Methods* **44**, 164–169 (2008).
43. S. K. Goswami, C. F. Frey, Manganous chloride spray reagent for cholesterol and bile acids on thin-layer chromatograms. *J. Chromatogr. A* **53**, 389–390 (1970).
44. A. Shokrollahi, F. Firoozbakht, Determination of the acidity constants of neutral red and bromocresol green by solution scanometric method and comparison with spectrophotometric results. *Beni. Suef Univ. J. Basic Appl. Sci.* **5**, 13–20 (2016).
45. E. Cífková, R. Hájek, M. Lísa, M. Holčapek, Hydrophilic interaction liquid chromatography-mass spectrometry of (lyso)phosphatidic acids, (lyso)phosphatidylserines and other lipid classes. *J. Chromatogr. A* **1439**, 65–73 (2016).
46. G. Keith, G. Gangloff, G. Dirheimer, Isolement des tRNATyr et tRNAAsp de levure de bière hautement purifiés. *Biochimie* **53**, 123–125 (1971).

BIOCHEMISTRY

Supplemental Figures
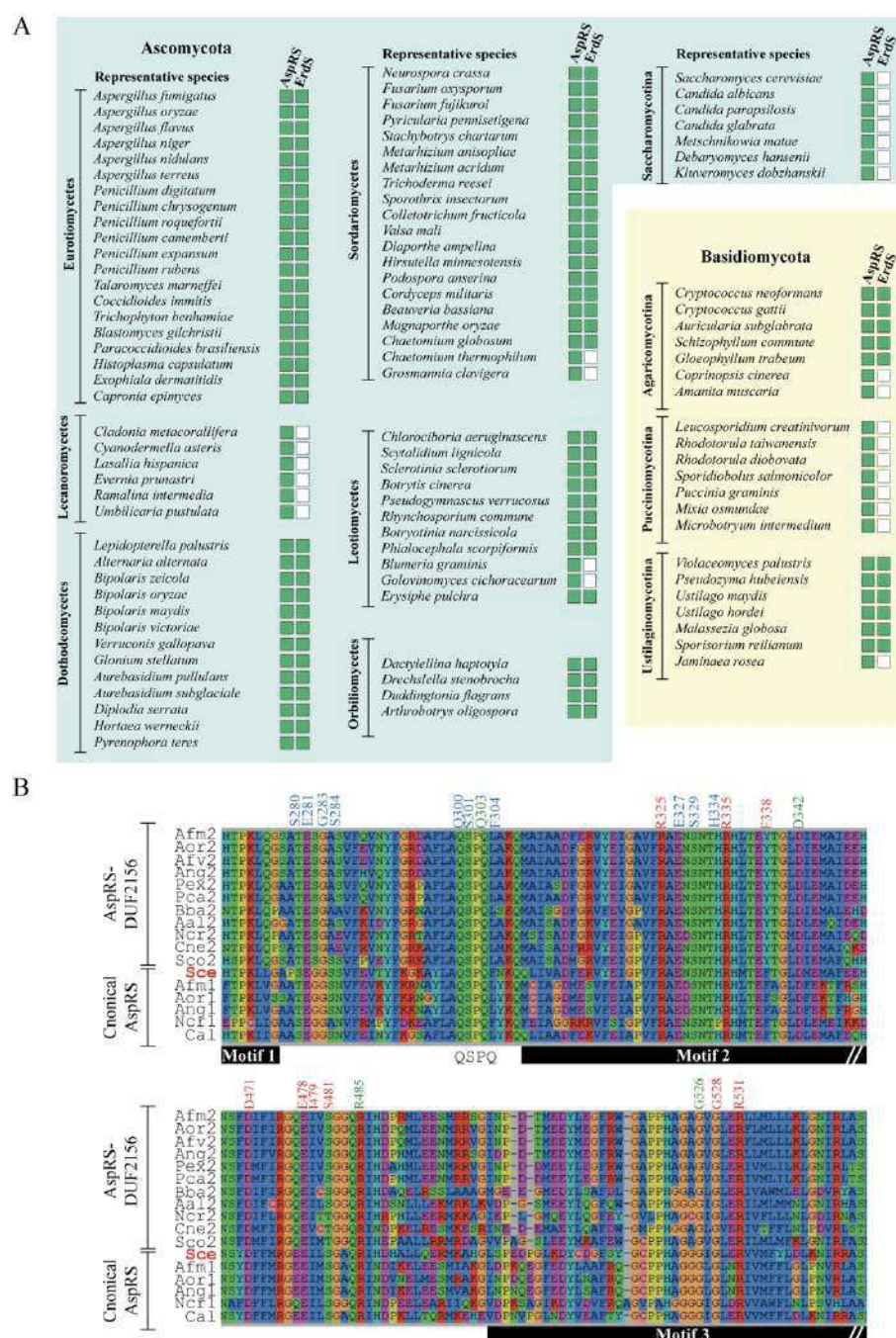
Figure S1: (**A**) Distribution in representative species of each class of Dikarya of the presence (green box) or absence (white box) of a canonical AspRS and ErdS. (**B**) Conservation of the consensus class II aaRS motifs 1, 2 and 3 in the alignment of 11 ErdS (AspRS-DUF2156) and 6 canonical AspRSs. *Afm: Aspergillus fumigatus, Aor: Aspergillus oryzae, Afv: Aspergillus flavus, Ang: Aspergillus niger, Pex: Penicillium expansum, Pca: Penicillium camemberti, Bba:*

Beauveria bassiana, Aal: Alternaria alternata, Ncr: Neurospora crassa, Cne: Cryptococcus neoformans, Sco: Schizophyllum commune, Sce: Saccharomyces cerevisiae, Cal: Candida albicans. Numberings are indicated relative to the *Sce* AspRS sequence. Residues involved in the recognition of ATP, and aspartate are indicated in red and green respectively, whereas residues responsible for the tRNA$^{\text{Asp}}$acceptor arm recognition through its 3'-CCA are indicated in blue.
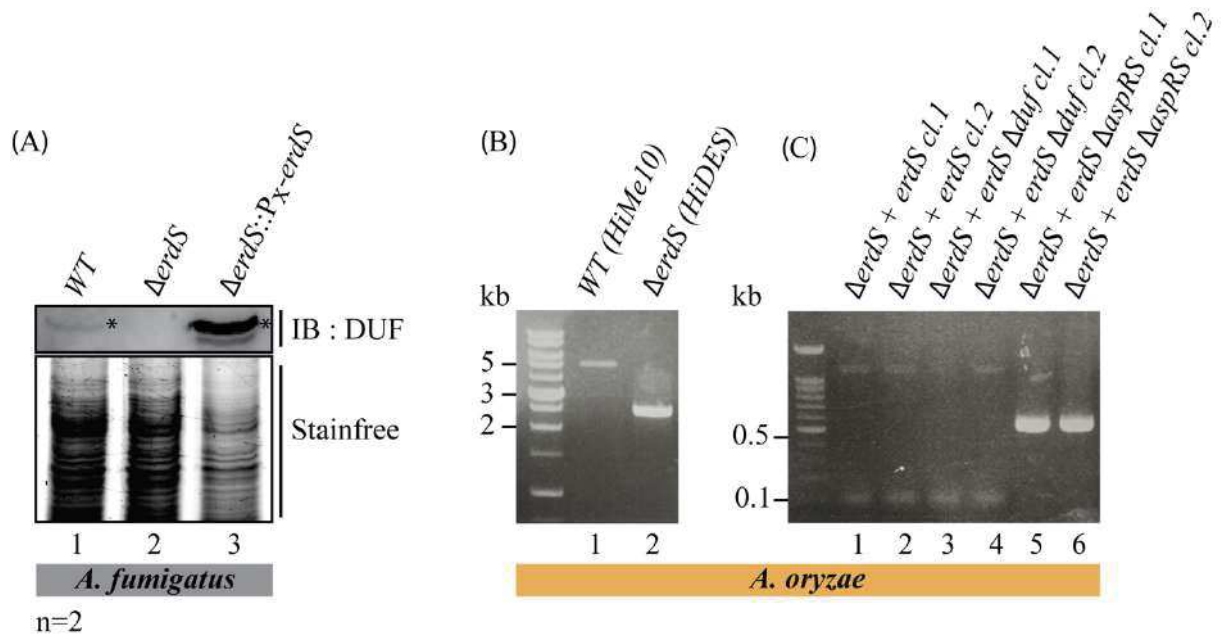
Figure S2: (**A**) Confirmation of *erdS* deletion in Δ*erdS* (lane 2) and complementation in Δ*erdS::*P$_X$-*erdS* (lane 3) extracts using immunodetection of ErdS with anti-ErdS polyclonal antibodies (WT as a control) (n=2). Stainfree: loading control. The uncropped Western Blot is shown in **Figure S8**. (**B**) Confirmation of the presence of *erdS* in *Aor* HiMe10 (lane 1) and *erdS* deletion in *Aor* HiDES (lane 2) by PCR amplification. (**C**) PCR confirmation of Δ*erdS* complemented with *erdS* (lanes 1 and 2), *erdSΔduf* (lanes 3 and 4) or *erdSΔaspRS* (lanes 5 and 6) in *Aor* HiDES. Molecular weight markers are indicated in kb. Primers used for construction verification are listed in **Table S1 and S2**.
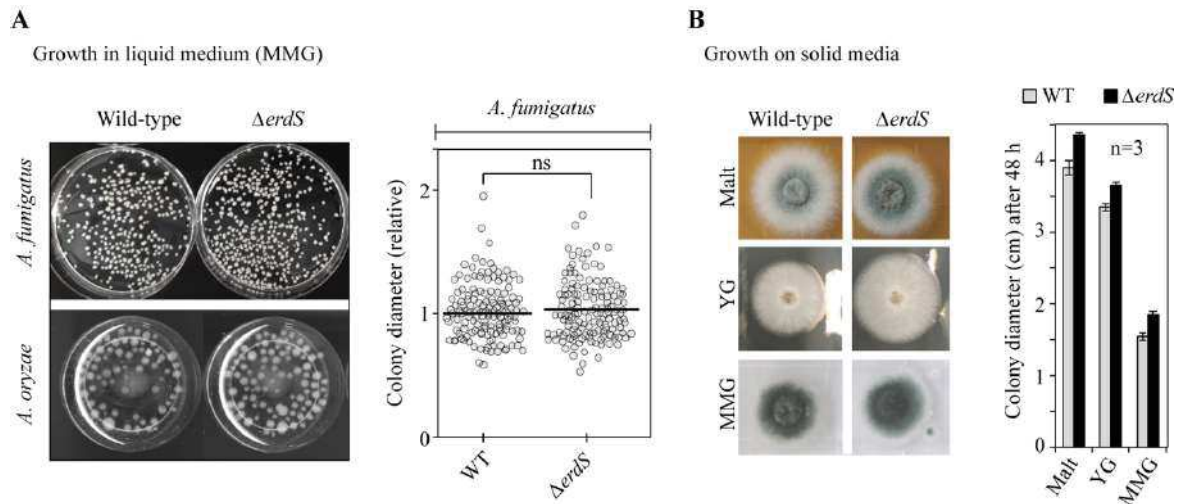
Figure S3: The *erdS* gene is not essential and its deletion does not affect growth or colony morphology. **(A)** *A. fumigatus* and *A. oryzae* WT and Δ*erdS* strains were grown in liquid media under agitation (200 rpm) at 37°C and the resulting spherical colonies (pellets) obtained after 24 hrs were photographed (left panel). In the case of *Afm*, 140 colonies (pellets) of the WT and Δ*erdS* strains were measured (pixel area of individual pellets) and each represented in a dot plot. The geometric mean of pellets' sizes of the WT strain was normalized to 1. No significant (ns, t-test) differences were detected between both strains, indicating the absence of growth defects in the Δ*erdS* strain. **(B)** Growth was also analyzed on solid agar plates containing 3 different media: Malt extract, YG (Yeast extract 0.5 % (w/v), Glucose 2 %) and MMG (*Aspergillus* minimal medium with 1 % glucose). Six μL of a freshly prepared 10^6 conidia/mL suspension were spotted on plates and growth monitored (37 °C) up to 4 days. Results after 48 hours of growth are represented. Colony diameters of mycelia were monitored. No significant difference between the WT and Δ*erdS* strains was detected, indicating that mycelia expansion is not significantly altered upon deletion of the *erdS* gene in *Afm*.
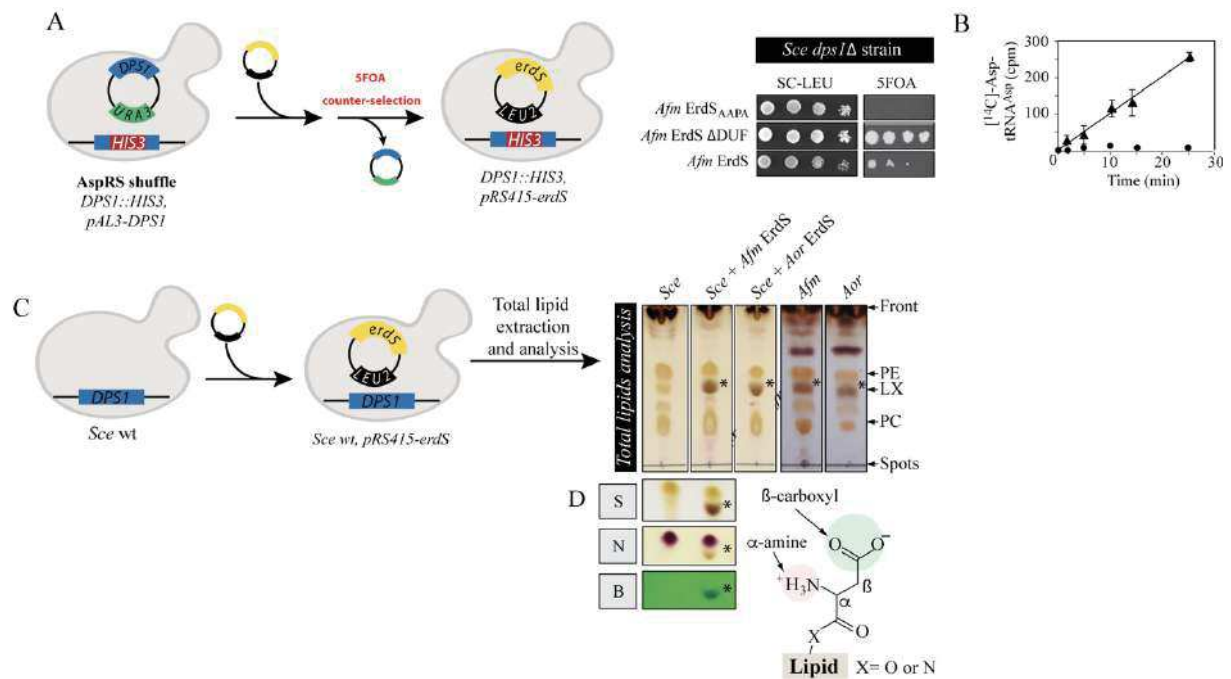
Figure S4:(A) Plasmid shuffling experiments in the Δ*dps1 Sce* strain. Drop tests were performed on SC-LEU and 5FOA media with Δdps1 strains carrying plasmids expressing the indicated *Afm* ErdS isoform: ErdS$_{AAPA}$ corresponds to ErdS mutated in the QSPQ motif of the AspRS domain, ErdS ΔDUF corresponds to ErdS with the DUF2156 domain deleted and ErdS corresponds to the full-length protein version. (**B**) *In vitro* tRNA^{Asp} aminoacylation assay performed with purified recombinant *Afm* ErdS (triangles) in the presence of pure *Sce* tRNA^{Asp}, ATP, and [^{14}C]-Asp. Circles: control without enzyme. (**C**) Total lipids were extracted from the 3 indicated *Sce* strains and from *Afm* and *Aor*, separated by TLC in the CHCl$_3$: MeOH: H$_2$O (130:50:8 v/v/v) solvent and stained with a MnCl$_2$/sulfuric acid treatment. The novel ErdS-dependent lipid (lipid X (LX), marked with *), also present naturally in *Afm* and *Aor* was detected. PE: phosphatidylethanolamine, PC: phosphatidylcholine. (**D**) An Asp residue is likely linked to any lipid via an ester (α-COO$^-$) or amide (N-containing) bond and have free α-NH$_3^+$ and β-COO$^-$ groups. TLCs of total lipids extracted from *Sce* strain expressing *Afm* ErdS were stained with MnCl$_2$/sulfuric acid (S), ninhydrin (N) or bromocresol green (B) dyes and supported that lipid X contained an amine and carboxyl groups.
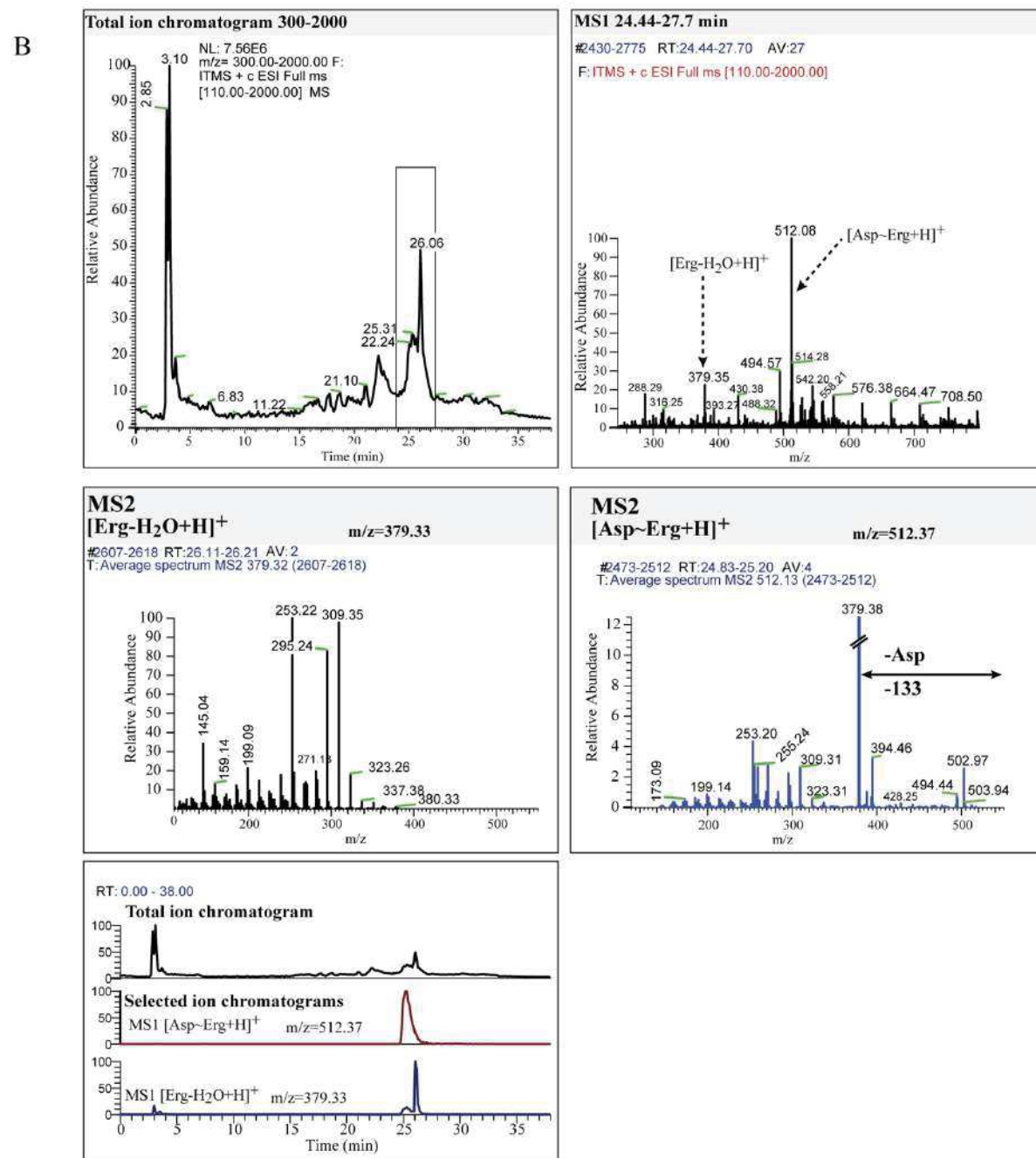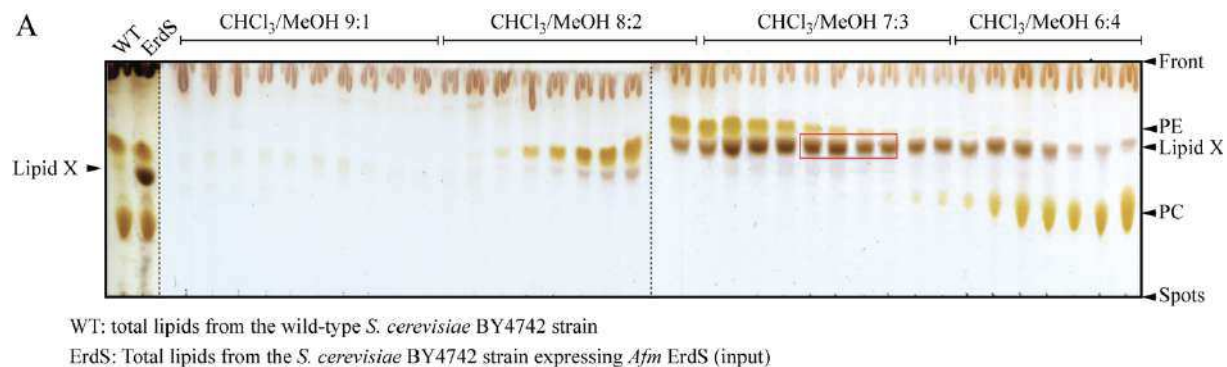
Figure S5: Purification of Erg-Asp from *Sce* and detection of Erg-Asp in total lipids from *Afm*.

(**A**) Erg-Asp was purified from *Sce* expressing the *Afm* ErdS protein. Total lipids were loaded

on a silica gel 60 glass column, washed with CHCl$_3$, followed by acetone, and polar lipids were eluted using CHCl$_3$/MeOH mixture varying from 9/1 to 6/4 ratio. Fractions enriched in Erg-Asp were collected, pooled, and analyzed by MS/MS. Total lipids from a WT *Sce* strain that does not produce Erg-Asp were treated equally, and fractions corresponding to the elution peak of Erg-Asp were collected, pooled and used as a negative control for MS/MS (see **Fig. 4**). (**B**) In parallel, total lipids from *Afm* were extracted and directly analyzed. The figure shows the LC-ESI-MS/MS analysis of total lipid extract from *Afm*. 10 µL of total lipids from *Afm* were analyzed with a liquid chromatograph Surveyor Plus coupled with a LTQ-XL ion trap analyzer (Thermo Finnigan). The column was a Cogent Diamond Hydride (250×4.6 mm, 4 µm, Microsolv, Eatontown, NJ, USA) ran in hydrophilic interaction chromatography (HILIC) conditions. Mass spectrometer was run in positive mode, and MS/MS spectra were acquired for the 15 most intense peaks. Erg-Asp and Erg were identified with their MSMS spectra. Selected ion chromatograms show that these lipids had a retention time of 24.1 and 26.1 min, respectively.

A

4-tBu-*N*-(Boc)-L-Asp   Ergosterol   Ergosteryl-3ß-*O*-(4-tBu-*N*-(Boc))-L-Asp   Ergosteryl-3ß-*O*-L-Asp

DCC / DMAP → TMSOTf / Et₃N

B

position	¹H(ppm)	¹³C(ppm)	position	¹H(ppm)	¹³C(ppm)
1		38,240	17		57,047
2		29,436	18	0.668, s	12,511
3		76,965	19	0.981, s	16,506
4		41,807	20		40,287
5		139,166	21	1.057, d	21,652
6	5.573, m	119,660	22	5.228, m	133,256
7	5.396, m	117,531	23	5.228, m	136,980
8		142,791	24		44,347
9		47,397	25		30,735
10		37,253	26	0.868, d	20,082
11		22,071	27	0.847, d	20,468
12		38,922	28	0.944, d	18,207
13		43,936	1'		172,663
14		55,691	2'	4.307, m	50,603
15		24,019	3'		34,368
16		28,844	4'		168,89

D

* Erg-Asp

Solvent system:
CHCl₃:MeOH:H₂O (130/50/8)

C

Figure S6: Chemical synthesis of Erg-Asp. (**A**) Two-step synthesis scheme of Erg-Asp (Ergosteryl-3β-*O*-L-aspartate) from Erg and 4-tBu-*N*-(Boc)-L-Asp. (**B**, **C**) NMR chemical shift assignments of synthetic Erg-Asp (synErg-Asp) and [¹³C] NMR spectrum of synthetic ergosteryl-3β-*O*-L-aspartate. (**D**) Comparison of synErg-Asp (lane 4) with Erg-Asp extracted from a *Sce* strain expressing *Afm*ErdS (lane 1), from *Afm* and *Aor* (lanes 2, 3).
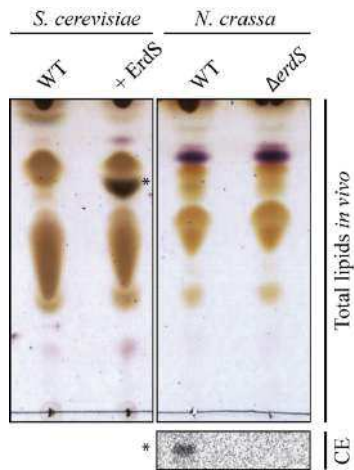
Figure S7: Total lipids from WT and Δ*erdS* strains of *Ncr* were extracted and separated by TLC with the CHCl₃(n=2): MeOH: H₂O (130:50:8 v/v/v) solvent and stained with a MnCl₂/sulfuric acid treatment. Control Sce strains that express (+) or not (WT)ErdS were used as controls. Erg-Asp is marked with *. The expression of ErdS was tested in crude protein extracts (CE) from the WT and Δ*erdS* strains of *Ncr* using the LA assay with [¹⁴C]-Asp to monitor Erg-[¹⁴C]Asp synthesis (n=2). To obtain a clear visualization of the Erg-[¹⁴C]Asp band, after reaction and separation in TLC, at least 8 hrs of exposure (phosphorimaging) were required, which suggested that ErdS was weakly expressed or that a putative Erg-Asp hydrolase was expressed and masked ErdS activity by cleaving the Erg-[¹⁴C]Asp product.
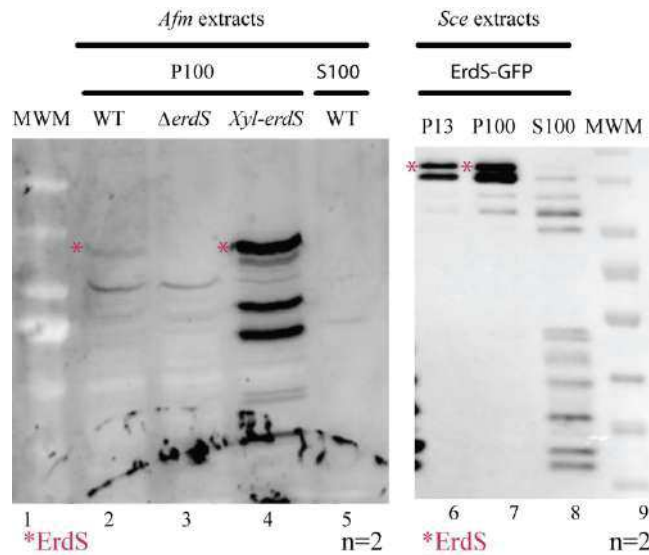
Figure S8: *Afm* ErdS colocalizes with membrane fractions. Western blot using anti-ErdS antibodies (1/1000 dilution) after 12 % SDS-PAGE (n=2). Lanes 1 &9: molecular weight marker; lanes 2 and 5: P100 andS100 fractions of the *Afm* WT strain extract; lane 3: P100 fraction of the *Afm* Δ*erdS* strain extract; lane 4: P100 fraction of an extract of the *Afm* Δ*erdS* strain complemented with the *erdS* gene under the dependence of a xylose promoter (overexpresses ErdS in the presence of xylose); lanes 6-8: P13, P100 andS100 fractions of an extract of the *Sce* strain overexpressing *Afm* ErdS. Note that lanes 2-4 represent the uncropped Western blot shown in Figure S2.
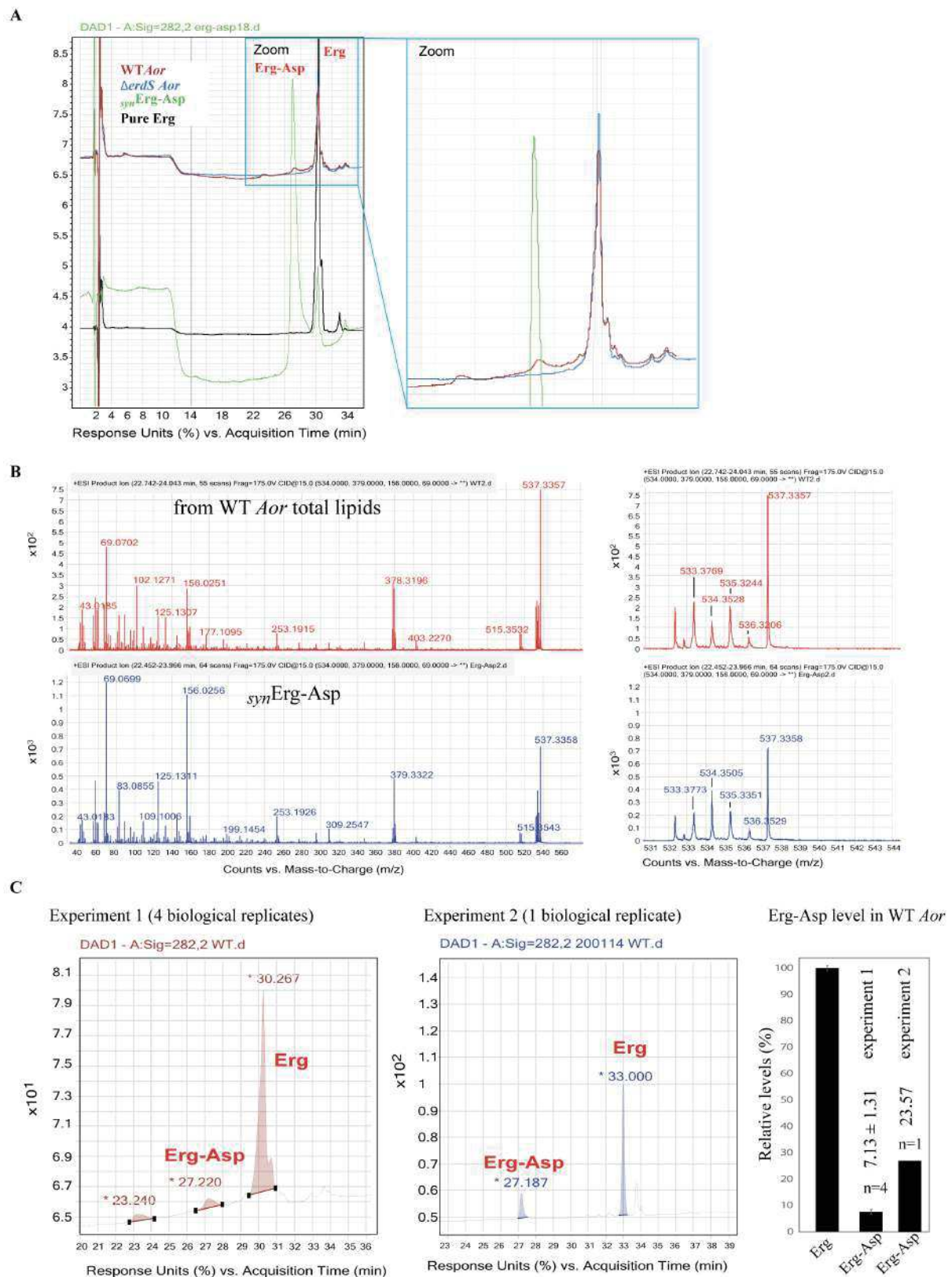
Figure S9:Detection and quantification of Erg-Asp in *Aor*.(A) Lipids extracted from *Aor* were fractionated on a TSKgel ODS80$_{TM}$ QA (C18) (2.0×150 mm, 5mm) column using a continuous gradient from 100 % MeOH:H$_2$O (4:1, v:v) (solvent A) to 100 % MeOH:CH$_2$Cl$_2$ (3:1, v:v)(solvent B) between 5 and 34 min at a flow rate of 0.2 mL/min at 25°C. Eluted compounds were monitored at 282 nm and

peaks of interest were submitted to an Accurate-Mass Q-TOF LC/MS (Agilent Technologies 6520) to confirm their identity **(B)** (upper spectrum: total lipids from WT *Aor* and bottom spectrum: $_{syn}$Erg-Asp). Lipids from a WT *Aor* strain (Erg and Erg-Asp present) and from a Δ*erdS* strain (no Erg-Asp) were analyzed and compared to the elution profile of pure Erg or of our synthetic (chemically synthesized) $_{syn}$Erg-Asp, as a reference (**A** and **B**).**(C)** Lipids from a WT *Aor* strain, having both Erg and Erg-Asp, were analyzed on a TSKgel ODS80$_{TM}$ QA (C18) (2.0×150 mm, 5mm) column with a continuous gradient from 100 % solvent A to 100 % B between 5 and 34 min and analyzed with an Accurate-Mass Q-TOF LC/MS (Agilent Technologies 6520) (experiment 1, 4 independent biological replicates). Quantification of peaks area showed that Erg-Asp represents 7.13±1.31 % of total Erg. Total lipids were also analyzed on a TSKgel ODS80$_{TM}$ QA (C18) (2.0×150 mm, 5mm) column in an independent biological replicate (experiment 2). In this case, quantification showed that Erg-Asp represented 27.2 % of total Erg. Discrepancies likely come from the solubility properties of Erg-Asp in extraction solvents, the amount found in experiment 2 representing an upper limit. Therefore, Erg-Asp is seemingly produced under standard growth conditions at levels between 7 and 20 %, but most likely ~10 % of total free Erg in *Aor*, which is in good correlation with TLC profiles obtained with *Aor* total lipids, but also with its close relative *Afm*.

Supplemental Tables

Table S1: Bacterial and fungi strains used in this study

REAGENT or RESOURCE	SOURCE	IDENTIFIER
Bacterial and Virus Strains		
Escherichia coli XL-1 Blue:endA1 gyrA96(nalR) thi-1 recA1 relA1 lac glnV44 F'[::Tn10 proAB+ lacIq Δ(lacZ)M15] hsdR17(r$_K$- m$_K$+)	Agilent (Stratagene)	Catalog#200249
Escherichia coli Rosetta-2: strain B F– *ompT gal dcmlonhsdSB(rB⁻mB⁻) λ(DE3 [lacI lacUV5-T7p07 ind1 sam7 nin5]) [malB⁺]K-12(λ^S))*, carrying the pRARE2 plasmid	Merck Millipore	71400-3
Escherichia coli DH5α: F⁻ endA1 glnV44 thi-1 recA1 relA1 gyrA96 deoRnupG purB20 φ80dlacZΔM15 Δ(lacZYA-argF)U169, hsdR17(r$_K$⁻ m$_K$⁺), λ⁻	Invitrogen	C404003
Organisms/Strains		
***Saccharomyces cerevisiae* strains**		
Saccharomyces cerevisiae BY4742: MATα his3Δ1 leu2Δ0 lys2Δ0 ura3Δ0	Euroscarf	
Saccharomyces cerevisiae YAL3 Δdps1: MATa ura3-52 lys2-801am trp1-63 his3-200 leu2-1 ade2-450 ade3-1483 dps1::HIS3	Dr. Gilbert Eriani	Ador *et al*, 1999
Saccharomyces cerevisiae BY4742: MATα his3Δ1 leu2Δ0 lys2Δ0 ura3Δ0 + pRS415-*erdSAfm*	This paper	N/A
Saccharomyces cerevisiae BY4742: MATα his3Δ1 leu2Δ0 lys2Δ0 ura3Δ0 + pRS415-*erdSAor*	This paper	N/A
Saccharomyces cerevisiae BY4742: MATα his3Δ1 leu2Δ0 lys2Δ0 ura3Δ0 + pRS415-*erdS ΔDUF2156Afm*	This paper	N/A
Saccharomyces cerevisiae BY4742: MATα his3Δ1 leu2Δ0 lys2Δ0 ura3Δ0 + pRS415-*erdSΔaspRSAfm*	This paper	N/A
Saccharomyces cerevisiae BY4742: MATα his3Δ1 leu2Δ0 lys2Δ0 ura3Δ0 + pRS415-*erdS$_{AAPA}$Afm*	This paper	N/A
Saccharomyces cerevisiae BY4742: MATα his3Δ1 leu2Δ0 lys2Δ0 ura3Δ0 + pRS414-*erdS ΔDUF2156Afm* (AspRSonly)+ pRS415-*erdS ΔaspRSAfm* (DUF2156 only)	This paper	N/A
Saccharomyces cerevisiae YAL3 Δdps1: MATa ura3-52 lys2-801am trp1-63 his3-200 leu2-1 ade2-450 ade3-1483 dps1::HIS3 + pRS415-*erdSAfm*	This paper	N/A

Saccharomyces cerevisiae YAL3 *Δdps1: MATa ura3-52 lys2-801am trp1-63 his3-200 leu2-1 ade2-450 ade3-1483 dps1::HIS3* + pRS415-*erdSAor*	This paper	N/A
Saccharomyces cerevisiae YAL3 *Δdps1: MATa ura3-52 lys2-801am trp1-63 his3-200 leu2-1 ade2-450 ade3-1483 dps1::HIS3* + pRS415-*erdS ΔDUF2156Afm*	This paper	N/A
Saccharomyces cerevisiae YAL3 *Δdps1: MATa ura3-52 lys2-801am trp1-63 his3-200 leu2-1 ade2-450 ade3-1483 dps1::HIS3* + pRS415-*erdSΔaspRSAfm*	This paper	N/A
Saccharomyces cerevisiae YAL3 *Δdps1: MATa ura3-52 lys2-801am trp1-63 his3-200 leu2-1 ade2-450 ade3-1483 dps1::HIS3* + pRS415-*erdS$_{AAPA}$Afm*	This paper	N/A
Saccharomyces cerevisiae YAL3 *Δdps1: MATa ura3-52 lys2-801am trp1-63 his3-200 leu2-1 ade2-450 ade3-1483 dps1::HIS3* + pRS415-*erdS* W785A *Afm*	This paper	N/A
Saccharomyces cerevisiae YAL3 *Δdps1: MATa ura3-52 lys2-801am trp1-63 his3-200 leu2-1 ade2-450 ade3-1483 dps1::HIS3* + pRS415-*erdS* W785A *Afm*	This paper	N/A
Saccharomyces cerevisiae YAL3 *Δdps1: MATa ura3-52 lys2-801am trp1-63 his3-200 leu2-1 ade2-450 ade3-1483 dps1::HIS3* + pRS415-*erdS* W785H *Afm*	This paper	N/A
Saccharomyces cerevisiae YAL3 *Δdps1: MATa ura3-52 lys2-801am trp1-63 his3-200 leu2-1 ade2-450 ade3-1483 dps1::HIS3* + pRS415-*erdS* R789A *Afm*	This paper	N/A
Aspergillus fumigatus strains		
Aspergillus fumigatus CEA17^{KU80}: *pyrG akuB::pyrG (ΔakuB^{KU80})*	Prof. J.-P. Latgé. Pasteur Institute, Paris, France	Da Silva Ferreira ME et al., 2006
Aspergillus fumigatus CEA17^{KU80}Δ*erdS (hph): pyrG akuB::pyrG (ΔakuB^{KU80})* **erd**S::*hph*	This paper	N/A
Aspergillus fumigatus CEA17^{KU80}Δ**erdS**: *pyrG akuB::pyrG (ΔakuB^{KU80})* Δ**erdS** (hph cassette excised)	This paper	N/A
Aspergillus fumigatus CEA17^{KU80}Δ**erd**S::P$_{xyl}$-**erd**S: *pyrG akuB::pyrG (ΔakuB^{KU80})* Δ**erdS**::*[5'-utr- P$_{xyl}$-**erd**S-trpCterm-hph-3'-utr]*	This paper	N/A
Aspergillus oryzae strains		
Aspergillus oryzae RIB40: *wild-type*	H. Nakajima. Meiji University, Tokyo, Japan	Kuroki Y *et al.*, 2002

Aspergillus oryzae HiMe10: *ΔligD::AnpyrG-300bp ΔpyrG*	H. Nakajima Meiji University, Tokyo, Japan	Kuroki Y *et al.,* 2002
Aspergillus oryzae HiDES*ΔerdS:* *ΔligD::AnpyrG-300bp,* Δ**pyrG,** Δ**AorErd***S::AnpyrG-300bp*	This paper	N/A
Aspergillus oryzae HiDEC *ΔerdS+aspRS:* *ΔligD::AnpyrG-300bp, ΔpyrG, ΔAo-erdS::AnpyrG-300bp, niaD::(AoaspRSniaDAnpyrG)*	This paper	N/A
Aspergillus oryzae HiDEC *ΔerdS+duf2156:* *ΔligD::AnpyrG-300bp, ΔpyrG, ΔAo-erdS::AnpyrG-300bp, niaD::(Aoduf2156 niaDAnpyrG)*	This paper	N/A
Aspergillus oryzae HiDEC *ΔerdS+erdS:* Δ**ligD::AnpyrG-300bp, ΔpyrG,** Δ**AoErd***S::AnpyrG-300bp,* **niaD::(Ao**erd*SniaDAnpyrG)*	This paper	N/A
Neurospora crassa strains		
Neurospora crassa 74-OR23-1VA : wild-type, *matA*	FGSC	FGSC #2489
*Neurospora crassa ΔerdS:***erd***S::hph, matA*	FGSC	FGSC #20236
*Neurospora crassa ΔeraH:***erd***H::hph, matA*	FGSC	FGSC #20235
Other fungal strains		
*Aspergillus flavus*CA14: *ΔpyrG Δku80*	FGSC	FGSC #A1421
Beauveria bassiana NRRL 20698*:* wild-type	ATCC	ATCC 90517
Schizophyllum commune H4-8*:* wild-type	FGSC	FGSC #9210
*Aspergillus niger:*wild-type	University of Strasbourg	N/A
*Candida albicans:*wild-type	University of Strasbourg	N/A
*Candida parapsilosis:*wild-type	University of Strasbourg	N/A
*Geotrichum candidum:*wild-type	University of Strasbourg	N/A
*Penicillium expansum:*wild-type	University of Strasbourg	N/A
*Penicillium camemberti:*wild-type	University of Strasbourg	N/A
*Alternaria alternata:*wild-type	University of Strasbourg	N/A
*Cryptococcus neoformans:*wild-type	University of Strasbourg	N/A

Final plasmid	DNA template	Primers (5' --> 3')
Construction of donor plasmids containing erdS variants - Gateway BP reactions		
pDONR221-erdS-afm_Sce_opt	pUC57-erdS-afm_Sce_opt	GW_s : GGGGACAAGTTTGTACAAAAAAGCAGGCTTCATG

(GW BP reaction)		
		GW_as : GGGGACTTTGTACAAGAAAGCTGGGTC
pDONR221-erdS-Δduf2156 (GW BP reaction)	pUC57-erdS-afm_Sce_opt	FF001 : GGGGACAAGTTTGTACAAAAAAGCAGGCTTCATGTCAATCAAGAGAGCATTATCC
		FF003 : GGGGACCACTTTGTACAAGAAAGCTGGGTCTCAAGGTGGAAAAGATTTTGGATC
pDONR221-erdS-ΔaspRS (GW BP reaction)	pUC57-erdS-afm_Sce_opt	dufssDRS_s : GGGGACAAGTTTGTACAAAAAAGCAGGCTTCatgAGACACCCTGAAAGTTCTACAATAGAACC
		GW_as : GGGGACTTTGTACAAGAAAGCTGGGTC
pDONR221-erdS-aor (GW BP reaction)	A. oryzaegDNA	GGGGACAAGTTTGTACAAAAAAGCAGGCTTCatgtccatcaaacgggccc
		GGGGACCACTTTGTACAAGAAAGCTGGGTCttagtcttcgaaaaagtgaagg
pDONR221-erdS-afm_Sce_opt (GW BP reaction)	pUC57-erdS-afm_Sce_opt	GW_s : GGGGACAAGTTTGTACAAAAAAGCAGGCTTCATG
		GW_as : GGGGACTTTGTACAAGAAAGCTGGGTC
pDONR221-erdS-Δduf2156 (GW BP reaction)	pUC57-erdS-afm_Sce_opt	FF001 : GGGGACAAGTTTGTACAAAAAAGCAGGCTTCATGTCAATCAAGAGAGCATTATCC
		FF003 : GGGGACCACTTTGTACAAGAAAGCTGGGTCTCAAGGTGGAAAAGATTTTGGATC
pDONR221-erdS-ΔaspRS (GW BP reaction)	pUC57-erdS-afm_Sce_opt	dufssDRS_s : GGGGACAAGTTTGTACAAAAAAGCAGGCTTCatgAGACACCCTGAAAGTTCTACAATAGAACC
		GW_as : GGGGACTTTGTACAAGAAAGCTGGGTC
pDONR221-erdS-aor (GW BP reaction)	A. oryzaegDNA	GGGGACAAGTTTGTACAAAAAAGCAGGCTTCatgtccatcaaacgggccc
		GGGGACCACTTTGTACAAGAAAGCTGGGTCttagtcttcgaaaaagtgaagg
pDONR221-erdS-afm_Sce_opt (GW BP reaction)	pUC57-erdS-afm_Sce_opt	GW_s : GGGGACAAGTTTGTACAAAAAAGCAGGCTTCATG
		GW_as : GGGGACTTTGTACAAGAAAGCTGGGTC
Construction of _S. cerevisiae_ expression plasmids - isoThermal assembly		
pRS415-GPD-erdS-aor	pDONR221-erdS-aor	#101 : gaactagtggatcccccatcacaagtttGTACAAAAAAGCAGGCTTC
		#102 : cttgatatcgaattcctgcagcccatcaCCACTTTGTACAAGAAAGCTGGGTC
	pRS415-GPD-X (LR recombined plasmid)	#104 : tgatgggctgcaggaattcgatatcaag
		#103 : aaacttgtgatgggggatccactagttc
pRS415-GPD-erdS-afm	pDONR221-erdS-afm	#101 : gaactagtggatcccccatcacaagtttGTACAAAAAAGCAGGCTTC
		#102 : cttgatatcgaattcctgcagcccatcaCCACTTTGTACAAGAAAGCTGGGTC
	pRS415-GPD-X	#104 : tgatgggctgcaggaattcgatatcaag
		#103 : aaacttgtgatgggggatccactagttc
pRS415-GPD-erdS-Δduf2156	pDONR221-erdS-Δduf2156	#101 : gaactagtggatcccccatcacaagtttGTACAAAAAAGCAGGCTTC
		#102 : cttgatatcgaattcctgcagcccatcaCCACTTTGTACAAGAAAGCTGGGTC
	pRS415-GPD-X	#104 : tgatgggctgcaggaattcgatatcaag
		#103 : aaacttgtgatgggggatccactagttc
pRS415-GPD-erdS-ΔaspRS	pDONR221-erdS-ΔaspRS	#101 : gaactagtggatcccccatcacaagtttGTACAAAAAAGCAGGCTTC
		#102 : cttgatatcgaattcctgcagcccatcaCCACTTTGTACAAGAAAGCTGGGTC
	pRS415-GPD-X	#104 : tgatgggctgcaggaattcgatatcaag
		#103 : aaacttgtgatgggggatccactagttc

pRS415-AspRS_{AAPA}-DUF2156	pRS415-GPD-erdS-afm	FF048 : TTTTAGCCGCTGCTCCTGCTTTGGCAAAGCAAATGGCCATC
		FF049 : CTTTGCCAAAGCAGGAGCAGCGGCTAAAAATGCATCTCTACCG
pRS415-GPD-erdS-aor	pDONR221-erdS-aor	#101 : gaactagtggatcccccatcacaagtttGTACAAAAAAGCAGGCTTC
Construction of *E. coli* overexpression plasmids - isoThermal assembly		
pMtevGWA-erdS-afm	pDONR221-erdS-afm	#142 : GGTACCGGATCTTACATCACAAGTTTGTACAAAAAAGCAGGCTTC
		#134 : GTGGTGGTGGTGCTCGAGGTACATCAACTTTGTACAAGAAAGCTGGGTC
	pMtevGWA-X	#114 : TGATGTACCTCGAGCACCACCACCAC
		#135 : AAACTTGTGATGTAAGATCCGGTACC
pMtevGWA-erdS-Δduf2156	pDONR221-erdS-Δduf2156	#142 : GGTACCGGATCTTACATCACAAGTTTGTACAAAAAAGCAGGCTTC
		#134 : GTGGTGGTGGTGCTCGAGGTACATCAACTTTGTACAAGAAAGCTGGGTC
	pMtevGWA-X	#114 : TGATGTACCTCGAGCACCACCACCAC
		#135 : AAACTTGTGATGTAAGATCCGGTACC
pMtevGWA-erdS-ΔaspRS	pDONR221-erdS-ΔaspRS	#142 : GGTACCGGATCTTACATCACAAGTTTGTACAAAAAAGCAGGCTTC
		#134 : GTGGTGGTGGTGCTCGAGGTACATCAACTTTGTACAAGAAAGCTGGGTC
	pMtevGWA-X	#114 : TGATGTACCTCGAGCACCACCACCAC
		#135 : AAACTTGTGATGTAAGATCCGGTACC
pMtevGWA-AspRS_{AAPA}-DUF2156	pMtevGWA-erdS-afm	FF048 : TTTTAGCCGCTGCTCCTGCTTTGGCAAAGCAAATGGCCATC
		FF049 : CTTTGCCAAAGCAGGAGCAGCGGCTAAAAATGCATCTCTACCG
pMtevGWA-erdH	*Afm*Genomic DNA	NY119 : AAGCAGGCTTCATGGCCTCTCATGCCCCTC
		NY120 : gAAAGCTGGGTCCTATCTGTCAAAAATCGC
	pMtevGWA-X	NY121 : GACAGATAGGACCCAGCTTTcttgtacaaagtgg
		NY122 : ATGAGAGGCCATGAAGCCTGCTTTTTTTGTACaaac
pMtevGWA-erdH-S153A	pMtevGWA-erdH	NY145 : TGAGTGGTTTCGCTGCGGGCGGCAACCTCGCTG
		NY146 : TTGCCGCCCGCAGCGAAACCACTCAGAGCAATTC
pMtevGWA-erdH-D277A	pMtevGWA-erdH	NY147 : TCTGCGAATGGGCTATGCTGATGAACGAGGGC
		NY148 : TTCATCAGCATAGCCCATTCGCAGATGTACAG
Deletion and complementation cassettes for *Afm* strains - isoThermal assembly		
pJET1.2-erdS délétion cassette *Afm*	pSK529 (Hartmann et al., 2010)	FF166 : TATAGGTCAATAGAGTATACTTATTTG
		FF167 : TATTATGCTCAACTTAAATGACCTAC
	*Afm*CEA17ΔakuB^{KU80}gDNA	FF168 : cccgggTACGTTGGTACGTGAAAGAAATGG
		FF169 : TAAGTATACTCTATTGACCTATAGGTGACGGATGAGAGACCACC
		FF170 : GGTCATTTAAGTTGAGCATAATAAGTGGCAGATGTACCAAGCCC
		FF171 : cccgggTACGCCGCCTCCCTTCCCATTGC
pJET1.2-Pxyl-erdS	pJET1.2-erdS deletion cassette *Afm*	FF271 : CAAAGCACGTTTGATCGACATCTGCAgttggttcttcgagtcgatgaatg
		FF272 : TGCACTTCTTTGAAGACTAAGGATCCCCGACGCCGACCAACACCGCC
	Afm CEA17ΔakuB^{KU80}gDNA	FF273 : ATGTCGATCAAACGTGCTTTGTCTAAG
		FF274 : TTAGTCTTCAAAGAAGTGCAGAACCG
pJET1.2-erdS délétion cassette *Afm*	pSK529 (Hartmann et al., 2010)	FF166 : TATAGGTCAATAGAGTATACTTATTTG
		FF167 : TATTATGCTCAACTTAAATGACCTAC
	*Afm*CEA17ΔakuB^{KU80}gDNA	FF168 : cccgggTACGTTGGTACGTGAAAGAAATGG
		FF169 : TAAGTATACTCTATTGACCTATAGGTGACGGATGAGAGACCACC
		FF170 : GGTCATTTAAGTTGAGCATAATAAGTGGCAGATGTACCAAGCCC
Afm ΔerdS strains verification		
	*Afm*CEA17ΔakuB^{KU80}gDNA	FF684 : GGAGATTGGATATGGATGAAGTGAAC
		FF685 : GTTGCCAACGTCGAGAAAACC
		NY15 : GAGCTGATGCTTTGGGCCGAGGACTGC
		NY16 : GCAGTCCTCGGCCCAAAGCATCAGCTC
	*Afm*CEA17ΔakuB^{KU80}gDNA	FF684 : GGAGATTGGATATGGATGAAGTGAAC
		FF685 : GTTGCCAACGTCGAGAAAACC
		NY15 : GAGCTGATGCTTTGGGCCGAGGACTGC

		NY16 : GCAGTCCTCGGCCCAAAGCATCAGCTC
Deletion and complementation cassettes for *Aor* strains - restriction and ligation		
pTAnpyrG	*A. nidulans* A26	AnpyrG-F : CCCCCCCGGGCTAGGCGCAATCCCTG
		AnpyrG-R : GGGGACTAGTGCCGGCTTAACCACAG
pAnpyrG-MR	pTAnpyrG	AnpyrG-SpeI-FF : CCCCACTAGTCTCGTCGGCTCTTTTCGCAA
		AnpyrG-SphI-FR : GGGGGCATGCGTAGAGGGTGCGGAGAACA
pUCdn	*Aor*RIB40*genomic DNA*	AoErdS-3'-SmaI-F : GACTAACCCGGGGCCTTCTTATGTTAGGCGTTTG
		AoErdS-3'-EcoRI-R : CTAGTCGAATTCTTCGAACCAGAATTAACGCTAC
pUCflk	*Aor*RIB40*genomic DNA*	AoErDS-5'-HindIII-F : ACCTGCAAGCTTCTTTAATATCCCGAGAATACTCG
		AoErDS-5'-PstI-R : TGATGACTGCAGTTGTGTAGCGGACGATAG
pDAor-ErDS	pAnpyrG-MR	AnpyrG-MR-SmaI-F primer : CTTCATCCCGGGCTAGGCGCAATCCCTGTC
		AnpyrG-MR-PstI-R primer : CTTCATCCCGGGCTAGGCGCAATCCCTGTC
pTAnpyrG	*A. nidulans* A26	AnpyrG-F : CCCCCCCGGGCTAGGCGCAATCCCTG
		AnpyrG-R : GGGGACTAGTGCCGGCTTAACCACAG
pAnpyrG-MR	pTAnpyrG	AnpyrG-SpeI-FF : CCCCACTAGTCTCGTCGGCTCTTTTCGCAA
		AnpyrG-SphI-FR : GGGGGCATGCGTAGAGGGTGCGGAGAACA
pUCdn	*Aor*RIB40*genomic DNA*	AoErdS-3'-SmaI-F : GACTAACCCGGGGCCTTCTTATGTTAGGCGTTTG
		AoErdS-3'-EcoRI-R : CTAGTCGAATTCTTCGAACCAGAATTAACGCTAC
pUCflk	*Aor*RIB40*genomic DNA*	AoErDS-5'-HindIII-F : ACCTGCAAGCTTCTTTAATATCCCGAGAATACTCG
		AoErDS-5'-PstI-R : TGATGACTGCAGTTGTGTAGCGGACGATAG
Deletant and complemented *Aor* strains verification		
	HiMe10, HiDES (gDNA)	P1 : AoErdS-5'-HindIII-F : ACCTGCAAGCTTCTTTAATATCCCGAGAATACTCG
		P4 : AoErdS-3'-EcoRI-R : CTAGTCGAATTCTTCGAACCAGAATTAACGCTAC
	HiDES + erdS, HiDES + erdSΔduf (gDNA)	P15 : AoErdS-486-F : TGCCAAGCTGGTTTTCCTTG
		P16 : AoErdS-575-R : ATGGCGATGGAATTCTTGCC
	HiDES + erdSΔaspRS (gDNA)	P10 :AoErdS-PmaCI-R : AGACACGTGTTAGTCTTCGAAAAAGTGAAGGACAG
		P17 : AoErdS-2274F : GGCGATCCTTTGTGCGATTC

Supplemental Materials and Methods

Media and growth conditions

For routine growth and maintenance of *Aspergillus fumigatus (Afm)* and *Aspergillus oryzae (Aor)*, fresh conidia were spread on Malt extract agar (ThermoScientific) plates or slants and incubated at 37 °C (*Afm*) or 30 °C (*Aor*). Mycelia were then incubated 7 days for *Afm* or 10 days for *Aor* until they produced enough conidia. *N. crassa* (*Ncr*) was grown in Vogel's agar medium. Nutrient-rich (NR) liquid or agar medium was composed of glucose 4 % (w/v), peptone 1 % (w/v) and yeast extract (YG) 1 % (w/v) (with 1.5 % w/v agar for plates or slants). Standard *Aspergillus* minimal medium Glucose (MMG) was composed as follow: For 1 L, it contained glucose (1 % w/v), ammonium tartrate dibasic(0.92 g, 5 mM, *i.e.*, 10 mM ammonium), salts (10 mL of a 50 X solution containing KCl 26 g/L, $MgSO_4$ $7H_2O$ 26 g/L, KH_2PO_4 76 g/L) and trace elements (0.5 mL of a 1000 X solution containing: $FeSO_4$ $7H_2O$ 1 g, Na_2EDTA 10 g, $ZnSO_4$ $7H_2O$ 4.4 g, H_3BO_3 2.2 g, $MnCl_2$ $4H_2O$ 1 g, $CoCl_2$ $6H_2O$ 0.32 g, $CuSO_4$ $5H_2O$ 0.32 g and Na_2MoO_4 0.8 g for 200 mL adjusted at pH 6.5). For MMX media, it contained 1 % (w/v) xylose as the carbon source. Solid media contained 1.5 % (w/v) agar. Agar plates or slants were incubated at 37°C (*Afm*) or 30 °C (*Aor*, *Ncr*) in the dark for indicated periods of time. Liquid cultures were incubated in glass flasks at 37 °C for *Afm* or 30 °C for *Aor*, *Ncr* and

all other filamentous fungi tested under shaking (220 rpm) for 24 (*Afm*) to 48 h (other fungi), until enough cells or mycelia were produced. *Sce*, *Candida* spp. and *C. neoformans* (*Cne*) were grown in NR medium for 24 h at 30 °C under agitation (220 rpm).

Spores/conidia preparation

Spores from 7 days for *Afm* or 10 days-old for *Aor* Malt agar slants were resuspended by addition of 5 mL sterile Tween 20-H_2O (0.05 % v/v) and vortexing, then the conidia were filtered with Cell Strainer filters (EASY strainer™ Greiner Bio-One), and the concentration was determined with a hemacytometer. Conidia were stored in Tween 20-H_2O (0.05 % v/v) at 4°C in the dark up to 1 week. For *Ncr*, conidia were harvested and treated similarly using 1 M sterile sorbitol.

Mycelia harvesting from liquid cultures

Liquid cultures to produce mycelia were inoculated with 10^6 to 10^7 conidia/mL in 50 mL liquid MMG for *Afm* or NR for *Aor*, incubated for 24 h at 37 °C (*Afm*) or 30° C (*Aor*) in the dark under agitation (220 rpm). Mycelia were then filtrated through two layers of gauze, rinsed twice with 50 mL sterile H_2O, and squeezed to eliminate excess water. Mycelia were directly used to extract total lipids.

Construction of cassettes for *A. fumigatus*

For the construction of Δ*erdS*mutants of *Afm*, 1000 bp of the 5'-upstream and of the downstream regions were amplified by PCR (using primer pairs FF#168 + FF#169 andFF#170 + FF#171, respectively) from *Afm*CEA17Δ*akuB*^{KU80}genomic DNA. Primers contained a 25 bp sequence at the 3' and 5' extremities, respectively, to obtain sequence tags corresponding to the 5' and 3' extremities of the *six*-P$_{xyl}$-β*rec-trpC-hygB-six* resistance cassette (1) flanked by *Sma*I restriction sites. The *six*-P$_{xyl}$-β*rec-trpC-hygB-six* resistance cassette was amplified by PCR (FF#166 and FF#167), and the 3 resulting fragments were fused using the Gibson method as described (2) to obtain the 5'-UTR-*six*-P$_{xyl}$-β*rec-trpC-hygB-six*-3'-UTR cassette flanked by the *Sma*I restriction sites. This cassette was ligated into a pJET1.2 plasmid using the CloneJET PCR Cloning Kit (ThermoScientific) following the manufacturer's instructions, to obtain the pJET1.2-Δ*erdS*deletion plasmid. The integrity of the deletion cassette was checked by PCR and sequencing. Thexylose-inducible *erdS* complementation cassette was constructed by replacing the β- *rec* gene in the 5'-UTR-*six*-P$_{xyl}$-β*rec-trpC-hygB-six*-3'-UTR cassette by the

wild-type *erdS* gene, so that it is under the control of the xylose promoter (P_{xyl}) (3) and the *trpC* terminator. The pJET1.2-Δ*erdS* plasmid was reverse-amplified with primers FF#271 and FF#272 to obtain the pJET1.2-Δ*erdS* open plasmid (pJET1.2-*eraS*-β*rec*$^{0, open}$) deprived of the β-*rec* gene. This PCR fragment was submitted to *Dpn*I digestion at 37 °C, 1 h, to remove the pJET1.2-Δ*erdS* matrix and purified using the Nucleospin Gel and PCR clean-Up Kit (Marcherey-Nagel). The *erdS* gene was amplified from *Afm*CEA17 24 ΔakuB^{KU80}enomic DNA using primers FF#273 and FF#274 with 20 pb 5'- and 3'-tags corresponding to the flanking regions of the β-rec gene. The pJET1.2-*eraS*-β*rec*$^{0, open}$ and *erdS* fragments were fused using the Gibson procedure (2) to obtain the pJET1.2-P_{xyl}-*erdS* (precisely, the pJET1.2 plasmid containing the 5'-UTR-*six*-P_{xyl}-*erdS*-*trpC*-*hygB*-*six*-3'-UTR cassette) integration plasmid. This cassette was designed to be integrated by homologous recombination at the Δ*erdS* locus. Because the β-*rec* gene was removed, once integrated at the Δ*erdS* locus, the 5'-UTR-*six*-P_{xyl}-*eraS*-*trpC*-*hygB*-*six*-3'-UTR cassette could not be excised.

Construction of mutants and complemented strains in *A. fumigatus*

Deletion of the *erdS* gene was obtained through homologous recombination with the deletion cassettes described above. Transformations of *Afm* were performed by electroporation of swollen conidia essentially as described (4) and we used 10 µg of linearized (*Sma*I-digested) deletion plasmid.

From the primary hygromycin-resistant colonies, conidia were isolated on individual Malt agar plates containing 150 µg/mL hygromycin B. After 3 days, conidia from single isolated colonies were scrapped and transferred on Malt agar slants containing 150 µg/mL hygromycin B and incubated 5 days at 37 °C. Genomic DNA was extracted (5)from mycelium cultures of Δ*erdS* mutants and the disruption of the *Afm-erdS* gene was confirmed by PCR (Primers FF#684 + NY#015 and NY#016 + FF#685) and by Western-blot. The hygromycin resistance cassette was then self-excised as described (1) on xylose-containing MM, and clones verified by PCR with primers FF#684 and FF#685.

To complement this Δ*erdS* strain, P_{xyl}-*erdS* cassette was inserted at the Δ*erdS* locus with the same protocol but the cassette could not be excised since, for this construct, the β-recombinase gene (1) was replaced by the *erdS* open reading frame.

Construction of cassettes for *A. oryzae*

For the disruption of *Aor-erdS* in *Aor*, *pyrG* marker recycling method was used (6). The first 300 bp of the coding sequence (starting from the ATG codon) of *Aspergillus nidulanspyrG* was amplified (AnpyrG-300 bp) and ligated to the 3' end of *pyrG* gene, immediately after the stop codon. This will bring the first 300 bp sequence directly attached to the 3' end of the *pyrG* gene in tandem repeats. The *pyrG* gene was amplified by PCR from *A. nidulans* A26 genomic DNA with the primers AnpyrG-F and AnpyrG-R. The PCR product was then ligated into pT7Blue using TA-cloning kit to yield pTAnpyrG. AnpyrG-300bp was amplified from pTAnpyrG with the primers AnpyrG-SpeI-FF and AnpyrG-SphI-FR. The resulting fragment was ligated into pTAnpyrG digested with *Spe*I and *Sph*I to yield the pAnpyrG-MR.

To construct the *Aor-erdS* gene disruption cassette, the upstream (1.0 kb) and the downstream (1.0 kb) flanking region of *Aor-erdS* ORF were amplified by PCR from *Aor*RIB40 genomic DNA using primer pairs AoErDS-5'-HindIII-F and AoErDS-5'-PstI-R for the upstream, and AoErDS-3'-SmaI-F and AoErDS-3'-EcoRI-R for the downstream regions. The downstream fragment was ligated into pUC118 vector digested with *Sma*I and *EcoR*I to yield the pUCdn, and then the upstream fragment was ligated into pUCdn digested with *Hind*III and *Pst*I to yield the pUCflk. The AnpyrG-MR was amplified from pAnpyrG-MR with the primers AnpyrG-MR-SmaI-F and AnpyrG-MR-PstI-R, and ligated into pUCflk digested with *Sma*I and *Pst*I to yield the pDAor-ErDS.

Construction of mutants and complemented strains in *A. oryzae*

The conidial suspension of *Aor*HiMe10was inoculated in 50 mL GPYU broth (2 % glucose, 1 % polypeptone, 0.5 % yeast extract, 0.1 % uridine, 0.1 % uracil) and incubated for 18 h at 30 °C and 160 rpm. Then mycelia were harvested by filtration with sterile Myracloth, washed with sterile distilled water and the cell walls digested with 1 % yatalase (Takara), 0.6 M $(NH_4)_2SO_4$, 50 mM maleate buffer (pH 5.5) at 30 °C for 3 h. Protoplast conversion was monitored by microscopic observation. After removing hyphal debris by filtration, the protoplast suspension was diluted 1:1 with Solution I (1.2 M sorbitol, 50 mM $CaCl_2$, 35 mM NaCl, 10 mM Tris-HCl, pH 7.5). Protoplasts were collected by centrifugation (2000 rpm, 8 min, 4 °C) and washed twice with Solution I. Finally, protoplasts were resuspended in Solution I at $2x10^7$ cells mL^{-1}. Of the protoplast suspension, 200 µL was mixed with 15 µg of linearized disruption cassette and incubated on ice for 30 min, then to the mixture was added 1.35 mL Solution II (60 % PEG4000, 50 mM $CaCl_2$, 10 mM Tris-HCl, pH 7.5). After 20 min incubation at room temperature (RT), the mixture was diluted with 5 mL Solution I and centrifuged (2000 rpm, 8 min, 4 °C). The precipitates were suspended in 250 µL Solution I and added in 5 mL Top agar (selective media

including 1.2 M sorbitol and 0.8 % agar) and then the transformation mix overlaid on selective agar media (3 % sucrose, 0.3 % NaNO$_2$, 0.1 % K$_2$HPO$_4$, 0.05 % MgSO$_4$·7H$_2$O, 0.05 % KCl, 0.001 % FeSO$_4$·7H$_2$O and 1.2 M sorbitol). The plates were incubated at 30 ˚C for seven days. From the primary transformation plates, conidia were isolated from individual colonies using a flamed loop and transferred on individual Czapek-Dox agar plates to allow isolated sporulating colonies to form. After isolating three times to a single colony, conidia were inoculated into 5 mL GPY broth and incubated for 18 h at 30 ˚C and 160 rpm. Mycelia were harvested by filtration through Miracloth, washed with water, subjected to genomic DNA extraction with the DNeasy Plant Mini Kit (Qiagen) following the manufacturer's instructions. After isolation, the disruption of the *Aor-eraS* gene was confirmed by PCR with QuickTaq HS DyeMix (TOYOBO)using primers AoEraS-F2 and AnpyrG-F2 that were designed based on homologous region and the AnpyrG-MR, respectively. The AnpyrG-MR was self-excised on PDU agar media containing 5-FOA. The resulting disruption mutant was named HiDES.

To complement the *Aor* Δ*eraS* disruption mutant, the plasmid pUAES was constructed, which harbors the *Aor-eraS* gene, the promoter region of *Aor-eraS* and the terminator of *agdA*. The *Aor-eraS* gene was amplified by PCR using the primers PEraS-Sse8387I-F and AoEraS-PmaCI-R digested with *Sse8387*I and *PmaC*I, and then ligated into pUenoP digested with *Pst*I and *Sma*I. The resulting pUAES plasmid containing the *niaD* gene was introduced into HiDES to obtain HiDEC. Clones were isolated and identified as described above.

Induction of *erdS* expression with xylose

Liquid cultures were performed as described in the previous section, and mycelia harvested similarly. Then washed mycelia were resuspended in fresh minimal media containing 1 % glucose (w/v) or 1 % xylose (w/v) as the sole carbon source, to induce or not ErdS and Erg-Asp overproduction in the Δ*erdS*::P$_{xyl}$-*erdS* strain of *Afm*. Mycelia were then harvested as described and lipids extracted as specified below.

Construction of *Sce* and *E. coli* expression plasmids

The *Afm erdS* open reading frame (*AFUA_1g02570*) was synthesized (Genscript®) with codon optimization for expression in *Sce*, amplified by PCR (Primers GW_s and GW_as) and cloned in a pDONR221-*ccdB* vector (kanamycin resistance marker) (Gateway technology) using a BP reaction as described (7). To construct the *erdS*Δ*duf2156* and *erdS*Δ*aspRS* variants, the *erdS* sequence was amplified with primers pairs FF#001/FF#003 and

Dufssdrs_sens/GW_as, respectively, that contained *attB1* and *attB25'*-tags, and introduced in the pDONR221-*ccdB* with a BP reaction, as described (7). To transfer the *erdS*, *erdSΔduf2156* and *erdSΔaspRS* constructs in destination vectors (pDEST was pRS415-Gpd or pRS414-Gpd), we first amplified the corresponding ORFs from the pDONR vectors with primers #101 and #102. We reverse-amplified a pDEST vector containing another unrelated ORF (already recombined) with primers #104 and #103 to obtain the open form of the plasmid without this unrelated ORF. Fragments (*erdS*, *erdSΔduf2156* and *erdSΔaspRS*) were introduced in the open pDEST form separately using the Gibson assembly procedure as described (2) and recombinant plasmids verified by PCR, restriction analysis and sequencing. The same procedure was used to clone the *erdS* gene from *Aor* (primers FF#099 and FF#100 to insert the ORF in the pDONR and primers #101 and #102 to transfer in the pDEST vectors).

To construct vectors enabling the expression of Maltose-binding protein fusions in *E. coli*, the codon-optimized *erdS* ORFs and variants were PCR-amplified using primers #142 and #134, and the pDEST (pMTevGWA) reverse-amplified with primers #114 and #135 before performing the Gibson assembly. The same was applied for the *erdH* gene (*AFUA_1g02580*, no introns) that was PCR-amplified from *Afm*KU80 with primers NY#119 and NY#120 and inserted directly in the pMTevGWA open vector generated by reverse-amplification with primers NY#121 and NY#122.

Site directed mutagenesis was performed with primer pairs containing selected mutations (indicated and described in supplementary table), as previously described (8).

Plasmid-shuffling complementation assays in *S. cerevisiae*

Plasmid shuffling experiments were conducted in the Δ*dps1 Sce* strain (9) rescued with a wild-type *DPS1* gene copy cloned in an *URA3*-bearing plasmid. All *Afm* or *Aor erdS* constructs to be tested were cloned in p415 (LEU) plasmids, transformed in the Δ*dps1* strain, and shuffled essentially as described (10, 11).

Proteins extraction and Western blots

For yeast crude extract preparation, 1 OD_{600nm} of cells were resuspended and incubated 10 min in 500 µL of pre-cooled NaOH 0.185 N, then precipitated by adding 50 µL of Trichloroacetic acid (TCA) 100 % and incubated 10 min on ice. Finally, the samples were centrifuged at 13, 000 x *g* for 15 min and the resulting pellets were resuspended in 100 µL of

Laemmli Sample Buffer. Then, 8 µL of each sample was then resolved on 10 % SDS-PAGE gels. Samples were separated by using a BioRad Mini-PROTEAN electrophoresis apparatus. For western blotting, proteins were transferred onto PVDF membranes that were blocked in 5 % (w/v) skimmed milk in TBS-Tween (TBS 1X, Tween-20 0.3 % (v/v)) for 1 h at RT. Primary antibodies (polyclonal anti-DUF2156, Covalab, France, anti-PGK) were incubated overnight at 4 °C and then washed several times with TBS-Tween. Membranes were then incubated for 1 h with HRP-conjugated secondary antibodies (Goat anti-rabbit for anti-DUF2156 and Goat anti-mouse for anti-PGK) at RT. Revelation was performed with the BioRad clarity western ECL Kit and monitored in a BioRad ChemiDoc Touch® apparatus.

Recombinant protein expression and purification

For recombinant protein purification, we modified the pMGWA vector (described in (7)) by introducing the Maltose Binding Protein (MBP) tag coding sequence 5' to a TEV cleavage site (TevCS). The gene encoding the protein of interest (*erdS*, *erdH* and mutants) was then cloned into this pMtevGWA using the above described cloning method. The resulting MBP-TevCS-X expression plasmids were then transformed in *E. coli* Rosetta-2 strains. Transformed bacteria were grown in LB medium containing ampicillin (150 µg/ml) and shaken at 37 °C, until an $OD_{600nm} \sim 0.5$-0.6 was reached. Cultures were then chilled on ice for 30 min and protein overexpression was induced with 0.1 mM IPTG for 12 h at 18 °C. Finally, cells were harvested by centrifugation (5000 x *g*, 15 min, 4 °C). The resulting cell pellet (~9 g) was resuspended in 30 mL of Tris-HCl pH 7 250 mM lysis buffer, containing NaCl 300 mM, KCl 30 mM, Glycerol 5 % (v/v), Tween 20 0.25 % (v/ v), TritonX-100 0.1 % (v/v), 2-mercaptoethanol 5 mM, Na_2EDTA 0.5 mM and a protease inhibitor cocktail (Roche Complete, EDTA-free). Cell lysis was performed by sonication (6 x 1 min, amplitude 28 %) (Vibracell, 72408) with intermediate cooling on ice. The lysate was centrifuged at 13, 000 x *g*, 20 min and the supernatant directly incubated with 1 mL of equilibrated amylose resin (NEB Amylose Resin, E8021S) at 4 °C on a rotating wheel. After transfer on an column (BioRad), the flow through was collected, beads where washed with 5 column volumes (CV) of wash buffer (Tris-HCl pH 7 50 mM, NaCl 300 mM, KCl 30 mM, Glycerol 5 % (v/v), Tween-20 0.25 % (v/v), 2-mercaptoethanol 10 mM) and the recombinant protein was eluted with 5 x 1 mL of elution buffer (Wash buffer supplemented with 2 % (p/v) of maltose monohydrate (Sigma-Aldrich). The collected fractions were then analyzed on 10 % SDS-PAGE gels. Fractions containing MBP-TevCS-X (X: ErdS, ErdH or mutants) protein were pooled. When required, the MBP-tag was cleaved off using the TEV

protease, as described. To separate the protein of interest from the MBP-tag and some other contaminants, fractions were injected on a HiLoad 16/600 Superdex 200 pg set up on a ÄKTA pure chromatography system (GE Healthcare). Finally, the fractions containing the protein of interest where pooled, concentrated to a final concentration of 1 mg/mL and stored at -20 °C with 30 % glycerol until use.

S. cerevisiae tRNA[Asp] purification

Extraction and purification of tRNA[Asp] from *Sce* was performed as described elsewhere (12).

In vitro tRNA[Asp] aspartylation assay

Aspartylation of tRNA[Asp] was performed as and adapted from (13, 14). Briefly, pure MBP-ErdS (or mutants) or ErdS (or mutants) without the N-terminal MBP tag were used. Aminoacylation reactions were performed in a Na-HEPES 100 mM pH 7.2 buffer containing KCl 30 mM, $MgCl_2$, 12 mM, ATP 10 mM, BSA 0.1 mg/mL, pure yeast tRNA[Asp] (10 µM), [U-^{14}C]-Asp (280 cpm/pmol, Perkin Elmer) in a final volume of 100 µL. Reactions were initiated by adding 1 µg of enzyme pre-incubated at 30°C, and incubated at 30 °C. At each time points, 10 µL of reaction mix were removed, spotted onto Whatman paper filters (2 x 2 cm) and plunged into a 5 % TCA solution in a glass beaker to precipitate [^{14}C]-Asp-tRNA[Asp]. Papers were washed 3 times for 15 min in 5 % TCA to remove residual free [^{14}C]-Asp, and 3 times 5 min in 100 % ethanol and air-dried. Radioactivity of precipitated [^{14}C]-Asp-tRNA[Asp] was counted in a scintillation counter. Control experiments were performed with a reaction mix deprived of enzyme to obtain the background counts.

Chemical synthesis of ergosteryl-3β-*O*-L-aspartate and NMR analyses
4-*tert*-Butyl-1-ergosteryl *N*-(*tert*-butoxycarbonyl)-*L*-aspartate

Ergosterol (400 mg) and 4-*tert*-butyl-*N*-(*tert*-butoxycarbonyl)-*L*-aspartate (300 mg in Et_2O (30 ml)) at RT was added *N,N'*-dicyclohexylcarbodiimide (300 mg) and *N,N*-dimethyl-4-aminopyridine (amount of catalyst) and stirred for 3 h at RT. The mixture was extracted with EtOAc and washed with 1N HCl, sat. $NaHCO_3$ and sat. brine. The organic layer was dried over Na_2SO_4. Removal of the organic solvent *in vacuo* gave the crude product. Purification by silica gel column chromatography (hexane/EtOAc = 15:1) gave the product (480 mg) in 70 % yield. NMR was measured using JEOL ECP-500 (^{1}H at 500 MHz, ^{13}C at 125 MHz) with $CDCl_3$ (99.8% atom ^{2}H, Kanto Chemical, Japan) as a solvent with a solvent signal of δ 7.26 ppm for ^{1}H and δ 77.0 ppm for ^{13}C as references for chemical shifts.

¹H NMR (300 MHz, CDCl₃): δ 0.617 (s, 3H), 0.814 (d, J = 6.60 Hz, 3H), 0.830 (d, J = 6.60 Hz, 3H), 0.908 (d, J = 6.60 Hz, 3H), 0.940 (s, 3H), 1.028 (d, J = 6.60 Hz, 3H), 1.438 (s, 9H), 1.446 (s, 9H), 2.704 (dd, J = 4.40, 16.86 Hz, 1H), 2.887 (dd, J = 4.77, 16.86 Hz, 1H), 4.475 (m, 1H), 4.762 (m, 1H), 5.190 (m, 2H), 5.368 (m, 1H), 5.545 (m, 1H).

¹³C NMR (75 MHz, CDCl₃): δ 12.022, 16.140, 17.571, 19.618, 19.930, 20.972, 21.073, 22.947, 28.020, 28.258, 28.291, 33.051, 36.405, 37.022, 37.786, 38.962, 40.417, 42.767, 42.768, 45.941, 50.192, 54.475, 55.642, 74.123, 79.861, 81.554, 116.214, 120.291, 131.941, 135.525, 138.197, 141.625, 155.518, 170.135, 170.653.

Ergosteryl-3β-*O*-L-aspartate

To 4-*tert*-Butyl-1-ergosteryl *N*-(*tert*-butoxycarbonyl)-*L*-aspartate (290 mg) in CH₂Cl₂ was added Et₃N (200 μL). After cooling with an ice bath, the mixture was added TMSOTf (300 μL) and stirred for 24 hrs at 0 °C. The mixture was extracted with CHCl₃ and washed with sat. NaHCO₃. The organic layer was dried over Na₂SO₄. Removal of the organic solvent *in vacuo* gave the crude product. Purification by silica gel column chromatography (CHCl₃ ~ CHCl₃/MeOH = 5:1) gave the product. NMR was measured with CD₃OD (99.8 % atom ²H, Merck, Switzerland) as a solvent with a tetramethylsilane signal of δ 0.00 ppm for ¹H and a solvent signal of δ 49.0 ppm for ¹³C as references for chemical shifts.

In silico analyses and determination of the phylogenomic distribution of ErdS

BLAST analyses

The protein sequence of the *Afm* AspRS-DUF2156 (ErdS) (encoded by the *AFUA_1G02570* gene in the Af293 strain) was used to perform PSI-BLAST searches (15) using non-redundant protein sequences databases and limited to fungi with 20,000 target sequences. Convergence was reached after 2 iterations. Sequences were then filtered using a home-made Python algorithm to recover only sequences of 250 to 2000 residues in length (7584 sequences) to exclude short and truncated versions of protein domains (AspRS and/or DUF2156). These filtered sequences were used to construct a protein size distribution plot in order to determine the average length of AspRS-DUF2156 proteins. Filtered sequences were then used to build a local BLAST database and a local BLAST search was performed using the sequence of the DUF2156 domain of *Afm* AspRS-DUF2156 as a query to detect DUF2156-containing proteins in the distribution plot (1006 sequences).

Phylogenomics analyses: To determine the phylogenomic distribution of AspRS-DUF2156 (ErdS), we used the *Afm* AspRS-DUF2156 sequence to retrieve by BLAST (15) all orthologs in each fungal class that belongs to the Dikarya sub-kingdom (Eurotio-, Lecanoro-, Xylono-, Dothideo-, Sordario-, Leotio-, Pezizo-, Orbioliomycetes, Saccharo- and Taphrinomycotina for ascomycetes, and in Agarico-, Puccinio- and Ustilagomycotina for basidiomycetes) and counted proteins containing a DUF2156 domain with length >750 residues, to take into account only complete and full-length AspRS-DUF2156 fusions, and not truncated forms that could account for sequencing or protein sequence prediction errors. No AspRS-DUF2156 fusions were detected outside Dikarya. We mapped the presence/absence of ErdS in each class onto the phylogenetic tree of fungi available at the JGI MycroCosm website (16). Distribution of ErdS was also monitored in the indicated selected species. In each case, we also indicated the presence of a canonical AspRS, involved in protein synthesis, for comparison.

Sequence alignments and analyses: Eleven ErdS (AspRS-DUF2156) protein sequences from *Aspergillus fumigatus*, *Aspergillus oryzae*, *Aspergillus flavus*, *Aspergillus niger*, *Penicilliumexpansum*, *Penicillium camemberti*, *Beauveria bassiana*, *Alternaria alternata*, *Neurosporacrassa*, *Cryptococcus neoformans* and *Schizophyllum commune* were used, together with 6 canonical AspRS sequences from *Saccharomyces cerevisiae*, *Candida albicans*, *A. fumigatus*, *A. oryzae*, *A. niger* and *N. crassa* to obtain a multiple alignment of all proteins with the Muscle program (17, 18) included in the Seaview package. Class II aaRS motifs 1, 2 and 3 (19) and the AspRS-specific QSPQ (20, 21) sequences were localized using the well characterized *S. cerevisiae*AspRS(20, 22). Residues known to be crucial for tRNA[Asp] acceptor arm, ATP, L-Asp or the Asp~AMP intermediate binding were identified according to the residues that had been experimentally identified in the yeast AspRS(9, 20, 23). The N-terminal extensions, AspRS and DUF2156 domains boundaries were determined according to the alignment.

Protein structure modelling and analysis: The amino acid sequence of the *Afm* AspRS-DUF2156 (ErdS) protein was used on the Phyre2 server (http://www.sbg.bio.ic.ac.uk/phyre2/html/page.cgi?id=index) (24) to obtain structurespredictions of either the AspRS (residues 1-593) or DUF2156 (residues 594-947) domains independently. Because sequence similarity with bacterial DUF2156 was very low (~20 %), the GNAT I and II subdomains – as well as the intercalated $\alpha^{(+)}$ helix – of the *Afm*DUF2156 (residues 594-947) were localized in the Phyre2 model by comparison with the

crystal structures of the DUF2156 domains of bacterial aaPGSs (25). The $\alpha^{(+)}$ helix of the DUF2156 domain was identified based on the model of the interaction inferred between tRNA$^{\text{Ala}}$ and the $\alpha^{(+)}$ helix of *P. aeruginosa* AlaPGS (25) where it was suggested to contact and recruit the Ala-tRNA$^{\text{Ala}}$ acceptor arm.

Supplemental References

1. T. Hartmann *et al.*, Validation of a self-excising marker in the human pathogen Aspergillus fumigatus by employing the beta-rec/six site-specific recombination system. *Appl Environ Microbiol***76**, 6313-6317 (2010).
2. D. G. Gibson *et al.*, Enzymatic assembly of DNA molecules up to several hundred kilobases. *Nat Methods***6**, 343-345 (2009).
3. I. Zadra, B. Abt, W. Parson, H. Haas, xylP promoter-based expression system and its use for antisense downregulation of the Penicillium chrysogenum nitrogen regulator NRE. *Appl Environ Microbiol***66**, 4810-4816 (2000).
4. K. Lambou, C. Lamarre, R. Beau, N. Dufour, J. P. Latge, Functional analysis of the superoxide dismutase family in Aspergillus fumigatus. *Mol Microbiol***75**, 910-923 (2010).
5. F. M. Muller *et al.*, Rapid extraction of genomic DNA from medically important yeasts and filamentous fungi by high-speed cell disruption. *J Clin Microbiol***36**, 1625-1629 (1998).
6. J. Maruyama, K. Kitamoto, Multiple gene disruptions by marker recycling with highly efficient gene-targeting background (DeltaligD) in Aspergillus oryzae. *Biotechnol Lett***30**, 1811-1817 (2008).
7. D. Busso, B. Delagoutte-Busso, D. Moras, Construction of a set Gateway-based destination vectors for high-throughput cloning and expression screening in Escherichia coli. *Anal Biochem***343**, 313-321 (2005).
8. S. N. Ho, H. D. Hunt, R. M. Horton, J. K. Pullen, L. R. Pease, Site-directed mutagenesis by overlap extension using the polymerase chain reaction. *Gene***77**, 51-59 (1989).
9. C. A. Ador L, Erbs P, Cavarelli J, Moras D, Gangloff J, Eriani G., Active site mapping of yeast aspartyl-tRNA synthetase by in vivo selection of enzyme mutations lethal for cell growth. *J Mol Biol***288**, 231-242 (1999).
10. L. Ador *et al.*, Active site mapping of yeast aspartyl-tRNA synthetase by in vivo selection of enzyme mutations lethal for cell growth. *J Mol Biol***288**, 231-242 (1999).
11. R. S. Sikorski, J. D. Boeke, In vitro mutagenesis and plasmid shuffling: from cloned gene to mutant yeast. *Methods Enzymol***194**, 302-318 (1991).
12. A. C. Dock *et al.*, Crystallization of transfer ribonucleic acids. *Biochimie***66**, 179-201 (1984).
13. F. Fischer *et al.*, The asparagine-transamidosome from Helicobacter pylori: a dual-kinetic mode in non-discriminating aspartyl-tRNA synthetase safeguards the genetic code. *Nucleic Acids Res***40**, 4965-4976 (2012).
14. H. Roy, M. Ibba, Monitoring Lys-tRNA(Lys) phosphatidylglycerol transferase activity. *Methods***44**, 164-169 (2008).
15. S. F. Altschul *et al.*, Gapped BLAST and PSI-BLAST: a new generation of protein database search programs. *Nucleic Acids Res***25**, 3389-3402 (1997).
16. I. V. Grigoriev *et al.*, MycoCosm portal: gearing up for 1000 fungal genomes. *Nucleic Acids Res***42**, D699-704 (2014).
17. R. C. Edgar, MUSCLE: a multiple sequence alignment method with reduced time and space complexity. *BMC Bioinformatics***5**, 113 (2004).

18. R. C. Edgar, MUSCLE: multiple sequence alignment with high accuracy and high throughput. *Nucleic Acids Res***32**, 1792-1797 (2004).

19. G. Eriani, M. Delarue, O. Poch, J. Gangloff, D. Moras, Partition of tRNA synthetases into two classes based on mutually exclusive sets of sequence motifs. *Nature***347**, 203-206 (1990).

20. E. G. Cavarelli J, Rees B, Ruff M, Boeglin M, Mitschler A, Martin F, Gangloff J, Thierry JC, Moras D (1994) The active site of yeast aspartyl-tRNA synthetase: structural and functional aspects of the aminoacylation reaction. in *EMBO J.*, pp 327-337.

21. B. H. Roy H, Reinbolt J, Kern D., When contemporary aminoacyl-tRNA synthetases invent their cognate amino acid metabolism. *Proc Natl Acad Sci U S A***100**, 9837-9842 (2003).

22. C. J. Eriani G, Martin F, Ador L, Rees B, Thierry JC, Gangloff J, Moras D., The class II aminoacyl-tRNA synthetases and their active site: evolutionary conservation of an ATP binding site. *J Mol Evol.***40**, 499-508 (1995).

23. K. S. Ruff M, Boeglin M, Poterszman A, Mitschler A, Podjarny A, Rees B, Thierry JC, Moras D., Class II aminoacyl transfer RNA synthetases: crystal structure of yeast aspartyl-tRNA synthetase complexed with tRNA(Asp). *Science***252**, 1682-1689 (1991).

24. L. Kelley, Mezulis, S, Yates, CM, Wass, MN, Sternberg, MJE (2015) The Phyre2 web portal for protein modeling, prediction and analysis. in *Nat Protocols*, pp 845-858.

25. S. Hebecker, Krauszeb,J , Hasenkampfa, T., Schneider, J., Groenewold, M., Reichelt, J., Jahn, D., Heinz, D.W., andMoser, J. (2015) Structures of two bacterial resistance factors mediating tRNA-dependent aminoacylation of phosphatidylglycerol with lysine or alanine. in *Proc Natl Acad Sci*, pp 10691–10696.

II. Additional results and discussions

II.1. Identification of functional residues of ErdS

II.1.1. The predicted structure of ErdS$_{Afm}$ reveals high similarities to bacterial aaLSs

In the accompanying paper we demonstrated through experimental procedures that fungal ErdSs aspartylate ergosterol through their DUF2156 domain in a tRNA dependent manner. To further decipher the molecular mechanism of those fungal proteins, we actually collaborate with Pr. O. Nureki's team to resolve the 3D structure of ErdS$_{Afm}$. Meanwhile, a prediction of the structure was obtained by submitting the 347 aa C-terminal sequence of ErdS$_{Afm}$ (i. e. ErdS$_{Afm}$-ΔAspRS containing the DUF2156 domain) to the Phyre2 server (Kelley *et al.*, 2015) and the closest experimentally established structures were detected with the Dali server (Holm and Rosenstrom 2010). As expected, the closest structural homologs found were DUF2156 domains of LysPGS from *B. licheniformis*, LysPGS from *Agrobacterium fabrum* and AlaPGS from *P. aeruginosa* (AlaPGS$_{Pae}$) [Protein Data Bank (PDB) entries 4V34, 4V36 and 5VRV respectively]. The predicted structure was superposed to AlaPGS$_{Pae}$ with Pymol and yield a rmsd of 11.2 Å when using normal align method without outlier rejection cycles and was decreased to 8.3 Å when setting 5 outlier rejection cycles. Because both proteins have low sequence similarity the cealign command is preferred and yielded a rmsd of 2.8 Å (**Figure S1-A**). Both structures seem very similar, but a closer look points out some variations in the positioning of secondary structure elements and the presence of inserted regions. Analyzing the secondary structures organizations show that the DUF2156 from ErdS$_{Afm}$ shares globally the same topological organization proposed for the bacterial AlaPGS (**Figure S-1B**) (Hebecker *et al.*, 2015). As detailed in the introduction, S. Hebecker and colleagues showed that a tunnel crosses bacterial DUF2156 domains and the latter is proposed to accommodate the aa-tRNA and the lipidic substrates at each extremity. In the center of this tunnel, a bottleneck allows the polar headgroup of PG to encounter the aa moiety (**Figures S-2C and S-2E**). A tunnel crossing the fungal DUF2156 domain was also present when analyzing its van der Waals surface but the bottleneck separating two cavities is absent or at least enlarged (**Figure S-2D**).

A
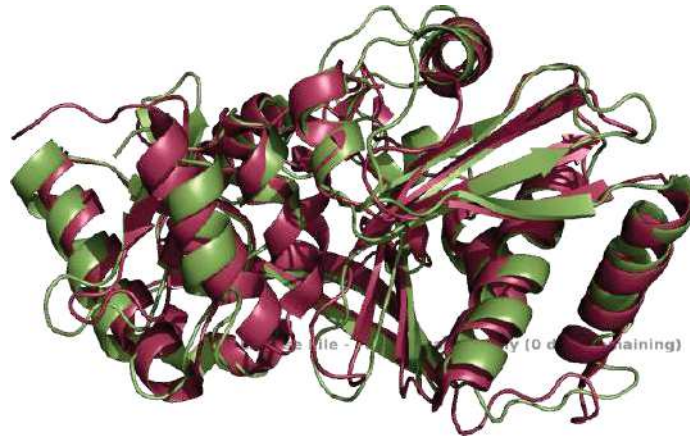
Resolved structure of the DUF2156 domain of AlaPGS from *P. aeruginosa*
Structure prediction of the DUF2156 domain of ErdS from A. fumigatus

B

GNAT domain 1

GNAT domain 2

INS 6-7

Positively charged helix ($\alpha^{(+)}$, binding of the acceptor stem of the tRNA)

★ Conserved residues of the PG pocket
★ Residues involved in binding the aa-tRNA's aa-moiety
★ Residues involved in binding the tRNA's 3'CCA end
* α-helix insertions in comparison to the consensus GNAT topology
* secondary structures predicted to be absent or severely shortened in ErdS$_{Afm}$

Figure S-1: Bacterial and fungal DUF2156 domains are predicted to share similar structural topology. (A) Structural superposition of DUF2156 domains (*i. e.* transferase domains) from AlaPGS$_{pae}$ (resolved structure, pdb: 4V34, raspberry) and from the fungal ErdS$_{Afm}$ (Phyre2 structure prediction, olive-green) was performed with the pymol cealign command and is shown in a wall-eye stereo view. **(B)** The Dupli-GNAT topology of AlaPGS$_{pae}$, presented in Figure I-17 (introduction), was implemented with additional details. GNAT domain 1 is in gray, GNAT domain 2 is in green and the positively charged α-helix ($\alpha^{(+)}$) delineating them is colored in blue. The DUF2156 domain of ErdS$_{Afm}$ is predicted to share similar topology as bacterial aaPGSs but α-helices 2 and 4 from GNAT domain 1 and α-helix 9 are predicted to be degenerated in the case of ErdS$_{Afm}$. **Figure B was modified from** Fields & Roy., 2018.

In addition to other bioinformatic predictions, these results strongly suggest that the fungal DUF2156 might also be composed of a tandem repeated GNAT fold were GNAT1 lacks the most N-terminally β-strand when compared to the consensus GNAT fold, while GNAT2 has two additional α-helices (8a and 9). However, α-helices 2 and 4 from GNAT domain 1 and α-helices 9 are predicted to be degenerated in the case of ErdS$_{Afm}$ (**Figures S-1B, S-2A and S-2B**).

Both GNAT domains of bacterial aaLSs are separated by an inserted positively charged α-helix ($\alpha^{(+)}$), considered as a signature feature common to all aa-tRNA transferases (ATT). Mutating basic residues (Lys, Arg) from this α-helix through inverting their charge (Glu) completely abolished the AlaPGS$_{Pae}$ activity (Hebecker *et al.,* 2015). As expected, $\alpha^{(+)}$ is also present in the structure prediction of ErdS$_{Afm}$ and in the present case both GNAT folds were delimited by this helix. In both structures the positively charged α-helix is thought to interact with the tRNA acceptor stem and is oriented perpendicular to the near located α-helix 8 which is also implicated in tRNA binding (**Figures S-2A and S-2B**).

The aa-tRNA cavity is mainly delineated by conserved secondary structure elements belonging to GNAT domain 2 which have equivalent features in the predicted structure of fungal DUF2156 (red in **Figure S-2A and S2B**). In AlaPGS$_{Pae}$ several residues forming this cavity were proposed to interact with the 3′-CCA of the tRNA (**Figure S1B**). The C-terminal extremity of α-helix 6, the N-terminal extremity of α-helix 7 and the extended loop (INS 6-7) between them contain highly conserved residues. Among them W712 of AlaPGS$_{Pae}$ found in α-helix 6 is in van der Waals distance from the tRNA 3′-CCA as shown through docking experiments (Hebecker *et al.,* 2015). Strikingly, the extended loop between α-helix 6 and 7 was also predicted in the fungal DUF2156 domain and **W785**, predicted in the C-terminus of α-helix 6 from ErdS$_{Afm}$-ΔAspRS, is proposed to interact with the tRNA 3′-CCA (**Figure S-2A and S-2B**). Importantly, the presence of an extended loop might be a characteristic feature of lipid aminoacylation factors regarding other ATT and is thought to be essential for the formation of a closed cavity ready to accept the lipid substrate. Due to its location, this feature might correspond to the interface between the aa-tRNA and lipid binding sites. Finally, α-helix 10 of AlaPGS$_{Pae}$ participates also to the aa-tRNA cavity formation and contains several conserved residues. Notably, F839, K840 and K842 were shown to be functionally relevant (most probably for binding of the 3′CCA of the tRNA (**Figures S-1B and S-2A**). This helix
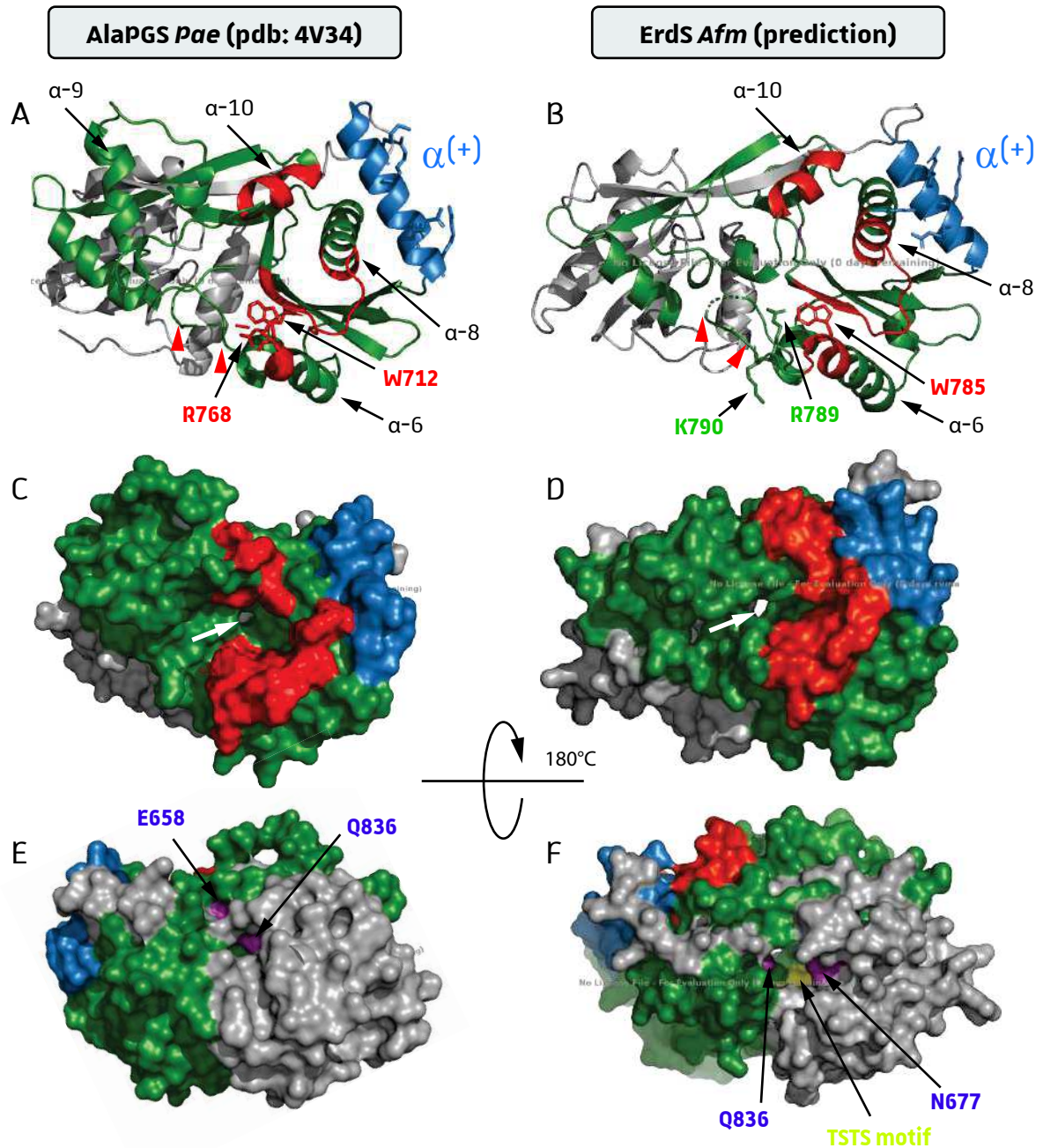
Figure S-2: Confronting the ErdS$_{Afm}$ DUF2156 domain (structure prediction, *right panel*) to AlaPGS$_{Pae}$ (4V34, *left panel*) as an early approach to identify functional residues. (A & B) Secondary structures of both proteins are shown as a cartoon. Residues of interest within $\alpha^{(+)}$ and within secondary structures delineating the tRNA-binding cavity (CAV$_{CCA-aa}$) are highlighted as well as some α-helices (α-6, α-8, α-9 and α-10) of particular interest. Based on this structural model, conserved residues W785, R789 and/or K790 from ErdS$_{Afm}$ are proposed to be functionally equivalent residues to AlaPGS$_{Pae}$ W712 and R768 (tRNA 3'CCA binding and catalysis). This is even more true for basic residues within $\alpha^{(+)}$, considered as the hallmark of ATT and thought to interact with the acceptor-stem of the substrate tRNA. The large loop inserted between helices 6 and 7 (INS 6-7) is indicated by red arrowheads. **(C & D)** ErdS$_{Afm}$ and AlaPGS$_{Pae}$ DUF2156 domains are in the same orientation as in (A & B) but their structures are shown as Van der Waals surfaces. This view suggests that ErdS$_{Afm}$ probably also forms a CAV$_{CCA-aa}$ to accommodate the charged acceptor stem of the tRNA as proposed for bacterial DUF2156 proteins. In addition, a tunnel traversing the protein is also predicted for ErdS$_{Afm}$ (white arrow, right panel) which suggests that the hydrophobic Erg substrate might probably enter the protein through a backdoor entrance (as proposed for bacterial aaPGS) in order to encounter the 3'CCA-aa of the aa-tRNA. (*continued*)

was also predicted in ErdS$_{Afm}$ and strikingly contains a well conserved sequence *i. e.* **F913**, **R914** and **K916** (**Figure S-2B**).

Concerning catalysis, AlaPGS$_{Pae}$ R768 residue (β-strand I) was bound to the α-carbonyl of the co-crystalized aa analog and was proposed to increase the electrophilicity of the aa-tRNA ester bond thereby favoring the nucleophilic attack of the lipid 3'OH (**Figure S-2A**). Such a key catalytic Arg (or even a closely related Lys) residue is absent from the fungal β-strand I but instead a "nearly" located **R789** pointing toward the aa-tRNA cavity was found in the internal loop **(Figure S-2B)**. Taken together, the recognition mechanism and the catalytic reaction might be achieved in similar ways by the DUF2156 GNAT domain 2 from bacterial and fungal aaLSs. Similar aa-tRNA recognition mechanisms were described in several ATT that contain at least one conserved GNAT fold with a positively charged helix (Moutiez *et al.,* 2017).

As explained in the general introduction, structural elements of ATT that are implicated in the second substrate recognition are generally less conserved. In dupli-GNAT-containing ATTs, it is assumed that several adaptations of GNAT domain 1 lead to the formation of the second substrate recognition site that can adopt various conformations (e. g. cleft formed by GNAT domain 1 of FemX to accommodate the UDP-MurNAc pentapeptide (Fonvielle *et al.,* 2013) vs. the lipid pocket of aaLSs). Because of the low conservation degree of GNAT domain 1 it is much more difficult to describe a general substrate recognition mechanism which might be idiosyncratic in each case. The situation might be similar in the present case since lipidic substrates of bacterial aaLSs (PG) and fungal ErdS (Erg) belong to distinct classes and their recognition modes, enabled through structural reorganization of GNAT domain 1, might differ. Numerous secondary structure elements of GNAT domains 1 and 2 participate to the formation of AlaPGS's lipid pocket that contains several conserved residues (Q636, E640, E658, S763, G800, M801 and R850) (**Figure S-1B and S-2E**). However, the analogy between both structures was not concluding for this purpose and multiple protein sequence alignments must be combined to structural predictions to target more efficiently residues involved in lipid recognition.

II.1.2. Identification of functional residues through mutagenesis

Even though the fungal DUF2156 from bacteria and from fungi are predicted to share several structural similarities, especially in the GNAT domain 2, their sequences vary considerably. When compared to its closest structural homologs (i. e. the DUF2156 domains of LysPGS from *B. licheniformis*, LysPGS from *Agrobacterium fabrum* and AlaPGS from *P. aeruginosa*), the 347 aa C-terminal sequence of ErdS$_{Afm}$ show only 14-16 % sequence identity. In addition, the inserted sequences mentioned above hinder the global alignment of bacterial and fungal DUF2156. In contrast, aligning DUF2156 sequences from filamentous fungi revealed several conserved residues as illustrated in (**Figure S-3**). Analysis of the present alignment combined to the predicted structure of ErdS$_{Afm}$-ΔAspRS allowed us to select a set of 29 residues potentially involved in lipid aminoacylation.

Mutated versions ErdS$_{Afm}$ were cloned, expressed in *Sce* and their lipid content was analyzed by TLC. The *in vivo* ErdS activities of mutants were evaluated by comparing their corresponding Erg-Asp spots to those found for *Sce* expressing the wt ErdS$_{Afm}$. However, total lipid amounts analyzed on TLC may vary from one sample to another. Thus Erg-Asp/PE ratio were estimated with ImageJ and values were classified into 4 classes: +++, activity comparable to wild type enzyme; +, moderately decreased activity (around 50 %); -, activity severally decreased and almost not detectable; --, no detectable ErdS$_{Afm}$ activity. 3 clones of each mutant were tested by TLC and equal expression of ErdS$_{Afm}$ was verified through WB. Results summarized in **Table S-1** were extracted from data presented on **Figure S-4**. Note that most mutant activities were unambiguously reproduced but, in few cases, (indicated in **Table S-1**) confronting the different experiments raised ambiguities. Note also the convenience of the employed acid sulfuric/MnCl2 based staining method which under UV light first greatly facilitates Erg-Asp (orange) recognition from other lipids and second allows to detect very low amounts of the modified lipid when compared to the ErdS wt associated level.

Figure S-2 (*continued*): **(E & F)** Structures from (A & B) were rotated at 180° as indicated. The backdoor entrance would be enabled by the CAV$_{Lip}$ that might accommodate the lipidic substrate as proposed by Hebecker *et al.*, 2015. Residues in purple are conserved and are proposed to interact with the lipid while the feature highlighted in yellow is a conserved motif foud in fungal ErdSs (**Figure S-3**) and might either directly participate in Erg recognition or to the formation of the corresponding CAV$_{Lip}$. GNAT domain 1 in gray; GNAT domain 2 in green; positively charged a-helix ($\alpha^{(+)}$) in blue; secondary structures delineating the tRNA-binding cavity (CAV$_{CCA\text{-}aa}$) in red; conserved residues within proposed CAV$_{Lip}$ in purple.
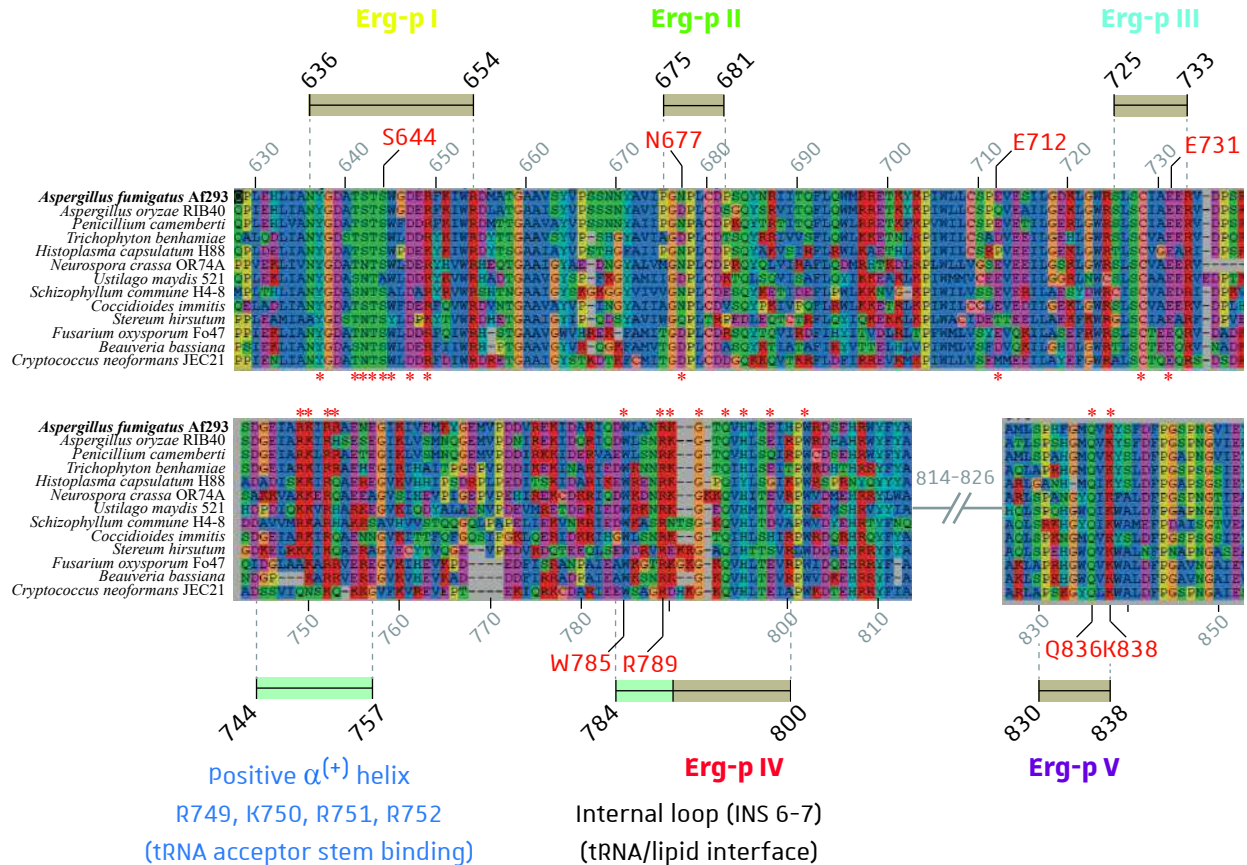
Figure S-3: Identification of conserved residues in the C-terminal DUF2156 domain of fungal ErdSs. DUF2156 domains of ErdS proteins from 13 representative fungal species were aligned. Numberings are indicated relative to the ErdS$_{Afm}$ sequence. Combining this approach with structure prediction described in **Figure S-2** reveals 5 ErdS regions suspected to be involved in the formation of the CAV$_{Lip}$ and/or in Erg-binding (Erg-p I to Erg-p V; see also **Figure S-4**). Candidate residues that were mutated and functionally tested (**Figure S-5** and **Table S-1**) are indicated by *. Sequences corresponding to Erg-p and to tRNA-binding motifs are highlighted by brown and cyan marks, respectively.

II.1.2.1. Identification of functional residues predicted to interact with the tRNA^{Asp} moiety.

We first wanted to assess the importance of the positively charged α-helix located between residues 744-757. Therefore, positive charges of R749, K750, R752 and R753 were neutralized or reversed by mutating them to Ala or Glu, respectively (mutants $\alpha^{(0)}$ and $\alpha^{(-)}$). No activity could be detected in mutants containing simultaneously the 4 mutated positions which further argued for the binding of aa-tRNA (probably the acceptor stem) by this helix (**Figure S-4 & Table S-1**). However, mutating simultaneously 4 residues might completely destabilize the secondary structure and according to mutagenesis studies performed on bacterial aaLS, single mutations of those residues to E might be enough to completely abolish the lipid modification activity. Therefore, it would be interesting to check whether the 4 single mutations of the fungal DUF2156 helix affect equally the activity.

The three above mentioned residues found in α-helix 10 and predicted to bind the 3'-CCA of the tRNA, were also selected for mutagenesis but we failed to express ErdS variants that are mutated at residues F913 and R914. In contrast **F916** is an essential functional residue as witnessed by the complete abolition of the activity through its mutation (**Figure S-4 & Table S-1**). Thus, α-helix 10 seems also to be relevant in fungal DUF2156 and testing F913 / R914 mutants should be repeated. Similarly, mutation of the highly conserved **W785**, the last residue of helix 6 preceding the large internal loop (INS 6-7), to its resembling His or to Ala, almost completely abolished the presence of Erg-Asp (**Figure S-4 & Table S-1**). Both identified residues are of high interest because their equivalent are present in bacterial aaLS and are assumed to interact with the 3'-CCA of the tRNA.

II.1.2.2. Identification of functional residues potentially involved in catalysis.

Regarding the catalytic Arg residue of AlaPGS$_{Pae}$ shown to interact with the α-carbonyl group of the aa substrate, **R789** and **K790** from ErdS$_{Afm}$ were ideal candidates as catalytic key players. Importantly, R789 is predicted to point toward the putative aa-tRNA binding-cavity while K790 points to the opposite direction (**Figure S-2B**). Therefore, R789 is more a favorable candidate
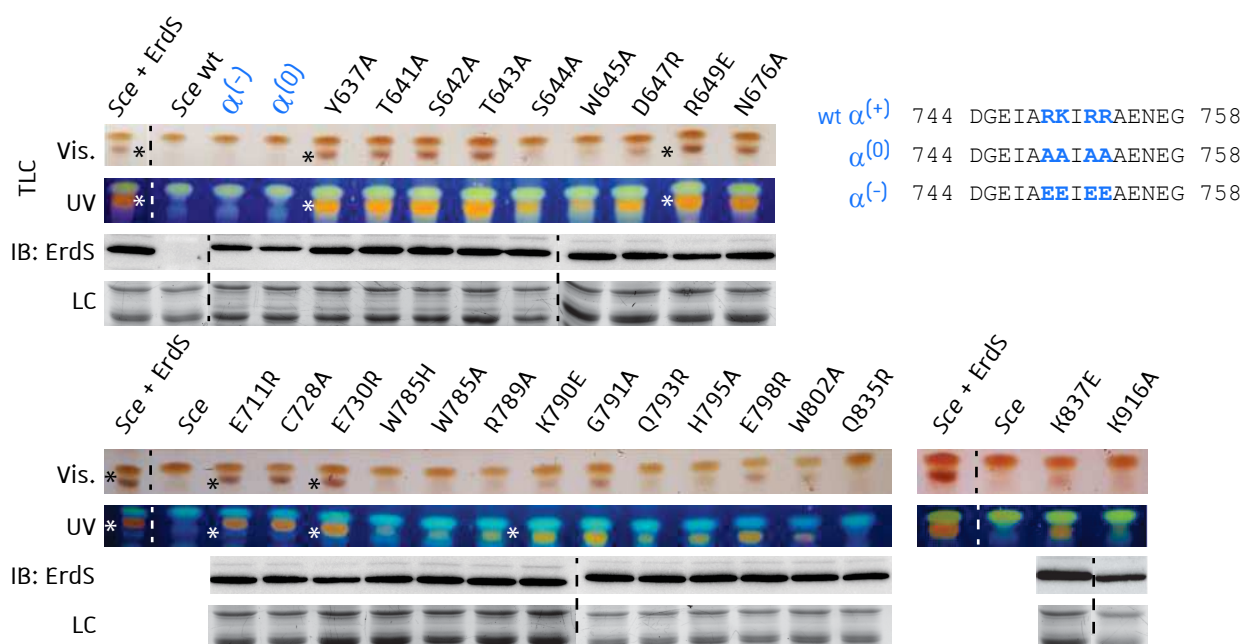
Figure S-4: Identification of functional residues in the DUF2156 domain of ErdS. Total lipids of *Sce* expressing the indicated ErdS$_{Afm}$ variants were separated by TLC and were observed under white light (Vis.) or under UV. TLC pictures were cropped to area of interest, equally treated, and images separated by dash lines arise from the same silica plate. In this way, total lipids from *Sce* expressing ErdS wt and *Sce* devoid of any ErdS form were spotted on each of the 3 TLCs presented here. Erg-Asp is colored in orange and indicated by *. Luminosity and brightness of images obtained under UV were treated to allow the detection of Erg-Asp traces. For example, a very slight orange coloration observed in W785 mutant indicates the presence of residual Erg-Asp amount, which is not detectable under Vis. The specific coloration allows also to distinct without ambiguity the modified lipid from other lipids. Crude extracts of Sce strains expressing the indicated ErdS mutant were submitted to SDS-PAGE. WB were performed with an anti-ErdS polyclonal antibody (IB: ErdS; LC: loading control). α(-) and α(0) correspond to mutants where basic residues (R,K) of α(+) were mutated to E or to A, as illustrated in the righ panel

Mutation	*in vivo* activity	Comments		Mutation	*in vivo* activity	Comments
Sce + ErdS wt	+++			C728A	+++	
Sce	--			E731R	+++	Erg-p 3
α(-)	--	tRNA acceptor stem		W785H	-	
α(0)	--	binding		W785A	-	tRNA 3'CCA binding
Y637A	+++			R789A	-	catalytic residue
T641A	+++			K790E	+	
S642A	+++			G791A	+++	
T643A	+++			Q793R	+	
S644A	+	Erg-p 1		H795A	+	Erg-p 4
W645A	+			E798R	+++	
D647R	+			W802A	+	
R649E	+++			Q836R	--	
N677A	+++	Erg-p 2		K838E	+	Erg-p 5
E712R	+++			K916A	--	tRNA 3'CCA binding

Table S-1: Identification of functional residues in the DUF2156 domain of ErdS. Results from figure S-5 were confronted to other TLC and mutants were classified into 4 classes; +++, activity comparable to wild type enzyme; +, moderately decreased activity (around 50 %); -, activity severally decreased and almost not detectable; --, no detectable ErdS$_{Afm}$ activity.

to ensure a catalytic role. Accordingly, mutating R789 to Ala severely decreased the Erg-Asp level but the residual activity is surprising since mutating the catalytic site should completely abolish the activity (**Figure S-4 & Table S-1**). It cannot be excluded that R789A mutation reorients partially К790 toward the aa-tRNA cavity, thereby enabling its interaction with the α-carbonyl of the cargo Asp which increases the electrophilicity of the ester bound of Asp-tRNA$^{\text{Asp}}$. In this hypothesis, К790 would partially complement the R789A mutant, explaining the observed residual activity. In comparison, К790E only showed a moderate decrease and one might speculate that the observed effect is due to the destabilization of the catalytic R789 residue. R789 and К790 are in the N-terminal region of the extended internal loop (INS 6-7) which contain several other conserved residues among fungal DUF2156.

II.1.2.3. Identification of functional residues potentially implicated in Erg accommodation.

We then focused on the recognition of the aa-acceptor (Erg) and we aimed to target features that participate to the formation of the putative Erg-pocket. Secondary structures of GNAT domain 1 are tilted together in bacterial aaLS and those and other adaptations are assumed to modulate the second substrate recognition. On the basis of the structural predictions and conserved sequences, we focused on five regions that might participate to structural rearrangement of the protein and the formation of the Erg-pocket indicated as "Erg-p" in **Figure S-3** and highlighted on **Figure S-5**. Some residues present in these features probably interact with Erg to favor the nucleophilic attack mediated by its hydroxyl group. Erg-p I harbors a highly conserved motif, enriched in polar but non-charged aa (mainly Ser/Thr), followed by an apolar aa, mainly Trp. In ErdS$_{Afm}$ it corresponds to T641-S642-T643-S644-W645 (**Figure S-2F** and **S-3**). Individual exchange of these residues to Ala showed an important *in vivo* activity decrease for **S644A** and **W645A** mutants. Results obtained for **D647R** and **R649E**, also located in the Erg-p I, are ambiguous and mutations in Erg-p III did not show their requirement for Ergosterol aspartylation. Note that Erg-p I and III are probably important for scaffolding GNAT domain I rather than for direct interaction with the substrates or for catalysis.

The internal loop between α-helices 6 and 7 might also participate to Erg accommodation. Mutants **G791A**, **E798R** and **W802A** did not significantly affect the Erg-Asp amount as compared to

α⁽⁺⁾

Erg-p I
Erg-p II
Erg-p III
Erg-p IV
Erg-p V
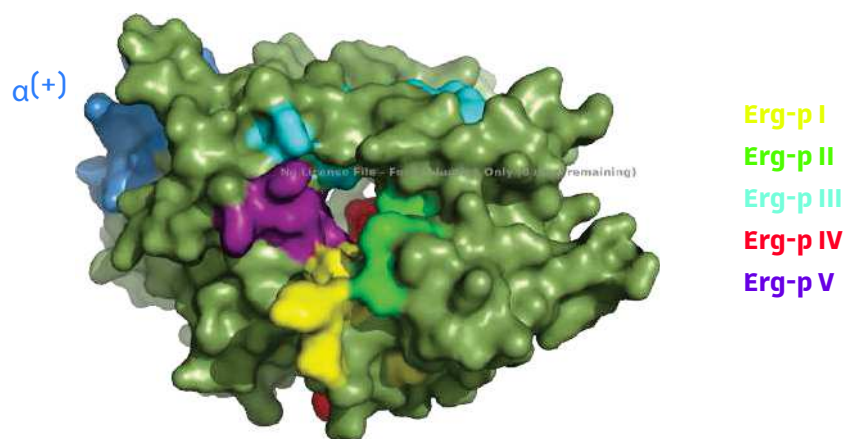
Figure S-5: Erg-p features face the predicted CAV$_{Lip}$ of fungal ErdSs. The predicted structure of ErdS$_{Afm}$ is presented in the same orientation as in **Figure S-2F**, showing the Erg-channel (*i. e.* CAV$_{Lip}$). Erg-p I-V are shown in the same colors as noted in **Figure S-3**. Beside the α$^{(+)}$-helix (blue), the rest of the protein is in olive-green without distinguishing both GNAT domains.

the wt level while **Q793R** and **H795A** severely decreased the lipid modification activity (Table S-1). However, both functional residues identified here are not predicted to be near or part of the Erg-pocket.

In contrast, Erg-p II and V might harbor residues pointing toward the Erg-pocket *stricto sensu* that probably interact with Erg. In bacterial AlaPGS, a highly conserved Gln residue (Q636) located in the lipid-binding pocket was identified (**Figure S-2E**). Similarly, **N677** of Erg-pocket II and **Q836** from Erg-pocket V are predicted to point toward the observed tunnel of ErdS (**Figure S-2F**). Strikingly, Q836R mutation completely abolished Erg-Asp synthesis while the result obtained for the N677A mutant is ambiguous and should be reinvestigated (Table S-1).

II.1.3. Conclusion and additional remarks

Taken together, results obtained here allowed the identification of several functional residues implicated in Erg-Asp synthesis by ErdS$_{Afm}$. The prediction of functional aa from the positively charged α-helix and from the GNAT domain 2 was much easier in comparison to the less conserved GNAT domain 1. Accordingly, the mechanism involved in Asp-tRNA^{Asp} recognition is probably achieved in a similar way to bacterial aaLS. In contrast aaLSs involving Erg were never described so far and thus the interaction mechanism between ErdS and Erg remains to be discovered. In comparison to the important knowledge about protein/aa-tRNA interaction, less is known concerning structural interaction between a protein and Erg. Interestingly, the binding mechanism of Cholesterol (structurally corresponding to Erg lacking the alkyl group at position 24 and presenting additional substitutions at positions 7 and 22) to proteins was described in some cases. Notably, membranous receptors have generally a linear consensus binding motif, called CRAK or CARK, involving 3 types of residues interacting with the different parts of Cholesterol: *1)* basic residues (Lys/Arg) interact with the polar hydroxyl group of Cholesterol, *2)* aromatic residues (Phe/Tyr) stack to the aliphatic rings and 3) aliphatic residues (Leu/Val) interact with the aliphatic chain of Cholesterol (Fantini *et al.*, 2016). Because of the high similarity between Erg and Cholesterol, it would be interesting to investigate if ErdS$_{Afm}$ uses a similar mechanism for lipid binding.

One important point that must be taken in consideration when analyzing this *in vivo* study, is that the Erg-Asp level was assumed to reflect the activity of ErdS variants. When the Erg-Asp spot significantly decreased or completely abolished, it was concluded that the corresponding aa is somehow important for lipid modification. In contrast, it is impossible to conclude when Erg-Asp levels of mutants were similar to those found for the wt ErdS using the *in vivo* approach since cultures were grown overnight without performing kinetics, and consequently, the modified lipid might accumulate even if the synthesis activity of ErdS is decreased. The bias introduced in the Erg-Asp-signal/ErdS-activity relation was also noticed during the extended mutagenesis study performed on AlaPGS which clearly showed that for some mutants the *in vivo* signals were comparable to the wt enzyme while *in vitro* analysis finally revealed significantly decreased activities associated for the same mutations (Hebecker *et al.,* 2011). Results obtained here must therefore be taken with care and other approaches assaying more directly the activity and facilitating their quantification will probably be more appropriate to investigate these aspects.

Furthermore, the molecular function of the herein identified residues can only be speculative and the result obtained here might be confronted in the next future to experimentally resolved (co-)structures and further biochemical experiments. For example, residues important for aa-tRNA binding can be identified by assaying the formation of protein/(aa-)tRNA complexes through Electrophoretic mobility shift assays (EMSA) or even through size exclusion chromatography. On another hand, lipid binding capacity of ErdS*Afm* mutants might be tested through other approaches such as lipid strip assays also called lipid-protein overlay assay (LPO) (Shirey *et al.,* 2017; Han *et al.,* 2020).

II.2.   Production of a tRNA^Asp transcript suitable for lipid modification by ErdS

tRNA transcripts are powerful tools to determine the substrate specificities of aaRSs or aa-tRNA utilizing enzymes. Previous studies have also used such approaches to characterize the tRNA determinants required for efficient aa-tRNA transferase activities (Hebecker *et al.*, 2011). During my thesis I principally used tRNAs purified from the yeast *Sce* for *in vitro* experiments assaying the lipid aminoacylation activities of fungal DUF2156 proteins. However, to further decipher their substrate specificities, I thought that it was a good strategy to obtain a transcribed tRNA^Asp from filamentous fungi that encode naturally ErdS. In this way, I focused myself on the unique tRNA^Asp found in *Afm* and I aimed to develop a tRNA^Asp transcript that will be used as a starting point for future characterizations of the aa-tRNA substrate specificity of ErdS.

II.2.1. Description and particularities of the tRNA^Asp from *Afm*

According to the Genomic tRNA database (Chan and Lowe 2009; Chan and Lowe 2016), *Afm* strains Af293 and A1163 contain 9 tRNA^Asp genes that all encode for tRNAs with an intron following position 37 (**Figure RT 1**). Surprisingly, the mature sequences of all encoded tRNA^Asp are identical and harbor a GUC anticodon; no isodecoders nor isoacceptors were detected. The unique mature tRNA^Asp is predicted to be composed of 75 nt's that forms canonical L-shape composed of an acceptor stem, anticodon and TΨC -stem-loops but some particularities were noticed in the D-stem-loop. The latter is formed by only 3 bp (instead of the canonical 4 bp), and the corresponding 10 bp loop lacks one nt between C_{12} and C_{17}. Finally, $G_{18}G_{19}U_{20}$ is followed by an additional C_{20A} and a 4 nt V-loop is predicted **(Figures RT1 & RT2)**.

Regarding the transcription assay, it is important to note that the mature sequence of tRNA^Asp~*Afm*~ contains an internal BstNI cleavage site. As explained in the Materials & Methods sections, plasmids containing the transcription template are linearized with BstNI prior transcription to obtain a 3'CCA extremity. Therefore, I aimed to mutate A_{50}-U_{64} bp which would avoid the internal BstNI restriction site. A_{50}-U_{64} bp is found in the unique tRNA^Asp from other *Aspergillus sp.* (*A. oryzae*, *A. clavatus* etc.) but several other species harboring ErdS activities too, such as *B. bassiana* (*Bba*) *N. crassa* (*Ncr*) and *P. camemberti* (*Pca*) as examples, have a G_{50}-C_{64} or C_{50}-G_{64} (**Figure RT 2**). The

A

| | 37 | | 38 | Intron | |
| 5' | | | | | 3' |

tRNA-Asp-1-1 UCCUCGAUGGUCUAACGGUCAUGAUUUCCGCUU**GUC**Acucaa-cagagaacgagGCGGGGAGACCAGGGUUCGACUCCCUGUCGGGGAG

tRNA-Asp-1-2 UCCUCGAUGGUCUAACGGUCAUGAUUUCCGCUU**GUC**Acucaa-cagagaacgagCGCGGGAGACCAGGGUUCGACUCCCUGUCGGGGAG

tRNA-Asp-1-3 UCCUCGAUGGUCUAACGGUCAUGAUUUCCGCUU**GUC**Acucca-acgagaacgagCGCGGGAGACCAGGGUUCGACUCCCUGUCGGGGAG

tRNA-Asp-1-4 UCCUCGAUGGUCUAACGGUCAUGAUUUCCGCUU**GUC**Acucca--agagaacgagCGCGGGAGACCAGGGUUCGACUCCCUGUCGGGGAG

tRNA-Asp-1-5 UCCUCGAUGGUCUAACGGUCAUGAUUUCCGCUU**GUC**Acucta-atgagaacgagCGCGGGAGACCAGGGUUCGACUCCCUGUCGGGGAG

tRNA-Asp-1-6 UCCUCGAUGGUCUAACGGUCAUGAUUUCCGCUU**GUC**Acuccg-atgagaacgagCGCGGGAGACCAGGGUUCGACUCCCUGUCGGGGAG

tRNA-Asp-1-7 UCCUCGAUGGUCUAACGGUCAUGAUUUCCGCUU**GUC**Acucga-atgagaacgagCGCGGGAGACCAGGGUUCGACUCCCUGUCGGGGAG

tRNA-Asp-1-8 UCCUCGAUGGUCUAACGGUCAUGAUUUCCGCUU**GUC**AcucaaattgagaacgagCGCGGGAGACCAGGGUUCGACUCCCUGUCGGGGAG

tRNA-Asp-1-9 UCCUCGAUGGUCUAACGGUCAUGAUUUCCGCUU**GUC**AcuctcaatgagaacgagCGCGGGAGACCAGGGUUCGACUCCCUGUCGGGGAG

B

tRNA^{Asp} from *Afm*   tRNA$^{Asp}_{Afm}$ (75 nt)

5' UCCUCGAUGGUCUAACGGUCAUGAUUUCCGCUUGUCACGCGGG<u>AGACC</u>AGGGUUCGACUCCCUGUCGGGGAGCCA 3'
                                                                   BstNI

Figure RT-1: Predicted tRNA^{Asp} sequences from *Afm*. (A) A total of 9 pre-tRNAAfm transcripts were predicted by the genomic tRNA database server (http://gtrnadb.ucsc.edu/) to occur in the *Afm* Af293 strain. Complementary sequences predicted to form the acceptor stem (red), the D-stem-loop (purple), the anticodon-stem-loop (green) and the T-stem-loop (cyan) are highlighted as well as the GUC anticodon (bold; positions 34, 35 and 36 of the mature tRNA) and the intron inserted between positions 37 and 38 (according to the consensus numbering of mature tRNAs). Sequence differences are only present in the intron that will be spliced during tRNA maturation. **(B)** The nucleotide sequence of the mature tRNA after splicing and addition of the 3'CCA is shown. The predicted secondary structure (cloverleaf representation) is found in **Figure RT-2**. The internal BstN1 restriction site is indicated.
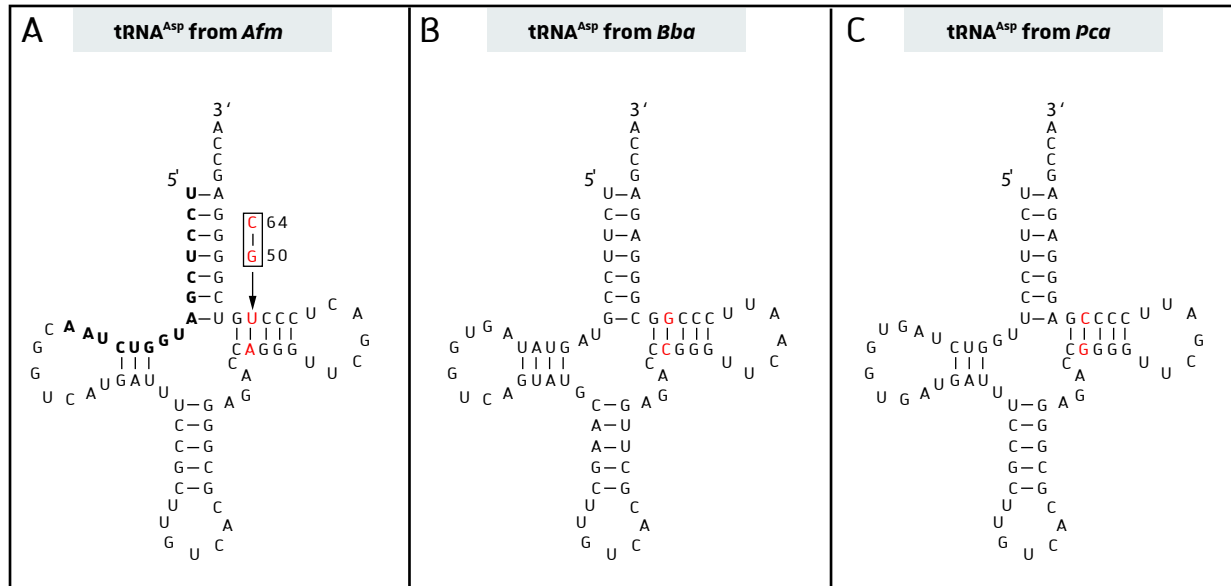
Figure RT-2: Covariance cloverleaf models of tRNA^{Asp} from fungi species encoding ErdS. (A) Secondary structure of *Afm* tRNA^{Asp}. The 5' sequence in bold was used as template for the design of HMH$_{wt}$-tRNA$^{Asp}_{Afm}$ tranzyme's stem I (see text and **Figures RT-3** and **RT-4**). For the present purpose, A50-C64 bp was mutated to G50-C64 to avoid the internal BstN1 restriction site. Our choice was supported by the fact that unique tRNA$_{Asp}$ found in *B. bassiana (Bba)* **(B)** and *P. camemberti (Pca)* **(C)** are degenerated at this position (red) and contain either C50-G64 or G50-C64, respectively. Because tRNA$^{Asp}_{Afm}$ sequence looks more like tRNA$^{Asp}_{Pca}$ and that both share the shortened D-stem (3 bp instead of the consensus 4 bp stem) I preferred to mutate tRNA$^{Asp}_{Afm}$ A50-C64 bp to G50-C64 rather than to C50-G64.

situation of *Pca* is particularly interesting because its tRNA^{Asp} is very similar to this of *Afm*; a unique isotype, composed of 75 nt, containing the same particularities in the D-stem-loop and harboring the GUC anticodon. Importantly, the tRNA^{Asp} from *Pca* contains G_{50}-C_{64} bp in the TΨC-stem instead of the A_{50}-U_{64} found in *Afm*. Therefore, I speculated that the N_{50}-N_{64} might not be essential, nor for tRNA aspartylation nor for Erg aspartylation mediated by ErdS. Accordingly, the TΨC-stem of bacterial tRNA does not contain determinants for its recognition by bacterial aaLSs, at least *in vitro* (Hebecker *et al.,* 2011). However, without further biochemical experiments I cannot certify that A_{50}-U_{64}, conserved in tRNA^{Asp} from *Aspergillus sp.*, is not involved for ergosterol aspartylation by ErdSs. Finally, I mutated A_{50}-U_{64} to G_{50}-C_{64} which allowed me to employ BstNI restriction enzyme for plasmid linearization before transcription.

II.2.2. Designing a construct for the synthesis of an accurate tRNA^{Asp} transcript

II.2.2.1. Fusing a ribozyme to overcome unfavorable 5' start of tRNA for transcription

The major strategy used to obtain a tRNA transcript is to clone the transfer DNA (tDNA) sequence downstream to the T7 promoter and to perform *in vitro* transcription as described in Materials & Methods. As a reminder, a BstNI restriction site is generated by adding two GG nt's after the terminal 3'CCA of the tDNA, and enzymatic restriction is performed before transcription to obtain a linearized template ending with CCA. Importantly, the produced tRNA transcript does not contain post-transcriptional modifications but remains suitable in most cases for *in vitro* aminoacylation assays. However, an absolute requirement for efficient T7 RNA polymerase transcription is the presence of nt G at the first tDNA position, and accordingly, G enriched 5' extremities further enhance the transcription process. For tDNA templates starting with unfavorable 5' nt (i. e. A, T or C), which is the case of tRNA$^{Asp}_{Afm}$ that starts with nt U, one ingenious solution is to fuse them adequately to an autocatalytic 5' *cis*-acting ribozyme, resulting to a so called transzyme (Fechter *et al.,* 1998) (**Figure RT 3A**). Basically, the principle of the transzyme is that a modified ribozyme moiety is fused upstream of the tRNA in order to generate a long transcript in which the tRNA 5' end is precisely generated by autocatalytic cleavage of the ribozyme. During transcription, the autocatalytic cleavage of the ribozyme releases a full-length
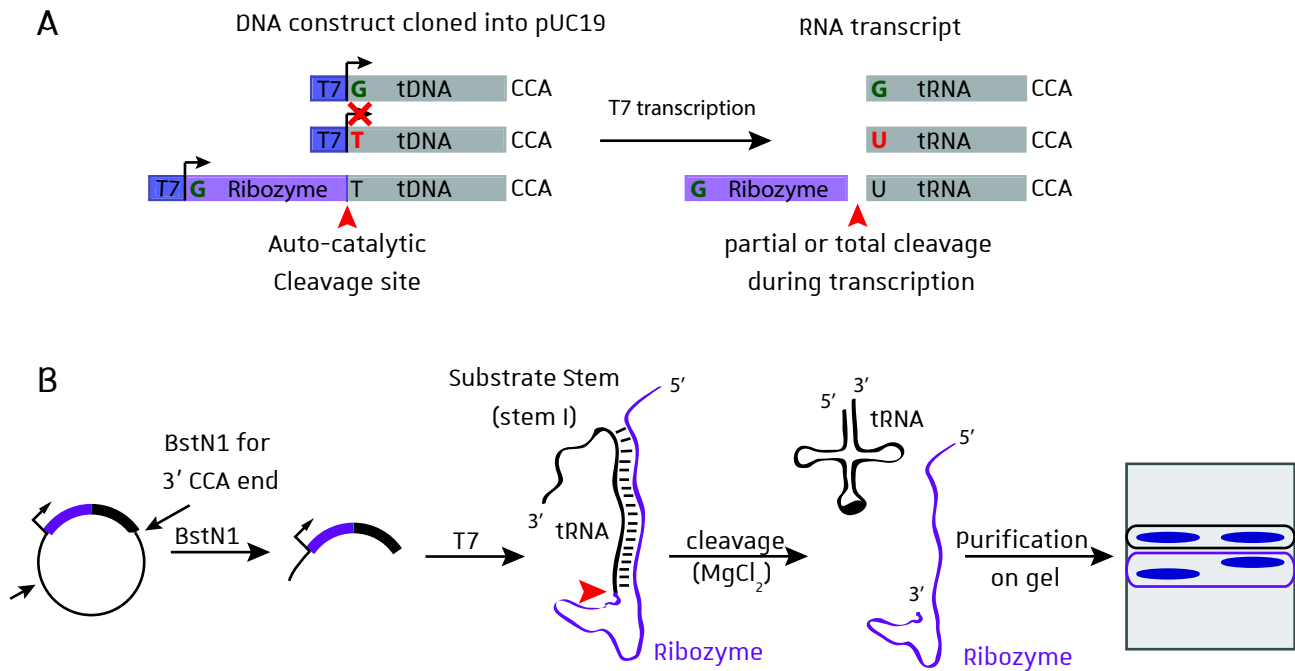
Figure RT-3: Transzymes as an alternative to overcome unfavorable 5' tRNA starts for transcription. (A) T7-mediated transcription is suitable for sequences starting with nt G at their 5' extremity (the complementary template ends with nt C at its 3' extremity). To overcome the issue of templates starting with unfavorable nts (e. g. tDNA encoding tRNA$^{Asp}_{Afm}$ starts with T) it is possible to fuse the sequence of interest (gray) to a ribozyme (purple) achieving auto-cleavage activity. During transcription, the autocatalytic activity of the fusion construction, called transzyme, results in cleaved ribozyme and free full-length tRNA. **(B)** Schematic representation of the strategy used in the present work. The Ribozyme-tRNA encoding-sequence is cloned in a plasmid under the control of a T7 promoter. Insertion of GG dinucleotide after the 3'CCA end of the tDNA forms a BstN1 restriction site. In this way, BstN1 treatment of the plasmid template enables to perform run-off transcription (mutating the internal BstN1 site within tRNA$^{Asp}_{Afm}$ was therefore a prerequisite). During transcription, the 5' sequence of the tRNA (total or partial according to the designed ribozyme) pairs with the 5' sequence of the ribozyme thereby forming the substrate stem. Importantly, the latter must be designed so that the cleavage-site (red arrowhead) is located between the last nt of the ribozyme and the first nt of the RNA of interest. Following cleavage, transcripts are separated by gel electrophoresis for analysis or for purification.

tRNA harboring a 5'OH extremity (**Figure RT 3B**). The latter is assumed to not significantly affect tRNA aminoacylation rate by aaRSs.

II.2.2.2. Description of the wt Hammerhead ribozyme and guidelines for designing transzymes.

The full-length HMH ribozyme, found in *Schistosoma* (HMH$_{wt}$) (Martick and Scott 2006) is composed of three stems, connected to each other by a three-way junction (**Figure RT 4A**). Both extremities of the ribozyme sequence (named here stem I 5' and 3' strands) form the stem I corresponding to the substrate stem, while stems II and III are closed by loops and form the catalytic core. The cleavage site is located at the phosphodiester bond, preceding the first nt of stem I's 3' strand. Importantly, the wild-type HMH contains an essential unpaired feature (bulge) found 6 nt after the cleavage site in its stem I. This bulge composed of $U_6A_7C_8$ faces a single U_{56} and interacts in *trans* through tertiary contacts with the loop of stem-loop 2. A second bulge is also found in the substrate stem and the presence of these unpaired secondary structures enhances by up to 1000-fold the autocatalytic cleavage activity when compared to HMH lacking these features (Canny *et al.*, 2004; Martick and Scott 2006; Meyer and Masquida 2014).

When designing a transzyme, the 3' strand of ribozyme's stem I must be replaced by the 5' sequence of the tRNA, so that the cleavage site immediately precedes the first nt of the tRNA part. Consequently, the sequence of the 5' strand of stem I must be adapted regarding Watson-Crick complementarity, but the design is complexified by the fact that both above mentioned bulges must be conserved. Partial base-pairing of the 5' sequence of the ribozyme with the 5' sequence of the tRNA acceptor stem, mimics the ribozyme stem 1 and determines the cleavage site.

M. Meyer and B. Masquida tested several versions of the HMH ribozyme and provided general guidelines for designing transzymes when using the HMH$_{wt}$. In this way, stem I's 5' strand should be composed by a dozen nt's and the tricky step takes places when predicting the unpaired features (bulges) found in stem I that must be preserved. Consequently, the 5' strand of stem I will only partially pair to the 5' sequence of the tRNA. In most cases it is not possible to predict the most efficient stem and therefore numerous constructs should be tested. Furthermore, the 5' sequence of stem I should start by three G residues to enhance transcriptional efficiency. Stem-
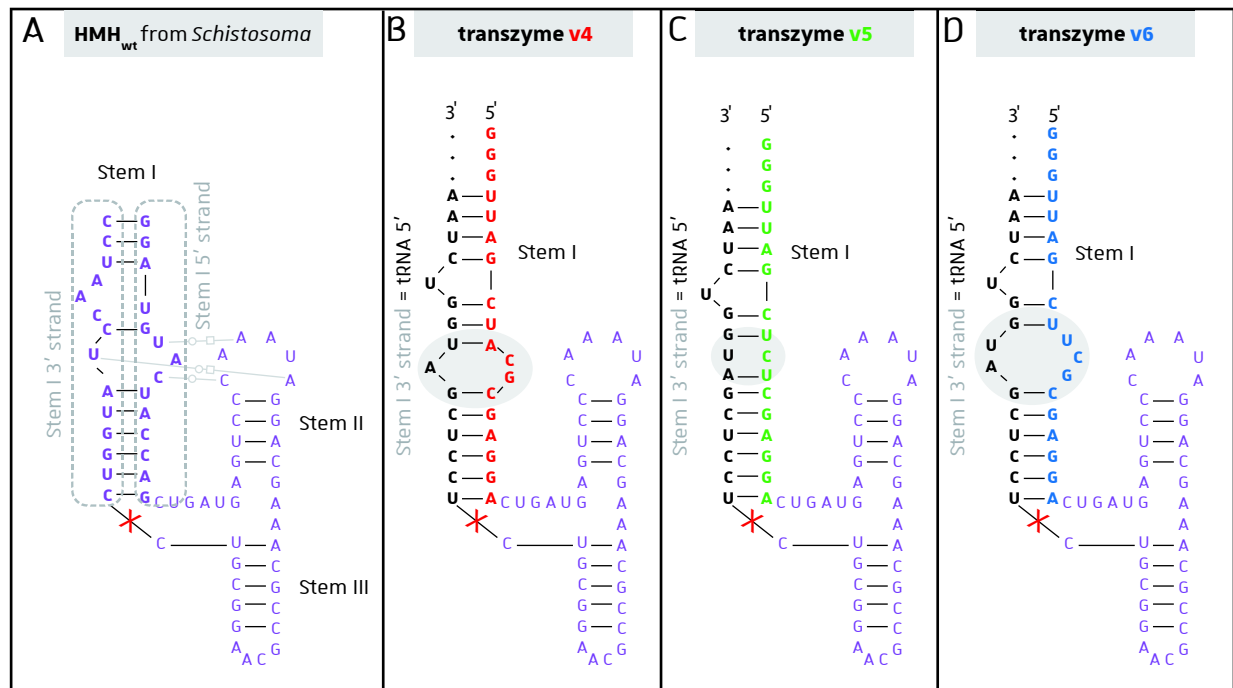
Figure RT-4: Secondary structure of the HMH$_{wt}$ ribozyme and covariance model folds of HMH$_{wt}$-tRNA$^{Asp}_{Afm}$ transzymes used in this study. (A) The wt sequence of the HMH ribozyme is in purple and stem I's (substrate stem) 5' and 3' strands are annotated. X indicates the cleavage site. **HMH$_{wt}$-tRNA$^{Asp}_{Afm}$** transzymes v4 **(B)**, v5 **(C)** and v6 **(D)** were designed using HMH$_{wt}$ as background. During the design, the 5' sequence of the tRNA (in black and bold) was fused to the HMHwt and the 5' strand (red for v4, green for v5 and blue for v6) of the substrate stem was adapted to obtain partial complementarity so that essential unpaired structures (bulges; see text) are conserved. In this way the 5' sequence of the tRNA dictates the sequence of the 3' strand of the expected ribozyme stem I.
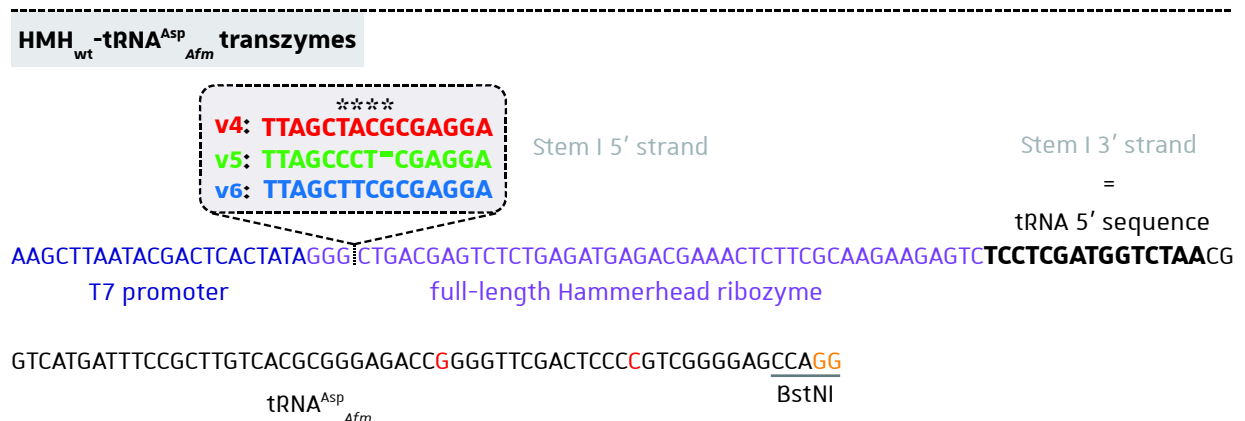
Figure RT-5: Engineering of HMH-tRNA expression constructs for T7 *in vitro* transcription. Stem I 5'strands of v4-, v5- and v6-transzymes are highlighted in the box and replace the 5'strand of the wt HMH's stem I (**Figure RT-4A**). The other HMH sequence (purple) remains unchanged. Positions varying between the 3 candidates are indicated by *. Mutated residues within the tRNA$^{Asp}_{Afm}$ (G50 and C64) are noted in red and the dinucleotide GG immediately following the 3'CCA extremity is in orange. When not indicated, same colors as in **Figure RT-4** are used.

loops 2 and 3, composing the catalytic core of the ribozyme, should be copied from the genuine HMH$_{wt}$ without any modifications (Meyer and Masquida 2014). The tRNA sequence is finally fused at the 3' end of the ribozyme sequence.

II.2.2.3. Design of stem I candidates for HMH$_{wt}$-tRNA$^{Asp}_{Afm}$ transzymes

According to the above recommendations, I designed *in silico* several HMH$_{wt}$-tRNA$^{Asp}_{Afm}$ candidates by using the mfold web server (Zuker 2003). Here I will only describe the 3 versions (v4, v5, v6) that were retained and experimentally tested. The sequence corresponding to the 15 nt's at the 5' extremity of the tRNA (7 nt from the 5' strand of the acceptor stem, U8, G9, 5' strand of the D-stem and the 3 first nt's of the D-loop) form the 3' strand of the ribozyme substrate stem. In all models the 5' strand of stem I starts with 5'UUAGCU3' which forms a stem composed of 6 bp and a single nt bulge. The following 4 nt's of the ribozyme 5' strand are involved in the formation of the crucial *trans*-interacting bulge and consequently, much attention should be paid when modeling this region. The accuracy of the putative bulge for scaffolding the ribozyme and subsequently the catalytic efficiency of the cleavage activity can only be determined through experimental procedures. The 3 candidates modeled here vary from each other exclusively in this 4 nt sequence and were designed so that positions A7 and/or U8 from tRNA$^{Asp}_{Afm}$ faces at least one C of ribozyme's 5' strand. In this way v4 and v6 might form bulges involving 3 and 5 nt's, respectively, while v4 has only an unpaired bp in this region. In all cases the variable 4 nt's are followed by 5'CGAGGA3' which are fully complementary to the 6 starting nt's of the tRNA and form together a stem, proximal to the ribozyme cleavage site (**Figures RT-4 B, C, D and 6**). Cloned sequences corresponding to HMH-tDNA constructs are detailed in (**Figure RT-5**)

II.2.3. Assaying *in vitro* transcription of HMH$_{wt}$-tRNA$^{Asp}_{Afm}$ v4, v5 and v6

The 3 HMH$_{wt}$-tRNA$^{Asp}_{Afm}$ transzymes (**v4**, **v5** and **v6**) were cloned and subjected to *in vitro* T7 transcription assays. The results on **Figure RT-6** unequivocally demonstrated the autocatalytic cleavage for HMH$_{wt}$-tRNA$^{Asp}_{Afm}$ v4, v5 and v6 during transcription. In facts, the upper band 1 is assumed to contain the remaining uncleaved HMH$_{wt}$-tRNA^{Asp}, while bands 2 and 3 contain the cleaved tRNA (75 nt) and the ribozyme, respectively. However, HMH$_{wt}$-tRNA$^{Asp}_{Afm}$ v5, containing 7 nt instead of 6 nt between the cleavage site and the critical bulge, presented an additional

	transzyme (1)	tRNA (2)	HMH (3)
v4	138	75	63
v5	137	75	62
v6	138	75	63
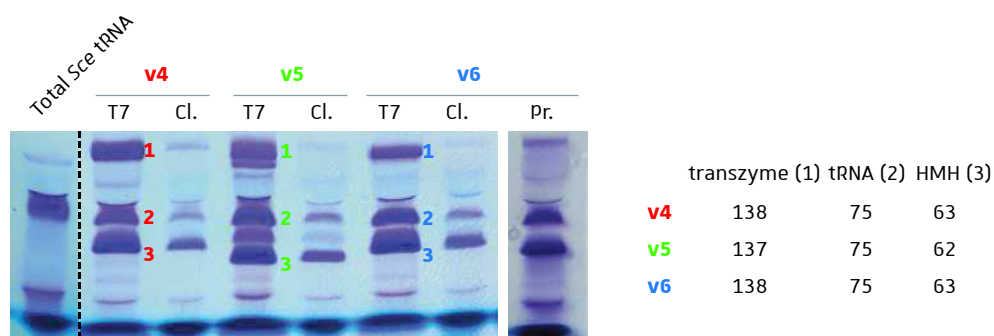
Figure RT-6: Transcripts analysis on 12 % (w/v) polyacrylamide gel containing 8 M urea. At the end of the transcription reaction, 5 volumes of transzyme buffer (50 mM Tris-HCl pH 8.0, 100 mM MgCl2) were added to yield higher cleavage rates. After incubation 1 h at 60 °C nucleic acids were precipitated. Aliquots before (T7) or after (Cl.) adding the transzyme buffer were analyzed on gel for each tested construct (v4, v5 and v6). An aliquot of precipitated products obtained with the v6 transzyme was also analyzed (Pr.). Bands of interest corresponding to non-cleaved transzymes (1), free tRNAs (2) and cleaved HMHs (3) are indicated and their expected size (bases) is specified in the right panel. The first lane corresponds to total tRNA from *S. cerevisiae* and served as indication of the molecular weight.

contaminant and was therefore excluded. In contrast, HMH$_{wt}$-tRNA$^{Asp}_{Afm}$ v4 and v6 showed slightly similar results but the ratio of cleaved transyme is higher for v6 than for v4. Finally, adding the transyme buffer further enhanced autocatalytic cleavage and removed almost completely the uncleaved forms as shown after precipitation of the v6 transcript. Taken together, HMH$_{wt}$-tRNA^{Asp} v6 seemed to be the most appropriate transyme construction to obtain purified transcript of tRNA$^{Asp}_{Afm}$. Consequently, HMH$_{wt}$-tRNA^{Asp} v6 transcript products were separated and purified "in-gel" using polyacrylamide gel electrophoresis as described in Materials & Methods sections. Around 100 µg of transcript tRNA$^{Asp}_{Afm}$ were obtained from 100 µg of linearized plasmid. This rate is lower than the common 500 µg described for yeast tRNAs transcripts (Fechter $et\ al.,$ 1998) but remains largely suitable for biochemical experiments.

Note that a minimal version of the Hammerhead (HMH$_{min}$) ribozyme was optimized especially for purifying transcript tRNAs starting with unfavorable nt at their 5' extremity (Fechter $et\ al.,$ 1998). Designing transymes with HMH$_{min}$ is much more convenient in comparison to the HMH$_{wt}$ that I used, since the chimeric stem I is fully paired but the cleavage activity of the minimal ribozyme is severally decreased in comparison to the HMH$_{wt}$ (Martick and Scott 2006). Without experimental procedures I cannot predict if the HMH$_{min}$ is suitable for the purification of tRNA^{Asp} but if it is the case, it will greatly facilitate the production of transcript tRNA^{Asp} mutants. Therefore, a transyme composed of a fusion between the correct HMH$_{min}$ and tRNA$^{Asp}_{Afm}$ should be tested.

II.2.4. The transcript tRNA$^{Asp}_{Afm}$ is well aminoacylated by the heterologous AspRS$_{Sce}$ and by the homologous ErdS$_{Afm}$

The ability of the heterologous yeast AspRS$_{Sce}$ and of the homologous ErdS$_{Afm}$ (the MBP-ErdS$_{Afm}\Delta$84 recombinant version was used here) to aminoacylate the transcript was tested (**Figure RT-7**). Aminoacylation assays were performed as described in the accompanying paper and the aminoacylation rate is defined here as the ratio between the concentration of Asp-tRNA^{Asp} at the plateau and the initial concentration of tRNA^{Asp}. The plateaus of the aminoacylation reaction showed that nearly 70 % of the transcript tRNA$^{Asp}_{Afm}$ was aspartylated by both tested enzymes. As expected, the cleaved ribozyme, used as a negative control, was not aminoacylated, while surprisingly only 18.4 % of native tRNA^{Asp} purified from Sce (REF) was charged in these conditions. Regarding former experiments performed in our lab, during which another batch of purified

A

min	tRNA$^{Asp}_{Sce}$ (2,5 μM)		tRNA$^{Asp}_{Afm}$ (2,5 μM)		cl. HMH$_{wt}$ v6 (5 μM)		tRNA$^{Asp}_{Afm}$ (5 μM)	
	cpm	μM	cpm	μM	cpm	μM	cpm	μM
0,5	705	0,29	47	0,02	n.d	n.d	n.d	n.d
1	900	0,38	60	0,03	n.d	n.d	73	0,06
3	1129	**0,47**	265	0,11	31	0,01	411	0,31
5	1142	**0,48**	1156	0,49	35	0,01	919	0,70
10	1063	**0,45**	2684	1,13	29	0,01	2631	1,99
15	n.d	n.d	n.d	n.d	31	0,01	n.d	n.d
20	1010	**0,42**	4017	**1,69**	31	0,01	3895	2,95
30	1117	**0,47**	3922	**1,65**	33	0,01	4537	**3,44**
45	1160	**0,49**	4082	**1,72**	n.d	n.d	4581	**3,47**
60	1077	**0,45**	4194	**1,77**	n.d	n.d	5172	3,92

[AspRS$_{Sce}$] = 1 μM

AS [^{14}C]Asp = 237 cpm/pmol

prec. aliquot: 10 μl

[ErdS$_{Afm}$] = 1 μM

AS [^{14}C]Asp = 264 cpm/pmol

prec. aliquot: 5 μl

B
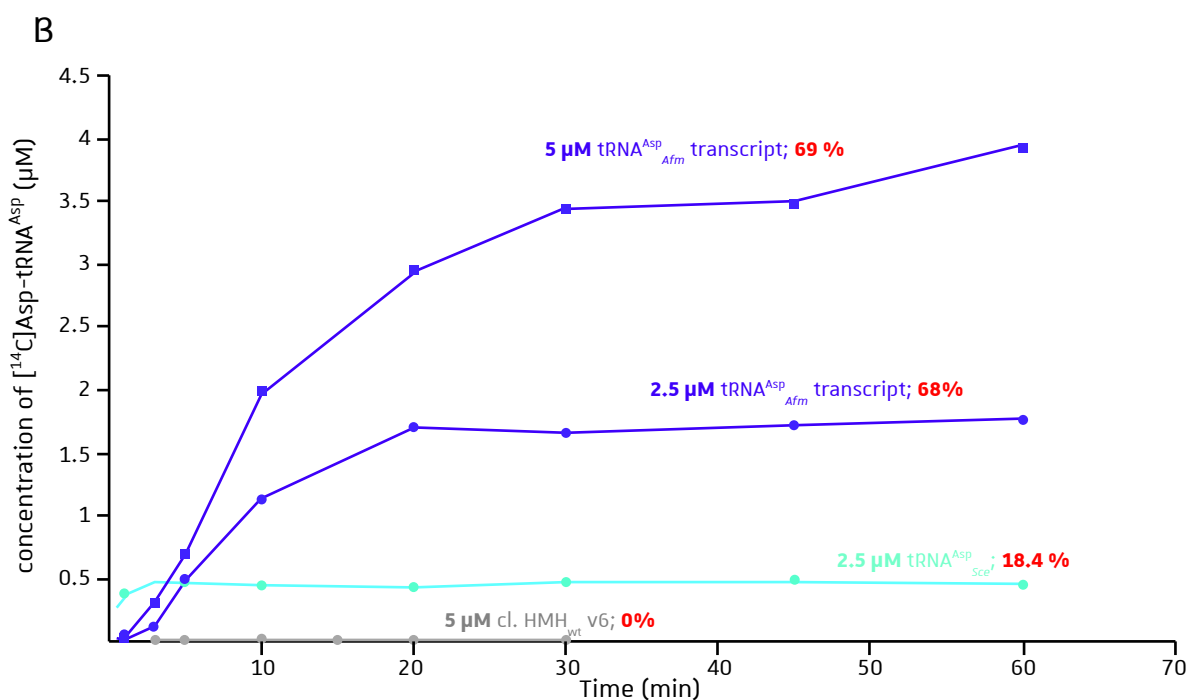
Figure RT-7: The transcript tRNA$^{Asp}_{Afm}$ is highly aminoacylable by ErdS$_{Afm}$ and by the cytosolic AspRS from *Sce*. (A) As explained in the Material & Methods sections of the accompanying paper, aliquots of the reaction mixture are precipitated onto Whatman papers at each indicated time plots. Uncharged [^{14}C]Asp is washed away and radioactivity signals (cpm) obtained after counting with a scintillation counter are issued from [^{14}C]Asp-tRNA$_{Asp}$. Raw values are divided by the specific activity (AS) to obtain the amount of aspartylated tRNAAsp and further dividing by the volume of the precipitated aliquot leads to the concentration of [^{14}C]Asp-tRNA$_{Asp}$ (μM). Identities of RNAs and their concentrations (in brackets) added at the beginning of the reaction are indicated at the top of each series. Note that data's result from two experiments (separated by dash lines) and that assays were performed in the presence of AspRS$_{Sce}$ or a recombinant version of ErdS$_{Afm}$, (MBP-ErdS$_{Afm}$Δ84) as indicated. (B) Graphical representation of aminoacylation kinetics obtained from data's in (A). Aminoacylation rates (red) correspond to the ratio between the mean of Asp-tRNA^{Asp} concentrations at the plateau (values in bold in (A)) and the initial concentration of RNA (bold in B). Purple, transcript tRNA$^{Asp}_{Afm}$; blue, tRNA$^{Asp}_{Sce}$; grey, cleaved HMH$_{wt}$ ribozyme; cl. HMH$_{wt}$v6, cleaved ribozyme part purified in gel.

tRNA$^{Asp}_{Sce}$ was used, I suspect that the tRNA$^{Asp}_{Sce}$ used here was partially degraded or denatured. These results clearly demonstrate that the transcript tRNA$^{Asp}_{Afm}$ is a highly suitable substrate for AspRS$_{Sce}$ and more importantly for ErdS.

These results also suggest that the velocity of tRNA$^{Asp}_{Afm}$ aspartylation by both tested AspRS homologs is low when compared to tRNA$^{Asp}_{Sce}$. Despite all substrates were set in excess (i. e. [tRNA] and [Asp] >> K$_M$) in addition to the increasing amount of added enzymes, the plateau was reached only after 10 to 20 minutes with AspRS$_{Sce}$ and even later by ErdS$_{Afm}$. These observations require more extensive investigations since the apparent slow reaction can be due to several reasons. One may speculate that the presence of the additional domain hijacking the aa-tRNA (i. e. DUF2156 domain) might hinder its release and delays the reaction. However, our preliminary data suggest that tRNA$^{Asp}_{Sce}$ is slowly aminoacylated by both, the full-length ErdS$_{Afm}$ and the ErdS$_{Afm}$-ΔDUF2156 (not shown). In addition to that, AspRS$_{Sce}$ presented low aminoacylation velocity only for the transcript tRNA$^{Asp}_{Afm}$ but not for its homologous tRNA$^{Asp}_{Sce}$. Because the several tRNA^{Asp}-genes from *A. fumigatus* encode a single version of tRNA^{Asp}, it will be interesting to compare the kinetic aminoacylation parameters for the cytoplasmic AspRS and for *Afm* ErdS. Such an approach combined to structural investigations could reveal how *Afm* partitions a pool composed by a unique tRNA$^{Asp}_{Afm}$ for lipid modification and protein biosynthesis.

II.2.5. The transcript tRNA$^{Asp}_{Afm}$ is used *in vitro* by ErdS$_{Afm}$ for lipid aminoacylation

The suitability of the transcript tRNA$^{Asp}_{Afm}$ for Erg aminoacylation was tested by an *in vitro* system and the general procedure used for this lipid aminoacylation assay (LA assay) is described in the accompanying paper. In the present case, the recombinant ErdS$_{Afm}$ was assayed as for the aminoacylation assay described in the previous section, but the reaction mixture was supplemented with 0.5 mg / ml of sonicated ergosterol. Reaction was stopped after 45 min by lipid extraction followed by separation on TLC. Finally, radiolabeled species were analyzed using a Typhoon TRIO variable Mode Imager (GE Healthcare) (**Figure RT-8**).

Results confirmed that [14C]-Asp is indeed transferred from the transcript tRNA$^{Asp}_{Afm}$ onto ergosterol. Surprisingly, when the experiment was conducted in the presence of tRNA^{Asp} from *Sce* the amount of aspartylated ergosterol was increased which suggest that ErdS has higher substrate

A **B**

tRNA$^{Asp}_{Afm}$	+	+	−		+	+	+	+
tRNA$^{Asp}_{Sce}$	−	−	+		−	−	−	−
RNase	−	+	−		−	+	+	+
ErdH	−	−	−		−	−	+	−
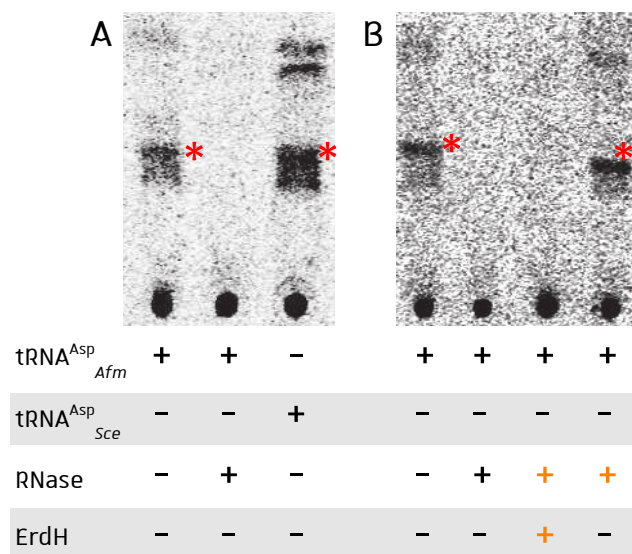
Figure RT-8: The transcript tRNA$^{Asp}_{Afm}$ is used by ErdS$_{Afm}$ for Erg aspartylation. (A) LA assays were conducted in the presence of MBP-ErdS$_{Afm}$Δ84 1 µM, [14C]Asp 10 µM, tRNA 5 µM and 0.5 mg / ml commercial Erg. (B) The same experiment was repeated, and 2 additional assays were incorporated to confirm that the tRNA$^{Asp}_{Afm}$ dependent product (i. e. Erg-Asp) is hydrolyzed by ErdH$_{Afm}$ (Lipid deacylation assay). In these cases, the assay was performed as in (A), but 1µl of RNase A (10 mg/ml) was added after 45 min, incubated for 5 min, supplemented or not with 1 µM of recombinant ErdH$_{Afm}$ and incubated for 30 min. *, Erg-Asp; -, absence; +, presence; +, added after 45 min of the reaction. For more details on the procedure, refer to the accompanying paper.

specificity for tRNA$^{Asp}_{Sce}$. However, the observed variation can be due to several reasons: first, the absence of tRNA post-transcriptional modifications and second, the mutated bp in the TΨC-stem (A$_{50}$-U$_{64}$ to G$_{50}$-C$_{64}$). Furthermore, the concentration of tRNA was identical in both experiments but, as shown above, their aminoacylation rates vary and the velocity of tRNA$^{Asp}_{Afm}$ and tRNA$^{Asp}_{Sce}$ aspartylation by the AspRS domain of ErdS was not compared yet. In our initial hypothesis we postulated that Asp-tRNA^{Asp} is channeled from the AspRS to the DUF2156 active site. The presence of the lipidic substrate and thus the transferase activity of the DUF2156 might regulate the velocity of the global reaction. To further complexify the situation, tRNA$^{Asp}_{Afm}$ and tRNA$^{Asp}_{Sce}$ and their aspartylated forms might be differently recognized by both domains constituting ErdS. These explanations illustrate well the complexity of the issue and the necessity to characterize enzymatically ErdS, especially which reaction, tRNA aminoacylation or lipid transfer, is rate-limiting.

II.2.6. Concluding remarks

In a more global reflection, the transcript tRNA$^{Asp}_{Afm}$ is suitable for both activities catalyzed by ErdS despite the mutation in the TΨC-stem (A$_{50}$-U$_{64}$ mutated to G$_{50}$-C$_{64}$), the lack of post-transcriptional modifications, and the 5' hydroxyl group (instead of the classical 5' mono-phosphate). As speculated here, further kinetic characterization of ErdS is needed (we plan to characterize the kinetic parameters of ErdS-ΔAspRS and ErdS-ΔDUF2156). Importantly, the transcript tRNA$^{Asp}_{Afm}$ obtained here constitutes a powerful tool to further decipher the substrate specificity of fungal DUF2156 proteins. Regarding the work done for bacterial aaPGSs, it will by particularly interesting to construct truncated versions of the tRNA (i. e. mini- and micro-helices) as well as single mutations in the acceptor stem. Finally, the herein obtained transcript is used by our collaborators from the laboratory of Pr. O. Nureki to resolve the 3D structure of ErdS$_{Afm}$ in complex with its tRNA.

III. Annex I: Adapting lipid analysis for the characterization of Erg-Asp and some additional results

In the accompanying paper we demonstrated that AspRS-DUF2156 from *Afm* has dual-activity which together result to the synthesis of Erg-Asp. In the present section I aimed to report many optimizations that were brought to the lipid analysis method that finally enabled the stepwise discovery of Erg-Asp. As a reminder, the primary goal in the early steps of the project was to determine if fungal DUF2156 proteins are responsible for the presence of an additional lipid. I studied both detected fungal DUF2156 proteins (initially called AspRS-DUF2156 and fDUF2156) in parallel but, as it will be highlighted in the present section, the characterization of fDUF2156 was more difficult and therefore we focused our efforts primarily on the AspRS-DUF2156 protein.

III.1.   Critical adaptations of TLC conditions enabling the detection of the AspRS-DUF2156 dependent lipid

III.1.1. The initial TLC conditions failed to reveal additional lipids in the presence of fungal DUF2156

Initially, AspRS-DUF2156 and fDUF2156 encoded by *Afm* were expressed in the heterologous yeast model *Sce* to determine if expression of AspRS-DUF2156 and fDUF2156 are responsible for the presence of additional lipids. Total lipids were extracted from the different *Sce* strains (adapted Bligh & Dyer; see Material & Methods) and analyzed by TLC. The experimental procedure was inspired to investigate phospholipid contents of total lipids, by using CHCl3 : MetOH : 25 % NH3 (68 : 35 : 5) as TLC eluent and ninhydrin or phosphomolybdate as staining reagents (**Figure AL-1A and B**). However, this strategy did not reveal the presence of an additional lipid despite numerous experimental adaptations, including lipid extraction and TLC conditions.

III.1.2. The MnCl2 / Sulfuric acid staining method, the trigger for the detection of AspRS-DUF2156 dependent lipid.

The previous experiment was repeated with the same lipid samples, but I switched to the MnCl2 / Sulfuric acid staining-method. My curiosity was aroused by the darker LA spot in total lipids
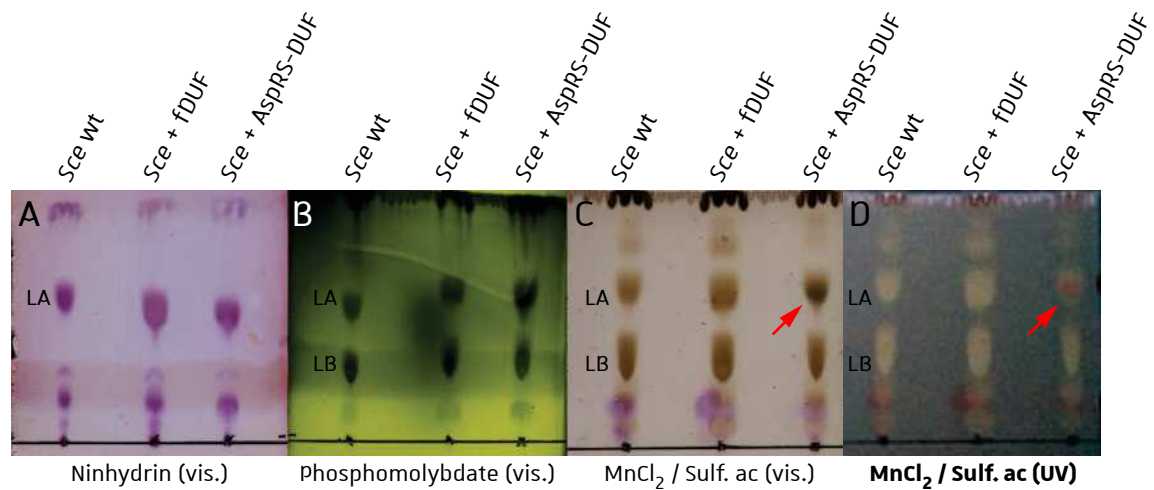
Figure AL-1: 1D-TLC analysis of total lipids and optimization of the TLC staining method. Total lipids from wt *Sce* or expressing heterologous DUF2156 proteins from *Afm* were extracted by the adapted Bligh & Dyer method and separated by TLC with the **CHCl$_3$: MeOH : NH$_3$ 68 : 35 : 5** (v : v : v) developing solvent. Chromatograms were revealed with the indicated staining methods and observed either under white light (vis.) or under UV. Red arrows indicate the AspRS-DUF2156 dependent lipid (LX1) modification that comigrates with spot LA. fDUF, fDUF2156; AspRS-DUF, AspRS-DUF2156.

from *Sce* expressing AspRS-DUF2156 when compared to *Sce* wt (**Figure AL-1C**) and strikingly, when the same plate was visualized under UV light the corresponding spot had a completely different color in comparison to the other spots (**Figure AL-1D**). This suggested that either a lipid from spot LA is modified without affecting its Retardation factor (Rf) or that the migration pattern of another lipid species, initially migrating at a different position, is relocated due to the presence of AspRS-DUF2156. Due to the poor quality of this result, another possibility was that the unstandardized amount of analyzed lipids lead to this distinct coloration. However, when the experiment was repeated, the quality of the result was remarkably increased, and it became much more convincing that spot LA might contain an additional lipid in the presence of AspRS-DUF2156 (**Figures AL-2A and AL-2B**).

The numerous variations observed between both results can be due to several reasons. In facts, both experiments were conducted identically except that the eluent (or the developing solvent) was not freshly prepared in each case. This and other factors, such as the environment temperature, might affect the saturation level of the TLC chamber and consequently the migration pattern of the lipid sample. Importantly, lipids were eluted in the same order. On another hand, chromatograms in **Figures AL-1D and AL-2A** were both stained with the MnCl2 / sulfuric acid solution and coloration differences observed between both results illustrate the consequences of overheating plates (**Figures AL-1D**) during revelation.

Note that in all cases, LX1 remains distinguishable from other lipids and that in optimal staining conditions, LX1 is colored in orange under UV light. Consequently, using this staining method is very convenient when aiming to study LX1, especially when analyzing total lipids. Furthermore, as witnessed by results presented in previous sections (*i. e.* concerning mutagenesis) the staining method used here allowed to distinguish the presence of the modified lipid even when its amount was severely decreased.

Unfortunately, these results did not reveal any modification in the total lipid pattern when fDUF2156$_{Afm}$ was expressed in *Sce*.
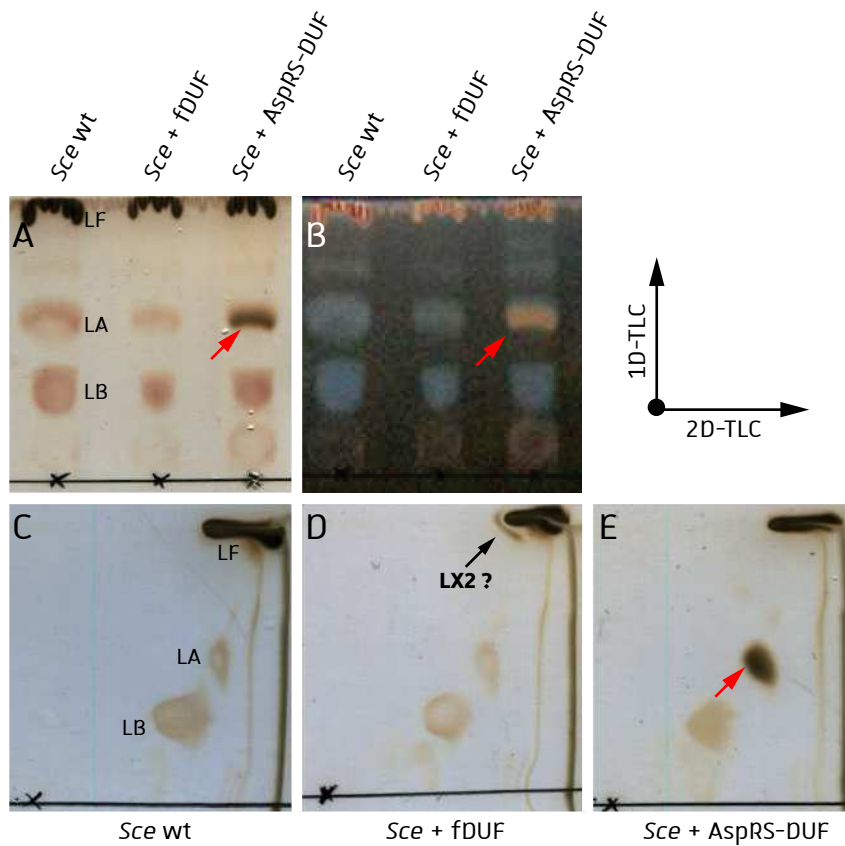
Figure AL-2: 2D-TLC analysis of total lipids from of *Sce* strains expressing fungal DUF2156 proteins. **(A)(B)** Lipids were extracted from the indicated *Sce* strains, separated by 1D-TLC and stained with the MnCl$_2$ / Sulfuric acid method. Note the characteristic dark brown and orange colorations of the AspRS-DUF2156 dependent lipid modification (red arrow) under white (A) and UV light (B), respectively. Concomitantly, total lipids from *Sce* wt **(C)** and *Sce* expressing heterologous fDUF2156$_{Afm}$ **(D)** or AspRS-DUF2156$_{Afm}$ **(E)** were separated by 2D-TLC. Note the presence of the additional spot with fDUF2156 (LX2) that migrates near to the cross formed by both migration fronts. 1D-TLC solvent: CHCl$_3$: MeOH : NH$_3$ 68 : 35 : 5 (v : v : v); 2D-TLC solvent: Hexane : MeOH : CHCl$_3$: glacial acetic acid 60 : 20 : 10 : 10 (v : v : v : v)

III.1.3. 2D-TLC fails to further resolve LX1 from spot LA.

The same lipid samples analyzed by 1D-TLC and presented in **Figures AL-2A** and **AL-2B** were concomitantly analyzed by 2D-TLC to verify if LX1 is separable from other specie(s) in the LA spot. Results further assessed the presence of an AspRS-DUF2156 dependent lipid modification but failed to separate lipid species from spot LA (**Figure AL-2E**).

Concerning fDUF2156, the 1D-TLC failed again to reveal a modified lipid, but interestingly an additional spot (LX2) was noticed near the crossing of both migration fronts after 2D-TLC. However, due to the low reproducibility of this result I unfortunately considered that this spot might correspond to an artefact (**Figure AL-2D**). Note also the dark brownish color of spot LF, corresponding to apolar lipids such as ergosterol.

III.1.4. Optimization of the 1D-TLC developing system separates LX1 from spot LA

Finally I succeed to further separate the AspRS-DUF2156 dependent lipid on 1D-TLC, by adapting the TLC developing buffer to CHCl3 : MeOH : H2O 130 : 50 : 8 (v : v : v). In these conditions, LX1 had a lower Rf than the LA spot but remarkably, when compared with total lipids extracted from *Sce* wt, LX1 still comigrates with another lipid species (**Figure AL-3A**). The latter is masked by the intense dark brownish coloration of LX1 in *Sce* expressing AspRS-DUF2156 and does not hinder the appreciation of the modified lipid nor under white light nor under UV light. Therefore the CHCl3 : MeOH : H2O 130 : 50 : 8 (v : v : v) was retained as main TLC developing buffer to observe the AspRS-DUF2156 dependent lipid. Importantly, the spot corresponding to LX1 but not the "masked" lipid was stained with ninhydrin, consistent with AspRS-DUF2156 dependent lipid being an aminoacylated lipid (**Figure AL-3B**).

Without going into details, the ninhydrin positive spot LA was attributed by MS experiments to PE (see the accompanying paper) and spot LB was attributed to PC by using *Sce* lipid biosynthesis deletion strains (see later). Comparing migration of commercial lipids indicated that the masked lipid might contain PG (not shown).
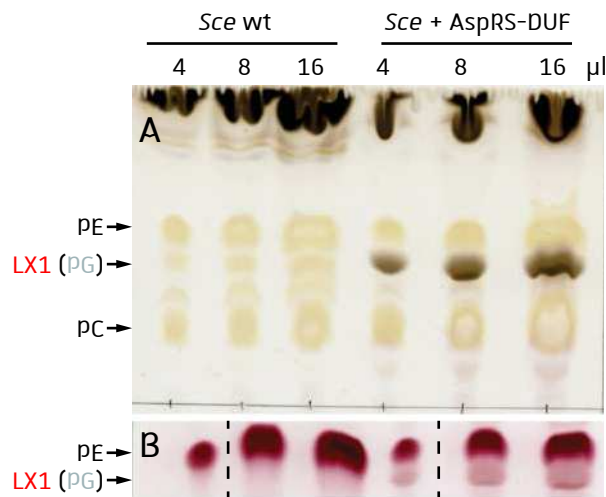
Figure AL-3: Separation of LX1 from PE by optimizing the 1D-TLC devlopping system. Lipids were extracted from the indicated *Sce* strains, resuspended in 50 μl and 4, 8 and 16 μl were spotted on Silca plates. 1D-TLC devlopping solvent was adapted to **CHCl$_3$: MeOH : H$_2$O 68 : 35 : 5 (v : v : v)** and stained with the MnCl$_2$ / Sulfuric acid method (A) or with the ninhydrin reagent. LX1 corresponds to the AspRS-DUF2156 dpendent lipid modification, which is separated from PE in these TLC conditions. The lipid migrating at the same position than LX1 is visible in total lipids from *Sce* wt strain but not in lipids extracted from *Sce* expressing AspRS-DUF2156 where it is probably masked by LX1. This masked lipid corresponds most probably to PG.

III.1.5. The adapted Folch method is also suitable for analysis of LX1.

Total lipids were extracted by the adapted Folch method (see Materials & Methods) and lipids were separated with the CHCl3 : MeOH : H2O 130 : 50 : 8 (v : v : v) system. Using this approach was also suitable and confirmed the presence of the AspRS-DUF2156 dependent lipid (LX1) (**Figure AL-4**).

III.1.6. Co-expression of *Afm* AspRS-DUF2156 and fDUF2156 in *Sce*

As detailed in the introduction to the topic, most species encoding the fDUF2156 version also encode the AspRS-DUF2156, while species encoding only fDUF2156 are rare. In *Afm* both proteins are encoded, which is why I speculated that the fDUF2156 activity might depend on the simultaneous presence of AspRS-DUF2156. LX1 could be for example an intermediate in the synthesis of a lipid subsequently modified by fDUF2156. To mimic the naturally encountered situation of *Afm*, AspRS-DUF2156 and fDUF2156 were co-expressed in the yeast model, lipids were extracted by the Bligh & Dyer procedure and TLC was performed in the presence of CHCl3 : MeOH : H2O 130 : 50 :8 (v : v : v). Unfortunately, this additional trial failed again to associate fDUF2156 to lipid modification (**Figure AL-5**).

III.1.7. Conclusion and additional remarks

The presented results clearly demonstrated that the heterologous expression of AspRS-DUF2156 is responsible for the presence of an additional lipid. The successful optimization of lipid analysis conditions reported here led us finally to standardize the TLC procedure when analyzing the AspRS-DUF2156 dependent lipid. In this way, lipids containing LX1 were from then on routinely separated with developing solvent CHCl3 : MeOH : H2O 130 : 50 : 8 (v : v : v) and stained with the MnCl2 / Sulfuric acid solvent. Regarding these results, it is also tempting to compare the amount of the modified lipid to other phospholipids. This might be possible if both compared spots contain the same class of lipids since the staining reagent reacts distinctly according to the considered lipid class. Albeit obvious, it was necessary to show that the lipid modification activity is dependent on the DUF2156 domain of AspRS-DUF2156. LX1 synthesis was not detected in a strain expressing

Sce wt — Sce + AspRS-DUF — Sce wt — Sce + AspRS-DUF

MnCl$_2$ / Sulf. ac (vis.)   **MnCl$_2$ / Sulf. ac (UV)**
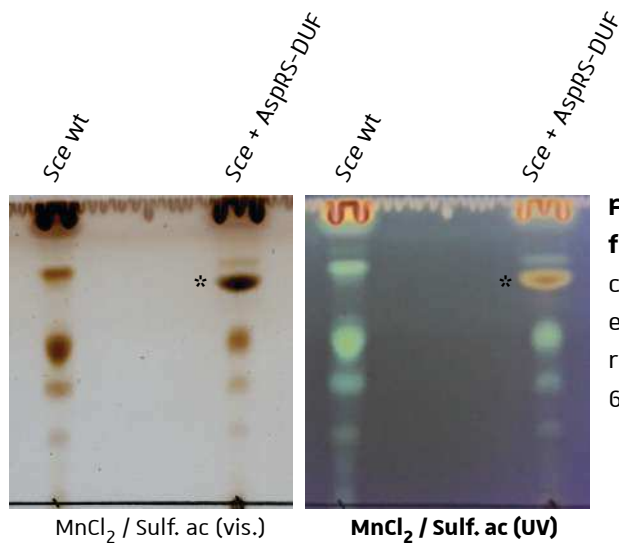
Figure AL-4: TLC analysis of total lipids extracted from *Sce* strains using the adapted Folch method. In contrast to all other presented results, lipids were extracted by the adapted Folch method in this experiment. TLC was performed with CHCl$_3$: MeOH : H$_2$O 68 : 35 : 5 (v : v : v). * indicates the presence of LX1.

Sce wt — Sce + fDUF — Sce + AspRS-DUF — Sce + AspRS-DUF + fDUF
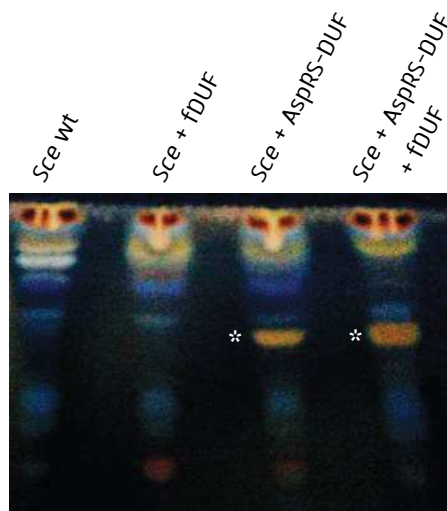
Figure AL-5: TLC analysis of total lipids extracted from *Sce* strains expressing one or both fungal DUF2156 proteins. Lipids were extracted from the indicated *Sce* strains by the Bligh & Dyer method, TLC was performed with CHCl$_3$: MeOH : H$_2$O 68 : 35 : 5 (v : v : v) and the result was observed under UV light. * indicates the presence of LX1.

the AspRS moiety of ErdS (ErdS-ΔDUF2156) but restored when the C-terminal domain (*i. e.* DUF2156) was co-expressed in *trans*. Moreover, expression of the DUF2156 domain alone or the AspRS-DUF2156$_{AAPA}$ variant (an AspRS catalytically inactive variant) were also able to sustain LX1 synthesis. The common point of all three cases reported here is that the DUF2156 domain is not fused to a catalytically active AspRS domain and that the LX1 level is strongly decreased when compared to the *Sce* expressing the full-length wt version of ErdS.

Failure to detect an additional lipid in the presence of fDUF2156, we decided to further concentrate our efforts on the AspRS-DUF2156. The function of fDUF2156 protein will be treated in a separate chapter.

III.2. Evidencing the presence of LX1 in fungi naturally encoding AspRS-DUF2156

At the start of the project we had no filamentous fungal strains expressing DUF2156 proteins nor strains in which AspRS-DUF2156 was deleted. However, we were able to isolate a filamentous fungus from a contaminated petri dish (later determined as belonging to *Penicillium*) and we purchased the insect pathogen strain *Beauveria bassiana* (*Bba*). Both are thought to express AspRS-DUF2156 and the dark-brownish spot, identified as LX1, was present in both cases. As expected, LX1 was absent from *Yarrowia lipolytica* (*Yli*), which does not encode AspRS-DUF2156. This was the first result that brought evidences that the modified lipid is present in naturally occurring fungi encoding AspRS-DUF2156 proteins without adding any stress condition during growth (**Figure AL-6**).
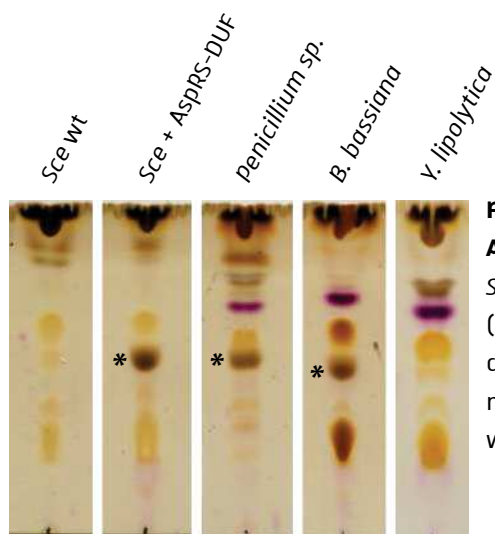
Figure AL-6: Detection of LX1 lipid in fungi encoding naturally AspRS-DUF2156. Total Lipids were extracted from the indicated *Sce* strains, from fungi encoding naturally AspRS-DUF2156 (*Penicillium sp.* and *B. bassiana*) and from *Y. lipolytica* which does not encode AspRS-DUF2156 (Bligh & Dyer). TLC was performed with CHCl$_3$: MeOH : H$_2$O 68 : 35 : 5 (v : v : v) and the result was observed under white light. * indicates the presence of LX1.

III.3. AspRS-DUF2156 activity is not abolished in phospholipid biosynthesis deletions strains of *Sce*.

III.3.1. Expression of AspRS-DUF2156*Afm* in PC, PS and PE biosynthesis deletions strains

Phospholipids are synthetized by two pathways in the *Sce* model organism (**Figure AL-7A**). In the CDP-DAG pathway, CDP-DAG is converted by the *CHO1*-encoded PS-synthase to PS, which is then decarboxylated to obtain the major lipid, PE (Henry *et al.,* 2012). In yeast, the latter reaction can be accomplished by two encoded homologs; the mitochondrial Psd1 which accounts for the large majority of phosphatidylserine decarboxylase activity and the multi-localized Psd2 (Golgi, Vacuole, Endosomes) (Trotter and Voelker 1995). Finally, PE undergoes 3 sequential methylations, the first of them catalyzed by Cho2 (Pem1) and the two remaining by Opi3 (Pem2), to synthetize PC, the other major phospholipid found in yeast membranes (McGraw and Henry 1989; Kodaki and Yamashita 1989). Beside PS decarboxylation, all other reactions transforming CDP-DAG to PC occur at the ER. Alternatively, yeast uptakes ethanolamine and/or choline from the media via the e HNM1-encoded choline/ethanolamine transporter (Nikawa *et al.,* 1986) and transforms them to their CDP-conjugate. ER located Ept1 and Cpt1 transfer the ethanolamine and choline moieties onto DAG, thereby producing respectively PE and PC through the so-called Kennedy pathway (Hjelmstad and Bell 1990; Henry *et al.,* 2012).

Under choline starvation, deletion of *OPI3* (*PEM2*) abolishes the synthesis of PC and induces important accumulation of phosphatidylmonomethylethanolamine (PMME) (McGraw and Henry 1989). AspRS-DUF2156 was expressed in this strain and total lipid analysis by TLC showed that the level of LX1 synthesis was similar to that found in the *Sce* wt strain (**Figure AL-7B**). From this result it was concluded that PC is not a substrate of AspRS-DUF2156.

For *ΔPSD2* it was not surprising that no changes occur concerning LX1 (**Figure AL-7B**), since even if PS would be implicated, the deleted gene accounts only for 4-12 % of the phosphatidylserine decarboxylase activity (Trotter and Voelker 1995). Therefore, the high amount of PE is assumed to be only slightly affected through *PSD2* deletion. The *Δpsd1Δpsd2* mutant is not capable to synthetize PE but this strain has ethanolamine auxotrophy. Testing this strain makes

A

CDP-DAG pathway   Kennedy pathway

B

AspRS-DUF2156 expressed in

Sce wt   Δ*OPI3*   Δ*PSD2*   Δ*GEP4*   Δ*CRD1*
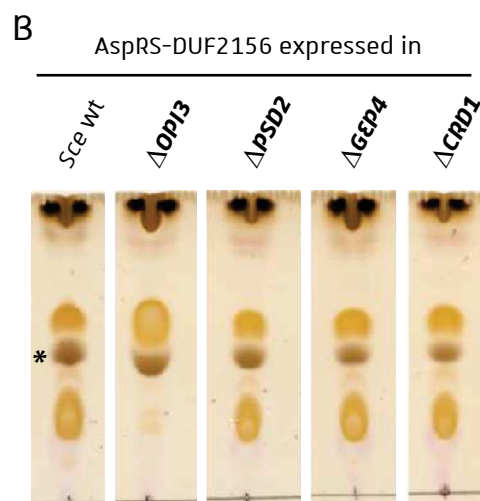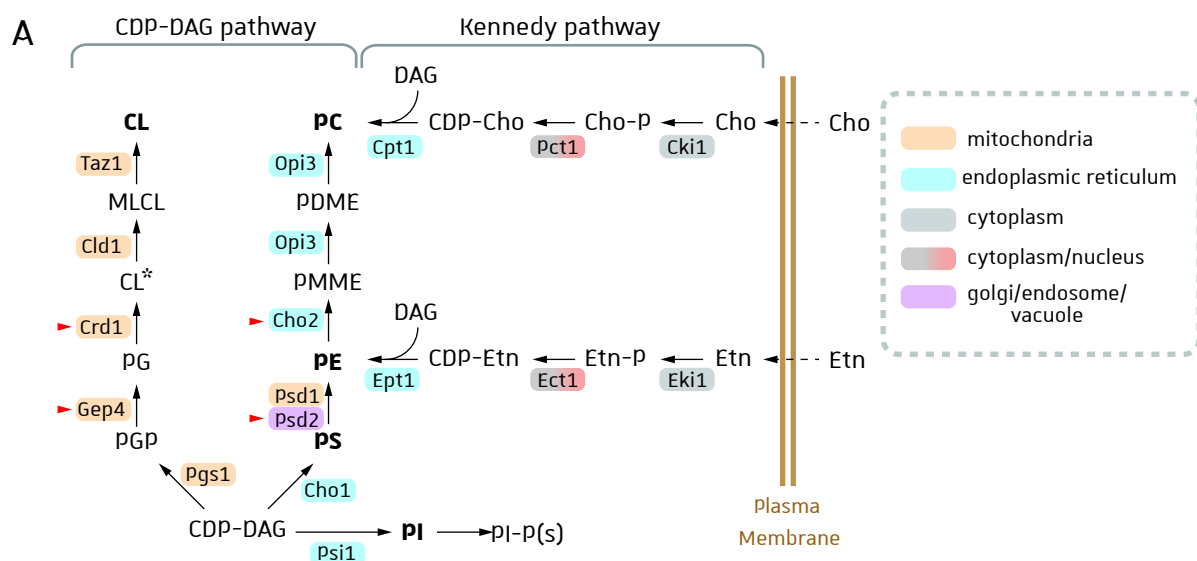
Figure AL-7: Assaying AspRS-DUF216 activity in vivo in phospholipid biosynthesis deletion strains of *Sce*. (A) Biosynthesis enzymes are boxed, and their associated colors indicate their sub-cellular localization (color code at the right). Most abundant lipids found in yeast are indicated in bold. Red arrowheads indicate enzymes lacking in deletion strains. The latter were transformed with plasmids expressing AspRS-DUF2156. **(B)** AspRS-DUF2156 was expressed in the indicated Sce strains and lipids extracted by the Bligh & Dyer method were analyzed by TLC as described in Figure AL-3.

CDP-DAG, CDP-diacylglycerol; DAG, diacylglycerol; PS, phosphatidylserine; PE, phosphatidylethanolamine; PG, phosphatidylglycerol; PGP phosphatidylglycerol phosphate; CL* precursor cardiolipin; MLCL, monolyso-cardiolipin; CL, mature cardiolipin; PMME, phosphatidylmonomethylethanolamine; PDME, phosphatidyl-dimethylethanolamine; PC, phosphatidylcholine; Cho, choline ; Etn, ethanolamine, Cho-P, choline phosphate; CDP-Cho, CDP-choline; Etn-P, ethanolamine phosphate; CDP-Etn, CDP-ethanolamine; PI-P(s), phosphatidylinositol-phosphate(s). Figure in (A) is reproduced and simplified from (Henry *et al.*, 2012).

no sense in the present case because adding ethanolamine in the media would enable synthesis of PE through the Kennedy pathway. The fact that PC and PE are not substrates of AspRS-DUF2156 mediated lipid aminoacylation is not surprising since *1)* PE, PC and PMME were never shown to be O-esterified by an aa and *2)* no hydroxyl group is susceptible to be aminoacylated in these phospholipids.

III.3.2. Expression of AspRS-DUF2156*Afm* in PG and CL biosynthesis deletions strains

On contrary to the above-mentioned phospholipids, CL and its precursor PG are only neo-synthesized from CDP-DAG, but this pathway occurs in mitochondrial membranes. Pgs1 catalyzes the transformation of CDP-DAG to Phosphatidylglycerolphosphate (PGP) which in turn is dephosphorylated by the mitochondrial inner-membrane associated Gep4 phosphatase to obtain PG. However, the latter is efficiently transformed to CL by Crd1 which condenses PG to another

CDP-DAG. The resulting product, corresponding structurally to CL, is then further modified by the *CLD1*-encoded cardiolipin-specific phospholipase and the *TAZ1*-encoded monolyso-cardiolipin acyltransferase to yield specific unsaturated CL species (Henry *et al.,* 2012). Deletion of *GEP4* abolishes synthesis of PG and CL and consequently accumulates PGP. Because DUF2156-dependent lipid-modification was shown to occur mainly on PG and CL in bacteria we were very surprised to see that AspRS-DUF2156 activity was not abolished in *ΔGEP4*. Accordingly, in the *ΔCRD1* which accumulates important amounts of PG (Osman *et al.,* 2010) no significant increase of LX1 was observed (**Figure AL-7B**).

III.4. Purification of LX1

To identify the modified lipid, I aimed to purify LX1 by chromatography on a silica column. This technic was already employed in a similar context by AM. Smith and colleagues to purify Ala-DAG found in *C. glutamicum* (Smith *et al.,* 2015). As detailed in Materials & Methods, *Sce* wt or *Sce* expressing AspRS-DUF2156 from *Afm* were grown in 500 mL and cells were harvested when OD_{600} reached 1.0. Lipids were extracted by the adapted Bligh Dyer method, resuspended in 200 µl of CHCl3 and loaded on the silica gel column. According to their polarity, and thus to their partition between the polar matrix and the mobile phase, lipids are gradually eluted from the column. This

experiment was first conducted with lipids from *Sce* wt to establish the general elution pattern. As expected, highly apolar lipids such as tri-acylglycerols, CL and sterols, are weakly or not retained by the polar resin and are consequently eluted with 100% CHCl$_3$ (**Figure AL-8**). Accordingly, these lipid species migrate in the front of the TLC. Glycolipids are eluted with acetone and are characterized through their intense pink coloration. Fractions collected during these early steps of the purification process do not contain detectable amounts of phospholipids which are polar lipids and bind therefore more strongly to the polar stationary phase. Their elution requires an increase of the eluent polarity which was achieved here by adding MeOH. However, elution with 100 % MeOH failed to separate the different phospholipid species. Because LX1 polarity is like those of phospholipids, it was necessary to refine the phospholipid eluent. In this way, the same experiment was repeated with lipids extracted from *Sce* expressing AspRS-DUF2156 from *Afm* but in this case, polar lipids were eluted with CHCl$_3$: MeOH mixtures ranging from 9 : 1 to 5 : 5 (v : v), thereby increasing stepwise the concentration of MeOH from 10 % to 50 % (**Figure AL-9A**). Elution

fractions collected with 9 : 1 contained the lipid (most probably PG) which is usually masked by LX1 when analyzing total lipids extracted from *Sce* expressing AspRS-DUF2156. PE elution started with 8 : 2 and was completely achieved with 7 : 3 while the other major lipid, PC, was mostly collected through elution with 6 : 4 and 5 : 5. LX1 was continually eluted with CHCl3 mixtures ranging from 8 : 2 to 5 : 5 but its highest amounts were obtained within 7 : 3 fractions. In these fractions, LX1 is contaminated almost only by PE but importantly, the enrichment of LX1 with respect to PE and PC is severely increased in the latest fractions eluted with 7 : 3 and the estimated LX1/(LX1 + PC + PE) ratio reached nearly 90 % as illustrated on **Figure AL-9B**.

Taken together, the silica column chromatographic approach was successful and severely increased the enrichment of LX1 with regard to apolar lipids, glycolipids, PC and probably other undetected lipids. Despite this success, fractions containing the highest amount of LX1 are contaminated by PE and further optimization of the purification procedure might help to avoid this contamination. Increasing the column volume (1 ml) should already increase the resolution of the separation but another approach that might overcome the PE contamination is to perform a second silica column and further refining the elution procedure.
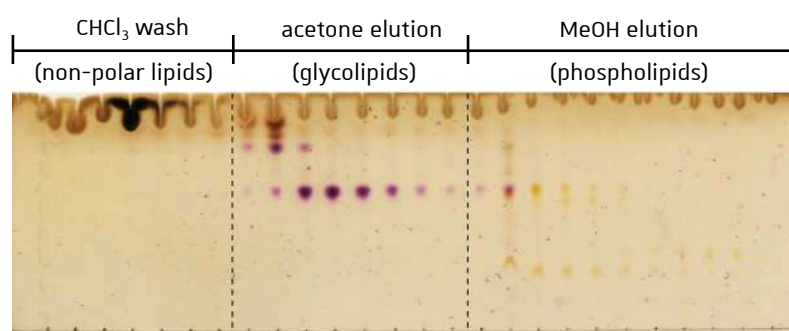
Figure AL-8: Fractionation of total lipids extracted from *Sce* by silica gel chromatography. Total lipids from Sce wt were extracted by the Bligh & Dyer method and submitted to Silica Gel chromatography. Fractionated lipids were analyzed by TLC as in Figure AL-3. Elution solvents are indicated at the top of the TLC and eluted lipid classes are indicated in brackets.

A

CHCl3 : MeOH 9 : 1   8 : 2   7 : 3   6 : 4   5 : 5   MeOH

B
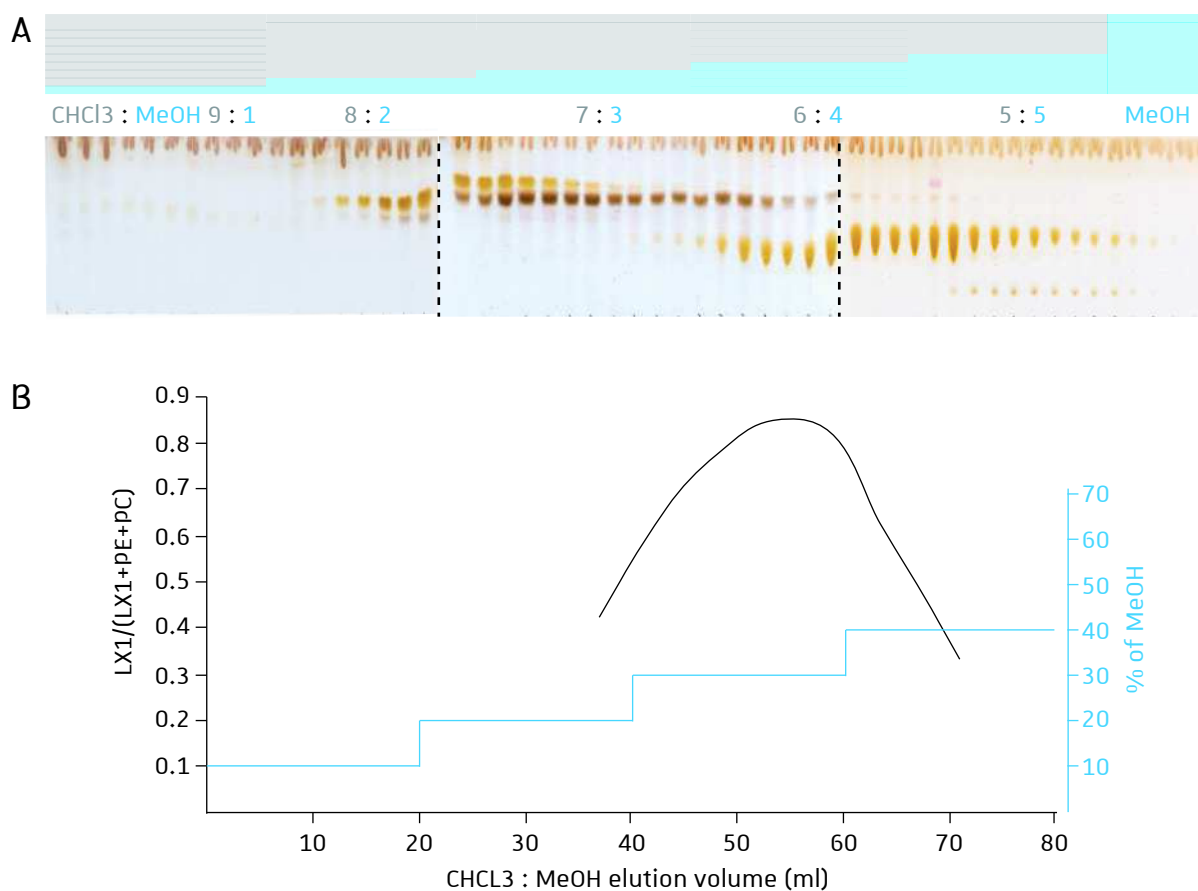
Figure AL-9: Purification of LX1 by silica gel chromatography. (A) Total lipids from *Sce* expressing AspRS-DUF2156 were extracted and submitted to Silica Gel column chromatography as in Figure 8 but the phospholipid elution was adapted. CHCl3 wash and acetone elution were performed but fractions were not collected. (A) Polar lipids (including mainly phospholipids and LX1) were fractionated with indicated CHCl3 : MeOH ratios and the increased step-gradient of MeOH is illustrated at the top of the figure. Fractions were vacuum dried, resuspended in CHCl3 : MeOH 1 : 1 (v : v) and 2/5 of each fraction was analyzed by TLC. Concerning the final elution performed with 100 % MeOH, only 5 fractions out of 10 were analyzed. (B) LX1, PE and PC signals were measured from TLC in fractions containing important amounts of LX1 with ImageJ. The background of the 3 TLCs was measured and subtracted from the corresponding spot signals. LX1/(LX1 + PE + PC) ratio was calculated and graphically represented as a function of the CHCl3 : MeOH elution volume. The MeOH step gradient is represented in blue.

III.5.   LX1 identification by MS

Results presented above clearly demonstrated that the AspRS-DUF2156 protein is responsible for the presence of an additional lipid, whose migration behavior and polarity is like phospholipids. However, the distinguishable coloration of LX1 as well as experiments performed with phospholipid biosynthesis deletion strains, strongly suggested that a lipid belonging to a distinct class is modified. Regarding the coloration similarity of LX1 to lipids migrating in the front it was assumable that AspRS-DUF2156 modifies an apolar lipid.

Finally, LX1 fractions partially purified and contaminated by PE were analyzed by MS in collaboration with Dr. H. Roy. To everyone's surprise LX1 was identified as being Ergosteryl-3-β-O-aspartate (Erg-Asp) and as detailed in the accompanying paper biochemical experiments confirmed that AspRS-DUF2156 (renamed Ergosteryl-aspartate Synthase or ErdS) transfers Asp from its cognate tRNA^{Asp} onto the non-polar Ergosterol. This result as well as the physiological implication of the Erg-Asp will be discussed in the discussion and perspective sections.

IV. Annex II: Purification of recombinant proteins

IV.1. Using the MBP-tag to overcome the strong intrinsic insolubility of fungal DUF2156 proteins

To characterize biochemical aspects of fungal DUF2156 proteins, we aimed to overexpress recombinant versions of them by using appropriate *E. coli* systems such as Rosetta™ 2 or Star 2. Therefore, the corresponding ORFs were cloned in bacterial expression vectors that would encode recombinant versions that are fused to a tag. Initially we tried to purify the proteins of interest in their most native forms, *i. e.* the ORF encoding AspRS-DUF2156 (ErdS) or fDUF2156 fused to an hexahistidine tag (His$_{6X}$) at their N-terminal extremity. Because bacterial aaLSs (i. e. MprF homologs) were 1) shown to be retained in the membrane through their N-terminal domain and 2) successfully purified using recombinant versions containing only the cytoplasmic C-terminal domain of various aaPGSs (i. e. DUF2156 domains) , we decided to delete the 200 residues from the N-terminal extension of fDUF2156. However, we were rapidly confronted to strong intrinsic protein insolubility which led to almost 100 % protein precipitation in the insoluble fraction when comparing to soluble fraction (**Figure P-1A**). Several culture and lysis conditions were tested to overcome this issue, but the recombinant proteins remained insoluble, probably as aggregates (not shown).

To overcome this critical issue, frequently encountered when investigating membrane associated proteins, many strategies exists but most of them consist of fusing larger tags that have solubility "enhancer" properties. Fusing this protein to Maltose binding protein (MBP) at its N-terminus increases considerably its solubility. More than that, once the "passenger" protein (i. e. the protein of interest) is correctly folded, the solubility enhancer is in many cases no longer required to maintain proper folding and can be removed (Kapust and Waugh 1999). The mode of action of MBP as a solubilizing-tag was discussed in several works, but I will not go into details because this is not the purpose here. However, note that in some cases the situation can be more complex, since a certain rate of the MBP-passenger fusion protein remains insoluble despite the presence of the tag (Raran-Kurussi and Waugh 2012).
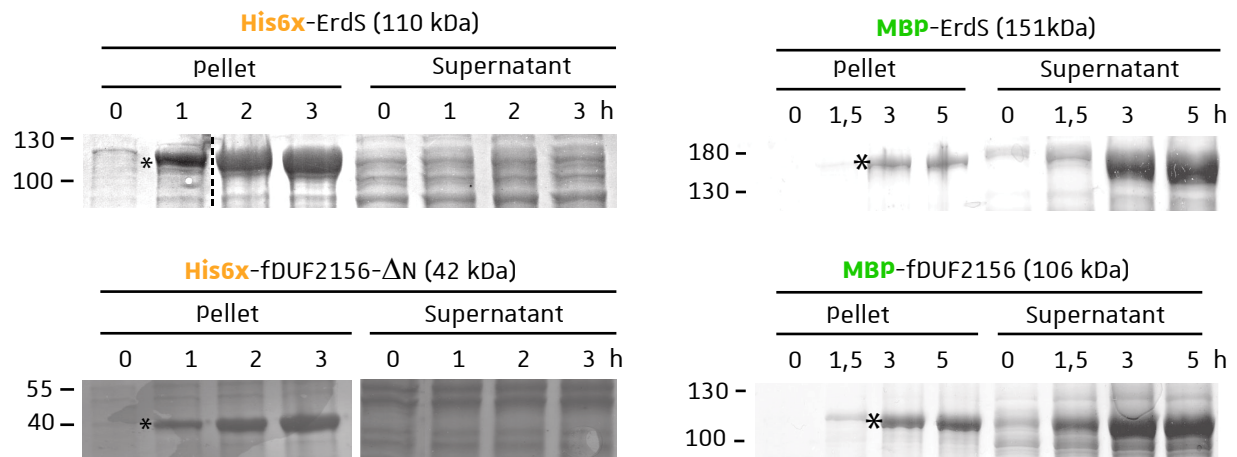
Figure P-1: Overexpression kinetics and solubility analysis of fungal DUF2156 proteins by SDS-PAGE. *E. coli* Rosetta 2 strains were grown in LB media supplemented with Amp 0,1 mg / ml at 37°C. Overexpression of the indicated construct was induced by adding 0.3 mM IPTG when OD_{600} reached 0.5. Aliquots were collected at different times after induction and cells were harvested by centrifugation (5000 × *g* for 10 min at 4 °C). Each crude extract obtained after cell disruption (sonication) was centrifuged at 10000 × *g* for 30 min and the resulting supernatant was transferred to a fresh tube. The pellet was resuspended in an equal volume and both fractions were analyzed by SDS-PAGE 10%. Gels were stained with Coomassie blue R250. Values at the left indicate the molecular weight in kDa

Fungal DUF2156 proteins were fused N-terminally to MBP-tag, cloned into bacterial expression plasmids and transformed in *E. coli* Rosetta™ 2. The MBP-tag solubilized fungal DUF2156 proteins, but a certain amount of the recombinant versions remained in the insoluble fractions as shown in **figure P-1B**. Overexpression kinetics indicate that the overexpression plateau was reached after 3h at 30°C.

IV.2. Purification of MBP-ErdS variants

IV.2.1. Enrichment of MBP-tagged ErdS variants by amylose resin affinity chromatography

As detailed in the Material & Method sections, *E. coli* strains overexpressing MBP-ErdS were incubated in 2 L culture, cells were disrupted by sonication and the resulting soluble fraction was submitted to amylose chromatography. MBP-ErdS, MBP-ErdS-$\alpha^{(0)}$ (basic residues of the positively charged α-helix mutated to Ala. This mutant is inactive when expressed in *Sce* (see **§ II.1.2.1.**)) and MBP-ErdS$_{AAPA}$ (the Q300-S301-P302-Q303 essential signature sequence of the AspRS domain was mutated to AAPA) were successfully enriched by atmospheric amylose resin affinity chromatography (**Figure P-2**). However, a major contaminant, presenting a MW similar to free MBP (40 kDa), is always co-eluted when purifying MBP-ErdS versions containing both functional domains. The ratio of recombinant MBP-ErdS versions in comparison to total proteins is estimated between 30-40 % and the concentration of enzyme added for qualitative *in vitro* assays was calculated on this basis. In contrast, when MBP-ErdS versions containing only one of both functional domains are purified (i. e. MBP-ErdS-ΔDUF2156 or MBP-ErdS-ΔaspRS), the purity of the protein is strongly increased and can reasonably be estimated to around 90 % (**Figure P-3**). More precise analysis of enrichments and yields are required but assuming that all mentioned proteins were purified from comparable cell mass and that the same purification procedure was applied it is reasonable to consider that the amount of purified MBP-ErdS-ΔaspRS protein is strongly increased in comparison to other ErdS variants mentioned here. The successful purification of the recombinant protein, containing the DUF2156 domain separated from the AspRS domain will be essential for the determination of its kinetic parameters, independently of the AspRS domain.

MBP-ErdS$_{\Delta 84}$ (141.5 kDa)

MBP   AspRS   DUF2156

TevCS

Overexpression in
E. coli Rosetta 2

Cell lysis
(sonication)

Low pressure affinity
chromatography
on amylose resin

GF75 column

TEV
Clivage

E1 E2 **E3 E4 E5 E6**

170 —
130 —

55 —

40 —

MBP-ErdS$_{\Delta 84}$

«MBP»

Size exclusion chromatography

Peak 1   Peak 2

MBP-ErdS$_{\Delta 84}$ ≈ 2 mg
ε = 1.28 M^{-1}.cm^{-1}
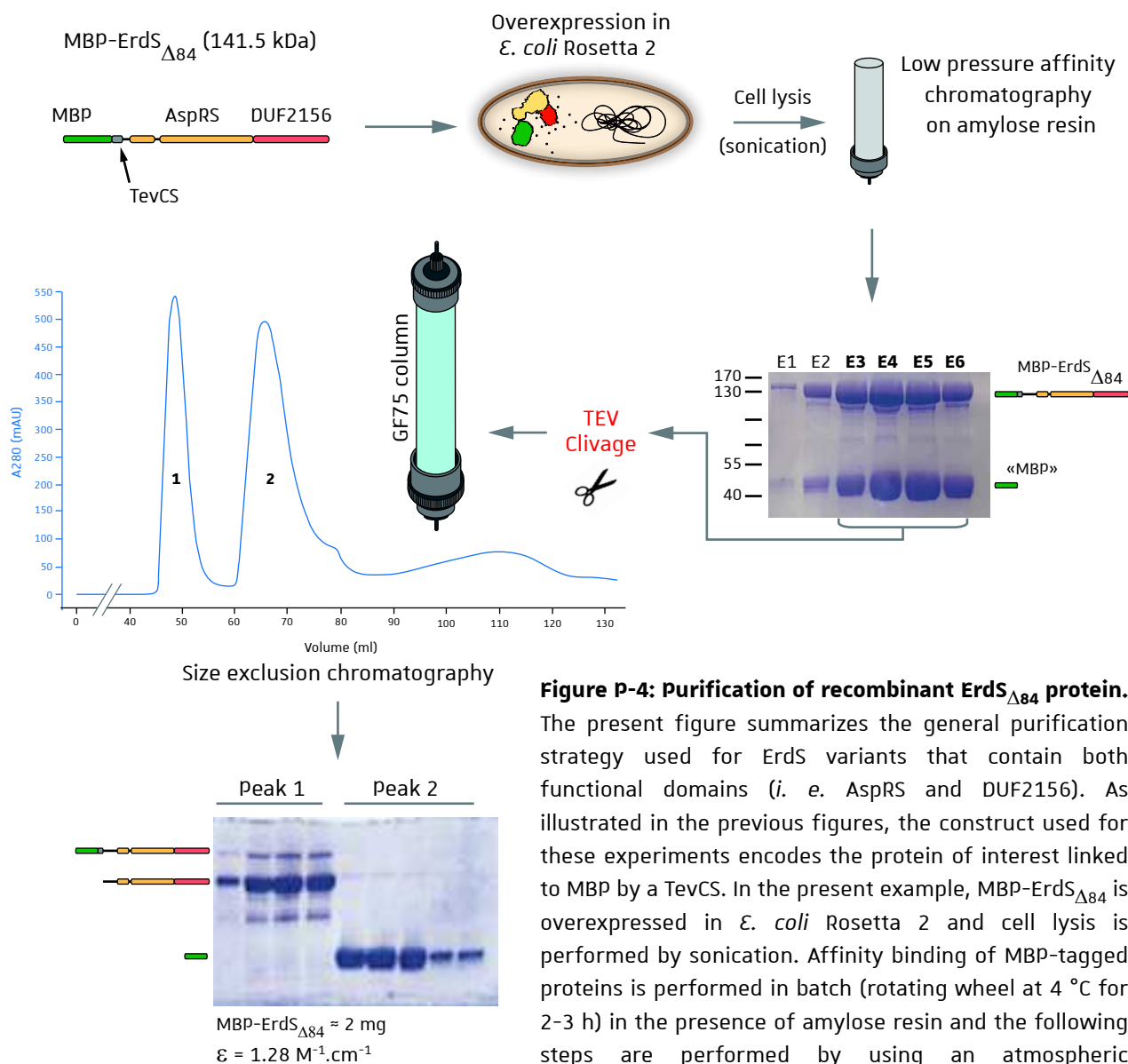
Figure P-4: Purification of recombinant ErdS$_{\Delta 84}$ protein. The present figure summarizes the general purification strategy used for ErdS variants that contain both functional domains (*i. e.* AspRS and DUF2156). As illustrated in the previous figures, the construct used for these experiments encodes the protein of interest linked to MBP by a TevCS. In the present example, MBP-ErdS$_{\Delta 84}$ is overexpressed in *E. coli* Rosetta 2 and cell lysis is performed by sonication. Affinity binding of MBP-tagged proteins is performed in batch (rotating wheel at 4 °C for 2-3 h) in the presence of amylose resin and the following steps are performed by using an atmospheric chromatography column support. Eluted fractions are analyzed by SDS-PAGE and it is noteworthy that in the present example the purification profile is very similar to those presented in figure P-2 *i. e.* MBP-ErdS$_{\Delta 84}$ enriched fractions are accompanied by the major contaminant supposed to correspond to abortive proteins such as "free"-MBP. Fractions E3-E6 are pooled together aliquoted by 190 µl fractions and submitted to proteolytic TEV-cleavage, as described in the Materials & Methods sections, pooled again and injected (1.8 ml) onto a homemade GF75 resin column (2.5 × 30 cm; Biorad, Econo-Column® #7372532), powered by an HPLC Äkta purifier system. All steps are performed in the presence of GF buffer containing 50 mM Tris-HCl pH 7 and 30 mM KCl. The flow is set to 0.2 ml/min and 1.4 ml fractions are collected. Selected fractions are analyzed by SDS-PAGE (10 %). After removal of aggregates by ultracentrifugation, the concentration of purified ErdS$_{\Delta 84}$ was measured by spectral absorbance at 280 nm and the total amount determined to around 2 mg.

IV.2.2. Purification of ErdS variants by size exclusion chromatography

The MBP-tag of our recombinant proteins is separated from the ErdS variants by a TevCS and can consequently be removed by proteolytic cleavage. Cleaved ErdS variants that have similar molecular weight to the full-length wt ErdS (151 kDa) can then be easily separated from minor contaminants including the MBP-tag by size exclusion chromatography. In addition, AspRSs are class II aaRS and therefore the AspRS domain of ErdS is assumed to dimerize, thereby further facilitating the discrimination of ErdS from MBP. To illustrate these purification aspects, I choose an ErdS variant in which the N-terminus was shortened. The AspRS domain of ErdS$_{Afm}$ is preceded by an N-terminal extension of 104 aa for which no domain homology was predicted. The sequence encoding 84 aa of the N-terminal extension was deleted and cloned into the pMtevGWA vector by using the Gibson isothermal assembly method. This construct might be useful to establish the tridimensional structure of the protein because the presence of labile or unfolded regions within the protein often hinders efficient crystallization.

MBP-ErdS$_{\Delta 84}$ was enriched on amylose resin with the classical procedure described in the corresponding Material & Methods sections. SDS-page analysis of fractions eluted from the amylose resin shows similar results in comparison to those obtained for the purification of full-length ErdS proteins (**Figure P-4**). Fractions were cleaved by the TEV-protease and injected into the homemade GF75 size exclusion column monitored by an Äkta purifier HPLC system. Analysis of the chromatograph on **figure P-4** confirms the presence of two peaks that were attributed to cleaved ErdS$_{\Delta 84}$ and MBP when analyzed by SDS-page. Micro aggregates were removed by ultracentrifugation at $100000 \times g$ for 1 h at 4 °C. The purity of ErdS$_{\Delta 84}$ is estimated to 96 % and the total amount was determined to be around 2 mg by measuring the OD$_{280}$. The same protocol is used for the purification of full-length MBP-ErdS, MBP-ErdS-$\alpha^{(0)}$ and MBP-ErdS$_{AAPA}$ (not shown).

Performing size exclusion chromatography following TEV protease cleavage is not suitable to discriminate the MBP-tag (40 kDa) from cleaved ErdS-ΔaspRS (39.3 kDa). To overcome this issue, it will be important either to find conditions in which the His-tagged version of this protein is soluble or to add a second tag. For example, GST-MBP- or His-MBP-tagged versions of ErdS-ΔaspRS may resolve this issue. The proposed strategy is to perform amylose affinity chromatography as described above, followed by TEV protease cleavage. Finally, the cleaved His-MBP- or GST-MBP-
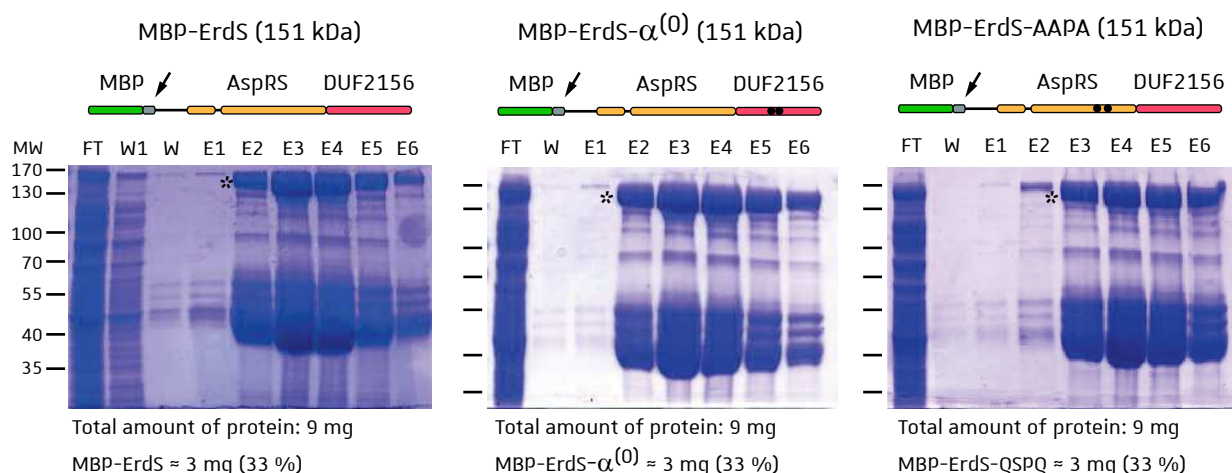
Figure P-2: Purification of full-length MBP-Erds variants on amylose resin. *E. coli* Rosetta 2 harboring pMtev-ErdS were grown and ErdS variants were overexpressed. Cells were resuspended in lysis buffer, disrupted by sonication, and cleared by centrifugation (see the Materials & Methods sections). The soluble fraction of the crude extract obtained from a 2 L pellet was put in the presence of 2 mL of equilibrated amylose resin placed on a rotating wheel for 2-3h at 4°C. The batch was poured into a column and the flow through (FT) was collected. Beads were washed with wash buffer several times and elution was performed with the same buffer supplemented with 3 % maltose. The FT, the last wash fraction (W) and eluted fractions (E) were analyzed by SDS-PAGE. MBP-Erds-$\alpha^{(0)}$ contains a catalytic null DUF2156 domain (R749, K750, R751 and R752 mutated to Ala). MBP-ErdS-AAPA contains a catalytic null AspRS domain (QSPQ signature sequence of AspRSs mutated to AAPA). Protein concentrations were measured by the Bradford method and the total amount of protein was deduced. Finally the ratio of the protein of interest on total proteins is approximatively 1/3. W1, first wash fraction; MW, molecular weight in kDa; black arrows indicate the TevCS; * indicate the band corresponding to the protein of interest**.**
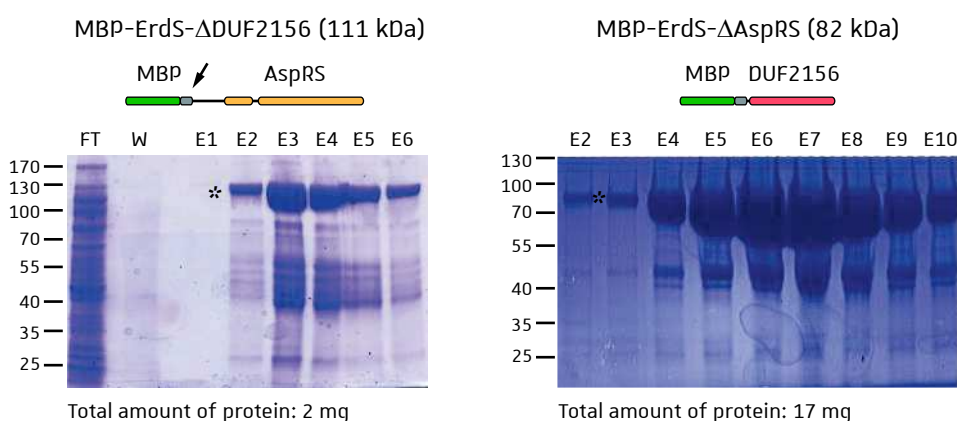
Figure P-3: Purification of truncated MBP-Erds variants on amylose resin. Proteins were purified as in figure P-2 (see legend and Materials & Methods sections). MBP-ErdS-DDUF2156 harbors ErdS only containing the AspRS domain and while MBP-ErdS-DAspRS corresponds to a fusion between the MBP-tag and the DUF2156 domain of ErdS. Note that both truncated forms are severally enriched with regard to the major contaminant copurified with full-length ErdS variants (Figure 2-P).

tag will be removed by a second affinity chromatography round (i.e. NiNTA or GSH resins), whereas the native ErdS-ΔaspRS would be recovered from the flow-through. One advantage if choosing the His-tag for this purpose is that the proposed strategy will also allow to remove the His-tagged TEV-protease from the purified protein in a single step. Unfortunately, I had not the time to test these strategies, but I already constructed expression plasmids allowing GST-MBP- or His-MBP-tagged versions of ErdS-ΔaspRS.

Finally, cleaved ErdS-ΔDUF2156 should dimerize since AspRSs belong to class II aaRS. Consequently, this ErdS variant should be easily discriminated from the MBP-tag by size exclusion chromatography.

IV.3. Assaying the lipid modification activity of recombinant ErdS proteins through *in vitro* lipid aminoacylation assay (LAA).

As a quality check, we wanted to verify if the purified ErdS versions sustain lipid aminoacylation by performing LAA described in the accompanying paper. Note that ErdS-ΔaspRS and MBP-ErdS-ΔDUF2156 were cleaved before the assay but the free MBP-tag was not removed from the enzyme fraction. In accordance with our expectations, full-length ErdS retained lipid aminoacylation activity which was not the case when ErdS-ΔDUF2156, ErdS-AAPA, ErdS-a[(0)] and ErdS-ΔaspRS were assayed **(Figure P-5)**. Combining ErdS-ΔaspRS and ErdS-ΔDUF2156 restored only a residual activity when compared to ErdS wt. Interestingly, when ErdS-ΔaspRS or MBP-ErdS-ΔaspRS were assayed in the presence of purified AspRS from *Sce* the lipid aminoacylation activity was similar to ErdS wt. Note also that the presence of the MBP-tag does not seem to affect the activity of the DUF2156 domain (which is very advantageous since cleaved ErdS versions tend to precipitate). Therefore, the enriched proteins were in most cases stored in their MBP-fused versions.

IV.4. Conclusion and preliminary optimizations of the purification procedure.

In the previous sections I reported the status of the purification procedure I reached during my thesis. The MBP-tag was successful to solubilize the ErdS and the amylose resin allowed the purification of sufficient amounts of protein to perform biochemical experiments. Furthermore,

A

tRNA^{Asp} + ATP

Lipid + [^{14}C]Asp $\xrightarrow{\hspace{2cm}}$ | ErdS | $\rightarrow$ [^{14}C]Asp-LipidX

tRNA^{Asp} + AMP + PPi

B

| 1 | 2 | 3 | 4 | 2+3 | 5 | 1 | 5+7 | 6+7 |

1 ErdS

2 ErdS-ΔDUF2156

3 ErdS-AAPA

4 ErdS-α(0)

5 MBP-ErdS-ΔAspRS

6 ErdS-ΔAspRS

7 *Sce* AspRS
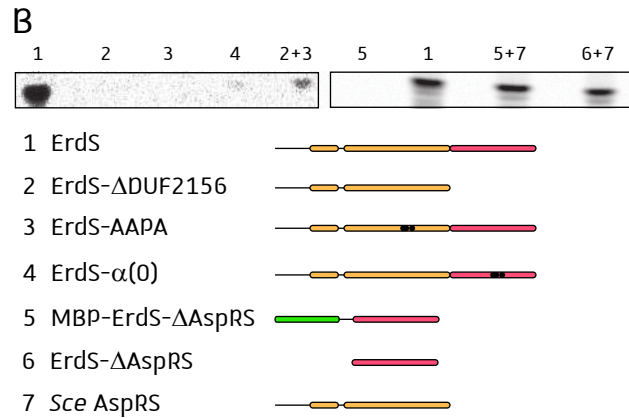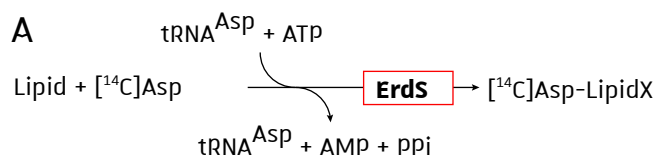
Figure P-5: Assaying lipid aminoacylation activities of recombinant ErdS variants. LAA was performed as described in the accompanying paper. The reaction is schematically represented in **(A)** and was performed in the presence of radiolabeled [^{14}C]Asp (20 μM), pure tRNA^{Asp} from *Sce* (10 μM) and total lipids from *Sce* (2 mg/ml). ErdS variants tested here are listed in **(B)** and their structural organizations are depicted. 1, 3 and 4 contain both functional domains found in ErdS while 2, 5 and 6 contain only one of them. Reactions were started by adding 0.1-0.5 μg of the enzyme and when mixed, enzymes were added in equimolar ratios. 5 and 6 contain the same ErdS construct but in 5 the MBP-tag was not removed. Finally, 7 corresponds to the recombinant cytoplasmic AspRS from *Sce*. Colors used are the same than in figure P-2. After 40 min, lipids were extracted by the adapted Bligh and Dyer procedure and separated by TLC (developing system: CHCl3 : MeOH : H2O 130 : 50 : 8 (v : v : v)). TLC plates were exposed onto an imaging plate (Fuji Imaging plate) and radiolabeled species were detected with a Typhoon TRIO variable Mode Imager (GE Healthcare).

the insertion of the TEV cleavage site enabled proteolytic cleavage of MBP fused proteins and the combination of this procedure with size exclusion chromatography lead to the purification of tag-free versions of ErdS. It is also important to note that the aim of obtaining recombinant ErdS proteins was to detect qualitatively the tRNA- and the lipid aminoacylation activities of the AspRS and the DUF2156 domains, respectively and to demonstrate that the Erg-Asp synthesis is tRNA and DUF2156 dependent. Regarding results presented here and in the accompanying paper, these goals were fully reached, but it will be important to investigate more in depth the molecular mechanism of ErdS. Therefore, the purification procedure must be further optimized, and other strategies should be tested or at least complementary purification steps, such as ion exchange chromatography should be tested. enduring the last benchwork days of my thesis I obtained some preliminary data that could help to further optimize the purification procedure.

IV.4.1. Optimization of culture and overexpression conditions

With regard to the major contaminant co-eluted from the amylose resin when purifying "full-length" ErdS variants, I aimed testing whether the overexpression conditions may affect the final purity of the protein of interest. For each condition, 250 ml LB supplemented with Ampicillin (100 mg / L) were incubated with *E. coli* Rosetta2 cells containing pMtevGWA-ErdS$_{\Delta 84}$ until OD600 reached 0.5. Differential overexpression conditions, including temperature, IPTG concentration and incubation time, were tested and proteins were enriched in parallel by a single affinity chromatography step (amylose). Increasing the concentration of IPTG for overexpression at 30 °C dramatically decreased the proportion of the MBP-ErdS version when compared to the major contaminant (**Figure P-6**) while overexpression at 18°C for 12 h with 0.1 mM IPTG was the most favorable condition to enrich MBP-ErdS$_{\Delta 84}$. Overexpression at 30 °C with 0.1 mM IPTG appears also to overcome this issue but the culture was stopped after only 1 h after induction which is why the amount of purified protein is low. Accordingly, our collaborators from Pr. O. Nureki's team even succeed to purify soluble His-tagged ErdS from *E. coli* when overexpression of the recombinant protein was induced with 0.1 mM IPTG at 20°C overnight (not shown). In the latter case, cells were resuspended and disrupted with lysis buffer containing NaCl 1 M. Consequently, ErdS variants containing both domains (AspRS and DUF2156) should be overexpressed regarding these conditions.
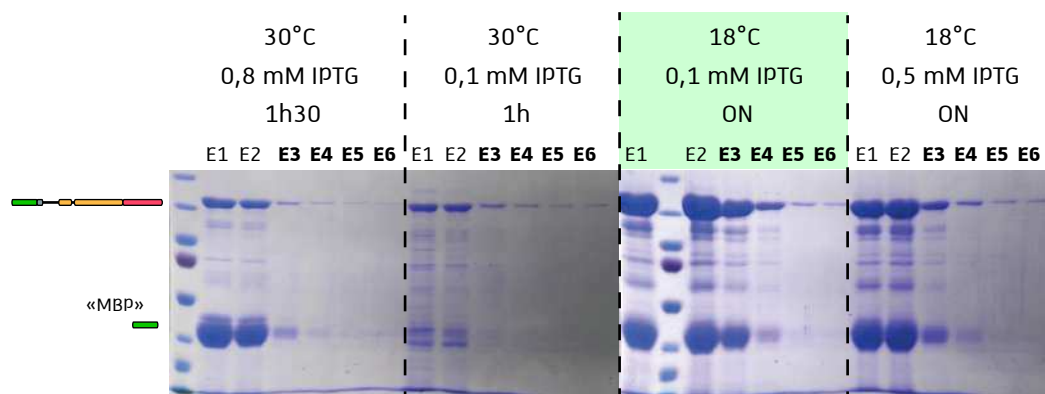
Figure P-6: Optimizing the overexpression conditions of recombinant ErdS variants. *E. coli* expressing MBP-ErdS$_{\Delta 84}$ was grown in 250 ml LB + Amp (100 mg/L) and when OD$_{600}$ reached 0.5, 4 different overexpression conditions were tested. In all cases the cold-shock (prior the conditions indicated above the gels) was maintained and the varying parameters include incubation temperature, concentration of IPTG for induction and duration of the overexpression. Cells were recovered by centrifugation, the MBP-ErdS$_{\Delta 84}$ was purified by affinity chromatography (amylose) as described previously and elution fractions (collected by 1 ml) were analyzed by SDS-PAGE (10 %). Note that in this case the column support was changed (Poly-Prep® Chromatography Columns, Biorad #7311550) and the volume of amylose resin was lowered to 500 µL.

IV.4.2. Optimization of GF

Later during my thesis, we purchased a newer HPLC system (Äkta pure, GE healthcare) which encouraged me to repeat the purification of ErdS by using a Hiload 16/600 Superdex 200pg column instead of the homemade GF75 column. In this experiment, *E. coli* expressing MBP-ErdS$_{\Delta84}$ was grown in 1 L culture and overexpression was induced with 0.1 mM IPTG for 12 h at 18°C. Fractions eluted from the amylose resin that contained MBP-ErdS$_{\Delta84}$ were pooled (total 4 ml) and concentrated as described in the Materials & Methods sections and the 2 ml fraction was injected onto the Hiload 16/600 Superdex 200pg (**Figure P-7**). Importantly, an additional peak arose when using this alternative in comparison to the two peaks obtained with the homemade GF75. Peaks 1 and 2 contain MBP-ErdS$_{\Delta84}$ and free MBP respectively while the situation of peak 1 is not clear. Intriguingly, the UV280/UV260 ratio of peak 1 is increased when comparing to peaks 2 and 3 and is near to 1. Further investigations are required but the enhanced absorption of UV260 might indicate the presence of nucleic acids, probably a tRNA co-purified from *E. coli* in complex with MBP-ErdS$_{\Delta84}$. Importantly, fractions from peaks 1 and 2 retained lipid aminoacylation *in vitro* but the activity of proteins from peak 1 is very low when compared to peak 2. Therefore, one might speculate that peak 1 contains majorly aggregates or misfolded forms of the protein rather than MBP-ErdS$_{\Delta84}$ in complex with a co-eluted tRNA. Through this strategy, 4.95 mg of uncleaved MBP-ErdS$_{\Delta84}$ were purified from a 4 g cell pellet.

Beside using size chromatography to purify DUF2156 proteins, similar strategies are also useful to study other aspects related to these proteins. Because ErdS contains a class II synthetase (i. e. AspRS), ErdS should at least dimerize. However, no standard proteins were injected to compare the size of proteins eluted with regard to the elution volume. Therefore, it is difficult to exploit the herein reported results to deduce the oligomerization state of the protein. Furthermore, to study such aspects, it will be more adapted to use Superdex™ 200 Increase 5/150 GL or Superdex™ 200 Increase 10/300 GL columns. Similar approaches will also be useful to investigate the binding affinities of the (Asp-)tRNA^{Asp} with ErdS but also with either the AspRS or the DUF2156 domains alone.

Protein amount in peak 2 (MBP-ErdSD84) = 4.95 mg
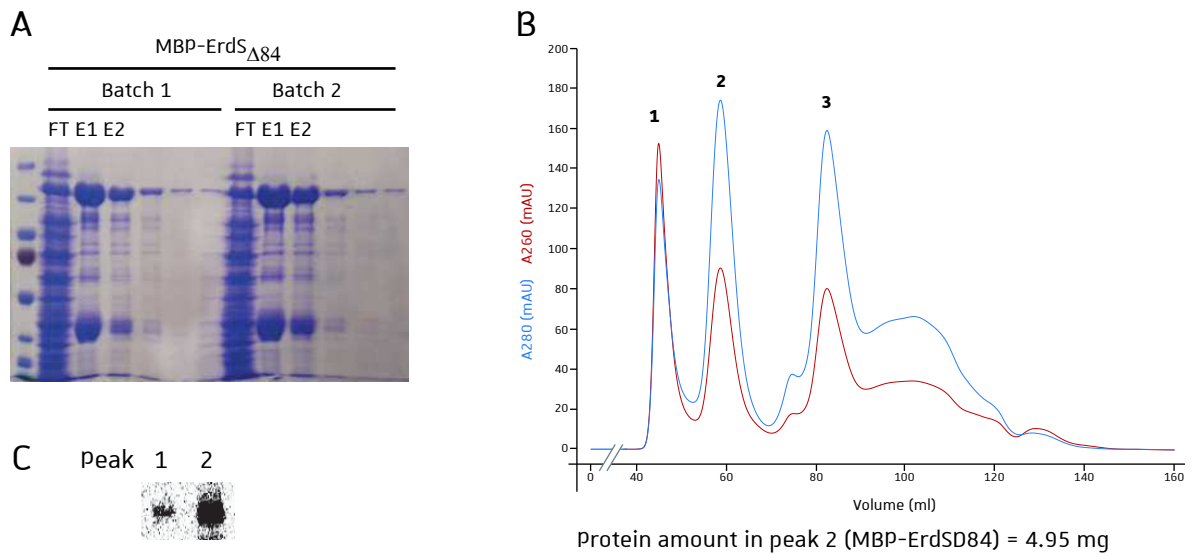
Figure P-7: Adapting size exclusion chromatography conditions. (A) *E. coli* harboring pMtev-ErdS$_{\Delta84}$ was grown in 1 L LB + Amp (100 mg/L) and MBP-ErdS$_{\Delta84}$ was overexpressed with 0.1 mM IPTG at 18 °C for 12 h. Cells were resuspended in 20 ml, disrupted by sonication, and the soluble fraction was split in two. Each fraction was treated separately; incubation in batch with 1 ml amylose resin (2h, 4 °C on rotating wheel), transfer onto a Poly-Prep® Chromatography Columns, Biorad #7311550 and elution fractions collected per 1ml. **(B)** E1 and E2 obtained from both batch were pooled and concentrated to a single 2 ml fraction. The latter was injected onto a Hiload 16/600 Superdex 200pg column conducted by Äkta pure HPLC system and the chromatograph is represented. Equilibration and size exclusion were performed with GF buffer (TrisHCl 50 mM, KCl 30 mM), the flow was set to 1 ml/min and fractions were collected per 0.8 ml. Fractions from peaks 1 and 2 were pooled separately and concentrated to 1 mg/ml. **(C)** Erg-Asp synthesis activities of peaks 1 and 2 were assayed by LAA in the presence of 0.5 mg/ml commercial Erg, as described in the accompanying paper (see also Figure P5).

IV.5.   Purification of MBP-ErdH$_{Afm}$

ErdH$_{Afm}$ and its associated mutants were fused to MBP and overexpressed in *E. coli*. Cells were grown in 250 mL LB + Amp and the pellet was resuspended in 10 ml lysis buffer. In contrast to the above described atmospheric affinity chromatography, the soluble fraction obtained after cell lysis was injected onto on a MBPTrap™ HP (GE healthcare, 28-9187) conducted by an Äkta Pure HPLC system. SDS-page analysis of eluted fractions confirmed the enrichment of recombinant proteins and in contrast to full-length ErdS variants, the major MBP contaminant was absent when purifying ErdH proteins (**Figure P-8**).
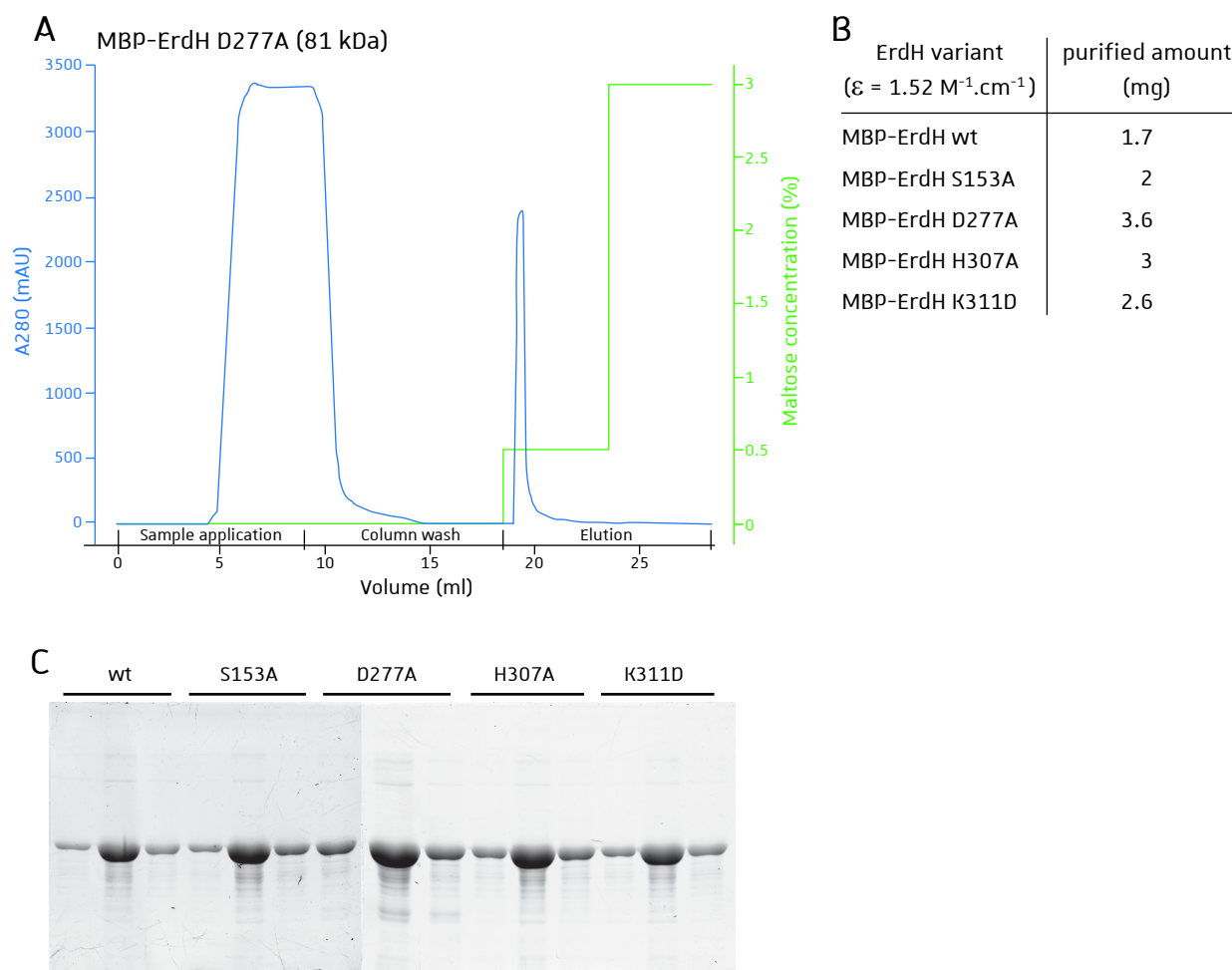
Figure P-8: Purification of ErdH variants. *E. coli* strains harboring pMtev-ErdH wt or mutants were grown in 250 mL LB + Amp (100 mg/mL) and overexpression was induced with 0.3 mM IPTG at 30 °C for 3 h. Cells were disrupted by sonication in the presence of 10 mL lysis buffer and the soluble fraction was injected into a MBPtrap 1mL affinity column, conducted by an Äkta pure HPLC system. Wash steps were performed with 10 ml of Wash buffer (Tris-HCl pH 7 50 mM, NaCl 300 mM, KCl 30 mM, Glycerol 5 % (v / v), Tween20 0.25 % (v / v), TritonX-100 0.1 % (v / v), β-mercaptoethanol 5 mM) and for elution the same buffer supplemented with a step gradient of maltose (5 ml at 0.5 % followed by 5ml at 3 %) was used. The flow rate was 1 ml/min during equilibration and column wash and was decreased to 0.5 ml/min for sample application and elution. Fractions were collected per 0.5 mL. The chromatograph is represented in (A) and total amounts of each ErdH variants recovered are summarized in (B). (C) Eluted fractions of each purified protein was separated by SDS-PAGE and bands were revealed by the stainfree method using ChemiDoc Imaging System (Biorad).

PART II: Discovery of a second tRNA dependent ergosterol aminoacylation pathway catalyzed by a free standing DUF2156

RNA-dependent synthesis of ergosteryl-3-β-O-glycine expands the diversity of steryl-amino acid conjugates in ascomycota. (*Article in preparation*) Yakobov *et al.*

Preliminary remarks

As introduced at the beginning of the present manuscript, the bioinformatic study performed by F. Fischer revealed in addition to ErdS another fungal DUF2156 protein, initially named fDUF2156. This protein is mostly distributed among Ascomycota and during my thesis I also aimed to characterize the function of this second protein that we supposed to be a lipid aminoacyation factor too. By using similar strategies as in our recently published work I detected an fDUF2156 dependent lipid and our tight collaboration with Dr. H. Roy's and Pr. T. Kushiro's teams allowed us finally to establish that fDUF2156 is an aminoacyl-tRNA transferase (ATT) that catalyzes the esterification of Gly onto Erg in a tRNA dependent manner. Thus, our study provides a novel pathway for the synthesis of ergosteryl-3-β-O-glycine (Erg-Gly), a so far never described lipid. Based on structural predictions and mutagenesis experiments we also show the essentiality of a positively charged helix, commonly found in DUF2156/ATTs and strongly suggested to be involved in aa-tRNA binding, for the lipid modification activity. In the coming months we plan to submit our discovery for publication and therefore we started the redaction of the article.

In the context of my thesis manuscript I nevertheless wanted to propose a preliminary draft even if incomplete. In this way, I adapted the draft "ErgS article draft" to my thesis and the reader should be aware that even if the main results are presented, some of them are incomplete or lack some controls. In addition, some experiments we would like to integrate are still lacking and depending on their outcomes (in the following month) the direction of the article might completely change. Note also that the following draft will refer to some parts of my thesis manuscript, particularly in the Materials & Methods section which is incomplete for the moment but for the convenience to the reader I tried to integrate all essential information required for the comprehension of the purpose. Regarding these preliminary remarks, I inserted several notes, written in [*Italic*] between rectangle brackets, in order to guide the reader. They will among others indicate complementary experiments that are ongoing or that must be performed prior to publication. Author contributions will also be indicated with the aim to point out my participation

during the past 4 years. Some figures (mainly supplementary figures) are in preparation and unfortunately, I was not able to integrate them at time. In those cases, the integrated notes will also guide the reader and sometimes an alternative illustration will be proposed. Finally, the Discussion section was the most challenging to redact since according to results that will be obtained in the coming month, its orientation might completely change. Therefore, in addition to discussing properly the characterization of ErgS and several other points, I also provided in this section a global analysis on the discovery of fungal lipid aminoacylation pathways by performing notably an analogy with bacterial systems. The discussion part can consequently be considered as the conclusion of my thesis work.

Taken together, the reader should consider the following ErgS article draft as a part of my thesis, in which several results from our collaborators or from other members of our lab were implemented, rather than the version that will be submitted for publication.

RNA-dependent synthesis of ergosteryl-3β-*O*-glycine expands the diversity of steryl-amino acid conjugates in ascomycota

Nathaniel Yakobov[1,§], Nassira Mahmoudi[1, §], Guillaume Grob[1], Daisuke Yokokawa[2], Hervé Roy[3], Bruno Senger[1], Tetsuo Kushiro[2], Hubert D. Becker[1,*]& Frédéric Fischer[1, *]

[1] Université de Strasbourg, CNRS, Génétique Moléculaire, Génomique, Microbiologie, UMR 7156, 4 Allée Konrad Röntgen, 67084 Strasbourg Cedex, France.[2]School of Agriculture, Meiji University, 1-1-1 Higashimita, Tama-ku, Kawasaki, Kanagawa 214-8571, Japan. [3]Burnett School of Biomedical Sciences, College of Medicine, University of Central Florida, Orlando, FL 32826, USA.

[§] Share first co-authorship

*Corresponding authors: Dr. Frédéric FISCHER, frfischer@unistra.fr and to Pr. Hubert BECKER, h.becker@unistra.fr

Key Words: aminoacyl-tRNA, ergosterol, ergosteryl-glycine, fungi, glycyl-tRNA synthetase, DUF2156, lipid aminoacylation, sterol conjugate

INTRODUCTION

Modification of membranes lipid components through the addition of D/L-amino acids (aa) or aa derivatives is a widespread mechanism in bacteria for glycerolipids (1), lipid A (2) or teichoic acids (3). Bacterial virulence factors termed MprF (for *Multiple Peptides Resistance Factors*) use aminoacyl-tRNAs (aa-tRNAs) —*e.g.* synthesized by aminoacyl-tRNA synthetases (aaRSs) (4)— rerouted from ribosomal protein synthesis to transfer the L-aa moiety that they carry onto one hydroxyl of an acceptor glycerolipid, yielding *O*-L-aminoacyl-esters of glycerolipids (AGLs) (5, 6). MprFs can use Lys-, Ala-and/or Arg-tRNAs (7, 8) and transfer the aa that they carry onto phosphatidylglycerol (PG), cardiolipin (CL) or diacylglycerol (DAG), yielding Lys- or AlaPG, LysCL or AlaDAG (5, 9). The aa-tRNA transferase activities carried by the C-terminal cytoplasmic *Domain of Unknown Function 2156* (DUF2156) of MprFs (5) that is fused to an N-terminal integral membrane domain with an AGL flippase activity (10-12) that transports the modified lipids from the inner leaflet of the plasma membrane, where they are produced, to the outer leaflet, where they are exposed (5, 10). AGLs intensify resistance of bacteria to cationic antimicrobial peptides (CAMPs), seemingly through charge repulsion, but also to other types of antimicrobials (9, 13). In bacteria, AGLs are degraded by dedicated hydrolases/esterases (14) that are periplasmic in diderm bacteria (15, 16) or extracytoplasmic and membrane-anchored in monoderms (17). The MprF/hydrolase couple is therefore central to the turnover of AGLs in bacterial membranes but also to proper antimicrobial resistance, pathogenicity and/or immune escape (5, 9, 16).

MprF-like proteins have been thought to be absent in eukaryotes, like AGLs or other forms of tRNA-dependently modified lipids (9, 14). However, we recently discovered that most of "higher" fungi —*i.e.* Dikarya— are equipped with MprF-like enzymes having DUF2156 domains (18). Unlike MprFs, they have no membrane domains, but the DUF2156 module is rather fused at the C-terminus of an aspartyl-tRNA synthetase (AspRS) paralog, *i.e.* the enzyme responsible for Asp-tRNA^{Asp} production (19). They are bifunctional enzymes capable of producing Asp-tRNA^{Asp} from free Asp, ATP and tRNA^{Asp} (AspRS activity) and use it in the appended DUF2156/Asp-tRNA transferase domain to acylate aspartate onto a lipid that is not a glycerolipid, but ergosterol (Erg), the major fungal membrane sterol, yielding ergosteryl-3β-*O*-L-aspartate (Erg-Asp) (18).Those bifunctional AspRS/Erg-Asp synthases (ErdSs)and Erg-Asp are widespread across Dikarya (KEGG orthology: K24278) and in a substantial number of occurrences, we evidenced that an Erg-Asp hydrolase (ErdH, KEGG orthology: K24279) can remove the Asp moiety of Erg-Asp, providing the first example of a sterol

aminoacylation/deacylation system in fungi (18).To date, the cellular function of Erg-Asp in the physiology of Dikarya remains unknown.

A wide range of mono- and diderm bacteria possess one or several combinations of MprF proteins, which, due to the catalytic diversity of the enzymes, expands the AGLs diversity within a given bacterial species (14). In *Clostridium perfringens*, two MprFs are present, with MprF2 being a LysPG synthase (specific for Lys-tRNA) and MprF1 an AlaPG synthase (specific for Ala-tRNA) (7), while in *Enterococcus* spp., MprF1 is a Lys/Arg/Ala-PG synthase of broad aa-tRNA specificity (8). Up to date, only Erg-Asp has been evidenced in fungi, and no other *O*-L-aminoacyl ester of Erg or of glycerolipids has been discovered, nor has a second type of DUF2156 protein.

Here we report the discovery in ascomycota —one of the two divisions of Dikarya— of a novel type of DUF2156 proteins. They are all free-standing DUF2156 domains (fDUF2156) phylogenetically related and paralogous to ErdS that, contrary to the latter (18), are not fused to an aminoacyl-tRNA synthetase. Using *Aspergillus fumigatus* (*Afm*), *Aspergillus oryzae* (*Aor*) and *Yarrowia lipolytica* (*Yli*) as models, we demonstrate that fungal fDUF2156 proteins have an enzymatic activity distinct from that of ErdS: they use glycyl-tRNA^{Gly} (Gly-tRNA^{Gly}) produced by glycyl-tRNA synthetase (GlyRS) to transfer Gly onto Erg, yielding ergosteryl-3β-*O*-glycine (Erg-Gly), another and previously undetected type of sterol conjugate of the aminoacyl-type. Therefore, fungal f-DUF2156 are genuine Erg-Gly synthases (ErgS, Er: ergosterol, g: glycine, S: synthase) that expand the repertoire of the newly discovered class of *O*-L-aminoacyl ester of sterols. We conclude that ErgS and ErdS both represent members of a novel enzyme family —ergosteryl-3β-*O*-amino acid synthases—that produce ergosteryl-3β-*O*-amino acids in a vast diversity of fungi.

RESULTS

A second type of aminoacyl-tRNA transferases in ascomycota [*in silico studies were mainly performed by Dr. F. Fischer & G. Grob*]

Upon detection of ErdS in Dikarya (18), we noticed that *Aspergillus fumigatus* (*Afm*) and *Aspergillus oryzae* (*Aor*) possess an additional protein that presented distant homology to the DUF2156/Asp-tRNA transferase domain of ErdS (~20 % identity) and that was unambiguously recognized as a DUF2156 protein, using the Protein FAMily database (PFAM) search tool (https://pfam.xfam.org/) (20). Both proteins —encoded by the *AFUA_8g01260* and *AO090011000521* genes in *Afm* and *Aor*, respectively— are free-standing DUF2156 domains

(fDUF2156), meaning that they are neither fused to an aaRS domain, nor to an N-terminal integral membrane flippase-like domains, which differs from fungal ErdS (18) and bacterial MprFs (5), respectively (**Fig. 1***A* and **1***B*). These fDUF2156 proteins were not restricted to *Afm* or *Aor*, but also detected in numerous other ascomycota, including various Eurotiomycetes (*Aspergillus* and *Penicillium* spp., among others) and Sordariomycetes (*Beauveria bassiana*, *Bba*, for example) (**Fig. 1***B* and *C*), as well as several Dothideo- and Leotiomycetes (**Fig. S1** [*figure in preparation but the reader can refer to* **Fig. S7** *which summarizes the landscape of fungal DUF2156 proteins*]). The fDUF2156 proteins seem absent in basidiomycota, except in *Trichosporon oleaginosus* (**Fig. S1** [*in preparation*]). Interestingly, while ErdS was absent in all Saccharomycotina (18), we detected one fDUF2156 in *Yarrowia lipolytica* (*Yli*) (Saccharomycete), encoded by the *YALI0E00330g* gene (**Fig. 1***B*).

Sequence analysis and structure prediction of *Afm*, *Bba* and *Yli* fDUF2156 (**Fig. 1***B*, *C*, **Fig. S2** [*Fig. S2 in preparation*]) shows that, like in the case of the DUF2156/Asp-tRNA transferase domain of ErdS (18) or the Ala- or Lys-tRNA transferase domain of MprFs (21), the proteins are all likely constituted of two Gcn5-like N-acetyltransferase (GNAT) subdomains separated by a positively charged $\alpha^{(+)}$ helix, a fold characteristic of aa-tRNA transferases of the DUF2156 family (5, 21, 22) (**Fig. 1***B*, **Fig. S2** [*Fig. S2 in preparation*]). Like in bacterial MprFs (21) or in ErdS, this $\alpha^{(+)}$ helix, together with the GNAT II domain, is expected to bind the aa-tRNA substrate, while the GNAT I subdomain recognizes the acceptor lipid. This architecture is conserved in all selected cases (**Fig. 1***B*). Depending on the species from which they originate, fDUF2156 proteins can have N terminal extensions of various sizes sharing neither homology with known proteins (**Fig. 1***B*), nor obvious signal sequences (PSORT II, https://psort.hgc.jp/form2.html). In the case of *Aor*, however, the fDUF2156 protein seems much shorter than its closest homologs found in *Afm* or in *Afv* (with which it shares close ancestry (23, 24)), and the GNAT II domain appears dramatically truncated, to the point that most of the putative aa-tRNA transferase active site would be absent, suggesting that the enzyme would be inactive (**Fig. 1***B* and see below).

Because fDUF2156 proteins are not fused to an aaRS, and because no consensus sequences have been determined to predict the substrate specificity of DUF2156 proteins (5), *in silico* determination of the aa-tRNA or acceptor lipid substrates were impossible. Phylogenetic reconstructions, however, evidenced that fungal DUF2156 (ErdS and fDUF2156) are related to the DUF2156 domains of bacterial MprFs, but more interestingly, that ErdS and fDUF2156 form two distinct and robust clades of different architectural types (**Fig. 1***D*), suggesting that they represent two distinct types of enzymes, possibly with different activities. These

evolutionary relationships of fDUF2156 with either ErdS or MprF, as well as its structural features, supported the hypothesis that it could modify lipids — glycerolipids or Erg— by a tRNA-dependent mechanism as well (5, 18). In consequence, we hypothesized that fDUF2156 might be able to bind an aa-tRNA of unknown identity, produced by an unknown aaRS, to use it in a tRNA-dependent lipid modification mechanism using an unknown lipid.

Attempts to delete the *fDUF2156* gene in *Aspergillus* spp [performed by Dr. N. Mahmoudi-Kaidi in our Lab, and by Pr. T. Kushiro's team*].*

In order to verify that fDUF2156 proteins are involved the tRNA-dependent aminoacylation of a lipid, and as we did for ErdS (18), we tried to construct Δ*fDUF2156* mutants in *Afm* and *Aor* by gene replacement to analyze and compare total lipids from WT and deletion strains by thin layer chromatography (TLC). Despite multiple attempts in *Afm* using electroporation (18, 25) to introduce the deletion cassette, or in *Aor* using either protoplast-PEG (18) or *Agrobacterium*-mediated transformation (26), we failed to isolate *bona fide* Δ*fDUF2156* mutants in both species. In *Afm*, we could only isolate one clone in which the *fDUF2156* was seemingly knocked out, but in which the fDUF2156 ORF was still detected by PCR, either suggesting that the region is not prone to deletion, or that the *fDUF2156* gene underwent duplication upon deletion, suggesting that it could be essential under the selection and/or growth conditions used (see below). Because gene deletion was unsuccessful, we could not evaluate whether the absence of fDUF2156 led to the loss of an aminoacylated lipid. We therefore used a different strategy to characterize fungal fDUF2156 proteins.

[*Note for the reader: Alternatively, we are going to try to obtain an Afm strain in which the fDUF2156 gene will be replaced by a copy under the control of a xylose-inducible promoter (P_{xyl}). If fDUF2156 is essential, at least in given time points of Afm's life cycle, the P_{xyl}-fDUF2156 strain should grow on minimal medium with xylose (MMX, induced conditions), but not in the presence of only glucose (MMG, non-induced conditions). This, if it happens, should prove fDUF2156 to be essential, at least in some circumstances, or under the growth conditions used. This would, of course, change the shape of the paper.*]

Freestanding DUF2156 proteins modify lipids [*the fDUF2156 dependent lipid was discovered by N. Yakobov. Results in **Fig. 2A, 2B, 2C** and **3B** were obtained by N. Yakobov*]

The impossibility to delete the *fDUF2156* in either *Afm* or *Aor* prompted us to express them heterologously in the yeast *Saccharomyces cerevisiae* (*Sce*) that, according to our *in silico* analyses, lacks both ErdS (18) and fDUF2156 proteins (**Fig. S1** [*figure in preparation. Please*

*refer to **Fig. S7** which summarizes the landscape of fungal DUF2156 proteins*]). Heterologous expression of ErdS in *Sce* facilitated the identification of its Erg-Asp product (18). We therefore chose the fDUF2156 proteins from *Afm* and *Aor* but also from *Bba* and *Yli* (**Fig. 1B**), to obtain information on diverse representatives within the fDUF2156 clade (**Fig. 1D**). Genes from *Afm*, *Bba* and *Yli* presented no introns, so they were PCR-amplified from genomic DNA and cloned directly in destination vectors for expression in *Sce*. In the case of *Aor*, the shortest form described above (**Fig. 1B**, **Fig. S3** [*Fig S3 in preparation*]) was unexpected. Closer examination revealed that in *Aor*'s genome, the *AO090011000521* (fDUF2156) gene (FundiDB: https://fungidb.org/fungidb/ app/record/gene/AO090011000521), of 1538 bp, contains one intron (398 bp) that, if spliced out, would produce an ORF of 1140 bp encoding a 380 aa-long protein corresponding to the annotated and truncated form of fDUF2156 (**Fig. 1A**). Of note, this intron is absent in *Afv* (AFLA_043480) that yet shares close ancestry with *Aor* (23, 24) and it does not interrupt the ORF (**Fig. S3** [*Fig S3 in preparation*]).Translation of the intron-containing ORF to the next stop codon —*e.g.* 24 bp downstream the annotated stop— gives a 1563 bp-long ORF that would encode a full-length fDUF2156 protein, closely related to those from *Afv* and *Afm*. We amplified the ORF from *Aor* cDNA and were able to obtain the longest form of 1563 bp that corresponds to the full-length fDUF2156 of *Afv*, indicating that the intron is not spliced out, probably wrongly annotated and that it simply does not exist. This long form was used for heterologous expression in *Sce*

[*Note for the reader: Western Blot with polyclonal antibodies raised against Afm fDUF2156 will be used to analyze Afm, Aor, Afv, A. nidulans and A. niger protein extracts, for which fDUF2156 share very close identity; this should clarify which protein form is expressed in Aor but also in A. nidulans, in which the same truncation was observed. Ongoing.*]

We first extracted total lipids from WT and *Afm* fDUF2156-expressing *Sce* strains and separated them by TLC, using a solvent system that was appropriate to visualize Erg-Asp, *i.e.* CHCl$_3$:MeOH:H$_2$O (130:50:8, v:v:v) (18). Comparison of the two strains revealed that a novel lipid, termed lipid Y (*Sce +Afm* fDUF), absent from the WT strain (*Sce*), was produced (**Fig. 2A**). Lipid Y displayed different migration properties than the Erg-Asp produced by *Afm* ErdS (*Sce + Afm* ErdS), suggesting that the two enzymes have distinct activities and produce distinct products. The fact that lipid Y migrated close to the solvent front, suggested that it was more hydrophobic than Erg-Asp. In order to better visualize lipid Y on TLC, we used a more suitable solvent, *i.e.* CHCl$_3$:MeOH:H$_2$O (130:16:1, v:v:v) (**Fig. 2B**). Under these conditions, lipid Y migrated approx. in the middle of the TLC, which enabled to highlight that *Afm*, *Aor*, *Bba* and *Yli* fDUF2156 proteins, when expressed in *Sce*, produced the exact same lipid Y, *e.g.* sharing

the same migration and staining properties (**Fig. 2C**) [*Note for the reader*: *A TLC with WT Sce and Sce expressing Aor fDUF2156, using the (130:16:1, v:v:v) solvent will be added*]. Finally, we analyzed total lipid extracts from WT strains of *Afm*, *Aor*, *Bba* and *Yli* and confirmed in each case that a lipid band with similar migration and staining properties as lipid Y was present (**Fig. 2D**), with the exception of *Bba* that, under the growth condition used, produced only barely detectable levels of lipid Y. Of note, all fDUF2156 seem to produce the same modified lipid Y, despite very different positions within the fDUF2156-specific clade (**Fig. 1D**). Importantly, lipid Y stained with a distinctive brownish color with a $MnCl_2/H_2SO_4$ solution (27), suggesting that it could also be an Erg or sterol derivative (**Fig. 2A**) (18). Furthermore, lipid Y weakly but positively stained with ninhydrin, and was degraded through alkaline treatment (**Fig 3B**), which supported the hypothesis that it was an aminoacylated lipid, likely an aminoacylated sterol (**Fig. 2A**).

[*Note for the reader: At the beginning we focused on the fDUF2156 from Afm. However as illustrated here the amounts of lipid Y produced in Sce expressing Afm fDUF2156 are very low in comparison to levels found in Sce expressing homologs from Yli or Bba. Consequently, it is more convenient to use the Sce strain expressing Yli fDUF2156 to purify higher amounts of the modified lipid as well as to appreciate with more facility the in vivo lipid aminoacylation activity in mutants (see below)*].

Lipid Y is an ergosteryl-3β-*O*-amino acid [*Total lipid extraction and Lipid Y purifications were performed by N. Yakobov; MS experiments, data collection and analysis were performed by H. Roy's team; synthetic Erg-Gly was produced by Pr. T. Kushiro*]

We reasoned that the determination of lipid Y's structure by LC-MS/MS would represent a step forward to the deciphering of their catalytic activity and to the identification of two substrates that they use. We therefore used total lipids from *Yli* —that naturally expresses fDUF2156 and produces appreciable amounts of lipid Y (**Fig. 2**)— to extract and purify lipid Y using Silica Gel column chromatography also called Flash chromatography (FC) (**Fig. 3A**, refer also to **Fig. S12**) (14, 18). LCMS^n analysis of the resulting fraction revealed the presence of protonated ions of dehydrated ergosterol ($[Erg-H_2O+H]^+$, *m/z*=379 (18, 28), as well as of a compound at a *m/z* of 907 (**Fig. 4A**). MS^n analysis of this latter compound revealed a fragmented ergosterol ion at *m/z*=379 (**Fig. 4E**) suggesting that the parent ion (*m/z*=907) may be a protonated dimeric ion of glycylated ergosterol ($[2Erg-Gly+H]^+$, *m/z*=907), which would imply that lipid Y would be, like Erg-Asp, an aminoacylated sterol, most likely an ergosteryl-3β-*O*-amino acid if fDUF2156 proteins function catalytically like ErdS (18). To test this hypothesis,

we synthesized ergosteryl-3β-*O*-glycine (Erg-Gly) chemically (**Fig. S4**) and analyzed it directly by the same methods. The synthesized Erg-Gly and a FC-purified fraction both exhibited a peak at *m/z*=907 and identical fragmented ion products upon MS^n analysis (**Fig. 4*A-F*** and compare **Fig. S5*A* to Fig. S5*B***). Tuning the instrument to the *m/z* peak at 907 using the synthetic Erg-Gly allowed detection of the monomeric protonated ion [ErgGly+H]$^+$ at *m/z*=454 both in the synthetic Erg-Gly preparation and in the FC-purified sample (**Fig. 4*A-F*, Fig. S5*A* and Fig. S5*B***). To confirm that fDUF2156 synthesizes Erg-Gly, LCMS^n analyses were carried out on total lipid extracts originating from the *Sce* strain expressing heterologously fDUF2156 from *Afm*, alongside the wild-type strain. Erg-Gly was detected in the dimeric ion form ([2GlyErg+H]$^+$, *m/z*=907) in the strain expressing fDUF2156, but was absent from the wild-type (**Fig S5*C*** and **S5*D***). Because fDUF2156 is a homolog of ErdS (18), these results suggest that fDUF2156 aminoacylates Erg using Gly-tRNA^{Gly} as an aa donor, making it an ergosteryl-3β-*O*-glycine synthase, or ErgS (Er: ergosterol, g: glycine, S: synthase) (**Fig. 4*G***).

fDUF2156 are ergosteryl-3β-*O*-glycine synthases [*the in vitro assays described in (18) was adapted for the present purpose by N. Yakobov which obtained results from **Fig. 5** and **S6***] To further characterize its molecular mechanism and more importantly to confirm its Erg-Gly synthesis activity, we aimed to perform *in vitro* lipid aminoacylation assays (LA assay). To this end we used a lipid aminoacylation assay (LA assay) adapted from that used for ErdS (18). Briefly, a total soluble extract from WT *Sce* (S100) was used as a source of glycyl-tRNA synthetase (GlyRS) that, in the presence of ATP, total tRNA from *Sce* (containing tRNA^{Gly} isoacceptors) and [^{14}C]Gly, produced [^{14}Gly]-tRNA^{Gly} (**Fig. 5*A***), expected to be used as a substrate for ErgS. Upon addition of cold Erg and fractions containing ErgS, reaction products were extracted by the Bligh & Dyer method, and separated on TLC, before visualization of radioactive compounds by phosphorimaging. As mentioned above, we initially focused on the characterization of the ErgS homolog encoded by *Afm*. Therefore, we expressed *Afm* ErgS (fDUF2156) in *E. coli* as Maltose-binding protein (MBP) fusion to improve solubility of the recombinant enzymes that otherwise are non-soluble and/or poorly expressed. However, LA assays failed to reveal Erg-Gly synthesis by *Afm* Ergs despite several trials (an example is provided in **Fig. S6**). Moreover, crude extracts prepared from *Sce* expressing ErgS from *Afm* were also inactive [*not shown, will be repeated before integration in the manuscript*] which was even more surprising since Erg-Gly was detected by TLC in *Sce* expressing *Afm* ErgS (but not in the *Sce* wt strain) (**Fig. 2*B***), and MS data confirmed the presence of the modified lipid in this strain (**Fig. S5*C***). The reason why *Afm* ErgS was inactive in the LA assay could not be

determined, but such peculiarity likely results from its own properties that also make it less active than *Yli* and *Bba* ErgS when expressed heterologously in *Sce* (**Fig. 2C**).

In front of this issue we changed the ErgS homolog to be tested and, because expression of the *Yli* ErgS seemed to be more active *in vivo*, we expressed this homolog as an MBP fusion in *E. coli* and purified it. Since the $\alpha^{(+)}$ helix seems critical for the activity of DUF2156 proteins (21), we also produced a mutated form of the enzyme, in which the positively charged R and K residues found in this helix were mutated to E, to produce a negatively charged $\alpha^{(-)}$ helix (see below for more details). Both recombinant enzymes were tested by LA assay and results showed that *Yli* ErgS, but importantly not the $\alpha^{(-)}$ mutant, was active *in vitro* and produced high amounts of Erg-[^{14}C]Gly from Erg and [^{14}C]Gly-tRNA^{Gly} (**Fig. 5B**). [*Same experiments with [^{3}H]Erg will be done soon*].

In the absence of Erg, or in the presence of RNase A, *Yli* ErgS failed to produce Erg-[^{14}C]Gly, demonstrating that it requires Erg and is strictly tRNA-dependent, as the DUF2156 of ErdS (18) (**Fig. 5B**). Interestingly, using [^{14}C]Gly-tRNA^{Gly} to produce Erg-[^{14}C]Gly is only possible in the presence of ErgS and not in the presence of ErdS, that is known to use Asp-tRNA^{Asp} to produce Erg-Asp (18), suggesting that both enzymes —the DUF2156/aa-tRNA transferase modules— are likely specific towards the aa-tRNA that they use (**Fig. 5C**). Because ErgS is not fused to GlyRS, this could expose the enzyme to other, unrelated aa-tRNAs *in vivo*. We therefore next tested whether ErgS was specific for Gly-tRNA^{Gly}*in vitro*. In the presence of total tRNA, ATP and a mix of 15 [^{14}C]aa (excluding Met, Cys, Trp, Asn and Gln), protein extracts from *Sce* —containing the 20 aaRSs, including the 15 necessary to the test—, produced the 15 possible aa-tRNAs, including [^{14}Gly]-tRNA^{Gly}. In the presence of Erg, *Yli* ErgS indeed produced Erg-[^{14}C]Gly. However, when non radioactive Gly (5 mM) was added to the mix during the aa-tRNA synthesis phase the Erg-[^{14}C]Gly band was absent after addition of Erg and *Yli* fDUF2156 (**Fig. 5D**). This likely resulted, as expected, from a strong isotopic competition that implies that ErgS, when in the presence of 15 aa-tRNA species, favors Gly-tRNA^{Gly} over other aa-tRNAs, including Asp-tRNA^{Asp}, making it a genuine Gly-tRNA transferase, distinct from ErdS in terms of specificity. Of note, a similar experiment conducted with ErdS confirmed that it uses only Asp to produce Asp-tRNA^{Asp} and then Erg-Asp, excluding that it could use Gly, or any other aa (**Fig. 5D**).

Altogether, results demonstrate that ErgS specifically recognizes Gly-tRNA^{Gly} and uses it to transfer Gly onto the 3β-OH group of Erg to produce Erg-Gly. [*tests on crude extracts from Afm, Aor, Bba and Yli will be done*].

The α⁽⁺⁾ helix is critical to the activity of Erg-aa synthases [*experiments design, structure predictions, selection of residues to mutate, experimental mutagenesis, lipid analyses etc. were performed by N. Yakobov and Dr. N. Mahmoudi-Kaidi*]

In bacterial MprFs, the $\alpha^{(+)}$ helix between subdomains GNAT I and II of the DUF2156 module (referred to as "the α_5 helix") has been postulated to bind the acceptor stem of the tRNA carrying the aa substrate (21). We mutated the putative $\alpha^{(+)}$ helix of *Afm* and *Yli* fDUF2156 proteins —that we delineated in the two predicted structures presented in **Fig. 1C**— by changing positively charged R and K residues to E, thereby modulating the global charge of the helix, with the expectation that negative charges brought about by E residues would "repel" the negatively charged backbone of the tRNA's acceptor stem. When expressed in *Sce*, *Afm* ErgS $\alpha^{(-/+)}$ (2 out of 4 positive residues are mutated to E), *Afm* ErgS R328E and *Afm* ErgS R335E mutants failed to produce Erg-Gly, which mimicked the behavior of equivalent mutants in bacterial MprFs (21)(**Fig. 6A**). However, because Erg-Gly levels are hardly appreciable even in *Sce* expressing the wt *Afm* ErgS in comparison to the wt *Yli* ErgS, we wonder if equivalent mutations in the latter would completely abolish or only partially reduce Erg-Gly levels. To this end, *Yli* ErgS $\alpha^{(-)}$, (all K and R residues are mutated to E), *Yli* ErgS $\alpha^{(-)2}$ and $\alpha^{(-)3}$ mutants, in which various combinations of R-to-E and/or K-to-E point mutations were introduced in the $\alpha^{(+)}$ helix, were tested in *Sce* and showed no detectable amounts of Erg-Gly (**Fig. 6B**). Because equivalent mutations have similar effects in bacterial MprFs (21), these results highlighted the crucial role of this $\alpha^{(+)}$ helix in aa-tRNA transferases of the DUF2156 fold.

[*Additional notes for the reader:*

1) *In the first part of my thesis I presented results obtained for ErdS mutants containing equivalent mutations in the $\alpha^{(+)}$ helix found in the DUF2156 module of ErdS: all R and K residues were mutated to E to generate an $\alpha^{(-)}$ —negative— helix, and to A to obtain an $\alpha^{(0)}$ —neutral— helix. In both cases, $\alpha^{(-)}$ and $\alpha^{(0)}$ mutations identically abrogated Erg-Asp production in Sce expressing the mutants, or in vitro with the $\alpha^{(0)}$ mutant. These results were not published for the moment but together with the herein presented results they further demonstrate the essential role of the $\alpha^{(+)}$ helix.*

2) *In addition to a(+) mutants I performed together with Dr. N. Mahmoudi-Kaidi a broader mutagenesis study on Afm ErgS that will not be presented here.*

3) *One important technical point that must be underlined is that the anti-ErgS antibody synthesized during my thesis in collaboration with Covalab France, seems to be specific*

to ErgS from Afm and failed to detect the expression of the Yli homolog. This is an additional reason why results obtained with Afm and Yli Ergs mutants were necessary at this state. In the future, recombinant versions of relevant Yli ErgS mutants will also be tested in vitro, as it was done for Yli ErgS $\alpha^{(-)}$. Tagged versions of this proteins should also be expressed in Sce to test simultaneously ErgS expression and Erg-Gly synthesis in each mutant.

4) Yli ErgS WT and $\alpha^{(-)}$ mutant will be purified to test interaction with tRNA^{Gly} transcripts (gel-filtration). Gly-tRNA^{Gly} will be used as well, to determine whether the Gly moiety is required for recognition by ErgS. Precisely, the goal is to determine if Yli ErgS $\alpha^{(-)}$ fails to interact with its substrate (tRNA^{Gly} or Gly-tRNA^{Gly}). The same can be done on the DUF2156 module of ErdS, deleted from the AspRS domain, to show the same thing, if required and/or relevant.]

DISCUSSION

[*Introducing remarks for the reader: As mentioned in the introducing remarks, the proposed ErgS article draft is very preliminary and according to the results we will obtain in the few coming month, the article might completely change. Similarly, I wrote the following discussion regarding my thesis work while the final version will probably completely be revised. In addition to that, I would like to aware the reader that in the following part I also included some remarks concerning the technical issues that I encountered during the characterization of this second lipid aminoacylation pathway. I will also provide an analogy between aminoacyl lipid synthases (aaLSs) from fungi and from bacteria which will highlight the main similarities/differences. Thus, the present part should be considered as a general discussion on the characterization of fungal aaLSs and their associated aminoacylated sterols (AS), which was the main task during my thesis.*]

RNA dependent lipid aminoacylation factors (*i. e.* MprF-like proteins achieving their aa-tRNA transferase (ATT) activity through a DUF2156) were thought for a long time to be restricted to bacteria. However, in our recent work we detected an AspRS-DUF2156 fusion protein in most higher fungi belonging to Ascomycota and Basidiomycota and showed it to synthesize ergosteryl-3-β-O-L-aspartate (Erg-Asp) in an Asp-tRNA^{Asp} dependent manner (18). The characterization of this Ergosteryl-aspartate Synthase (ErdS) was to our knowledge the only

RNA dependent lipid aminoacylation factor described in eukaryotes. In our initial study we also characterized an Erg-Asp hydrolase (ErdH) as being responsible to regulate the homeostasis of Erg-Asp, thereby highlighting a novel sterol derivate synthase/hydrolase mechanism (18). In the continuity if this work, we aimed to further investigate the landscape of fungal DUF2156 proteins in eukaryotes. Indeed, in the present study we detected through *in silico* analyzes a second fungal DUF2156, which, in contrast to ErdS, is mostly restricted to Ascomycota and importantly is not fused to an aaRS. We demonstrated that this so far uncharacterized freestanding fDUF2156 is a genuine ATT that transfers Gly onto the 3-β-O-hydroxyl of Erg in a tRNA dependent manner, making it an Ergosteryl-3-β-O-glycine synthase (ErgS). To our knowledge, Erg-Gly was never described before and its discovery enlarges the repertoire of 3-β-O-modified sterols in fungi. Importantly, the physiological function of fungal aminoacylated sterols (AS) remains to be discovered but it is noteworthy that for the moment we dramatically failed to delete *ergS* in *Afm* and our collaborators from Pr. T. Kushiro's team, are confronted to the same issues in the context of *Aor*. Therefore, we question ourselves if this gene is essential at least in *Aspergillus* spp. In order to circumvent this issue, ongoing experiments in our lab aim to replace *ergS* by inducible versions but we also undertake to verify if the *ergS* can more easily be deleted in the *Afm ΔerdS* strain. Establishing that *Afm ΔerdS ΔergS* double deletant is viable but not *Afm ΔergS* would indicate a strong functional correlation between both encoded enzymes and could indicate that in addition to ErdH, the balance between Erg-Asp and Erg-Gly is crucial for Erg-aa homeostasis.

1) Main issues encountered during the identification of the ErgS dependent lipid and strategy adaptations to overcome them.

The functional characterization of ErgS was much more complex, even using *Sce* as a model organism. First the detection of an additional lipid in *Sce* expressing Ergs*Afm* in comparison to *Sce* wt through TLC failed for a long time and the main reason for that was that the ErgS dependent lipid is more apolar than Erg-Asp. Consequently, the ErgS dependent lipid was often stacked in the migration front of the TLC and was therefore difficult to appreciate. Furthermore, for a yet undetermined reason, the level of ErgS dependent lipid was much lower than Erg-Asp levels in *Sce* strains expressing ErdS. Fortunately, we realized this and optimizations of TLC conditions, in particular the migration solvent and the visualization method, enabled finally the

unambiguous detection of **a fDUF2156 dependent lipid that, importantly, behaved distinctly to Erg-Asp** with regard to its migration by TLC. In contrast, this modified lipid was stained similarly to Erg-Asp i. e. both lipids shared the distinguishable coloration observed for Erg and Erg sterols under UV light in comparison to phospholipids. This observation was indicative for that the lipidic part of the fDUF2156 dependent lipid corresponds also to Erg.

The fact that ErgS is not fused to the aaRSfurther complexified its characterization mainly for 3 reasons. First, the eventuality that this protein modifies the lipid through another modification than aminoacylation could not be excluded, even if the *in-silico* detection of the DUF2156 strongly suggested that the protein might have an ATT activity. Second, even if ErgS achieves ATT activity, the hypothesized aa moiety was not predictable. Third, in contrast to ErdS for which the AspRS domain served as "quality control" to confirm that the purified protein or the crude extract tested through *in vitro* experiments contain an ErdS at least partially active, nothing could attest that ErgS (purified or from crude extracts) was active in the tested sample. In an attempt to identify the supposed aa esterified on the ErgS dependent lipid, we performed several *in vitro* assays (LAA) notably with the recombinant ErgS*Afm* (e. g. **Fig. S6**), as well as crude extracts from *Sce* expressing or not ErgS*Afm*. However, despite many trials, we failed to detect the expected lipid aminoacylation activity of fDUF2156*Afm in vitro*. We also tried to identify the lipid by MS. As for Erg-Asp, we aimed to purify the fDUF2156 dependent lipid from *Sce* expressing ErgS from *Afm* [*refer to the material & methods section of the thesis manuscript*]. The procedure for silica column chromatography was optimized but even though the modified lipid was successfully enriched, MS analysis failed dramatically to identify the lipid, probably due to the apolar nature, the low ionization rate, and the insufficient amount of the targeted lipid. Finally the situation was unlocked by switching to the ErgS homolog from *Y. lipolytica* (*Yli*), which to our knowledge is the sole saccharomycotina encoding a DUF2156 protein and the sole species in which the fDUF2156 (ErgS) version was detected but not the AspRS-DUF2156 (ErdS). This strategy adaptation was promising due to that levels of the modified lipid are severally increased in both, *Sce* expressing heterologously ErgS*Yli* and in *Yli*. This suggested that the fDUF2156 homolog found in *Yli* is either more stable, more active, or more efficiently expressed when present in *Sce* in comparison to the fDUF2156 homolog found in *Afm*. Following these observations, the unknown lipid was purified from *Yli* by silica column

chromatography which was then again submitted to MS analysis (LC-MS/MS/MS). Hervé Roy also considered synthetic aminoacylated-Erg (Erg-aa) derivates that were synthesized by another one of our collaborators, Pr. Tetsuo Kushiro. Comparison of spectra obtained from MS analysis finally strongly supported that *Yli* **contains ergosteryl-3-β-O-glycine (Erg-Gly)**. While m/z corresponding to Erg-Gly and (Erg-Gly)$_2$ were detectable in MS1 spectra and expected Erg ions were detected in MS2/MS3 spectra, no Gly ions were detectable nor in MS2 nor in MS3. This might be due to the known limitations of using iontrap MSs for which relative signal intensities corresponding to low masses significantly decreases with the number of MS rounds (MSn). The identification of Gly as being the aminoacylated lipid was indirectly deduced from MS data according to the m/z differences, as regularly done for proteomics but also in some cases in lipidomics (28). Therefore, it was even more necessary to confirm the lipid identity through biochemical experiments. To this end we adapted the LAA and confirmed *in vitro* that the ErgS homolog from *Yli* transfers specifically Gly onto Erg in a tRNA and DUF2156 dependent manner. Surprisingly, this activity remained undetectable when the recombinant fDUF2156 form *Afm* was assayed (**Fig S6**) which was surprising since Erg-Gly was also detected by TLC and by MS data in *Sce* **expressing fDUF2156**$_{Afm}$ but not in the *Sce* wt strain. Nevertheless, Erg-Gly was detected by TLC in several other fungi and its presence will also be verified in the future by other approaches including MS analyses. Taken together, our data demonstrated that fungal **fDUF2156 are Erg-Gly synthase, abbreviated ErgS**, and this enzyme as well as the synthesized Erg-Gly lipid were to our knowledge never described before.

2) AaRS fused- and freestanding- aaLS are encoded by bacteria and fungi but their distribution/occurrence differ

It is striking to note that as in bacteria, fungal species encode two distinct aaLS that differ in that they are either fused or not with an aaRS. However, their occurrence differs importantly, since, in bacteria aaRS-fused MprF are restricted to only one bacteria phylum (i. e. actinobacteria) while "freestanding" MprFs are majorly found in bacteria (14). In contrast, the main eukaryotic aaLS is the aaRS fused one (i. e. ErdS) which is found in almost all filamentous fungi, while the freestanding version (i. e. ErgS) is less widespread and restricted to Ascomycota (**Fig. S7**). Concerning their co-occurrence, fungi encode either both aaLSs or only

the bifunctional ErdS while species harboring only the freestanding ErgS protein are very rare. Furthermore, species from both kingdoms can harbor more than one aminoacylated lipid (aaL), but in bacteria distinct aaLs are produced either by aaLS that contain broad range specificities or by expressing distinct aaLSs, each containing strict substrate specificities (8, 9, 14, 29). In comparison, our results showed that in fungi, ErdS and ErgS have strict substrate specificities for Asp-tRNA^{Asp} and Gly-tRNA^{Gly}, respectively (**Fig. 5C and 5D**). The mechanism by which aaLS restrict their specificities for the aa-tRNA is not known nor in bacteria neither in fungi. In fact, Hebecker and colleagues showed that AlaPGS from *P. aeruginosa* and LysPGS from *B. licheniformis* only use Ala-tRNA^{Ala} and Lys-tRNA^{Lys}, respectively but no marked differences explaining the recognizing mechanism were evidenced (21). In accordance, the phylogenetic study performed by Smith and colleagues did not reveal phylogenetic discriminations between bacteria MprF-homologs harboring distinct substrate specificities (14). In our lab, F. Fischer and G. Grob aimed to study the phylogeny of fungal DUF2156 domains and to this end they recovered erdS and ergS sequences cleared from their AspRS domain and their N-terminal extensions. Without going into details their result indicates that fungal DUF2156 form ErdSs and from ErgSs are phylogenetically related but, in contrast to bacterial aaLSs, they are separated in distinct clusters according to their experimentally demonstrated or predicted substrate specificities (**Fig. 1**). Because this study also included DUF2156 sequences from bacteria species, F. Fischer and G. Grob also showed that fungal and bacterial DUF2156 domains are phylogenetically related.

3) Implementing aa-tRNAs for lipid aminoacylation in addition to protein biosynthesis: A poorly understood issue.

In the cases of actinobacteria encoding bifunctional LysPGSs proteins that are directly fused to a LysRS (30) it is assumed that Lys-tRNA^{Lys} might be directly channeled from the aaRS to the MprF-like domain. Notably, LysX from *M. tuberculosis* (encoded by *Rv1640c* gene) synthesizes LysPG and both functional domains, i. e. the LysRS and the MprF-like domain, were shown to be essential for lipid aminoacylation (30). Importantly, the *Rv1640c* gene is not essential for viability and can be deleted since this species encodes a distinct housekeeping LysRS (*Rv3598c*) to provide Lys-tRNA^{Lys} for protein biosynthesis. Because the housekeeping LysRS is essential (31) it is assumed that LysX cannot supply Lys-tRNA^{Lys} for protein

biosynthesis and that its LysRS activity is strictly restricted for LysPG synthesis (32). Consequently, both LysRS homologs found in *M. tuberculosis* are restricted to their distinct functions.

In comparison, we showed ErdS from filamentous fungi to be a bi-functional protein that synthesis Erg-Asp in an Asp-tRNA^{Asp} dependent manner (18) and as for LysX from *M. tuberculosis*, the *erdS* gene is (at least in *Afm*, *Aor* and *Ncr*) not essential. This correlates with the fact that, in addition to ErdS (*AFUA_1G02570*), *Afm* encodes for 3 additional AspRSs; *AFUA_2G02590* is predicted to encode the cytoplasmic AspRS that synthesizes Asp-tRNA^{Asp} for protein biosynthesis while AspRSs encoded by *AFUA_8G00100* and *AFUA_4G08330* are annotated as being implicated in mitochondrial biogenesis (at least one of them might ensure Asp-tRNA^{Asp} synthesis for mitochondrial protein biosynthesis). The essentiality of *AFUA_2G02590* gene, encoding the cytoplasmic AspRS, was not verified in our recent study and because ErdS was shown to complement the loss of the housekeeping AspRS from *Sce* it would be interesting to clarify this matter (18). Even though it was not clearly demonstrated, we proposed that Asp-tRNA^{Asp} synthesized by the AspRS moiety of ErdS might be directly channeled to its fused DUF2156 for Erg-Asp synthesis. [*Note for the reader: It is important to remind that in our published study, ErdS was constitutively overexpressed in Sce (p415 plasmids with GPD promoter) which seemed not be the case in Afm. Therefore, it is tempting to speculate that in physiological conditions the cytoplasmic AspRS encoded by AFUA_2G02590 might be essential for protein biosynthesis*].

In contrast, the fungal freestanding DUF2156 (ErgS), can be compared to the bacterial freestanding MprF, and fungi expressing ErgS might somehow deal with a pool of Gly-tRNA^{Gly} for cytoplasmic protein biosynthesis and for lipid modification. Very little is known concerning how cells deal to provide aa-tRNA substrates for both, translation and ATT pathways, from a single aa-tRNA pool. In very few cases it was shown that some tRNA isoacceptors are specifically used for the ATT activity but not for translation (33). This is notably the case for *S. aureus* FemABX protein, involved in the tRNA-dependent remodeling of the peptidoglycan sacculus found in the bacterial cell wall (34). *S. aureus* encodes five tRNA^{Gly} isoacceptors but three of them were shown to be used for cell wall remodeling but not for translation (35).

In bacteria, the DUF2156 domain of freestanding MprFs is assumed to hijack aa-tRNAs synthesized by the housekeeping aaRS to transfers the aa-moiety onto the lipid (9). In accordance, studies suggested that bacteria do not use specific tRNA species to discriminate aa-tRNA for protein biosynthesis or for lipid aminoacylation (7). Thus, it is assumed that aaRSs from bacteria provide a single pool of aa-tRNA suitable for both aa-tRNA utilizing pathways, but this aspect remains largely to be investigated.

In the case of the herein characterized fungal ErgS, one basic possibility is that the cellular machinery provides sufficient Gly-tRNA^{Gly} levels to ensure both mechanisms without specifically discriminating distinct pools. This might be possible by finely regulating ErgS expression so that basal levels of Gly-tRNA^{Gly} are highjacked from the translation machinery. Alternatively, ErgS could be overexpressed in specific conditions during which protein biosynthesis is down-regulated, thereby bearing higher levels of Gly-tRNA^{Gly} for Erg glycylation. However, several fungal species (if not all) encoding ErgS, encode at least two tRNA^{Gly} isoacceptors and therefore it cannot be excluded that some of them are specifically dedicated to provide a Gly-tRNA^{Gly} pool dedicated to ErgS activity.

Finally, another possibility, is that GlyRS interacts directly with ErgS, enabling thereby Gly-tRNA^{Gly} channeling from the aaRS domain to the DUF2156 protein. Formation of similar ternary complexes involving aaRS.tRNA was demonstrated in other mechanisms. For example, selenocysteine (Sec) is an amino acid that is incorporated during protein biosynthesis into so-called selenoproteins, which are involved in oxidoreductions, redox signaling and antioxidant defense (36, 37). To this end Seryl-tRNA synthetase catalyzes the formation of a non-cognate Ser-tRNA^{Sec} intermediate. In bacteria, the selenocysteine synthase SelA achieves subsequently Ser to Sec conversion in the presence of selenophosphate, yielding cognate Sec-tRNA^{Sec} which is carried to the ribosome by SelB factor (38). Importantly, OH. Thiemann's team demonstrated recently that the synthesis of Sec-tRNA^{Sec} involves the formation of a SerRS.tRNA^{Sec}.SelA ternary complex in *E. coli* (39). Another case of ternary complex formation was also shown to occur during indirect Asn-tRNA^{Asn} synthesis pathway in *H. pylori*. In this pathway tRNA^{Asn} is mis-aspartylated by a non-discriminating AspRS (ND-AspRS), and the mis-charged Asp is converted to Asn though a trimeric amidotransferase complex, called GatCAB. F. Fischer and

colleagues demonstrated that the formation of GatCAB.tRNA^{Asp} is a prerequisite for the recruitment of the ND-AspRS and consequently for synthesis of non-cognate Asp-tRNA^{Asn} immediately followed by its conversion to Asn-tRNA^{Asn} through transamidation (40). The GatCAB.tRNA^{Asp}.ND-AspRS complex is called transamidosome and enables channeling of the aa-tRNA from one active site to the other, thereby preventing mis-incorporations of Asp at Asn codons during protein biosynthesis (41). In *H. influenza* mis-charged Cys-tRNA^{Pro} is edited by Ybak which also requires the formation of ProRS.Ybak.tRNA ternary complex (42, 43). Note also that beside aaRS.tRNA containing ternary complexes that are involved in translation (i. e. indirect aa-tRNA synthesis/editing of non-cognate aa-tRNAs) similar complex formations were also shown to occur between aaRS.tRNA and metabolic factors. Notably, tRNA dependent Glu-1-semialdehyde formation during heme synthesis in bacteria and chloroplasts involves GluRS.tRNA^{Glu} interaction with the metabolic glutamyl-tRNA-reductase (GluTR) (44).

With regard to the available literature, we question ourselves about the potential interactions between GlyRS, (Gly-)tRNA and ErgS and if they form a ternary complex. To this end a recombinant version of the *Yli* GlyRS will be purified and a transcript tRNA^{Gly} will be produced. Binary or ternary interactions will also be tested using coIP with Sce strains expressing tagged versions of *Yli* ErgS and *Yli* GlyRS. RNA-dependency of the interaction can be tested by adding tRNA in total protein extracts, or by adding RNase A. In combination to these approaches, two hybrid assays in *Sce* will be attempted if required/relevant.

Another important point that we revealed in the present work is the essentiality of the positively charged α$^{(+)}$ helix found in the DUF2156 domain of ErgS for lipid aminoacylation activity. As explained in the introduction, this helix, found in all Dupli-GNAT/ATTs, is assumed to participate to aa-tRNA binding (33) and was also shown in bacterial aaLSs to be essential for their activity (21). However, the formation of the protein-tRNA complex was never experimentally demonstrated to be α$^{(+)}$ helix dependent. To shed light on the functional role of this helix, we also plan assay the formation of ErgS.tRNA complexes in α$^{(+)}$ helix mutants with similar strategies cited in the previous paragraph, including size exclusion, CoIPs and also Electrophoretic mobility shift assays (EMSA).

4) Erg-Gly catabolism seems not to be regulated by ErdH

In our recent work we reported that the divergent gene located immediately upstream to *Afm erdS* gene encodes for a genuine ergosteryl-aspartate hydrolase (ErdH). Investigations of the synteny of both genes revealed that the ErdH α/β hydrolase is specifically present in species encoding *erdS* and that the *erdH-erdS* cluster is conserved in most species. Even though, ErdH might regulate Erg-Asp homeostasis, it remains to be established how is ErdS/ErdH enzymatic pathway is regulated and integrated in fungal cells physiology. Importantly, no ergosteryl-glycine hydrolase (ErgH) was detected for the moment but we suppose that such Erg-Gly might be regulated somehow. This is notably supported by the facts that *1)* aaLs homeostasis was shown to be essential for cellular processes as well as for virulence in bacteria (14-16), *2)* other sterol 3-β-O modifications, including glycosylation (45), acylation by fatty acids (46) and acetylation were all shown to be regulated by reversible mechanisms (47).

One possibility was that ErdH has dual-specificities with regard to the aa-moiety and could hydrolyze Erg-Gly in addition to Erg-Asp. To verify this, we synthesized Erg-Gly *in vitro* and tested its ability to be degraded by ErdH by performing a lipid deacylation assay (as described in (18)). The preliminary result presented in **Fig. S8** however suggest that Erg-Gly is not substrate of ErdH, suggesting that a specific ErgH remains to be discovered. This result gave already an important indication concerning the substrate specificity of ErdH since the only difference between both Erg-aa species is the lateral chain of the aminoacid (R(L-Asp): -CH$_2$-COOH; R(Gly): -H). Thus, the lateral chain of the aa-moiety of Erg-aa seems to be determinant for hydrolysis by ErdH. Furthermore, we also tested ErdH in the presence of commercially available Cholesteryl-hemisuccinate (Cho-HS). Erg and cholesterol (Cho) are structurally very similar and Cho-HS is composed by a Cho molecule esterified on its 3-β-OH group with succinate. Importantly the latter is identical to Asp with notable difference that it does not contain the amine group (-NH$_3^+$) on the C$_\alpha$, which is consequently no more chiral. According to our very preliminary result, Cho-HS was at least partially hydrolyzed by ErdH (not shown), which further indicates that the lateral -CH2-COOH, but not the -NH$_3^+$ group of the modified sterols, is important for substrate recognition or hydrolysis by ErdH.

[*Note to the reader: Those results lack important controls and must be taken with great hindsight. Experiments will be repeated in the lab to clarify these preliminary results.*]

5) aaLS from bacteria and from fungi differ in their substrate specificity for the lipid

In addition to the unexpected discovery that aaLS are also found in fungi species we were very surprised that fungal aaLSs modify Erg since bacteria aaLSs were shown to only modify glycerolipids. In facts, even if their synthesis pathway remains in some cases not totally established, aaPG, aaCL and aaDAG were described in bacteria (9). However, Hebecker and colleagues showed that aaLS from bacteria have *in vitro* broad specificities for the lipid substrate and the molecular recognition mechanism remains largely to be determined (48). It must also be taken in consideration that eukaryotes have a larger repertoire of lipid species and classes when compared to bacteria and therefore might use other lipids than glycerolipids to modulate their membrane properties. Furthermore, in bacteria it is assumed that remodeling the PM through lipid aminoacylation pathways, in particular through the synthesis of the cationic LysPG, reduces the global negative charge of the cell surface, thereby increasing bacterial resistance to CAMPs by charge repulsion (6). Lipid aminoacylation was also involved in several other pathways and it was largely suggested that other mechanism beyond charge repulsion might be involved (9). Importantly, cytoplasmic membranes of eukaryotes are enriched in zwitterionic and apolar lipids while anionic PG levels for example are very low, explaining that they are less susceptible to CAMPs. Therefore, we speculate that fungal DUF2156 proteins might be involved in other mechanism than CAMP resistance. Nevertheless, it is interesting to note that as commonly described in bacteria, fungal aaLs are either zwitterionic (Erg-Asp between pH 3.86 and 9.82) or cationic (Erg-Gly [+1] below pH 9.6) under physiological pH.

Concluding remarks

Beside the several points that I discussed here and notably the comparison with bacterial aaLS, they're other points that can be further discussed. Notably, bacteria MprFs contain a variable number of TMH at their N-terminal extremity which anchors the protein to the membrane (14). In few species it was demonstrated that aminoacylated glycerolipids, synthesized by the C-terminal cytoplasmic synthase domain (i. e. the DUF2156 domain), are translocated from the inner leaflet of the plasma membrane to the outer leaflet (10, 12). The molecular basis of this flippase activity is poorly understood but it was nevertheless was shown to be mediated by the membranous N-terminal domain. It is striking to note that fungal ErdS and ErgS contain N-

terminal extensions for which no domain were predicted but more surprisingly, no transmembrane helices (TMH) were predicted. This important difference raises the question of how fungal DUF2156 proteins are associated to membranes were their lipidic substrate is thought to be found. Even though the localization of ErdS and ErgS remains to be investigated, we reported already some evidences that that ErdS is associated to membranes (18). Similar preliminary experiments suggest that this might also be the case for ErgS (**Fig S9**), thereby comforting the expectation that eukaryotic lipid aminoacylation factors are associated to membranes, even if their identity remains to be determined.

Even though we are relatively advanced in the functional characterization of fungal lipid aminoacylation activities and, in a lesser extent, of fungal aaLs homeostasis, we are still only at the beginning of the "fungal DUF2156" project and several aspects surrounding the topic remain poorly investigated. One of them, the most obvious and probably the most important one, is the physiological function of Erg-Asp and Erg-Gly. More globally, how are ErdS/ErdH and ErgS pathways integrated in cell's physiology? [*Note for the reader: this point will be discussed in the next part of the manuscript*]

MATERIALS AND METHODS

Media and growth conditions

For the routine growth and maintenance, *Y. lipolytica* (*Yli*) and *S. cerevisiae* (*Sce)* wt were grown in YPD agar (Yeast Peptone Dextrose, MP). *Sce* strains BY4742 (*MATα his3Δ1 leu2Δ0 lys2Δ0 ura3Δ0*) carrying vectors (with the LEU marker) expressing *Yli*, *Beauveria bassiana* (*Bba*) or *Afm* ErgS were grown in SC-Leu (MP™ Biomedicals) agar. Cultures were incubated at 30°C overnight under agitation (220 rpm) and cells were harvested by centrifugation at 5000 × g for 5 min at 4 °C when OD_{600} was 0.6-1, depending on the experiment.

Concerning *Aspergillus* spp., the CEA17 Δ*akuB*[KU80] strain of *Afm* (49) and the RIB40 strain of *Aor* (50) have been used as wild-type strains. *Aspergillus* spp. were maintained as follows: fresh conidia (asexual spores) were spread on Malt extract agar (Thermoscientific) plates or slants and incubated in the dark at 37 °C for 7 days until they produced enough mature conidia. Standard *Aspergillus* minimal medium (MM) was composed (for one liter) of glucose (1% w:v),

10 mM ammonium tartrate dibasic, 20 mL of salts (50X solution containing KCl 26 g/L, $MgSO_4$, 7 H_20 26 g/L, KH_2PO_4 76 g/L) and 1 mL of trace elements (1000x solution containing $FeSO_4$, 7 H_2O 1 g, $CuSO_4$, 5 H_2O 0.32 g and Na_2MoO_4 0.8 g for 200 mL adjusted at pH 6.5). Solid media contained 1.5 % (w/v) agar. Agar plates or slants were incubated at 37 °C (*Afm*) or 30°C (*Aor*) in the dark for indicated periods of time. Liquid cultures were incubated in glass flasks at 37 °C (*Afm)* or 30°C (*Aor*) under shaking (220 rpm) for 24 (*Afm*) to 48 hrs (*Aor*), until enough mycelia were produced.

Plasmid constructions for heterologous expression in *Sce* and *E. coli*, and site directed mutagenesis [*performed by N. Yakobov and Dr. N. Mahmoudi-Kaidi*]

The *Afm* ORF encoding ErgS (*AFUA_8g01260*) was synthetized with codon optimized sequences for expression in *Sce*, flanked by attB1 and attB2 sequences and cloned into pUC57 (Genscript®). All other ORF's described here, including ErgS from *Yli* CLIB 99 (ORF identical to YALI0_E00330g from CLIB122 strain) and from *Bba* 80.2, were recovered from the corresponding genomic DNA by PCR. ORF's were then cloned into *Sce* expression plasmids (p415GPD-ccdB) either by Gateway technologies (51) or by the isothermal Gibson assembly method (isoT) (52). For overexpression in *E. coli*, ORF's were cloned by isoT into pMtevGWA plasmid as previously described (18), thereby leading to the expression of a maltose-binding protein (MBP)-fused recombinant proteins. For *ergS* mutagenesis, we applied the isoT mutagenesis method previously described (18, 53). All described plasmids were transformed in *E. coli* DH5α and selected on Luria-Bertani (LB) medium supplemented with 100 µg/mL ampicillin (LB-Amp). The p415GPD- *ergS_Yli* and p415- *ergS_Afm* plasmids were transformed in *Sce* strain as described previously (18) for heterologous expression of the fDUF2156/ErgS proteins. The pMtev-*ergS Yli* and pMtev-*ergS Afm* plasmids were transformed in *E. coli* Rosetta-2 strains for expression and purification of recombinant MBP-tagged ErgS proteins.

[*For more details please refer to the Materials & Methods sections of the thesis manuscript. Primers, templates, and final constructs used in this study are summarized in* **Table MMX** *of the thesis manuscript. Note also that during my thesis I constructed cassettes for the deletion and the complementation of ergS gene in Afm (detailed in Materials & Methods sections of the thesis manuscript). These cassettes were then used by Dr. N. Mahmoudi-Kaidi and Dr. F. Fischer for the several attempts to constructs recombined Afm strains*].

Overexpression of recombinant MBP-ErgS [*performed by N. Yakobov*]

[*Please refer to the Materials & Methods sections of the thesis manuscript*]. Briefly, overexpression of MBP-ErgS (and mutants) was performed by transforming pMtev-*ergS_Yli* pMtev-*ergS_Afm* plasmid in the *E. coli* Rosetta-2 strain. A single colony was inoculated in 50 mL of LB containing 150 µg/mL ampicillin overnight (ON) at 37°C. Bacteria were diluted 200-fold in 500 mL LB-Amp medium and incubated at 37°C, until OD_{600} reached 0.5-0.6. The culture was then incubated on ice (15 min) and overexpression of the MBP-ErgS protein induced by adding IPTG at a final concentration of 0.3 mM. Cultures were incubated 3 h at 30 °C under agitation (200 rpm). Then, cells were harvested by centrifugation (4000 x *g*, 10 min, 4 °C), the pellet washed once in Phosphate Buffer Saline (PBS), and stored at -80°C until use.

MBP-ErgS variants purification [*performed by N. Yakobov*]

1. **Purification of MBP-ErgS-*Afm* (Fig. S10)**

The pellet resulting from 2L culture (around 4 g) was resuspended in 20 mL lysis buffer composed of Tris-HCl pH 7 250 mM, NaCl 300 mM, KCl 30 mM, glycerol 5 % (v/v), Tween20 0.25 % (v/ v), TritonX100 0.1 % (v/v), β-mercaptoethanol 5 mM, Na2EDTA 10 mM, protease inhibitor cocktail (Roche Complete, EDTA-free), benzamidine 2 mM, pMSF 0.5 mM. Cells disruption is conducted by sonication (Bioblock Scientific, VibraCell; 8 × 1 min 1 sec on / 1 sec off, amplitude 30 %, on ice) and the lysate is centrifuged at 10000 × *g* for 30 min at 4°C. The supernatant is incubated with 2 mL amylose resin (NEB, E8021S), previously equilibrated with lysis buffer, and placed on a rotating wheel for 2-3 h at 4°C. The flow-through is collected using a 1.5 × 10 cm chromatography column (Biorad, Econo-Column® #7371512), beads are washed several times (at least 5-15 column volumes) with wash buffer (Tris-HCl pH 7 50 mM, NaCl 300 mM, KCl 30 mM, glycerol 5 % (v/v), Tween20 0.25 % (v/v), TritonX-100 0.1 % (v/v), β-mercaptoethanol 5 mM). Elution is achieved with the wash buffer supplemented with 2,5 % maltose monohydrate (p/v). 0.5 mL fractions were collected and analyzed by SDS-page. Eluted proteins were stored with glycerol 50 % (v / v) at -20°C or -80°C.

2. **Purification of MBP-ErgS-*Yli* versions (Fig. S11)**

ErgS-*Yli wt* and the ErgS-*Yli*-α(0) mutant were fused to MBP and overexpressed in *E. coli*. The pellet resulting from 1 L culture (around 3 g) was resuspended in 25 mL lysis buffer and disrupted as described in the previous section. Sonicated cells were centrifuged at 9000 x *g* for 30 min at 4°C. Supernatants were transferred in a clean tube and centrifuged 30 min at 100,000 x *g* at 4°C. Clarified supernatants were then loaded on a MBPTrap™ HP (GE healthcare, 28-

9187) mounted on an Äkta Pure FPLC system, equilibrated with wash buffer (composition detailed in the previous section), at a flow rate of 1 mL/min. Sample application was performed at 0.5 mL/min and the column was washed with 10 column volumes of wash buffer. MBP-tagged proteins were then eluted using a maltose-monohydrate gradient (0% - 3% p/v) in wash buffer at a flow rate of 0.5 mL/min. Fractions (0.8 mL) were collected and analyzed by SDS-PAGE 10%. The total protein amount in the eluted peak was 3.3 mg and 5 mg for MBP-ErgS-*Yli wt* and MBP-ErgS-*Yli*-α(0) respectively. Chromatograms, SDS-PAGE and their description are found in the supplementary materials.

Spores preparation of *Aspergillus fumigatus* [*performed by Dr. N. Mahmoudi-Kaidi*]

Conidia from 7 days-old (*Afm*) Malt agar slants were resuspended in 5 mL sterile Tween 20-H_2O (0.05 % v/v) using a vortex (3x30 sec), filtered using Cell Strainer filters (Grosseron, EASY strainer^{TM} Greiner Bio-One), and concentration of the suspension determined with a hemacytometer. Conidia were stored in Tween 20-H_2O (0.05 % v/v) at 4°C in the dark for up to 1 week.

Liquid cultures for lipid extraction

For the lipid extraction of *Yli, Sce* WT and *Sce* expressing ErgS, liquid cultures were performed in YPD or SC-Leu (MP™ Biomedicals) for 24 hrs at 30°C under agitation (220 rpm), then harvested by centrifugation (5000 x *g*, 5 min, 4°C), either directly used for lipid extraction or stored at -20°C until used. For *Afm*, liquid cultures were inoculated with 10^6conidia/mL in 50 mL liquid MM and incubated for 24 hrs at 37°C in the dark under agitation (220 rpm). Mycelia were then filtrated through two layers of gauze, rinsed twice with 50 mL sterile H_2O, and squeezed to eliminate excess water. Mycelia were either directly used to extract total lipids or stored at -20°C until used.

Total lipid extraction from *Sce, Yli* and *Afm*. [*mainly performed by N. Yakobov. N. Mahmoud-Kaidi and F. Fischer participated*]

Lipid extraction protocol for fungi (*Sce, Sce* expressing *ergS of Yli or Afm, Afm and Yli)* was adapted from the Bligh and Dyer procedure and as previously described (18, 54). Briefly, 50 DO_{600} of *Sce* cells or an equivalent amount of *Yli* cells were resuspended in 500 µL of 120 mM Na-Acetate pH 4.5. Then, 1.875 mL of $CHCl_3$:MetOH (2: 1) and 1.5 mL of glass beads (ø 0.25-0.5 mm, Roth) were added for mechanical cell lysis in a FastPrep Instrument (MP™

Biomedicals, Serial N° 10020698) at 1 min 5.5 m/s repeated 6 times. To improve lipid extraction, cells were put on a rotating wheel ON. Finally, 625 µL of $CHCl_3$ and 120 mM Na-Acetate pH 4.5 were sequentially added, the samples were vortexed 1 min between each step. Then, phases separation was performed by centrifugation (9000 g; 30 min; 4°C). The organic lower phase containing lipids was transferred into a clean tube and dried by using a SpeedVac vacuum concentrator. To avoid oxidation, it is recommended to complete this drying step under argon flow. Lipids are finally stored at -20°C or resuspended in 50-100 µL of $CHCl_3$:MetOH (1:1) for lipid analysis by Thin Layer Chromatography (TLC) by depositing 25 µL on a TLC silica plate for TLC analysis.

For *Afm*, the mechanic cell lysis is performed as described by elsewhere (18) by using FastPrep (6 times 1 min at 5.5 m/s) and then incubated ON in rotating wheel. Briefly, 2g of fresh dried on towel paper of mycelia was resuspended in 1 mL of 120 mM Na-Acetate pH 4.5 as the first step of the above described procedure. The rest of the above described procedure stays unchanged.

Lipid analysis by Thin layer chromatography (TLC) [*mainly performed by N. Yakobov. N. Mahmoud-Kaidi and F. Fischer participated*]

TLC plates were developed in a chamber saturated either with $CHCl_3$: MetOH : H_2O 130 : 16 : 1 or 130 : 50 : 8 (v : v : v). The migration of total lipids was performed for 10 min, then the TLC plates were dried. To visualize total lipids species, we used routinely the Sulfuric acid / $MnCl_2$ staining method (Sulfuric acid 9 mL, $MnCl_2.4H_2O$ 0.8 g, Methanol 120 mL, H_2O 120 mL) which is particularly interesting because of its differential sterol coloration (27). With this coloration, the lipids appear yellow under white light while the sterols are dark brown. When specified, TLC were also stained either with ninhydrin for the primary amines detection. Ninhydrin 0.4 % (w/v) (Sigma-Aldrich) was prepared in absolute ethanol. Reagents were sprayed on plates that were air-dried. In the case of $MnCl_2$/sulphuric acid and ninhydrin stains, plates were heated at 100°C until coloration developed and imaged under natural light or under UV light (254 or 315 nm).

Lipid Y (Erg-Gly) purification by silica column chromatography (Fig. 3 and Fig. S12) [*performed and adapted by N. Yakobov*]

Yli and *Sce wt* were grown in YPD and *Sce* expressing ErgS-*Yli* is grown in SC-Leu. Cultures were diluted to OD600 = 0.1, grown O/N and the next morning cells were harvested by

centrifugation at 5000 × g for 15 min at 4°C. 5 g of cells were obtained from a 500 ml culture of *Yli*; 3.5 g of cells were obtained from a 500 ml culture of *Sce* wt; 4 g of cells were obtained from a 1 L culture of *Sce* expressing *Yli* ErgS. In all cases, cells are resuspended in 15 ml Na-acetate 120 mM pH 4.5 and mechanically lysed with a FastPrep-24 apparatus in the presence of glass beads (ø 0.25 mm to 0.5 mm, Roth) at 6 m/s, for 1 min repeated 5 times, with cooling on ice between each step. 28.125 mL of MetOH : CHCl3 2 : 1 are added, then 3 additional shacking runs are performed and another 28.125 ml of MetOH : CHCl3 2 : 1 is added (Total volume of MetOH : CHCl3 2 : 1 added = 56.25 mL). Tubes are placed on a rotating wheel at 4 °C for 3 h. Finally, 18,75 mL of CHCl$_3$ and 120 mM Na-Acetate pH 4.5 were sequentially added, the samples were vortexed 1 min between each step. Then, phases separation was performed by centrifugation (9000 x *g*; 30 min; 4°C). The organic lower phase containing lipids was transferred into a clean tube and dried by using a SpeedVac vacuum concentrator.

To purify the lipid of interest from total lipid fractions, obtained as described in the previous section, we built a silica gel column as in (18). However, the size of the column was increased since 8 mL of Silica Gel were poured into a 1 cm x 20 cm chromatography column. The stationary phase was washed with 4 column volumes of CHCl$_3$ and total lipids, resuspended in 500 µl ultrapure CHCl$_3$, were injected manually on the top of the silica gel. Volumes used to elute lipids are increased so that each collected fraction corresponds to 1 column volume. In this way lipids were then gradually eluted as follow: 4 x 8 mL CHCl$_3$; 3 x 8 mL CHCl$_3$: MetOH (144:1); 3 x 8 mL CHCl$_3$: MetOH (72:1) and 2 x 8 mL CHCl$_3$: MetOH (36:1). Lipids were dried as previously described, resuspended in 200 µL CHCl$_3$: Methanol (1:1) and analyzed by TLC.

[Note for the reader: *Initially I used this protocol to purify Lipid Y from total Yli wt total lipids. However, for the moment we have not obtained the Yli ΔergS strain and therefore, determining the ErgS dependent lipid was challenging. Comparing the lipid profiles to this of Sce expressing Yli ErgS was helpful but not sufficient. Therefore, I decided to repeat the experiment on total lipids extracted from Yli wt, Sce expressing Yli ErgS and from Sce wt which does not produce Lipid Y (**Fig. S12**). Comparing the profiles obtained in these three cases greatly facilitated the determination of the ErgS dependent lipid in Yli even if, being rigorous, the deletant strain remains essential to conclude. The reproducibility of the elution profiles obtained here also shows the suitability for Lipid Y purification, which will probably be important in further steps of the topic.*]

Identification of Ergosteryl-3β-*O*-glycine (lipid X) by mass spectroscopy [*performed by Dr. H. Roy's team*]

LCMS analyses of total lipid extracts were performed on a liquid chromatograph Surveyor Plus with autosampler connected to a LTQ-XL ion trap analyzer mounted with an Ion Max ESI probe (Thermo Finnigan). Lipid sample were resuspended in chloroform/methanol 2/1 and diluted three times with injection solvent (isopropanol/acetonitrile/water, IPA/ACN/water, 6.5/3/0.5). 10 µL were injected on a Ascentis Express C18 (10 cm × 2.1 mm, 2.7 µm, Sigma-Aldrich) HPLC column at a temperature of 45°C as described in (55) with minor modifications. Elution was performed at a flow rate of 260 µL/min with a binary gradient where A was 60:40 water: ACN and B was 90:10 IPA:ACN. Both solutions contained 0.1% formic acid and 10 mM of aqueous ammonium formate. Elution was performed with a 16 min gradient; from 0 to 1 min B was maintained at 32%, from 1 to 2.5 min B was increased to 62%, from 2.5 to 14 min to 99%, and B was maintained at 99% for 2 min. Before identification of Gly-Erg, the instrument was tuned with cholesterol in solvent B (Sigma Aldrich, [M-H2O+H]+ m/z = 369). The LC-MS experiment shown in this manuscript and in the supplemental section were acquired with the instrument tuned with synthesized Gly-Erg in solvent B ([2M +H]+ m/z = 907). Drying gas flow rate was 20 units and temperature of the ESI was 380°C. Full-scan spectra were collected in the 110–2000 m/z range in positive mode, and data-dependent MS2 spectra were acquired on the 15 most intense MS1 peaks. MS3 spectra were acquired on the MS2 peak at m/z=379. MSn data was acquired with a Collision-induced dissociation energy set at 35. Data were analyzed with Xcalibur Qual Browser.

Preparation of soluble *Sce* extract fraction (S100) [*performed by N. Yakobov*]

Cells were grown in 500 mL YPD on a rotary shaker at 30 °C and harvested when OD600 = 1 by centrifugation at 5000 × g for 5 min at 4 °C. The pellet was resuspended in 5 mL of lysis buffer containing 50 mM Na-HEPES pH 7, 30 mM KCl (or 140 mM NaCl), 10 % glycerol, 0.1 mM EDTA, 1 % (w/v) Triton X100, 0.3 % (w/v) NP40, 5mM ß-mercaptoethanol and protease inhibitors tablet (Roche). 1 volume of glass beads (Ø 0.25-0.5 mm, Roth) was added and cell lysis was performed with a FastPrep®-24 apparatus (6 × 1 min at 6.5 m/s, with 1 min on ice between each cycle). Cells debris were removed by centrifugation at 500 × g for 10 min at 4 °C and the supernatant is centrifuged at 100000 × g for 1 h. The resulting soluble fraction

(S100) is recovered, then dialyzed O/N against the storage buffer (50 mM Na-HEPES pH 7, 30 mM KCl (or 140 mM NaCl), 50 % glycerol, 0.1 mM EDTA) and kept at – 20 °C.

Aminoacylation assay [*adapted and performed by N. Yakobov*]

tRNA^{Gly} aminoacylation was performed in the presence of 100 mM Na-HEPES pH 7, 10 mM MgCl$_2$, 30 mM KCl, 0.1 mg/mL BSA, 10 mM ATP, radiolabeled [C^{14}]-glycine 70 µM (AS = 89 cpm/pmol), 5 µL of soluble *Sce* S100 fraction (3 mg/mL) and either 4 mg/mL unfractionated tRNA from *Sce* or 10 µM of tRNA^{Gly} resulting from the countercurrent fractionation (56). Alternatively, the radiolabeled [C^{14}]-glycine was replaced by a mixture of 15 radiollabelled amino acids that includes notably [C^{14}]-glycine. The reaction volume was set up to 50 µL and the temperature to 30°C. To assess rates of aminoacylated tRNA^{Gly} we performed kinetics as described (57). [*Some additional specification concerning this procedure are found in the Materials & Methods sections of the thesis manuscript*].

Lipid aminoacylation assays (LAA) [*adapted and performed by N. Yakobov*]

An aliquot of commercial Erg, (solubilized in EtOH 100 % and stored at 20 mg/mL at -20 °C), was dried by evaporation at 60 °C and solubilized by sonication in an adequate volume of R buffer (100 mM Na-HEPES, 30 mM KCl, 10 mM MgCl2) to yield a 5 mg/mL preparation. The principle of LA assay used in this study is similar this one described in our recent work (18), but in the present case, Gly-tRNA^{Gly} was synthesized in a reaction volume of 50 µL for 1 hour (as described in the precedent section), then 10 µL of Erg (final concentration, 0.5 mg/mL) and 5-7 µg of MBP-ErdS enriched fractions were added to the reaction mixture. The volume was completed to 100 µL with R buffer and the assay was further incubated at 30 °C for 40 min **(Fig 5A)**. Then, the reaction was stopped by adding 500 µL of CHCl$_3$: MetOH : 120 mM Na-Acetate pH 4.5 (1 : 2 : 0.8). The samples were mixed, vortexed for 1 min and then 130 µL of CHCl$_3$ and 120 mM Na-Acetate pH 4.5 were sequentially added. The samples were vortexed 20 secs for each step. Phases separation was performed by centrifugation (13000 g; 3 min; room temperature). The organic lower phase containing lipids was transferred into a clean tube and dried by using a SpeedVac vacuum concentrator. Lipids were resuspended in 50 µLCHCl$_3$ or CHCl$_3$: MetOH (2 : 1) and 25 µL were spotted on a TLC silica gel plate. Finally, radiolabeled lipid species were revealed by exposing the Silica plates to a storage phosphor screen and submitted to a phosphoimager (Typhoon). [*Some additional specification concerning this procedure are found in the Materials & Methods sections of the thesis manuscript*]

Protein extraction and Western blots [*performed by N. Yakobov*]

Sce WT and *Sce* expressing ErgS of *Afm* were grown at 30°C until OD_{600} reached 1. 1 OD_{600} of *Sce* cells were resuspended in 500 µL of pre-cooled NaOH 0.185 N for alkaline lysis. After 10 min, proteins were precipitated by adding 50 µL of TCA 100% for another 10 min. Finally, the precipitate was harvested by centrifugation (13000 x *g*, 15 min, 4°C) and resuspended in 100 µL of Laemmeli sample buffer. For the Western-Blot, 8 µL of each crude extract were resolved/separated using SDS-PAGE 10 %. The proteins were transferred onto PVDF membranes, then the membranes blocked with 5% (w/v) skimmed milk in TBS-Tween (TBS 1X, Tween-20 0.3% (v/v)) for 1h at RT. Primary antibodies (anti-ErgS, anti-PGK) incubation was performed ON at 4°C, followed by several TBS-Tween washing steps. Membranes were then incubated 1 h with an HRP-conjugated secondary antibody (goat anti-rabbit for anti-ErgS, and goat anti-rabbit for anti-PGK antibodies) at RT. Revelation was performed with the BioRad clarity western ECL Kit and monitored in a BioRad ChemiDoc Touch® apparatus. The anti-ErgS polyclonal antibody was obtained from the serum of a rabbit immunized with the purified recombinant ErgS protein from *Afm* (Covalab, France, https://www.covalab.com/).

Phylogenetic analyses [*performed by F. Fischer an G. Grob*]

The amino acid sequence of *Afm* ErdS (AFUA_1g02570), annotated in the KEGG database (https://www.kegg.jp/) was used to extract the sequence of the DUF2156 domain (*A. fumigatus* Af293, residues 588-946) and the latter was used for a PSI-BLAST search (58) (default parameters) (National Center for Biotechnology Information, NCBI, https://www.ncbi.nlm.nih.gov/) in *A. fumigatus* strains Af293 and A1160 and in *A. oryzae* RIB40. As expected, 3 proteins, corresponding to full-length ErdS (946 aa, identity 100 %, E=0), matched the query in the 3 strains. However, 3 others proteins, shorter than ErdS (549 aa in *Afm* Af293, 492 in *Afm* A1160 and 379 in *Aor* RIB40), with only low sequence identity (20.25 % for *Afm* strains and 22.88 % in *Aor*, E=6E-10 and E=0.004, respectively), were also detected. Interestingly, those 3 sequences were not detected using classical BLAST searches, using the BlastP program (58). Sequence analysis using the Protein Family Database (PFAM, https://pfam.xfam.org/) (20) showed that they all contained a DUF2156 domain (E=2.1E-24 for *Afm* Af293, E=7.7E-25 for *Afm* A1160 and E=3E-15 for *Aor*), but no other identifiable domains, reason for which we named them free-standing DUF2156 (fDUF2156). Given the low sequence identity between ErdS and fDUF2156, we first used the fDUF2156 sequence from *Afm* Af293 (549 aa, the longest form) and performed a BLAST search across non-redundant protein sequences in all Eukaryotes (taxid:2759) with default parameters and a maximum of 5,000

sequences. A set of 42 sequences with identity >20 % and E<0.004 was retrieved and added to a list of 99 sequences of DUF2156 domains from *bona fide* ErdSs (18) and 29 sequences of DUF2156 sequences from bacterial MprFs, representative of the major clades described in Smith *et al* (14). The 170 sequences were aligned using the MUSCLE software (59) in the Seaview package and the resulting alignment trimmed using the BMGE software (60), with a BLOSUM 30 substitution matrix. Maximum likelihood (ML) tree of DUF2156 sequences was then reconstructed using IQ-TREE (61) and the LG+G4 model. The resulting tree was visualized using the FigTree software (http://tree.bio.ed.ac.uk/software/figtree/). Since a limited number of fungi (only Dikarya) possess DUF2156 proteins, while they are abundant and widespread in bacteria (5, 14), we chose the bacterial DUF2156 (MprF) sequences as a root, when necessary.

Sequence alignments [*performed by F. Fischer an G. Grob*]

Sequences used were identified as described above. Eleven fDUF2156/ErgS sequences were chosen: *Aspergillus fumigatus* (*Afm*), *Aspergillus oryzae* (*Aor*), *Aspergillus flavus* (*Afv*), *Penicillium expansum* (*Pex*), *Penicillium camemberti* (*Pac*), *Beauveria bassiana* (*Bba*), *Yarrowia lipolytica* (*Yli*), *Aspergillus fischeri* (*Afi*), *Exophiala sideris* (*Esi*), *Exophiala oligosperma* (*Eol*) and *Aspergillus lentulus* (*Ale*) [NCBI IDs: gi_66844705, XP_023093537, XP_002377810, gi_700469555, gi_902275081, gi_701770216, gi_49649238, gi_119409904, gi_759204124, gi_759263934, gi_952546312, respectively]. In the case of the fDUF2156/ErgS sequence from *Aor*, the protein was shorter (379 aa) compared to others and truncated in the GNAT II domain. We used the cDNA-amplified sequence of Aor's gene and noticed that the intron annotated in the second part of the gene (see FungiDB, the AO090011000521 gene, link: https://fungidb.org/fungidb/app/record/gene/AO09001100 0521) actually did not exist, since it was not spliced out in the cDNA sequence. This is identical to the situation found in *Aor*'s closest relative *Afv* (FungiDB, gene: AFLA_043480, link: https://fungidb.org/fungidb/app/record/gene/AFLA_043480#Sequences). Translating the ORF from the start (ATG) codon to the next stop codon (with the intron in the sequence) resulted in a full-length fDUF2156/ErgS sequence identical to that of *Aspergillus flavus*, the closest relative of *Aor*. Therefore, the intron was considered misannotated. This full-length sequence was used for *Aor* ErgS. Alignments were performed using MUSCLE (59).

Structure predictions [*performed by F. Fischer, N. Yakobov and G. Grob*]

The full-legnth fDUF2156/ErgS sequences from *A. fumigatus*, *A. oryzae*, *B. bassiana* and *Y. lipolytica* were used in the Phyre2 software (http://www.sbg.bio.ic.ac.uk/~phyre2/html/page.cgi?id=index) (62) with default parameters in the normal and intensive mode to obtain structure prediction of the proteins. Results were identical in both modes. Resulting predictions were visualized using PyMol (https://pymol.org/2/) and compared to Phyre2-predicted structure of the DUF2156 module of *Afm* ErdS (18) (residues 588-946) and to the crystal structure of the DUF2156 domain of *Bacillus licheniformis* MprF (21) (PDB: 4V36). Predicted structures were used, together with alignments (see above), to map the $\alpha^{(+)}$ helices, GNAT I and GNAT II of fDUF2156/ErgS proteins, by comparison with MprF's structure.

Phylogenomics [*performed by F. Fischer an G. Grob*]

Sequences of fDUF2156/ErgS proteins were searched across all Eukaryotes (Non redundant protein sequences) using the BlastP program (58), hosted at the NCBI (https://www.ncbi.nlm.nih.gov/). As ErdS, they were detected only in Fungi (kingdom). More specifically, fDUF2156/ErgS were detected only in division Ascomycota (whereas ErdS was present in both Ascomycota and Basidiomycota), which included the subdivisions Pezizomycotina and Saccharomycotina. Only one species in Saccharomycotina (*Yarrowia lipolytica*) possessed fDUF2156/ErgS, while all others were Pezizomycotina. fDUF2156/ErgS were searched in all classes of Pezizomycotina: Eurotiomycetes, Lecanoromycetes, Xylonomycetes, Dothideomycetes, Sordariomycetes, Leotiomycetes, Pezizomycetes, Orbiliomycetes, and representative organisms of each class were used to illustrate the diversity of species having fDUF2156/ErgS. The presence/absence of ErdS was also indicated in each selected species using the same approach, as in Yakobov & Fischer *et al* (18). Results (presence/absence of ErgS and/or ErdS) were mapped onto the phylogenetic tree of Ascomycota provided at the JGI Genome Portal (63), together with information on the detection of Erg-Asp (from our previous work (18)) and Erg-Gly (this sudy).

1.   Geiger O, Gonzalez-Silva N, Lopez-Lara IM, & Sohlenkamp C (2010) Amino acid-containing membrane lipids in bacteria. *Prog Lipid Res* 49(1):46-60.
2.   Hankins JV, Madsen JA, Giles DK, Brodbelt JS, & Trent MS (2012) Amino acid addition to Vibrio cholerae LPS establishes a link between surface remodeling in gram-positive and gram-negative bacteria. *Proc Natl Acad Sci U S A* 109(22):8722-8727.
3.   Brown S, Santa Maria JP, Jr., & Walker S (2013) Wall teichoic acids of gram-positive bacteria. *Annu Rev Microbiol* 67:313-336.

4.   Rubio Gomez MA & Ibba M (2020) Aminoacyl-tRNA Synthetases. *RNA*.

5.   Fields RN & Roy H (2018) Deciphering the tRNA-dependent lipid aminoacylation systems in bacteria: Novel components and structural advances. *RNA Biol* 15(4-5):480-491.

6.   Peschel A*, et al.* (2001) Staphylococcus aureus resistance to human defensins and evasion of neutrophil killing via the novel virulence factor MprF is based on modification of membrane lipids with l-lysine. *J Exp Med* 193(9):1067-1076.

7.   Roy H & Ibba M (2008) RNA-dependent lipid remodeling by bacterial multiple peptide resistance factors. *Proc Natl Acad Sci U S A* 105(12):4667-4672.

8.   Roy H & Ibba M (2009) Broad range amino acid specificity of RNA-dependent lipid remodeling by multiple peptide resistance factors. *J Biol Chem* 284(43):29677-29683.

9.   Slavetinsky C, Kuhn S, & Peschel A (2017) Bacterial aminoacyl phospholipids - Biosynthesis and role in basic cellular processes and pathogenicity. *Biochim Biophys Acta Mol Cell Biol Lipids* 1862(11):1310-1318.

10.   Ernst CM*, et al.* (2009) The bacterial defensin resistance protein MprF consists of separable domains for lipid lysinylation and antimicrobial peptide repulsion. *PLoS Pathog* 5(11):e1000660.

11.   Slavetinsky CJ, Peschel A, & Ernst CM (2012) Alanyl-phosphatidylglycerol and lysyl-phosphatidylglycerol are translocated by the same MprF flippases and have similar capacities to protect against the antibiotic daptomycin in Staphylococcus aureus. *Antimicrob Agents Chemother* 56(7):3492-3497.

12.   Ernst CM*, et al.* (2015) The lipid-modifying multiple peptide resistance factor is an oligomer consisting of distinct interacting synthase and flippase subunits. *mBio* 6(1).

13.   Ernst CM & Peschel A (2011) Broad-spectrum antimicrobial peptide resistance by MprF-mediated aminoacylation and flipping of phospholipids. *Mol Microbiol* 80(2):290-299.

14.   Smith AM*, et al.* (2015) tRNA-dependent alanylation of diacylglycerol and phosphatidylglycerol in Corynebacterium glutamicum. *Mol Microbiol* 98(4):681-693.

15.   Arendt W, Groenewold MK, Hebecker S, Dickschat JS, & Moser J (2013) Identification and characterization of a periplasmic aminoacyl-phosphatidylglycerol hydrolase responsible for Pseudomonas aeruginosa lipid homeostasis. *J Biol Chem* 288(34):24717-24730.

16.   Groenewold MK*, et al.* (2019) Virulence of Agrobacterium tumefaciens requires lipid homeostasis mediated by the lysyl-phosphatidylglycerol hydrolase AcvB. *Mol Microbiol* 111(1):269-286.

17.   Smith AM, Harrison JS, Sprague KM, & Roy H (2013) A conserved hydrolase responsible for the cleavage of aminoacylphosphatidylglycerol in the membrane of Enterococcus faecium. *J Biol Chem* 288(31):22768-22776.

18.   Yakobov N*, et al.* (2020) RNA-dependent sterol aspartylation in fungi. *Proc Natl Acad Sci U S A*.

19.   Ruff M*, et al.* (1991) Class II aminoacyl transfer RNA synthetases: crystal structure of yeast aspartyl-tRNA synthetase complexed with tRNA(Asp). *Science* 252(5013):1682-1689.

20.   El-Gebali S*, et al.* (2019) The Pfam protein families database in 2019. *Nucleic Acids Res* 47(D1):D427-D432.

21.   Hebecker S*, et al.* (2015) Structures of two bacterial resistance factors mediating tRNA-dependent aminoacylation of phosphatidylglycerol with lysine or alanine. *Proc Natl Acad Sci U S A* 112(34):10691-10696.

22.   Favrot L, Blanchard JS, & Vergnolle O (2016) Bacterial GCN5-Related N-Acetyltransferases: From Resistance to Regulation. *Biochemistry* 55(7):989-1002.

23. Chang PK & Ehrlich KC (2010) What does genetic diversity of Aspergillus flavus tell us about Aspergillus oryzae? *Int J Food Microbiol* 138(3):189-199.

24. Amaike S & Keller NP (2011) Aspergillus flavus. *Annu Rev Phytopathol* 49:107-133.

25. Lambou K, Lamarre C, Beau R, Dufour N, & Latge JP (2010) Functional analysis of the superoxide dismutase family in Aspergillus fumigatus. *Mol Microbiol* 75(4):910-923.

26. He B*, et al.* (2019) Functional Genomics of Aspergillus oryzae: Strategies and Progress. *Microorganisms* 7(4).

27. Goswami SK & Frey CF (1970) Manganous chloride spray reagent for cholesterol and bile acids on thin-layer chromatograms. *J Chromatogr* 53(2):389-390.

28. Munger LH, Boulos S, & Nystrom L (2018) UPLC-MS/MS Based Identification of Dietary Steryl Glucosides by Investigation of Corresponding Free Sterols. *Front Chem* 6:342.

29. Arendt W, Hebecker S, Jager S, Nimtz M, & Moser J (2012) Resistance phenotypes mediated by aminoacyl-phosphatidylglycerol synthases. *J Bacteriol* 194(6):1401-1416.

30. Maloney E*, et al.* (2009) The two-domain LysX protein of Mycobacterium tuberculosis is required for production of lysinylated phosphatidylglycerol and resistance to cationic antimicrobial peptides. *PLoS Pathog* 5(7):e1000534.

31. Sassetti CM, Boyd DH, & Rubin EJ (2003) Genes required for mycobacterial growth defined by high density mutagenesis. *Mol Microbiol* 48(1):77-84.

32. Ravishankar S*, et al.* (2016) Essentiality Assessment of Cysteinyl and Lysyl-tRNA Synthetases of Mycobacterium smegmatis. *PLoS One* 11(1):e0147188.

33. Moutiez M, Belin P, & Gondry M (2017) Aminoacyl-tRNA-Utilizing Enzymes in Natural Product Biosynthesis. *Chem Rev* 117(8):5578-5618.

34. Dare K & Ibba M (2012) Roles of tRNA in cell wall biosynthesis. *Wiley Interdiscip Rev RNA* 3(2):247-264.

35. Green CJ & Vold BS (1993) Staphylococcus aureus has clustered tRNA genes. *J Bacteriol* 175(16):5091-5096.

36. Bock A & Stadtman TC (1988) Selenocysteine, a highly specific component of certain enzymes, is incorporated by a UGA-directed co-translational mechanism. *Biofactors* 1(3):245-250.

37. Forchhammer K & Bock A (1991) Selenocysteine synthase from Escherichia coli. Analysis of the reaction sequence. *J Biol Chem* 266(10):6324-6328.

38. Hemmerle MW, M.; Grob, G.; Yakobov, N.; Mahmoudi, N.; Senger, B.; Debard, S.; Fischer, F.; Becker, H. (2020) Noncanonical inputs and outputs of tRNA aminoacylation. *The Enzymes*).

39. de Freitas Fernandes A, Serrao VHB, Scortecci JF, & Thiemann OH (2020) Seryl-tRNA synthetase specificity for tRNA(Sec) in Bacterial Sec biosynthesis. *Biochim Biophys Acta Proteins Proteom* 1868(8):140438.

40. Fischer F*, et al.* (2012) The asparagine-transamidosome from Helicobacter pylori: a dual-kinetic mode in non-discriminating aspartyl-tRNA synthetase safeguards the genetic code. *Nucleic Acids Res* 40(11):4965-4976.

41. Bailly M, Blaise M, Lorber B, Becker HD, & Kern D (2007) The transamidosome: a dynamic ribonucleoprotein particle dedicated to prokaryotic tRNA-dependent asparagine biosynthesis. *Mol Cell* 28(2):228-239.

42. An S & Musier-Forsyth K (2005) Cys-tRNA(Pro) editing by Haemophilus influenzae YbaK via a novel synthetase.YbaK.tRNA ternary complex. *J Biol Chem* 280(41):34465-34472.

43. Ling J, Reynolds N, & Ibba M (2009) Aminoacyl-tRNA synthesis and translational quality control. *Annu Rev Microbiol* 63:61-78.

44.   Paravisi S, *et al.* (2009) Kinetic and mechanistic characterization of Mycobacterium tuberculosis glutamyl-tRNA synthetase and determination of its oligomeric structure in solution. *FEBS J* 276(5):1398-1417.

45.   Rella A*, et al.* (2015) Role of Sterylglucosidase 1 (Sgl1) on the pathogenicity of Cryptococcus neoformans: potential applications for vaccine development. *Front Microbiol* 6:836.

46.   Korber M, Klein I, & Daum G (2017) Steryl ester synthesis, storage and hydrolysis: A contribution to sterol homeostasis. *Biochim Biophys Acta Mol Cell Biol Lipids* 1862(12):1534-1545.

47.   Tiwari R, Koffel R, & Schneiter R (2007) An acetylation/deacetylation cycle controls the export of sterols and steroids from S. cerevisiae. *EMBO J* 26(24):5109-5119.

48.   Hebecker S*, et al.* (2011) Alanyl-phosphatidylglycerol synthase: mechanism of substrate recognition during tRNA-dependent lipid modification in Pseudomonas aeruginosa. *Mol Microbiol* 80(4):935-950.

49.   da Silva Ferreira ME*, et al.* (2006) The akuB(KU80) mutant deficient for nonhomologous end joining is a powerful tool for analyzing pathogenicity in Aspergillus fumigatus. *Eukaryot Cell* 5(1):207-211.

50.   Machida M*, et al.* (2005) Genome sequencing and analysis of Aspergillus oryzae. *Nature* 438(7071):1157-1161.

51.   Busso D, Delagoutte-Busso B, & Moras D (2005) Construction of a set Gateway-based destination vectors for high-throughput cloning and expression screening in Escherichia coli. *Anal Biochem* 343(2):313-321.

52.   Gibson DG*, et al.* (2009) Enzymatic assembly of DNA molecules up to several hundred kilobases. *Nat Methods* 6(5):343-345.

53.   Mitchell LA*, et al.* (2013) Multichange isothermal mutagenesis: a new strategy for multiple site-directed mutations in plasmid DNA. *ACS Synth Biol* 2(8):473-477.

54.   Bligh EG & Dyer WJ (1959) A rapid method of total lipid extraction and purification. *Can J Biochem Physiol* 37(8):911-917.

55.   Bird SS, Marur VR, Sniatynski MJ, Greenberg HK, & Kristal BS (2011) Serum lipidomics profiling using LC-MS and high-energy collisional dissociation fragmentation: focus on triglyceride detection and characterization. *Anal Chem* 83(17):6648-6657.

56.   Keith GG, J.; Dirheimer, G. (1971) Isolement des tRNA[Try] et tRNA[Asp] de levure de bière hautement purifiés. *Biochimie* 53(1):123-125.

57.   Kern D, Giege R, Robre-Saul S, Boulanger Y, & Ebel JP (1975) Complete purification and studies on the structural and kinetic properties of two forms of yeast valyl-tRNA synthetase. *Biochimie* 57(10):1167-1176.

58.   Altschul SF*, et al.* (1997) Gapped BLAST and PSI-BLAST: a new generation of protein database search programs. *Nucleic Acids Res* 25(17):3389-3402.

59.   Edgar RC (2004) MUSCLE: a multiple sequence alignment method with reduced time and space complexity. *BMC Bioinformatics* 5:113.

60.   Criscuolo A & Gribaldo S (2010) BMGE (Block Mapping and Gathering with Entropy): a new software for selection of phylogenetic informative regions from multiple sequence alignments. *BMC Evol Biol* 10:210.

61.   Nguyen LT, Schmidt HA, von Haeseler A, & Minh BQ (2015) IQ-TREE: a fast and effective stochastic algorithm for estimating maximum-likelihood phylogenies. *Mol Biol Evol* 32(1):268-274.

62. Kelley LA, Mezulis S, Yates CM, Wass MN, & Sternberg MJ (2015) The Phyre2 web portal for protein modeling, prediction and analysis. *Nat Protoc* 10(6):845-858.

63. Grigoriev IV*, et al.* (2014) MycoCosm portal: gearing up for 1000 fungal genomes. *Nucleic Acids Res* 42(Database issue):D699-704.
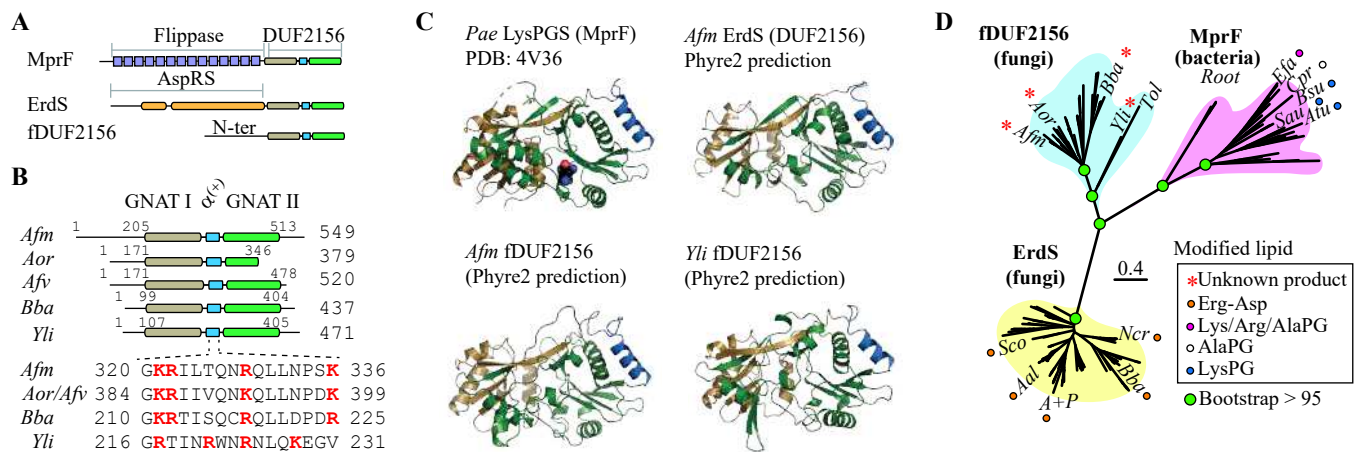
Figure 1: **In silico characterization of a novel type of fungal free-standing DUF2156 proteins**. **(A)** Architecture of bacterial MprFs, with the N-terminal flippase (14 TMH represented by grey squares) and the DUF2156/aa-tRNA transferase domain. Fungal ergosteryl-aspartate synthases (ErdS) have an aspartyl-tRNA synthetase (AspRS) domain and a DUF2156/Asp-tRNA transferase domain. Fungal free-standing DUF2156 (fDUF2156) proteins have neither flippase nor aminoacyl-tRNA synthetase domains. **(B)** Examples of fDUF2156 proteins from *Afm*, *Aor*, *Afv*, *Bba* and *Yli*. The two Gcn5-N-acetyltransferase (GNAT) domains separated by the positively charged α(+) helix, that constitute the DUF2156 fold, are detailed (boundaries indicated, with the length of the proteins indicated on the right). Positively charged residues (K, R) are shown in red. **(C)** Structure of the DUF2156 of MprF (LysPG synthase from *Bacillus licheniformis*, PDB: 4V36) and predicted structures of the DUF2156 domain of *Afm* ErdS and of *Afm* and *Yli* fDUF2156 (Phyre2 predictions). **(D)** Maximum likelihood phylogenetic reconstruction of bacterial (MprF) and fungal (ErdS, fDUF2156) DUF2156 domains. Three clades are visible, that match bacterial MprF- (purple background), ErdS- (yellow background) and fDUF2156- (blue background) specific architectural groups. Positions of *Afm*, *Aor*, *Bba* and *Yli* fDUF2156 proteins are indicated by a red asterisk. Several example organisms are presented for other clades. Modified lipids produced by the proteins are indicated, when known.*Afm*: *Aspergillus fumigatus, Aor*: *Aspergillus oryzae, Afv*: *Aspergillus flavus, Bba*: *Beauveria bassiana* and *Yli*: *Yarrowia lipolytica*, *Tol*: *Trichosporon oleaginosus*, *Sco*: *Schizophyllum commune, Aal*: *Alternaria alternata, Ncr*: *Neurospora crassa*, A+P: *Aspergillus and Penicillium spp.*, *Efa*: *Enterococcus faecium, Cpr*: *Clostridium perfringens, Bsu*: *Bacillus subtilis, Sau*: *Staphylococcus aureus, Atu*: *Agrobacterium tumefaciens*.
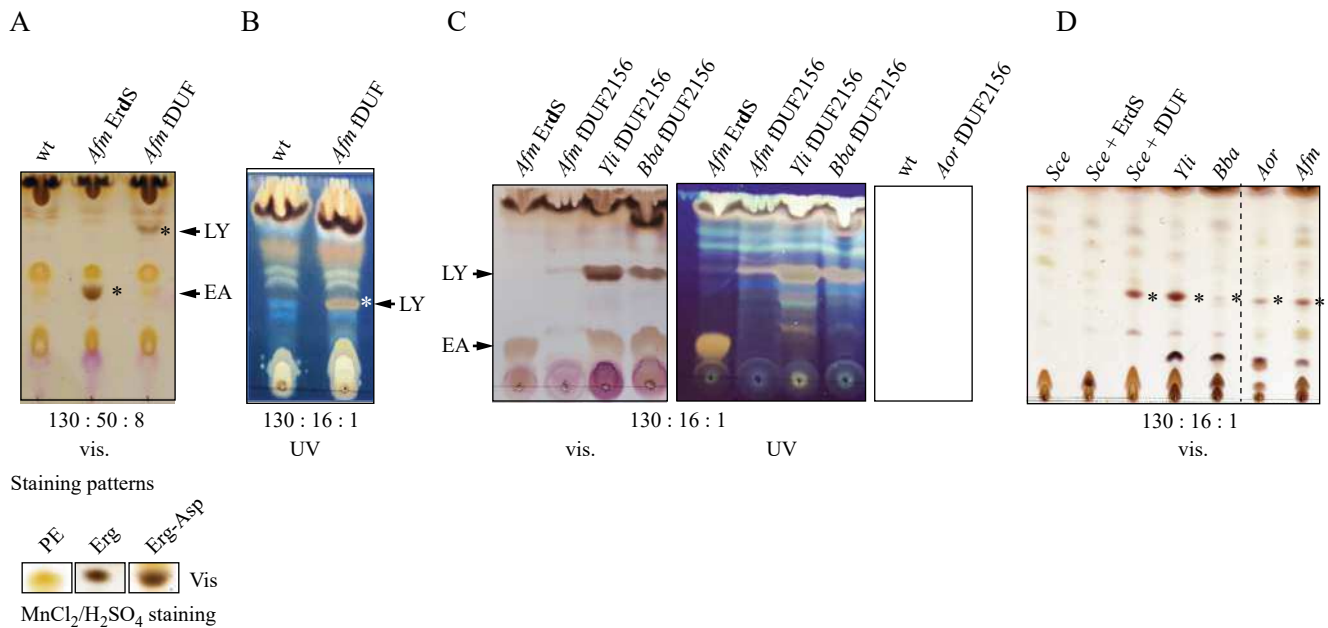
Figure 2: Ascomycetes possess a free-standing DUF2156 protein (fDUF2156) whose heterologous expression in *S. cerevisiae* enables the production of a possible aminoacylated lipid. **(A)** Heterologous expression of *Afm* ErdS (Erg-Asp synthase) and fDUF2156 in *Sce*. TLC analysis of total lipids extracted from the indicated *Sce* strains: lipids were separated with a CHCl₃:MeOH:H2O solvent with the indicated composition (130:50:8, v:v:v), stained with an MnCl2/H2SO4 solution and visualized under white light (vis.). Below, control lipid bands (PE: phosphatidylethanolamine, Erg, Erg-Asp) were stained with the same solution to illustrate the brown staining of sterols. LY: lipid Y, EA: Erg-Asp. * Indicates the position of EA and LY. **(B)** Lipids extracted from a *wt* and *Afm* fDUF2156 strains and separated by TLC using the CHCl₃:MeOH:H2O (130:16:1, v:v:v) solvent to better resolve the LY band. TLC was visualized under UV light. **(C)** TLC analysis of total lipids extracted from Sce strains expressing the indicated proteins: ErdS (control of Erg-Asp production), *Afm*, *Bba*, *Yli* and *Aor* fDUF2156. **(D)** Separation on HP-TLC plates, with the CHCl₃:MeOH:H2O (130:16:1, v:v:v), of total lipids from the indicated *wt* strains (*Afm*, *Aor*, *Bba* and *Yli*) compared to the control *Sce wt*, ErdS- and fDUF2156-expressing strains. A lipid band similar to lipid Y (LY) is present in those fungi, and is indicated by an asterisk (*) in each case.
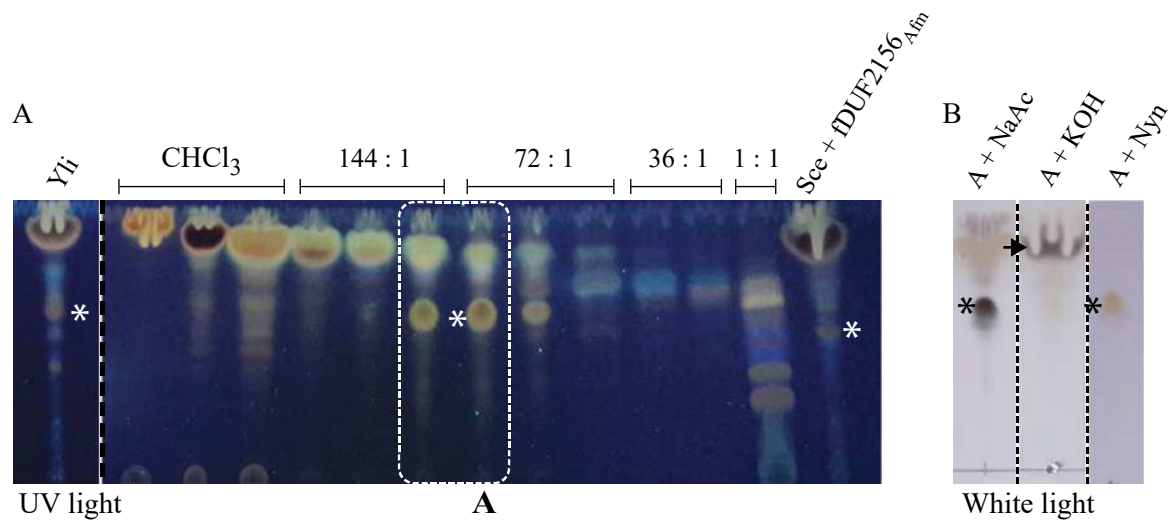
Figure 3: Enrichment of Lipid Y from *Yli*. **(A)** Lipid Y was purified from *Yli* by Flash chromatography (FC). Total lipids were loaded on a silica gel 60 glass column, washed with $CHCl_3$, and lipids were eluted using $CHCl_3$/MeOH mixture varying from 144 : 1 to 36 : 1 ratios (v : v). A final elution step was performed with $CHCl_3$/MeOH 1 : 1 (v : v). **(B)** An aliquot of fraction A was submitted to alkaline treatment (KOH 1 M at 37°C for 1h) which hydrolyzes ester bonds. As a negative control an aliquot was treated equally but KOH was replaced by Na-Acetate pH 4.5 24 mM (lane 1). Through alkaline treatment Lipid Y disappears and a dark brownish spot (indicated by the dark arrow), probably corresponding to free ergosterol appears near the front. Another aliquot of fraction A separated by TLC but instead of the routinely used $MnCl2$/Sulfuric acid staining method, lipids were stained with ninhydrin (lane 3). Asterisks indicate Lipid Y. Fractions enriched in Lipid Y (indicated by the dash rectangle in (A)) were collected and analyzed by LC-MSn (**Fig. 4** and **Fig. S5**).
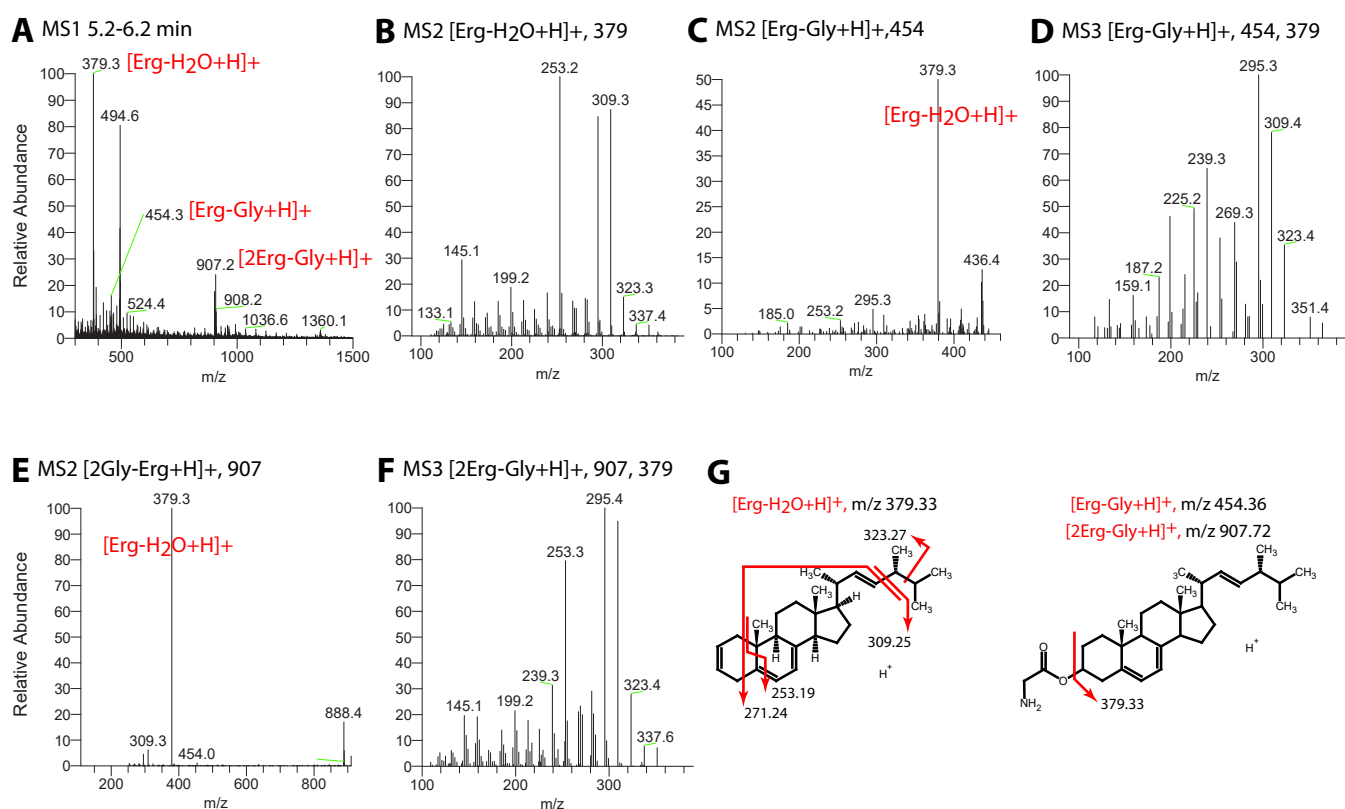
Figure 4: LC-MSn analysis of Lipid Y, enriched from *Yli* total lipids by Flash chromatography (FC) . (A) MS1 spectrum between 5.2-6.2 min **(B)**. MS2 spectrum of ergosterol [Erg-H2O+H]+ at m/z=379 **(C)**. MS2 spectrum of glycyl-ergosterol [Erg-Gly+H]+ at m/z=454 **(D)**, and its MS3 spectrum at m/z=379 (454→379). **(E)** MS2 spectrum of the ion complex glycyl-ergosterol [2Gly-Erg+H]+ at m/z=907, and **(F)** its MS3 spectrum at m/z=379 (907→379). **(G)** Structure of the ions of ergosterol [Erg-H2O+H]+, ergosteryl-3β-O-glycine [Erg-Gly+H]+ and MS2 fragmentations. MSn data are shown for peaks annotated in red. MS2 fragmentation of ergosterol is identical to that previously described (e.g. (28)).
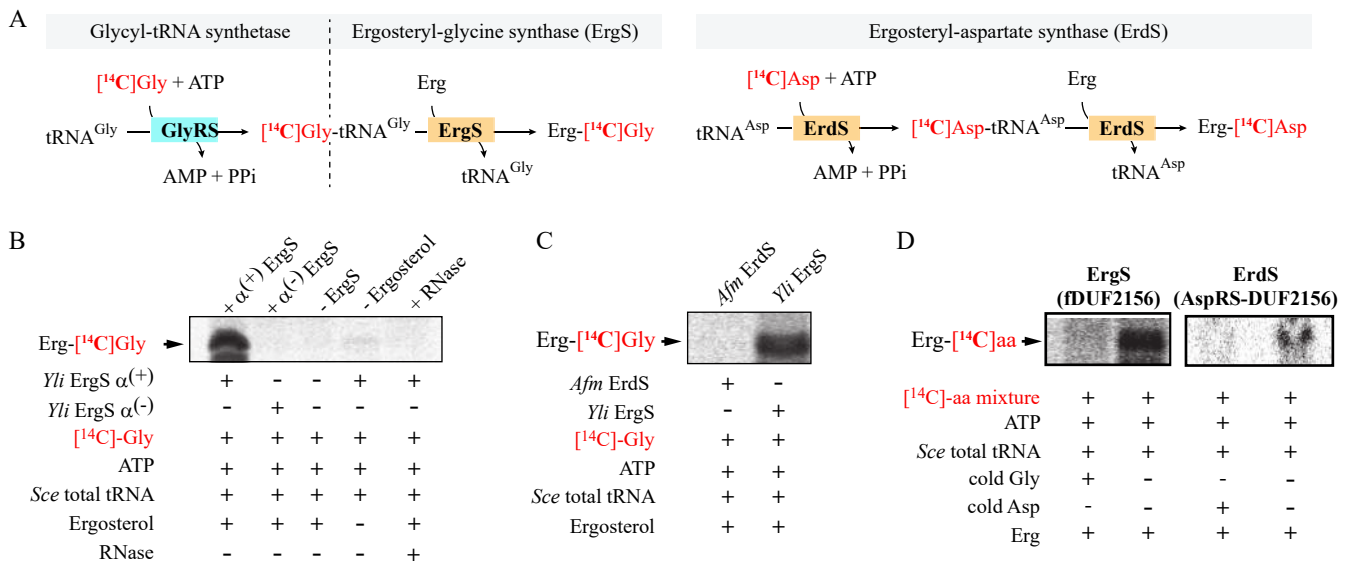
Figure 5: *In vitro* characterization of ergosteryl-glycine synthases (ErgS). (A) Schematized reaction performed for the LA assay. Left: glycyl-tRNA synthetase (GlyRS, provided by crude extracts from *Sce*) is used to produce [14C]Gly-tRNAGly from [14C]Gly, ATP and tRNA^{Gly} (provided by total tRNA from *Sce*). [14C]Gly-tRNA^{Gly} is used in a second reaction in the presence of Erg and ErgS to produce Erg-[14C]Gly. Right: in the case of ErdS, the aspartyl-tRNA synthetase activity (Asp-tRNA^{Asp} production from [14C]Asp, ATP and tRNAAsp in total tRNA from *Sce*) and the Erg-[14C]Asp synthase activity are carried by the same bifunctional protein and no extraction step is required to isolate Asp-tRNA^{Asp}, that is used directly by the DUF2156 module of ErdS upon synthesis. **(B)** The Erg-[14C]Asp synthesis was measured by LA assay in the presence of purified *Yli* ErgS, *Sce* total tRNA, radiolabeled [14C]Gly in the presence (+) or absence (−) of the indicated enzyme (WT or α(-)), or of the indicated substrates. Tests included addition (+) or not (−) of RNase A to verify the tRNA-dependency of the reaction. **(C)** The same LA assay allows to visualize that only ErgS is capable of Erg-[14C]Gly synthesis from [14C]Gly-tRNA^{Gly}, while ErdS cannot use this aa-tRNA. **(D)** Isotopic competition assay. A mixture of 15 [14C]aa-tRNAs was first synthesized using total tRNA, ATP and 15 [14C]aa in the presence of the 15 corresponding aaRSs of an *Sce* crude protein extract. After extraction, the 15 [14C]aa –tRNAs were provided to either ErgS or ErdS to produce Erg-[14C]Gly and Erg-[14C]Asp, respectively. The same was performed in the presence of excess (5 mM) cold L-Gly or L-Asp to produce isotopically diluted [14C]aa-tRNAs. In this case, no Erg-[14C]Gly was observed in the presence of cold Gly for ErgS, and no Erg-[14C]Asp in the presence of cold Asp in the case of ErdS demonstrating that both ErgS and ErdS are specific towards one aa for the synthesis of Erg-Gly and Erg-Asp respectively.
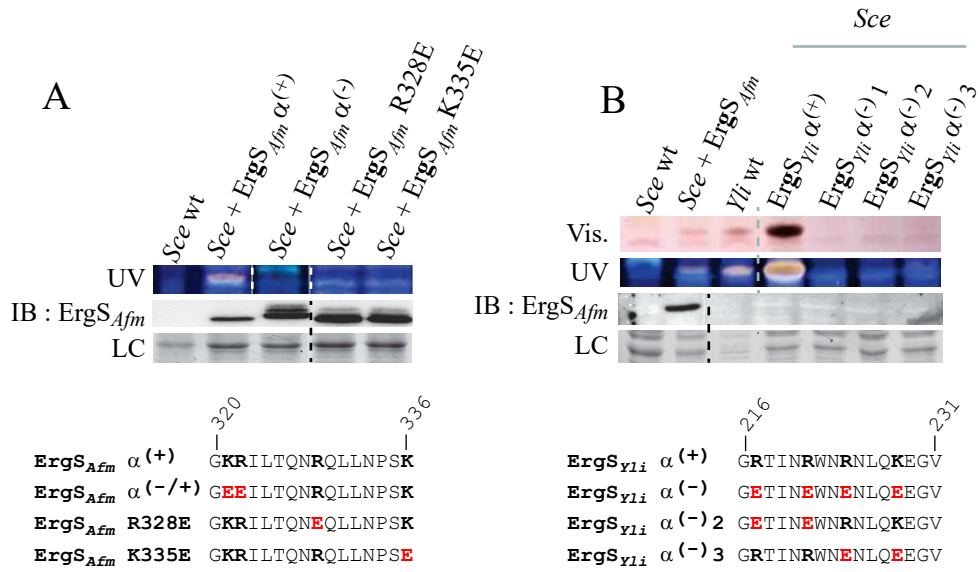
Figure 6: The positively charged α helix of ErgS is essential for Erg-Gly synthesis. On the basis of structure predictions and sequence alignments, the positively charged α helix of ErgS was delimited as described in Fig 1B. α(+) variants correspond to the wt versions where the helix was not mutated. Positively charged residues within this helix, indicated in dark and bold in lower panels of (A) and (B), were mutated to negatively charged residues (in red) and transformed in *Sce*. Total lipids from *Sce* wt (negative control), *Yli* wt and *Sce* expressing indicated *Afm* ErgS (A) or *Yli* ErgS (B) were extracted and *in vivo* activities of ErgS variants were analyzed by TLC. The eluent was ChCl3 : MeOH : H2O 130 : 16 : 1 (v : v : v), plates were stained with the MnCl2 / Sulfuric acid solution and results were captured either under UV- or white light. Total protein extracts were prepared from each indicated strain and ErgS variants expression was analyzed by Western blot with an anti-Afm ErgS polyclonal antibodies (IB:ErgS*Afm*). The SDS-PAGE was used as loading control (LC) before the protein transfer onto PVDF membranes.

Supporting informations

Supplementary Materials & Methods

Sub-cellular fractionation on *Sce* cells [*performed by N. Yakobov*]

Cells are inoculated O/N in the appropriate medium on a rotary shaker at 30 °C and the obtained pre-culture is diluted to OD600 = 0.1. The culture is incubated at 30 °C under rotation until OD600 reaches 0.8-1 and 20 OD600 equivalent units of cells are harvested by centrifugation at 5000 × g for 5 min at 4 °C. The following steps must all be done at 4 °C. Cells are washed twice with ice cold 1 × PBS (Phosphate-Buffered Saline) supplemented with 0.2 M sorbitol. The pellet is resuspended in 800 µl lysis buffer (1 × PBS, 0.2 M sorbitol, protease inhibitors tablet (Roche)), 1 volume of beads (Ø 0.25-0.5 mm, Roth) are added and cells are broken with a FastPrep®-24 apparatus (6 × 30 sec at 6.5 m/s, with 1 min on ice between each cycle). Cell debris are removed by centrifugation at 300 × g for 5 min at 4 °C, and the supernatant subjected to another centrifugation at 13000 × g for 15 min at 4°C. The resulting P13 pellet is resuspended in an equal volume of lysis buffer whereas the S13 supernatant is further fractionated by ultracentrifugation at 100000 × *g* for 1 h at 4°C. The soluble fraction is transferred in a fresh tube and the P100 is resuspended in an equal volume. For protein analysis, aliquots of obtained P13, P100 and S100 fractions are supplemented with 1 × Laemmli buffer and 10 µl are analyzed by SDS-PAGE and eventually subsequent immunoblots.

Ergosteryl-3β-*O*-glycine synthesis [*performed by Pr. T. Kushiro's team*]

Esterification of ergosterol and amino acid: Ergosterol （1 mmol） and 1 eq. of *N*-(*tert*-butoxycarbonyl)-glycine in CH₂Cl₂ （30 mL） at room temperature was added *N*,*N*′ Dicyclohexylcarbodiimide （300 mg） and *N*,*N*-dimethyl-4-aminopyridine （amount of catalyst） and stirred for 3 h at room temperature. The mixture was extracted with CHCl₃ and washed with 1*N*-HCl, sat. NaHCO₃ and sat. brine. The organic layer was dried over Na₂SO₄. Removal of the organic solvent *in vacuo* gave the crude product. Purification by silica gel column chromatography (hexane/ethylacetate = 5:1) gave the product in 48% yield.

Deprotection: 1-Ergosteryl *N*-(*tert*-butoxycarbonyl)-glycine （0.24 mmol） in CH₂Cl₂ was added Et₃N (1 mL). The mixture was added TMSOTf (excess) and stirred for 20 h at room temperature. The mixture was extracted with CHCl₃ and washed with cold sat. NH₄Cl and sat. NaHCO₃. The organic layer was dried over Na₂SO₄. Removal of the organic solvent *in vacuo*

gave the crude product. Purification by silica gel column chromatography (CHCl$_3$/MeOH = 100:1 ~ 10:1) gave the product in 88% yield. A schematic representation of the 2-step synthesis of Erg-Gly is shown in **Fig S4**.

1-Ergosteryl *N*-(*tert*-butoxycarbonyl)-glycine: ^{1}H NMR (300 MHz, CDCl$_3$): δ 0.605 (s, 3H), 0.801 (d, *J* = 6.97 Hz, 3H), 0.816 (d, *J* = 6.6 Hz, 3H), 0.895 (d, *J* = 6.6Hz, 3H), 0.927 (s, 3H), 1.105 (d, *J* = 6.6 Hz, 3H), 1.432 (s, 9H), 3.864 (d, *J* = 5.5, 1H), 4.75 (m, 1H), 5.177 (m, 2H), 5.356 (m, 1H), 5.544 (dd, 1.83 Hz, 5.5 Hz).

^{13}C NMR (75 MHz, CDCl$_3$): δ12.587, 14.733, 16.664, 18.152, 20.182, 20.495, 21.555, 21.646, 23.520, 28.575, 28.855, 32.126, 33.614, 37.083, 37.584, 38.365, 39.549, 40.988, 43.330, 43.355, 46.544, 55.052, 56.244, 60.897, 74.485, 80.387, 116.826, 120.953, 132.510, 136.078, 138.651, 142.103, 156.258, 170.298.

1-Ergosterylglycine: ^{1}H NMR (300 MHz, CDCl$_3$): δ 0.620 (s, 3H), 0.820 (d, *J* = 6.6 Hz, 3H), 0.836 (d, *J* = 6.97 Hz, 3H), 0.915 (d, *J* = 6.6 Hz, 3H), 0.941 (s, 3H), 1.032 (d, *J* = 6.23 Hz, 3H), 3.987 (s, 1H), 4.751 (m, 1H), 5.192 (m, 2H), 5.37 (m, 1H), 5.558 (dd, *J* = 2.2 Hz, 5.5 Hz 1H).

^{13}C NMR (75 MHz, CDCl$_3$): δ 12.645, 16.705, 18.218, 20.248, 20.552, 21.605, 21.720, 23.586, 28.608, 33.680, 37.108, 37.650, 38.423, 39.615, 41.062, 42.169, 43.018, 43.043, 43.388, 43.421, 46.602, 55.110, 56.310, 74.715, 116.892, 121.010, 132.593, 136.127, 138.741, 171.342.

Supplemental Figures

Figure S1 [*in preparation. The reader may refer to Fig. S7*]

Figure S2 [*in preparation*]

Figure S3 [*in preparation*]
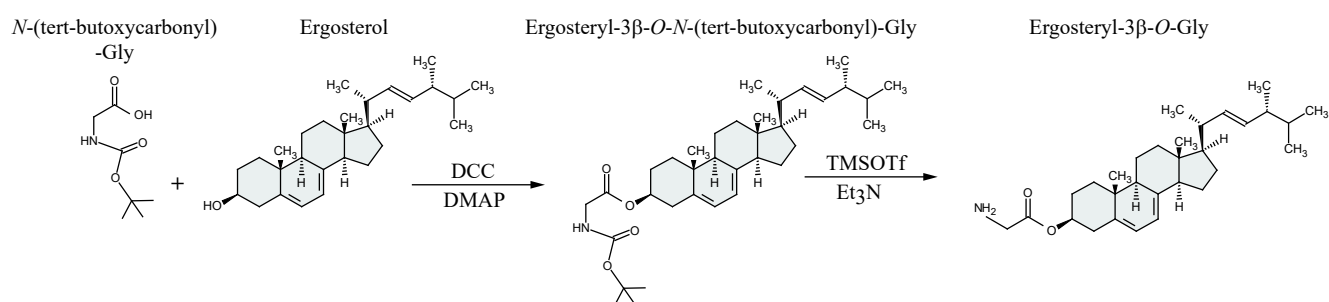
Figure S4: Chemical synthesis of Erg-Gly. Two-step synthesis scheme of Erg-Gly (Ergosteryl-3β-O-Glycine) from Erg and 4-tBu-N-(Boc)-Gly. For more details see the supplementary Materials & Methods section.
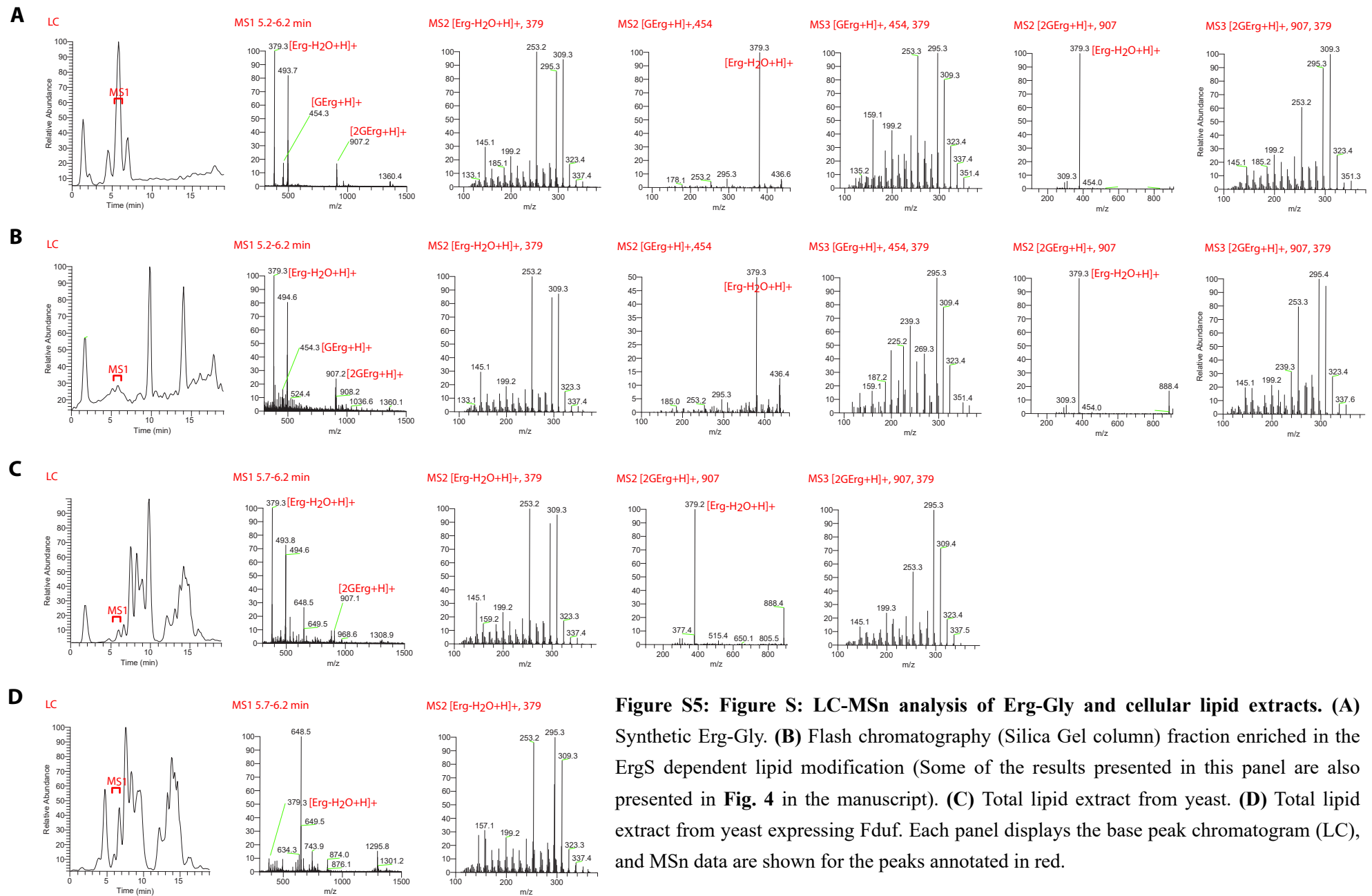
Figure S5: Figure S: LC-MSn analysis of Erg-Gly and cellular lipid extracts. (A) Synthetic Erg-Gly. **(B)** Flash chromatography (Silica Gel column) fraction enriched in the ErgS dependent lipid modification (Some of the results presented in this panel are also presented in **Fig. 4** in the manuscript). **(C)** Total lipid extract from yeast. **(D)** Total lipid extract from yeast expressing Fduf. Each panel displays the base peak chromatogram (LC), and MSn data are shown for the peaks annotated in red.

Erg-[^{14}C]Gly →

Yli ErgS	−	−	−	+
Afm ErgS	−	+	+	−
[^{14}C]-Gly	+	+	+	+
Sce S100	+	+	+	+
ATP	+	+	+	+
Sce total tRNA	+	+	+	+
Ergosterol	+	+	+	+
RNase	−	−	+	−
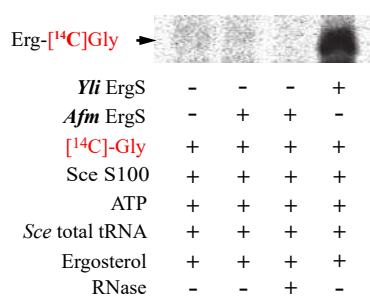
Figure S6: *Afm* ErgS is inactive in vitro for the synthesis of Erg-Gly. (A) GlyRS, provided by the soluble extracts from *Sce* (S100), is used to produce [^{14}C]Gly-tRNA^{Gly} from [^{14}C]Gly, ATP and tRNA^{Gly} (provided by total tRNA from *Sce*). After 1 h incubation enriched *Afm* ErgS, *Yli* ErgS and/or Erg were added in the appropriate assays (as indicated) and Erg-[^{14}C]Gly synthesis was measured by LA assays. Tests included addition (+) or not (−) of RNase A to verify the tRNA-dependency of the reaction.
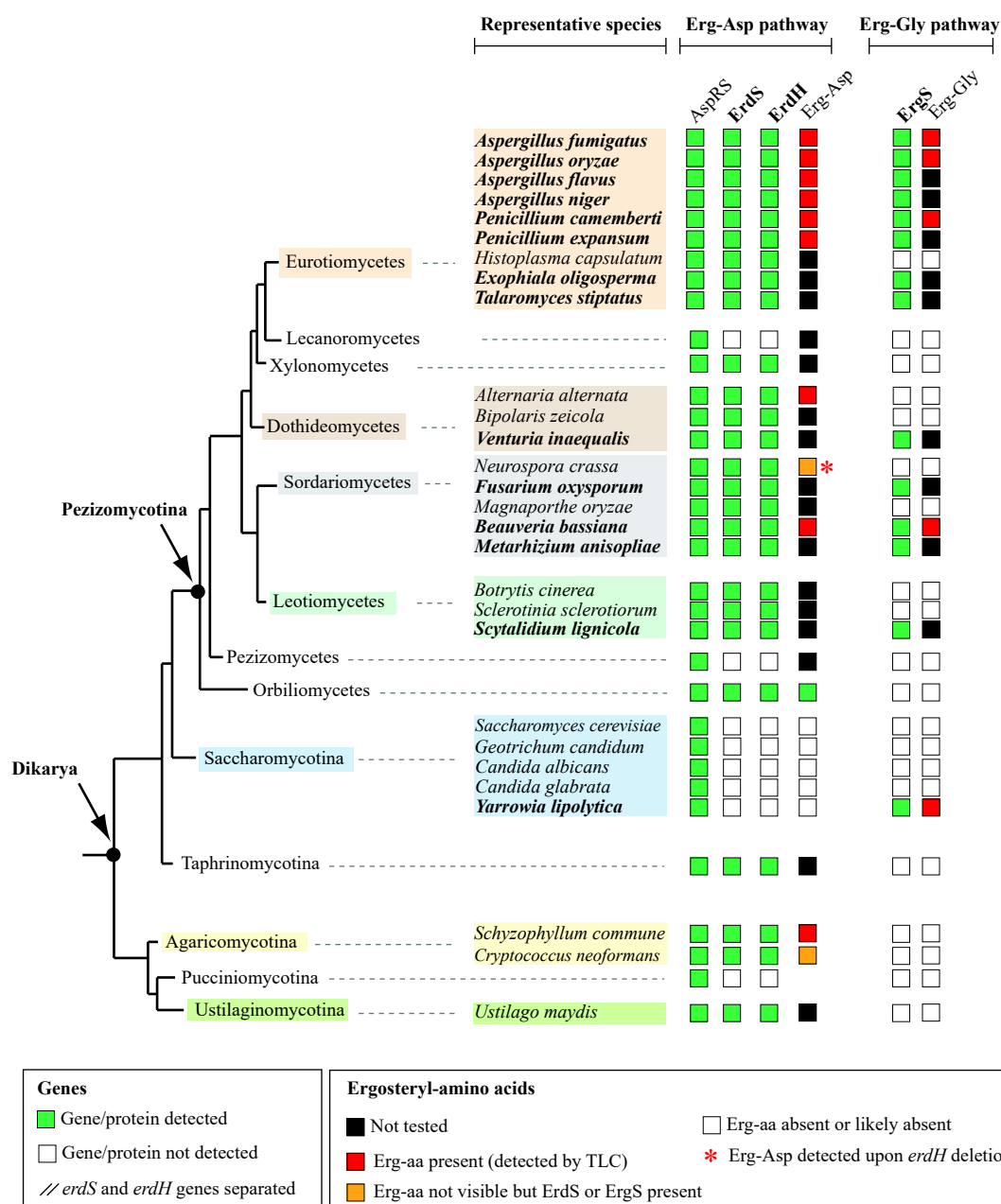
Figure S7: Distribution and co-occurrence of Erg-Asp and Erg-Gly pathway among fungi.
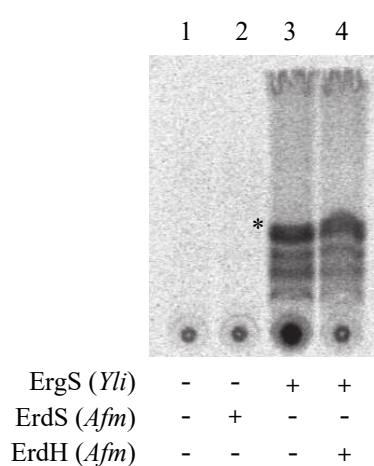
Figure S8: Assaying Erg-Gly hydrolysis activity of ErdH. Erg-[^{14}C]Gly was synthesized as in Fig. 5 (LA assay) in the presence of purified *Yli* ErgS, *Sce* total tRNA from *Sce*, radiolabeled [^{14}C]Gly, ATP, *Sce* S100 and Erg (lanes 3 & 4). At the end of the LA assay, synthesis of Erg-Gly was stopped in assays 3 and 4 by adding RNase A, and 0.1 μM of purified recombinant ErdH were added in assay 4 but not in assay 3. Both assays were further incubated for 30 min at 30 °C to test ErdH dependent Erg-Gly hydrolysis. Note that the TLC presented here correspond to the uncropped result of Fig 5C. Thus, lane 1 (LA assay without added enzymes) and 2 (LA assay in the presence of ErdS) are negative controls for the synthesis of Erg-Gly.

[*Please note that the activity of the recombinant ErdH assayed here was tested the day before the experiment by performing a Lipid deacylation assay on in vitro synthesized Erg-Asp. Consequently, the present result strongly suggests that Erg-Gly is not a substrate of ErdH. However, for more rigor, it is essential to repeat the experiment by using the same reaction mixture (including enzymes and substrates) at the same time for the positive control (i. e. lipid deacylation assay on Erg-Asp). Ongoing.*]
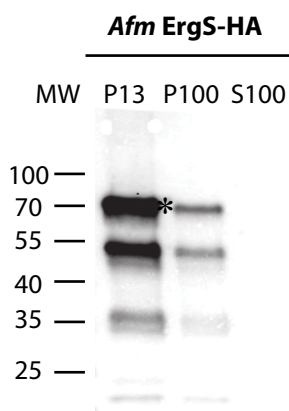
Figure S9: *Afm* **ErgS colocalizes with membrane fractions.** *Afm* ErgS was fused to a HA-tag and expressed in *Sce*. Sub-cellular fractionation was performed and provided P13, P100 and S100 fractions which were then separated by SDS-PAGE and analyzed by WB using anti-HA antibodies (1/3000).
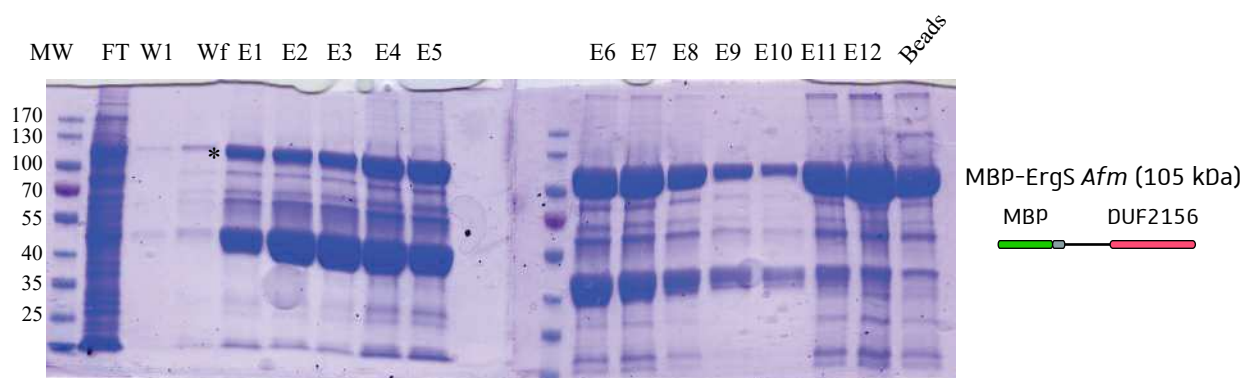
Figure S10: Enrichment of full-length MBP-Ergs *Afm* by amylose resin affinity. *E. coli* Rosetta 2 harboring pMtev-ErgS *Afm* were grown and the construct of interest was overexpressed. Cells were resuspended in lysis buffer, disrupted by sonication, and cleared by centrifugation (see the Materials & Methods sections). The soluble fraction of the crude extract obtained from a 2 L pellet was put in the presence of 2 mL of equilibrated amylose resin and incubated on a rotating wheel for 2-3h at 4°C. The batch was poured into a column and the flow through (FT) was collected. Beads were washed with wash buffer several times and elution was performed with the same buffer supplemented with 3 % maltose. 10 elution fractions (E1-E10) of 0.5 mL were initially collected. Then beads were incubated O/N with 3 mL of elution buffer at 4°C and the next morning, two additional fractions (E11, E12) of 1 mL were collected. The FT, the first (W1) and the last wash fraction (Wf), the eluted fractions (E1-E10) and an aliquot of beads were analyzed by SDS-PAGE. MW, molecular weight in kDa; * indicate the band corresponding to the protein of interest.

Note that eluted fractions were enriched in MBP-ErgS$_{Afm}$ but a major contaminant, probably corresponding to free MBP (40 kDa), is present. The amount of eluted MBP-ErgS$_{Afm}$ decreased after 11 elution fractions but surprisingly, important amounts of the protein were eluted after O/N incubation with the elution buffer. Furthermore, analysis of proteins retained on the beads following the several elution steps clearly showed that MBP-ErgS$_{Afm}$ was not fully eluted from amylose. These results indicate that MBP-ErgS$_{Afm}$ is strongly retained on the amylose resin and suggest that MBP-ErgS$_{Afm}$ either partially precipitates during the purification or has an affinity for the amylose resin. This might partially explain our failures to detect any in vitro lipid aminoacylation activity of the recombinant ErgS$_{Afm}$ protein (**Fig S6**). Importantly, note that fractions E1-E8 were polled together and the resulting fraction was used for the *in vitro* assay, presented in **Fig. S6**.

ErgS variant (95 kDa) (ε = 1.45 M^{-1}.cm^{-1})	purified amount (mg)
MBP–ErgS$_{Yli}$ wt	3.3
MBP–ErgS$_{Yli}$ $\alpha^{(-)}$	5
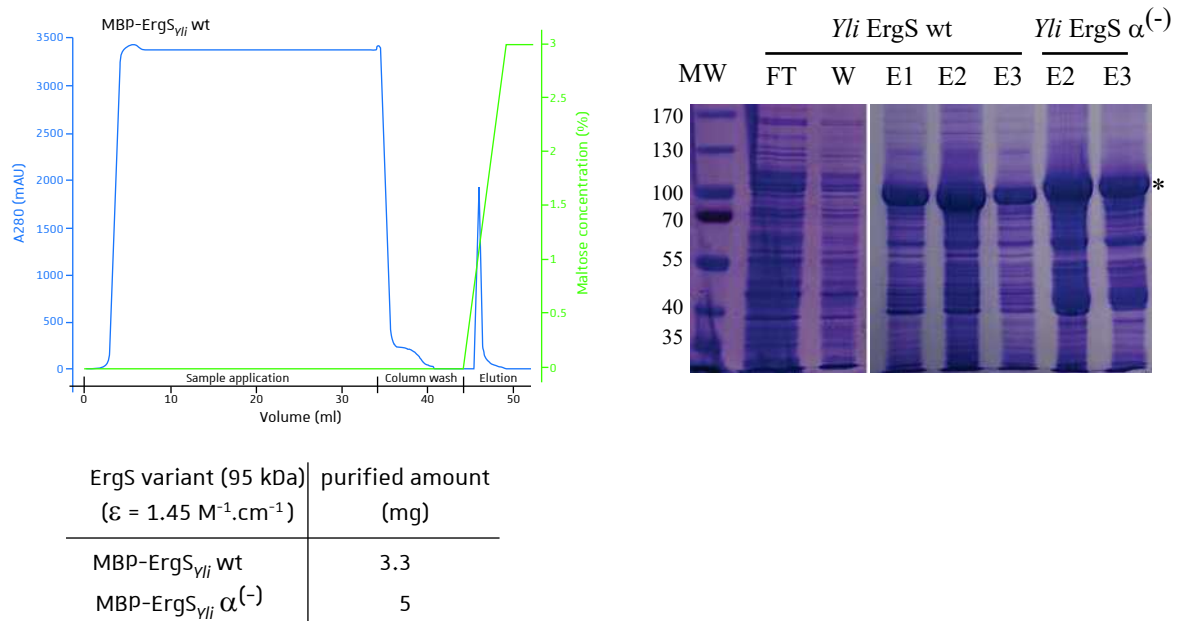
Figure S11: Enrichment of MBP-ErgS *Yli* variants by MBPtrap affinity column. *E. coli* strains harboring the adequate plasmid were treated as described in legend of (Fig. S10) but the volume culture was lowered to 1 L. The soluble fraction was injected onto a MBPtrap 1mL affinity column, conducted by an Äkta pure HPLC system (for more details see the Material & Methods section). Wash steps were performed with 10 column volumes of Wash buffer and elution was achieved with a gradient of maltose (0% - 3% p/v) in Wash buffer. The flow rate was 1 ml/min during equilibration and column wash and was decreased to 0.5 ml/min for sample application and elution. Elution fractions were collected per 0.5 mL. The chromatograph for MBP-ErgS *Yli* wt is represented in **(A)** and those for the MBP-ErgS *Yli* mutant yield similar profile (not shown). Total amounts of protein recovered in the elution peak are summarized below the chromatograph. **(B)** The flow through (FT), the single wash fraction collected (W), as well as eluted fractions of both enriched proteins were analyzed by SDS-PAGE.*

Even though eluted fractions are enriched in recombinant ErgS protein it is clear that the purity of the protein remains largely to be improved. However, the aim of purifying recombinant *Yli* ErgS versions was at this state mainly to detect and to confirm the ErgS activity. Since no *Yli* deletant strain was available to confirm ErgS dependency for lipid Y (Erg-Gly) synthesis we used the enriched fraction of *Yli* ErgS $\alpha^{(-)}$ KO mutant as a negative control.
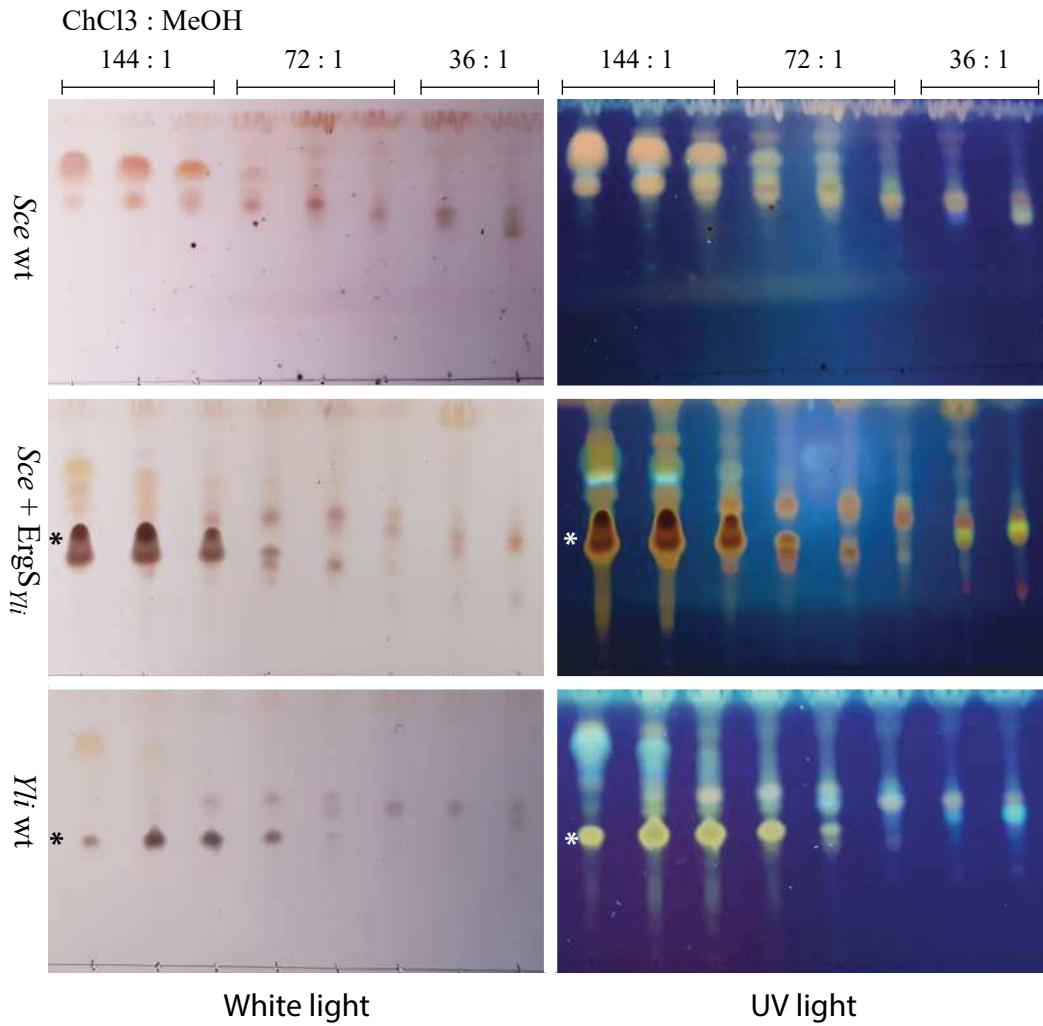
Figure S12: Enrichment of Erg-Gly by Silica column chromatography. Total lipids from *Sce*, *Sce* expressing *Yli* ErgS and *Yli* wt were extracted, then fractionated by Silica column chromatography with CHCl$_3$ and CHCl$_3$: MeOH (v : v) mixtures ranging from 144 : 1 to 36 : 1. Finally fractions collected through elution with CHCl$_3$: MeOH mixtures were analyzed by TLC using CHCl$_3$: MeOH : H$_2$O 130 : 16 : 1 (v : v: v). Plates were stained with the MnCl$_2$ / Sulfuric acid method and visualized either under white light or under UV light. Asterisks indicate Erg-Gly. Note the absence of the dark-brownish spot (Erg-Gly) in fractions obtained from total lipids extracted from *Sce* wt.

Conclusions & Perspectives
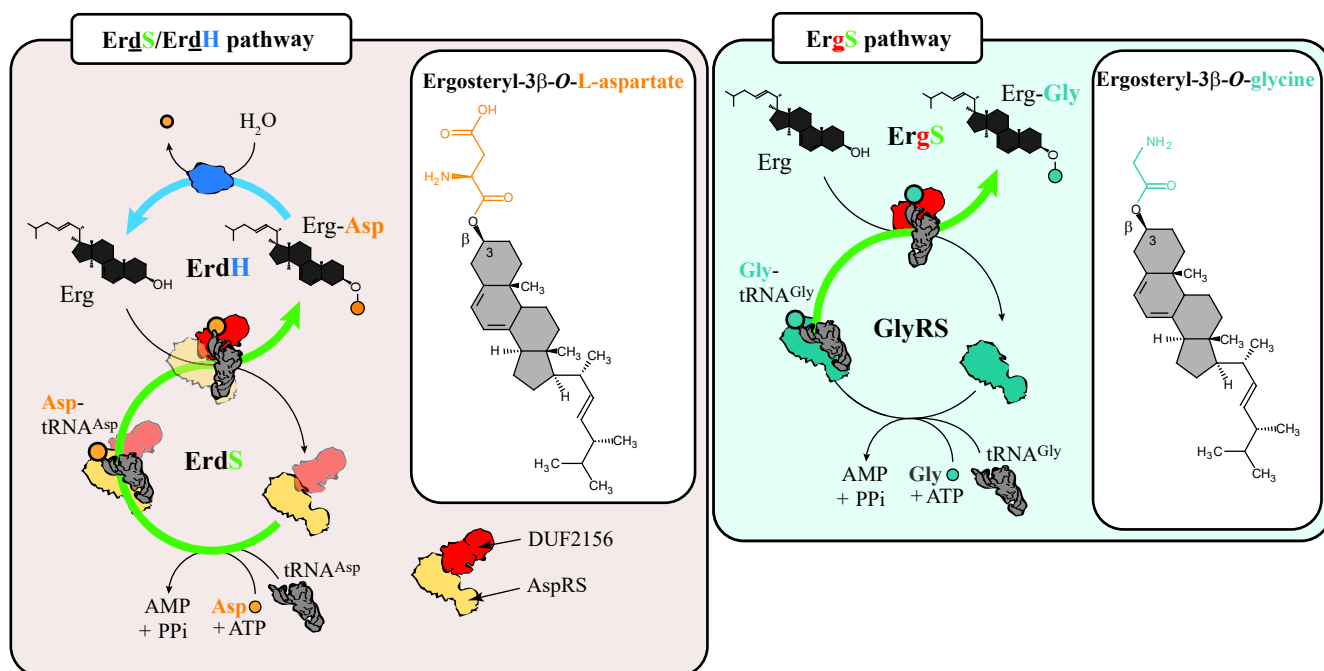
Figure CP-1: Graphical summary of both fungal Erg-aa pathways discovered during my thesis. (A) The bifunctional Er**d**S protein synthesizes Asp-tRNA^{Asp} assumed to be directly channeled from the AspRS domain to the DUF2156 domain for Erg aspartylation. **(B)** In contrast, Er**g**S is not fused to the cognate GlyRS and might therefore compete with the translational machinery for the Gly-tRNA^{Gly} substrate to synthesize Erg-Gly. Green arrows indicate ATT activities of ErdS and ErgS while the blue arrow highlights Erg-aa hydrolysis, only discovered for the Erg-Asp pathway so far.

I. Conclusion of my thesis work: The DUF2156 domain is a tRNA-dependent ergosteryl-amino acid (Erg-aa) synthase in filamentous fungi

The study described in this manuscript describes the functional characterization of a domain of unknown function called DUF2156 widespread among filamentous fungi. Through a combination of approaches we were able to attribute a role to this domain that lead to major changes of paradigms in the fields of tRNA aminoacylation and fungal sterol metabolism.

The results I obtained concerning the identification of enzymatic activity of the AspRS-DUF2156 protein allowed me to prove that this bifunctional enzyme is an ergosteryl-aspartate synthase (ErdS) which combines an aspartyl-tRNA synthetase that produces an Asp-tRNA^{Asp}, to an aminoacyl-tRNA transferase (ATT) that transfers the tRNA-bound Asp onto ergosterol releasing ergosteryl-aspartate (Erg-Asp) (**Figure CP-1A**). This work also shows that sterol aminoacylation is dynamic since we identified a dedicated Erg-Asp hydrolase (ErdH) that removes Asp from Erg (**Figure CP-1A**). Although we concentrated our efforts on two species of filamentous fungi, our study suggests that most of the higher fungi use this novel tRNA-dependent ergosterol-modifying pathway. The widespread distribution of this pathway among fungi insinuates that it might play an important physiological role despite the fact that ErdS is not essential to the viability in the species in which we knocked out the gene, at least in the phenotypic conditions we screened.

The study of the free-standing DUF2156 (fDUF2156) enzyme shows that, again, the DUF2156 protein is an ATT responsible for the aminoacylation of ergosterol. However, it transfers Gly from Gly-tRNA^{Gly} onto Erg thereby generating ergosteryl-glycine (Erg-Gly); we therefore named it ergosteryl-glycine synthase (ErgS) (**Figure CP-1B**). Unlike Erg-Asp, Erg-Gly isn't deacylated by ErdH and we haven't yet characterized the hydrolase that would remove Gly from Erg-Gly, but we still don't know whether production of Erg-Gly is, like that of Erg-Asp, dynamic and involves a dedicated Erg-Gly hydrolase. However, like our Japanese collaborator, Pr. T. Kushiro (Meiji University), we failed in isolating *ergS* deletion mutants suggesting that there is a possibility that Erg-Gly synthesis could be essential at least in the two fungal species in which we tried to delete the genes, *Afm* and *Aor*. I started to map, by site-directed mutagenesis, the residues of the double GNAT domain of ErdS that might be important for aa-tRNA and ergosterol binding; I could

identify several residues putatively involved in aa-tRNA- or ergosterol-binding that upon mutagenesis severely decreased Erg-aa synthesis, but ran out of time to fully characterize the mutants.

Like probably most of my fellow PhD student, I'm left with the feeling that the most important discoveries to be made on these tRNA-dependent ergosterol aminoacylating pathways are ahead of us and I have outlined in the next part of my manuscript, the leads I would follow if I were given more years to continue on this project. For me, the obvious most crucial question that needs to be answered is what physiological role these new sterol conjugates play in fungi and especially in pathogenic species. However, before detailing those perspectives I will first briefly introduce the life cycle of *Afm* and give and overview about Erg biosynthesis and its physiological functions.

II. The life cycle of *A. fumigatus*

Fungi species are found in almost all ecological niches which allowed them to learn how to adapt to several environmental and stress conditions (Latge and Chamilos 2019). *A. fumigatus* is a saprotrophic fungus that adopts various morphological states during its life cycle (**Figure CP-2**). As a common feature of filamentous fungus, its vegetative form is composed of a network of branched hyphae and is called mycelium (Tekaia and Latge 2005). Conidiophores are specialized hyphae that emerge from the mycelium and produce separate phialides at their extremities (Park and Yu 2016). Phialides are vase-shaped cells specialized and responsible to produce asexual spores called conidia. Conidia from *Afm* are pigmented (dark green) and are defined as propagules since they correspond to the form by which they spread (Park and Yu 2016). *Afm* was believed for a long time to reproduce only by asexual sporulation and genetic diversity was proposed to be generated through hyphal fusion in the absence of meiosis (Latge 1999; Debeaupuis *et al.,* 1997). However, since the 70's, evidences arguing for the existence of a cryptic sexual cycle were brought (Latge and Chamilos 2019). Production of asci containing sexual propagules (ascospores) occur in specialized structures, namely cleistothecia, emerging at hyphae junctions between two parental isolates (Dyer and O'Gorman 2012). This sexual reproduction involves MAT1-1 and MAT1-2 genes from the heterothallic *Afm* species (Poggeler 2002; Paoletti *et al.,* 2005; Bain *et al.,* 2007). to form
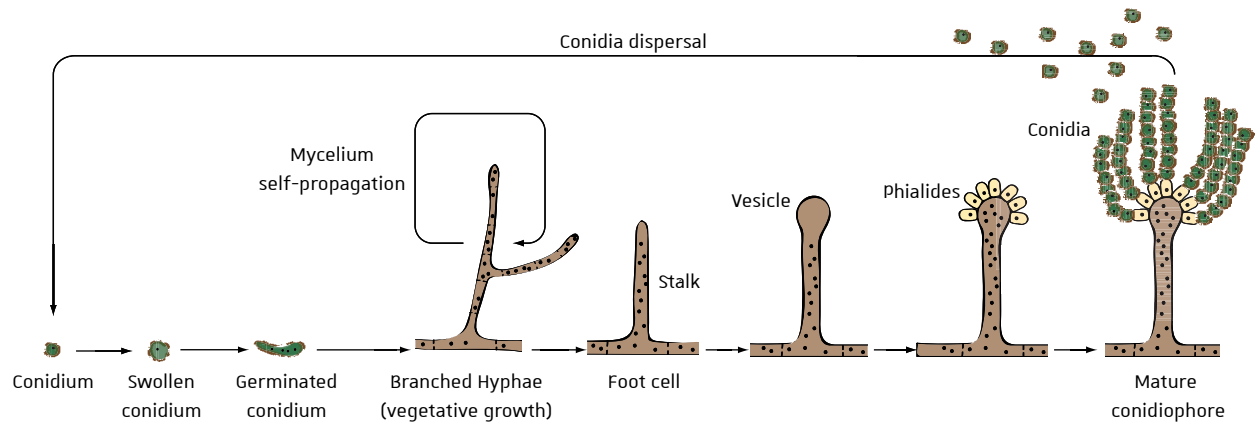
Figure CP-2: The asexual life cycle of _Afm_.

sexual propagules called ascospores. However, sexual reproduction occurs under very specific conditions that are rarely encountered in nature (O'Gorman *et al.,* 2009).

III. Introduction to Erg, the main fungal sterol

III.1.   Erg biosynthesis

Erg, a 5,7-diene oxysterol, is the functional fungal analog of cholesterol (Cho) and is the most abundant sterol in fungal cell membranes (Jacquier and Schneiter 2012; Rodrigues 2018; Jorda and Puig 2020). Most erg biosynthesis steps are assumed to be conserved but some species-specific deviations were described. Notably, lanosterol, the first sterol synthesized during erg biosynthesis, is converted either to eburicol in *Afm* or to zymosterol in *Sce* (**Figure CP-3**). Both pathways converge then to the synthesis of fecosterol which is successively transformed to episterol, Ergosta-5,7,24(28)-trienol, Ergosta-5,7,22,24(28)-trienol and finally Erg (Dhingra and Cramer 2017). Successive reactions catalyzing the transformation of squalene to the final Erg occur mainly in the endoplasmic reticulum where Erg biosynthesis enzymes are mostly located but some of the latter can be multi-localized and be found for example in lipid particles which is the universal lipid storage compartment (Mullner *et al.,* 2004; Kristan and Rizner 2012) (Jorda and Puig 2020). Once synthesized in the ER Erg is distributed to its final destinations, mainly the PM, but Erg significant amounts were also detected in mitochondria, endoplasmic reticulum, vacuoles, and peroxisomes (Schneiter *et al.,* 1999; Zweytick *et al.,* 2000; Kristan and Rizner 2012). Erg is distributed all along the PM, mainly in the cytoplasmic leaflet (Solanko *et al.,* 2018; Martzoukou *et al.,* 2017), but enriched features, called sterol-rich domains (SRD) are located at hyphal tips and septa in filamentous fungi, or at bud and mating projection tips in various yeast species (Alvarez *et al.,* 2007). Sphingolipids are also enriched in those structures and were suggested to have important roles in membrane organization, fungal cell polarization and other important processes (Maxfield and Tabas 2005; Fischer *et al.,* 2008; Douglas and Konopka 2014).
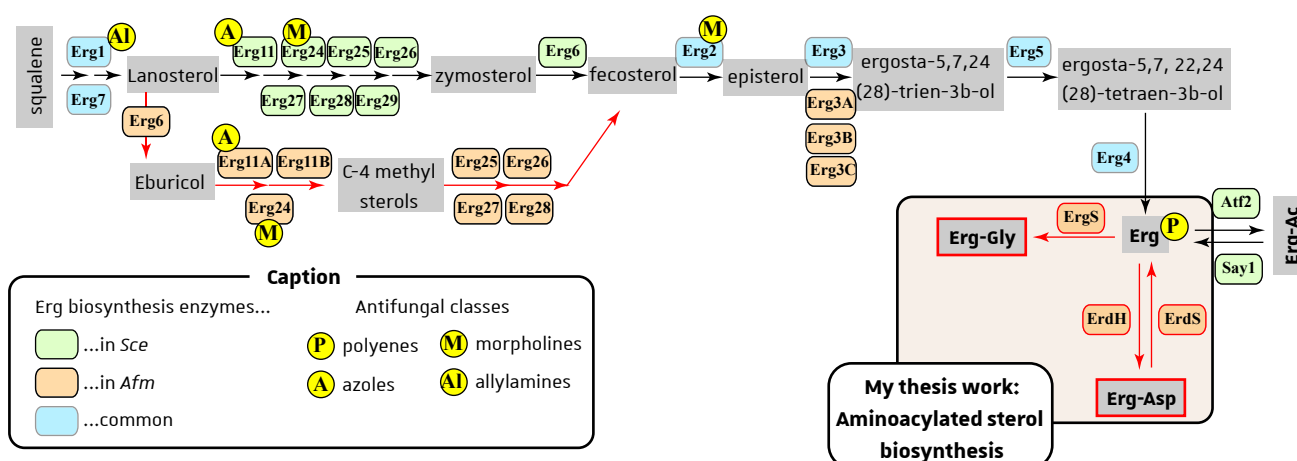
Figure CP-3: Erg, Erg-acetate and Erg-aa biosynthesis pathways. Gray boxes indicate Erg, Erg intermediates or Erg derivates. Erg biosynthesis steps in *Sce* and *Afm* are indicated by black and red arrows, respectively. Erg-aa and enzymes responsible for their homeostasis are highlighted in red-surrounded boxes. A pathway enabling Erg-Gly hydrolysis might exist in fungi but no factor achieving this activity was revealed so far. Erg-Ac, ergosteryl-acetate.

III.2.   The central role of Erg in fungal species illustrated by its implication several processes

Erg is critical to regulate the permeability, the fluidity and the thickness of the PM (Daum *et al.*, 1998; Douglas and Konopka 2014; Kodedova and Sychrova 2015) and is involved in several cellular process, including growth (Kodedova and Sychrova 2015; Bhattacharya *et al.*, 2018), regulation of membrane associated proteins activities (V-ATPase (Zhang *et al.*, 2010), G-protein-coupled receptor (GPCR) (Morioka *et al.*, 2013) and Multidrug Resistance Pumps (Kodedova and Sychrova 2015)), sporulation, pheromone signaling, endocytosis (Heese-Peck *et al.*, 2002; Jin *et al.*, 2008) mitochondria DNA maintenance (Cirigliano *et al.*, 2019). Beside its critical role in several cellular processes, Erg has been reported to be important for adaptation to several stressors since increased amounts of Erg raise the resistance to low temperature, low sugar, alcohol and oxidative stresses while osmotic stresses were associated to decreased Erg levels. The importance of Erg was also pointed out during hypoxia, iron and salt stresses (Shakoury-Elizeh *et al.*, 2010; Montanes *et al.*, 2011; Hu *et al.*, 2017; Liu *et al.*, 2019; Jorda and Puig 2020). Numerous studies investigated the effect of sterol levels on drug susceptibility notably by deleting *erg* genes. M. Kodedova and colleagues showed that most deletion strains were more susceptible to cationic drugs (hygromycin B and tetramethylammonium) while resistance to antifungal drugs (cycloheximide, nystatin and several azole derivates) was either increased or decreased according to the deletion strain and to the tested component (Kodedova and Sychrova 2015). In addition, S. Bhattacharya and colleagues used *Sce* strains overexpressing erg genes and tested their susceptibility in the presence of a large range of drugs. They confirmed that deletion strains show various susceptibilities to drugs, a fact that was also true when overexpressing *erg* genes. For example, *ERG6* overexpression lead to higher susceptibilities to polyenes targeting Erg (Nystatin and Amphotericin B (AmB)) while the corresponding deletion strain was more susceptible to lovastatin (targeting Hmg1p protein) and more resistant to fluconazole (targeting *ERG11*) (Bhattacharya *et al.*, 2018). Finally, Erg has recently been shown to trigger the NLRP3-Casp1/11-mediated pyroptosis of macrophages, an inflammatory programmed cell death pathway (Koselny *et al.*, 2018).

The very brief and non-exhaustive report of the plethora of processes in which Erg is implicated, demonstrates the essentiality of this metabolite in fungal cells. Moreover, the impact

of sterol variation on several cellular, adaptative and resistance pathways perfectly illustrates the importance of maintaining accurate sterol levels in fungal cells and thus their homeostasis. Moreover, fungal sterols like Erg can be esterified thereby enlarging their functional repertoire.

III.3. 3β-O-modified sterols in fungi

Sterol esterification with acyl chains is widely found in eukaryotic species and contributes to its homeostasis (Korber *et al.,* 2017). *Sce* uptakes exogenous sterols, which are transported by Aus1p and Pdr11p (ABC transporters) from the PM to the ER (Li and Prinz 2004). At this location, acyl-CoA:sterol acyltransferases (Are1p and Are2p) were shown to esterify mainly Erg and its precursor Lanosterol (Yang *et al.,* 1996; Yu *et al.,* 1996; Zweytick *et al.,* 2000). Acylated sterols are then stored in lipid droplets, the universal lipid storage compartment (Kuhnlein 2012). Homeostasis of acylated sterols is ensured by steryl ester hydrolases that mainly belong to the α/β hydrolase family and their activity releases free fatty acids and non-esterified sterols (Korber *et al.,* 2017). In *Sce* three steryl ester hydrolases were identified, namely, Yeh1p and Tgl1p, located at lipid droplets, and Yeh2p, located at the PM (Koffel *et al.,* 2005). [For review refer to (Korber *et al.,* 2017)]

Another sterol esterification mechanism participating to sterol homeostasis was described in *Sce* (but not in *Afm*) and consists of sterol acetylation (**Figure CP-3**). Beside Erg, *Sce* can uptake exogenous sterols including cholesterol. Furthermore, under certain conditions *Sce* must deal with accumulated amounts of sterols, including Erg, which became toxic for the cell. In order to detoxify, *Sce* has inherited an alcohol acetyltransferase, Atf2, which acetylates sterols (Tiwari *et al.,* 2007) that are then transported from the ER to the PM and subsequently exported from the cell by Pry1p and Pry2p (Choudhary and Schneiter 2012). This esterification is reversible through the action of Say1 that also harbors an α/β hydrolase fold (Tiwari *et al.,* 2007). Importantly, Atf2-acetylated sterols such as Erg intermediates or analogs are not deacetylated by Say1 and are therefore efficiently removed from membranes. In contrary, Erg is efficiently deacetylated and transported to the PM but not exported (Choudhary *et al.,* 2014; Tiwari *et al.,* 2007). This detoxification mechanism regulated by Atf2/Say1 cycle participates also to the removal of damaged lipids and was shown to confer resistance and growth advantage in the presence of eugenol (Choudhary and Schneiter 2012).

Another interesting class of modified sterols are steryl-glucosides (SG) that are found in bacteria, plants, fungi, and animals. Here, modification of sterols is achieved by a UDP-sugar:sterol glycopyranosyltransferases or NDP-sugar:steryl glycoside glycosyltransferases. As for the above reported examples, this mechanism can be reversed by the antagonist action of SG hydrolases [For reviews refer to (Grille *et al.,* 2010)]. In fungi the most abundant SG is ergosterol-3β-glucoside (Sakaki *et al.,* 2001; Watanabe *et al.,* 2015) and UDP-glucose:sterol glycosyltransferases (Atg26), were described in various species including *Sce*, *P. pastoris*, *C. albicans* and *D. discoideum* *(Warnecke et al., 1999; Warnecke et al., 1997; Warnecke and Heinz 1994)*. In some of them, steryl-β-glucosides were shown to be important for peroxisome degradation and are thus implicated in macroautophagy, most likely through the recruitment of protein partners onto the nascent autophagosome (Yamashita *et al.,* 2006; Grille *et al.,* 2010). Notably, a recent study investigated the physiological relevance of Atg26 in the filamentous fungi, *A. oryzae* and showed its requirement for autophagy of peroxisomes, mitochondria, and nuclei (Kikuma *et al.,* 2017). SG hydrolases were described more recently in fungi, notably, Sgl1 from *C. neoformans* and Egh1 from *Sce*. In recent years, SGs have attracted much interest because of their implication in fungal virulence notably as regulators of the host immune response (Rella *et al.,* 2016). Deletion of the sterylglucosidase *sgl1* in *C. neoformans* lead to SGs accumulation which abolished the pathogenicity of this strain, but even more remarkable is the fact that high levels of SG act as a vaccine against *C. neoformans* in murine mice models (Rella *et al.,* 2015). Thus, Sgl1 is an important virulence factor and the SG synthesis/degradation cycle further illustrates the importance of finely regulating sterol homeostasis in fungi. Beyond fungal infections, administration of SG was suggested to confer a beneficial effect in patients with allergic issues, pulmonary tuberculosis (Donald *et al.,* 1997; Bouic 2001) and the effect of SGs on cancer are under investigations (Bouic 2001; Kunimoto *et al.,* 2003; Jayaprakasha *et al.,* 2010).

The three examples of Erg modification further illustrate the multifunctionality of Erg and the difficulty to predict the physiological functions of aminoacylated lipids that we discovered. Even though each of those 3 mechanisms shows specific features, they share important features not only between them but also with the ErdS/ErdH pathway that I described during my thesis. Notably, they all modify ergosterol on its hydroxyl group (at position 3) and more importantly they all include hydrolases to regulate lipid homeostasis which is was undoubtedly an essential aspect.

The important role of such hydrolases was also demonstrated in the context of bacterial MprFs notably for the virulence of *M. tuberculosis*. This also strongly suggests that a yet unidentified Erg-Gly hydrolase might be present in species encoding ErgS.

Regarding this brief overview, my thesis work not only enlarges the repertoire of 3-b-O sterols but introduces a new class of modified lipids, namely aminoacylated sterols.

IV. Perspectives aiming to uncover the physiological function of aminoacylated sterols (AS)

IV.1. How are fungal DUF2156 proteins and ASs integrated in *Afm* cell's physiology?

With regard to the available literature and the knowledge about sterols and modified sterols, the Erd-aa pathways discovered during my thesis can potentially be involved in several physiological processes including trafficking, signaling, autophagy, drug resistance, cell wall remodeling, pathogenesis and virulence among others. One critical point that must be taken in consideration is the regulation of AS homeostasis. The imbalance of Erg-aa species might be toxic and this is supported by our preliminary experiments performed on the complemented *Afm* strain in which overexpression of *erdS* (induced with xylose) triggers high accumulation of Erg-Asp and strongly reduces growth rate (not shown). Similarly, *Sce* strains expressing *Yli ergS* show reduced growth under standard conditions. Because such a growth defect was not observed for *Sce* expressing *Afm ergS*, producing relatively low amounts of Erg-Gly, it is tempting to speculate that the observed phenotype is directly correlated to the AS levels (not shown). These results further support that Erg-aa might be involved in central cellular processes.

Because little is known about AS physiological role, it will be necessary to start with approaches to decipher the physiological landscape in which those modified lipids are involved in. In the coming sections I will present some questions that the lab aims to investigate and some strategies that we plan to use.

IV.1.1. Determining the sub-cellular localization of Erg-aa synthases and hydrolases

Because co-expression of *erdS* and *erdH* would lead to futile synthesis/degradation cycle, we suspect that both genes might be differentially expressed under defined conditions. Another possibility is that both genes are co-expressed, but Erg-Asp synthesis and degradation might occur at different locations or their activity might be controlled, for example, by a specific kinase. Sub-cellular fractionation indicated that ErdS (Yakobov *et al.,* 2020) and ErgS (ErgS draft article) are associated with membranes and wherever they are located, they might point toward the cytoplasm where their (aa-)tRNA substrates are available. Accordingly, ErdS was predicted to be cytoplasmic while ErdH$_{Afm}$ contains a putative mitochondrial targeting sequence (Wolf PSort, MitoProt II). Note that, mitochondria contain also aa-tRNA for organellar protein biosynthesis and to date it is not possible to exclude that Erg-Asp synthesis occurs in mitochondria, given that substantive amounts of Erg are also present in this organelle. In order to clarify ErdS and ErdH location the lab plans to use a integrative cassette to replace the endogenous *erdS-erdH* locus by a synthetic locus from which ErdS-GFP and ErdH-mCherry will be expressed in *Afm* under their endogenous promoters (the cassette is already available). In a first approach, the recombined strain will be grown under various conditions, including stressors, and the localization of both proteinswill be analyzed by fluorescence microscopy. Fluorescent probes targeting specific compartments will then be used for co-localization experiments. Additionally, subcellular fractionations and purification of specific organelles can be performed, and their ErdS/H content analyzed by WB.

Similar approaches will be used to investigate the localization of ErgS. During my thesis I aimed to study the localization of ErgS$_{Afm}$-CFP, heterologously expressed in *Sce*, by fluorescence microscopy. In this case results indicated that ErgS$_{Afm}$-CFP co-localizes with Sec7-GFP which is a specific marker of the Golgi apparatus (not shown). ErgS localization at Golgi vesicles is surprising with regard to its activity since to our knowledge Erg is not located in this compartment and the transport of Erg from the ER to the PM is assumed to be performed by lipid binding/transport proteins rather than vesicular transport (Sokolov *et al.,* 2019; Jorda and Puig 2020). However, it cannot be excluded that ErgS localization at Golgi vesicles is transitory and that the vesicular transport is used to reach its final destination where the Erg substrate is located.

IV.1.2. Determining ErdS/ErdH/ErgS interacting partners

Another important task that will help to understand how the whole fungal lipid aminoacylation/deacylation system is integrated in cell's physiology will be to determine **ErdS/ErdH/ErgS interacting partners**. To this end the lab plans to use an integrative cassette to replace the endogenous *erdS-erdH* locus by a synthetic locus from which TAP-tagged ErdS and ErdH-HA$_3$ will be expressed in *Afm* under their endogenous promoters (the cassette is already available). The tandem affinity purification (TAP) strategy was initially described to purify interacting partners in *Sce* but the strategy was adapted and is suitable for experiments on filamentous fungi (Bayram *et al.,* 2012). Interactants will be identified by MS and should deliver hints with respect to the cellular pathway in which ErdS/ErdH are involved. Most relevant interactions will then be validated through other experiments including co-immunoprecipitations (co-IP).

IV.1.3. Investigating the transcriptional regulation of the *erd* locus

In our recent publication we showed that under standard growth conditions, Erg-Asp synthesis surpasses degradation (by ErdH) in *Afm wt* and *Aor wt* while the tendency seems to be reversed in *Ncr wt* were Erg-Asp was absent from total lipids. Nevertheless, ErdS activity was detectable in crude extracts prepared from *Ncr wt* and more importantly high Erg-Asp levels accumulated in *Ncr ΔerdH.* Analysis of *erdS-erdH* synteny also revealed that both genes tend to cluster, as frequently found for other genes with metabolically-related functions in fungi (Nutzmann *et al.,* 2018). This suggests that *erdS* and *erdH* expressions are regulated at the transcriptional level and it is tempting to speculate that they might be differentially regulated with regard to their antagonist activities.

Monitoring the expression of genes in fungi can be achieved by using firefly and Gaussia princeps luciferases as reporters (Paul *et al.,* 2013; Krappmann 2015). In this way we plan to use an integrative cassette to replace the endogenous *erdS-erdH* locus by divergent luciferases under the control of the common *erd* promoter. However, the genomic sequence separating both divergent genes is less than 1 kb. There is a risk of truncating some important regulatory elements that overlap erdS and ergS ORF's. Therefore, the herein proposed approach must be combined to other transcriptomic analysis strategies, notably RNA-seq or qRT-PCR. Expression patterns will be determined under several growth conditions including variations of carbon and nitrogen sources,

hypoxia, liquid or solid growths, nutrient-rich or nutrient-depleted media, autophagy-inducing conditions, etc. Response to stresses (osmotic, oxidative) including to the presence of antifungals, cell wall or membrane disrupting agents, etc. will also be tested. Finally, we will also test the activity of the *erd* promoter at growth stages: conidia, swollen or germinating conidia, mycelia, conidiation/sporulation. Obviously, *ergS* promoter will also be integrated in this study and it would be particularly interesting to verify transcriptional correlations between the *erd* locus and *ergS*. Anti-ErdS and -ErgS antibodies developed during my thesis will also be used to correlate transcriptional effects to the expression of ASSs at the protein level. Finally, lipid analyzes will be done to verify if AS and protein levels correlate (analytical analysis by TLC and if needed quantitative analysis by MS (lipidomics))

IV.1.4. Genome-wide analysis of transcriptional changes induced by ASs.

As mentioned above, AS could be potentially implicated in several pathways including central regulatory processes known to be regulated by sterol metabolism. To screen the largest range of pathways potentially affected by AS, we plan perform whole genome transcriptomics on *Afm* strains in which AS levels are known to vary. The most obvious will be to start those RNA-seq experiments with *Afm wt* and deletion strains (*ΔerdS, ΔerdH*) as well as with our recombinant strain engineered to overexpress ErdS. Comparing data obtained for the different strains will highlight genes whose expression is affected by the presence, excess or absence of Erg-Asp. Hits will be ranked and confronted to databases to delineate the regulatory landscape of AS. RT-qPCR, Northern-blots and luciferase reporter system will be used for data validation. Alternatively, and only if relevant, global transcriptomic analysis will also be performed under growth conditions that were determined in the previous section.

IV.2. Do ASs participate in trafficking and signaling pathways

No obvious phenotypes affect *Afm ΔerdS* strain under standard growth conditions but some preliminary results, obtained by Dr. F. Fischer and Dr. N. Mahmoudi-Kaidi, showed an increased accumulation of autophagosomes in vacuoles which is typical of autophagy activation. This was surprising because, when using a nutriment rich media, autophagy is normally repressed (Klionsky *et al.,* 2016). This suggest that Erg-Asp might act as an autophagy repressor. As described

above, another 3-β-OH modified sterol, namely Erg-Glc regulates the onset of macroautophagy most likely through the recruitment of protein partners onto the nascent autophagosome. (Kikuma et al., 2017). Therefore, a potential crosstalk between glycosylated and aminoacylates sterols exist. Furthermore, depleting the media from the nitrogen source reduced Erg-Asp levels in *Afm wt* strain (not shown), indicative for a potential role of ASs as a signaling molecule for example by being aa level indicators (Klionsky *et al.*, 2016).

Finally, Atf2/Say1 pathway, responsible for sterol and steroid export in *Sce* (Tiwari *et al.*, 2007), was not described in *Aspergillus* spp. and no evidences were brought for the presence of an analogous detoxification pathway. Due to their similarities with the ErdS/ErdH pathway it will be interesting to consider the hypothesis that sterol aminoacylation could play analogous function to sterol acetylation. In a first attempt ASSs or AS hydrolase will be expressed in *Sce Δatf2* and *Δsay1* strains (available in the lab) to investigate if their reported phenotypes (e. g. susceptibility to eugenol) are complemented. *In vivo* synthesis of radiolabeled sterols will be performed as in (Tiwari *et al.*, 2007) and export of sterols will be assayed by analyzing radiolabeled species in the cell media after culture.

To investigate the participation of ASs to trafficking and signaling pathways we propose the following strategies in combination with tasks presented in **§ IV.1**.

IV.2.1. Determination of AS interacting partners

One additional task that will probably be determinant to unwind these hypotheses is the determination of Erg-Asp and Erg-Gly interacting partners. Resin-immobilized sterols were used previously in pull-down experiments (Nedelcu *et al.*, 2013) or for affinity purification of sterol-binding proteins (Satsangi and Mott 1992). As described in our published work and in the ErgS draft article, our collaborators from Pr. T. Kushiro's team that have strong expertise in sterol chemistry and synthesized a collection of AS ($_{syn}$AS) that already proved to be very useful for our work. In the next future we will try to obtain chromatographic supports conjugated to AS or unmodified sterol to perform pull-down experiments with crude extracts from *Afm* strains. The sterol backbone that will be used is still a matter of debate since Cho for example might be more suitable than Erg due to its higher stability (Chauhan *et al.*, 2020). ASs interactants will be identified by proteomic

analysis, hits will be ranked, and interactions validated through protein/lipid binding assays (Saliba *et al.,* 2015) and column affinity-binding assays with radiolabeled Ass (Darwiche and Schneiter 2017). Of note, the first known Erg-Asp interactant is ErdH that hydrolyses Erg-Asp (Yakobov *et al.,* 2020). However, the immobilized aminoacylated sterols should be non-hydrolysable.

IV.2.2. Determining Erg-Asp localization

A widely used marker of cholesterol (Bittman and Fischkoff 1972) and ergosterol (Van Leeuwen *et al.,* 2008) is filipin which binds to sterols in a 3-β-OH dependent manner and is therefore not suitable to stain esterified sterols (Maekawa 2017). An interesting strategy that will be considered to study AS trafficking in living cells is to develop **fluorophore labeled sterols** as previously proposed to study cellular dynamics of cholesterol (BODIPY-sterols) (Holtta-Vuori *et al.,* 2008) (Wustner *et al.,* 2016). However, care must be taken because addition of a fluorophore to a sterol can change its physiological behavior (e. g. distribution and dynamics) (Solanko *et al.,* 2013) and such dyes do not distinguish lipids from both membranous bilayers (Maekawa 2017). On another hand, sterol binding proteins/domain fused to fluorescent proteins were developed and one valuable advantage is that they can either be directly added to the media to label sterols at the cell surface, or expressed/microinjected into the cell, thereby labeling intracellular membrane-associated sterols (Maekawa 2017). For example, the D4 domain of Perfringolysin O fused to GFP or mCherry was used in several studies but unfortunately this fusion protein recognizes the hydroxyl group at the position 3 of cholesterol and might therefore not be suitable for esterified sterols (e. g. AS) (Sato *et al.,* 2013; Heuck *et al.,* 2007; Maekawa *et al.,* 2016). Therefore, we aim to develop our in-house fluorescent dye, specifically targeting Erg-Asp by fusing a catalytic null mutant of ErdH (e. g. ErdH S153A) to a fluorescent protein. As described for the D4-GFP, the fluorescent ErdH-GFP or ErdH-mCherry will have the advantage to specifically stain surface or intracellular sterols. Similarly, the discovery of a specific hydrolase targeting Erg-Gly (if it exists) would enable us to study the trafficking and the localization of both AS.

IV.3. Do AS participate in resistance to antifungal drugs?

Changes in sterol composition were widely shown to modulate the resistance to antifungal drugs. This was notably illustrated by the above-mentioned work of S. Bhattacharya and colleagues, but several other studies demonstrated that dysregulations of the Erg biosynthetic pathway leads either to resistance or to accurate sensibility to antifungal drugs (Young *et al.,* 2003; Sanglard *et al.,* 2003; Bhattacharya *et al.,* 2018). Being eukaryotes, fungal cells resemble strongly to its host cells and several physiological pathways were shown to be conserved between them, thereby complexifying the task of establishing fungal-specific targets. Erg has attracted much attention because it is essential, and its synthesis slightly differs from that of Cho in humans (Alcazar-Fuoli and Mellado 2012). Accordingly, Erg and its biosynthetic pathway are often considered as the target of choice for novel antifungal drugs and notably two out of the three main antifungal classes used to combat fungal infections (including invasive aspergillosis), target Erg or its biosynthetic pathway. Polyenes (e. g. AmB and nystatin) bind directly to Erg (**Figure CP-3**) and despite their mode of action is not completely established, it is accepted that they act by forming pores in the PM, leading to membrane permeabilization, inhibition of aerobic and anaerobic respiration, accumulation of reactive oxygen species (ROS) and leakage of small molecules (Gray *et al.,* 2012; Mesa-Arango *et al.,* 2014; Valiante *et al.,* 2015; Dhingra and Cramer 2017). Emergence of resistance mechanisms against AmB were reported in few cases, notably in *Candida* spp. harboring low ergosterol levels (Young *et al.,* 2003; Vandeputte *et al.,* 2008; Gray *et al.,* 2012) and the increased resistance observed in *A. terreus* was attributed to increased expression of catalases (Blum *et al.,* 2013). However, polyenes were also shown to interact with Cho and induce cytotoxicity in host cells (Perfect 2017). Importantly, the 3-β-hydroxyl of Erg is important for its interaction with AmB (Kaminski 2014) which is why Erg aminoacylation could interfere with tolerance to polyenes.

Azole derivates constitute the other main class of clinically used antifungal drugs that targets Erg11 (**Figure-CP3**) leading to depletion of ergosterol and accumulation of lanosterol and toxic 14-α-methylated sterols in the plasma membrane (Kelly *et al.,* 1997; Dhingra and Cramer 2017; Bhattacharya *et al.,* 2018). Unfortunately, resistance to azole derivates were reported to emerge through distinct mechanisms in several fungal species, including point mutations within

erg11 leading to reduced affinity to azoles (Parker *et al.,* 2014), overexpression of *erg11* either induced by tandem repeats in the 5'UTR (Verweij *et al.,* 2016) or by point mutations of transcription factors that bind to the 5'UTR CGAAT motif (Gsaller *et al.,* 2016; Dhingra and Cramer 2017). Other drugs exists, notably, Allylamines (inhibit the squalene epoxidase Erg1 (**Figure CP-3**)) (Krishnan-Natesan 2009) and Morpholines (targeting Erg2 and Erg24 (**Figure CP-3**)) are used as agricultural fungicides (White *et al.,* 1998)) but beside the Erg pathway additional fungal pathways/constituent were also used as target of antifungal drugs. For example, the synthesis of β-1,3-glucan, an essential component of the fungal cell-wall, is inhibited by echinocandins (Onishi *et al.,* 2000) and recent advances in the characterization of the fungal sphingolipid biosynthesis pathway revealed potential targets for the development of novel antifungal drugs (McEvoy *et al.,* 2020).

Due to the importance of Erg and Erg biosynthesis pathway and its strong relation with resistance mechanisms we questioned if ASS and AS could participate to the tolerance/resistance to antifungal drugs but also if they may be involved in cell-wall remodeling. To this end I performed antibiograms in 96 well-plates in the presence of AmB or fluconazole and I tested the viability of available *Afm* strains by using the colorimetric Alamar blue dye, as described elsewhere (Monteiro *et al.,* 2012). The results are very preliminary and may lead to erroneous conclusions and will therefore not be presented here. Nevertheless they suggest that *Afm* Δ*erdS* has increased tolerance to fluconazole and AmB and interestingly this tendency was supported by the fact that the *Afm* P$_{xyl}$-erdS strain (in which Erg-Asp accumulation is severely increased in the presence of xylose) had a marked increased susceptibility to antifungals when grown in xylose containing media but not in the absence of xylose. However, xylose induced *Afm* P$_{xyl}$-erdS strain also showed strongly reduced growth in the absence of antifungals, indicating that Erg-Asp influences developmental circuits rather than resistance.

In the future, we plan to perform several experiments by using **resazurin based viability tests** (Alamar blue) and **disk diffusion tests** to assay drug sensitivities of *Afm* strains that vary in their AS levels. The **analysis of transcriptional patterns** and the **determination of interacting partners** will certainly also provide important information regarding AS function. Interestingly global transcriptomic analyzes reported *erdS* regulation by calcineurin and decreased expression of *erdS* through exposition to AmB (Gautam *et al.,* 2008) and calcium (Soriani *et al.,* 2008). Given

the central role of calcium and its binding proteins (including calcineurin) in *Afm* cell's physiology this data further suggest that Erg-Asp might somehow interfere with pathways involved in drug tolerance/resistance (Hayes *et al.,* 2014; Latge and Chamilos 2019). Strikingly, transcriptome analysis revealed that *ergS* expression is strongly increased in the presence of azoles notably voriconazole (da Silva Ferreira *et al.,* 2006).

The cell wall of fungi is another important barrier for those organisms and its integrity is regulated by the central MAPK pathway (Valiante *et al.,* 2015). Therefore, it would be interesting to see whether AS pathway interfere with the regulation or the synthesis of the cell-wall. Note that preliminary data obtained by Dr. N. Mahmoudi-Kaidi suggest that *Afm ΔerdS* strain, in contrary to the WT, become sensitive to Congo Red, indicative of changes in the cell-wall composition, a phenotype reversed to WT by re-complementation with ErdS.

IV.4. Implication of ASs in virulence and pathogenesis

As briefly mentioned in the introduction to Erg (**§ III.3.**), Erg has recently been shown to be immunologically active. In response to pathogens, macrophages assemble the canonical inflammasome, which results in pyroptosis, a necrotic and proinflammatory programmed cell death induced by inflammatory caspases (Man *et al.,* 2017). The recent study of K. Koselny and colleagues evidenced that Erg itself induces pyropotosis of macrophages in an NLRP3-Casp1/11-dependent manner, and author proposed that cell-wall proteins interacting directly with Erg (mannoprotein Dan1 and manosyltransferases) might be involved in this process (Koselny *et al.,* 2018; Rodrigues 2018). During our **interactome experiments** (**§ IV.1.2** and **IV.2.1**) it will be therefore interesting to investigate ASSs and ASs interactions with proteins from the cell-wall and factors involved in the immune response.

IV.4.1. Evaluating the immune response of macrophages to ASs

The ability of ASs to elicit or to inhibit pyroptosis and the inflammatory response in immune cells will be monitored as in (Koselny *et al.,* 2018) by exposing macrophages to **liposomes containing free Erg, Erg-Asp or Erg-Gly**. **Evaluation of the immune response** will be done by **analyzing casp1/11-dependent macrophage lysis** (followed with the release of lactate

dehydrogenase) and by **quantifying the secretion of interleukins** (e. g. IL1-β and IL-6). If relevant, similar experiments will be performed by **exposing macrophages to conidia** from our different *Afm* strains. Moreover, our preliminary experiments indicate that Cho is aspartylated *in vitro* by ErdS in comparable amounts to Erg and it is tempting to speculate that this broader substrate specificity might also occur in vivo when cells uptake Cho from their environment. Interestingly, it is well known that Cho induce NLRP3-mediated pyroptosis (Ordovas-Montanes and Ordovas 2012) which is why the proposed experiments will also be done with Cho-Asp or Cho-Gly.

IV.4.2. Monitoring phagocytosis of conidia

Conidia from WT or recombinant *Afm* strains will be stained by FITC and their phagocytosis will be monitored by fluorescence, confocal and/or NANOLIVE microscopy in combination with flow cytometry quantification. Preliminary experiments were already done on mouse macrophages by Dr. N. Mahmoudi-Kaidi and the outcomes of future experiments will evidence if AS pathways are involved in immune escape.

IV.4.3. Testing virulence using insect and/or mouse models of infection

G. mellonella is an insect model of infection that has been validated as a good alternative to the mouse model to study some aspects of aspergillosis, including for clinical strains (Sheehan et al., 2018). Spores from WT and mutant Afm strains will be injected into *G. mellonella* larvae and the Lethal Doses (LD$_{90}$/LD$_{50}$) will be measured to quantify their virulence. Various strategies are planned to evaluate the response of the insect immunity, notably quantification of hematocytes and monitoring phagocytosis of fluorescent labeled conidia.

Materials & Methods

I. Biological materials

E. coli, *S. cerevisiae* (*Sce*) and other fungal strains used during my thesis are listed at the end of the Materials and Methods sections in **Table MM-1**.

II. Molecular biology for gene amplification and cloning

II.1. Bacteria growth media

XL1 or DH5α strains were grown in liquid LB-Miller medium (peptone 10 g/L, yeast extract 5g/L, NaCl 5 g/L) supplemented with ampicillin 100 mg/L (LB + Amp) or kanamycin 50 mg/L (LB + Kan). For growth on solid media, the same preparations were supplemented with 15 mg/L of Agar-agar.

II.2. Preparation of competent bacteria cells

A single colony is incubated O/N at 37°C in LB medium. The next morning cells are diluted to OD_{600} = 0.2 (250 mL) and grown at 18°C until OD600 reaches 0.6. All following steps must be performed at 4 °C on ice. The culture is transferred in a precooled centrifugation vial and placed on ice for 10 min. Cells are collected by centrifugation (2500 × *g*, 10 min at 4°C) and resuspended in 80 mL cold TBjap buffer (10 mM Na-PIPES, pH 6.7, 15 mM CaCl2 , 250 mM KCl, 55 mM MnCl2 , 2 % (v/v) DMSO (added just before use)). The suspension is kept on ice for 10 min. Cells are harvested by centrifugation (2500 × *g*, 10 min at 4°C) and resuspended in 20 mL TBjap buffer supplemented with 7 % (v/v) DMSO and incubated for another 10 min on ice. Competent cells are aliquoted in 100 μl fractions and immediately flash-frozen in liquid nitrogen and stored at -80 °C until use.

II.3. Transformation of competent bacteria cells

Competent bacteria cells are thawed on ice and appropriate amounts of intact plasmid DNA (around 1 ng) or ligation mixture are added to the cells. The tube is incubated on ice for 30 min, then a heat-shock is performed at 42 °C for 45 sec and the mixture is put back on ice for 2 min. For transformation of plasmids encoding the kanamycin resistance cassette it is recommended to

incubate the mixture with 500 µl of LB at 37 °C to allow the resistance protein to be expressed before adding the antibiotic. Finally, the mixture is spread out onto solid LB-medium supplemented with the appropriate antibiotic by using glass beads. Plates are incubated O/N at 37 °C.

II.4. Plasmid extraction from bacteria cells

II.4.1. Minipreparation of plasmid DNA

Cells from a single colony are incubated O/N at 37 °C in 3 mL LB supplemented with the appropriate antibiotic. Cells are harvested by centrifugation at $10000 \times g$ for 2 min and plasmid DNA is extracted with the EZ-10 Spin Column Plasmid DNA Miniprep kit (BIO BASIC) following supplier's instructions.

II.4.2. Maxipreparation of plasmid DNA

E. coli XL1 transformed with the plasmid of interest, is inoculated in 250 mL of LB supplemented with antibiotic at 37°C O/N. Bacteria are harvested by centrifugation ($4000 \times g$, 10 min at 4°C) and the pellet is resuspended in 5 mL of solution I (Glucose 50 mM, EDTA 10 mM, Tris-HCl pH8 25 mM). Cells are then lysed by adding 10 mL of freshly prepared lysis buffer (NaOH 0,2 N, SDS 1 % v / v) for 10 minutes at room temperature and neutralization of alkaline lysis is achieved through adding 7,5 mL of precooled neutralization buffer ($AcNH_4$ pH6,5 7,5 M) for 7 minutes on ice. Cell debris are removed by centrifugation ($4000 \times g$, 15 min at 4°C) and the supernatant (SN) is transferred in another clean tube. 0.6 volumes of isopropanol are added to the SN and incubated for 10 minutes at RT. Upon centrifugation ($4000 \times g$, 15 minutes, RT), the pellet is washed with 1 mL EtOH 70 %, air dried and resuspended in 500 µl of TE (Tris-HCl pH 8 25 mM, EDTA 10 mM). RNA contaminations are removed by adding 1 µL of DNase-free RNase A (10 mg/mL stock solution) for 30 min at RT (in the meantime, the remaining debris are removed by centrifugation ($13000 \times g$, 5 minutes, RT)). Then, DNA is precipitated by addition of 500 µl of a solution containing NaCl 1.6 M and PEG_{6000} 17.5 %. The tube is immediately vortexed and centrifugated at $13000 \times g$, for 5 min at 4°C. Finally, the pellet is resuspended in 400 µl TE buffer. To remove any protein contaminations, the DNA sample is extracted once with phenol, twice with phenol/chloroform (1/1 v/v) and once with chloroform. Nucleic acids within the resulting aqueous phase are precipitated with 250 mM

NaCl and 2.5 volumes of ice-cold ethanol 100 %, either at -20°C O/N or at -80°C for 30 min. Finally, nucleic acids are recovered by centrifugation (13000 × g, 15 min, 4°C), washed with ethanol 70 %, driedand either stored at -20°C or resuspended in an adequate volume of TE buffer.

This purification yields high amounts of protein- and RNA-free plasmid DNA's, required for example for *in vitro* transcription by T7 RNA polymerase or for filamentous fungi transformations.

II.5.   Amplification of DNA fragments by polymerase chain reaction (PCR)

DNA fragments were amplified by PCR using primer pairs designed according to the cloning strategy. I used mainly the PrimeSTAR Max® kit (Takara, R045B) but in some cases were amplification failed I changed to SapphireAmp® Fast PCR Master Mix (Takara, RR350B). PCR amplification are performed with a thermocycler (C1000 Touch™ Thermal Cycler from Bio-Rad) and protocols are described in tables from **Figure MM-1**. Primers and templates are listed in **Table MM-2** at the end of the Materials and Methods sections.

II.6.   Enzymatic restriction

I used FastDigest restriction enzymes purchased from Thermo Scientific. Around 1 µg of plasmid DNA was digested in the presence of 0.5 µl of each restriction enzyme in a final volume of 20 µl. Depending on the restriction enzyme and the supplier's indications, digestions were incubated at the recommended temperature for 30-40 min.

II.7.   Analysis of DNA fragments by agarose gel electrophoresis

1 % (w/v) agarose was dissolved in TAE buffer (Tris-base 40 mM, acetic acid 20 mM, EDTA 5 mM) by heating in a microwave and gels were casted in an appropriate support. DNA fragments resulting from PCR amplification or from enzymatic restriction are supplemented with 1x loading buffer (Thermofisher, R0611) when needed loaded on the gel, and submitted to electrophoresis at 110 V for 20-30 min. The developed gel is placed in a BET bath (0.5µg/mL) for 15-20 min, washed with water and DNA bands are visualized under UV light with an imaging system (Syngene, G:BOX Chemi XT).

A

PCR mix composition	
Enzyme (kit)	PrimeStar Max / SapphireAmp
Fwd primer (µM)	0.5
Rv primer (µM)	0.5
Template DNA (ng)	plasmid DNA: 0.5-1 gDNA: 50-200
Enzyme Mix (µl)	10
H2O qsp 20 µl	up to 20 µl

B

Cycling protocol		
	Temperature (°C)	Time
Initial denaturation	98	2 min
Denaturation	98	10 sec
Annealing	55-65 depending on primer's Tm	10 sec
Elongation	72 °C	PrimeStar Max 5 sec/kb[*] SapphireAmp : 10 sec/kb[*]
Final extension	72 °C	2 min

30 cycles

Figure MM-1: PCR mix composition (A) and thermocycling protocol (B). [*] elongation time per kb doubled when the template to amplify exceeds 4 kbs.

II.8.   Cloning strategies

The *Afm* ORF's encoding ErdS (*AFUA_1g02570*) and ErgS (*AFUA_8g01260*) were synthetized with codon optimized sequences for expression in *Sce*, flanked by attB1 and attB2 sequences and cloned into pUC57 (Genscript®). All other ORF's described in the present manuscript, including ErdH from *Afm* (*AFUA_1g02580*) and ErgS from *Yli* CLIB 99 (ORF identical to YALI0_E00330g from CLIB122 strain) and from *Bba* 80.2, were recovered from the corresponding genomic DNA by PCR. Depending on the type of cloning and the material available in the laboratory I used two different cloning strategies to design yeast and bacteria expression plasmids as well as recombination cassettes for *Afm*: The Gataway strategy (Busso *et al.,* 2005) and the isothermal Gibson assembly method (Gibson *et al.,* 2009; Gibson 2011). Constructs, PCR templates and primers are listed and described in **Table MM-2** found at the end of the Materials & Methods sections.

II.8.1. Gateway™ cloning

A gene of interest (GOI) is amplified by PCR using primers flanked by attB1 (forward; fwd) and attB2 (reverse; rv) sites. The PCR product is cloned into pJET1.2 blunt plasmid using the CloneJETPCR Cloning Kit (Thermo Scientific) following supplier's instructions. 1 µg of the resulting pJET1.2-GOI is linearized in a 20 µl reaction assay and the restriction enzyme is heat-inactivated. 5 µl of this mixture are added to 150 ng of pDONR221 "donor vector" for the BP recombination with the Gateway™ BP Clonase™ II Enzyme mix (Thermo Scientific). After O/N incubation at 25 °C, 5 µL of the recombination mix are transformed into competent bacterial DH5α cells (using LB+Kan plates). The resulting "entry plasmid", obtained through non-homologous recombination between aatB sequences of the linearized plasmid (harboring the GOI) and attP sequences found in the donor vector, is used to shuttle the GOI into several destination vectors (pDEST) through LR recombination reaction without any additional cloning steps (**Figure MM-2**). For the LR recombination, 150 ng of each plasmid (pDONR221-GOI and destination vector) are mixed in 10 µL of LR recombinase buffer with the Gateway™ LR Clonase™ Enzyme mix (Thermo Scientific). After 2 h of incubation at 25 °C, 2 µL of the LR recombination mix is used to transform competent bacterial cells. Positive clones are selected onLB agar plates supplemented with ampicillin (100 mg/L). This strategy is particularly
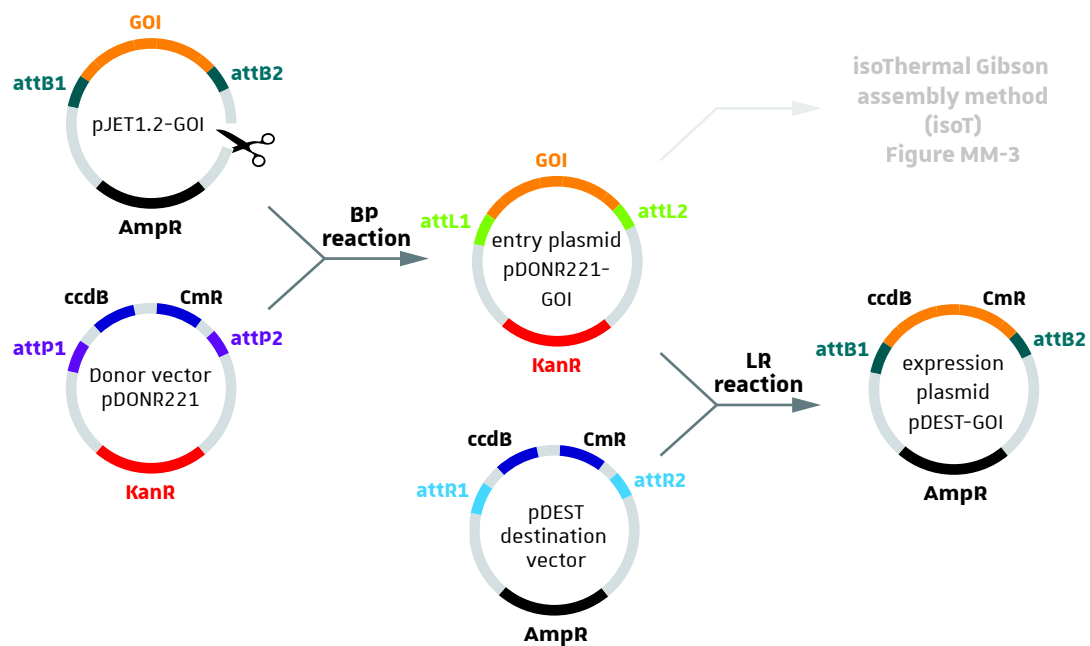
Figure MM-2: Schematic representation of the Gateway cloning strategy. GOI flanked by attB1/B2 sites is cloned into pJET1.2 and the resulting plasmid is linearized. During BP reaction, attB1/B2 sites recombine with attP1/P2 sites from the donor vector, thereby generating the entry plasmid in which the GOI is flanked by attL1/L2 sites. Non-homologous recombination of those sites with attR1/R2 found in Gateway destination vectors generates attB1/B2 sites.

convenient when starting the characterization of a new protein, since it provides rapidly a collection of expression plasmids encoding native, recombinant, or tagged versions of this protein.

II.8.2. Isothermal Gibson assembly (isoT) method

The principle of the isoT cloning method consist of assembling DNA fragments through complementary base pairing. As illustrated in **Figure MM-3A**, the gene of interest (GOI) is amplified from genomic or plasmid DNA with primers that contain overlapping sequences of the destination plasmid. The latter was in most cases amplified by PCR, but it can also be obtained by restriction enzymes. Importantly, overlapping regions at 5' and 3' extremities of the amplified GOI and of the linearized plasmid are at least 25 bp long. Assembling of DNA fragments is as described (**Figure MM-3B**).

Experimentally, a 5x concentrated isoT buffer is prepared, diluted, and supplemented with the 3 enzymes described in figure MM-3B to obtain an isoT reaction mix 2x (preparation detailed in **Figure MM-4A and B**) (Gibson 2011). The latter is aliquoted in 11 µl fractions that can be stored at -20 °C or -80 °C until use. Equimolar amounts of DNA fragments to be assembled are added to a 11 µl aliquot of isoT reaction mix 2x in a final volume of 20 µl and tubes are placed at 50 °C for 25 min (**Figure MM-4C**). The 1x isoT reaction mix is composed of Tris-HCl pH 7.5 100 mM, $MgCl_2$ 10 mM, DTT 10 mM, NAD^+ 1mM, 0.2 mM of each dNTP, PEG_{8000} 5 % (w/v), T5 exonuclease 7.5 U/mL, Phusion DNA polymerase 25 U/mL and Taq DNA ligase 4000 U/mL. When fragments were amplified with similar efficiencies, 1 µl of each PCR product was simply added to the isoT reaction assay without performing any DNA cleaning up steps. Amounts of added DNA fragments were adapted in cases were PCR efficiencies differed importantly, according to the intensities of DNA bands visually analyzed on agarose gels. However, the amount of each DNA fragment should be comprised between 10 and 100 ng. DNA templates used for amplification should be specifically degraded, either through Dpn I (Thermo Scientific, FD1703) treatment of PCR products prior to the isoT reaction or by performing the DpnI digestion on the final isoT reaction. Finally, Dpn I is inactivated at 90 °C for 20 min and 5 µl of the mixture are transformed into competent bacteria cells (**Figure MM-4C**). Additional DNA cleaning steps are optional.
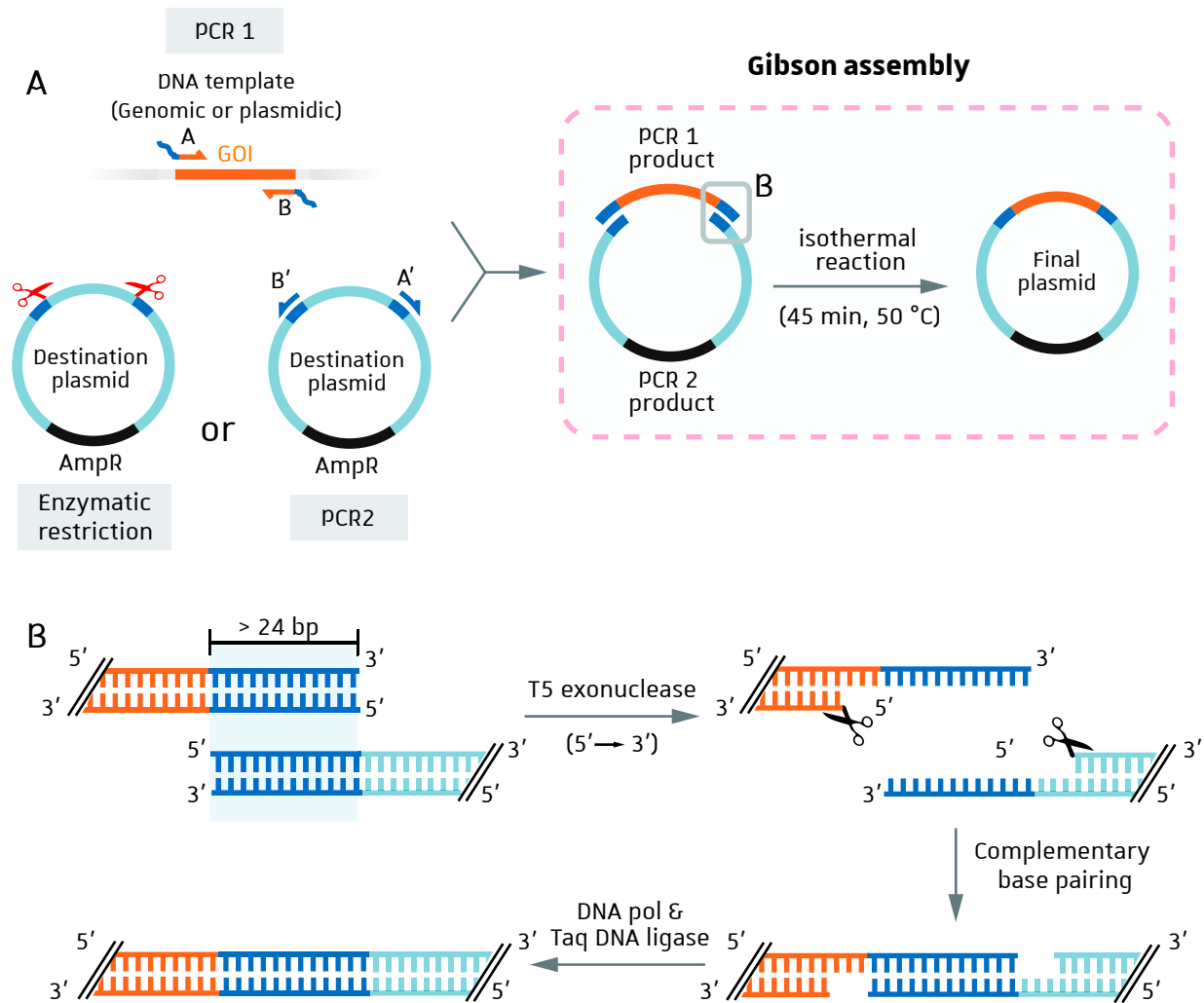
Figure MM-3: Overview of assembling DNA fragments by the isoT cloning method. (A) The gene of interest (GOI) is amplified with primers A and B that contain isoT overhangs (dark blue) and yields a linear DNA fragment flanked by homologous extremities present in the destination plasmid. The destination plasmid is amplified with primers A' and B' or cleaved by restriction enzymes, so that 5' and 3' extremities of the linearized plasmid overlap with the 3' and 5' extremities of the amplified GOI, respectively. The extremities of both linearized fragments are assembled by the isothermal Gibson assembly method (isoT), detailed in B, and results in a final plasmid in which the GOI is cloned. **(B)** The 3' and 5' extremities of the linearized GOI and the destination plasmid, respectively, are colored in dark blue and the homologous overlap is indicated by the transparent blue rectangle. The "chaw-back" step is achieved during the first step of isoT assembly by the T5 exonuclease which releases 3' single stranded extremities, thereby enabling complementary base-pairing. The remaining gaps are filled in and sealed through the combined activities of a thermostable DNA pol and the Taq DNA ligase. All these steps are combined in a single assay that leads to the fact that the isoT assembly can be considered as a one-step reaction performed at 50°C for 25 min.

A

5x isoT buffer (6 ml)

Component	amount	concentration	supplier
Tris-HCl pH 7,5 1M	3 mL	0,5 M	
$MgCl_2$ 2 M	150 µl	50 mM	
dNTP 100 mM each	60 µl	1 mM	Promega, U1515
DTT 1 M	300 µl	50 mM	
NAD^+ (663.43 g/mol)	20 mg	5 mM	Sigma-Aldrich N1511
PEG_{8000}	1.5 g	25 % (w/v)	Euromedex PB0433
H_2O qsp 6 mL			

The resulting 5x isoT buffer is mixed until all components are completely dissolved. Aliquots of 320 µl (around 18 tubes) are prepared and can be stored at -20 °C or -80 °C for at least 1 year.

B

isoT reaction mix 2x

Component	volume (µl)	concentration	supplier
5x isoT buffer	320		
T5 exonuclease (10 U/µL)	1.2	15 U/ml	NEB, M0363S
Phusion DNA pol (2 U/µl)	20	50 U/ml	Finnzymes, F-530S
Taq DNA ligase (40 U/µl)	160	8000 U/ml	NEB, M0208S
H_2O qsp 800 µl	300		

The resulting 2x isoT reaction mix is mixed and aliquots of 10 µl (around 80 tubes) are stored at -20 °C or -80 °C until use.

C

isoT reaction assay

isoT reaction mix 2x	11 µl	
PCR products	1 µl/fragment*	10 to 100 ng max
plasmid	1 µl/plasmid*	10 to 100 ng max
H_2O qsp 20 µl		

* volumes can be increased up to 10 µl but the reaction volume must not exceed 20 µl.

Incubation at 50 °C for 45 min

If all fragments to be assembled result from PCR amplification: DNA template(s) degradation by Dpn I treatment at 37 °C for 1 h.
Alternatively Dpn I treatment is performed on PCR product prior to the isoT reaction.

Heat-inactivation of Dpn I (90 °C for 20 min)

5 µl are used for plasmid transformation into competent bacteria cells

Figure MM-4: Procedure of the isothermal Gibson assembly (isoT) method: (A) Composition of the 5x concentrated isoT buffer used for the preparation of the 2x concentrated isoT reaction mix described in **(B)**. **(C)** Step by step description of the isoT cloning assay. DNA cleaning up steps are optional and can be performed on the PCR products and/or the linearized plasmid prior isoT cloning assay or on the assembled product before to transformation in *E. coli*. For more details see {Gibson, 2011 #604}{Gibson, 2009 #603} and https://wiki.med.harvard.edu/SysBio/Megason/MakingIsothermalAssemblyAliquots.

II.8.3. Site directed mutagenesis

The procedure used for site directed mutagenesis can be considered as a direct application of the above described isoT cloning strategy and was previously described to mutate several residues within a sequence through a single cloning step (Mitchell *et al.,* 2013). The principle of the method that I used is to amplify the entire plasmid in 2 (or more) linear DNA fragments by performing separate PCR reactions. As illustrated in **Figure MM-5**, PCR 1 and PCR 2 are performed with primer pairs A (fwd)/B (rv) and B′ (fwd)/A′ (rv), respectively where primers A and A′ on one hand and primers B and B′ on the other hand share at least 25 nt overlapping sequences that are complementary with respect to WC base pairing. Primers A (fwd from PCR 1) and A′ (rv from PCR 2) anneal into the GOI to be mutated and encode reverse complementary primers with base substitution(s). Primers A and A′ were designed so that the mutated nt(s) is at least 17 nts (generally 19) upstream to the last nt in 3′ and the 5′ sequence preceding the mutation is generally 11-13 nts. B (rv) and B′ (fwd) encode reverse complementary primers too and can be used to incorporate mutation at another region of the plasmid. However, during my thesis, I used primers B and B′ (FF060/FF061) that anneal into the gene encoding the Amp resistance protein (*ampR*) without any base substitutions. In this way, the amplified PCR 1 product contains the 5′-sequence of the GOI and the 3′-sequence of *ampR* while PCR 2 product contains the 5′-sequence *ampR* and the 3′-sequence of the GOI. Moreover, both linear DNA's share homologous extremities which enable the assembly of both truncated genes through the isoT assembly method and thus the reconstitution of a full-length *ampR*, encoding for the corresponding resistance activity, and a full-length GOI, nevertheless containing the incorporated mutation(s). This strategy achieving simultaneous reconstitutions of the resistance gene and of the GOI might strongly favorize the selection of positive clones on selective media. Finally, degrading the common PCR template with Dpn I treatment (before or after isoT reaction) is even more crucial during mutagenesis to avoid transformation of non-mutated plasmid which are mostly non distinguishable from the mutated version by enzymatic restriction. Using this strategy for mutagenesis yields almost 100 % positive clones which is why I generally tested only 3 clones of which at least 2 were always positives.
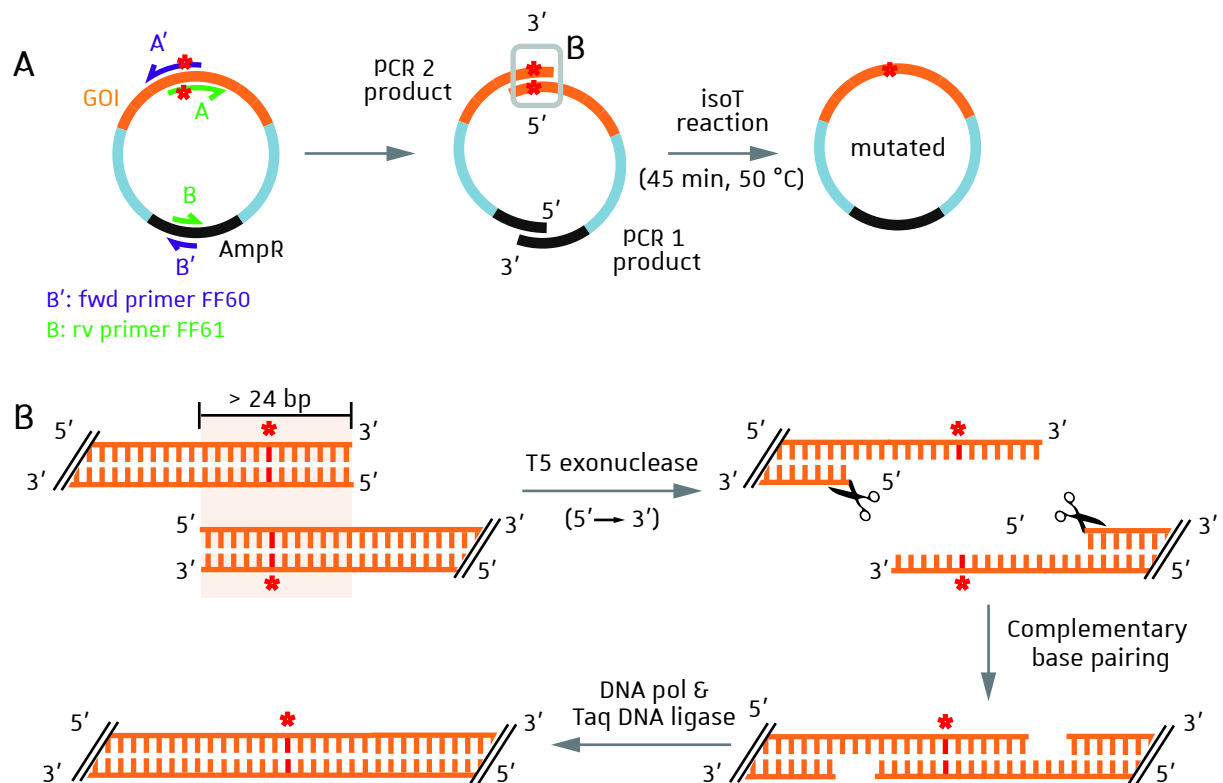
Figure MM-5: Overview of site directed mutagenesis by the isoT assembly method. (A) Primers A (fwd) and A' (rv) anneal in the GOI sequence (orange) and contain base substitution(s) (✱) similarly as for QuickChange primers described elsewhere {Liu, 2008 #606}. Primers B' (fwd; FF060) and B (rv; FF060) are fully complementary and anneal into ampR (black). Inverse partnering of primers A/B and A'/B' during PCR splits the GOI and the AmpR gene and results in the amplification of PCR 1 and PCR 2 products that share homologous extremities (overlapping lines in the middle panel). Base substitutions are incorporated in the homologous 5' and 3' extremities of PCR 1 and PCR 2 products, respectively. The isoT reaction (isoT), detailed in (B) assembles homologous extremities of both PCR products and yields the final plasmid harboring the inserted mutation. **(B)** Depiction of the assembly occurring during the isoT reaction between 5' and 3' homologous extremities (light orange box) of PCR 1 and PCR 2, respectively. For more details see the text and Figure MM-3.

II.8.4. Construction of deletion and complementation cassettes for *Afm*

Procedures used to construct *erdS* and *ergS* replacement cassettes for *Afm* are detailed in the published article (Yakobov *et al.*, 2020) and the article in preparation, and the aim of this section is to briefly describe the cloning strategies that I used.

II.8.4.1. Description of self-excising cassettes suitable for gene deletion and re-complementation by homologous recombination

To delete genes from *Afm* we constructed recombination cassettes that contain a resistance cassette flanked by 1kb upstream and downstream sequences of the ORF to be deleted. The flanking sequences are termed here 5' and 3' UTR's (untranslated regions) even if they overlap on adjacent ORF's. The herein used resistance cassette, contains a selection marker (in the present case *hygR* gene under the control of gpdA promoter confers resistance to hygromycin B) but in addition it also comprises a β-rec/six-site specific recombination system (**Figure MM-6A**). The β-rec gene is under the control of a xylose inducible promoter (Pxyl) and is followed by the trpC transcriptional terminator from *A. nidulans*. Finally, the whole resistance cassette is flanked by six-sites (required for self-excision of the cassette) as depicted in **Figure MM-6A**. The complete deletion cassette (resistance cassette flanked by 1 kb UTR's) is transformed in *Afm*, as described in the accompanying paper (Yakobov *et al.*, 2020) and recombines the targeted locus through homologous recombination. Once the deletant is selected on the selective media, the corresponding colony can be shifted onto hygromycin-free media in the presence of xylose to induce the six-site specific recombination, achieved by the overexpressed β-rec. In this way the self-excised resistance cassette described here is recyclable and can be used for tandem deletions within the same strain. The suitability of this ingenious self-excising cassette was described elsewhere (Hartmann *et al.*, 2010) and the resistance cassette was obtained from pSK529 plasmid (gift from J-P Latgé) through PCR. To construct complementation cassettes, the same strategy is used but the b-rec gene is replaced by the GOI ORF. Consequently, when transformed and recombined at the corresponding locus (deleted or not), GOI overexpression is inducible in media containing xylose but the complementation cassette is no more excisable.
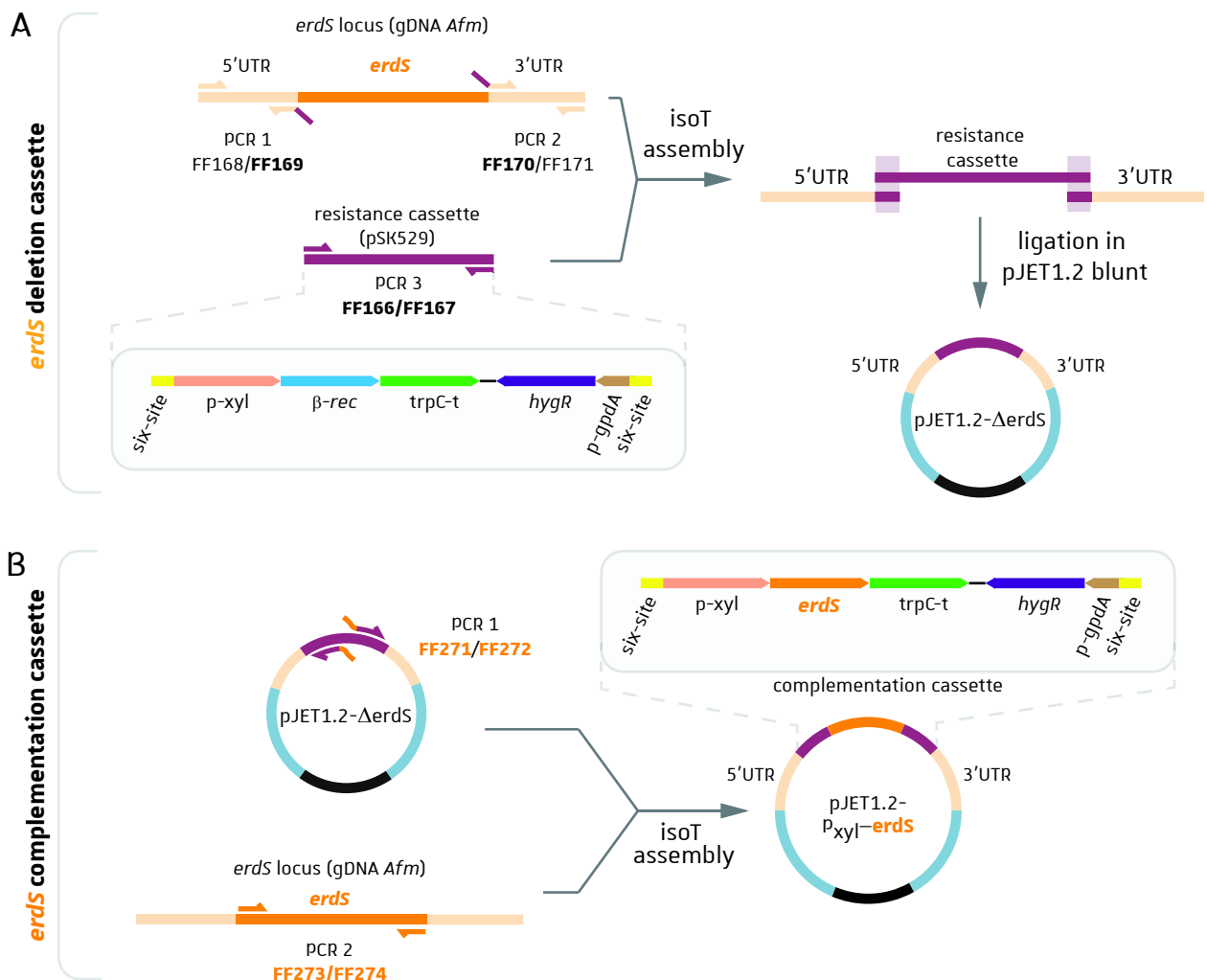
Figure MM-6: Overview of isoT cloning strategies used to construct *erdS* replacement cassettes for *Afm*. (A) To construct the *erdS* deletion cassette, 5' and 3' UTR's (light orange) were amplified by PCR with primer pairs FF168/FF169 and FF170/FF171, respectively. FF169 and FF170 contain overhangs designed so that the amplified 5' and 3' UTR's contain 3' or 5' tags homologous to the 5' or 3' extremities of the resistance cassette (grape), respectively. The later is amplified with primer pair FF166/FF167 and the three linear DNA fragments are assembled by the isoT reaction. The resulting *erdS* deletion cassette is finally ligated into pJET1.2 plasmid. The organization of the resistance cassette is depicted in the grey box and contains the β-rec/six-site recombination system and the hygR gene which confers hygromycin resistance. Homologous sequences at the extremity of linear DNA's that assemble are indicated by the light grape squares. **(B)** The PJET1.2-ΔerdS deletion cassette described in (A) and the *erdS* ORF were reverse amplified with the indicated primer pairs and assembled by isoT to obtain the pJET1.2-Pxyl-erdS plasmid. The core of the complementation cassette (whithout flanking UTR's) is depicted in the gray box and shows the presence of *erdS* ORF replacing β-rec. Primers are colored according to the DNA sequence to which they are complementary. trpC-t, trpC transcriptional terminator; p-gpdA, gpdA promoter.

II.8.4.2.   *erdS* deletion and complementation cassettes

1 kb of the erdS 5'UTR (primers FF168/FF169) and of the 3'UTR (primers FF170/FF171) were amplified with isoT overhangs at their 3' and 5' extremity, respectively. The sequence corresponding to these overhangs are homologous to the 5' and 3' extremities of the resistance cassette, amplified from pSK529 plasmid with primers FF166/FF167. The three amplified sequences were assembled by the isoT cloning method, then PCR templates were degraded by Dpn I treatment and the resulting *erdS* deletion cassette was ligated into pJET 1.2 using the CloneJETPCR Cloning Kit (Thermo Scientific) following supplier's instructions (**Figure MM-6A**). To construct the complementation cassette, the plasmid containing the obtained pJET1.2-ΔerdS was reverse amplified (FF271/FF272) and the *β-rec* was replaced by the *erdS* ORF (amplified from *Afm* gDNA with primers FF273/FF274) through isoT (**Figure MM-6B**).

II.8.4.3.   *ergS* deletion and complementation cassettes

The *ergS* deletion cassette was also cloned by isoT but the strategy differs slightly. In this case the 5'UTR (primers fD-5'UTR-fwd/rv) and the 3'UTR (primers fD-3'UTR-fwd/rv) 1 kb sequences were amplified with isoT overhangs at their 3' and 5' extremity, respectively, and both products were separately ligated into pJET 1.2 plasmids. Clones where the 5'UTR and the 3'UTR were ligated in the same orientation were selected for the next cloning step. Sequences from both plasmid containing their respective UTR's and a truncated part of *ampR* were amplified with isoT overhangs homologous to the amplified resistance cassette and the three sequences were assembled by isoT (**Figure MM-7A**). To construct the complementation cassette, the pJET1.2-DergS plasmid was amplified with primers NY041/FF061 or with NY040/FF060 and both PCR products were assembled through isoT with the ergS ORF amplified with NY042/NY043. The resulting complementation cassettes contains the *ergS* ORF in place of the *β-rec*, in comparison to the deletion cassette (**Figure MM-7B**).
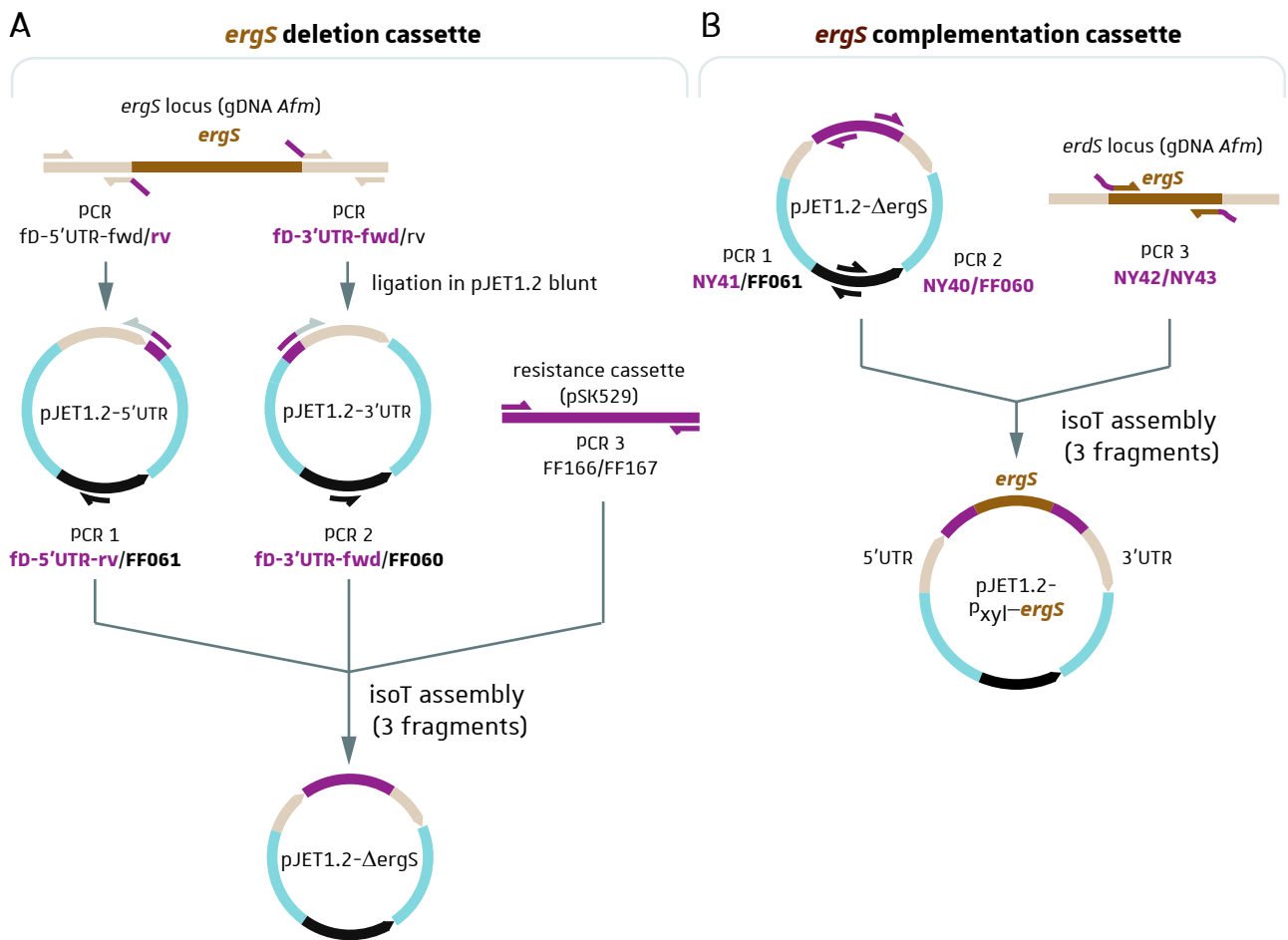
Figure MM-7: Construction of *ergS* recombination cassettes for *Afm*. (A) To construct the ΔergS deletion cassette, 5' and 3'UTR's were amplified from *Afm* gDNA and ligated into separate pJET1.2 plasmids. Plasmids containing the 5'UTR or the 3'UTR in the same direction were reverse amplified and the resistance cassette was amplified from pSK529 plasmid. The 3 PCR products were assembled in a single isoT reaction to obtain pJET1.2-ΔergS. **(B)** The *ergS* complementation cassette was obtained similarly as for the *erdS* complementation cassette, described in the previous figure, but in the present case pJET1.2-ΔergS was reverse amplified in two separate DNA fragments. Both resulting fragments and the ergS ORF, which was amplified from *Afm* gDNA with isoT overhangs-containing primers, were assembled by isoT. The nomenclature is the same as in Figure MM-6.

III. Procedures used for *Sce* cells

III.1. *Sce* growth media

Sce can be grown in either in liquid media or on solid agar-agar plates. The composition of the growth medium depends on the experiment and on the genetic background of the *Sce* strain. Depending on their composition, two types of media are used for yeast cells growth: rich media such as YPD (Yeast Extract-Peptone-Dextrose) or minimal media such as SC (Synthetic Complete). YPD (**Table MM-3**) contains all aa and nucleotides (nt) and is therefore not suitable for auxotrophic selection. SC contains also all aa and nt but auxotrophic selection can be performed by preparing SC lacking specific aa or nt. In this way, non-transformed *Sce* strains that has autotrophies were grown in YPD or SC media. In contrast, *Sce* strains transformed with plasmids encoding the *LEU2* (p415- plasmids) or the *TRP1* (p414- plasmids) marker were selected and grown on SC-Leu (SC medium lacking Leu) and SC-Trp (SC medium lacking Trp), respectively. Accordingly, strains that are co-transformed with two plasmids, one encoding the *LEU2* marker and the other encoding the *TRP1* marker were selected on SC lacking Trp and Leu (SC-Leu-Trp). Finally, the 5-fluoroorotic acid (5-FOA) containing media is used for plasmid shuffling experiments, assayed on *Sce* YAL3 *Δdps1* strains (Ador *et al.,* 1999) that were transformed with various ErdS variants, as detailed in our published work (Yakobov *et al.,* 2020). Media compositions are described in **Tables MM-3 and MM-4**.

III.2. *Sce* transformation

The lithium-based transformation procedure was adapted from (Gietz and Woods 2002). For this procedure, all steps must be performed in a sterile environment and all buffers are sterile. Cells to be transformed are grown until the stationary phase is reached, then cells are collected by centrifugation at 5000 × *g* for 5 min at 4°C and washed twice with sterile water. The pellet is resuspended in an appropriate volume so that 50 µl contain 3 OD_{600} equivalent units. For each transformation 50 µl are transferred in a sterile tube, and 10 µl of boiled (95 °C) and sonicated single-stranded DNA (10 mg/mL) is added to cells. Tubes are vigorously mixed (vortex), then 1-2 µg of plasmid DNA and 350 µl of transformation mix (240 µL of PEG 4000, 36 µL LiAc 1M, 70 µL water) are added. Then the tubes are mixed again by vortex mixing and finally incubated at 42°C

	Components	Concentration	Comments
YPD	Peptone	2 % (w/v)	Source of nitrogen, carbon, minerals and vitamins
	Yeast extract	1 % (w/v)	Supplies vitamin-B complex
	Dextrose (D-glucose)	2 % (w/v)	Fermentable carbon source
	Agar-Agar (for solid media)	2 % (w/v)	

Table MM-3: Composition of YPD rich medium

	Components	Concentration	Comments
Common components for SC derived media	Yeast Nitrogen Base (YNB) with ammonium sulfate	6.7 g/L	Source of nitrogen, salts, trace elements and vitamins
	Dextrose (D-glucose)	2 % (w/v)	Fermentable carbon source
	Agar-Agar (for solid media)	2 % (w/v)	
+ Components specific to each media			
SC	Complete Supplement Mixture (CSM)	0.79 g/L	Supplies adenine, uracil and all aa
SC-Leu	CSM minus Leu	0.69 g/L	Supplies adenine, uracil and all aa except Leu
SC-Trp	CSM minus Trp	0.74 g/L	Supplies adenine, uracil and all aa except Trp
SC-Leu-Trp	CSM minus Leu & Trp	0.64 g/L	Supplies adenine, uracil and all aa except Leu and Trp
SC+5-FOA	5-Fluoroorotic Acid	2.5 mM	Used to select the loss of vectors carrying the URA3 marker

Table MM-4: Composition of SC derived media

for 45 min in a water bath. Cells are centrifuged at 10000× g for 30 sec, the supernatant is removed and traces of LiAc and PEG4000 are washed away with 1 mL of water. Cells are resuspended in 150 µl water and spread onto the appropriate selective plates and incubated at 30 °C for 2-3 days. Finally, transformants from single colonies are transferred onto fresh solid media and incubated again for 2-3 days.

III.3. Drop tests on *Sce* cells

Appropriate liquid medium is inoculated with *Sce* cells O/N at 30 °C. The next morning the OD_{600} is measured (spectrophotometer DU® 730, Beckman Coulter), then the pre-culture is diluted to OD_{600} = 0.1 in fresh media and cells are grown at 30 °C until OD_{600} reaches 0.5-0.6. Cells are centrifuged, washed with water, and adjusted to OD_{600} = 0.5. Ten-fold serial dilution are prepared in water (10^1-10^5) and 7 µl of each dilution is spotted on solid medium. Plates are incubated at 25 °C, 30 °C or 37 °C for several days and photographed each day.

III.4. Preparation of *Sce* crude extracts (EB) for total protein analysis

Pre-cultures from *Sce* are performed in the appropriate media and cells are diluted the next morning to OD600 = 0.1. The culture is grown until OD_{600} reaches 1.0 and 1-1.5 unit of cells is collected in a fresh tube and centrifuged at 13000 × g for 1 min. Alkaline cell lysis is performed by resuspending the pellet in 500 µl of ice cold NaOH 0.185 M and tubes are incubated on ice for 10 min. Total proteins are then precipitated by adding Trichloroacetic acid (TCA) to a final concentration of 10 % and cells are incubated for another 10 min on ice. Finally, tubes are centrifuged at 13000 × g for 10 min at 4 °C, the supernatant is removed properly and the resulting EB is resuspended in 100 µl of 1 × Laemmli buffer (125 mM Tris-HCl pH 6.8, 2 % (w/v) SDS, 10 % (w/v) glycerol, 2 % (v/v) β-mercaptoethanol, 0.0125 % (p/v) bromophenol blue). By doing so, the coloration of the sample might turn to orange, due to remaining TCA traces. In these cases, 3-5 µl of Tris base 1 M are added to re-equilibrate the pH. 10 µl of this preparation are loaded on polyacrylamide gel for SDS-PAGE analysis and subsequent immunoblots.

III.5.   Soluble protein extract (S100)

Cells were grown in 500 mL YPD on a rotary shaker at 30 °C and harvested when OD600 = 1 by centrifugation at 5000 × g for 5 min at 4 °C. The pellet was resuspended in 5 mL of lysis buffer containing 50 mM Na-HEPES pH 7, 30 mM KCl (or 140 mM NaCl), 10 % glycerol, 0.1 mM EDTA, 1 % (w/v) Triton X100, 0.3 % (w/v) NP40, 5mM β-mercaptoethanol and protease inhibitors tablet (Roche). 1 volume of glass beads (Ø 0.25-0.5 mm, Roth) was added and cell lysis was performed with a FastPrep®-24 apparatus (6 × 1 min at 6.5 m/s, with 1 min on ice between each cycle). Cells debris were removed by centrifugation at 500 × g for 10 min at 4 °C and the supernatant is centrifuged at 100000 × g for 1 h. The resulting soluble fraction (S100) is recovered, then dialyzed O/N against the storage buffer (50 mM Na-HEPES pH 7, 30 mM KCl (or 140 mM NaCl), 50 % glycerol, 0.1 mM EDTA) and kept at − 20 °C.

III.6.   Sub-cellular fractionation

Cells are inoculated O/N in the appropriate medium on a rotary shaker at 30 °C and the obtained pre-culture is diluted to OD_{600} = 0.1. The culture is incubated at 30 °C under rotation until OD_{600} reaches 1 and 20 OD_{600} equivalent units of cells are harvested by centrifugation at 5000 × g for 5 min at 4 °C. The following steps must all be done at 4 °C. Cells are washed twice with ice cold 1 × PBS (Phosphate-Buffered Saline) supplemented with 0.2 M sorbitol. The pellet is resuspended in 800 µl lysis buffer (1 × PBS, 0.2 M sorbitol, protease inhibitors tablet (Roche)), 1 volume of beads (Ø 0.25-0.5 mm, Roth) are added and cells are broken with a FastPrep®-24 apparatus (6 × 30 sec at 6.5 m/s, with 1 min on ice between each cycle). Cell debris are removed by centrifugation at 300 × g for 5 min at 4 °C, and the supernatant subjected to another centrifugation at 13000 × g for 15 min at 4°C. The resulting P13 pellet is resuspended in an equal volume of lysis buffer whereas the S13 supernatant is further fractionated by ultracentrifugation at 100000 × g for 1 h at 4°C. The soluble fraction is transferred in a fresh tube and the P100 is resuspended in an equal volume. For protein analysis, aliquots of obtained P13, P100 and S100 fractions are supplemented with 1 × Laemmli buffer and 10 µl are analyzed by SDS-PAGE and eventually subsequent immunoblots.

IV. Procedures used for *Afm*

As explained in the introduction to my topic, I focused my thesis work on the characterization of fungal proteins by using mainly the yeast *Sce* as a model while experiments on filamentous fungi were performed in almost all cases by Dr. Nassira Mahmoudi-Kaidi or by Dr. Frédéric Fischer. Most of those procedures are detailed in our published article (Yakobov *et al.*, 2020) but during my thesis I used and adapted few of them as described in the coming sections.

IV.1.   Routine growth conditions

Afm strains were grown in defined MMG media composed of 1 % (w/v) glucose, 0.92 g/L ammonium tartrate dibasic, salts (10 mL of a 50 × solution containing KCl 26 g/L, $MgSO_4.7H_2O$ 26 g/L, KH_2PO_4 76 g/L) and trace elements (0.5 mL of a 1000 × solution containing: $FeSO_4.7H_2O$ 1 g, Na_2EDTA 10 g, $ZnSO_4.7H_2O$ 4.4 g, H_3BO_3 2.2 g, $MnCl_2$ $4H_2O$ 1 g, $CoCl_2$ $6H_2O$ 0.32 g, $CuSO_4$ $5H_2O$ 0.32 g and Na_2MoO_4 0.8 g for 200 mL adjusted at pH 6.5). 50 mL liquid MMG was inoculated with 10^6 - 10^7 conidia and incubated for 22 hours at 37 °C in the dark under agitation (220 rpm). When the *Afm* Pxyl-ErdS strain was used, *erdS* overexpression was then induced by supplementing the media with 1 % xylose (w/v) for 1 additional hour. Mycelia were then filtrated through two layers of gauze, rinsed twice with 50 mL sterile H_2O, squeezed, and dried on towel paper to eliminate excess water.

IV.2.   Genomic DNA (gDNA) extraction

Mycelia equivalent to 200 - 250 µL was transferred in a screw cap microtube and 400 µL of lysis buffer (2% TritonX100, 1 % SDS, 100 mM NaCl, 100 mM Tris-HCl pH 8 and 1 mM EDTA) were added. 200 µL of phenol and 200 µL of $CHCl_3$ were then added and mechanical disruption was performed with an FastPrep®-24 apparatus (6 × 1 min at 6.5 m/s, with 1 min on ice between each cycle) in the presence of 200 µL of glass beads (Ø 0.25-0.5 mm, Roth). Tubes were centrifuged at 10000 g for 2 min at RT and the upper aqueous phase was transferred in a clean tube. DNA was precipitated with 1.2 mL of ice cold EtOH 100 % and 40 µL of Na-Acetate 3M at -80 °C for 30 min. After centrifugation at 10000 × *g* for 10 min at 4°C, the pellet is dissolved in 400 µL of TE (10 mM Tris-HCl pH 8, 1 mM Na_2-EDTA) and RNA contamination are removed through RNase treatment (add

3 µl at 10 mg / mL and incubate at 37 °C for 20 min). Finally, DNA are precipitated again, as described above, and the pellet is resuspended in 50 – 100 µl of TE buffer.

IV.3. Preparation of crude extracts (EB)

4.5 – 5 g of dried mycelia were frozen in liquid nitrogen and grinded with mortar and pestle until the biological material became a fine powder. The latter is transferred to a Falcon 50 mL tube together with 7 mL of lysis buffer (50 mM Tris-HCl pH 7,5, 30 mM KCl, 0.1 % TritonX100, 0.5 mM Na$_2$-EDTA, 2 mM phenylmethylsulfonyl fluoride (pMSF), 2 mM Benzamidine, protease inhibitors tablet (Roche)) and 5 g of glass beads (Ø 0.25-0.5 mm, Roth). The mycelia is further disrupted with a FastPrep®-24 apparatus (6 × 1 min at 6.5 m/s, with 1 min on ice between each cycle) and the lysate is carefully transferred in a clean tube in order to remove most glass beads. If nothing is specified, the obtained EB was cleared by centrifugation at 500 × g for 5 min and stored at -20 °C with 30 % glycerol.

V. Protein analysis

V.1. SDS-PAGE

Polyacrylamide gels used for SDS-PAGE are composed of a lower layer (separating gel) and an upper layer (stacking gel). The separating gel is composed of 10 % (v/v) acrylamide:bisacrylamide (37,5:1 ROTIPHORESE®Gel 30, Roth), 375 mM Tris-HCl pH 8.8, SDS 0.1 % (w/v). The stacking gel is composed of 5 % (v/v) acrylamide:bisacrylamide (37,5:1 ROTIPHORESE®Gel 30, Roth), 125 mM Tris-HCl pH 6.8, 0.1 % (w/v) SDS. Polymerization of both layers are initiated with 1 % (v/v) of ammonium persulfate (APS) 10 % (w/v) and 0.1 % (v/v) of N,N,N',N'-tetramethylethylene-diamine (TEMED, Roth) and gels are poured between two glass plates (10 × 8 cm) separated by 1 mm integrated spacers (Mini-PROTEAN® Spacer Plates, BioRad).

If nothing is specified, protein samples were supplemented with 1 × Laemmli buffer (125 mM Tris-HCl pH 6.8, 2 % (w/v) SDS, 10 % (w/v) glycerol, 2 % (v/v) β-mercaptoethanol, 0.0125 % (p/v) bromophenol blue), briefly mixed and boiled at 95 °C. 10 µl of each fraction was loaded on gel and electrophoresis was performed in TGS buffer (25 mM Tris, 192 mM glycine, 0.1 % (w/v)

SDS, pH 8.5) at 200 V for 30 – 45 min using MiniPROTEAN® Tetra Vertical Electrophoresis Cell (BioRad).

Proteins are visualized either by staining gels with Coomassie blue or by using the stainfree imaging technology available on our ChemiDoc™ Touch imager (BioRad). Note that for the second option, 0.5 % of 2,2,2-Trichloroethanol (TCE) must be incorporated into polyacrylamide gels before polymerization.

V.2.   Immunoblotting (or western blots; WB)

Proteins were electroblotted to Polyvinylidene fluoride (PVDF) membranes using a Trans-Blot Turbo™ transfer system (BioRad) (7 min at 25 V (2.5 A)) and the blot was then activated with EtOH 100 % for a few sec. The blot was then briefly washed with TBS-Tween (TBS 1X, Tween-20 0.3 % (v/v)) and blocked with 5 % skimmed milk (p/v) dissolved in TBS-Tween at RT for 1 hour. Incubation with primary antibodies, diluted in TBS-Tween buffer supplemented with in 5 % (w/v) skim milk, were performed O/N at 4 °C (serum / antibody and dilutions are specified for each presented blot). The next morning, the blot was washed 3 times for 10 min with TBS-Tween buffer and incubated with the secondary antibody (rabbit anti-mouse or goat anti-rabbit horseradish peroxidase (HRP) conjugate at 1 / 3000 dilution) at RT for 1 hour. Finally, the blot was washed as described above, the Clarity Western ECL substrate kit was used according to supplier's instructions chemiluminescence signals were captured with the ChemiDoc™ Touch imager (BioRad).

VI. Purification of recombinant fungal proteins

VI.1.   Construction of clones overexpressing recombinant DUF2156 related proteins fused to MBP.

ORFs encoding ErdS and ErgS variants from *Afm* were amplified from the codon optimized sequences, flanked with gateway attB sequences, and cloned into pDONR221 using Gateway technologies (Gateway® BP Clonase™ II Enzyme Mix) as described in previous sections (see **§ II.8.1**). The ORF was then shuttled through LR reaction into pHtevGWA corresponding to pGGWA in which GST was replaced by an His6x tag followed by an TEV protease cleavage site (TevCS). To express MBP-tagged versions, ErdS$_{Afm}$ and ErgS$_{Afm}$ were amplified from the entry plasmid (i.e. pDONR221-

GOI) and cloned downstream to the MBP-TevCS ORF found in pMtevGWA vector (*i. e.* pMGWA gateway vector in which we inserted an TevCS at the 3' end of MBP) using the isoT cloning method. The same procedure was employed to obtain plasmids for the expression of MBP-ErdH*Afm*, MBP-ErgS*Yli* but in those cases ORFs were amplified from gDNAs. Primers, PCR templates and final plasmids expressing recombinant proteins are listed in **Table MM-2** at the end of the present manuscript. *E. coli* Rosetta2 cells where transformed with pHtevGWA-X of pMtevGWA-X expression plasmids, where X corresponds to the ORF of interest.

VI.2. Solubility check of recombinant proteins

E. coli Rosetta2 cells expressing recombinant proteins were grown in liquid LB supplemented with Amp (100 µg/ml) at 37°C until OD_{600} reached 0.5. MBP- and His-tagged proteins overexpression was induced with 0.3 mM IPTG and aliquots were collected at different times to follow overexpression kinetics. Culture was stopped by centrifugation at 5000 × *g* for 10 min at 4 °C. Cells were resuspended in lysis buffer (Tris-HCl pH 7 250 mM, NaCl 300 mM, KCl 30 mM, Glycerol 5 % (v/v), Tween20 0.25 % (v/ v), β-mercaptoethanol 5 mM, Na₂-EDTA 10 mM, protease inhibitor cocktail (Roche Complete, EDTA-free), disrupted by sonication and the resulting lysate was centrifugated at 10000 × *g* for 30 min at 4°C. The supernatant was transferred to a new tube and the pellet was resuspended in an equal volume of lysis buffer. Finally, 10 µL of each fraction, supplemented with 1 × Laemmli buffer and boiled at 95°C, were analyzed by SDS-page. Further informations and obtained data are presented and discussed elsewhere (**Results & Discussions Part I § IV.1.**).

VI.3. Purification of MBP-tagged ErdS and ErgS variants

VI.3.1. Culture and overexpression conditions

Cells were grown in liquid LB supplemented with Amp (100 µg/mL) and when OD_{600} reached 0.5, flasks were placed on ice for 30 min. Overexpression of recombinant proteins was induced with 0.3 mM IPTG for 3h at 30°C and the culture was finally stopped by centrifugation at 5000 × *g* for 10 min at 4°C. Note that later during my thesis I tested various overexpression conditions and

the results revealed that induction with 0.1 mM at 18 °C for 12 h yield higher amounts of the recombinant proteins (**Results & Discussions, Part I, § IV.4.1.**).

VI.3.2. Enrichment of MBP-tagged proteins on amylose resin

The pellet resulting from 2L culture (around 5 g) was resuspended in 15-20 mL lysis buffer composed of Tris-HCl pH 7 250 mM, NaCl 300 mM, KCl 30 mM, glycerol 5 % (v/v), Tween20 0.25 % (v/ v), TritonX100 0.1 % (v/v), β-mercaptoethanol 5 mM, Na_2EDTA 10 mM, protease inhibitor cocktail (Roche Complete, EDTA-free), benzamidine 2 mM, PMSF 0.5 mM. Cells disruption is conducted by sonication (Bioblock Scientific, VibraCell; 8 × 1 min 1 sec on / 1 sec off, amplitude 30 %, on ice) and the lysate is centrifuged at 10000 × g for 30 min at 4°C. The SN is incubated with 2 mL amylose resin (NEB, E8021S), previously equilibrated with lysis buffer, and placed on a rotating wheel for 2-3 h at 4°C. The flow-through is collected using a 1.5 × 10 cm chromatography column (Biorad, Econo-Column® #7371512), beads are washed several times (at least 5-15 column volumes) with wash buffer (Tris-HCl pH 7 50 mM, NaCl 300 mM, KCl 30 mM, glycerol 5 % (v/v), Tween20 0.25 % (v/v), TritonX-100 0.1 % (v/v), β-mercaptoethanol 5 mM). Elution is achieved with the wash buffer supplemented with 2,5 % maltose monohydrate (p/v). 0.5 mL fractions are generally collected and 10 µL of each is analyzed by SDS-page. Eluted proteins were stored with glycerol 50 % (v / v) at -20°C or -80°C.

This protocol stands as the reference protocol and can be used for all MBP-tagged proteins cited in the present manuscript. However, during my thesis I also used an MBPTrap™ HP (GE healthcare, 28-9187) conducted by an Äkta Pure HPLC system instead of the atmospheric amylose resin chromatography. In those cases, equilibration and wash steps were performed at a flow rate of 1 mL/min while sample application was performed at 0.5 mL/min and proteins were eluted with a gradient of maltose (0-3 % maltose (w/v) at 0.5 mL/min. Note that the MBPTrap™ HP alternative yield very low efficiencies for ErgS$_{Afm}$ and ErdS$_{Afm}$ purification (not shown). Consequently, I used the MBPTrap™ HP only to purify recombinant versions of ErgS from *Yli* (ErgS$_{Yli}$) and of ErdH from *Afm* (ErdH$_{Afm}$). In these cases, volumes of the culture and consequently of the lysis buffer used to resuspend cells were modified as specified in the result sections.

Further informations and obtained data are present and discussed elsewhere (**Results &** **Discussions Part I § IV.2. and Part II** (ErgS article draft)).

VI.3.3. TEV protease cleavage

Fractions eluted from the amylose resin that contain the protein of interest were pooled to obtain a homogenous concentration and aliquoted into fractions of 190 µL to which 10 µL of TEV buffer 20 × (1M Tris-HCl pH 7.5 and 10 mM Dithiothreitol (DTT)) were added. This concentrated buffer can be stored at -20 °C or at -80 °C. 2 µL of DTT at 100 mM were added to the reaction tubes and cleavage was started with 8-10 µg of purified TEV protease. Reaction tubes were incubated at 18°C for 5h or at 4 °C O/N. In some cases, when the rate of cleaved proteins was not satisfying, the concentration of the protein was diluted to 1 mg / mL and the cleavage assay was repeated. This was applied to show that both, the MBP-fused and the cleaved version of ErdS versions are active.

VI.3.4. Purification of ErdS$_{\Delta 84}$ by size exclusion chromatography

One goal during my thesis was to purify a version of ErdS$_{Afm}$ that would facilitate its crystallization to resolve the tridimensional structure. As described in the accompanying paper, the AspRS domain of ErdS$_{Afm}$ is fused to a N-terminal (Nt) extension of 104 aa in which no domain of known function was predicted. Furthermore, Phyre2 failed to predict structural features in the Nt extension, which advocates for a labile region susceptible to hinder the obtention of X-ray crystal structures of ErdS. In a first attempt I deleted 84 aa from the Nt extension by using pMtevGWA-erdS-Afm plasmid as template and two purification strategies were tested. The construct is termed (MBP-)ErdS$_{\Delta 84}$.

In the first case, the usual culture, overexpression, lysis, amylose purification, and proteolytic cleavage procedures described above were used. A homemade gel filtration column, made of Superdex 75 resin casted in a 2.5 × 30 cm chromatography column (Biorad, Econo-Column® #7372532), was mounted on an Äkta purifier HPLC system. Column equilibration and size exclusion chromatography were performed in the presence of buffer GF (50 mM Tris-HCl pH 7 and 30 mM KCl) and the flow rate was set to 0.2 ml / min. 1.8 ml of enriched and cleaved ErdS$_{\Delta 84}$ were injected and fractions of 1.4 ml were collected.

In the second case I brought several modifications to the purification protocol. The culture was performed in 1 L and overexpression was induced with 0.1 mM IPTG for 12 h at 18 °C. The resulting pellet (4 g) was resuspended in 20 ml of lysis buffer and sonication was performed as described above. The lysate was centrifuged at 13000 × g for 30 min and the supernatant was incubated with 2 ml of amylose resin at 4 °C for 2 h on a rotating wheel. The batch was split into two fractions that were separately poured into distinct Poly-Prep® Chromatography Columns (Bio-rad). The flow-through was collected, beads were washed several times and proteins were eluted with 5 × 1 ml of wash buffer supplemented with 3 % maltose monohydrate. A total of 4 fractions were pooled and concentrated to 2 ml (Centricon Amicon Ultra-4, 10 kDa) and importantly, the MBP-tag was not removed in this case. The concentrated fraction was subjected to a Hiload 16/600 Superdex 200pg (GE healthcare) monitored by another Äkta pure HPLC system (ÄKTA pure Chromatography System, GE healthcare). The GF buffer was (50 mM Tris-HCl pH 7 and 30 mM KCl), the flow rate was 1 mL / min and fractions were collected in 0.8 mL fractions.

Further informations and obtained data are present and discussed elsewhere (**Results & Discussions, Part I § IV. and Part II** (ErgS article draft)).

VII. Purification of TEV-protease (Tobacco Etch Virus)

The procedure used here was adapted from (Kapust *et al.*, 2001). *E. coli* Rosetta 2 was transformed with a plasmid pRK793 that encodes for TEV protease fused at the N-terminal extremity to a MBP-tag. In addition, both sequences are separated by an internal Tev cleavage site (TevCS) followed by a heptahistidine tag (His7X). During expression and purification, autocleavage of the MBP-TevCS-His$_{7X}$-TEV protein leads to an His7X tagged TEV protease (**Figure MM-8**) that can be purified as described in the following sections.

VII.1. Culture and overexpression

Liquid LB medium supplemented with 100 mg/L Amp and 34 mg/L Chloramphenicol (LB + Amp + Chl) is seeded with *E. coli* cells carrying the expression plasmid. This pre-culture is incubated O/N at 37°C under constant shaking at 200 rpm. The next morning, the preculture is diluted to OD$_{600}$ = 0.05 in 2 × 1L LB + Amp + Chl and the cultures are grown at 37°C until OD$_{600}$ = 0.5 − 0.6. The flasks
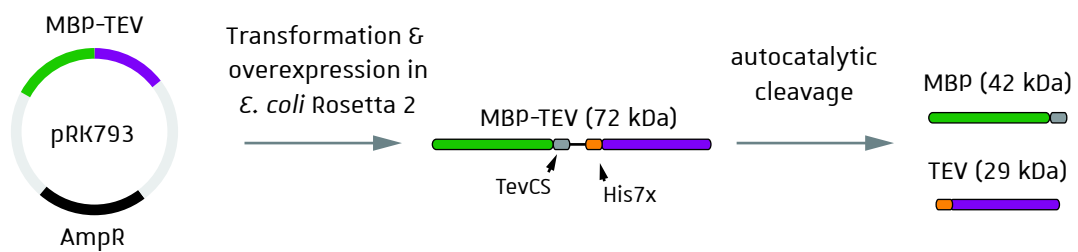
Figure MM-8: Representation of the pRK793 plasmid and its encoded self-cleavable MBP-TEV protein. pRK793 plasmid encodes for a recombinant MBP-TEV protein and was transformed in *E. coli* Rosetta 2. The N-terminal MBP-tag and the C-terminal TEV protease are separated by a TevCS and a His7x-tag. During overexpression and purification, the autocatalytic activity of the protein releases a free MBP and his-tagged TEV protease.

are then transferred at 30°C for 1 hour and overexpression of MBP-TevCS-His6X-TEV is induced with 0.5 mM isopropyl β-D-1-thiogalactopyranoside (IPTG). After 3h, cells are harvested by centrifugation at 5000 × g for 10 min, washed once with PBS and stored at -20°C.

VII.2. Enrichment of His7X-TEV by Ni-NTA by affinity chromatography and purification by size exclusion chromatography

Each 1 L pellet is resuspended in 40 mL ice-cold lysis buffer (25 mM NaH_2PO_4 pH 8.5, 300 mM NaCl, 10 % glycerol, 0.01 % NP40 and 7 mM β-mercaptoethanol) and transferred in a glass tube. Cell disruption is conducted by sonication (Bioblock Scientific, VibraCell; 1 min 1 s on / 1 s off, amplitude 30 %, on ice) and the lysate is centrifugated at 10000 × g for 30 min at 4°C. The supernatant (SN) is incubated with 2 ml Ni-NTA beads (protino Ni-NTA Agarose, Machery-Nagel), previously equilibrated with lysis buffer, and placed on a rotating wheel for 1h at 4°C. Beads are washed with 50 ml lysis buffer supplemented with 15 mM Imidazole, elution is achieved with 12 ml lysis buffer supplemented with 300 mM Imidazole and the resulting eluted fraction is concentrated to 2 ml by using an centrifugal filter unit (Centricon Amicon Ultra-4, 10 kDa). This first purification step provides a fraction highly enriched in cleaved His6X-TEV (28,5 kDa) but an important amount of uncleaved MBP-TevCS-His6X-TEV (72 kDa) is also present. The concentrated fraction is therefore injected onto a Hiload 16/600 Superdex 200pg (GE healthcare) and monitored by a High-Performance Liquid Chromatography (HPLC) system (ÄKTA pure Chromatography System, GE healthcare) according to manufactured recommendations. GF buffer is composed of 25 mM NaH_2PO_4 pH 8,5, 200 mM NaCl, 10 % glycerol and 1 mM β-mercaptoethanol, the flowrate during equilibration and elution was set to 1 mL/min and the volume of collected fractions was 1 mL.

As explained above, I performed the experiment on 2 × 1 L culture and both pellets were treated successively at the same day. Surprisingly, the elution profile obtained by size exclusion differed from one experiment to the other. In fact, chromatograms on **Figure MM-9** clearly show that the relative amount of peak 2 is severally increased in comparison to peak 1 during the second experiment (compare **Figures MM-9A and MM-9B**). This might be due to the fact that the percentage of cleaved protein was higher at the time when the second sample was submitted to Ni-NTA or/and when it was submitted to size exclusion. In fact, the fraction eluted from Ni-NTA

A Experiment 1

B Experiment 2
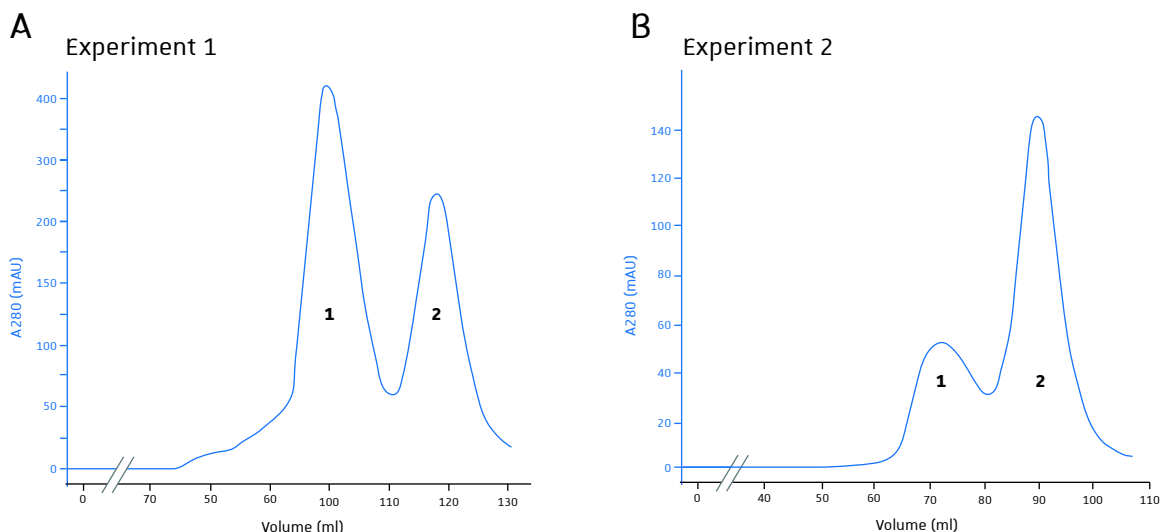
Figure MM-9: Purification of TEV protease by size exclusion chromatography. The 12 mL fraction eluted from the Ni-NTA resin was concentrated to 2 mL and then injected onto a Hiload 16/600 Superdex 200pg monitored by HPLC. The purification process was repeated on two equally treated cell pellets, with the unique difference that due to technical reasons, purification steps during the second experiment were delayed. Size exclusion chromatograms obtained during experiment 1 and 2 are presented in **(A)** and **(B)**, respectively. GF buffer: 25 mM NaH2PO4 pH 8,5, 200 mM NaCl, 10 % glycerol and 1 mM β-mercaptoethanol; flowrate, 1 mL/min; fractions volume, 1 mL. **(C)** The SDS-PAGE presented here was performed on fractions collected during experiment 2. Fractions eluted from the Ni-NTA resin (last lane) and from the size exclusion column were analyzed.
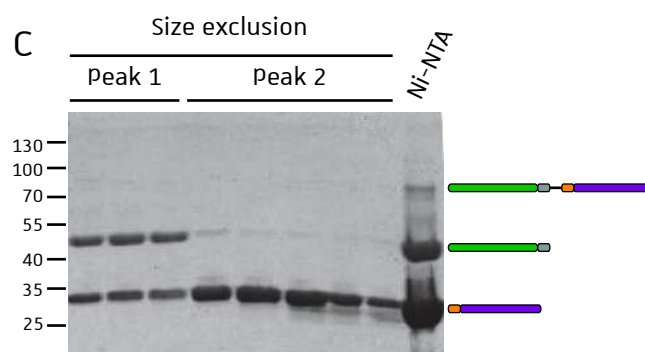
during the second experiment shows that MBP-TEV was almost completely cleaved (**Figure MM-9C**). Unfortunately, SDS-PAGE analysis were not performed during the first experiment and therefore no conclusions can be made. Anyway, fractions from peaks 1 and 2 obtained during the second size-exclusion experiment were analyzed by SDS-PAGE and clearly show that the cleaved TEV protease is separated in the second peak (**Figure MM-9C**). Consequently, fractions from peak 2 (form both experiments), containing pure and cleaved TEV protease are pooled together, supplemented with 50 % glycerol (v / v), aliquoted and stored at -80 °C at a concentration of 0.5 mg/ml.

VIII. Production of polyclonal antibodies against ErdS and ErgS from *Afm*.

VIII.1. Preparation of ErdS and ErgS antigens

Developing antibodies that recognize specifically fungal DUF2156 proteins was another important goal during my thesis. Antigen used for immunizations were either the full-length ErgS$_{Afm}$ or the ErdS-*ΔaspRS*. For the latter, the goal was in fact to obtain polyclonal antibodies specifically recognizing the DUF2156 domain rather than the AspRS domain. One option that often induce good antibody response is to elute protein antigens directly from SDS-page (Greenfield *et al.*, 2019).

MBP-ErgS$_{Afm}$ was purified as described above, but here a maltose gradient was used to elute proteins (**Figure MM-10A**). The eluate (9,5 ml) was concentrated to 2 ml with a Centricon (Amicon Ultra-4, 30 kDa). During this concentration step no precipitation was observed. The MBP-tag was removed by performing proteolytic cleavage mediated by the TEV-protease, as described above, with the notable difference that the reaction was incubated O/N at RT (**Figure MM-10B**). An aliquot of the concentrated protein was incubated in the same conditions without adding TEV-protease, which further confirmed that the cleaved version but not the MBP-tagged protein precipitates (Shown ou not shown ??). Proteins were supplemented with Laemmli buffer 1 ×, boiled at 95 °C and mixed until no remaining precipitate was visible. As described later, the development of polyclonal antibodies was performed in collaboration with Covalab which required at least 500 µg of the antigen (enclosed in polyacrylamide gel) to perform all immunization steps. Therefore,

Figure MM-10

MBP-ErgS (105 kDa)

MBP ↗ DUF2156

A

1 ml | 0.5 ml

0.25 | 0.5 | 1 | 3 % (p/v)

FT E1 **E2 E3 E4 E5 E6 E7 E8 E9 E10 E11 E12**

170 —
130 —
100 —
70 —
55 —
40 —
35 —

*

Amylose resin affinity

B

TEV − + − +
vol (µl) 10 2

170 —
130 —
100 —
70 —
55 —
40 —
35 —

*
*

TEV cleavage

C

MBP-ErgS (105 kDa)

ErgS (63 kDa)

MBP (40 kDa)

large scale SDS-PAGE 15 x 15 cm
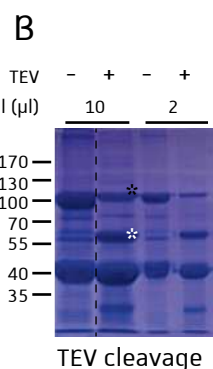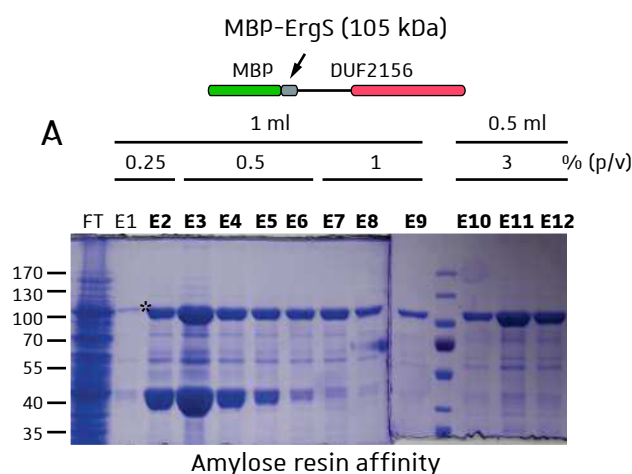
Figure MM-10: Preparation of the ErgS antigen for immunization. (A) Plasmid pMtev-ErgS-Afm was transformed in *E. coli Rosetta2*, cells were grown in 2 L culture until OD_{600} reached 0.5 and overexpression of MBP-ErgS$_{Afm}$ was induced with 0.3 mM IPTG for 3 h at 30 °C. Cells were disrupted by sonication, and the recombinant protein enriched on amylose resin on low pressure column. The volume of eluted fraction and % (p / v) used for the maltose step gradient are indicated. 10 µl of each fraction supplemented with Laemmli buffer 1 × was analyzed by SDS-PAGE. **(B)** Fractions E2-E12 were concentrated to 2 mL final, an aliquot of 100 µl was put to side as control the rest was submitted to TEV protease. Aliquots of treated (+) or non-treated (-) fractions were analyzed by SDS-PAGE after O/N incubation at RT. The black star indicates non-cleaved MBP-ErgS and the white star indicates cleaved ErgS. **(C)** 400 µl of TEV treated fraction was loaded on a large 1 well polyacrylamide gel (15 x 15 cm) 10 % and separated by SDS-PAGE. Note that due to the low separation quality, I repeated the SDS-PAGE, which gave better resolution and the band corresponding to ErgS was cut out of the gel (not shown). MW, molecular weight; FT, flowthrough; E, Elution fractions

Figure MM-11

GST-MBP-ErdS-ΔAspRS (108 kDa)

A

GST MBP ↗ DUF2156

E1 **E2 E3 E4 E5 E6 E7 E8**

130 —
100 —
70 —

Amylose resin affinity

B

170 —
130 —
100 —
70 —
55 —
40 —
35 —

GST-MBP-ErdS-ΔAspRS (108 kDa)

GST-MBP (67 kDa)

ErdS-ΔAspRS (40 kDa)

TEV cleavage

C

large scale SDS-PAGE 15 x 15 cm

D

ErdS-ΔAspRS

cuting out the band of interest
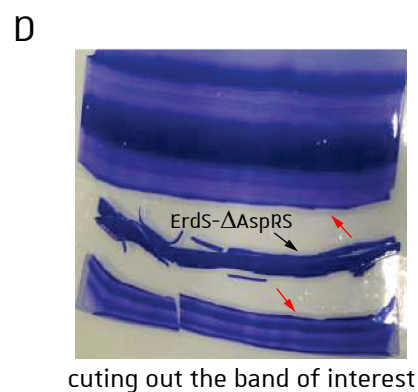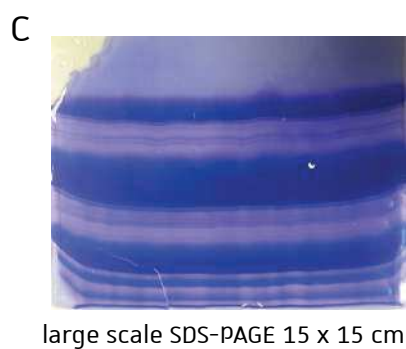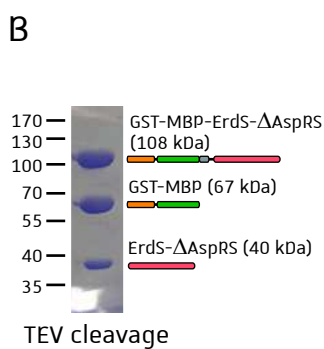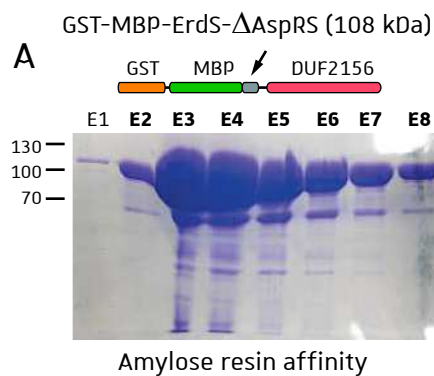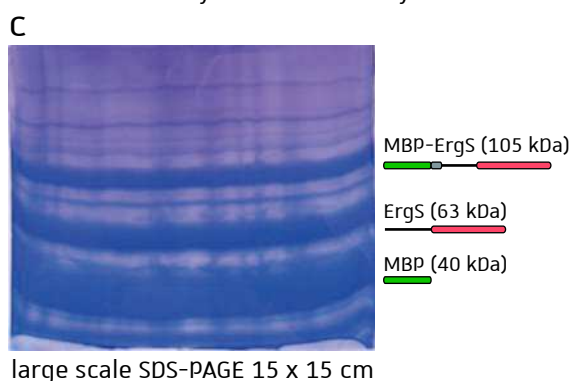
Figure MM-11: Preparation of the ErdS antigen for immunization. (A) MBP-ErdS$_{Afm}$ was enriched as for MBP-ErgS$_{Afm}$ (see legend of the previous figure) except that elution was performed continually with maltose 3 %. Elution fractions were analyzed by SDS-PAGE. **(B)** Fractions E3 and E4 were first pooled and then submitted to TEV protease. An aliquot was analyzed by SDS after 4 h incubation at RT but the cleavage was not satisfying which is why tubes were further incubated O/N. **(C)** 250 µl of TEV treated fraction was loaded on a large polyacrylamide (15 x 15 cm) 10 % gel and separated by SDS-PAGE. **(D)** Cutting out the band corresponding to cleaved ErdS$_{Afm}$. Red arrows indicate the outlines of the excised band.

around 400 µL were loaded onto a large 10 % polyacrylamide gel (15 × 15 cm), proteins were resolved by electrophoresis and the gel was finally stained with Coomassie Blue R-250 (**Figure MM-10C**). The band corresponding to cleaved ErgS*Afm* was cut out of the gel, sliced, grinded into fine pieces, and submerged with 4 ml PBS buffer 1 ×.

For the second antigen, the MBP-ErdS-*ΔaspRS* version was not suitable for this purpose since ErdS-*ΔaspRS* and MBP have quasi identical MW (39.3 and 40.5 kDa respectively), thereby hindering their separation on by SDS-PAGE. Therefore, I fused an additional tag at the N-terminus of the constructions which increases the size of the tag (66.3 kDa). The resulting GST-MBP-ErdS-*ΔaspRS* (108 kDa) was purified on amylose resin (**Figure MM-11A**) and two elution fractions containing the highest amount of the purified protein were submitted to TEV protease at RT (**Figure MM-11B**). After 4 h incubation a fraction was analyzed by SDS-PAGE but the cleavage efficiency was low and tubes were further incubated O/N. The partial cleavage might be due to the high concentration of the target protein but for technical reasons I wanted to avoid dilutions. Finally, proteins were separated by SDS-PAGE using on a large polyacrylamide gel and the band corresponding to cleaved ErdS-*ΔaspRS* was prepared as described above (**Figure MM-11C and MM-11D**). Importantly, when cutting the band of interest from the gel it is recommended to not surpass the band outlines.

VIII.2.   General protocol for the immunization of rabbits against antigens (Covalab France).

ErdS and ErgS antigens were prepared as described above and sent to Covalab France that performed all immunization steps. The pipeline of the procedure is presented in **Figure MM-12**. Note that at this stage of the project we aimed to develop antibodies mainly to detect ErdS and ErgS variants by Western blots (WB). Therefore, we assumed that it would be sufficient to produce polyclonal antibodies and we decided to realize the immunizations against our antigens of interest on New Zeeland White rabbits. One important step was to select the appropriate rabbits to inject and in the present case the choice was done by testing pre-immunized serums by WB. These serums are indicated as SXXX_PI, were XXX correspond to the 3 last numbers of rabbit's identification matricula. At day 0 the serum is again collected and will be used as negative control (indicated as SXXX_D0). The first immunization step performed the same day through intradermal

covalab
R&D in Biotechnology

gm
Génétique Moléculaire ▪ Génomique ▪ Microbiologie
(In our lab)

Collecting 4-5 ml of pre-immune serums of 4
New Zeeland White rabbits (**SXXX_PI**)

Testing the reactivity of SXXX_PI by WB and
choosing two rabbits to be immunized

Day 0
Collecting control serums (**SXXX_D0**)
&
Intradermal injection (1 mL / rabbit)
0.5 mL antigen + 0.5 mL complete Freund's adjuvant

Day 14
Intradermal injection (1 mL / rabbit)
0.5 mL antigen + 0.5 mL complete Freund's adjuvant

Day 28
Intradermal injection (1 mL / rabbit)
0.5 mL antigen + 0.5 mL complete Freund's adjuvant

Day 39
Collecting 4-5 mL of test serums (**SXXX_D39**)

Confirming the induction of an immune response
against the antigen by testing SXXX_D39 through
WB. SXXX-D0 are used as controls.

Day 42
Subcutaneous injection (1 mL / rabbit)
0.5 mL antigen + 0.5 mL complete Freund's adjuvant

Day 53
Collecting 10-15 mL of test serums (**SXXX_D53**)

Evaluation of the immune response
Confirmation of the presence of primary antibodies
specifically recognizing the antigen
Validating the suitability of immunized serums for
planned experiments.

Day 67
Sacrificing rabbits and collecting final serums
(**SXXX_final**)

Figure MM-12: Pipeline of the procedure used for the production of polyclonal antibodies. The left side describes the immunization steps performed by Covalab France and the abbreviation of the collected serums are indicated in bold between brackets. XXX corresponds to the suffix of rabbit's identification numbers. At different stages of this immunization protocol, Covalab provided us serum fractions that were tested by WB to evaluate the production of primary antibodies against the antigen (right side).

injection of the antigen, and this injection is repeated after 14 and 28 days. A few mL of each tested serum is sampled at day 39 (indicated as SXXX_D39) to verify whether an immune response was triggered. If so, the latter is boosted by subcutaneous injection of the antigen at day 42 and serums are again sampled at day 53 (indicated as SXXX_D53). The suitability of the obtained serum to perform the whished experiments (*i. e.* mainly WB in the present case) is tested and the rabbits are sacrificed at day 67 to collect the final serum (indicated as SXXX_final).

VIII.3. Evaluation of the immunization against ErdS by immunoblotting

The ability of serums, collected at different stages of the immunization, to specifically recognize ErdS was tested by WB. Preparation of Crude extracts (EB) from Sce strains, SDS-PAGE and WB were performed as described in (Yakobov *et al.*, 2020). Sera extracted from the rabbits contain primary antibodies and dilutions that were assayed are specified in the following sections and in the accompanying figures. The secondary antibody used for all WB presented, corresponds to HRP-conjugated goat anti-rabbit and was diluted to 1 / 3000.

Pre-immune sera of 4 naïve New Zeeland White rabbits (1831**003**, 1831**005**, 1831**026** and 1831**029**) were collected and their reactivity was tested by WB in the presence of EB obtained from *Sce* wt, *Sce* expressing ErdS$_{Afm}$ and *Afm* wt (**Figure MM-13**). Pre-immune sera from rabbits 1831005 (S005_PI) and 1831029 (S029_PI) showed less background signals, in particular at sizes neighboring those of full-length ErdS, and were finally retained for immunization with ErdS-ΔAspRS.

Sera were collected from both selected rabbits just before immunization (S005-D0 and S029_D0) or after 39 days immunization (S005_D39 and S029_D39) and immunoblots were performed on EB from *Sce* strains or on recombinant MBP-ErdS purified from *E. coli* (**Figure MM-14**). Blots performed with S005_D39 and S029_D39 (dilution: 1 / 3000) on EB from *Sce* revealed an additional band, migrating at the expected MW which was specific to the presence of ErdS$_{Afm}$ (**Figure MM-14A**). These results confirmed that both injected rabbits were successfully immunized and produce antibodies specifically recognizing ErdS$_{Afm}$. However, the signal corresponding to ErdS$_{Afm}$ seemed to be more important with S005_D39 in comparison to S029_D39 which is why further tests were performed with S005_D39. Moreover, the intensity of the specific signal was only slightly higher in comparison to non-specific bands revealed by S005_D39. The same result

Selection of PRE-immune serums

S003_PI | S029_PI | S026_PI | S005_PI
1 2 3 | 1 2 3 | 1 2 3 | 1 2 3

MW
— 170
— 130
— 100
— 70

1 : *Afm wt*
2 : *Sce* + ErdS$_{Afm}$
3 : *Sce wt*

WB with PRE-immune serums (**PI**); 1/1000
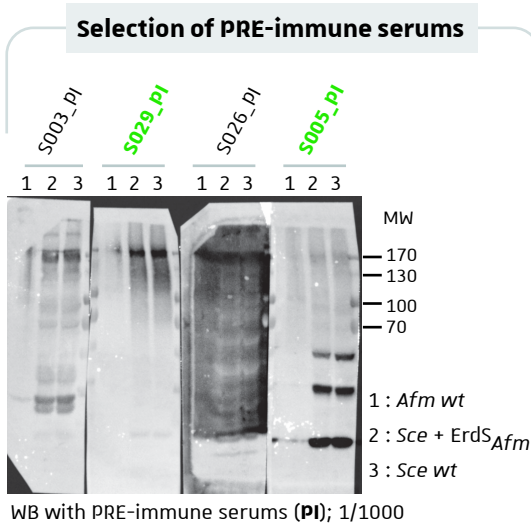
Figure MM-13: Assaying pre-immune serums by WB for the selection of appropriate rabbits to be immunized against ErdS$_{Afm}$. EB from Afm wt (1), *Sce* expressing ErdS$_{Afm}$ (2) and *Sce* wt were prepared and separated by SDS-page. Proteins were transferred onto PVDF membrane and WB were performed using SXXX_PIs as primary antibody (1 / 1000) and an HRP-conjugated goat anti-rabbit secondary antibody at 1/3000 dilution. Rabbits containing serums indicated in green were selected for the immunization against ErdS. MW, molecular weight in kDa.

D39 | **D53** | **Final**

A | **B** | **C** | **D**

WB with serums at **D0** and **D39** after immunization; 1/3000

Samples: 1 : *Sce wt*

　　　　　2 : *Sce* + ErdS Afm (108 kDa)

　　　　　3 : MBP-ErdS (5 µg) (151 kDa)

WB with S005_**D39**; 1/3000
Samples: MBP-ErdS (µg)

WB with S005_**D53**;
1/5000

WB with S005_**final** 1/5000
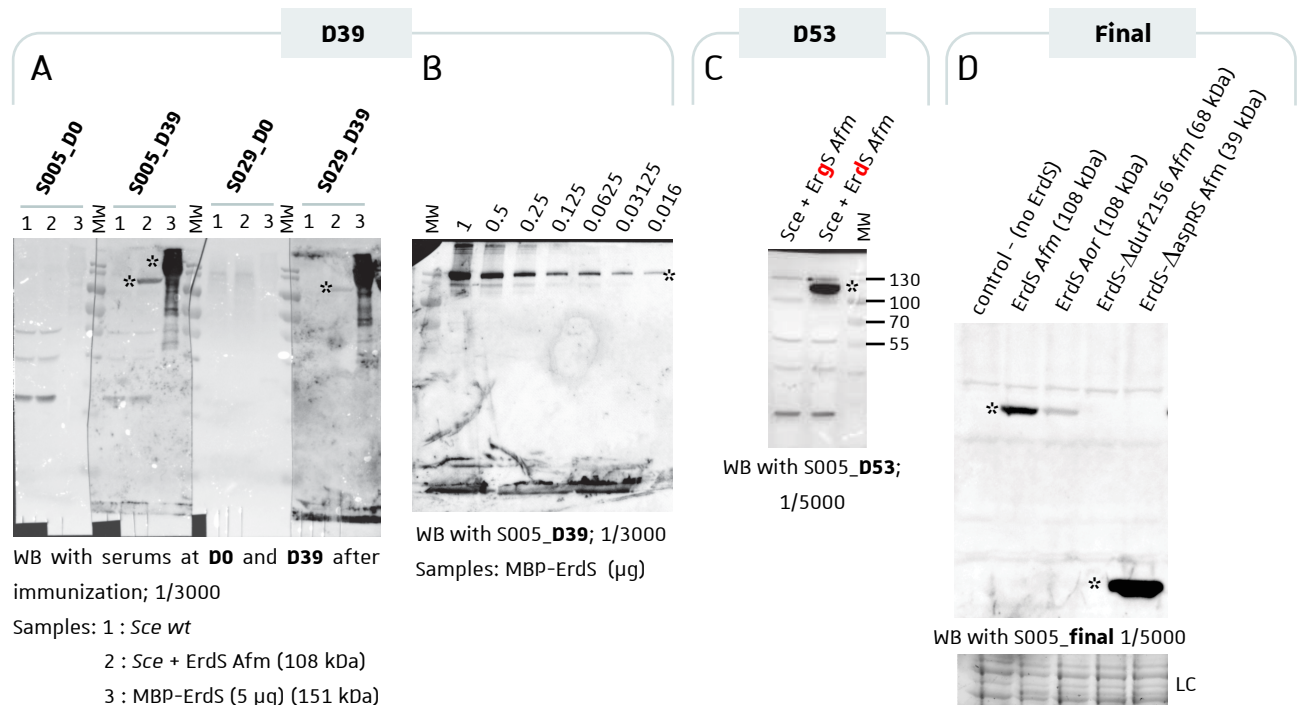
Figure MM-14: Evaluation of ErdS$_{Afm}$ immunized serums collected at days 0, 39, 53 and 67 (final) by WB. (A) WB were performed on EB from *Sce* wt (1) or from *Sce* expressing ErdS$_{Afm}$ (2) and on purified MBP-ErdS (3). The tested serums are indicated at the top of the result. **(B)** S005_D39 was tested in the presence of decreasing amounts of recombinant MBP-ErdS$_{Afm}$ (indicated in µg at the top of the blot). **(C)** S005_D53 was tested in this case on EB obtained from *Sce* expressing one of both DUF2156 proteins from *Afm* (i. e. ErdS and ErgS). Antibodies from this serum do not cross react with ErgS. Note the increased intensity of the expected band in comparison to the contaminants (compare with S005_D39 in (A)). **(D)** With regard to the results obtained in (C), the immunization procedure was stopped at day 67 and the final serum was collected. Testing EB from the indicated *Sce* strains confirmed that antibodies from S005_final interact specifically with the DUF2156 domain but not with the AspRS domain of ErdS. The presented results also indicate that interaction strength between the antibodies and ErdS from *A. oryzae* (ErdS$_{Aor}$) is lowered in comparison to ErdS$_{Afm}$. * indicate the expected band; LC, loading control. Serums dilutions are indicated at the bottom of each result and the secondary antibody was in all cases HRP-conjugated goat anti-rabbit used at 1/3000 dilution.

shows also that MBP-ErdS is also detected by both tested sera but due to the loaded amounts it is not possible to compare the efficiencies of both serums. In addition, amounts of MBP-ErdS ranging from 1 to 0.016 µg were successfully detected by WB performed with S005_D39 and the acquired signal decreased as expected proportionally to the amount of protein (**Figure MM-14B**).

A subcutaneous injection of the antigen injection was performed at day 42 and sera were collected at day 53 (D53). EB from *Sce* expressing Er**d**S*Afm* or Er**g**S*Afm* were prepared to test potential cross-recognition and serum S005_D53 obtained from rabbit 1831005 was tested by WB at 1 / 5000 dilution. Importantly, ErgS*Afm* was not detected in these conditions, which witnesses the specificity of S005(-D53) antibodies for ErdS*Afm* recognition. Moreover, this result also shows that the ErdS specific signal is severely increased when compared to unspecific bands (**Figure MM-14C**).

At day 67 after immunization, rabbits were sacrificed and the final serums (S005_final and S029_final) were collected. **Figure MM-14D** shows the result obtained by WB performed with S005_final on EB that were obtained from *Sce* expressing distinct ErdS variants. As expected, ErdS-ΔaspRS was also detected but not ErdS-Δduf2156 which confirms the specificity of polyclonal antibodies from S005_final for the DUF2156 domain of ErdS. In this experiment an EB obtained from Sce expressing the homologous ErdS from *Aor* was also included. Antibodies from S005_final recognized this homolog but surprisingly the intensity of the band was severally decreased. Because the size of the corresponding band is similar to those obtained for ErdS*Afm*, it might be that the avidity of the antibodies for ErdS*Aor* is weaker than for ErdS*Afm*.

Finally, EB obtained from *Afm* strains were also tested but the detection of ErdS was much more compromised. Here I selected two experiments where the signal suspected to correspond to ErdS recognition was appreciable. Culture were grown as described in (Yakobov *et al.*, 2020), EB were prepared as described above (**Materials & Methods, § IV.3.**) and aliquots were clarified by centrifugation at 1000 × *g* or 4000 × g for 10 min at 4 °C (S1). The resulting S1 and S4 supernatants were supplemented with Laemmli buffer 1.5 ×, boiled at 95 °C and vortexed until complete solubilization, loaded on 10 % polyacrylamide gel and developed by SDS-PAGE. Proteins were transferred onto a PVDF membrane and WB was performed with S005_final diluted at 1/1000. The dilution of the HRP-conjugated goat anti-rabbit (secondary antibody) remains unchanged (1 /

3000). The result in (**Figure MM-15A**) shows that ErdS was specifically detected in EB from *Afm* wt but the corresponding signal was very slight. In addition, an important non-specific band with size between 70 and 100 kDa was revealed in all tested samples.

In the second experiment EB from *Afm* wt, *Afm ΔerdS*, and *Afm* Pxyl-*erdS* (*Afm ΔerdS* strain complemented with the *erdS* gene under the dependence of a xylose promoter) were tested. Overexpression of *erdS* in the latter strain was performed after 22 h culture at 37 °C by adding xylose 1 % (w / v) and the culture was incubated at 37 °C for an additional hour. EB were prepared and clarified by centrifugation at 500 g for 5 min. The pellet was removed, and 3 mL of each supernatant was fractionated by ultracentrifugation at 100000 × g for 1 h at 4 °C. The soluble fraction (S100) was transferred in a fresh tube and an aliquot was supplemented with Laemmli buffer 1 ×. The pellet (P100) was resuspended in 200 µL of lysis buffer supplemented with 1% N-Lauroylsarcosine sodium salt. An aliquot of each P100 fraction is supplemented with Laemmli buffer 1 × boiled at 95 °C and vortexed until total solubilization. 10 µl of each fraction are finally loaded on SDS-PAGE for further analysis by WB treated with S005_final (**Figure MM-15B**). A slight ErdS signal was detected in the P100 fraction of *Afm* wt, but not in *Afm ΔerdS*. In contrast, ErdS was not detected in the corresponding S100 fraction and one might speculate that this is due to the poverty of the loaded protein amount. Strikingly, three intense bands were revealed in P100 from *Afm* Pxyl-*erdS* that were not present in the corresponding S100 fraction (**Figure MM-15B**). The upper band is assumed to contain the full-length ErdS protein and the presence of both lower bands might correspond to cleaved products that harbour the DUF2156 domain. As detailed in (Yakobov *et al.*, 2020) this preliminary result advocates for the membranous localization of ErdS and this point will be discussed in the conclusion and perspectives sections.

To conclude the S005_final, containing polyclonal antibodies specifically recognizing the DUF2156 domain of ErdS, is suitable for WB performed on *Sce* strains expressing ErdS in the tested conditions. The situation is more complex when aiming to detect ErdS in *Afm* and it is not determined if this is due to potentially low avidity of the antibodies or to the very low expression level of *erdS* in the tested condition. Finally, some tests were also performed with S029_final including WB on EB from *Afm* strains and results seem to be similar (not shown).
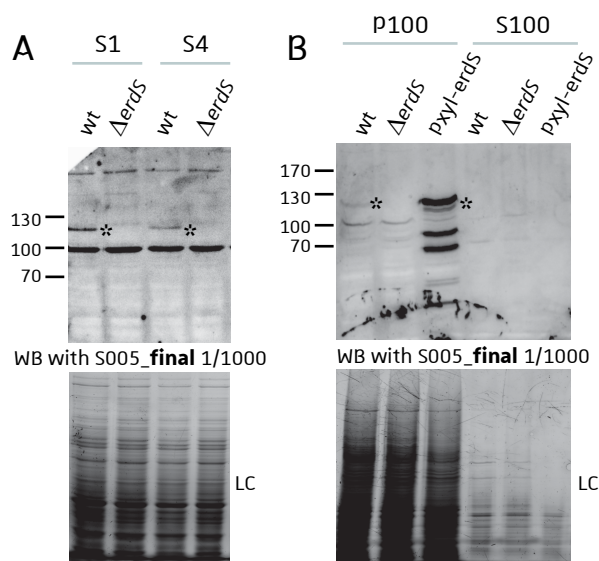
Figure MM-15: Detecting ErdS in Afm with S005_final. (A) EBs from *Afm* wt and *Afm*-ΔerdS were prepared as described in the corresponding Materials & Methods section and were clarified either with centrifugations at 1000 *x g* or at 4000 *x g* (10 min at 4 °C). 10 µl of each fraction was separated by SDS-PAGE and analyzed by WB. **(B)** In addition to both EB mentioned in (A), the *Afm* strain overexpressing erdS under the xylose inducible promoter (Pxyl-erdS) was also considered. In this experiment, EB were fractionated by ultracentrifugation (100000 *x g*, 1 h, 4 °C) and aliquots of the pellet (P100) and of the supernatant (S100) were analyzed by WB. * indicate the expected band; LC, loading control. Serums dilutions are indicated at the bottom of each result and the secondary antibody was in all cases HRP-conjugated goat anti-rabbit used at 1/3000 dilution.

VIII.4. Evaluation of the immunization against ErgS by immunoblotting

The same immunization protocol was applied to develop polyclonal antibodies against ErgS$_{Afm}$ and sera collected at different stages were assayed by WB mainly on EB obtained from *Sce* expressing ErgS$_{Afm}$ or *Sce* wt. Prior to injection of the ErgS antigen, pre-immune serums from naïve New Zeeland White rabbits (1906**008**, 1906**009**, 1906**012** and 1906**014**) were tested to select serums presenting the lowest non-specific signals on WB (1 / 3000) (**Figure MM-16**). Serum from rabbits 1906**008** and 1906**009** showed several non-specific bands in the presence of EB from *Sce* and even in a fraction of partially purified ErgS$_{Afm}$. The latter corresponds to the same fraction used to prepare the antigen and contains non-cleaved MBP-ErdS$_{Afm}$ (105 kDa), cleaved ErdS$_{Afm}$ (63 kDa) and free MBP (40 kDa). Intriguingly, the pre-immune serum from rabbit 1906008 (S009_PI) contains antibodies against MBP since MBP-ErdS$_{Afm}$ and MBP were revealed but not the cleaved ErdS$_{Afm}$. In contrast, serum from rabbit 1906**012** (S012_PI) seemed to be the most appropriate choice and ErgS$_{Afm}$, cutted out from the resolved polyacrylamide gel, was injected in this rabbit. As a second choice I selected rabbit 1906**014** (S014_PI) even though this serum interacts with a band that migrates at similar size than ErdS$_{Afm}$.

Sera were collected at D39 and D53 after immunization from rabbits 1906**012** and 1906**014** and at the beginning I planned to test the resulting S012_D39 and S014_D39 at dilution of 1 / 1000. However, the membrane treated with S012_D39 completely burned when the revelation solution (BioRad clarity western ECL Kit) was added (not shown) which is why dilutions were adapted. S012_D39 and S012_D53 were used at 1 / 10000 or 1 /20000 which revealed the presence of an additional band, migrating at the expected size, in EB sample from *Sce* expressing ErdS$_{Afm}$ but not in *Sce* wt (**Figure MM-17A**). Despite the high dilution, the corresponding band was quite intense which advocates for the strong immune response against ErgS$_{Afm}$. Minor non-specific interactions were also present but beside this there was always an important smear at the top of the blot when EB from yeast were tested. The reason for that is unclear especially that when the final S012 serum was collected, two independent clones of *Sce* + Er**g**S$_{Afm}$ and *Sce* + Er**d**S$_{Afm}$ were assayed by WB (1/10000) and the contamination was present in one experiment but not in the other (**Figure MM-17B**). Using *Sce* + Er**d**S$_{Afm}$ as a control showed that in this case too, S012_final recognizes specifically Er**g**S and does not cross-interact with Er**d**S. Concerning the second immunized rabbit

WB with PRE-immune serums (**PI**); 1/3000

1 : recombinant ErgS (62 kDa; 1 μg)

2 : *Sce* + ErgS$_{Afm}$

3 : *Sce* wt
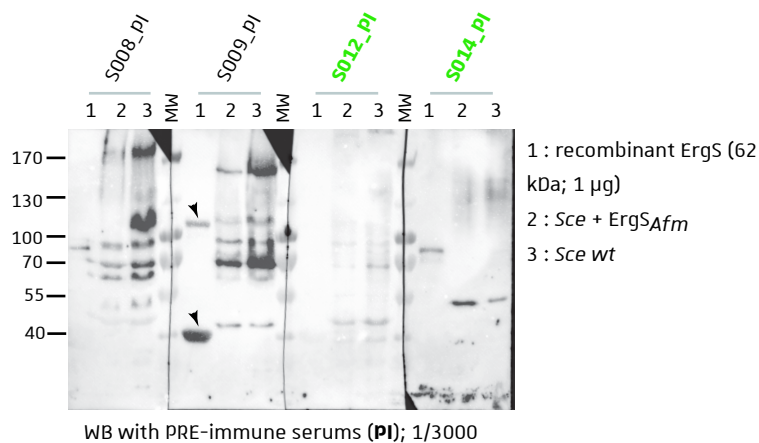
Figure MM-16: Assaying pre-immune serums by WB for the selection of appropriate rabbits to be immunized against ErgS$_{Afm}$. Serums were tested as in Figure MM-13. Samples that were assayed are indicated at the top. Arrowheads shows bands corresponding to non-cleaved MBP-ErgS (105 kDa) and free MBP. Rabbits containing serums indicated in green were selected for the immunization against ErgS MW are indicated in kDa.

Samples

1 : *Sce* + Er**g**S$_{Afm}$ (62 kDa)

2 : *Sce* wt

3 : Sce +Er**d**S$_{Afm}$ (108 kDa)
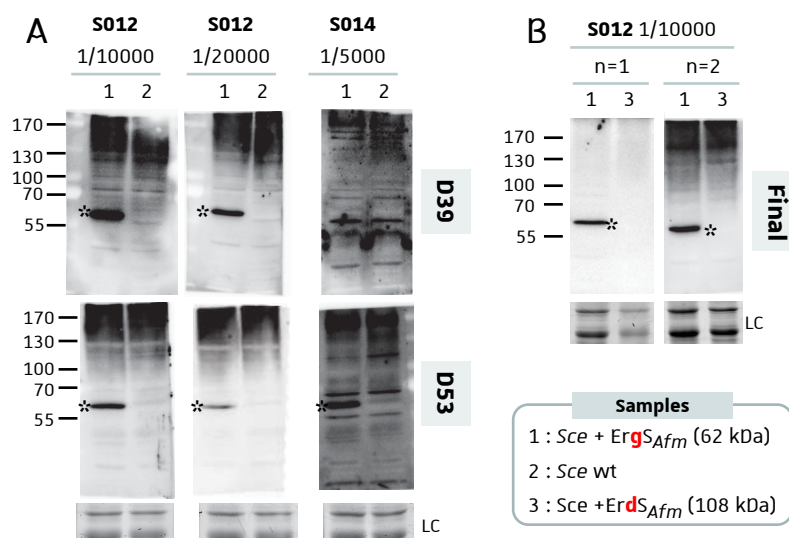
Figure MM-17: Evaluation of ErgS$_{Afm}$ immunized serums collected at different steps of the procedure. (A) Serums from rabbits 1906012 (S012) and 1906014 (S014) were collected at days 39 or 53 (indicated in grey boxes) and tested by WB on *Sce* expressing ErgS$_{Afm}$ (1) or on *Sce* wt (2). S012 was used at 1 / 10000 or 1 / 20000 dilutions and S014 was diluted at 1 / 5000. **(B)** The final serum from rabbit 1906012, collected at day 67 was tested on *Sce* expressing one of both DUF2156 proteins from *Afm* (i. e. ErgS (1) or ErdS (2)) attesting that antibodies interacting with ErgS$_{Afm}$ do not cross-recognize ErdS$_{Afm}$. LC, loading control; MW, molecular weight in kDa.

(1906**014)**, ErgS was surprisingly not detected by WB incubated with S014_D39 even though the dilution was 1 / 5000 (**Figure MM-17A**). In contrast, the injection performed at day 42 triggered an immune response against the injected ErgS*Afm* antigen as shown when using S014_D53 on WB. However, important non-specific bands surrounding the ErgS band are present and in view of the strong reactivity of immunized S012 serums I preferred to retain the latter for all experiments done during my thesis. Finally, preliminary tests started to be done with EB obtained from *Afm* but since for the moment we failed to construct the *Afm ΔergS* strain the results are difficult to interpret and are not shown here.

VIII.5.   Conclusion

The strategy used here in collaboration with Covalab France was successful to immunize rabbits against fungal DUF2156 proteins since specific polyclonal antibodies appeared during the immunization process and were extracted in form of serums. The qualitative characterization (affinity, avidity, and specificity) of those antibodies is difficult since they were not further purified, and the corresponding sera undoubtedly also interacts with contaminants. However, regarding the presented tests, the immunized sera are largely suitable for WB and give appreciable results especially in the presence of EB obtained from Sce. Furthermore, sera immunized against ErdS do not cross-interact with ErgS and vice versa, despite both contain a DUF2156 domain. For immunoblots performed in the presence of EB prepared from Afm further investigations are needed but from preliminary results it appears that fungal DUF2156 proteins may be present in low amount in the tested conditions. Further tests should be performed to characterize the selected serums and it is also probable that other strategies (e. g. monoclonal antibodies) will be necessary in the future to develop improved antibodies. However, in the meantime, I retained immunized S005 sera (S005_D53 or S005_final) as "primary antibody" against ErdS for all WB shown in the present manuscript, while S012 sera (S012_D39, S012_D53 or S012_final) are used to detect ErgS.

IX. In vitro lipid aminoacylation assays (LAA)

In vitro tRNA aminoacylation assays, LAA by fungal DUF2156 proteins and lipid deacylation assays by ErdH are fully described in (Yakobov *et al.*, 2020) and in the article in preparation. Thus, the aim of the present section is to provide some practical precisions when assaying *in vitro* the transfer of Asp or Gly onto Erg.

IX.1. Erg-Asp synthesis

In order to synthesize radiolabeled Erg-Asp species, we first adapted the LAA described elsewhere (Roy and Ibba 2008a), as follow: A 2 × concentrated reaction mix was prepared and contained 200 mM Na-Hepes pH 7.2, 60 mM KCl, 24 mM MgCl2, 20 mM ATP, 0.2 mg/mL bovine serum albumin (BSA), 20 µM pure yeast tRNA^{Asp} (46), 40 µM [U-14C]- Asp (280 cpm/pmol, Perkin-Elmer, NEC268E050UC). Commercial sterols species and total lipids from yeast were first solubilized in EtOH 100 % and CHCl3, respectively. Reaction tubes were prepared, 25 µg of commercial sterols or 100 µg of total lipids from yeast were added and the organic solvent was evaporated by heating tubes at 60 °C. 25 µl of the 2 × concentrated reaction mix was added and lipids were resuspended by sonication for 30 sec in a sonicator bath at RT. Finally, 0.1 to 0.5 µg of purified (MBP-)ErdS variants or 20 µg of total proteins from crude extracts were added, the volume was completed to 50 µL with H$_2$O and assays were incubated at 30 °C for 40-60 min. In this way a reaction assay is composed of 100 mM Na-Hepes pH 7.2, 30 mM KCl, 12 mM MgCl2, 10 mM ATP, 0.1 mg/mL bovine serum albumin (BSA), 10 µM pure yeast tRNA^{Asp} (46), 20 µM [U-14C]-Asp (280 cpm/pmol, Perkin-Elmer, NEC268E050UC), 0.5 mg/mL of total lipids from yeast or 2 mg/mL of commercial sterols and 2 - 10 µg/mL of purified (MBP-)ErdS or 0.4 mg/mL of total proteins from crude extracts. By doing this, both involved reactions (*i. e.* tRNA^{Asp} aspartylation and the subsequent transfer of Asp onto Erg) are coupled from the very start of the reaction.

IX.2. Erg-Gly synthesis

In contrast to ErdS, the other fungal DUF2156 protein, ErgS, is not fused to GlyRS. To optimize our chances to synthesize Erg-Gly in appreciable amounts, I adapted the above described

procedure. In this case, the LAA was performed in two steps: tRNA^{Gly} was first aminoacylated and Erg-Gly synthesis was initiated after the tRNA^{Gly} aminoacylation plateau was reached.

IX.2.1. Step 1: tRNA^{Gly} aminoacylation assay

The 2 × concentrated reaction mix was prepared and contained 200 mM Na-Hepes pH 7.2, 60 mM KCl, 20 mM MgCl2, 20 mM ATP, 0.2 mg/mL bovine serum albumin (BSA) and 140 µM [U-14C]-Gly (100 cpm/pmol). Total tRNA from yeast was purchased from Sigma-Aldrich (R8759) and dissolved in water to 46 mg/mL. 4.3 µL of total tRNA from yeast were added to 25 µl of 2 × concentrated mix and the volume was completed to 45 µl. tRNA^{Gly} aminoacylation was initiated by adding 5 µl of a S100 soluble fraction, prepared from *Sce*, and the assay was incubated at 30 °C for 1 hour. Kinetics were performed as described in (Yakobov *et al.*, 2020) to confirm the synthesis of Gly–tRNA^{Gly}.

IX.2.2. Step 2: LAA

An aliquot of commercial Erg, (solubilized in EtOH 100 % and stored at 20 mg/mL at -20 °C), was dried by evaporation at 60 °C and solubilized by sonication in an adequate volume of R buffer (100 mM Na-HEPES, 30 mM KCl, 10 mM MgCl2) to yield a 5 mg/mL preparation. As described in the previous section, Gly-tRNA^{Gly} was pre-synthesized in a reaction volume of 50 µL for 1 hour, then 10 µL of Erg (final concentration, 0.5 mg/mL) and 5-7 µg of MBP-ErdS enriched fractions were added to the reaction mixture and the volume was completed to 100 µL with R buffer. Finally, the assay was further incubated at 30 °C for 40 min.

In all cases the reaction assays were thereafter stopped by extracting lipids and radiolabeled species were revealed as described in (Yakobov *et al.*, 2020).

X. tRNA synthesis by *in vitro* transcription

X.1.   Cloning Ribozyme-tDNA constructs for *in vitro* transcription

Several ribozyme-tRNA versions were designed *in silico* using the mfold web server and 3 of them, termed v4, v5 and v6, were experimentally cloned. 4 overlapping primers, encompassing together the T7 promoter, the HMH_{wt} ribozyme, and the tDNA^{Asp}_{Afm} (corresponding to the DNA

sequence encoding the tRNA) were designed (**Table MM-5**). One of them is specific to each construction (NY183 for v4, NY184 for v5 and NY185 for v6) while the 3 remaining primers (NY186, NY187 and NY188) are common to all constructs tested here. NY188 was designed so that a dinucleotide GG is incorporated immediately downstream the 3'CCA of the tDNA, thereby generating a BstNI restriction site (CC^AGG) for run-off transcription. Importantly, tRNA$^{Asp}_{Afm}$ contains an internal BstNI restriction site, which is why A50-U64 base-pair was mutated to G50-C64. Plasmids containing HMH$_{wt}$-tDNA constructs were obtained by performing successively two isoT cloning reactions (**Figure MM-18**). However, the T5 exonuclease activity was inactivated before the first reaction (isoT 1) by pre-incubating the isoT mix 1 × at 50°C for 15 min. Then the adequate primer combinations, detailed in **Table MM-2**, were added to the pre-incubated mix (1µl of each primer at 10 µM) and primers were annealed at 50 °C for 45 min. The resulting HMH$_{wt}$-tDNA constructs are amplified by PCR with primers NY189 and NY190 and inserted through a second isoT step (isoT 2) into BamHI/HindIII double-digested pUC19 (**Figure MM-18**). Finally, isoT 2 products are transformed in *E. coli* XL1. The obtained HMH$_{wt}$-tDNA sequences and further important information's are detailed and discussed in the corresponding result sections (**Results & Discussions, Part I, § II.2.**).

X.2.   *In vitro* transcription of ribozyme-tRNA constructs

For this procedure important amounts of template plasmid are needed. 150 µg of plasmid pUC19 containing the transcription template downstream the T7 promoter, were digested O/N at 60 °C with BstNI (NEB Biolabs) (100 µl BstNI, 250 µl Buffer 3.1, 150 µg of DNA in a final reaction volume of 2.5 ml). Linearized nucleic acids are purified by phenol/chloroform extraction and precipitated as described above. For each assay, 50 µg of DNA are transcribed in TMSDT buffer 1 × (40 mM Tris-HCl pH 8.0, 30 mM MgCl2, 0.01 % (v/v) Triton X100, 0.2 mM spermidine, 1 mM DTT) supplemented with 4 mM of each RiboNucleotides Tri-Phosphates (rNTPs) stabilized at pH 8.0 (ATP, UTP, GTP and CTP) and 16 mM GMP in a total volume of 500 µL. The excess of GMP is important to favorize 5'-monophosphate ended transcripts. Finally, around 5 µg of T7 RNA polymerase are added and transcription is performed at 37°C for at 3 h. The appearance of a white precipitate, corresponding to magnesium pyrophosphate, evidences tRNA T7 polymerase activity and can be removed by adding 10 units of inorganic pyrophosphatase. Reaction assays are pooled together

Name	Sequence 5' to 3'	Used as/for
NY183	TAATACGACTCACTATAGGGTTAGCTACGCGAGGACTGACGAGTCTCTGAG	Primer 1 for **v4** (fwd)
NY184	TAATACGACTCACTATAGGGTTAGCCCTCGAGGACTGACGAGTCTCTGAG	Primer 1 for **v5** (fwd)
NY185	TAATACGACTCACTATAGGGTTAGCTtCGCGAGGACTGACGAGTCTCTGAG	Primer 1 for **v6** (fwd)
NY186	GACTCTTCTTGCGAAGAGTTTCGTCTCATCTCAGAGACTCGTCAGTCCTC	Primer 2 for **v4**, **v5**, **v6** (rv)
NY187	aactcttcgcaagaagagtctcctcgatggTCTAACGGTCATGATTTCCGCTTGTCACGCGGGAG	Primer 3 for **v4**, **v5**, **v6** (fwd)
NY188	tattttt**CCTGG**CTCCCCGACgGGGAGTCGAACCCcGGTCTCCCGCGTGACAAGCGGAAATC	Primer 4 for **v4**, **v5**, **v6** (rv)
NY189	AATTCGAGCTCGGTACCCGGggatccTAATACGACTCACTATAGGG	Amplification of isoT 1 product (fwd)
NY190	atgaccatgattacgccaagctTtattttt**CCTGG**CTCCCCGACgG	Amplification of isoT 1 product (fwd)

Table MM-5: List of primers used to construct HMH$_{wt}$-tDNA transzymes. Primers NY183, NY184 and NY185 are specific to v4, v5 and v6 respectively while the remaining primers are used for three constructs, either for the annealing step (isoT 1) or to amplify isoT 1 products prior to isoT 2. The BstNI restriction site generated by inserting dinucleotide CC in primer NY188 is shown in bold. Fwd, forward primer; rv, reverse primer.
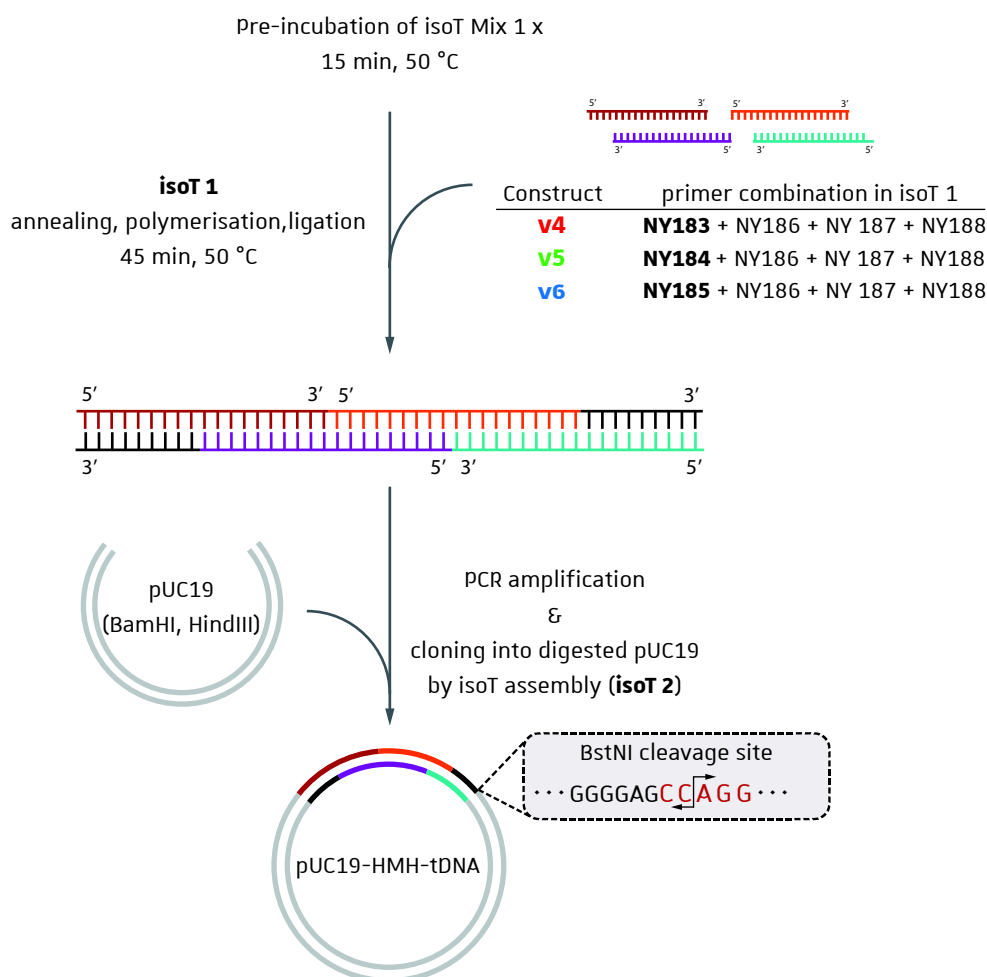
Figure MM-18: Constructing pUC19-HMH$_{wt}$-tDNA plasmids by two step isoT assembly method. Primer combinations annealed in the presence of the preincubated isoT mix are indicated a for each construction. The variable primer 1, specific for each construction is indicated in bold. Once assembled, the isoT 1 product is amplified with primers NY189/190 and the PCR product is cloned into the linearized pUC19.

and to favorize the ribozyme mediated autocatalytic cleavage, 5 volumes of transzyme buffer (50 mM Tris-HCl pH 8.0, 100 mM MgCl$_2$) are added and incubated for 1 h at 60 °C. Finally, nucleic acids are precipitated in the presence of 250 mM NaCl and 3 volumes ice-cold ethanol 100% O/N. The pellet is washed with ethanol 70 %. Note that phenol/chloroform and chloroform extractions are recommended but since the transcripts are further purified on gel (see below) these procedures are not mandatory.

Aliquots of the reaction before and after cleavage are mixed to loading buffer (95 % formamide, 1 mM EDTA, 0.025 % (w/v) bromophenol blue and xylene cyanol) and analyzed on 12 % (w/v) polyacrylamide gel containing 8 M urea.

X.3.   Purification of tRNA transcripts

To separate and purify tRNA transcripts from other contaminants present in the transcription reaction (DNA template, free nucleotides, cleaved ribozyme, remaining uncleaved ribozyme-tRNA, abortive and extended transcripts), samples are mixed to the above mentioned loading buffer, loaded on a large gel (33 cm × 40 cm × 0,2 cm) composed of 12 % (w/v) polyacrylamide (acrylamide:bisacrylamaide 29:1) and 8 M urea, and electrophoresis is achieved at 550 V (75 mA) in TBE buffer until the upper migration indicator (xylene cyanol) reaches the bottom of the gel. The gel is carefully unmolded, placed on a phosphorescent plate and observed under UV light. Each band of interest is cut out of the gel, rigorously ground, and transferred in an Schleicher & Schuell (Dassel, Germany) Biotrap in which 2 BT1 impermeable membranes delimit the cell, while an additional BT2 semi-permeable membrane, inserted adjacent to one of both BT1 membranes forms as small chamber. The cell is then placed in a tank filled with TBE and electroelution is achieved at 250 V (100 mA) for 4h at 4 °C. The transcript, which migrate between the adjacent BT1 and BT2 membranes, is recovered, purified by phenol/chloroform and chloroform extractions, precipitated, and finally resuspended in water. Note that at least a certain fraction of the obtained transcripts might be in a denatured form. To recover the scaffold of the RNA, transcripts are heated at 90 °C and slowly cooled at RT prior to *in vitro* assays.

XI. Lipid analysis and purification of aminoacylated ergosterol species

XI.1. Total lipid extraction from yeast and filamentous fungi

XI.1.1. The Bligh and Dyer method

Several lipid extraction protocols exist [reviewed in (Fuchs *et al.,* 2011)] but the "Bligh & Dyer" (Bligh and Dyer 1959) and the "Folch" (Folch *et al.,* 1957) methods remain the most widely used. A common point to all lipid extraction procedures is the employment of organic solvents. According the Bligh & Dyer procedure, lipids are extracted in a solvent mixture, composed of chloroform ($CHCl_3$) and methanol (MeOH), that must form a single homogenous phase together with the aqueous phase enclosed in the biological sample. Consequently, volumes of organic solvents that must be added are directly determined by the aqueous phase retained in the biological tissue. E. G. Bligh and W. J. Dyer determined that to yield optimal extraction, the ratio of $CHCl_3$: MeOH : aqueous phase must be 1 : 2 : 0.8 (v : v : v) . Once the extraction process is achieved, the sample is diluted to obtain a final $CHCl_3$: MeOH : aqueous phase ratio of 2 : 2 : 1.8 (v : v : v), thereby enabling phase separation. The upper aqueous phase is removed, and the lower organic phase encloses the extracted lipid content. Importantly, to avoid plastic contaminants in the lipid sample, all steps should be performed using glass equipment's, especially when preparing samples for subsequent MS analysis.

XI.1.2. Adapting the Bligh and Dyer method to samples containing aminacylated species

The standard procedure is detailed in the accompanying paper (Yakobov *et al.,* 2020) and the aim of this section is to provide some additional precisions. When investigating aaLs, the hydrolysis of the ester bond between the aa and the lipid must absolutely be prevented. This is the reason why the introduction of an acidic buffer (e. g. Na-acetate pH 4.5) is critical during lipid extraction. Furthermore, the aqueous phase of the biological sample was not taken in consideration here and lipid extraction was performed in all cases by adding a mixture of $CHCl_3$: MeOH : Na-acetate 120 mM pH 4.5 1 : 2 : 0.8 (v : v : v). In practice, *Sce* cells corresponding to 15

equivalent OD_{600} are resuspended in 0.1 mL of Na-acetate 120 mM pH 4.5 and 3.75 volumes (referring to the volume of Na-acetate added) of MeOH : $CHCl_3$ 2 : 1 (v : v) are then added. Furthermore, the cell-wall surrounding the fungi cell renders them more resistant to cell lysis which is why 1 volume of glass beads (ø 0.25 mm to 0.5 mm, Roth) are added to the mixture and mechanical cell disruption is performed in a FastPrep-24 apparatus at 6 m/s for 1 min, repeated 6 times with cooling on ice between each step. Tubes are then placed on a rotating wheel at 4 °C for 2-3 h. Additions of 1.25 volume of $CHCl_3$ and of Na-acetate 120 mM pH 4.5 are each followed by vigorous mixing (vortex for 30 sec), and phase separation is then achieved by centrifugation at 4000 × g for 10 min at 4 °C. Finally the lower phase is transferred in a clean tube, vacuum dried and either stored at -20 °C or resolubilized in an adequate volume of $CHCl_3$ or $CHCl_3$: MeOH 1 : 1 (v : v) prior to lipid analysis or lipid purification. Non-lipid contaminants can be extracted from the lipid samples with H2O, NaCl 0.5 M, KCl 0.12 M or Na-acetate 120 mM pH 4.5 added to the recovered organic phase and followed by phase separation. However, such procedures were not taken to consideration here. Importantly, as explained the volume of Na-acetate 120 mM pH 4.5 used to resuspend the biological sample, determines all other volumes added during lipid extraction and is therefore critical. This procedure was successfully scaled for the extraction of lipids from samples ranging from 50 to 2000 OD_{600} equivalent yeast cell pellets.

Similar procedures were applied to filamentous fungi, either to extract total lipids from mycelia or from conidia, but early steps of the procedure was adapted due to difficulties encountered when breaking the biological sample. After growth, mycelium is washed with sterile water and rigorously dried with towel paper. Around 2 g of it are frozen with liquid nitrogen and the mycelia is ground in a mortar with a pestle. The resulting fine powder is resuspended in 1 ml of Na-acetate 120 mM pH 4.5, 3.75 mL of MeOH : $CHCl_3$ 2 : 1 (v : v) and 2 mL of glass beads are added and the biological material is further disrupted with a FastPrep-24 apparatus (6 m/s, for 1 min repeated 8 times with cooling on ice between each cycle). The other steps of the procedure remain unchanged. Finally, a sample of 10^9 conidia is resuspended in 500 µl of Na-acetate 120 mM pH 4.5 and the following steps are adapted in consequence.

XI.1.3. Adapting the Folch method to samples containing aminacylated species

The above described protocol, adapted from the Bligh and Dyer method, was used for all lipid extractions performed during my thesis, except in one case where I wanted to test another procedure, adapted from the Folch technique, which was successfully used by M. Atila, Y. Luo to get maximal yields of aaLs (Atila and Luo 2016). In this experiment, cell pellets equivalent to 80 OD_{600} were resuspended in 0.53 mL of Na-acetate 120 mM pH 4.5 and 2 mL of MeOH : $CHCl_3$ 1 : 2 (v : v) and the mixture was vortexed for 1 min. Successive additions of 0.66 ml (0.53 mL × 1.25) of MeOH and 0.66 ml of Na-acetate 120 mM pH 4.5 were each followed by 1 min vortexing. Tubes were placed on a shaking table for 3h at 4°C and phase separation was then assisted by centrifugation at 13000 × g for 5 min. The lower organic phase was transferred in a clean tube and lipids remaining in the upper aqueous phase were further extracted by adding 0.66 ml of chloroform followed by vortexing for 1 min and by phase separation (centrifugation at 13000 × g for 5 min). Both organic phases recovered are pooled together and the sample is cleared from contaminants as follows. 0.33 ml of H_2O is added to the organic phase, the mixture is vortexed for 1 min and the organic phase is transferred in a new tube after centrifugation. Finally, the sample is dried in an argon stream. Note that in this case the amount of recovered lipids appeared me to be very low when comparing to the material usually recovered with the adapted Bligh and Dyer method. This is probably because mechanical cell disruption was omitted.

XI.2. Separation of lipids by Thin layer chromatography (TLC) and analysis

XI.2.1. The principle of the technic

One important challenge to which biochemist are often confronted is the separation of components from a complex molecular mixture. To overcome such challenges, several chromatography techniques were developed and each of them are defined by specific physicochemical properties, thereby enabling them to separate molecules according to a specific feature. Depending on the employed technique, molecules can be discriminated through their size, their affinity, their ionic charge, their solubility, or their polarity. However, the common point to all chromatography techniques is the distribution of the molecular mixture between a stationary

phase and a mobile phase. TLC belongs to this category and is widely used to separate lipids according to their polarity and their solubility. The most widespread stationary phase is silica gel (SiO$_2$), coated on glass or aluminum foils, when separating lipids by TLC. The size of the coated particles distinguishes TLC (10-50 μm) from High-performance TLC (HPTLC; 5 μm) which consequently offers better resolution. Samples are spotted near to the bottom of the silica plate, thereby defining the "starting line" (**Figure MM-19A**). Once loaded, the chromatographic support is placed in a closed tank that contain a layer of the mobile phase, also called eluent or developing solvent. The latter, which is highly apolar when analyzing lipid mixtures, raises up through capillarity and the components of the sample are differentially partitioned between the polar stationary phase and the apolar mobile phase. The more a lipid is polar, the less it is soluble in the mobile phase, the more it is strongly adsorbed to the stationary phase and the less it migrates from the starting point (**Figure MM-19B**). In contrast, apolar lipids that are even more soluble in the mobile phase, bind less tightly to the stationary phase and migrate further. In this way, each lipid has a defined retardation factor (Rf) that corresponds to the ratio between the migration distance of the lipid and the migration front (**Figure MM-19B**). Obviously, the Rf of a given compound depends on the solvent used but varies also according the ambient temperature and the saturation inside the TLC chamber. Consequently, the developing solvent must be adapted for each class of lipids and must be judiciously chosen according to the aim of the experiment. Those and several other aspects related to lipid analysis by TLC are discussed in the excellent review by B. Fuchs and colleagues (Fuchs *et al.*, 2011). Finally, lipids that migrate in the same spot after one-dimensional-TLC can be further separated through two-dimensional-TLC. In this case, the same chromatogram is dried, turned at 90 ° and submitted to a second TLC run with another eluent (**Figure MM-19C**).

XI.2.2. Monitoring TLC analysis of total lipids in the present work

Resolubilized lipids are spotted μl per μl onto 10 × 20 cm or 10 × 10 cm (height × width) silica gel TLC Al foils (Sigma-Aldrich) at 2 cm from the bottom. The quantity of spotted lipid depends to each case and must be adapted by the manipulator. It depends notably if the aim of the experiment is analytical or preparative for further analysis e. g. by MS. Furthermore, the abundance of each lipid or at least of each lipid class may vary depending on growth conditions.
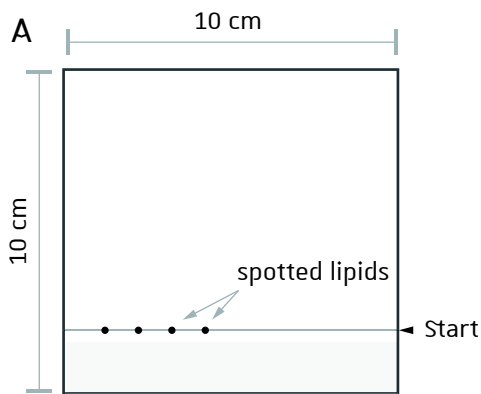
Figure MM-19: Schematic representation of lipid separation by thin layer chromatography (TLC). (A) Aluminum foils coated with silica gel were used. Resolubilized lipids are spotted µl per µl at 2 cm from the bottom and define the starting line of lipid separation. Once spotted, silica plates are placed in a closed tank containing a layer (< 2 cm) of the developing solvent (or eluent; in light grey). **(B)** Solvent A, used for 1D-TLC, migrates through up the silica plate and separates lipids according to their polarity. Each lipid has a Rf when separated with a given developing system in defined atmospheric conditions. In this illustration the Rf of lipid X is given by calculating the ratio between migration distances a and f. **(C)** Components that were not optimally separated by 1D-TLC (illustrated by green and red spots in (B)) can be further separated by 2D-TLC. The chromatogram obtained by 1D-TLC is rotated at 90 °C and 2D-TLC is achieved with a different solvent (light blue).
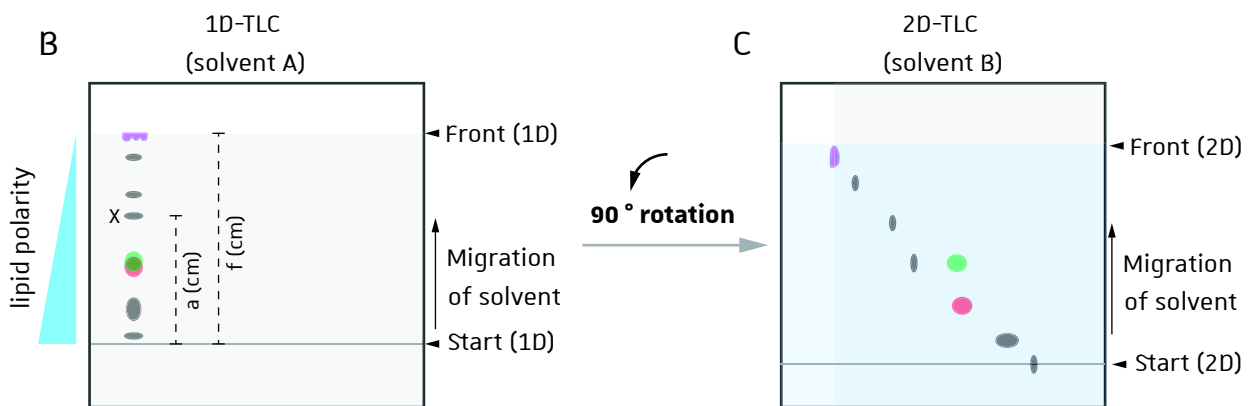
In general, lipids from *Sce* samples equivalent to 50 OD_{600} are rigorously resuspended in 50 µl ($CHCl_3$ or $CHCl_3$: MeOH 1 : 1 (v : v)) and 10 µl are spotted for TLC when targeting the Erg-Asp (≈ lipids from 10 equivalent OD_{600}). The situation is more complex when analyzing the ErgS dependent lipid and depends on the origin of the overexpressed enzyme. In fact, the relative amount of Erg-Gly recovered from *Sce* expressing ErgS*Yli* or ErgS*Bba* is high and lipids from 10 equivalent OD_{600} are largely sufficient to identify the lipid. In contrast the amount of Erg-Gly recovered from *Sce* expressing ErgS*Afm* is much lower and therefore the analyzed amount of total lipids is increased to 25 equivalent OD_{600}. This amount was not further increased because it hindered TLC migration and resolution. Note that the quantities of spotted lipids indicated here are suitable when staining thin layer chromatographs are revealed with the MnCl2 / sulfuric acid containing solution (see below). When staining the chromatograms with other reagents, the lipids of interest (i. e. Erg-Asp and Erg-Gly) were sometimes more difficult to visualize, which is why the amount of spotted lipids may increase 3-4-fold.

Lipids are separated through 1D-TLC in a 20 cm × 20 cm TLC developing chamber previously saturated with the developing system. Several solvent mixtures were assayed but the predilected developing system to visualize Erg-Asp and Erg-Gly are $CHCl_3$: MetOH : H2O 130 : 50 : 8 (188 ml) and 130 : 16 : 1 (147 ml), respectively. Other solvent systems used in this work are specified in result sections. The spotted Silica plate is placed into the chamber and separation is stopped after 10 min at RT by removing the plate from the chamber. By doing this, the migration front is optimally located about 8-8.5 cm from the bottom. Finally, thin layer chromatograms are dried. For 2D-TLC, each sample is analyzed on a distinct silica plate and the developing system used for the second elution is hexane : MeOH : $CHCl_3$: glacial acetic acid 60 : 20 : 10 : 10 (v : v : v : v).

XI.2.3. Silica plates staining procedures

Obviously, choosing the adapted staining method is important, and during my thesis this point came out to be critical as discussed in the results sections. The standard procedures are detailed in the accompanying paper (Yakobov *et al.,* 2020). Note that several lipid staining methods exists with some of them considered as universal, while other reveal specifically a class of lipid [main technics reviewed in (Fuchs *et al.,* 2011) and exhaustively listed in (Mahida 2019)]. For example, Ninhydrin and Bromocresol green reveal specifically the presence of amine and carboxyl

containing lipids while α-Naphthol, 5-Hydroxy-1-tetralone and orcinol are used to detect glycolipids. Phosphomolybdate reveals phospholipids and iodine vapor stains unsaturated compounds.

Interestingly, a staining solution containing acid ferric chloride and sulfuric acid, was shown to stain Cholesterol (closely related to Ergosterol) in red to violet dots but free Cholesterol is more rapidly stained than Cholesterol esters. This staining method does also reveal fatty acid containing lipids but in distinguishable colors. A very similar staining method, based on manganese chloride ($MnCl_2$) and sulfuric acid was also described to stain distinctly cholesterol and bile acids on TLC (Goswami and Frey 1970). Importantly, the $MnCl_2$ based technic stains Cholesterol and Cholesterol esters in pink, Ergosterol and Ergosterol esters in dark brown and phospholipids light brown under white light. Moreover, thin layer chromatograms stained with the latter technic can be visualized under UV light (254 or 315 nm). In this case Ergosterol and esters of it become even more distinguishable from other lipids and are revealed in orange.

The $MnCl_2$ / Sulfuric acid staining solution is composed of 0,8 mg $MnCl_2$ tetrahydrate, 9 ml concentrated sulfuric acid, 120 ml MeOH and 120 ml H_2O and was predominantly used in this work. Plates are dipped for few seconds in the solution and heated at 100 °C until the lipid spots appeared appreciably enough. Overheating burns the lipidic spots, thereby rendering them unexploitable. Alternatively, the plates can be sprayed with the solution and then heated. However, there was a debate if the spraying and dipping methods give identical results (Vasta 2008). For enhanced precision and reproducibility, it is recommended to privilege the dipping method especially when samples are compared, but in this case particular care should be taken regarding the solubility of analyzed compounds in the staining solution (Mahida 2019).

XI.2.4. Additional remarks

The quantities of total lipids extracted from a biological sample, and thus the standardization of TLC, are more difficult to determine in comparison to well-established methods for protein and nucleic-acid analysis. One reason for that is the important heterogeneity of lipid classes especially in eukaryotic cells. Some techniques exist to overcome this issue such as the Sulfo-Phospho-Vanillin assay (SPVA) which is a colorimetric technique commonly used to

determine relative amounts of unsaturated lipids in solution (Chabrol 1937; Knight *et al.,* 1972; McMahon *et al.,* 2013). An important advantage of this technique is that the chromophore produced during the colorimetric reaction absorbs at 535 nm and is therefore quantifiable with a spectrophotometer. However, because the lipids of interest are sterols here and for other reasons that will not be discussed, I did not quantify the amounts of extracted lipids prior to TLC analysis. For comparative studies, such as analysis of lipids from strains expressing proteins with single or domain mutations, total lipids were extracted at the same time from equivalent cell pellets. Lipids were resuspended in equal volumes and spotted on the same silica plate. Despite this, TLC results clearly showed heterogeneities in the amounts of extracted lipids. Consequently, variations of modified Erg species are standardized once the chromatogram is stained as described below.

Separated lipids also can be quantified directly from the developed and stained chromatogram. One possibility that will probably be very useful in the future of this project is to use filipin, a strong fluorophore known to interact with sterols such as cholesterol and ergosterol (Smejkal *et al.,* 1996). In this case, developed plates are stained with a filipin solution and spots are visualized and quantified under UV light at 365 nm. The quantification was reported to be linear for cholesterol amounts ranging from 5 to 3000 ng. Both quantification method should be taken in consideration in the future to determine the amount total lipids extracted and to estimate the ratio of aminoacylated ergosterol. Note also that filipin is widely used as a marker of ergosterol from conidia and mycelia membranes (Van Leeuwen *et al.,* 2008).

In this work however we choose another alternative that allowed as encompass *1)* the above-mentioned issue concerning the difficulty to standardize the amount of lipids spotted on TLC and *2)* the relative variations of aminoacylated lipids with respect to the tested conditions or the expressed enzyme versions (i. e. mutants). Quantification of spots containing DUF2156 dependent lipids (LX), PE, or PG was performed using the ImageJ software. Lipid spots signals (number of pixels, N) were normalized to that of PE (N_{LX}/N_{PE}). Furthermore, in the absence of LX, PG becomes visible at the same position; the PG/PE signal thus represents the background signal in the absence of LX.

XI.3.   Purification of aminoacylated lipids

Lipids of interest are purified by column chromatography with a stationary phase consisting of Silica Gel and consequently, the separation principle is very similar to TLC. The mobile phases used to elute successively different class of lipids are composed of $CHCl_3$ and MeOH which are both volatile. Therefore, all solutions are prepared in glass bottles just before the experiments. Before starting one should ensure that the glass column is free from any trace of aqueous liquids and the empty column, including the sinter, is washed several times with CHCl3. The column is placed on a support and all collecting tubes are annotated and placed on an adequate rack. An adequate amount of Silica Gel is resuspended in CHCl3 100 % so that the initially white powder becomes translucid, and volumes of this suspension are sequentially poured into a glass column until the required volume of packed silica beads is reached. From then on, the stationary phase should always be recovered by liquid mixtures since drying out the column would destabilize the chromatographic procedure. Furthermore, to prevent the packed resin to be resuspended, all added solutions are slowly flowed along the column wall. The resin is equilibrated with 5 column volumes of $CHCl_3$ and the lipid sample, resolubilized in $CHCl_3$, is slowly applied when the liquid level of the last wash forms a thin meniscus above the stationary phase. Once the sample is absorbed into the column, lipid classes are sequentially eluted with organic solvents according to their polarity. Lipid fraction are vacuum dried, resuspended in CHCl3 or CHCl3 : MetOH (1 : 1), spotted onto Silica plates, separated by TLC with the adequate developing system and finally revealed with the MnCl2 / Sulfuric acid containing staining solution. Fractions are dried again and stored at -20 °C.

XI.3.1. Erg-Asp purification

Sce strains expressing ErdS are grown in 500 mL SC-Leu media and culture is stopped by centrifugation (4,000 × *g* for 15 min at 4 °C) when the culture reaches OD_{600} = 1.0. Total lipids are extracted as described above and resolubilized in 200 μl of $CHCl_3$ extemporaneously. The column bed volume is 1.5 ml of Silica Gel, prepared and equilibrated as described above, and the total lipid sample is then manually applied. Afterwards, nonpolar lipids and glycolipids are washed away by adding 10 mL of CHCl3 followed by 10 mL acetone, respectively. 20 mL of CHCl3 : MetOH ratios

ranging from 9 : 1 to 5 : 5 (v : v) are then sequentially added and collected in 2 mL fractions. Finally, the purification is achieved with 20 mL of MetOH also collected in fractions of 2 mL. A total of 60 fractions are vacuum dried, resuspended in 35 µl of chloroform and 10 µl is analyzed by TLC performed with developing solution CHCl3 : MetOH : H2O 130 : 50 : 8.

XI.3.2. Erg-Gly purification from *Sce* expressing ErgS*Afm*

Sce wt and the strain expressing ErdS*Afm* are grown in 1 L SC-Leu media and culture is stopped by centrifugation (4,000 × *g* for 15 min at 4 °C) when the culture reaches OD600 = 1.0. Total lipids are extracted as described above and in the present case it is extremely important to completely dry the lipid sample, thereby removing any traces of methanol. The $CHCl_3$: MetOH mixtures used here contain very low proportions of methanol which gradually increases during elution by a 2-fold factor. To avoid errors and to enhance de reproducibility of the results, CHCl3 : MetOH mixtures with ratios going from 18 : 1 to 288 : 1 (v : v) are prepared by performing serial dilutions from an initial CHCl3 : MetOH 9 : 1 (v : v) solution. The column is prepared identically as for Erg-Asp purification (*i. e.* column bed volume: 1.5 mL) and the lipid sample, extemporaneously resolubilized in 400 µl of $CHCl_3$, is applied onto the Silica resin. 15 mL of $CHCl_3$ are added and collected in 3 fractions of 5 mL. The same procedure is sequentially repeated with $CHCl_3$: MetOH mixtures with ratios 144 : 1 to 72 : 1 (v : v). The resulting fractions, containing 5 mL eluates, are vacuum dried, lipids are resuspended in 100 µl of $CHCl_3$ and an aliquot of each fraction is analyzed by TLC (developing buffer $CHCl_3$: MetOH : H2O 130 : 16 : 1 (v : v)) (**Figure MM-20A**).

Fractions containing the highest amount of the modified lipid are pooled together and subjected to a second Silica Gel chromatography round. The column is freshly prepared as described above, lipids are absorbed onto the Silica resin, elution is performed successively with 15 mL of chloroform and 15 mL of CHCl3 : MetOH 288 : 1 (v : v) and eluates are collected into 1 mL fractions. Dried lipids are resuspended in 50 µl of CHCl3 and 25 µl are analyzed by TLC (**Figure MM-20B**).

XI.3.3. Erg-Gly extraction and purification from *Yli* and from *Sce* expressing ErgS*Yli*

Yli and *Sce* wt are grown in YPD and *Sce* expressing ErgS*Yli* is grown in SC-Leu. Cultures were diluted to OD_{600} = 0.1, grown O/N and the next morning cells were harvested by centrifugation at 5000 × g for 15 min at 4°C. 5 g of cells were obtained from a 500 ml culture of *Yli* harvested at OD_{600} = 3.8; 3.5 g of cells were obtained from a 500 ml culture of *Sce* wt harvested at OD_{600} = 4.5; 4 g of cells were obtained from a 1 L culture of *Sce* expressing ErgS*Yli* harvested at OD_{600} = 2. In all cases, cells are resuspended in 15 ml Na-acetate 120 mM pH 4.5 and mechanically lysed with a FastPrep-24 apparatus in the presence of glass beads (ø 0.25 mm to 0.5 mm, Roth) at 6 m/s, for 1 min repeated 5 times, with cooling on ice between each step. In this cases the 3.75 volumes of MetOH : CHCl3 2 : 1 (i. e. 56.25 mL) are added in two steps. First 28.125 ml ((15 × 3.75) / 2) of MetOH : CHCl3 2 : 1 are added and 3 additional shacking runs are performed. Then, the 3.75 volumes of MetOH : CHCl3 2 : 1 are completed by adding another 28.125 ml and tubes are placed on a rotating wheel at 4 °C for 3 h. The following total lipid extraction step remain unchanged with respect to the general procedure described in previous sections.

To purify the lipid of interest from total lipid fractions, obtained as described in the previous section, we built a silica gel column as in (Yakobov *et al.*, 2020). However, the size of the column was increased since 8 mL of Silicia Gel were poured into a 1 cm x 20 cm chromatography column. The stationary phase was washed with 4 column volumes of CHCl3 and total lipids, resuspended in 500 µl ultrapure CHCl3, were injected manually on the top of the silica gel. Volumes used to elute lipids are increased so that each collected fraction corresponds to 1 column volume. In this way lipids were then gradually eluted as follow: 4 x 8 mL CHCl3; 3 x 8 mL CHCl3: MetOH (144:1); 3 x 8 mL CHCl3: MetOH (72:1) and 2 x 8 mL CHCl3: MetOH (36:1). Lipids were dried as previously described, resuspended in 200 µL CHCl3: Methanol (1:1) and analyzed by TLC.

XII. Appendix: Table MM-1: List of strains
Table MM-2: List of plasmids and primers

Table MM-1: List of strains. All strains that were stored in the strain collection of Pr. H. Becker's Lab are listed (Labcollector). Note that some strains, in particular E. coli strains used for overexpression and purification of proteins (i.e. E. coli Rosetta-2 or Star-2 strains) and some S. cerevisiae strains, were not stored. To avoid any confusion, both ergosteryl-aminoacid synthases are distinguished as ErgS and ErdS. Tags are highlighted with distinct colors. For more information on those strains please refer to Labcollector of Pr. H. Becker's Lab.

LabCollector	Genotype	Comments
Bacterial strains for plasmid storage	
	ε. coli XL-1 Blue : *endA1 gyrA96(nalR) thi-1 recA1 relA1 lac glnV44 F'[::Tn10 proAB+ lacIq Δ(lacZ)M15] hsdR17(rK- mK+)*	
	ε. coli TOP10 : *F- mcrA Δ(mrr-hsdRMS-mcrBC) φ80lacZΔM15 ΔlacX74 nupG recA1 araD139 Δ(ara-leu)7697 galε15 galK16 rpsL(StrR) endA1 λ-*	
	ε. coli DH5 α : *F– endA1 glnV44 thi-1 recA1 relA1 gyrA96 deoR nupG purB20 φ80dlacZΔM15 Δ(lacZYA-argF)U169, hsdR17(rK–mK+), λ–*	
	ε. coli DB3.1 : *F- gyrA462 endA1 glnV44 Δ(sr1-recA) mcrB mrr hsdS20(rB-, mB-) ara14 galK2 lacY1 proA2 rpsL20(Smr) xyl5 Δleu mtl1*	
702	**ε. coli XL-1 Blue + pUC57-ErdS**	
703	**ε. coli XL-1 Blue + pUC57-Er *g* S**	
719	**ε. coli TOP10 + p415ADH-ErdS**	
720	**ε. coli TOP10 + p415ADH-Er *g* S**	
721	**ε. coli TOP10 + pDONR221-ErdS wo stop codon**	
722	**ε. coli TOP10 + pDONR221-Er *g* S wo stop codon** (clone 17)	
723	**ε. coli TOP10 + pDONR221-Er *g* S wo stop codon** (clone 18)	
724	**ε. coli TOP10 + pDONR221-Er *g* S** (clone 25)	
725	**ε. coli TOP10 + pDONR221-Er *g* S** (clone 27)	
726	**ε. coli XL-1 Blue + p415GPD-ErgS- HA** (clone 14)	
727	**ε. coli XL-1 Blue + p415GPD-ErgS- HA** (clone 20)	
728	**ε. coli XL-1 Blue +p415GPD-ErdS- Δ duf2156- HA** (clone 2) **[KO]**	AspRS encoded by this plasmid is inactive and does not complement Sce Δdps1. For ErdS-Δduf2156 active forms see: 1382-1389
729	**ε. coli XL-1 Blue +p415GPD-ErdS- Δ duf2156- HA** (clone 8) **[KO]**	
730	**ε. coli TOP10 + pDONR221-ErdS-Δdrs** (clone 2)	
731	**ε. coli TOP10 + pDONR221-ErdS-Δdrs** (clone 8)	
732	**ε. coli TOP10 + pDONR221-ErdS-Δduf2156** (clone 2) **[KO]**	AspRS encoded by this plasmid is inactive and does not complement Sce Δdps1. For ErdS-Δduf2156 active forms see: 1382-1389
733	**ε. coli TOP10 + pDONR221-ErdS-Δduf2156** (clone 5) **[KO]**	
734	**ε. coli TOP10 + pDONR221-ErdS-Δdrs wo stop codon** (clone 4)	
735	**ε. coli TOP10 + pDONR221-ErdS-Δdrs wo stop codon** (clone 5)	
748	**ε. coli TOP10 + pDONR221-ErdS-Δduf2156 wo stop codon**	AspRS encoded by this plasmid is inactive and does not complement Sce Δdps1. For ErdS-Δduf2156 active forms see: 1382-1389
749	**ε. coli TOP10 + pDONR221-ErdS-Δduf2156 wo stop codon** (clone 15) **[KO]**	
751	**ε. coli TOP10 + pRS415-ErdS-Δdrs- HA** (clone 2)	
752	**ε. coli TOP10 + pRS415-ErdS-Δdrs- HA** (clone 7)	
753	**ε. coli TOP10 + pRS415-ErdS-Δdrs** (clone 4)	
754	**ε. coli TOP10 + pRS415-ErdS-Δdrs** (clone 12)	
755	**ε. coli TOP10 + pRS415-ErdS-Δduf2156- HA** (clone 1) **[KO]**	AspRS encoded by this plasmid is inactive and does not complement Sce Δdps1 . For ErdS-Δduf2156 active forms see: 1382-1389
756	**ε. coli TOP10 + pRS415-ErdS-Δduf2156- HA** (clone 10) **[KO]**	
757	**ε. coli TOP10 + pRS415-ErdS-Δduf2156** (clone 1) **[KO]**	
758	**ε. coli TOP10 + pRS415-ErdS-Δduf2156** (clone 2) **[KO]**	
761	**ε. coli TOP10 + pRS415-ErdS-Δduf2156- HA** (clone 4)	
762	**ε. coli TOP10 + pRS415-ErdS-Δduf2156- HA** (clone 8)	
766	**ε. coli XL1 blue + pDONR221-ErdS** (clone 8)	
767	**ε. coli XL1 blue + pDONR221-ErdS** (clone 11)	
782	**ε. coli XL1 blue + pRS415GPD-ErdS** (clone 1)	
783	**ε. coli XL1 blue + pRS415GPD-ErdS** (clone 2)	
790	**ε. coli XL1 blue + pRS414GPD-Er *g* S**	

791	*E. coli XL1 blue + pRS414GPD-ErdS- Δdrs*	
799	*E. coli XL1 blue + pRS415GPD-ErdS- GFP*	
800	*E. coli XL1 blue + pRS415GPD-Er g S- GFP*	
801	*E. coli XL1 blue + pGGWA-ErdS*	ErdS with GST-tag at its Nt and His6x-tag at its Ct
802	*E. coli XL1 blue + pGGWA-Er g S*	ErgS with GST-tag at its Nt and His6x-tag at its Ct
875	*E. coli XL1 blue + pRS415GPD-Cer-Er g S (clone 5)*	
876	*E. coli XL1 blue + pRS415GPD-Cer-Er g S (clone 6)*	
883	*E. coli DH5α + p His6x -tev-GWA-ErdS- His6X*	
884	*E. coli DH5α + p His6x -tev-GWA-Er g S- His6X*	
929	*E. coli DH5α + pDONR221- Δ192-Er g S*	
930	*E. coli DH5α + pDONR221- Δ192-Er g S wo stop codon*	
947	*E. coli DH5α + p His6x -tev-GWA-Δ192-Er g S*	
948	*E. coli DH5α + p His6x -tev-GWA-Δ192-Er g S- His6X*	
955	*E. coli DH5α + pRS415GPD-ErdS- Δdrs- EGFP*	
956	*E. coli DH5α + pRS415GPD-Δ192-Er g S- EGFP*	
990	*E. coli DH5α + pRS415GPD- EGFP -ErdS*	
1037	*E. coli XL1 blue + pJET-Nt192-Er g S wo stop codon*	Nt192: 192 first residues of ErgS protein
1038	*E. coli XL1 blue + pJET-Nt192-Er g S*	
1047	*E. coli DH5α + pDONR221-Nt192-Er g S wo stop codon*	
1048	*E. coli DH5α + pDONR221-Nt192-Er g S*	
1053	*E. coli DH5α + pRS415GPD-Nt192-Er g S- HA*	
1054	*E. coli DH5α + pRS415GPD-Nt192-Er g S- EGFP*	
1055	*E. coli DH5α + pRS425GPD-ErdS-TAP*	
1056	*E. coli DH5α + pRS425GPD-Er g S-TAP*	
1058	*E. coli DH5α + pRS415GPD-Er g S-TAP*	
1059	*E. coli DH5α + pRS415GPD-ErdS-TAP*	
1081	*E. coli DH5α + pDONR221-Nt139-Er g S wo stop codon*	Nt139: 139 first residues of ErgS protein
1082	*E. coli DH5α + pDONR221-Nt(139-163)-Er g S wo stop codon*	Nt(139-163): residues 139 to 163 of ErgS Nt extension
1084	*E. coli DH5α + pRS414GPD- Cer -Nt192-Er g S*	
1085	*E. coli DH5α + pRS414GPD- Cer -Nt139-Er g S wo stop codon*	
1086	*E. coli DH5α + pRS414GPD- Cer -Nt(139-163)-Er g S wo stop codon*	
1087	*E. coli DH5α + pRS414GPD- Cer -Nt(163-199)-Er g S wo stop codon*	
1088	*E. coli XL1 blue + pRS415GPD-Nt139-Er g S- EFP*	
1089	*E. coli DH5α + pRS415GPD-Nt(139-163)-Er g S- EFP*	
1090	*E. coli DH5α + pRS415GPD-Nt(163-199)-Er g S- EFP*	
1120	*E. coli DH5α + p M GWA-ErdS- His6X*	
1021	*E. coli DH5α + p M GWA-Er g S- His6X*	
1022	*E. coli DH5α + p M GWA- Δ192-Er g S- His6X*	
1183	*E. coli DH5α + p M tevGWA-ErdS*	
1184	*E. coli DH5α + p M tevGWA-Er g S*	
1372	*E. coli DH5α + pRS415GPD- Δ192-Er g S*	
1377	*E. coli DB3.1 + p M tevGWA-ccdB*	
1383	*E. coli DH5α + pDONR221-ErdS- Δduf2156 wo stop codon [OK]*	
1384	*E. coli DH5α + pDONR221-Δ84-ErdS- Δduf2156 [OK]*	
1385	*E. coli DH5α + pDONR221-Δ84-ErdS- Δduf2156 wo stop codon [OK]*	
1386	*E. coli DH5α + pRS414GPD-Δ84-ErdS- Δduf2156 [OK]*	
1387	*E. coli DH5α + pRS414GPD-ErdS-Δduf2156 [OK]*	
1388	*E. coli DH5α + pRS415GPD-ErdS-Δduf2156 [OK]*	
1389	*E. coli DH5α + pRS415GPD-Δ84-ErdS- Δduf2156 [OK]*	
1390	*E. coli DH5α + pRS415GPD-ErdS AAPA*	ErdS with QSPQ signature sequence of AspRS mutated to AAPA
1391	*E. coli DH5α + pRS415GPD-ErdS-KR α5A*	ErdS residues R749, K750, R752, R753 mutated to A
1392	*E. coli DH5α + pRS415GPD-ErdS-KR α5E*	ErdS residues R749, K750, R752, R753 mutated to E

1393	*E. coli DH5α + pRS415GPD-ErdS-W785A*	
1394	*E. coli DH5α + pRS415GPD-ErdS-W785H*	
1395	*E. coli DH5α + pRS415GPD-ErdS-R789E*	
1417	*E. coli DH5α + pCOLDI (from Takara)*	
1418	*E. coli DH5α + pCOLDI-ErdS_Aor*	
1421	*E. coli DH5α + pRS415GPD-ErdS _{AAPA} - HA*	ErdS with QSPQ signature sequence of AspRS mutated to AAPA
1422	*E. coli DH5α + pRS415GPD-ErdS-KR α5A- HA*	ErdS residues R749, K750, R752, R753 mutated to A
1423	*E. coli DH5α + pRS415GPD-ErdS-KR α5E- HA*	ErdS residues R749, K750, R752, R753 mutated to E
1424	*E. coli DH5α + pRS415GPD-ErdS-W785A- HA*	
1425	*E. coli DH5α + pRS415GPD-ErdS-W785H- HA*	
1426	*E. coli DH5α + pRS415GPD-ErdS-R789E- HA*	
1443	*E. coli DH5α + pRS415GPD-ErdS- Δduf2156- HA*	
1444	*E. coli DH5α + pMtevGWA-ErdS-Δduf2156*	
1447	*E. coli DH5α + pDONR221-ErdS_Aor*	
1448	*E. coli DH5α + pDONR221-ErdS_Aor wo stop codon*	
1449	*E. coli DH5α + pRS415GPD-ErdS_Aor- EGFP*	
1450	*E. coli DH5α + pRS415GPD-ErdS_Aor- HA*	
1452	*E. coli DH5α + pDONR221-ErdS-N677A*	
1453	*E. coli DH5α + pDONR221-ErdS-E712R*	
1454	*E. coli DH5α + pDONR221-ErdS-E731R*	
1455	*E. coli DH5α + pDONR221-ErdS-Q836R*	
1456	*E. coli DH5α + pDONR221-ErdS-K838E*	
1457	*E. coli DH5α + pDONR221-ErdS-Q836-K838E*	
1458	*E. coli DH5α + pMtevGWA-ErdS_Aor*	
1464	*E. coli DH5α + pRS415GPD-ErdS-N677A*	
1465	*E. coli DH5α + pRS415GPD-ErdS-E712R*	
1466	*E. coli DH5α + pRS415GPD-ErdS-E731R*	
1467	*E. coli DH5α + pRS415GPD-ErdS-Q836R*	
1468	*E. coli DH5α + pRS415GPD-ErdS-K838E*	
1469	*E. coli DH5α + pRS415GPD-ErdS-Q836-K838E*	
1504	*E. coli DH5α + pJet-DerdS K7*	K7 for deletion of erdS in *Afm*
1513	*E. coli DH5α + pRS415GPD- Δ30-ErdS*	
1514	*E. coli DH5α + pRS415GPD- Δ60-ErdS*	
1515	*E. coli DH5α + pRS415GPD- Δ84-ErdS*	
1519	*E. coli DH5α + pRS415GPD- Δ30-ErdS- HA*	
1520	*E. coli DH5α + pRS415GPD- Δ60-ErdS- HA*	
1521	*E. coli DH5α + pRS415GPD- Δ84-ErdS- HA*	
1522	*E. coli DH5α + pRS415GPD- Δ30-ErdS-Δduf2156- HA*	
1523	*E. coli DH5α + pRS415GPD- Δ60-ErdS-Δduf2156- HA*	
1524	*E. coli DH5α + pRS415GPD- Δ84-ErdS-Δduf2156- HA*	
1525	*E. coli DH5α + p M tevGWA-ErdS-Q836R*	
1528	*E. coli DH5α + pJET-er g S_Yli deletion K7* (clone 2)	
1529	*E. coli DH5α + pJET-er g S_Yli deletion K7* (clone 3)	
1530	*E. coli DH5α + pJET-5'[1.5kb]-er g S_Yli*	
1531	*E. coli DH5α + pJET-3'[1.5kb]-er g S_Yli*	
1569	*E. coli DH5α + p M tevGWA- Δ84-ErdS*	
1620	*E. coli DH5α + pJET-ATG1[-/+1kb]_Afm* (clone 4)	
1621	*E. coli DH5α + pJET-ATG1[-/+1kb]_Afm* (clone 6)	
1648	*E. coli DB3.1 + p G M tevGWA-ccdB*	
1649	*E. coli DH5α + p G M tevGWA-ErdS-Δdrs*	
1650	*E. coli DH5α + p G M tevGWA-ErdS*	
1651	*E. coli DH5α + pJET- GFP -ATG8_Afm*	
1703	*E. coli DH5α + pPKS529a-5'[1kb]- GFP -ATG8_Afm-K7* (clone7)	5'[1kb] = ATG8_Afm 1 kb upstream sequence
1704	*E. coli DH5α + pPKS529a-5'[1kb]- GFP -ATG8_Afm-K8* (clone23)	

1705	*E. coli DH5α + p G M tev-Er g S*	
1707	*E. coli DH5α + PKS529a*	pKS529 in which KanR was replaced by AmpR
1740	*E. coli DH5α + pPKS529a-5'[1kb]- GFP -ATG8_Afm-3'[1kb] K7*	
1749	*E. coli DH5α + pPTRI (from Takara)*	A. fumigatus - E.coli shuttle vector
1750	*E. coli DH5α + pPTRII (from Takara)*	A. fumigatus - E.coli shuttle vector
1831	*E. coli XL1 blue + pRS415GPD-ErdS-T643A*	
1832	*E. coli XL1 blue + pXyl-Er g S⁕R* (clone 23)	early stop codon mutated to R
1833	*E. coli XL1 blue + pXyl-Er g S⁕R* (clone 29)	early stop codon mutated to R
1834	*E. coli XL1 blue + pRS415GPD-ErdS-Y637F*	
1835	*E. coli XL1 blue + pRS415GPD-ErdS-T641A*	
1836	*E. coli XL1 blue + pRS415GPD-ErdS-S642A* (clone 3)	
1837	*E. coli XL1 blue + pRS415GPD-ErdS-S642A* (clone 5)	
1849	*E. coli XL1 blue + pRS415GPD-ErdS-S644A* (clone 5)	
1850	*E. coli XL1 blue + pRS415GPD-ErdS-W645A*	
1851	*E. coli XL1 blue + pRS415GPD-ErdS-D647R*	
1852	*E. coli XL1 blue + pRS415GPD-ErdS-R649E*	
1853	*E. coli XL1 blue + pRS415GPD-ErdS_Aor(1-603)*	ErdS_Aor-Δduf2156
1854	*E. coli XL1 blue + pPTRII-ErdS[-/+1kb]*	
1855	*E. coli XL1 blue + pRS415GPD-ErdS-C728A*	
1856	*E. coli XL1 blue + pRS415GPD-ErdS-K790E*	
1857	*E. coli XL1 blue + pRS415GPD-ErdS-G791A*	
1858	*E. coli XL1 blue + pRS415GPD-ErdS-Q793R*	
1859	*E. coli XL1 blue + pRS415GPD-ErdS-H795A*	
1860	*E. coli XL1 blue + pRS415GPD-ErdS-E798R*	
1861	*E. coli XL1 blue + pRS415GPD-ErdS-W802A*	
1862	*E. coli XL1 blue + pRS415GPD-ErdS-F913A*	
1913	*E. coli XL1 blue + pUC-Ribozyme-tRNA$^{Asp}_{Afm}$ [KO]*	Ribozyme sequence based on Fechter *et al*. 1998. Please take care, some essential residues are lacking in the ribozyme sequence (refer to the attached plasmid map). Not suitable for tRNA$^{Asp}_{Afm}$ transcript synthesis.
1914	*E. coli XL1 blue + pRS415GPD-ErdS-Y637F*	same than 1834
1915	*E. coli XL1 blue + pRS415GPD-ErdS-K916E*	
1937	*E. coli XL1 blue + pRS414GPD-ErdH*	
1938	*E. coli XL1 blue + pRS414GPD- EGFP -ErdH*	
1939	*E. coli XL1 blue + pMtevGWA-ErdH*	
1940	*E. coli XL1 blue + pJET1.2- GFP -ATG8-hygR (pGA8H)*	
1941	*E. coli XL1 blue + pJET1.2- GFP -ATG8-hygR-AMA1 (pGA8HA1)* (clone 9)	*AMA1* amplified from pPTRII and subcloned into pGA8H
1942	*E. coli XL1 blue + pJET1.2- GFP -ATG8-hygR-AMA1 (pGA8HA1)* (clone 11)	
1961	*E. coli XL1 blue + pRS425GPD-Er g S-K321E-R322E*	
1962	*E. coli XL1 blue + pRS425GPD-Er g S-Q326A-N327A-R328E-Q329A*	
1963	*E. coli XL1 blue + pRS425GPD-Er g S-R368E*	
1964	*E. coli XL1 blue + pRS425GPD-Er g S-Q375R*	
1965	*E. coli XL1 blue + pRS425GPD-Er g S-R409E*	
1966	*E. coli XL1 blue + pRS425GPD-Er g S-N332A-K335E*	
1967	*E. coli XL1 blue + pRS425GPD-Er g S-D420R*	
1969	*E. coli XL1 blue + pMtevGWA-Er g S-His6X* (clone5)	
1970	*E. coli XL1 blue + pMtevGWA-Er g S-His6X* (clone6)	
1977	*E. coli XL1 blue + pRS425GPD-Er g S*	
????	*E. coli XL1 blue + p M tevGWA-ErdH-S153A*	
1978	*E. coli XL1 blue + p M tevGWA-ErdH-D277A*	
1979	*E. coli XL1 blue + p M tevGWA-ErdH-H307A*	
1980	*E. coli XL1 blue + p M tevGWA-ErdH-K311D*	

1994	*E. coli XL1 blue + pRS415GPD-* **MBP** *-Er* **g** *S-* **His6X**	
1995	*E. coli XL1 blue + pRS415GPD-* **MBP** *-Er* **g** *S*	
1996	*E. coli XL1 blue + pRS425GPD-Er* **g** *S-W364A*	
1997	*E. coli XL1 blue + pRS425GPD-Er* **g** *S-R365E*	
2009	*E. coli XL1 blue + pRS425GPD-Er* **g** *S-R328E*	
2010	*E. coli XL1 blue + pRS425GPD-Er* **g** *S-N332A*	
2011	*E. coli XL1 blue + pRS425GPD-Er* **g** *S-K335E*	
2012	*E. coli XL1 blue + pRS425GPD-Er* **g** *S-R328E-K335E*	
2014	*E. coli XL1 blue + pPKS529a-Er d S recomp K7*	not pXyl overexpression
2017	*E. coli XL1 blue + p* **M** *tevGWA-ErdS-* Δ*drs-KRa5E*	
2018	*E. coli XL1 blue + pRS415GPD-Er* **g** *S*	
2041	*E. coli XL1 blue + pRS414GPD-ErdH-* **EGFP**	
2042	*E. coli XL1 blue + pRS414GPD-ErdH-* **EGFP**	
2043	*E. coli XL1 blue + p* **His6X** *-* **M** *tev-ErdS*	
2044	*E. coli XL1 blue + p* **His6X** *-* **M** *tev-ErdS*	
2060	*E. coli XL1 blue + pUC19-Ribozyme-tRNA$^{Asp}_{Afm}$ - G50-C64* **[KO]** (clone 1)	Ribozyme sequence based on Fechter *et al*. 1998. Please take care, some essential residues are lacking in the ribozyme sequence (refer to the attached plasmid map). Not suitable for tRNA^{Asp}
2061	*E. coli XL1 blue + pUC19-Ribozyme-tRNA$^{Asp}_{Afm}$ - G50-C64* **[KO]** (clone 2)	transcript synthesis. A50-C64 mutated to G50-C64.
2098	*E. coli XL1 blue + pRS415GPD-Er* **g** *S_Bba*	
2099	*E. coli XL1 blue + pRS415GPD-Er* **g** *S_Yli*	
2112	*E. coli XL1 blue + pUC19-Ribozyme* **V4** *-tRNA$^{Asp}_{Afm}$ - G50-C64*	
2113	*E. coli XL1 blue + pUC19-Ribozyme* **V5** *-tRNA$^{Asp}_{Afm}$ - G50-C64*	
2114	*E. coli XL1 blue + pUC19-Ribozyme* **V6** *-tRNA$^{Asp}_{Afm}$ - G50-C64*	
2198	*E. coli DH5 α + p* **M** *tev-Er* **g** *S_Yli* (clone 2)	
2199	*E. coli DH5 α + p* **M** *tev-Er* **g** *S_Yli* (clone 4)	
2200	*E. coli XL1 blue + pRS415GPD-Er* **g** *S_Yli-R217E-R221E-R224E-K228E*	basic residues from the α(+) helix mutated to E
2201	*E. coli XL1 blue + pRS415GPD-Er* **g** *S_Yli-R217E-R221E*	
2202	*E. coli XL1 blue + pRS415GPD-Er* **g** *S_Yli-R224E-K228E*	
2203	*E. coli XL1 blue + p* **M** *tev-Er* **g** *S_Yli-R217E-R221E-R224E-K228E*	
2204	*E. coli XL1 blue + p* **M** *tev-Er* **g** *S_Yli-R217E-R221E*	
2205	*E. coli XL1 blue + p* **M** *tev-Er* **g** *S_Yli-R224E-K228E*	
2253	*E. coli DH5 α + pJET1.2-* Δ*er* **g** *S-K7*	K7 for deletion of ergS in *Afm*
2403	*E. coli DH5 α + p* **His10X** *-* **M** *tevGWA-Er* **g** *S_Yli*	
2409	*E. coli XL1 blue + pRS414-GlyRS_Yli-b11*	GlyRS ORF from Yli tagged with b11
2410	*E. coli XL1 blue + pRS415-* **HA** *-Er* **g** *S_Yli* (clone 17)	
2411	*E. coli XL1 blue + pRS415-* **HA** *-Er* **g** *S_Yli* (clone 26)	
2432	*E. coli XL1 blue + pE-* **SUMO** *-ErdS*	plasmids for bacterial overexpression of SUMO-tagged ErdS versions. D86ErdS = ErdS deleted from its 86 N-ter residues. From O. Nreki's Lab.
2433	*E. coli XL1 blue + pE-* Δ*86-* **SUMO** *-ErdS*	
2437	*E. coli DH5α + p441-* **His6X** *-ULP1*	plasmid for bacterial overexpression and purification of His6x tagged SUMO-protease (ULP1/YPL020C from *Sce*)
2439	*E. coli XL1 blue + pRS415GPD-* **HA** *-Er* **g** *S_Yli-R217E-R221E-R224E-K228E*	
2440	*E. coli XL1 blue + pRS415GPD-* **HA** *-Er* **g** *S_Yli-R217E-R221E*	
2441	*E. coli XL1 blue + pRS415GPD-* **HA** *-Er* **g** *S_Yli-R224E-K228E*	

Table MM-1 *(continued)*

	Bacterial strains for recombinant protein overexpression
	E. coli **Rosetta-2** : *strain B F− ompT gal dcmlonhsdSB(rB−mB−)* *λ(DE3 [lacI lacUV5-T7p07 ind1 sam7 nin5]) [malB+]K-12(λS))* ,
	E. coli **Star2** : *F- ompT hsdSB (rB-mB-) gal dcm rne131 (DE3),* carrying the pRARE2 plasmid
867	*E. coli Rosetta-2 + pGGWA-ErdS*
868	*E. coli Rosetta-2 + pGGWA-Er g S*
949	*E. coli Star2 + p His6x -tev-GWA-Δ192-Er g S*
950	*E. coli Star2 + p His6x -tev-GWA-Δ192-Er g S- His6X*
2415	*E. coli Rosetta-2 + p M tevGWA-Er g S_Yli*
2416	*E. coli Rosetta-2 + p His6X - M tevGWA-Er g S_Yli*

	S. cerevisiae (*Sce*) strains	
	Sce strains for Δ*dps1* complementation assays	
700	*Sce YAL3 Δdps1:* MATα ura3-52 lys2-801am trp1-63 his3-200 leu2-1 ade2-450 ade3-1483 dps1::HIS3 (clone 7)	Gift from G. Eriani
701	*Sce YAL3 Δdps1:* MATα ura3-52 lys2-801am trp1-63 his3-200 leu2-1 ade2-450 ade3-1483 dps1::HIS4 (clone 8)	Gift from G. Eriani
957	*Sce YAL3 Δdps1 + pRS415GPD-ErdS*	
958	*Sce YAL3 Δdps1 + pRS415GPD-ErdS- HA*	
959	*Sce YAL3 Δdps1 + pRS415GPD-ErdS- Δ duf2156* [KO]	AspRS encoded by this plasmid is inactive and does not complement
960	*Sce YAL3 Δdps1 + pRS415GPD-ErdS-Δduf2156- HA* [KO]	*Sce Δdps1* . For ErdS-Δduf2156 active forms see: 1382-1389
961	*Sce YAL3 Δdps1 + pRS415GPD-ccdB*	
995	*Sce YAL3 Δdps1 + pRS415GPD-ErdS- EGFP*	
996	*Sce YAL3 Δdps1 + pRS415GPD- EGFP -ErdS*	
1408	*Sce YAL3 Δdps1 + pRS415GPD-ErdS-Δduf2156* [OK]	
1409	*Sce YAL3 Δdps1 + pRS415GPD-Δ84-ErdS-Δduf2156* [OK]	
1410	*Sce YAL3 Δdps1 + pRS415GPD-ErdS AAPA*	
1411	*Sce YAL3 Δdps1 + pRS415GPD-ErdS-KRα5A*	
1412	*Sce YAL3 Δdps1 + pRS415GPD-ErdS-KRα5E*	
1413	*Sce YAL3 Δdps1 + pRS415GPD-ErdS-W785A*	
1414	*Sce YAL3 Δdps1 + pRS415GPD-ErdS-W785H*	
1415	*Sce YAL3 Δdps1 + pRS415GPD-ErdS-R789A*	
1503	*Sce YAL3 Δdps1 + pRS414GPD-ErdS- Δduf + pRS415GPD-ErdS-Δdrs*	
1545	*Sce YAL3 Δdps1 + pRS414GPD-ErdS- N677A*	
1546	*Sce YAL3 Δdps1 + pRS414GPD-ErdS-E712R*	
1547	*Sce YAL3 Δdps1 + pRS414GPD-ErdS-E731R*	
1548	*Sce YAL3 Δdps1 + pRS414GPD-ErdS- Q836R*	
1549	*Sce YAL3 Δdps1 + pRS414GPD-ErdS- K838E*	
1550	*Sce YAL3 Δdps1 + pRS414GPD-ErdS- Q836R_K838E*	
1559	*Sce YAL3 Δdps1 + pRS415GPD- Δ30-ErdS-Δduf2156- HA*	
1560	*Sce YAL3 Δdps1 + pRS415GPD- Δ60-ErdS-Δduf2156- HA*	
1561	*Sce YAL3 Δdps1 + pRS415GPD- Δ84-ErdS-Δduf2156- HA*	
1562	*Sce YAL3 Δdps1 + pRS415GPD-ErdS_Aor*	
1563	*Sce YAL3 Δdps1 + pRS415GPD- Δ30-ErdS- HA*	
1564	*Sce YAL3 Δdps1 + pRS415GPD- Δ60-ErdS- HA*	
1565	*Sce YAL3 Δdps1 + pRS415GPD- Δ84-ErdS- HA*	

Table MM-1 *(continued)*

	Sce BY4742/w strains	
63	*Sce* **BY4742:** *MATα ; his3Δ 1; leu2Δ 0; lys2Δ 0; ura3Δ 0*	
602	*Sce* **BY4742W:** *MATα ; his3Δ 1; leu2Δ 0; lys2Δ 0; ura3Δ 0;* *trp1::hygro*	
1998	*Sce* **BY4742 atg 26::KanMX4**	Euroscarf-116B10; YLR189C/ATG26
1999	*Sce* **BY4742 egh1::KanMX4**	Euroscarf-142D2; YIR007W/EGH1
2000	*Sce* **BY4742 atf2::KanMX4**	Euroscarf-113D3; YGR177C/ATF2
2001	*Sce* **BY4742 say1::KanMX4**	Euroscarf-130A8; YGR263C/SAY1
2026	*Sce* **BY4742 erg2::KanMX4**	Euroscarf-104D5; YMR202W/ERG2
2027	*Sce* **BY4742 erg3::KanMX4**	Euroscarf-102D7; YLR056W/ERG3
2028	*Sce* **BY4742 erg4::KanMX4**	Euroscarf-126D5; YGL012W/ERG4
2029	*Sce* **BY4742 erg5::KanMX4**	Euroscarf-170A6; YMR015C/ERG5
2030	*Sce* **BY4742 erg6::KanMX4**	Euroscarf-103D6; YML008C/ERG6
881	*Sce* **RH4889 (Sec24ts) + pRS415GPD-Er g S- EGFP**	
882	*Sce* **BY4742 + pUSE**	Sec7-GFP integrated at the genome with *URA3* marker
951	*Sce* **BY4742 + pUSE + pRS415GPD- Cer -Er g S**	
952	*Sce* **BY4742W + pRS415GPD-Er g S- EGFP**	
953	*Sce* **BY4742W + pRS415GPD-ErdS- EGFP**	
954	*Sce* **BY4742W + pRS415GPD-ErdS + pRS414GPD-Er g S**	
962	*Sce* **BY4742W + pRS415GPD-ErdS**	
963	*Sce* **BY4742W + pRS415GPD-ErdS- HA**	
964	*Sce* **BY4742W + pRS415GPD-Er g S- HA**	
965	*Sce* **BY4742W + pRS415GPD-Er g S**	
966	*Sce* **BY4742W + pRS415GPD-ErdS-Δduf2156 [KO]**	AspRS encoded by this plasmid is inactive and does not complement
967	*Sce* **BY4742W + pRS415GPD-ErdS-Δduf2156- HA [KO]**	*Sce* Δdps1. For ErdS-Δduf2156 active forms see: 1382-1389
968	*Sce* **BY4742W + pRS415GPD-ErdS-Δdrs**	
969	*Sce* **BY4742W + pRS415GPD-ErdS-Δdrs- HA**	
991	*Sce* **BY4742W + pRS415GPD-Δ192-Er g S- EGFP**	
992	*Sce* **BY4742W + pRS415GPD-ErdS-Δdrs- EGFP**	
1396	*Sce* **BY4742W + pRS414GPD-Δ84-ErdS-Δduf2156**	
1397	*Sce* **BY4742W + pRS415GPD-ErdS-Δduf2156**	
1398	*Sce* **BY4742W + pRS415GPD-Δ84-ErdS-Δduf2156**	
1399	*Sce* **BY4742W + pRS415GPD-ErdS AAPA**	ErdS with QSPQ signature sequence of AspRS mutated to AAPA
1400	*Sce* **BY4742W + pRS415GPD-ErdS-KR α5E**	ErdS residues R749, K750, R752, R753 mutated to E
1401	*Sce* **BY4742W + pRS415GPD-ErdS-W785A**	
1402	*Sce* **BY4742W + pRS415GPD-ErdS-W785H**	
1403	*Sce* **BY4742W + pRS415GPD-ErdS-R789A**	
1404	*Sce* **BY4742W + pRS414GPD-ErdS- Δduf2156**	
1405	*Sce* **BY4742W + pRS415GPD-ErdS-KR α5A**	
1416	*Sce* **BY4742W + pRS425GPD-Er g S**	
1493	*Sce* **BY4742W + pRS425GPD-Er g S + pRS424GPD-DRS- β 11**	
1494	*Sce* **BY4742W + pRS425GPD-Er g S + pRS424GPD-RRS- β 11**	
1495	*Sce* **BY4742W + pRS425GPD-Er g S + pRS424GPD-TRS- β 11**	
1496	*Sce* **BY4742W + pRS425GPD-Er g S + pRS424GPD-GRS- β 11**	
1497	*Sce* **BY4742W + pRS425GPD-Er g S + pRS424GPD-YRS- β 11**	
1498	*Sce* **BY4742W + pRS425GPD-Er g S + pRS424GPD-QRS- β 11**	
1499	*Sce* **BY4742W + pRS415GPD-Er g S + pRS424GPD-ccdB**	
1500	*Sce* **BY4742W + pRS425GPD-Er g S + pRS424GPD-SRS- β 11**	
1501	*Sce* **BY4742W + pRS425GPD-Er g S + pRS424GPD-KRS- β 11**	
1502	*Sce* **BY4742W + pRS425GPD-Er g S + pRS424GPD-ccdB**	
1516	*Sce* **BY4742W+ pRS415GPD- Δ30-ErdS**	
1517	*Sce* **BY4742W + pRS415GPD- Δ60-ErdS**	
1518	*Sce* **BY4742W + pRS415GPD- Δ84-ErdS**	

1534	*Sce BY4742W + pRS415GPD- Δ30-ErdS-* **HA**
1535	*Sce BY4742W + pRS415GPD- Δ60-ErdS-* **HA**
1536	*Sce BY4742W + pRS415GPD- Δ84-ErdS-* **HA**
1537	*Sce BY4742W + pRS415GPD-ErdS-Δduf2156-* **HA**
1538	*Sce BY4742W + pRS415GPD- Δ30-ErdS-Δduf2156-* **HA**
1539	*Sce BY4742W + pRS415GPD- Δ60-ErdS-Δduf2156-* **HA**
1540	*Sce BY4742W + pRS415GPD- Δ84-ErdS-Δduf2156-* **HA**
2062	*Sce BY4742W + pRS425GPD-Er* **g** *S-K321E-R322E*
2063	*Sce BY4742W + pRS425GPD-Er* **g** *S-Q326A-N327A-R328E-Q329A*
2064	*Sce BY4742W + pRS425GPD-Er* **g** *S-N332A-K335E*
2065	*Sce BY4742W + pRS425GPD-Er* **g** *S-R368E*
2066	*Sce BY4742W + pRS425GPD-Er* **g** *S-Q375R*
2067	*Sce BY4742W + pRS425GPD-Er* **g** *S-R409E*
2068	*Sce BY4742W + pRS425GPD-Er* **g** *S-R420E*
2069	*Sce BY4742W + pRS425GPD-Er* **g** *S-R365E*
2070	*Sce BY4742W + pRS425GPD-Er* **g** *S-R328E*
2071	*Sce BY4742W + pRS425GPD-Er* **g** *S-N332A*
2072	*Sce BY4742W + pRS425GPD-Er* **g** *S-K335E*
2073	*Sce BY4742W + pRS425GPD-Er* **g** *S-R328E-K335E*
2074	*Sce BY4742W + pRS415GPD-ErdS-N677*
2075	*Sce BY4742W + pRS415GPD-ErdS-E712R*
2076	*Sce BY4742W + pRS415GPD-ErdS-E731R*
2077	*Sce BY4742W + pRS415GPD-ErdS-Q836R*
2078	*Sce BY4742W + pRS415GPD-ErdS-K838E*
2079	*Sce BY4742W + pRS415GPD-ErdS-T643A*
2080	*Sce BY4742W + pRS415GPD-ErdS-Y637F*
2081	*Sce BY4742W + pRS415GPD-ErdS-T641A*
2082	*Sce BY4742W + pRS415GPD-ErdS-S642A*
2083	*Sce BY4742W + pRS415GPD-ErdS-S644A*
2084	*Sce BY4742W + pRS415GPD-ErdS-W645A*
2085	*Sce BY4742W + pRS415GPD-ErdS-D647R*
2086	*Sce BY4742W + pRS415GPD-ErdS-R649E*
2087	*Sce BY4742W + pRS415GPD-ErdS-R649E*
2088	*Sce BY4742W + pRS415GPD-ErdS-K790E*
2089	*Sce BY4742W + pRS415GPD-ErdS-G791A*
2090	*Sce BY4742W + pRS415GPD-ErdS-Q793R*
2091	*Sce BY4742W + pRS415GPD-ErdS-H795A*
2092	*Sce BY4742W + pRS415GPD-ErdS-E798R*
2093	*Sce BY4742W + pRS415GPD-ErdS-W802A*
2094	*Sce BY4742W + pRS415GPD-ErdS-K916E*

A. fumigatus (Afm) strains	
Afm CEA17^{KU80} **:** *pyrG akuB::pyrG (Δ akuB*^{KU80} *)*	
Afm CEA17^{KU80} **Δe rdS (hph):** *pyrG akuB::pyrG (ΔakuB*^{KU80} *) erdS::hph*	erdS ORF deleted by homologous recomb. Del. K7 contains hygR.
Afm CEA17^{KU80} **Δe rdS:** *pyrG akuB::pyrG (ΔakuB*^{KU80} *) Δ erdS*	Deletion K7 excised
Afm CEA17^{KU80} **Δ erdS::P**$_{xyl}$ **-erdS:** *pyrG akuB::pyrG (ΔakuB*^{KU80} *) ΔerdS::[5'-utr- P*$_{xyl}$ *erdS-trpCterm-hph-3'-utr]*	Afm CEA17^{KU80} ΔerdS complemented with an xylose inducible

Table MM-1 *(continued)*

A. oryzae (Aor) strains (from T. Kushiro's Lab)	
Aor RIB40 wt	
Aor HiMe10: *ΔligD::AnpyrG-300bp ΔpyrG*	
Aor HiDES: *ΔligD::AnpyrG-300bp, ΔpyrG, ΔAorɛrdS::AnpyrG-300bp*	
Aor HiDEC (ΔerdS + aspRS): *ΔligD::AnpyrG-300bp, ΔpyrG, ΔAorɛrdS::AnpyrG-300bp niaD::(AoaspRSniaDAnpyrG)*	
Aor HiDEC (ΔerdS + duf2156): *ΔligD::AnpyrG-300bp, ΔpyrG, ΔAorɛrdS::AnpyrG-300bp niaD::(Aoduf2156niaDAnpyrG)*	
Aor HiDEC (ΔerdS + erdS): *ΔligD::AnpyrG-300bp, ΔpyrG, ΔAorɛrdS::AnpyrG-300bp niaD::(AoerdSniaDAnpyrG)*	
N. crassa (Ncr) strains (from the FGSC)	
Neurospora crassa 74-OR23-1VA wt, matA	FGSC #2489
Neurospora crassa ΔerdS: *erdS::hph, matA*	FGSC #20236
Neurospora crassa ΔerdH: *erdH::hph, matA*	FGSC #20235
Other fungal species	
Aspergillus flavusCA14 : *ΔpyrG Δku80*	FGSC #A1421
Beauveria bassiana NRRL 20698 wt	ATCC 90517
Schizophyllum commune H4-8 wt	FGSC #9210
Aspergillus niger wt	Gift from UdS
Candida albicans wt	Gift from UdS
Candida parapsilosis wt	Gift from UdS
Geotrichum candidum wt	Gift from UdS
Penicillium expansum wt	Gift from UdS
Penicillium camemberti wt	Gift from UdS
Alternaria alternata wt	Gift from UdS
Cryptococcus neoformans wt	Gift from UdS
Yarrowia lipolytica	Gift from UdS

Table MM-2 : List of plasmids, and primers used to obtain them. The following table is organized in sections (black rows) and sub-sections (light orange rows). The cloning method for each section is specified. The first column describes the final plasmids, the second column lists templates for amplification by PCR and the last column details the primer pairs that were used to obtain each construction. The first primer of each pair used for PCR amplification corresponds to the forward primer and the second corresponds to the reverse primer. Plasmid descriptions containing "-X" correspond to a LR recombined destination plasmid. If not specified, the origin of the cloned genes corresponds to *Afm*. For isothermal cloning, products from PCR 1 & PCR 2 (and in few cases PCR 3) were assembled as described in the Materials and Methods sections. In cases where PCR 1 and PCR 2 involve primers FF060/FF061, both amplified products contain a truncated part of AmpR, reconstituted later during the isothermal Gibson assembly. Replacement cassettes used for genomic recombination in *Aspregillus* spp. are described at the end of this table. pJET1.2 in bold, indicate that the corresponding PCR product or the linear isothermally assembled intermediate was cloned into pJET1.2 by using the CloneJET PCR Cloning Kit (Thermofisher, K1231). Please note that *Afm erdS* and *ergS* genes were codon optimized for their expression in *Sce*. This is only specified in the first section of the present table but note that all plasmids used for expression in Sce and *E. coli* contain those optimized sequences.

Final plasmid	Template	Primers (5' --> 3')
Construction of donnor plasmids containing erdS or ergS variants - *Gateway BP reactions*		
pDONR221-ErdS-*Afm* (*Sce* _opt_seq)	pUC57-ErdS-*Afm* (*Sce* _opt_seq)	GW_s : GGGGACAAGTTTGTACAAAAAAGCAGGCTTCATG GW_as : GGGGACTTTGTACAAGAAAGCTGGGTC
pDONR221-ErdS-Δduf2156 (Sce_opt_seq)	pUC57-ErdS-*Afm* (*Sce* _opt_seq)	FF001 : GGGGACAAGTTTGTACAAAAAAGCAGGCTTCATGTCAATCAAGAGAGCATTATCC FF003 : GGGGACCACTTTGTACAAGAAAGCTGGGTCTCAAGGTGGAAAAGATTTTGGATC
pDONR221-ErdS-Δ*aspRS* (*Sce* _opt_seq)	pUC57-ErdS-*Afm* (*Sce* _opt_seq)	dufssDRS_s : GGGACAAGTTTGTACAAAAAAGCAGGCTTCatgAGACACCCTGAAAGTTCTACAATAGAACC GW_as : GGGGACTTTGTACAAGAAAGCTGGGTC
pDONR221-ErdS-*Aor*	*A. oryzae (Aor)* gDNA	GGGGACAAGTTTGTACAAAAAAGCAGGCTTCatgtccatcaaacgggccc GGGGACCACTTTGTACAAGAAAGCTGGGTCttagtcttcgaaaaagtgaagg
pDONR221-ErgS-*Afm* (*Sce* _opt_seq)	pUC57-ErgS-*Afm* (*Sce* _opt_seq)	GW_s : GGGGACAAGTTTGTACAAAAAAGCAGGCTTCATG GW_as : GGGGACTTTGTACAAGAAAGCTGGGTC
Construction of *S. cerevisiae* expression plasmids - *isoThermal assembly*		
ErdS wt and mutatnts		
pRS415-GPD-ErgS-*Aor*	pDONR221-ErgS-*Aor* (PCR 1)	#101 : gaactagtggatcccccatcacaagtttGTACAAAAAAGCAGGCTTC #102 : cttgatatcgaattcctgcagcccatcaCCACTTTGTACAAGAAAGCTGGGTC
	pRS415-GPD-X (LR recombined plasmid) (PCR 2)	#104 : tgatgggctgcaggaattcgatatcaag #103 : aaacttgtgatgggggatccactagttc
pRS415-GPD-ErgS-*Afm*	pDONR221-ErgS-*Afm* (PCR 1)	#101 : gaactagtggatcccccatcacaagtttGTACAAAAAAGCAGGCTTC #102 : cttgatatcgaattcctgcagcccatcaCCACTTTGTACAAGAAAGCTGGGTC
	pRS415-GPD-X (PCR 2)	#104 : tgatgggctgcaggaattcgatatcaag #103 : aaacttgtgatgggggatccactagttc
pRS415-GPD-ErgS-Δduf2156	pDONR221-ErdS-Δduf2156 (PCR 1)	#101 : gaactagtggatcccccatcacaagtttGTACAAAAAAGCAGGCTTC #102 : cttgatatcgaattcctgcagcccatcaCCACTTTGTACAAGAAAGCTGGGTC
	pRS415-GPD-X (PCR 2)	#104 : tgatgggctgcaggaattcgatatcaag #103 : aaacttgtgatgggggatccactagttc
pRS415-GPD-erdS-Δ*aspRS*	pDONR221-erdS-Δ*aspRS* (PCR 1)	#101 : gaactagtggatcccccatcacaagtttGTACAAAAAAGCAGGCTTC #102 : cttgatatcgaattcctgcagcccatcaCCACTTTGTACAAGAAAGCTGGGTC
	pRS415-GPD-X (PCR 2)	#104 : tgatgggctgcaggaattcgatatcaag #103 : aaacttgtgatgggggatccactagttc
pRS415GPD-erdS-AAPA	pRS415-GPD-ErdS-*Afm* (PCR 1)	FF048 : TTTTAGCCGCTGCTCCTGCTTTGGCAAAGCAAATGGCCATC FF061 : TTTTCTGTGACTGGTGAGTACTCAACC
	pRS415-GPD-ErgS-*Afm* (PCR 2)	FF060 : TTGAGTACTCACCAGTCACAGAAAAGC FF049 : CTTTGCCAAAGCAGGAGCAGCGGCTAAAAATGCATCTCTACCG

Table MM-2 (*continued*)

pRS415GPD-erdS-α(0) R749, K750, R751, R752 to A	pRS415-GPD-ErgS-*Afm* (PCR 1)	FF050 : GCAGCAGCAATAGCAGCAGCCGAAAACGAAGGTATTAAAATCG FF061 : TTTTCTGTGACTGGTGAGTACTCAACC
	pRS415-GPD-ErdS-*Afm* (PCR 2)	FF060 : TTGAGTACTCACCAGTCACAGAAAAGC FF051 : GCTGCTGCTATTGCTGCTGCAATTTCACCGTCAGAAGCGGCTTG
pRS415GPD-ErdS-α(-) R749, K750, R751, R752 to E	pRS415-GPD-ErdS-*Afm* (PCR 1)	FF052 : GCAGAAGAAATAGAAGAAGCCGAAAACGAAGGTATTAAAATCG FF061 : TTTTCTGTGACTGGTGAGTACTCAACC
	pRS415-GPD-ErdS-*Afm* (PCR 2)	FF060 : TTGAGTACTCACCAGTCACAGAAAAGC FF053 : GGCTTCTTCTATTTCTTCTGCAATTTCACCGTCAGAAGCGGCTTG
pRS415GPD-ErdS-Y637F	pRS415-GPD-ErgS-*Afm* (PCR 1)	NY050 : GATCGCCAACTTTGGTGACGCTACAAGTACC FF061 : TTTTCTGTGACTGGTGAGTACTCAACC
	pRS415-GPD-ErdS-*Afm* (PCR 2)	FF060 : TTGAGTACTCACCAGTCACAGAAAAGC NY051 : TAGCGTCACCAAAGTTGGCGATCAAATGTTC
pRS415GPD-ErdS-T641A	pRS415-GPD-ErdS-*Afm* (PCR 1)	NY052 : CGGTGACGCTGCTAGTACCTCTTGGGGTGACG FF061 : TTTTCTGTGACTGGTGAGTACTCAACC
	pRS415-GPD-ErdS-*Afm* (PCR 2)	FF060 : TTGAGTACTCACCAGTCACAGAAAAGC NY053 : AAGAGGTACTAGCAGCGTCACCGTAGTTGGC
pRS415GPD-ErdS-S642A	pRS415-GPD-ErgS-*Afm* (PCR 1)	NY054 : TGACGCTACAGCTACCTCTTGGGGTGACG FF061 : TTTTCTGTGACTGGTGAGTACTCAACC
	pRS415-GPD-ErdS-*Afm* (PCR 2)	FF060 : TTGAGTACTCACCAGTCACAGAAAAGC NY055 : CCCAAGAGGTAGCTGTAGCGTCACCGTAG
pRS415GPD-ErdS-S643A	pRS415-GPD-ErdS-*Afm* (PCR 1)	NY056 : CGCTACAAGTGCTTCTTGGGGTGACGAAAG FF061 : TTTTCTGTGACTGGTGAGTACTCAACC
	pRS415-GPD-ErdS-*Afm* (PCR 2)	FF060 : TTGAGTACTCACCAGTCACAGAAAAGC NY057 : CACCCCAAGAAGCACTTGTAGCGTCACCG
pRS415GPD-ErdS-S644A	pRS415-GPD-ErgS-*Afm* (PCR 1)	NY058 : TACAAGTACCGCTTGGGGTGACGAAAGATTC FF061 : TTTTCTGTGACTGGTGAGTACTCAACC
	pRS415-GPD-ErdS-*Afm* (PCR 2)	FF060 : TTGAGTACTCACCAGTCACAGAAAAGC NY059 : CGTCACCCCAAGCGGTACTTGTAGCGTCACC
pRS415GPD-ErdS-W645A	pRS415-GPD-ErdS-*Afm* (PCR 1)	NY060 : AAGTACCTCTGCTGGTGACGAAAGATTCAAG FF061 : TTTTCTGTGACTGGTGAGTACTCAACC
	pRS415-GPD-ErdS-*Afm* (PCR 2)	FF060 : TTGAGTACTCACCAGTCACAGAAAAGC NY061 : TTTCGTCACCAGCAGAGGTACTTGTAGCGTC
pRS415GPD-ErdS-D647R	pRS415-GPD-ErgS-*Afm* (PCR 1)	NY062 : CTCTTGGGGTAGAGAAAGATTCAAGATTTGG FF061 : TTTTCTGTGACTGGTGAGTACTCAACC
	pRS415-GPD-ErdS-*Afm* (PCR 2)	FF060 : TTGAGTACTCACCAGTCACAGAAAAGC NY063 : TGAATCTTTCTCTACCCCAAGAGGTACTTG
pRS415GPD-ErdS-R649E	pRS415-GPD-ErdS-*Afm* (PCR 1)	NY064 : GGGTGACGAAGAATTCAAGATTTGGAGAGAC FF061 : TTTTCTGTGACTGGTGAGTACTCAACC
	pRS415-GPD-ErdS-*Afm* (PCR 2)	FF060 : TTGAGTACTCACCAGTCACAGAAAAGC NY065 : AAATCTTGAATTCTTCGTCACCCCAAGAGG
pRS415GPD-ErdS-C728A	pRS415-GPD-ErgS-*Afm* (PCR 1)	NY070 : ATCATTGTCCGCTATTGCTGAAGAAAGAGTAG FF061 : TTTTCTGTGACTGGTGAGTACTCAACC
	pRS415-GPD-ErdS-*Afm* (PCR 2)	FF060 : TTGAGTACTCACCAGTCACAGAAAAGC NY071 : CTTCAGCAATAGCGGACAATGATCTCCAACC
pRS415GPD-ErdS-W785A	pRS415-GPD-ErdS-*Afm* (PCR 1)	FF054 : ATACAAGATGCTTTGGCAAACAGAAAGGGTACTCAAGTTC FF061 : TTTTCTGTGACTGGTGAGTACTCAACC
	pRS415-GPD-ErdS-*Afm* (PCR 2)	FF060 : TTGAGTACTCACCAGTCACAGAAAAGC FF055 : GTTTGCCAAAGCATCTTGTATTCTAGCGTCAATCTTTTC
pRS415GPD-ErdS-W785H	pRS415-GPD-ErgS-*Afm* (PCR 1)	FF056 : ATACAAGATCATTTGGCAAACAGAAAGGGTACTCAAGTTC FF061 : TTTTCTGTGACTGGTGAGTACTCAACC
	pRS415-GPD-ErdS-*Afm* (PCR 2)	FF060 : TTGAGTACTCACCAGTCACAGAAAAGC FF057 : GTTTGCCAAATGATCTTGTATTCTAGCGTCAATCTTTTC

pRS415GPD-ErdS-R789A	pRS415-GPD-ErdS-*Afm* (PCR 1)	FF058 : TTGGCAAACGCAAAGGGTACTCAAGTTCATTTGTCAGAAATAC
		FF061 : TTTTCTGTGACTGGTGAGTACTCAACC
	pRS415-GPD-ErdS-*Afm* (PCR 2)	FF060 : TTGAGTACTCACCAGTCACAGAAAAGC
		FF059 : AGTACCCTTTGCGTTTGCCAACCAATCTTGTATTCTAGCGTC
pRS415GPD-ErdS-K790E	pRS415-GPD-ErgS-*Afm* (PCR 1)	NY072 : GGCAAACAGAGAAGGTACTCAAGTTCATTTG
		FF061 : TTTTCTGTGACTGGTGAGTACTCAACC
	pRS415-GPD-ErdS-*Afm* (PCR 2)	FF060 : TTGAGTACTCACCAGTCACAGAAAAGC
		NY073 : CTTGAGTACCTTCTCTGTTTGCCAACCAATC
pRS415GPD-ErdS-G791A	pRS415-GPD-ErdS-*Afm* (PCR 1)	NY074 : AAACAGAAAGGCTACTCAAGTTCATTTGTC
		FF061 : TTTTCTGTGACTGGTGAGTACTCAACC
	pRS415-GPD-ErdS-*Afm* (PCR 2)	FF060 : TTGAGTACTCACCAGTCACAGAAAAGC
		NY075 : GAACTTGAGTAGCCTTTCTGTTTGCCAACC
pRS415GPD-ErdS-Q793R	pRS415-GPD-ErgS-*Afm* (PCR 1)	NY076 : AAAGGGTACTAGAGTTCATTTGTCAGAAATAC
		FF061 : TTTTCTGTGACTGGTGAGTACTCAACC
	pRS415-GPD-ErdS-*Afm* (PCR 2)	FF060 : TTGAGTACTCACCAGTCACAGAAAAGC
		NY077 : ACAAATGAACTCTAGTACCCTTTCTGTTTGC
pRS415GPD-ErdS-H795A	pRS415-GPD-ErdS-*Afm* (PCR 1)	NY078 : TACTCAAGTTGCTTTGTCAGAAATACACCCTTG
		FF061 : TTTTCTGTGACTGGTGAGTACTCAACC
	pRS415-GPD-ErdS-*Afm* (PCR 2)	FF060 : TTGAGTACTCACCAGTCACAGAAAAGC
		NY079 : TTTCTGACAAAGCAACTTGAGTACCCTTTCTG
pRS415GPD-ErdS-E798R	pRS415-GPD-ErgS-*Afm* (PCR 1)	NY080 : TCATTTGTCAAGAATACACCCTTGGAGAGATTC
		FF061 : TTTTCTGTGACTGGTGAGTACTCAACC
	pRS415-GPD-ErdS-*Afm* (PCR 2)	FF060 : TTGAGTACTCACCAGTCACAGAAAAGC
		NY081 : AAGGGTGTATTCTTGACAAATGAACTTGAGTAC
pRS415GPD-ErdS-W802A	pRS415-GPD-ErdS-*Afm* (PCR 1)	NY082 : AATACACCCTGCTAGAGATTCCGAACATAGATG
		FF061 : TTTTCTGTGACTGGTGAGTACTCAACC
	pRS415-GPD-ErdS-*Afm* (PCR 2)	FF060 : TTGAGTACTCACCAGTCACAGAAAAGC
		NY083 : CGGAATCTCTAGCAGGGTGTATTTCTGACAAATG
pRS415GPD-ErdS-F913A	pRS415-GPD-ErgS-*Afm* (PCR 1)	NY084 : AAAATCAGAGGCTAGAGCCAAGTTAGGTGCTC
		FF061 : TTTTCTGTGACTGGTGAGTACTCAACC
	pRS415-GPD-ErdS-*Afm* (PCR 2)	FF060 : TTGAGTACTCACCAGTCACAGAAAAGC
		NY085 : ACTTGGCTCTAGCCTCTGATTTTCTAACCAAG
pRS415GPD-ErdS-R914E	pRS415-GPD-ErdS-*Afm* (PCR 1)	NY086 : ATCAGAGTTTGAAGCCAAGTTAGGTGCTCATG
		FF061 : TTTTCTGTGACTGGTGAGTACTCAACC
	pRS415-GPD-ErdS-*Afm* (PCR 2)	FF060 : TTGAGTACTCACCAGTCACAGAAAAGC
		NY087 : CTAACTTGGCTTCAAACTCTGATTTTCTAACC
pRS415GPD-ErdS-K916E	pRS415-GPD-ErgS-*Afm* (PCR 1)	NY088 : GTTTAGAGCCGAATTAGGTGCTCATGAAGAAC
		FF061 : TTTTCTGTGACTGGTGAGTACTCAACC
	pRS415-GPD-ErdS-*Afm* (PCR 2)	FF060 : TTGAGTACTCACCAGTCACAGAAAAGC
		NY089 : GAGCACCTAATTCGGCTCTAAACTCTGATTTTC

	ErdH wt and mutants	
pRS414GPD-ErdH or pRS414GPD-EGFP-ErdH	Afm Genomic DNA (PCR 1)	NY119 : AAGCAGGCTTCATGGCCTCTCATGCCCCTC
		NY120 : gAAAGCTGGGTCCTATCTGTCAAAAATCGC
	pRS414GPD-X or pRS414GPD-EGFP-X (PCR 2)	NY121 : GACAGATAGGACCCAGCTTTcttgtacaaagtgg
		NY122 : ATGAGAGGCCATGAAGCCTGCTTTTTTGTACaaac
pRS414GPD-EGFP-ErdH	pRS414GPD-X-EGFP (PCR 1)	NY169 : TGAAAGCGATTTTTGACAGAGACCCAGCTTTcttgtacaaagtgg
		FF061 : TTTTCTGTGACTGGTGAGTACTCAACC
	pRS414GPD-ErdH (PCR 2)	NY170 : gtacaagAAAGCTGGGTCTCTGTCAAAAATCGCTTTCATGTCCG
		FF060 : TTGAGTACTCACCAGTCACAGAAAAGC

Table MM-2 (*continued*)

		ErgS wt and mutants
pRS415-GPD-ErgS-*Afm* or pRS414-GPD-ErgS-*Afm*	pDONR221-ErgS-*Afm* (PCR 1)	#101 : gaactagtggatcccccatcacaagtttGTACAAAAAAGCAGGCTTC
		#102 : cttgatatcgaattcctgcagcccatcaCCACTTTGTACAAGAAAGCTGGGTC
	pRS415-GPD-X or pRS414-GPD-X (PCR 2)	#104 : tgatgggctgcaggaattcgatatcaag
		#103 : aaacttgtgatgggggatccactagttc
pRS415-GPD-ErgS-*Afm* -α(-) K321, R322 to E	pRS415-GPD-ErgS-*Afm* (PCR 1)	NY125 : AACTTCAGGTGAAGAAATATTAACACAAAACAGAC
		FF061 : TTTTCTGTGACTGGTGAGTACTCAACC
	pRS415-GPD-ErgS-*Afm* (PCR 2)	FF060 : TTGAGTACTCACCAGTCACAGAAAAGC
		NY126 : GTGTTAATATTTCTTCACCTGAAGTTTCTAACAAAAC
pRS415-GPD-ErgS-*Afm* Q326A, N327A, R328E, Q329A	pRS415-GPD-ErgS-*Afm* (PCR 1)	NY127 : AATATTAACAGCTGCTGAAGCTTTGTTGAACCCTTCAAAAG
		FF061 : TTTTCTGTGACTGGTGAGTACTCAACC
	pRS415-GPD-ErgS-*Afm* (PCR 2)	FF060 : TTGAGTACTCACCAGTCACAGAAAAGC
		NY128 : GGTTCAACAAAGCTTCAGCAGCTGTTAATATTCTTTTACCTG
pRS415-GPD-ErgS-*Afm* N332A, K335E	pRS415-GPD-ErgS-*Afm* (PCR 1)	NY129 : ACAATTGTTGGCTCCTTCAGAAGGTGGTATAACTTTGCATATC
		FF061 : TTTTCTGTGACTGGTGAGTACTCAACC
	pRS415-GPD-ErgS-*Afm* (PCR 2)	FF060 : TTGAGTACTCACCAGTCACAGAAAAGC
		NY130 : TTATACCACCTTCTGAAGGAGCCAACAATTGTCTGTTTTGTG
pRS415-GPD-ErgS-*Afm* R328E	pRS415-GPD-ErgS-*Afm* (PCR 1)	NY157 : TAACACAAAACGAACAATTGTTGAACCCTTCAAAAG
		FF061 : TTTTCTGTGACTGGTGAGTACTCAACC
	pRS415-GPD-ErgS-*Afm* (PCR 2)	FF060 : TTGAGTACTCACCAGTCACAGAAAAGC
		NY158 : GTTCAACAATTGTTCGTTTTGTGTTAATATTCTTTTAC
pRS415-GPD-ErgS-*Afm* N332A	pRS415-GPD-ErgS-*Afm* (PCR 1)	NY159 : GACAATTGTTGGCTCCTTCAAAAGGTGGTATAAC
		FF061 : TTTTCTGTGACTGGTGAGTACTCAACC
	pRS415-GPD-ErgS-*Afm* (PCR 2)	FF060 : TTGAGTACTCACCAGTCACAGAAAAGC
		NY160 : CCTTTTGAAGGAGCCAACAATTGTCTGTTTTGTG
pRS415-GPD-ErgS-*Afm* K335E	pRS415-GPD-ErgS-*Afm* (PCR 1)	NY161 : TGAACCCTTCAGAAGGTGGTATAACTTTGCATATC
		FF061 : TTTTCTGTGACTGGTGAGTACTCAACC
	pRS415-GPD-ErgS-*Afm* (PCR 2)	FF060 : TTGAGTACTCACCAGTCACAGAAAAGC
		NY162 : GTTATACCACCTTCTGAAGGGTTCAACAATTGTC
pRS415-GPD-ErgS-*Afm* R328E, K335E	pRS415-GPD-ErgS-*Afm* (PCR 1)	NY163 : GAACAATTGTTGAACCCTTCAGAAGGTGGTATAACTTTGCATATC
		FF061 : TTTTCTGTGACTGGTGAGTACTCAACC
	pRS415-GPD-ErgS-*Afm* (PCR 2)	FF060 : TTGAGTACTCACCAGTCACAGAAAAGC
		NY164 : TTCTGAAGGGTTCAACAATTGTTCGTTTTGTGTTAATATTCTTTTAC
pRS415-GPD-ErgS-*Afm* W364A	pRS415-GPD-ErgS-*Afm* (PCR 1)	NY143 : CTATGACGAAGCTAGAATGGCCAGAAATAAGTC
		FF061 : TTTTCTGTGACTGGTGAGTACTCAACC
	pRS415-GPD-ErgS-*Afm* (PCR 2)	FF060 : TTGAGTACTCACCAGTCACAGAAAAGC
		NY144 : CTGGCCATTCTAGCTTCGTCATAGATTGCACATAATTC
pRS415-GPD-ErgS-*Afm* R365E	pRS415-GPD-ErgS-*Afm* (PCR 1)	NY133 : TGACGAATGGGAAATGGCCAGAAATAAGTCTG
		FF061 : TTTTCTGTGACTGGTGAGTACTCAACC
	pRS415-GPD-ErgS-*Afm* (PCR 2)	FF060 : TTGAGTACTCACCAGTCACAGAAAAGC
		NY134 : TTCTGGCCATTTCCCATTCGTCATAGATTGCAC
pRS415-GPD-ErgS-*Afm* R368E	pRS415-GPD-ErgS-*Afm* (PCR 1)	NY135 : GAGAATGGCCGAAAATAAGTCTGGTAGATTGC
		FF061 : TTTTCTGTGACTGGTGAGTACTCAACC
	pRS415-GPD-ErgS-*Afm* (PCR 2)	FF060 : TTGAGTACTCACCAGTCACAGAAAAGC
		NY136 : CAGACTTATTTTCGGCCATTCTCCATTCGTC
pRS415-GPD-ErgS-*Afm* Q375R	pRS415-GPD-ErgS-*Afm* (PCR 1)	NY137 : GGTAGATTGAGAGCCTTTATTACAGAATACG
		FF061 : TTTTCTGTGACTGGTGAGTACTCAACC
	pRS415-GPD-ErgS-*Afm* (PCR 2)	FF060 : TTGAGTACTCACCAGTCACAGAAAAGC
		NY138 : TAATAAAGGCTCTCAATCTACCAGACTTATTTC
pRS415-GPD-ErgS-*Afm* R409E	pRS415-GPD-ErgS-*Afm* (PCR 1)	NY139 : TGCTGCATTAGAATGGATAGGTGAAAAGAATG
		FF061 : TTTTCTGTGACTGGTGAGTACTCAACC
	pRS415-GPD-ErgS-*Afm* (PCR 2)	FF060 : TTGAGTACTCACCAGTCACAGAAAAGC
		NY140 : CACCTATCCATTCTAATGCAGCAAAACCGTTTAC

Table MM-2 (*continued*)

pRS415-GPD-ErgS-*Afm* D420R	pRS415-GPD-ErgS-*Afm* (PCR 1)	NY141 : TTATCACGTCAGACCTTGCATCGCCGCTCCTAG FF061 : TTTTCTGTGACTGGTGAGTACTCAACC
	pRS415-GPD-ErgS-*Afm* (PCR 2)	FF060 : TTGAGTACTCACCAGTCACAGAAAAGC NY142 : CGATGCAAGGTCTGACGTGATAACCATTCTTTTC
pRS415GPD-ErgS-*Bba*	*B. bassiana* genomic DNA (PCR 1)	NY177 : AAGCAGGCTTCATGATGCTGAGAAACTATC NY178 : gAAAGCTGGGTCCTATACCCGTTTCCGAGAG
	pRS415-GPD-X (LR recombined plasmid) (PCR 2)	NY179 : ACGGGTATAGGACCCAGCTTTcttgtacaaagtgg NY180 : TCAGCATCATGAAGCCTGCTTTTTTGTACaaac
pRS415GPD-ErgS-Yli	*Y. lipolytica* genomic DNA (PCR 1)	NY173 : AAGCAGGCTTCATGTGGTTCAACTGCTGCC NY174 : gAAAGCTGGGTCTTATGCGGCGACAGGAGGG
	pRS415-GPD-X (LR recombined plasmid) (PCR 2)	NY175 : CGCCGCATAAGACCCAGCTTTcttgtacaaagtgg NY176 : TTGAACCACATGAAGCCTGCTTTTTTGTACaaac
pRS415GPD-ErgS_*Yli* -α(-) 1 R217, R221, R224, K228 to E	pRS415GPD-ErgS_*Yli* (PCR 1)	NY201 : GAAACCATCAACGAATGGAACGAAAACCTGCAGGAAGAGGGCGTCAGCCTCAATGTG FF061 : TTTTCTGTGACTGGTGAGTACTCAACC
	pRS415GPD-ErgS_*Yli* (PCR 2)	FF060 : TTGAGTACTCACCAGTCACAGAAAAGC NY202 : TTCCTGCAGGTTTTCGTTCCATTCGTTGATGGTTTCGCCAAAACCGGGGTTGGTCTG
pRS415GPD-ErgS_*Yli* -α(-) 2 R217, R221 to E	pRS415GPD-ErgS_*Yli* (PCR 1)	NY203 : TTGGCGAAACCATCAACGAATGGAACCGAAACCTGCAGAAGGAGG FF061 : TTTTCTGTGACTGGTGAGTACTCAACC
	pRS415GPD-ErgS_*Yli* (PCR 2)	FF060 : TTGAGTACTCACCAGTCACAGAAAAGC NY204 : TTCCATTCGTTGATGGTTTCGCCAAAACCGGGGTTGGTCTGGGGG
pRS415GPD-ErgS_*Yli* -α(-) 3 R224, K228 to E	pRS415GPD-ErgS_*Yli* (PCR 1)	NY205 : GGAACGAAAACCTGCAGGAAGAGGGCGTCAGCCTCAATGTGTACTC FF061 : TTTTCTGTGACTGGTGAGTACTCAACC
	pRS415GPD-ErgS_*Yli* (PCR 2)	FF060 : TTGAGTACTCACCAGTCACAGAAAAGC NY206 : CCCTCTTCCTGCAGGTTTTCGTTCCATCGGTTGATGGTTCGGCC

Table MM-2 (*continued*)

Construction of *E. coli* overexpression plasmids - *isoThermal assembly*		
Constructions for protein purification of recombinant ErdS variants		
pMtevGWA-ErdS-*Afm*	pDONR221-ErdS-*Afm* (PCR1)	#142 : GGTACCGGATCTTACATCACAAGTTTGTACAAAAAAGCAGGCTTC
		#134 : GTGGTGGTGGTGCTCGAGGTACATCAACTTTGTACAAGAAAGCTGGGTC
	pMtevGWA-X (PCR2)	#114 : TGATGTACCTCGAGCACCACCACCAC
		#135 : AAACTTGTGATGTAAGATCCGGTACC
pMtevGWA-ErdS-Δduf2156	pDONR221-ErdS-Δduf2156 (PCR1)	#142 : GGTACCGGATCTTACATCACAAGTTTGTACAAAAAAGCAGGCTTC
		#134 : GTGGTGGTGGTGCTCGAGGTACATCAACTTTGTACAAGAAAGCTGGGTC
	pMtevGWA-X (PCR2)	#114 : TGATGTACCTCGAGCACCACCACCAC
		#135 : AAACTTGTGATGTAAGATCCGGTACC
pMtevGWA-ErdS-ΔaspRS	pDONR221-ErdS-ΔaspRS (PCR1)	#142 : GGTACCGGATCTTACATCACAAGTTTGTACAAAAAAGCAGGCTTC
		#134 : GTGGTGGTGGTGCTCGAGGTACATCAACTTTGTACAAGAAAGCTGGGTC
	pMtevGWA-X (PCR2)	#114 : TGATGTACCTCGAGCACCACCACCAC
		#135 : AAACTTGTGATGTAAGATCCGGTACC
pMtevGWA-ErdSΔ84-*Afm*	pMtevGWA-ErdS-*Afm* (PCR1)	DN_84 : GCCAACTTTGTACAAAAAAGCAGGCTTCATGTCAGATGACTCCGA
		FF061 : TTTTCTGTGACTGGTGAGTACTCAACC
	pMtevGWA-ErdS-*Afm* (PCR2)	FF060 : TTGAGTACTCACCAGTCACAGAAAAGC
		DN_rv : GAAGCCTGCTTTTTTGTACAAAG
pMtevGWA-AspRS~AAPA~-DUF2156	pMtevGWA-ErdS-*Afm* (PCR1)	FF048 : TTTTAGCCGCTGCTCCTGCTTTGGCAAAGCAAATGGCCATC
		FF061 : TTTTCTGTGACTGGTGAGTACTCAACC
	pMtevGWA-ErdS-*Afm* (PCR2)	FF060 : TTGAGTACTCACCAGTCACAGAAAAGC
		FF049 : CTTTGCCAAAGCAGGAGCAGCGGCTAAAAATGCATCTCTACCG
pMtevGWA-ErdS-α(0) R749, K750, R751, R752 to A	pMtevGWA-ErdS-*Afm* (PCR1)	FF050 : GCAGCAGCAATAGCAGCAGCCGAAAACGAAGGTATTAAAATCG
		FF061 : TTTTCTGTGACTGGTGAGTACTCAACC
	pMtevGWA-ErdS-*Afm* (PCR2)	FF060 : TTGAGTACTCACCAGTCACAGAAAAGC
		FF051 : GCTGCTGCTATTGCTGCTGCAATTTCACCGTCAGAAGCGGCTTG
p**His**MtevGWA-ErdS variant (insertion of His8x-tag at the Nt of the encoded MBP-ErdS)	pMtevGWA-ErdS variant (PCR 1)	His_fwd : ATGCACCACCACCACCACCACCACCACATGGGTACCAAAACTGAAGAAGGTA
		FF061 : TTTTCTGTGACTGGTGAGTACTCAACC
	pMtevGWA-ErdS variant (PCR 2)	FF060 : TTGAGTACTCACCAGTCACAGAAAAGC
		His_rev : GTGGTGGTGGTGGTGGTGGTGGTGCATGGTATATCTCCTTCTTAAAGTTAAA
p**G**MtevGWA-erdS-ΔaspRS (insertion of GST-tag at the Nt of the encoded MBP-ErdS)	pGGWA (PCR 1)	NY011 : GTTTAACTTTAAGAAGGAGATATACCATGGGTACCTCCCCTATACTAGGTTATTG
		NY012 : CCTTCTTCAGTTTTGGTACCCATATCCGATTTTGGGGGATGGTCGCCAC
	pMtevGWA-ErdS-ΔaspRS (PCR 2)	NY013 : ATGGGTACCAAAACTGAAGAAGG
		NY014 : GGTATATCTCCTTCTTAAAGTTAAAC

Constructions for protein purification of recombinant ErdH variants		
pMtevGWA-ErdH	Afm Genomic DNA (PCR1)	NY119 : AAGCAGGCTTCATGGCCTCTCATGCCCCTC
		NY120 : gAAAGCTGGGTCCTATCTGTCAAAAATCGC
	pMtevGWA-X (PCR2)	NY121 : GACAGATAGGACCCAGCTTTcttgtacaaagtgg
		NY122 : ATGAGAGGCCATGAAGCCTGCTTTTTTGTACaaac
pMtevGWA-ErdH-S153A	pMtevGWA-ErdH (PCR 1)	NY145 : TGAGTGGTTTCGCTGCGGGCGGCAACCTCGCTG
		FF061 : TTTTCTGTGACTGGTGAGTACTCAACC
	pMtevGWA-ErdH (PCR 2)	FF060 : TTGAGTACTCACCAGTCACAGAAAAGC
		NY146 : TTGCCGCCCGCAGCGAAACCACTCAGAGCAATTC
pMtevGWA-ErdH-D277A	pMtevGWA-ErdH (PCR 1)	NY147 : TCTGCGAATGGGCTATGCTGATGAACGAGGGC
		FF061 : TTTTCTGTGACTGGTGAGTACTCAACC
	pMtevGWA-ErdH (PCR 2)	FF060 : TTGAGTACTCACCAGTCACAGAAAAGC
		NY148 : TTCATCAGCATAGCCCATTCGCAGATGTACAG
pMtevGWA-ErdH-H307A	pMtevGWA-ErdH (PCR 1)	NY149 : AAAAAGCCCGAGCTGCCTGGGACAAGTCCCCG
		FF061 : TTTTCTGTGACTGGTGAGTACTCAACC
	pMtevGWA-ErdH (PCR 2)	FF060 : TTGAGTACTCACCAGTCACAGAAAAGC
		NY150 : TGTCCCAGGCAGCTCGGGCTTTTTCAATCATC
pMtevGWA-ErdH-K311D	pMtevGWA-ErdH (PCR 1)	NY151 : TGCCTGGGACGATTCCCCGAATCCCTTCCGAG
		FF061 : TTTTCTGTGACTGGTGAGTACTCAACC
	pMtevGWA-ErdH (PCR 2)	FF060 : TTGAGTACTCACCAGTCACAGAAAAGC
		NY152 : GGATTCGGGGAATCGTCCCAGGCATGTCGGGC

Table MM-2 (*continued*)

Constructions for protein purification of recombinant ErgS variants		
pMtevGWA-ErgS-*Afm*	pDONR221-ErgS-*Afm* (PCR1)	#142 : GGTACCGGATCTTACATCACAAGTTTGTACAAAAAAGCAGGCTTC
		#134 : GTGGTGGTGGTGCTCGAGGTACATCAACTTTGTACAAGAAAGCTGGGTC
	pMtevGWA-X (PCR2)	#114 : TGATGTACCTCGAGCACCACCACCAC
		#135 : AAACTTGTGATGTAAGATCCGGTACC
pMtev-ErgS_Yli	*Y. lipolytica* genomic DNA (PCR 1)	NY173 : AAGCAGGCTTCATGTGGTTCAACTGCTGCC
		NY174 : gAAAGCTGGGTCTTATGCGGCGACAGGAGGG
	pMtevGWA-X (PCR2)	NY175 : CGCCGCATAAGACCCAGCTTTcttgtacaaagtgg
		NY176 : TTGAACCACATGAAGCCTGCTTTTTTGTACaaac
pRS415GPD-ErgS_Yli-α(-) 1 R217, R221, R224, K228 to E	pMtev-ErgS_*Yli* (PCR 1)	NY201 : GAAACCATCAACGAATGGAACGAAAACCTGCAGGAAGAGGGCGTCAGCCTCAATGTG
		FF061 : TTTTCTGTGACTGGTGAGTACTCAACC
	pMtev-ErgS_*Yli* (PCR 2)	FF060 : TTGAGTACTCACCAGTCACAGAAAAGC
		NY202 : TTCCTGCAGGTTTTCGTTCCATTCGTTGATGGTTTCGCCAAAACCGGGGTTGGTCTG

Deletion and complementation cassettes for *Afm* strains - *isoThermal assembly & ligation in pJet*		
pJET1.2-erdS deletion cassette *Afm*	pSK529 (Hartmann et al., 2010) (PCR 1)	FF166 : TATAGGTCAATAGAGTATACTTATTTG
		FF167 : TATTATGCTCAACTTAAATGACCTAC
	Afm CEA17ΔakuBKU80 gDNA (5'-UTR) (PCR 2)	FF168 : cccgggTACGTTGGTACGTGAAAGAAATGG
		FF169 : TAAGTATACTCTATTGACCTATAGGTGACGGATGAGAGACCACC
	Afm CEA17ΔakuBKU80 gDNA (3'-UTR) (PCR 3)	FF170 : GGTCATTTAAGTTGAGCATAATAAGTGGCAGATGTACCAAGCCC
		FF171 : cccgggTACGCCGCCTCCCTTCCCATTGC
pJET1.2-Pxyl-erdS	pJET1.2-erdS deletion cassette Afm (PCR1)	FF271 : CAAAGCACGTTTGATCGACATCTGCAgttggttcttcgagtcgatgaatg
		FF272 : TGCACTTCTTTGAAGACTAAGGATCCCCGACGCCGACCAACACCGCC
	Afm CEA17ΔakuBKU80 gDNA (PCR 2)	FF273 : ATGTCGATCAAACGTGCTTTGTCTAAG
		FF274 : TTAGTCTTCAAAGAAGTGCAGAACCG
pJET1.2-5'UTR from ergS-*Afm*	Afm CEA17ΔakuBKU80 gDNA	fD-5'UTR-fwd : CCCGGGTGTGGATCAAACCTTAGATAGCC
		fD-5'UTR-rv : GGACCTGAGTGATGCGCAGTAATGTTTTAACAATCGCAAGTTCC
pJET1.2-3'UTR from ergS-*Afm*	Afm CEA17ΔakuBKU80 gDNA	fD-3'UTR-fwd : GGTCCATCTAGTGCGCAGGCATCGGTACCGTTCCTGCAAAAGTCC
		fD-3'UTR-rv : CCCGGGGCCTACGAATCAGAAGCCCTGC
pJET1.2-ergS deletion cassette Afm	pJET1.2-5'UTR from ergS-Afm (PCR 1)	FF061 : TTTTCTGTGACTGGTGAGTACTCAACC
		fD-5'UTR-rv : GGACCTGAGTGATGCGCAGTAATGTTTTAACAATCGCAAGTTCC
	pSK529 (Hartmann et al., 2010) (PCR 2)	hygroK7-fwd : TACTGCGCATCACTCAGGTCC
		hygroK7-rv : TGCCTGCGCACTAGATGGACC
	pJET1.2-5'UTR from ergS-Afm (PCR 3)	fD-3'UTR-fwd : GGTCCATCTAGTGCGCAGGCATCGGTACCGTTCCTGCAAAAGTCC
		FF060 : TTGAGTACTCACCAGTCACAGAAAAGC
pJET1.2-Pxyl-ergS	pJET1.2-ergS deletion cassette Afm (PCR 1)	NY041 : Cagttggttcttcgagtcgatgaatg
		FF061 : TTTTCTGTGACTGGTGAGTACTCAACC
	Afm CEA17ΔakuBKU80 gDNA (PCR 2)	NY042 : cattcatcgactcgaagaaccaacTGATAGCCTGTCTGGGCTGGAACTTGCG
		NY043 : GCGGTGTTGGTCGGCGTCGGGGATCCTCATTGCGGGACCGCAGGCTTGGAAC
	pJET1.2-ergS deletion cassette Afm (PCR 3)	NY040 : GGATCCCCGACGCCGACCAACACCGC
		FF060 : TTGAGTACTCACCAGTCACAGAAAAGC

Afm ΔerdS strains verification by PCR	
Afm CEA17ΔakuBKU80 gDNA	FF684 : GGAGATTGGATATGGATGAAGTGAAC
	FF685 : GTTGCCAACGTCGAGAAAACC
	NY15 : GAGCTGATGCTTTGGGCCGAGGACTGC
	NY16 : GCAGTCCTCGGCCCAAAGCATCAGCTC

Table MM-2 (*continued*)

Deletion and complementation cassettes for *Aor* strains - *restriction and ligation* (*T. Kushiro's team*)		
pTAnpyrG	*A. nidulans* A26	AnpyrG-F : CCCCCCCGGGCTAGGCGCAATCCCTG
		AnpyrG-R : GGGGACTAGTGCCGGCTTAACCACAG
pAnpyrG-MR	pTAnpyrG	AnpyrG-SpeI-FF : CCCCACTAGTCTCGTCGGCTCTTTTCGCAA
		AnpyrG-SphI-FR : GGGGGCATGCGTAGAGGGTGCGGAGAACA
pUCdn	*Aor* RIB40 *genomic DNA*	AoErdS-3'-SmaI-F : GACTAACCCGGGGCCTTCTTATGTTAGGCGTTTG
		AoErdS-3'-EcoRI-R : CTAGTCGAATTCTTCGAACCAGAATTAACGCTAC
pUCflk	*Aor* RIB40 *genomic DNA*	AoErDS-5'-HindIII-F : ACCTGCAAGCTTCTTTAATATCCCGAGAATACTCG
		AoErDS-5'-PstI-R : TGATGACTGCAGTTGTGTAGCGGACGATAG
pDAor-ErDS	pAnpyrG-MR	AnpyrG-MR-SmaI-F primer : CTTCATCCCGGGCTAGGCGCAATCCCTGTC
		AnpyrG-MR-PstI-R primer : CTTCATCCCGGGCTAGGCGCAATCCCTGTC

Verification of deletant and complemented *Aor* strains by PCR (*T. Kushiro's team*)		
HiMe10, HiDES (gDNA)		P1 : AoErdS-5'-HindIII-F : ACCTGCAAGCTTCTTTAATATCCCGAGAATACTCG
		P4 : AoErdS-3'-EcoRI-R : CTAGTCGAATTCTTCGAACCAGAATTAACGCTAC
HiDES + erdS, HiDES + erdSDduf (gDNA)		P15 : AoErdS-486-F : TGCCAAGCTGGTTTTCCTTG
		P16 : AoErdS-575-R : ATGGCGATGGAATTCTTGCC
HiDES + erdSDaspRS (gDNA)		P10 : AoErdS-PmaCI-R : AGACACGTGTTAGTCTTCGAAAAAGTGAAGGACAG
		P17 : AoErdS-2274F : GGCGATCCTTTGTGCGATTC

Additional publications

Review Article

Yakobov *et al.*, 2018

Cytosolic aminoacyl-tRNA synthetases: Unanticipated relocations for unexpected functions
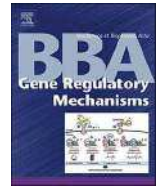
Cytosolic aminoacyl-tRNA synthetases: Unanticipated relocations for unexpected functions

Nathaniel Yakobov, Sylvain Debard, Frédéric Fischer, Bruno Senger, Hubert Dominique Becker*

Génétique Moléculaire, Génomique, Microbiologie, UMR 7156, CNRS, Université de Strasbourg, Institut de Botanique, 28 rue Goethe, 67083 Strasbourg Cedex, France

ABSTRACT

Prokaryotic and eukaryotic cytosolic aminoacyl-tRNA synthetases (aaRSs) are essentially known for their conventional function of generating the full set of aminoacyl-tRNA species that are needed to incorporate each organism's repertoire of genetically-encoded amino acids during ribosomal translation of messenger RNAs. However, bacterial and eukaryotic cytosolic aaRSs have been shown to exhibit other essential nonconventional functions. Here we review all the subcellular compartments that prokaryotic and eukaryotic cytosolic aaRSs can reach to exert either a conventional or nontranslational role. We describe the physiological and stress conditions, the mechanisms and the signaling pathways that trigger their relocation and the new functions associated with these relocating cytosolic aaRS. Finally, given that these relocating pools of cytosolic aaRSs participate to a wide range of cellular pathways beyond translation, but equally important for cellular homeostasis, we mention some of the pathologies and diseases associated with the dis-regulation or malfunctioning of these nontranslational functions.

1. Introduction

Aminoacyl-tRNA synthetases (aaRSs) belong to a family of ubiquitous and essential enzymes. Their primary task is to supply the protein synthesis machineries (cytosolic and organellar) with the full set of aminoacyl-tRNAs (aa-tRNAs) necessary to translate all messenger RNA codons into their corresponding amino acids (aa) [1]. In theory, a given organism has to encode at least one aaRS for each genetically-encoded aa, which means that a prokaryotic species that uses for protein synthesis the standard genetic code composed of 20 aa, would need 20 genes encoding the 20 required aaRSs. However, depending on the organism's origin and genetic code repertoire, the number of aaRSs that can be found in a given organism ranges from 18 to 23 in prokaryotes [2] to nearly 45 in eukaryotes [3]. Despite their essential biochemical function the majority of prokaryotes and all eukaryotic organelles have less unique aaRSs than genetically-encoded aa, because these organisms (or compartments) can compensate the lack of an essential aaRS by alternative routes to generate the aa-tRNA species corresponding to the orphan tRNA/codon pair ([4–6] and reviewed in [7,8]). Paradoxically, prokaryotes and mainly bacteria also quasi-systematically encode more aaRSs than the necessary set for decoding the genetic code repertoire because the majority of bacterial genomes harbor more than one gene for a given aaRS [2]. Although the majority of the bacteria present one or several duplicated aaRSs (and even triplicated ones), the reason for

the presence of 2 aaRSs of the same aa and tRNA-charging specificity in a given species has rarely been studied. However, in the few cases that were studied, it was found that one of the two forms is usually expressed under specific environmental or stress conditions and that this stress-induced aaRS possesses specific catalytic traits allowing formation of the cognate aa-tRNA in these particular physiological conditions [9–14].

In eukaryotes, the presence of at least 2 different translationally-active and membrane-separated compartments, the cytosol and mitochondria, makes already the situation more complex with respect to the number of aaRSs that these organisms have to possess; and becomes even more complicated if the organism possesses additional organelles besides the mitochondria. Because the organellar and cytosolic translation machineries are of different phylogenetic origins, each eukaryote carries several compartment-specific pools of aaRSs, one for cytosolic translation and one for each organelle (reviewed in [15]). While both sets of genes are encoded by the nuclear genome and translated by the cytosolic protein synthesis machinery, the organellar pools are easily distinguishable from the cytosolic one because they are of prokaryotic origins and because these aaRSs possess, usually in the N-terminus, an organelle-specific targeting sequence that directs their import into the corresponding compartment (reviewed in [15]). However, even if in theory, a eukaryotic species using the standard 20 aa-containing genetic code and that possesses mitochondria would have to encode 40 aaRS

genes, there is not a single eukaryotic species that has been proposed so far to encode 2 complete and unique compartment-specific sets of 20 aaRSs [5,15]. Depending on the species that was studied, up to 17 mitochondria-specific aaRS genes can be missing (reviewed in [15]) from the nuclear genome in certain species. To compensate this apparent lack of mitochondrial aaRSs, eukaryotes essentially utilize two different strategies: i) they use an alternate two-steps route to generate the aa-tRNA species for which the cognate aaRS is missing [6,16,17] or ii) they import the corresponding cytosolic aaRS making this enzyme a dual-localized aaRS both cytosolic and mitochondrial (reviewed in [15,18]). When both the cytosolic and mitochondrial aaRS are encoded by a single gene, both forms are either translated from two mRNAs of different length generated through different processes (see below). While using a dual-localized aaRS encoded from a single gene makes perfect sense when the gene encoding the mitochondria-specific aaRS is missing, there are examples in higher plants and *S. cerevisiae* (*Sce*), where a cytosolic aaRS can be targeted to mitochondria even if the corresponding mitochondrial ortholog encoded by a separate gene already exists (reviewed in [15]). The rational for having duplicated mitochondrial aaRS (one strictly organellar and one dual-localized) has been clarified in yeast [6] but has so far not been ruled out in higher plants. However, it was shown that some of these plant dual-localized aaRSs are not able to charge tRNA inside the mitochondria [19], suggesting that they might have a nonconventional role inside this compartment that has yet to be identified. Interestingly, in plants the cytosolic aaRSs that are dual-localized are strictly shared with the mitochondria and never with the chloroplast, however the majority of the mitochondrial aaRSs are dual-targeted both in the mitochondria and the chloroplasts because they harbor an ambiguous organellar targeting sequence [20].

The other common trait of eukaryotic cytosolic aaRSs that influences their subcellular localization is the capacity of some of them to form so-called Multi-Synthetase Complexes (MSCs). These complexes were found in all species studied so far ranging from fungi to mammals ([21–24] and reviewed in [25]). They are all composed of cytosolic aaRS and 1 to 3 auxiliary assembly factors also called Aminoacyl-tRNA synthetase Interacting Multifunctional Proteins (AIMPs). The number of aaRSs and AIMPs that build up these MSCs varies from 2 aaRSs and 1 AIMP in the *S. cerevisiae* AME complex to 9 aaRSs and 3 AIMPs (AIMP1, AIMP2 AIMP3 also called p43, p38 and p18 respectively) in the human, MARS complex. With the exception of the yeast AME MSC (reviewed in [26]), the association of cytosolic aaRSs into MSC does not impact the catalytic efficiency of the participating aaRSs but rather regulates the alternative subcellular localization and non-conventional function that some of them have been shown to display. The studies that have been published over the past 2 decades uniformly show that these MSCs can be considered as cytosolic retention platforms for aaRSs that can be released from these complexes under specific physiological or stress conditions to relocate into other subcellular compartments in which they can exert nonconventional functions (reviewed in [27–30]). Additionally, the AIMPs can also be released from MSCs to be targeted to other compartments (reviewed in [31]). The additional compartments that these MSC-released cytosolic aaRSs or AIMPs can reach and the repertoire of atypical physiological processes to which these proteins can participate is in constant expansion ([29], reviewed in [32]). Studies show that MSCs-released aaRSs can i) stay in the cytosol by building other non-MSC complexes, ii) be imported into mitochondria or nuclei, iii) bind to membranes or even iv) be secreted (reviewed in [18]). Once relocated, they can exert a myriad of regulatory or signaling functions that impact processes among which gene expression, angiogenesis, apoptosis, inflammation, adiposity, nutrient signaling, cell-to-cell crosstalk or even resveratrol-mediated poly(ADP-ribose) polymerase 1 (PARP1) activation (reviewed in [28–31], [33]). Their involvement in these processes is far from being trivial since in human, malfunctioning of these aaRSs' additional roles, inevitably leads to diseases [31,34].

At the molecular level, the release of an aaRS or AIMP from the MSC is usually mediated by posttranslational modification of the protein that includes chemical modification or proteolytic cleavage of the aaRSs at a specific residue [35]. More rarely, the release of an aaRS can be initiated by decreasing the quantity of the AIMP binding the aaRS [36]. There are 2 types of molecular mechanism by which these aaRSs exert their atypical function, either they bind to one or several new protein partners that deviates the aaRS from aa-tRNA formation or they accumulate a by-product or intermediate of the tRNA aminoacylation reaction (reviewed in [27–30]) or both. Note that in human and yeast some of the cytosolic aaRSs that do not belong to the MSCs have also been shown or predicted to be able to relocate to other subcellular compartments and, in some cases, their atypical role has been characterized.

In the present review we give a detailed overview of all the subcellular compartments that free-standing or MSC-participating cytosolic aaRSs can reach. We mention the mechanisms, strategies and and physiological or stress conditions that trigger their relocation and the unexpected cellular processes to which relocated cytosolic aaRSs participate. We have subdivided relocating aaRSs into two categories: those who keep their canonical function in their new subcellular destination, meaning formation of an aa-tRNA intermediate or end-product that supplies the translation machinery and those who exert a nonconventional function that does not require formation of an aa-tRNA species.

2. Membrane-localized aaRSs in bacteria

Prokaryotic cells are composed of distinct compartments that differ according to their phylogenetic origin. In all cases, the cytoplasm, in which transcription and translation of genetic information occur, is engulfed by a negatively charged plasma membrane made up of various lipid species, ranging from phospholipids to hopanoids [37,38]. The structure of the outer shell of prokaryotes differs between Gram-positive [39] and Gram-negative [40] bacteria, and between phylogenetical groups of archaea [41], but to date, no aaRS has been detected outside the cytoplasm, where the 20 enzymes find their substrates (ATP, aa, tRNAs) and perform their canonical aminoacylation function. Several studies, however, have shown that aaRS can sometimes be localized at membranous structures (see below).

Central and essential biological functions depend on the integrity of plasma membranes, such as respiration, electron transport, proton translocation, mechanical stresses resistance, nutrients and exogenous molecules selection and transport, interaction with the environment or host macromolecules, etc. [37–41]. Because of their relatively uniform negative charge, bacterial membranes are targeted by and sensitive to cationic antimicrobial peptides (CAMPs) synthesized and secreted by other bacteria or fungi, or by immune cells within a host [42]. Various CAMPs exist, but they often target bacteria through charge interaction, leading to membrane disruption and ultimately to bacterial death [42]. Bacteria possess CAMPs resistance factors of various types [43,44], and among them, aminoacyl-phosphatidylglycerol synthases (aaPGSs) [45,46]. AaPGSs are composed of two separated domains, an integral membrane N-terminal domain with 2 to 14 transmembrane helices, with a phospholipid flippase activity, and a C-terminal soluble domain of the DUF2156 family that has an aa-tRNA transferase activity. AaPGSs catalyze the transfer of an aa from an aa-tRNA to a second substrate, phosphatidylglycerol (PG) or cardiolipin (CL) [45]. For example, LysPGS transfers Lys from K-tRNA^K to PG, leading to a lysylated PG (K-PG), whose overall charge is $+1$, in comparison to PG (-1). AaPGSs can be specific of one aa (KPGS, APGS), bispecific (A/KPGS) or multi-specific (R/A/KPGS) and transfer corresponding amino acids onto PG or CL, providing aminoacylated phospholipids with modified charge properties. Such modifications change the overall properties of membranes such as permeability to various compounds (metals, antimicrobials, *etc*.), rigidity and, of course, global charge. AaPGSs have
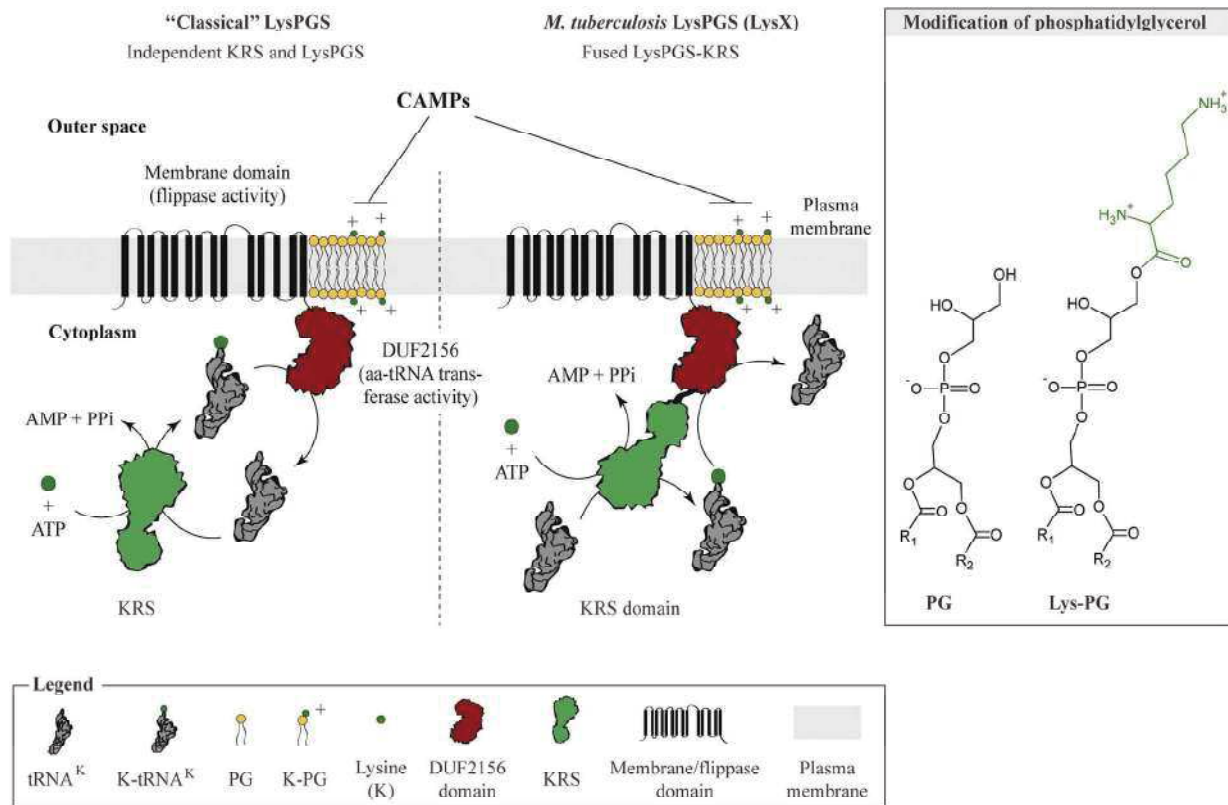
Fig. 1. Aminoacyl-phosphatidylglycerol synthases. "Classical" aaPGS, like the LysPGS from *S. aureus* is composed of an N-terminal integral membrane domain with 14 transmembrane helices (TMH, black), that targets the enzyme to the plasma membrane, and a C-terminal soluble domain, facing the cytoplasm (red), which belongs to the DUF2156 family of aa-tRNA transferases. The DUF2156 domain utilizes K-tRNA^K, produced independently by a "canonical" KRS (green), and catalyzes the transfer of K (green cicle) from tRNA^K to a hydroxyl group of phosphatidylglycerol (PG). Resulting K-PG can then be transferred to the outer leaflet of the plasma membrane by the N-terminal membrane domain that displays a phospholipid flippase activity. Changes in membrane charge properties participate in resistance against CAMPs. In *M. tuberculosis*, the LysX gene product is a LysPGS-KRS fusion protein, with the N-terminal flippase/membrane (black) and middle DUF2156 (red) domains of classical aaPGSs, followed by a KRS C-terminal domain (green). This domain is responsible for the synthesis of K-tRNA^K that is subsequently used by the DUF2156 and flippase domains to produce surface exposed K-PG molecules. The aaPGS part of the protein cannot scavenge K-tRNA^K produced by the second "canonical" KRS in *M. tuberculosis*. The right panel presents structures of PG and K-PG. (For interpretation of the references to color in this figure legend, the reader is referred to the web version of this article.)

been demonstrated to increase resistance against CAMPs in various model pathogens such as *Staphylococcus aureus*, *Listeria monocytogenes*, *Pseudomonas aeruginosa* and others and have been related to virulence phenotypes. Those virulence factors have thus been named Multiple Peptide Resistance Factors [45,46].

In *Mycobacterium tuberculosis* and numerous Actinobacteria [45], two KRS genes are detected. One of them (*lysS*, Rv3598c) encodes a canonical KRS with an N-terminal anticodon-binding domain (ABD) and a C-terminal catalytic core, while the second (*lysX*, Rv1640c) is composed of an N-terminal MprF-like domain (flippase and DUF2156 domains) followed by a KRS domain (ABD and catalytic domains) ([47], Fig. 1 and Table 1).

This KRS localizes at the plasma membrane, through the flippase-like domain, and has been shown to be a *bona fide* KPGS [47,49]. Interestingly, the "classical" MprF part of the protein cannot scavenge K-tRNA^K synthesized by the second, canonical KRS, when deprived of the KRS appended domain, in contrast to other "classical" aaPGS. The KRS domain thus specifically synthesizes K-tRNA^K for use in membrane modification. The LysX protein is, like other aaPGSs, involved in membrane remodeling, CAMPs resistance and virulence [47].

In cyanobacteria, specialized membrane structures separated from the plasma membrane, called thylakoids, are involved in oxygenic photosynthesis, in particular in the assembly and functioning of photosystems. Proteins and protein complexes can be targeted within the thylakoid lumen, or at the surface of the organelle-like compartment, and perform various functions related to oxygenic photosynthesis. For

example, F_1F_0 ATP synthase is assembled and functions at the surface of thylakoids [50,51]. Recent work highlighted that among 279 sequenced cyanobacteria, 102 contain one or several aaRSs that are anchored to the outer leaflet of thylakoid membranes [52]. Thylakoid-specific targeting of aaRSs depends on the presence of a CAAD (for Cyanobacterial Aminoacyl-tRNA synthetases Appended Domain) domain that has been detected in 7 different aaRSs (ERS, VRS, LRS, IRS, CRS, MRS, RRS) at various positions within the protein sequences. CAAD is found at the very C-terminus of ERS, but in a C-terminal internal region in other aaRSs [52]. In all cases, no other paralogs of CAAD-containing aaRSs is found in proteomes, which suggested that they are all active in spite of unusual membrane localization [52–54]. Phylogenetic studies suggest that only cyanobacteria contain aaRSs with a CAAD domain, and that insertion of this module in aaRSs corresponds to several independent evolutionary events [52,53]. The CAAD domain shares homology with the CURT1/TMP14/PSI-P-family proteins, found in chloroplasts of plants. They are all membrane proteins involved in the organization of thylakoids and grana in chloroplasts, by influencing curvature of lipid bilayers [53]. AaRS-CAAD domains have not been shown to be involved in modulating thylakoid curvature and/or ultrastructure, but have been experimentally demonstrated to anchor aaRSs in thylakoid membranes [52,54]. It is to be noted that VRS-CAAD, that is thylakoid-bound, relocates at cell poles of mature heterocysts (specialized and differentiated cyanobacterial cells) upon nitrogen starvation [52]. A combination of *in vivo* and *in vitro* experiments showed that VRS-CAAD is active and found only in membrane fractions of cyanobacteria, while

ARTICLE IN PRESS

N. Yakobov et al.
BBA - Gene Regulatory Mechanisms xxx (xxxx) xxx–xxx

Table 1

Non-canonical functions and relocalizations of aaRS: AaRSs that exert nontranslational functions are grouped as a function of the subcellular compartment to which they relocate: (C, cytoplasm; N, nucleus; M, mitochondria; C. mb, cytoplasmic membrane; L, lysosome; V, vacuole), or when they are extracellularly secreted (HIV, human immunodeficiency virus; RSV, Rous sarcoma virus; Exo, exosomes; EC, extracellular (secreted); S, (host) serum). Organisms or groups of organisms in which the aaRS relocalizations where reported in this review are abbreviated as follows: Mam, mammalian; Vert, vertebrates; High. Euk, higher eukaryotes; *Hsa*, *Homo sapiens*; *Sce*, *Saccharomyces cerevisiae*; Zf, zebrafish; *Bma*, *Brugia malayi*; *Mtu*, *Mycobacterium tuberculosis*. The schematized structural organization of each aaRS was designed based on pfam 31.0 (http://pfam.xfam.org/), NCBI blastp, recent reviews [29,48] and the cited references (domains are not at scale). Orange and blue boxes correspond to anticodon/tRNA binding domains and catalytic core respectively, gray boxes correspond to additional domains and green boxes to WHEP domains. Red marks indicate the position of the residue that is post-translationally modified and/or domains involved in relocalization. p, phosphorylation; ac, acetylation; n.d., not determined; Nt ext., N-terminal extension; Ct, C-terminal; Transmb, transmembrane domain; cat, Catalytic; tRNA bd, tRNA binding domain.

Comp.	Organism	aaRS	Structural organisation	(Re)loc. mec	domain(s) involved	Physiological funtion	References
C.	*Hsa*	EPRS		pS886/pS999	WHEP	Translation regulation (GAIT element)	[32], [35], [83-87]
	Hsa, Mmu	EPRS		pS990	WHEP	antiviral immunity	[88]
	Hsa	QRS		MARS released	Catalytic	Anti-apoptotic	[89-92]
	Mam	RRS		Alternative AUG	Nt. Zn finger	Protein degradation	[93-98]
N.	*Hsa*	KRS		pS207	tRNA bd.	Transcription activation (MITF)	[103-105]
	Mam. Zf	YRS		acK244	NLS tRNA bd.	DNA damage response	[109-112]
	Vert.	WRS		NLS	WHEP	p53 signaling	[113-115]
	Vert.	SRS		NLS	UNE-S	Anti-angiogenic	[28], [116], [120], [121]
	Vert.	TRS		n.d.	not UNE-T	Anti-angiogenic	[122]
	Hsa	MRS		NLS	Nt ext. (GST)	rRNA transcription	[123]
	Sce	MRS		NLS	GST-like	*ATP1* transcription regulation	[36]
	Sce	DRS		NLS (Nt)	Nt ext.	DRS-mRNA translational regulation	[116], [125]
M.	*Sce*	ERS		MTS	GST-like	ATP9 translation regulation	[36]
C. mb.	*Hsa*	KRS		pT52	ABD + ext.(1-72)	Promotes Cell-migration	[126-128]
	Hsa, Mmu	EPRS		pS999	WHEP	Adiposity and lifespan regulation	[32]
	Mtu	KRS		Transmb.	Flippase, Duf2156	Virulence and cAMP resistance	[45-47]
L.	Mam.	LRS		VPS34 (cat. site)	catalytic, UNE-L	Lysosomal mTORC1 activation	[136], [137]
V.	*Sce*	LRS		Gtr1	editing domain	Vacuolar mTORC1 activation	[139]
HIV	*Hsa*	KRS		pS207 / Gag	Helix H7	Primer tRNA^K packaging	[140-144],[145]
RSV	*Hsa*	WRS		n.d.	n.d.	Primer tRNA^W packaging	[146]
E.	*Hsa*	KRS		Syntenin	cleavage site, PDZ d.	TNFa and cell migration in macrophages	[147], [148]
EC.	High. Euk.	YRS		n.d.	Mini-YRS	Pro-angiogenic (IL8 like)	[151], [152], [154-156]
	High. Euk.	YRS		n.d.	EMAPII like Ct d.	Pro-inflammatory cytokine	[148], [153], [163]
	High. Euk.	WRS		n.d.	Mini-WRS	Angiostatic	[153], [154] [158-162]
	Hsa	WRS		n.d.	WHEP	Early immune response	[164]
	Hsa	TRS		n.d.	n.d.	Endothelial cell migration	[165], [166]
S.	*Hsa*	GRS		n.d.	n.d.	Defense against tumor formation (ERK)	[173], [174]
S.	*Bma*	NRS		secreted	UNE-N	Host Pro Inflammatory	[167-172]

deletion of the CAAD domain renders the protein soluble without impacting its kinetic activity. Importantly, a series of pull-down experiments coupled with LC-MS/MS characterizations conducted in *Anabaena* sp. PCC 7120 strongly support that VRS-CAAD directly interacts with the F_1F_0-ATP synthase in thylakoid membranes in a CAAD-dependent manner. Interaction between VRS-CAAD and F_1F_0-ATP synthase does not influence aminoacylation activity, and no impact on the overall ATP production, used as a proxy of ATP synthase activity, could be evidenced. However, authors propose several hypotheses relating CAAD-containing aaRSs and nutrient sensing (in particular nitrogen through aa sensing), or possible moonlighting functions that have yet still to be experimentally addressed [52].

3. Eukaryotic relocating aaRSs with conventional functions

The intracellular space of eukaryotic cells has a complex organization and displays more than one translationally active compartment. It is therefore questionable to ask if there is a specific aaRS for each compartment or if a single polypeptide chain can be found at multiple localizations within a cell. In this section, we examine how each translationally-active compartment is supplied with a complete set of aa-tRNA synthesizing activities and how cytosolic aaRS are distributed throughout the cell. The latter are generally considered as soluble enzymes but it is known for decades that they may be associated with ribosomes, organelles or lipids ([55] and references therein) and nowadays a growing number of publications lead to the conclusion that cytosolic aaRSs exert their canonical functions at multiple locations within the cell.

3.1. Nuclear translocation of aaRS and tRNA nuclear export

Eukaryotic precursors tRNAs are transcribed in the nucleus and undergo several maturation steps before being fully functional for aminoacylation in the form of L-shaped and fully modified tRNAs. Those include 5′ and 3′ processing, CCA addition and post-transcriptional base modifications [56]. A majority of maturation steps take place within the nucleus. Classically, all tRNAs are then transported through nuclear pores to reach the cytosol where they are aminoacylated by cognate cytosolic aaRSs, and participate in ribosomal protein synthesis [57,58]. Experiments conducted in the mid-eighties surprisingly showed that a fraction of the Phenylalanyl-tRNA-synthetase pool (FRS) relocalizes into the nucleus, although its function inside the

organelle was not clearly understood [59]. The presence of an aaRS in the nucleus, where tRNAs are synthesized and processed led to the attractive hypothesis that aminoacylation of nuclear tRNAs by aaRSs could be a quality control step to assess their structural and functional integrity prior to export [60,61]. In correlation to that, aminoacylation has been experimentally demonstrated for tRNA^Y and initiator tRNA^M (tRNA$_i^M$) in *X. laevis* oocytes [60]. However, for a putative quality control mechanism involving aminoacylation to occur in the nucleus for all tRNAs, the corresponding aaRSs should be all able to enter the nucleus as well. This hypothesis was reinforced by the detection of nuclear localization sequences (NLS) in most of these enzymes [18,62]. Incidentally, results obtained in the yeast *S. cerevisiae* showed nuclear tRNA aminoacylation activity for MRS, IRS and YRS [61,63]; and more recently 19 tRNA species have been detected in the form of aa-tRNAs in the nucleus [64]. Most of aa-tRNA are exported [65] to fuel cytosolic protein synthesis, but it has been demonstrated that 30% are retained inside the nucleus, where they might be involved in protein modification, especially in the case of R-tRNA^R, that participates in the N-end rule degradation pathway [66]. Several authors also suggested that nuclear pools of cytosolic aaRSs might assemble into molecular complexes [67,68]. Finally, nuclear relocalization of many cytosolic aaRSs seems to be a frequent feature across organisms and translocation of cytosolic aaRSs through the nuclear pores is accomplished by the classical import machinery (NLS/importins), although various other strategies to reach the nucleus [69]. Finally, their canonical function is only one of the many roles they exhibit inside this compartment.

3.2. Addressing cytosolic aaRS to mitochondria through MTS acquisition

In all organisms studied so far, no gene encoding mitochondrial aaRSs was found in any of the mitochondrial genomic DNAs. All mitochondrial aaRSs are nuclear-encoded [70,71], aside the 20 cytosolic aaRS genes. Importantly, the full set of the 20 mitochondrial aaRS genes has never been detected in any nuclear genomes so far [15,72,73]. Indeed, some aaRSs genes originating from mitochondria (or plastids in photosynthetic organisms and apicomplexans) have been lost during evolution. Consequently, mitochondrial aminoacylation activities have to be fulfilled by other aaRS, namely the cytosolic aaRSs. In this case, mitochondrial targeting sequences (MTS) are found at the N-terminus of the mitochondrial-targeted cytosolic aaRSs (Fig. 2). Addition of MTS can be achieved through different mechanisms such as alternative splicing of the aaRS transcript (human KRS) [74] or from an alternative translation start (AUG) site within the same transcript (human GRS) [75]. Moreover, both forms can be translated from mRNA transcripts that differ only in the 5′ regions. For example, the yeast *HTS1* gene, coding for the sole HRS, has two in-frame translational starts separated by an alternative transcriptional start leading, upon translation, to two isoforms of HRS, a longer (mitochondrial) and a shorter (cytosolic) one [76]. A similar strategy has been evidenced for yeast VRS [77]. Alternatively, experiments showed that the gene encoding the two isoforms of yeast ARS is translated from a single mRNA, where the mitochondrial isoform is initiated from an upstream atypical ACG start codon, and the cytoplasmic isoform from a classical AUG start codon [78]. This dual-targeting mechanism, that involves synthesis of two protein isoforms from a single mRNA seems to be the rule in multi organellar organisms like *A. thaliana* [3,79] or apicomplexan parasites [80].

3.3. Mitochondrial-cytosolic dual-localization of a single aaRS

Apart from synthesizing two protein isoforms (one with and one without an MTS) from expression of a single gene, another strategy to generate a cytosolic/mitochondrial dual-localized protein is to produce a mitochondrial protein (harboring an MTS) and to retain it within the cytosol through interaction with an anchoring protein. For example, the yeast cytosolic ERS is imported into the mitochondria even if it does not harbor an identifiable targeting signal [6]. Experiments demonstrated that mitochondrial import of cytosolic ERS compensates the absence of mitochondrial QRS. Indeed, mitochondrial Q-tRNA^Q cannot be synthesized directly, but *via* the indirect transamidation route. In this pathway, aminoacylation of mt-tRNA^Q is specifically performed by the mitochondria-localized cytosolic ERS, which produces a physiologically misacylated E-$_{mt}$tRNA^Q. This intermediate is further converted to
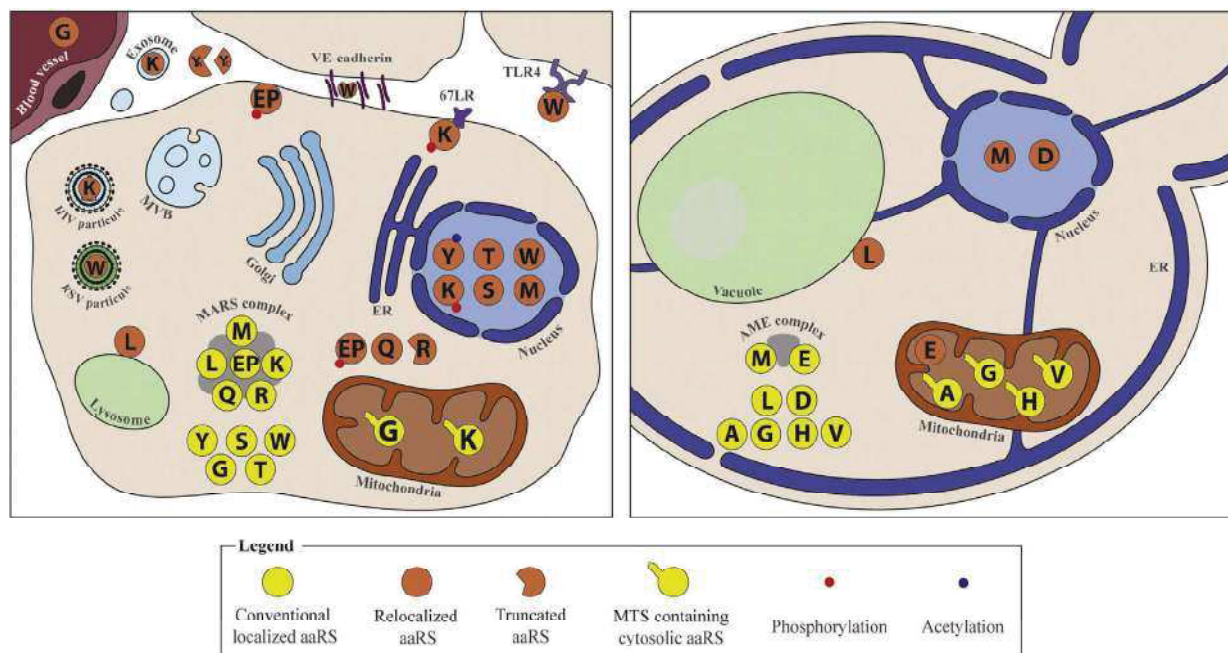
Fig. 2. Multiple subcellular localizations of mammalian (left) and yeast cytosolic aaRSs (right). Only mammalian and *S. cerevisiae* cytosolic aaRSs that relocate from the cytosol to a different compartment or that can be released from the MARS MSC and stay in the cytosol are shown. Only aaRSs that relocate to the nucleus and which are exerting non-conventional functions are represented on the figure.

Q-$_{mt}$tRNA^Q by the tRNA-dependent GatFAB amidotransferase in yeast [6]. In *A. thaliana* and mammals [16,17], a *bona fide* mitochondrial ERS, called non-specific, produces *E*-$_{mt}$tRNA^Q in addition to the cognate E-$_{mt}$tRNA^E, and the misacylated intermediate is converted to Q-$_{mt}$tRNA^Q by the mitochondrial GatCAB amidotransferase. Mitochondrial translocation of cytosolic ERS is triggered by a non-canonical MTS located after the first 190 residues [6]. Yeast cytosolic ERS is essential in both the cytosol and mitochondria, and regulation of its localization has been proven to be crucial during diauxic shift (transition from fermentation to respiration). Both yeast ERS and MRS are associated to the cytosolic anchoring protein Arc1p [22], preventing nuclear accumulation of the two aaRSs [81]. Upon diauxic shift, levels of soluble Arc1p decrease significantly, which triggers simultaneous release of both MRS and ERS [36]. While cytosolic MRS relocates into the nucleus (see Section 4.2.7), cytosolic ERS translocates into mitochondria, where it generates Q-tRNA^Q and controls the overall rate of mitochondrial protein synthesis.

4. Eukaryotic relocating cytosolic aaRSs with nonconventional functions

As mentioned in the introduction, the primary function of an aaRS is to aminoacylate its cognate isoacceptor tRNAs in the translationally active compartment where the aaRS is supposed to be localized. In eukaryotes, where several organelles and compartments are found, defining the exact subcellular localization of a given aaRS is not an easy task, since some aaRSs are free-standing enzymes while other are found in an MSC (Multi-"Synthetase" Complex), *i.e.* the human MARS-complex or the yeast AME complex. Furthermore, MSC-associated aaRSs can be released from the complex under specific physiological or stress conditions, and/or upon posttranslational modification. One of the remarkable feature of aaRSs is that they are modular enzymes. Some of them inherited additional domains, that are sometimes only be found in aaRSs, upon various evolutionary events, [29]. Some of those additional domains are necessary to ensure the specificity of the tRNA aminoacylation ("conventional") reaction (*i.e.* Connective Peptide of the editing domains), whereas other domains are involved in "non-canonical" (and sometimes non-translational) functions that these enzymes can carry out. Interestingly, some additional domains are required for both conventional and non-canonical functions in a single aaRS.

In this context, the additional domain can harbor the non-canonical function by itself or can be the target of a post-translational modification, required for aaRS relocalization. Indeed, to fulfil their non-canonical function(s), aaRSs often have to relocate from the cytoplasm (that is, their "canonical" localization) towards a new compartment. Alternatively, an MSC-associated aaRS can stay within the cytosol but be released from the MSC. In this section, we sorted the cytosolic aaRSs as a function of the subcellular compartment in which they exert their non-canonical functions. All the aaRS relocalizations reported in this section are summarized in Table 1 and Fig. 2.

4.1. aaRSs released from the MSC but staying in the cytoplasm

4.1.1. Human glutamyl-prolyl-tRNA-synthetase (EPRS) in response to IFNγ stimulation

In higher eukaryotes and notably human, ERS is fused to PRS by a non-catalytic linker that contains 3 so-called WHEP repeats. The phylogenetic origins of these WHEP domains (present in tryptophanyl-(W) histidinyl-(H) glycyl-(G) and glutamyl-prolyl-tRNA synthetase (EP) where explored by Ray et al. [82] who focused their work on this unique case of fused bi-functional aaRSs called EPRS. In the human MARS complex these WHEP repeats interact with AIMP3 and lysyl-tRNA-synthetase (KRS). However, EPRS can be released from the MARS complex upon sequential bi-phosphorylation of serine residues within the WHEP domain. For instance, in myeloid cells Serine 886 (S886) is

phosphorylated by the Cyclin-dependent kinase Cdk5/p35 kinase [83] and Serine 999 (S999) is phosphorylated by the mammalian Target Of Rapamycin 1 (mTORC1) activated p70 ribosomal protein S6 kinase 1 (S6K1) [32]. These phosphorylations occur upon interferon gamma (IFNγ) stimulation and trigger the release of EPRS. The phosphorylated WHEP repeats then sequentially interact with NSAP1, GAPDH, phosphorylated ribosomal L13a and the Gamma Interferon Inhibitor of Translation (GAIT) elements that can be found in the 3′-end of some mRNAs leading to the assembly of the so-called GAIT complex. This cytoplasmic GAIT complex then interacts with the translation initiation factor eIF4G, which inhibits translation of the mRNAs targeted by the GAIT complex [35,83–86].

Because, this translation inhibition was shown to be suppressed 14–16 h after IFNγ stimulation, Yao and coworkers [87] investigated the mechanism underlying the recovery of the translation of the mRNAs targeted by the GAIT complex. They discovered an alternative route which allows mRNAs that display GAIT-elements to be basally translated even after GAIT-complex assembly. This mechanism involves an EPRS isoform called EPRS^{N1} which is translated from a truncated EPRS mRNA. This shorter EPRS mRNA is generated through an alternative polyadenylation pathway that changes an UAU (encoding tyrosine 864) to a stop codon (UAA). This EPRS^{N1} isoform is composed of the ERS core followed by approximatively two WHEP domains. Consequently, the region of the WHEP domain that can be biphosphorylated is missing in EPRS^{N1}, preventing association of this EPRS variant to the GAIT complex. However, EPRS^{N1} being still able to bind to the mRNA GAIT-elements, it competes with the GAIT-complex for binding to these mRNAs, leading to a basal expression of pro-inflammatory mRNA.

4.1.2. Human glutamyl-prolyl tRNA-synthetase (EPRS) in response to viral infection

The mitochondrial antiviral signaling protein (MAVS) is considered as a central regulator of responses to viral infections through its capacity to block virus replication. MAVS is inhibited by poly(rC)-binding protein 2 (PCBP2)-dependent ubiquitination and is activated through viral RNA genome sensors such as RIG-I and MDA5. Lee and coworkers [88] showed that following viral infection, EPRS is phosphorylated at S990 which triggers its release from the MSC and promotes its interaction with PCBP2. This interaction prevents MAVS ubiquitination and sustains in this way antiviral immunity. Thus, EPRS is also an important factor of antiviral immunity.

4.1.3. Human glutaminyl-tRNA-synthetase (QRS)

The human QRS, which participates to the MARS MSC by binding to AIMP1 and arginyl-tRNA-synthetase (RRS) has been shown to possess an anti-apoptotic action. Apoptosis can be triggered by different factors (*i.e.* Tumor Necrosis Factor (TNF), Fasl, Reactive Oxygen Species (ROS)) and different pathways (*i.e.* c-Jun N-terminal kinase (JNK) and p38), and an essential factor for apoptosis is the Apoptosis Signal-regulating Kinase 1 (ASK1). To prevent apoptosis and to enhance cell survival, the QRS catalytic domain interacts directly with the ASK1 catalytic domain, in a glutamine-dependent manner. The QRS unique N-terminal domain (UNE-Q) does not seem to be involved in this aaRS-dependent anti-apoptotic pathway. Furthermore, because QRS can be released from the MARS MSC [89], Ko et al. [90] proposed that there is an equilibrium between the interaction of QRS with the MARS complex and with ASK1. On the opposite, Hwang et al. [91] showed that the translocation of ASK1 into the nucleus through its interaction with the Apoptosis-Linked Gene 2 (ALG2), also prevents apoptosis. However, no functional link between the QRS- and ALG2-dependent anti-apoptotic pathways was further revealed so far. Finally, Shao et al. [92] demonstrated that the microRNA miR-US4-1 encoded by the Human Cytomegalovirus (CMV) genome targets human QRS and induces cell apoptosis.

4.1.4. Mammalian RRS

During evolution, mammalian RRSs have inherited two leucine-

zippers in their N-terminal extension, and like for other aaRSs, these leucine-zippers were shown to be involved in binding with AIMPs or other aaRSs in order to participate to the MARS complex. However, beside the full-length RRS, an alternative AUG translation start allows synthesis of a 74-residues shorter RRS isoform, in which the leucine zippers are missing [93–95]. Consequently, this isoform cannot bind to the MSC and is found in free form in the cytoplasm [96–98]. Both RRS isoforms present similar aminoacylation activities [99] but it was suggested that R-tRNA^{R}s produced by the shorter isoform are rerouted from protein synthesis to provide activated arginyl moiety for the Arg-dependent protein degradation pathway ("N-end rule") [100–102].

4.2. Cytosolic aaRSs translocating to the nucleus

4.2.1. Human lysyl-tRNA-synthetase KRS (Mast Cells)

Many non-canonical functions were discovered for cytosolic KRS this past decade. For example, mast cells are known to be implicated in allergenic and anaphylaxis responses and also in some immune disorders. Through allergen recognition by the immunoglobulin E high affinity receptor, IgE-FcεRI, activated mast cells accumulate diadenosine tetraphosphate (Ap4A) also called "alarmone" or "second messenger". This second messenger binds to Histidine triad nucleotide-binding protein 1 (Hint1) which in turn releases the Microphthalmia-associated Transcription Factor (MITF) leading to its activation and the subsequent upregulation of the transcription of subset of genes (i.e. tryptophan hydroxylase and mast-cell protease 5) [103–106]. Recent structural investigations revealed that the pathway that activates MITF involves the phosphorylation of KRS at S207 (located at the ABD) by the MAPK/ERK kinase which is itself activated after allergen stimulation. The subsequent KRS conformational change induces i) its dissociation from the MARS complex (AIMP2) ii) inhibition of its aminoacylation capacity and iii) its translocation into the nucleus. Inside the nucleus, the exposed C-terminal domain of KRS interacts with the MITF which in turn dissociates from Hint1. Furthermore, KRS synthetizes Ap4A (KRS is responsible for the synthesis of about 70–80% of cellular Ap4A) which inhibits Hint1, leading to MITF-KRS-dependent upregulation of gene transcription under allergenic stimulation [107,108]. Interestingly, a very recent study reported that HIV1 infection in human cells induces similar LysRS translocation into the nucleus (see below Section 4.5.1).

4.2.2. Zebrafish and mammalian tyrosyl-tRNA-synthetase (YRS)

Such an aaRS-dependent transcription-regulation was also shown for mammalian and zebrafish YRS. Angiogenin, nicotinamide and oxidative stress were shown to trigger YRS translocation into the nucleus. This relocalization occurs trough a hexapeptide NLS which is located into a tRNA binding domain which is not the Anticodon Binding Domaine (ABD) of YRS [109]. Under stress conditions, resveratrol fits into the YRS active site by mimicking tyrosine and triggers i) inhibition of YRS's capacity to aminoacylate tRNA^Y (YRS null mutant like) [110] and ii) an increase in acetylation of YRS's lysine 244 (K244) by the p300/CBP-associated factor (PCAF acetylase vs. SIRT1 deacetylase) [111]. This acetylation induces a conformational change that exposes YRS's NLS and triggers its nuclear translocation. Interestingly, Fu et al., [109] showed that binding of tRNA^Y prevents nuclear relocation of YRS, which is in agreement with the fact that early acetylation occurs into the YRS tRNA-binding domain (K244). Following nuclear import, YRS binds to TRIM28 (which notably represses the transcription factor E2F1) and to its associated Histone Deacetylase 1 (HDAC1) [112]. Trough acetylation, E2F1 is activated and improves expression of genes involved in DNA damage repair (i.e. Breast Cancer 1 BRCA1 and the recombinase RAD51). Furthermore, two studies showed that YRS is able to stimulate NAD$^+$-dependent PARP1 activity which is well known for its participation to the DNA damage response [110,112]. Taken altogether, nuclear YRS seems to be an important factor to prevent DNA damages.

4.2.3. Vertebrate tryptophanyl-tRNA-synthetase (WRS)

Liu and coworkers [113] showed, in 2004, the presence of 5 WRS mRNA splice variants in human cells which are translated into 2 different WRS isoforms: the full length (residues 1 to 471) and the mini-WRS (residues 48–471). Both, WRS and mini-WRS can be further processed by extracellular elastases to produce T1-WRS (residues 71–471) and T2-WRS (residues 94–471). For instance, the full-length WRS (component of the MARS complex) harbors an additional N-terminal WHEP domain which is either in a "locked" conformation (presence of Trp ~ AMP into the active site) or "open" conformation (absence of W ~ AMP into the active site). Furthermore, WRS is a class 1 aaRS that homodimerizes (α2) and harbors a C-terminal NLS. WRS was already shown in 1993 [114] to be imported into the nucleus and later studies [115] showed that nuclear WRS increases upon IFN-γ treatment (anti-angiogenic and anti-proliferative). Upon IFN-γ stimulation, the WHEP domain from the nuclear WRS homodimer "opens" and serves as a bridge between PARP1 and DNA-dependent protein kinase (DNA-PKc), which is essential for DNA-PKc-ADP-ribosylation by PARP1 and p53 phosphorylation (Ser15). Consequently, phosphorylated p53 triggers cell death.

4.2.4. Vertebrate seryl-tRNA-synthetase (SRS)

SRS, that belongs to class 2 aaRSs, was also shown to be imported into the nucleus [116]. This import requires a robust NLS located into a unique C-terminal domain called UNE-S [28,117] which is conserved in all vertebrate SRSs from fish to human. In human cells (HUVE-C = endothelial cells, HEK293T cells), the amount of nuclear SRS was estimated to be 10% of the total SRS content [116]. In 2009, two studies [118,119] identified different SRS mutations that could lead to deletion or sequestration of the NLS (into the UNE-S domain). These mutants have deficiencies in SRS nuclear import and anomalies in angiogenesis. This phenotype was explained by an original "Yin-Yang" mechanism whereby nuclear SRS competes with c-Myc for binding to the promoter of Vascular Endothelial Growth Factor (VEGFa); c-Myc binds to the promoter of VEGFa and recruits a histone acetyltransferase which increases chromatin decondensation at VEGFa locus and its expression. Contrariwise, nuclear SRS binding to the VEGFa promoter can recruit Sirtuin 2 (SIRT2) which deacetylates histones at the VEGFa locus and represses its expression [120]. Beside this Yin-Yang mechanism that acts on the proximal cis regulation element (CRE) which avoids abnormal vascularization, a recent study proposed the existence of a distal CRE regulation mechanism. Notably, they demonstrated that nuclear SRS binds a transcription factor Yin-Yang1 (YY1), building a complex that represses VEGFa expression. As described for the SRS-SIRT2 complex, the recently identified SRS-YY1 complex competes with the Nuclear Factor kappa B (NFκB) which binds the same distal CRE to enhance VEGFa expression [121].

4.2.5. Vertebrates from zebrafish to human threonyl-tRNA-synthetase (TRS)

Recently Cao and coworkers [122] reported the capacity of human (HUVEC) and zebrafish TRSs to relocate to the nucleus. Based on a newly identified taARS^{cq16} mutant in zebrafish, they show that TRS down-regulates VEGFa expression to prevent abnormal vascular development. Interestingly, this regulatory function resembles that of the human SRS described in the previous section. The fact that taARS^{cq16} mutant phenotype could not be abolished by SRS mRNA injection suggests that TRS-mediated regulation of angiogenesis proceeds through a different mechanism. However, there were able to swap the Zebrafish TRS by its human ortholog, indicating that this new non-canonical regulatory function is conserved in human.

4.2.6. Human methionyl-tRNA synthetase (MRS)

MRS is another MSC-participating aaRS capable of relocating to the nucleus and more precisely to the nucleolus where ribosomal RNA (rRNA) are transcribed. Compared to prokaryotic MRSs, human MRS

possesses an N-(267 amino-acids) and a C-terminal extension, in the latter of which a NLS was found. Ko and coworkers [123] showed that nucleolar translocation of human MRS requires rRNA and RNA polymerase I activity and that this relocation upregulates rRNA biogenesis when cells are proliferating upon treatment with growth factors like insulin, Platelet-Derived Growth Factor (PDGF) or Epidermal Growth Factor (EGF). Finally, the mechanism that triggers release of MRS from the MARS complex remains unclear but Ko and coworkers anticipated that phosphorylation of the MRS N-terminal extension through casein kinase II could be the event initiating nucleolar relocation of MRS. This hypothesis is supported by the fact that this kinase is involved in cell growth and rRNA biogenesis. However, to our knowledge the exact pathway and mechanism of MRS nucleolar relocation still needs to be verified experimentally.

4.2.7. S. cerevisiae MRS

As mentioned above, the yeast AME composed of Arc1 ERS and MRS has been shown to constitute a cytosolic retention platform for the two participating aaRSs. In fermenting yeast cells (high glucose concentration), the majority of MRS and ERS are found bound onto Arc1 that enhances their cognate tRNA aminoacylation efficiency [22]. However, upon switch to the respiratory metabolism (low glucose concentration), *ARC1* transcription is downregulated by the Snf1/4 kinase pathway (glucose-sensing pathway), which leads to synchronous release of MRS and ERS from Arc1. Released ERS then relocates to the mitochondria and indirectly controls accumulation of the Atp9 subunit of the F_O domain of the mitochondrial ATP synthase (ATPase). Simultaneously, dissociation of MRS from the AME complex unmasks a bipartite NLS located in the MRS N-terminus and its subsequent nuclear translocation. Nuclear MRS then regulates transcription of Atp1 subunit of the F_1 domain of ATPase. Taken together the AME complex dissociation allows a synchronous synthesis and assembly of a functional ATPase and thus mitochondrial ATP synthesis [36].

4.2.8. S. cerevisiae aspartyl-tRNA-synthetase (DRS)

It was first suggested that, *in vivo*, DRS could interact with its own mRNA (mRNA^{DRS}) through the 70-amino-acid N-terminal extension that contains a lysine-rich RNA binding motif [124]. A second study by Frugier and coworkers [125] confirmed the nuclear translocation of DRS through a NLS that was shown to be located in this N-terminal extension. They proposed a mechanism by which the superfluous amount of DRS that is produced by yeast cells, enters into the nucleus and bind its own mRNA thereby inhibiting its expression and stopping further accumulation of the enzyme.

4.3. Cytoplasmic aaRSs that are targeted to the cytoplasmic membrane

4.3.1. Human lysyl-tRNA synthetase (KRS)

In most human organs, laminin is found as an extracellular matrix support for surrounding cells, which interact with laminin through membranous integrins. However, in cancer cells, laminin bound to integrin induces p38-MAPK (Mitogen Activated Protein Kinase) activation which in turn phosphorylates the threonine 52 (T52) located in the N-terminal extension of KRS. T52 phosphorylation induces a conformational change of this part of KRS that triggers its release from the MARS complex and allows its interaction with the membranous 67LR laminin receptor. This interaction occurs between the KRS N-terminal domain composed of the ABD and N-terminal extension (1–72) and the C-terminal domain of the 67LR. By doing so, KRS inhibits Nedd4-mediated ubiquitination of 67LR, enhancing laminin-dependent cell migration and cell dissemination which is considered as a marker of metastasis [126]. Kim and coworkers [127] also identified a compound (BC-KYH16899) that inhibits the KRS-dependent 67LR-mediated cell migration without affecting the aminoacylation capacity of KRS. This BC-KYH16899 compound is thus a promising molecule that could selectively inhibit cancer cells dissemination without affecting the

proteinogenic role of KRS. Finally, Nam and coworkers [128] investigated the molecular steps occurring downstream this KRS – 67LR interaction and showed that KRS-dependent cell-dissemination is done through cell-cell and cell-extracellular matrix interactions.

4.3.2. Mouse and human EPRS

In higher eukaryotes, ERS is fused to PRS by a non-catalytical linker that contains 3 WHEP repeats. This bifunctional EPRS was well characterized notably in human cells in which it participates to the MARS complex by interacting with AIMP2, KRS and DRS [30,129,130]. We already described in a preceding section the non-canonical function that EPRS exhibits in myeloid cells. However, Arif et al. [32] recently reported another relocation for MARS-released EPRS and a new non-translational function of this aaRS. In contrast to myeloid cells in which EPRS WHEP repeats are phosphorylated at S886 by Cdk5/p35 kinase, and at S999 by S6 kinase 1 (S6K1), in adipocytes EPRS was only shown to be phosphorylated at S999 making unclear whether S886 phosphorylation is also required in this cell type. Furthermore, contrary to mast cells, in adipocytes, the mTORC1-dependent S6K1 kinase that belongs to AGC kinases, is activated under insulin stimulation (mTORC1: mammalian Target Of Rapamycin Complex 1). Phosphorylated EPRS (at S999) interacts then with the cytoplasmic Fatty Acid Transport Protein 1 (FATP1). Formation of the EPRS-FATP1 complex is followed by its relocation to plasma membrane where it induces Long Chain Fatty Acid (LCFA) uptake. Thus, in adipocytes (but not in myeloid cells), and under insulin stimulation (but not under IFNγ stimulation), EPRS regulates adiposity and lifespan in a S6K1-dependent manner.

4.4. Yeast and human cytoplasmic aaRSs that are targeted to the vacuole and the lysosome

4.4.1. Mammalian leucyl-tRNA-synthetase (LRS)

In eukaryotes, TOR complexes (TORC) were shown to be involved in many processes such as cell growth, differentiation and metabolism, but increasing evidences suggest that its regulation is far from being fully understood. Indeed, different studies showed that amino acids and especially leucine [131–133], glutamine [133–135] and arginine [131] participate to activation of mTORC1. To be activated, mTORC1 requires a combination of Rag GTPases (component of the RAGULATOR complex) that are themselves regulated by a set of Guanine nucleotide Exchange Factors (GEFs) and GTPase-Activating Proteins (GAPs). It was suggested that LRS serves as a GAP for one of these Rag GTPases [136,137]. Beside these combinations of Rag-GTPases, mTORC1 activation at the lysosomes requires phosphatidic acid which is obtained by phospholipase D1-dependent (PLD1) hydrolysis of phosphatidylcholine. PLD1 recruitment to the lysosome is done by direct interaction with phosphatidylinositol-3P (PI3P) which is synthetized at the lysosome through the vacuolar protein sorting 34 (VPS34), a class 3 PI3-kinase which phosphorylates phosphatidylinositol and which is known to be involved in autophagy [138]. Yoon and coworkers [137] demonstrated that LRS interacts directly *via* its catalytic domain with VPS34 and activates it *via* its unique C-terminal extension called UNE-L. Furthermore, leucine binding but not tRNA binging nor tRNA aminoacylation is required for mTORC1 activation. Finally, Yoon and coworkers performed immunoprecipitation assays which suggest that this non canonical role of LRS requires the release of the enzyme from the MARS complex and its relocation at the lysosomal surface.

4.4.2. S. cerevisiae leucyl-tRNA synthetase (LRS)

In the Yeast *S. cerevisiae* two TOR complexes (TORC1 and TORC2) are also found and TORC1 is regulated by GTPases. Like for mammals, LRS was shown to be involved in vacuolar TORC1 regulation but this regulation is achieved through a different mechanism than the one detailed in the previous section. In yeast, LRS interacts with one of the GTPases (Gtr1) from the EGO complex (corresponding to the

mammalian RAGULATOR) *via* its non-essential connective peptide that corresponds to the editing domain (a domain involved in non-cognate aa-tRNA hydrolysis). When a non-canonical amino-acid is charged on tRNA^L, a conformational change occurs that disrupts the LRS-Gtr1 interaction and inhibits vacuolar TORC1. Bonfils and coworkers [139] proposed that in *S.cerevisiae*, LRS serves as GAP for Gtr1 GTPase and thus participates to the inactivation of TORC1.

4.5. Cytoplasmic aaRS that are targeted outside the cell

Many aaRSs were reported to be targeted/secreted outside the intracellular space. In the present section we decided to describe aaRSs that are either incorporated into viruses or secreted. For secreted aaRSs, we describe those which are secreted to the intercellular space *via* the Multi Vesicular Body MVB/exosome pathway, *via* the Endoplasmic Reticulum RE/Golgi pathway or *via* a yet unidentified pathway. Finally, we mention the aaRSs that have been found in the human serum.

4.5.1. Human KRS is encapsidated into HIV virions

During HIV1 infection, a key step for viral replication is the reverse transcription (RT) of the genomic RNA. This step requires a primer which has been shown to be the human tRNA^{Lys3} (tRK3). Cen and coworkers [140] showed that, in addition to tRK3, the human KRS is also encapsidated into HIV1 particles by interacting with the viral Gag precursor. Whereas other studies [141–143] brought evidences that tRK3 incorporation is regulated by KRS, Liu and coworkers [Anticodon-like binding of the HIV-1 tRNA-like element to human lysyl-tRNA synthetase] investigated the interaction of LysRS with the viral genome. Furthermore Dewan et al. [144] demonstrated that the H7 helix located in the class II motif 1of human KRS, and which is responsible for KRS dimerization, is also responsible for the interaction with HIV1 Gag protein.

As mentioned in a previous section (Section 4.2.1), a very recent study [145] investigated further the implication of KRS after HIV1 infection in human cells. This study shows that following HIV1 infection, phosphorylated KRS (S207P) is released from the MSC and translocates into the nucleus. Like in mast cells, phosphorylated KRS is deprived of its capacity to aminoacylate its cognate tRNA but retains its ability to bind the tRNA. Although nuclear LysRS function was not yet clearly established, this study strongly suggests that translocation into the nucleus of the phosphorylated LysRS-tRK3 complex *i*) occurs before the reverse transcription of HIV1 genome and *ii*) is important for tRK3 packaging and for HIV1 infectivity. Finally, in agreement with the previously described EPRS antiviral function (Section 4.1.2), Duchon and coworkers could detect a low amount of released EPRS upon HIV1 infection.

4.5.2. Human WRS is encapsidated into Rous sarcoma virus (RSV)

In the previous paragraph, we reported that KRS and the tRK3 are incorporated into HIV1 particles. Cen and coworkers [146] described a similar situation concerning the Rous sarcoma virus, except that tRNA^W is used as primer for reverse transcription of the viral genomic RNA. Like for HIV1 the aaRS homologous to the tRNA species used as a primer, in this case human WRS, is also encapsidated. Interestingly, the Moloney Murine Leukemia Virus that uses tRNA^P as primer for reverse transcription of its genomic RNA, does not encapsidate the cognate PRS into the viral particles. The reason why certain viruses encapsidate a given aaRS alone or together with its cognate tRNA, has so far, not been ruled out.

4.5.3. Human KRS is secreted via exosomes

Park and coworkers [147] showed that under starvation and stimulation by Tumor Necrosis Factor α (TNFα), the human KRS can be secreted from human cells and interacts with macrophages to induce their TNFα secretion and cell migration. However, the KRS secretion pathway and its detailed molecular steps remained unclear until

recently. Kim and coworkers [148] showed that, during evolution human KRS inherited a unique N-terminal extension which harbors a Caspase 8-specific cleavage site, and a C-terminal PDZ-binding domain. Whereas many proteins that harbor a localization signal are secreted by the ER-Golgi pathway, the human KRS interacts *via* its PDZ-binding domain to syntenin which guides KRS from de MARS complex into exosomes and more precisely in their lumen, prior to its release from the cell. Note that this KRS-syntenin interaction had already been suggested previously by Meershaert and coworkers [149] and Baietti and coworkers [150]. Kim and coworkers also showed the importance of the N-terminal caspase 8-specific cleavage site in this KRS secretion pathway and proposed a mechanism in agreement with the published 3D structure of KRS [107]; KRS is a class II aaRS that forms homodimers in which the caspase 8 cleavage site that is located in the N-terminal extension of one of the monomers masks the syntenin interaction site located in the C-terminal domain from the second monomer, thus inhibiting exosomal KRS secretion. Under starvation conditions, Caspase 8 cleaves the KRS N-terminal domain which allows KRS–syntenin interaction and subsequent incorporation of the enzyme into exosomes.

4.5.4. From insect to vertebrates, the balance between mini-YRS and -WRS regulates angiogenesis

We already reported in the previous sections that nuclear imported WRS, SRS and TRS are important angiogenesis regulators. However, secreted forms of YRS and WRS are also key players of angiogenesis regulation. In comparison to prokaryotic YRS, insect and vertebrates YRS have inherited an C-terminal Endothelial-monocyte-activating polypeptide II (EMAPII) like domain that can be cleaved by extracellular proteases (elastases) from the remaining core of YRS called "mini-YRS" [151]. This mini-YRS has similarities with the CXC chemotactic factor interleukin 8 (IL8), in particular with the ELR motif (Glu-Leu-Arg) harbored by pro-angiogenic chemokines. The evolutionary close WRS can similarly be cleaved into a "mini-WRS" (where translation starts at M48 due to alternative splicing or extracellular cleavage inside the WHEP domain) but the cleaved product doesn't harbor the ELR motif. As such, it was shown that in endothelial cells (HUVEC) and in polymorphonuclear leukocytes (PMN), extracellular mini-YRS induces cell migration and angiogenesis [152], whereas extracellular WRS has opposite effects [153,154]. Extracellular mini-YRS is increased through TNFα secretion and in endothelial cells mini YRS induces phosphorylation of Src, Akt, ERK (Extracellular Signal Regulated Kinase), and VEGF-receptor 2, required for angiogenesis [155,156]. Because IL8 is known to act on the CXCR1/2 receptor, My-Nuong Vo et al., [157] verified whether this is also the case for mini-YRS. This study showed, that under low mini-YRS secreted concentrations, mini-YRS is monomeric and induces cell migration *via* CXCR1/2 whereas under high mini-YRS secreted concentrations, mini-YRS is dimeric and inhibits cell migration (antagonistic effect). On the other hand, mini-WRS exerts its angiostatic activity by binding the first extracellular (EC1) domain of VE-cadherin (vascular endothelial cadherin). Recent studies [158,159] showed that mini-WRS K153 residue binds VE-cadherin and that VE-cadherin residues W2 and W4 are docked into the empty W-AMP pocket. Through this interaction, *i*) VE-cadherin interaction with activated VEGF receptor 2 (VEGFR2) is disrupted and *ii*) the subsequent activation of Akt that, in the absence of mini-WRS leads to angiogenesis, is inhibited [160,161]. However, the mechanism by which VEGFR2 is activated by mini-YRS remains unclear and Zeng et al. [162] in human umbilical vein endothelial cells in hypoxia suggested a yet unknown trans-activation mechanism. Thus, mini-WRS and mini-YRS cytokine-like antagonistic effects belongs to a pathway that fine tunes cell migration and angiogenesis.

4.5.5. From insect to vertebrates, YRS EMAPII-like domain

Compared to their prokaryotic homologs, insects and vertebrates YRSs inherited a additional C-terminal EMAPII-like domain. When YRS is secreted, this domain is cleaved by extracellular elastases from the

remaining "mini-YRS". This cleavage occurs during the apoptotic state and the EMAPII-like peptide will exert 2 different functions *i*) it carries chemo-attractive capacities which allows the recruitment of phagocytes to the apoptotic site and phagocytosis in order to prevent damages for surrounding cells; and *ii*) it induces TNFα secretion by leucocytes [151,153,163]. Finally, it was suggested that in the full-length YRS, EMAPII-like blocks IL-8 proangiogenic activity by preventing it recognition by IL8 receptor.

4.5.6. Secreted human full-length WRS (but not the mini-WRS) induces early innate immune response

Human WRS contains a unique 154 aa-long N-terminal domain that includes a WHEP domain (residues 8–64). Recently Ahn and coworkers [164] discovered a new function for the full-length WRS (FL-WRS) but not for the mini-WRS that we described previously. They showed that early after infection by pathogens, FL-WRS is secreted from monocytes and interacts with macrophages to induce innate immune stimulation (phagocytosis and cytokine production). Based on the available WRS crystal structure, Ahn et al. showed that in order to activate this type of immune response, FL-WRS binds to Toll-Like-Receptor 4 (TLR4) - MD2 complexes and probably also to TLR2 *via* its N-terminal extension. Finally, binding and activation was also showed with the 154 aa-long N-terminal domain alone.

4.5.7. Secreted human TRS regulates also angiogenesis

Similar to the above-mentioned mini-YRS angiogenic function, human TRS is also secreted under TNFα or VEGF stimulation and induces endothelial cell migration. However, it has not been elucidated if TRS cleavage or posttranslational modification is necessary for this non-canonical function [165]. Furthermore, Wellman and coworkers [166] found a link between stress-induced overexpression of TRS, angiogenesis and ovarian cancer.

4.5.8. Brugia malayi asparaginyl-tRNA-synthetase (NRS)

Brugia malayi is a filarial nematode which is a human parasite responsible for filariasis that causes chronic infections and elephantiasis. *Brugia malayi* NRS (BmNRS) is secreted from this intravascular worm parasite into patient's serum [167,168] and acts as immunodominant antigen. *Bm*NRS presents a 110 aa-long N-terminal extension (compared to prokaryotic NRSs) that harbors a 80-long IL8-like domain. Different studies demonstrated that *Bm*NRS induces several physiological responses *via* binding to 2 different types of receptors: IL8 CXCR1/2 receptors and purine receptors [168–172]. Recently Jothi and coworkers added to this list: endothelial cell proliferation, migration, ring and tube formation, vasodilation and angiogenesis which are also usually induced by VEGF.

4.5.9. Mouse and human glycyl-tRNA-synthetase GRS

Concerning GRS, Park and coworkers [173] recently showed that Fas-ligand secreted from cancer cells induces GRS secretion which can then circulate in the serum. Normally, phosphatase 2 (PP2A)-dependent ERK inhibition is blocked by its interaction to the membrane protein cadherin 6 (CDH6). However, binding of GRS to CDH6 *via* its extracellular domain, releases PP2A which inhibits ERK and provokes tumor cell death. Furthermore, this study provides *in vivo* data (mouse models) on GRS-mediated antitumor effects and suggests that this aaRS, by having this cytokine-like function, is a key player in an endogenous tumor surveillance mechanism. Finally, the mechanism by which GRS is secreted remains so far unknown, but He and coworkers [174] suggested that GRS is secreted by the exosomal pathway.

5. Concluding remarks

As described herein, the functional plasticity of relocating cytosolic aaRS is really remarkable for enzymes once considered to be restricted to the production of the ribosomes' aa-tRNA substrates. However, the

repertoire of nontranslational functions carried by these enzymes is probably even greater, especially in human, if one considers all the possible isoforms that that have been predicted to be produced by alternative splicing or initiation of translation [175]. The majority of these splice variants are catalytic nulls meaning that the alternative splicing event partially or entirely removed the functional parts responsible for aa-tRNA synthesis, leaving, usually, only domains that were added to the aaRS core in the course of evolution. These pieces of aaRSs have been found to have a tissue-specific expression profile and do not contribute or participate to the aminoacylation reaction. However, a strong selection pressure led to their conservation throughout evolution most probably because they exert a specific biological function that has nothing to do with protein synthesis but nevertheless equally essential. When tested in cell-based assay designed to check their involvement in cytoprotection, immunomodulation, acute inflammatory response, transcriptional regulation, regenerative responses, cell differentiation and cholesterol transport, almost 90% of these catalytically null pieces of aaRSs where shown to exert at least one specific biological activity. Given the type of physiological role they might be playing and their tissue-specific expression one can easily imagine that malfunctioning of their functions or a change in their expression will very likely be associated with diseases. Indeed, it has already been shown that malfunctioning of the nontranslational functions that cytosolic relocating aaRSs exert, triggers a wide spectrum of diseases in human [31,34]. The pathologies to which these aaRSs have been connected to, include for example *i*) neuronal syndromes like type-2 Charcot Mary Tooth [174,176–178] and Amyotrophic Lateral Sclerosis [179], *ii*) susceptibility to cancers [180–182], diabetes [183,184] or other abnormal metabolic conditions [32] and *iii*) auto-immune disorders [185–189]. The latter example is particularly interesting since auto-antibodies against 9 cytosolic aaRSs have been found in patients with autoimmune disorders among which inflammatory myopathies, interstitial lung diseases and rheumatoic arthritis [190,191]. Despite a growing number of reports describing the clinical features of these subtypes of autoimmune diseases also called the "antisynthetase syndrome" the physiological conditions and molecular mechanism by which these aaRSs become an antigen are still unknown.

Transparency document

The http://dx.doi.org/10.1016/j.bbagrm.2017.11.004 associated with this article can be found, in online version.

References

[1] M. Ibba, D. Söll, Aminoacyl-tRNA synthesis, Annu. Rev. Biochem. 69 (2000) 617–650.

[2] A. Chaliotis, P. Vlastaridis, D. Mossialos, M. Ibba, H.D. Becker, C. Stathopoulos, G.D. Amoutzias, The complex evolutionary history of aminoacyl-tRNA synthetases, Nucleic Acids Res. 45 (2017) 1059–1068.

[3] A.-M. Duchêne, A. Giritch, B. Hoffmann, V. Cognat, D. Lancelin, N.M. Peeters, M. Zaepfel, L. Maréchal-Drouard, I.D. Small, Dual targeting is the rule for organellar aminoacyl-tRNA synthetases in *Arabidopsis thaliana*, Proc. Natl. Acad. Sci. U. S. A. 102 (2005) 16484–16489.

[4] M. Wilcox, M. Nirenberg, Transfer RNA as a cofactor coupling amino acid synthesis with that of protein, Proc. Natl. Acad. Sci. U. S. A. 61 (1968) 229–236.

[5] A. Schön, C.G. Kannangara, S. Cough, D. Söll, Protein biosynthesis in organelles

requires misaminoacylation of tRNA, Nature 331 (1988) 187–190.

[6] M. Frechin, B. Senger, M. Braye, D. Kern, R.P. Martin, H.D. Becker, Yeast mitochondrial Gln-tRNAGln is generated by a GatFAB-mediated transamidation pathway involving Arc1p-controlled subcellular sorting of cytosolic GluRS, Genes Dev. 23 (2009) 1119–1130.

[7] K. Sheppard, J. Yuan, M.J. Hohn, B. Jester, K.M. Devine, D. Söll, From one amino acid to another: tRNA-dependent amino acid biosynthesis, Nucleic Acids Res. 36 (2008) 1813–1825.

[8] M. Frechin, A.-M. Duchêne, H.D. Becker, Translating organellar glutamine codons: a case by case scenario? RNA Biol. 6 (2009) 31–34.

[9] T.M. Henkin, B.L. Glass, F.J. Grundy, Analysis of the Bacillus subtilis tyrS gene: conservation of a regulatory sequence in multiple tRNA synthetase genes, J. Bacteriol. 174 (1992) 1299–1306.

[10] J. Gilbart, C.R. Perry, B. Slocombe, High-level mupirocin resistance in Staphylococcus aureus: evidence for two distinct isoleucyl-tRNA synthetases, Antimicrob. Agents Chemother. 37 (1993) 32–38.

[11] A. Brevet, J. Chen, F. Lévêque, S. Blanquet, P. Plateau, Comparison of the enzymatic properties of the two *Escherichia coli* lysyl-tRNA synthetase species, J. Biol. Chem. 270 (1995) 14439–14444.

[12] H.D. Becker, J. Reinbolt, R. Kreutzer, R. Giegé, D. Kern, Existence of two distinct aspartyl-tRNA synthetases in *Thermus thermophilus*. Structural and biochemical properties of the two enzymes, Biochemistry 36 (29) (1997) 8785–8797.

[13] S. Skouloubris, L. Ribas de Pouplana, H. De Reuse, T.L. Hendrickson, A noncognate aminoacyl-tRNA synthetase that may resolve a missing link in protein evolution, Proc. Natl. Acad. Sci. U. S. A. 100 (2003) 11297–11302.

[14] M.Á. Rubio, M. Napolitano, J.A.G. Ochoa de Alda, J. Santamaría-Gómez, C.J. Patterson, A.W. Foster, R. Bru-Martínez, N.J. Robinson, I. Luque, Trans-oligomerization of duplicated aminoacyl-tRNA synthetases maintains genetic code fidelity under stress, Nucleic Acids Res. 43 (2015) 9905–9917.

[15] J.L. Huot, L. Enkler, C. Megel, L. Karim, D. Laporte, H.D. Becker, A.-M. Duchêne, M. Sissler, L. Maréchal-Drouard, Idiosyncrasies in decoding mitochondrial genomes, Biochimie 100 (2014) 95–106.

[16] C. Pujol, M. Bailly, D. Kern, L. Marechal-Drouard, H. Becker, A.-M. Duchene, Dual-targeted tRNA-dependent amidotransferase ensures both mitochondrial and chloroplastic Gln-tRNAGln synthesis in plants, Proc. Natl. Acad. Sci. 105 (2008) 6481–6485.

[17] A. Nagao, T. Suzuki, T. Katoh, Y. Sakaguchi, T. Suzuki, Biogenesis of glutaminyl-mt tRNAGln in human mitochondria, Proc. Natl. Acad. Sci. 106 (2009) 16209–16214.

[18] S. Debard, G. Bader, J.-O. De Craene, L. Enkler, S. Bär, D. Laporte, P. Hammann, E. Myslinski, B. Senger, S. Friant, H.D. Becker, Nonconventional localizations of cytosolic aminoacyl tRNA synthetases in yeast and human cells, Methods 113 (2016) 91–104.

[19] A.M. Duchêne, N. Peeters, A. Dietrich, A. Cosset, I.D. Small, H. Wintz, Overlapping destinations for two dual targeted glycyl-tRNA synthetases in *Arabidopsis thaliana* and *Phaseolus vulgaris*, J. Biol. Chem. 276 (2001) 15275–15283.

[20] E.G.A.K. Berglund, C. Pujol, A.M. Duchêne, Defining the determinants for dual targeting of amino acyl-tRNA synthetases to mitochondria and chloroplasts, J. Mol. Biol. 393 (2009) 803–814.

[21] A.K. Bandyopadhyay, M.P. Deutscher, Complex of aminoacyl-transfer RNA synthetases, J. Mol. Biol. 60 (1971) 113–122.

[22] G. Simos, A. Segref, F. Fasiolo, K. Hellmuth, A. Shevchenko, M. Mann, E.C. Hurt, The yeast protein Arc1p binds to tRNA and functions as a cofactor for the methionyl- and glutamyl-tRNA synthetases, EMBO J. 15 (1996) 5437–5448.

[23] S. Havrylenko, R. Legouis, B. Negrutskii, M. Mirande, *Caenorhabditis elegans* evolves a new architecture for the multi-aminoacyl-tRNA synthetase complex, J. Biol. Chem. 286 (2011) 28476–28487.

[24] J.M. van Rooyen, J.-B. Murat, P.-M. Hammoudi, S. Kieffer-Jaquinod, Y. Coute, A. Sharma, H. Pelloux, H. Belrhali, M.-A. Hakimi, Assembly of the novel five-component apicomplexan multi-aminoacyl-tRNA synthetase complex is driven by the hybrid scaffold protein Tg-p43, PLoS One 9 (2014) e89487.

[25] D. Laporte, J.L. Huot, G. Bader, L. Enkler, B. Senger, H.D. Becker, Exploring the evolutionary diversity and assembly modes of multi-aminoacyl-tRNA synthetase complexes: lessons from unicellular organisms, FEBS Lett. 588 (2014) 4268–4278.

[26] M. Frechin, D. Kern, R.P. Martin, H.D. Becker, B. Senger, Arc1p: anchoring, routing, coordinating, FEBS Lett. 584 (2010) 427–433.

[27] P.S. Ray, A. Arif, P.L. Fox, Macromolecular complexes as depots for releasable regulatory proteins, Trends Biochem. Sci. 32 (2007) 158–164.

[28] M. Guo, X.-L. Yang, P. Schimmel, New functions of aminoacyl-tRNA synthetases beyond translation, Nat. Rev. Mol. Cell Biol. 11 (2010) 668–674.

[29] M. Guo, X.-L. Yang, Architecture and metamorphosis, Top. Curr. Chem. 344 (2014) 89–118.

[30] M. Guo, P. Schimmel, Essential nontranslational functions of tRNA synthetases, Nat. Chem. Biol. 9 (2013) 145–153.

[31] S.G. Park, P. Schimmel, S. Kim, Aminoacyl tRNA synthetases and their connections to disease, Proc. Natl. Acad. Sci. U. S. A. 105 (2008) 11043–11049.

[32] A. Arif, F. Terenzi, A.A. Potdar, J. Jia, J. Sacks, A. China, D. Halawani, K. Vasu, X. Li, J.M. Brown, J. Chen, S.C. Kozma, G. Thomas, P.L. Fox, EPRS is a critical mTORC1–S6K1 effector that influences adiposity in mice, Nature 542 (2017) 357–361.

[33] M. Sajish, P. Schimmel, A human tRNA synthetase is a potent PARP1-activating effector target for resveratrol, Nature 519 (2014) 370.

[34] P. Yao, P.L. Fox, Aminoacyl-tRNA synthetases in medicine and disease, EMBO Mol. Med. 5 (2013) 332–343.

[35] A. Arif, J. Jia, R. Mukhopadhyay, B. Willard, M. Kinter, P.L. Fox, Two-site phosphorylation of EPRS coordinates multimodal regulation of noncanonical

[36] M. Frechin, L. Enkler, E. Tetaud, D. Laporte, B. Senger, C. Blancard, P. Hammann, G. Bader, S. Clauder-Münster, L.M. Steinmetz, R.P. Martin, J.-P. di Rago, H.D. Becker, Expression of nuclear and mitochondrial genes encoding ATP synthase is synchronized by disassembly of a multisynthetase complex, Mol. Cell 56 (2014) 763–776.

[37] I.M. López-Lara, O. Geiger, Bacterial lipid diversity, Biochim. Biophys. Acta 1862 (2016) 1287–1299.

[38] A. Caforio, A.J.M. Driessen, Archaeal phospholipids: structural properties and biosynthesis, Biochim. Biophys. Acta 1862 (2016) 1325–1339.

[39] M. Rajagopal, S. Walker, Envelope structures of gram-positive bacteria, Curr. Top. Microbiol. Immunol., Springer, Cham, 404 2015, pp. 1–44, , http://dx.doi.org/10.1007/82_2015_5021.

[40] J.C. Henderson, S.M. Zimmerman, A.A. Crofts, J.M. Boll, L.G. Kuhns, C.M. Herrera, M.S. Trent, The power of asymmetry: architecture and assembly of the gram-negative outer membrane lipid bilayer, Annu. Rev. Microbiol. 70 (2016) 255–278.

[41] S.-V. Albers, B.H. Meyer, The archaeal cell envelope, Nat. Rev. Microbiol. 9 (2011) 414–426.

[42] A. Peschel, H.-G. Sahl, The co-evolution of host cationic antimicrobial peptides and microbial resistance, Nat. Rev. Microbiol. 4 (2006) 529–536.

[43] K.L. Nawrocki, E.K. Crispell, S.M. McBride, Antimicrobial peptide resistance mechanisms of gram-positive bacteria, Antibiot. (Basel, Switzerland) 3 (2014) 461–492.

[44] V.I. Band, D.S. Weiss, Mechanisms of antimicrobial peptide resistance in gram-negative bacteria, Antibiot. (Basel, Switzerland) 4 (2015) 18–41.

[45] R.N. Fields, H. Roy, Deciphering the tRNA-dependent lipid aminoacylation systems in bacteria: novel components and structural advances, RNA Biol. (2017) 1–12, http://dx.doi.org/10.1080/15476286.2017.1356980 [Epub ahead of print].

[46] C. Slavetinsky, S. Kuhn, A. Peschel, Bacterial aminoacyl phospholipids – biosynthesis and role in basic cellular processes and pathogenicity, Biochim. Biophys. Acta 1862 (2016) 1310–1318.

[47] E. Maloney, D. Stankowska, J. Zhang, M. Fol, Q.-J. Cheng, S. Lun, W.R. Bishai, M. Rajagopalan, D. Chatterjee, M.V. Madiraju, The two-domain LysX protein of mycobacterium tuberculosis is required for production of lysinylated phosphatidylglycerol and resistance to cationic antimicrobial peptides, PLoS Pathog. 5 (7) (2009) e1000534.

[48] M. Mirande, The aminoacyl-tRNA synthetase complex, Subcell. Biochem. 83 (2017) 505–522.

[49] E. Maloney, S. Lun, D. Stankowska, H. Guo, M. Rajagoapalan, W.R. Bishai, M.V. Madiraju, Alterations in phospholipid catabolism in *Mycobacterium tuberculosis* lysX mutant, Front. Microbiol. 2 (2011) 19.

[50] K.M. Frain, D. Gangl, A. Jones, J.A.Z. Zedler, C. Robinson, Protein translocation and thylakoid biogenesis in cyanobacteria, BBA-Bioenergetics 1857 (2016) 266–273.

[51] J. Nickelsen, W. Zerges, Thylakoid biogenesis has joined the new era of bacterial cell biology, Front. Plant Sci. 4 (2013) 458.

[52] J. Santamaría-Gómez, J.A.G. Ochoa de Alda, E. Olmedo-Verd, R. Bru-Martínez, I. Luque, Sub-cellular localization and complex formation by aminoacyl-tRNA synthetases in cyanobacteria: evidence for interaction of membrane-anchored ValRS with ATP synthase, Front. Microbiol. 7 (2016) 857.

[53] I. Luque, J.A. Ochoa de Alda, CURT1, CAAD-containing aaRSs, thylakoid curvature and gene translation, Trends Plant Sci. 19 (2014) 63–66.

[54] E. Olmedo-Verd, J. Santamaría-Gómez, J.A.G. Ochoa de Alda, L. Ribas de Pouplana, I. Luque, Membrane anchoring of aminoacyl-tRNA synthetases by convergent acquisition of a novel protein domain, J. Biol. Chem. 286 (2011) 41057–41068.

[55] L. Dimitrijevic, Intracellular localization of yeast (*Saccharomyces cerevisiae*) lysyl-tRNA synthetase, FEBS Lett. 79 (1977) 37–41.

[56] T. Ohira, T. Suzuki, Precursors of tRNAs are stabilized by methylguanosine cap structures, Nat. Chem. Biol. 12 (2016) 648–655.

[57] J.D. Aitchison, M.P. Rout, The yeast nuclear pore complex and transport through it, Genetics 190 (2012) 855–883.

[58] M. Zasloff, tRNA transport from the nucleus in a eukaryotic cell: carrier-mediated translocation process, Proc. Natl. Acad. Sci. U. S. A. 80 (1983) 6436–6440.

[59] M. Mirande, D. Le Corre, D. Louvard, H. Reggio, J.-P. Pailliez, J.-P. Waller, Association of an aminoacyl-tRNA synthetase complex and of phenylalanyl-tRNA synthetase with the cytoskeletal framework fraction from mammalian cells, Exp. Cell Res. 156 (1985) 91–102.

[60] E. Lund, J.E. Dahlberg, Proofreading and aminoacylation of tRNAs before export from the nucleus, Science 282 (1998) 2082–2085.

[61] S. Sarkar, A.K. Azad, A.K. Hopper, Nuclear tRNA aminoacylation and its role in nuclear export of endogenous tRNAs in *Saccharomyces cerevisiae*, Proc. Natl. Acad. Sci. U. S. A. 96 (1999) 14366–14371.

[62] P. Schimmel, C.-C. Wang, Getting tRNA synthetases into the nucleus, Trends Biochem. Sci. 24 (1999) 127–128.

[63] A.K. Azad, D.R. Stanford, S. Sarkar, A.K. Hopper, Role of nuclear pools of aminoacyl-tRNA synthetases in tRNA nuclear export, Mol. Biol. Cell 12 (2001) 1381–1392.

[64] M. Steiner-Mosonyi, D. Mangroo, The nuclear tRNA aminoacylation-dependent pathway may be the principal route used to export tRNA from the nucleus in *Saccharomyces cerevisiae*, Biochem. J. 378 (2004) 809–816.

[65] H. Grosshans, E. Hurt, G. Simos, An aminoacylation-dependent nuclear tRNA export pathway in yeast, Genes Dev. 14 (2000) 830–840.

[66] K. Rothbarth, D. Werner, Amino-acid-transfer reactions in isolated nuclei of Ehrlich ascites tumor cells, Eur. J. Biochem. 155 (1986) 149–156.

[67] L. Nathanson, M.P. Deutscher, Active aminoacyl-tRNA synthetases are present in

nuclei as a high molecular weight multienzyme complex, J. Biol. Chem. 275 (2000) 31559–31562.

[68] C.L. Wolfe, J.A. Warrington, S. Davis, S. Green, M.T. Norcum, Isolation and characterization of human nuclear and cytosolic multisynthetase complexes and the intracellular distribution of p43/EMAPII, Protein Sci. 12 (2003) 2282–2290.

[69] M. Christie, C.-W. Chang, G. Róna, K.M. Smith, A.G. Stewart, A.A.S. Takeda, M.R.M. Fontes, M. Stewart, B.G. Vértessy, J.K. Forwood, B. Kobe, Structural biology and regulation of protein import into the nucleus, J. Mol. Biol. 428 (2016) 2060–2090.

[70] C.R. Woese, G.J. Olsen, M. Ibba, D. Söll, Aminoacyl-tRNA synthetases, the genetic code, and the evolutionary process, Microbiol. Mol. Biol. Rev. 64 (2000) 202–236.

[71] B. Brindefalk, J. Viklund, D. Larsson, M. Thollesson, S.G.E. Andersson, Origin and evolution of the mitochondrial aminoacyl-tRNA synthetases, Mol. Biol. Evol. 24 (2007) 743–756.

[72] D. Diodato, D. Ghezzi, V. Tiranti, The mitochondrial aminoacyl tRNA synthetases: genes and syndromes, Int. J. Cell Biol. 2014 (2014) 787956.

[73] M. Sissler, L.E. González-Serrano, E. Westhof, Recent advances in mitochondrial aminoacyl-tRNA synthetases and disease, Trends Mol. Med. 23 (2017) 693–708.

[74] E. Tolkunova, H. Park, J. Xia, M.P. King, E. Davidson, The human lysyl-tRNA synthetase gene encodes both the cytoplasmic and mitochondrial enzymes by means of an unusual alternative splicing of the primary transcript, J. Biol. Chem. 275 (2000) 35063–35069.

[75] J. Alexandrova, C. Paulus, J. Rudinger-Thirion, F. Jossinet, M. Frugier, Elaborate uORF/IRES features control expression and localization of human glycyl-tRNA synthetase, RNA Biol. 12 (2015) 1301–1313.

[76] G. Natsoulis, F. Hilger, G.R. Fink, The HTS1 gene encodes both the cytoplasmic and mitochondrial histidine tRNA synthetases of S. cerevisiae, Cell 46 (1986) 235–243.

[77] B. Chatton, P. Walter, J.P. Ebel, F. Lacroute, F. Fasiolo, The yeast VAS1 gene encodes both mitochondrial and cytoplasmic valyl-tRNA synthetases, J. Biol. Chem. 263 (1988) 52–57.

[78] H.-L. Tang, L.-S. Yeh, N.-K. Chen, T. Ripmaster, P. Schimmel, C.-C. Wang, Translation of a yeast mitochondrial tRNA synthetase initiated at redundant non-AUG codons, J. Biol. Chem. 279 (2004) 49656–49663.

[79] G. Souciet, B. Menand, J. Ovesna, A. Cosset, A. Dietrich, H. Wintz, Characterization of two bifunctional Arabdopsis thaliana genes coding for mitochondrial and cytosolic forms of valyl-tRNA synthetase and threonyl-tRNA synthetase by alternative use of two in-frame AUGs, FEBS J. 266 (1999) 848–854.

[80] K.G. Saman Habib, Suniti Vaishya, Translation in organelles of apicomplexan parasites, Trends Parasitol. 32 (2016) 939–952.

[81] K. Galani, H. Grosshans, K. Deinert, E.C. Hurt, G. Simos, The intracellular location of two aminoacyl-tRNA synthetases depends on complex formation with Arc1p, EMBO J. 20 (2001) 6889–6898.

[82] P.S. Ray, P.L. Fox, Origin and evolution of glutamyl-prolyl tRNA Synthetase WHEP domains reveal evolutionary relationships within holozoa, PLoS One 9 (2014) e98493.

[83] A. Arif, J. Jia, R.A. Moodt, P.E. DiCorleto, P.L. Fox, Phosphorylation of glutamyl-prolyl tRNA synthetase by cyclin-dependent kinase 5 dictates transcript-selective translational control, Proc. Natl. Acad. Sci. U. S. A. 108 (2011) 1415–1420.

[84] P. Sampath, B. Mazumder, V. Seshadri, P.L. Fox, Transcript-selective translational silencing by gamma interferon is directed by a novel structural element in the ceruloplasmin mRNA 3′ untranslated region, Mol. Cell. Biol. 23 (2003) 1509–1519.

[85] P. Sampath, B. Mazumder, V. Seshadri, C.A. Gerber, L. Chavatte, M. Kinter, S.M. Ting, J.D. Dignam, S. Kim, D.M. Driscoll, P.L. Fox, Noncanonical function of glutamyl-prolyl-tRNA synthetase: gene-specific silencing of translation, Cell 119 (2004) 195–208.

[86] J. Jia, A. Arif, P.S. Ray, P.L. Fox, WHEP domains direct noncanonical function of glutamyl-prolyl tRNA synthetase in translational control of gene expression, Mol. Cell 29 (2008) 679–690.

[87] P. Yao, A.A. Potdar, A. Arif, P.S. Ray, R. Mukhopadhyay, B. Willard, Y. Xu, J. Yan, G.M. Saidel, P.L. Fox, Coding region polyadenylation generates a truncated tRNA synthetase that counters translation repression, Cell 149 (2012) 88–100.

[88] E.-Y. Lee, H.-C. Lee, H.-K. Kim, S.Y. Jang, S.-J. Park, Y.-H. Kim, J.H. Kim, J. Hwang, J.-H. Kim, T.-H. Kim, A. Arif, S.-Y. Kim, Y.-K. Choi, C. Lee, C.-H. Lee, J.U. Jung, P.L. Fox, S. Kim, J.-S. Lee, M.H. Kim, Infection-specific phosphorylation of glutamyl-prolyl tRNA synthetase induces antiviral immunity, Nat. Immunol. 17 (2016) 1252–1262.

[89] E. Pahuski, M. Klekamp, T. Condon, A.E. Hampel, Altered aminoacyl-tRNA synthetase complexes in CHO cell mutants, J. Cell. Physiol. 114 (1983) 82–87.

[90] Y.G. Ko, E.Y. Kim, T. Kim, H. Park, H.S. Park, E.J. Choi, S. Kim, Glutamine-dependent antiapoptotic interaction of human glutaminyl-tRNA synthetase with apoptosis signal-regulating kinase 1, J. Biol. Chem. 276 (2001) 6030–6036.

[91] I.-S. Hwang, Y.-S. Jung, E. Kim, Interaction of ALG-2 with ASK1 influences ASK1 localization and subsequent JNK activation, FEBS Lett. 529 (2002) 183–187.

[92] Y. Shao, Y. Huang, Z. Liu, X. Guo, S. Jiang, Z. Sun, Q. Ruan, Human cytomegalovirus-encoded miR-US4-1 promotes cell apoptosis and benefits discharge of infectious virus particles by targeting QARS, J. Biosci. 41 (2016) 183–192.

[93] M. Lazard, M. Mirande, Cloning and analysis of a cDNA encoding mammalian arginyl-tRNA synthetase, a component of the multisynthetase complex with a hydrophobic N-terminal extension, Gene 132 (1993) 237–245.

[94] A.A. Girjes, K. Hobson, P. Chen, M.F. Lavin, Cloning and characterization of cDNA encoding a human arginyl-tRNA synthetase, Gene 164 (1995).

[95] Y.-G. Zheng, H. Wei, C. Ling, M.-G. Xu, E.-D. Wang, Two forms of human cytoplasmic arginyl-tRNA synthetase produced from two translation initiations by a single mRNA, Biochemistry 45 (2006) 1338–1344.

[96] M.P. Deutscher, R. Chang Ni, Purification of a low molecular weight form of rat liver arginyl-tRNA synthetase, J. Biol. Chem. 257 (1982) 6003–6006.

[97] G. Vellekamp, R.K. Sihags, M.P. Deutscherq, Comparison of the complexed and free forms of rat liver arginyl-tRNA synthetase and origin of the free form, J. Biol. Chem. 260 (1985) 9843–9847.

[98] J.-P.W. Beyazit Cirakoglu, Multiple forms of arginyl- and lysyl-tRNA synthetases in rat liver: a re-evaluation, Biochim. Biophys. Acta Protein Struct. Mol. Enzymol. 829 (1985) 173–179.

[99] M. Lazard, P. Kerjan, F. Agou, M. Mirande, The tRNA-dependent activation of arginine by arginyl-tRNA synthetase requires inter-domain communication, J. Mol. Biol. 302 (2000) 991–1004.

[100] T. Tasaki, S.M. Sriram, K.S. Park, Y.T. Kwon, The N-end rule pathway, Annu. Rev. Biochem. 81 (2012) 261–289.

[101] A. Varshavsky, The N-end rule pathway and regulation by proteolysis, Protein Sci. 20 (2011) 1298–1345.

[102] S.V. Kyriacou, M.P. Deutscher, An important role for the multienzyme aminoacyl-tRNA synthetase complex in mammalian translation and cell growth, Mol. Cell 29 (2008) 419–427.

[103] H. Nechushtan, E. Razin, The function of MITF and associated proteins in mast cells, Mol. Immunol. 38 (2002) 1177–1180.

[104] E. Razin, Z.C. Zhang, H. Nechushtan, S. Frenkel, Y.N. Lee, R. Arudchandran, J. Rivera, Suppression of microphthalmia transcriptional activity by its association with protein kinase C-interacting protein 1 in mast cells, J. Biol. Chem. 274 (1999) 34272–34276.

[105] I. Carmi-Levy, N. Yannay-Cohen, G. Kay, E. Razin, H. Nechushtan, Diadenosine tetraphosphate hydrolase is part of the transcriptional regulation network in immunologically activated mast cells, Mol. Cell. Biol. 28 (2008) 5777–5784.

[106] Y.-N. Lee, H. Nechushtan, N. Figov, E. Razin, The function of lysyl-tRNA synthetase and Ap4A as signaling regulators of MITF activity in FcRI-activated mast cells, Immunity 20 (2004) 145–151.

[107] Y. Ofir-Birin, P. Fang, S.P. Bennett, H.-M. Zhang, J. Wang, I. Rachmin, R. Shapiro, J. Song, A. Dagan, J. Pozo, S. Kim, A.G. Marshall, P. Schimmel, X.-L. Yang, H. Nechushtan, E. Razin, M. Guo, Structural switch of lysyl-tRNA synthetase between translation and transcription, Mol. Cell 49 (2013) 30–42.

[108] N. Yannay-Cohen, I. Carmi-Levy, G. Kay, C.M. Yang, J.M. Han, D.M. Kemeny, S. Kim, H. Nechushtan, E. Razin, LysRS serves as a key signaling molecule in the immune response by regulating gene expression, Mol. Cell 34 (2009) 603–611.

[109] G. Fu, T. Xu, Y. Shi, N. Wei, X.-L. Yang, tRNA-controlled nuclear import of a human tRNA synthetase, J. Biol. Chem. 287 (2012) 9330–9334.

[110] M. Sajish, P. Schimmel, A human tRNA synthetase is a potent PARP1-activating effector target for resveratrol, Nature 519 (2015) 370–373.

[111] X. Cao, C. Li, S. Xiao, Y. Tang, J. Huang, S. Zhao, X. Li, J. Li, R. Zhang, W. Yu, Acetylation promotes TyrRS nuclear translocation to prevent oxidative damage, Proc. Natl. Acad. Sci. U. S. A. 114 (2017) 687–692.

[112] N. Wei, Y. Shi, L.N. Truong, K.M. Fisch, T. Xu, E. Gardiner, G. Fu, Y.-S.O. Hsu, S. Kishi, A.I. Su, X. Wu, X.-L. Yang, Oxidative stress diverts tRNA synthetase to nucleus for protection against DNA damage, Mol. Cell 56 (2014) 323–332.

[113] J. Liu, E. Shue, K.L. Ewalt, P. Schimmel, A new gamma-interferon-inducible promoter and splice variants of an anti-angiogenic human tRNA synthetase, Nucleic Acids Res. 32 (2004) 719–727.

[114] V.I. Popenko, N.E. Cherny, S.F. Beresten, J.L. Ivanova, V.V. Filonenko, L.L. Kisselev, Immunoelectron microscopic location of tryptophanyl-tRNA synthetase in mammalian, prokaryotic and archaebacterial cells, Eur. J. Cell Biol. 62 (1993) 248–258.

[115] M. Sajish, Q. Zhou, S. Kishi, D.M. Valdez, M. Kapoor, M. Guo, S. Lee, S. Kim, X.-L. Yang, P. Schimmel, Trp-tRNA synthetase bridges DNA-PKcs to PARP-1 to link IFN-γ and p53 signaling, Nat. Chem. Biol. 8 (2012) 547–554.

[116] X. Xu, Y. Shi, H.-M. Zhang, E.C. Swindell, A.G. Marshall, M. Guo, S. Kishi, X.-L. Yang, Unique domain appended to vertebrate tRNA synthetase is essential for vascular development, Nat. Commun. 3 (2012) 681.

[117] M. Guo, P. Schimmel, X.-L. Yang, Functional expansion of human tRNA synthetases achieved by structural inventions, FEBS Lett. 584 (2010) 434–442.

[118] H. Fukui, R. Hanaoka, A. Kawahara, Noncanonical activity of seryl-tRNA synthetase is involved in vascular development, Circ. Res. 104 (2009) 1253–1259.

[119] W. Herzog, K. Müller, J. Huisken, D.Y.R. Stainier, Genetic evidence for a noncanonical function of seryl-tRNA synthetase in vascular development, Circ. Res. 104 (2009) 1260–1266.

[120] Y. Shi, X. Xu, Q. Zhang, G. Fu, Z. Mo, G.S. Wang, S. Kishi, X.-L. Yang, tRNA synthetase counteracts c-Myc to develop functional vasculature, elife 3 (2014) e02349.

[121] C.-Y. Fu, P.-C. Wang, H.-J. Tsai, Competitive binding between Seryl-tRNA synthetase/YY1 complex and NFKB1 at the distal segment results in differential regulation of human vegfa promoter activity during angiogenesis, Nucleic Acids Res. 45 (2017) 2423–2437.

[122] Z. Cao, H. Wang, X. Mao, L. Luo, Noncanonical function of threonyl-tRNA synthetase regulates vascular development in zebrafish, Biochem. Biophys. Res. Commun. 473 (2016) 67–72.

[123] Y.G. Ko, Y.S. Kang, E.K. Kim, S.G. Park, S. Kim, Nucleolar localization of human methionyl-tRNA synthetase and its role in ribosomal RNA synthesis, J. Cell Biol. 149 (2000) 567–574.

[124] M. Frugier, R. Giegé, Yeast aspartyl-tRNA synthetase binds specifically its own mRNA, J. Mol. Biol. 331 (2003) 375–383.

[125] M. Frugier, M. Ryckelynck, R. Giegé, tRNA-balanced expression of a eukaryal aminoacyl-tRNA synthetase by an mRNA-mediated pathway, EMBO Rep. 6 (2005) 860–865.

[126] D.G. Kim, J.W. Choi, J.Y. Lee, H. Kim, Y.S. Oh, J.W. Lee, Y.K. Tak, J.M. Song,

E. Razin, S.-H. Yun, S. Kim, Interaction of two translational components, lysyl-tRNA synthetase and p40/37LRP, in plasma membrane promotes laminin-dependent cell migration, FASEB J. 26 (2012) 4142–4159.

[127] D.G. Kim, J.Y. Lee, N.H. Kwon, P. Fang, Q. Zhang, J. Wang, N.L. Young, M. Guo, H.Y. Cho, A.U. Mushtaq, Y.H. Jeon, J.W. Choi, J.M. Han, H.W. Kang, J.E. Joo, Y. Hur, W. Kang, H. Yang, D.-H. Nam, M.-S. Lee, J.W. Lee, E.-S. Kim, A. Moon, K. Kim, D. Kim, E.J. Kang, Y. Moon, K.H. Rhee, B.W. Han, J.S. Yang, G. Han, W.S. Yang, C. Lee, M.-W. Wang, S. Kim, Chemical inhibition of prometastatic lysyl-tRNA synthetase-laminin receptor interaction, Nat. Chem. Biol. 10 (2014) 29–34.

[128] S.H. Nam, D. Kim, M.-S. Lee, D. Lee, T.K. Kwak, M. Kang, J. Ryu, H.-J. Kim, H.E. Song, J. Choi, G.-H. Lee, S.-Y. Kim, S.H. Park, D.G. Kim, N.H. Kwon, T.Y. Kim, J.P. Thiery, S. Kim, J.W. Lee, Noncanonical roles of membranous lysyl-tRNA synthetase in transducing cell-substrate signaling for invasive dissemination of colon cancer spheroids in 3D collagen I gels, Oncotarget 6 (2015) 21655–21674.

[129] S. Bae Rho, M.J. Kim, J.S. Lee, W. Seol, H. Motegi, S. Kim, K. Shiba, Genetic dissection of protein–protein interactions in multi-tRNA synthetase complex, Genetics 96 (1999) 4488–4493.

[130] M. Kaminska, S. Havrylenko, P. Decottignies, P. Le Maréchal, B. Negrutskii, M. Mirande, Dynamic organization of aminoacyl-tRNA synthetase complexes in the cytoplasm of human cells, J. Biol. Chem. 284 (2009) 13746–13754.

[131] K. Hara, K. Yonezawa, Q.P. Weng, M.T. Kozlowski, C. Belham, J. Avruch, Amino acid sufficiency and mTOR regulate p70 S6 kinase and eIF-4E BP1 through a common effector mechanism, J. Biol. Chem. 273 (1998) 14484–14494.

[132] Y. Sancak, T.R. Peterson, Y.D. Shaul, R.A. Lindquist, C.C. Thoreen, L. Bar-Peled, D.M. Sabatini, The rag GTPases bind raptor and mediate amino acid signaling to mTORC1, Science 320 (2008) 1496–1501.

[133] P. Nicklin, P. Bergman, B. Zhang, E. Triantafellow, H. Wang, B. Nyfeler, H. Yang, M. Hild, C. Kung, C. Wilson, V.E. Myer, J.P. MacKeigan, J.A. Porter, Y.K. Wang, L.C. Cantley, P.M. Finan, L.O. Murphy, Bidirectional transport of amino acids regulates mTOR and autophagy, Cell 136 (2009) 521–534.

[134] S.G. Kim, G.R. Buel, J. Blenis, Nutrient regulation of the mTOR complex 1 signaling pathway, Mol. Cell 35 (2013) 463–473.

[135] R.V. Durá, W. Oppliger, A.M. Robitaille, L. Heiserich, R. Skendaj, E. Gottlieb, M.N. Hall, Glutaminolysis activates rag-mTORC1 signaling, Mol. Cell 47 (2012) 349–358.

[136] J.M. Han, S.J. Jeong, M.C. Park, G. Kim, N.H. Kwon, H.K. Kim, S.H. Ha, S.H. Ryu, S. Kim, Leucyl-tRNA synthetase is an intracellular leucine sensor for the mTORC1-signaling pathway, Cell 149 (2012) 410–424.

[137] M.-S. Yoon, K. Son, E. Arauz, J.M. Han, S. Kim, J. Chen, Leucyl-tRNA synthetase activates Vps34 in amino acid-sensing mTORC1 signaling, Cell Rep. 16 (2016) 1510–1517.

[138] M.-S. Yoon, G. Du, J.M. Backer, M.A. Frohman, J. Chen, Class III PI-3-kinase activates phospholipase D in an amino acid-sensing mTORC1 pathway, J. Cell Biol. 195 (2011) 435–447.

[139] G. Gory Bonfils, M. Jaquenoud, S.V. Bontron, C. Ostrowicz, C. Ungermann, C. De Virgilio, Leucyl-tRNA synthetase controls TORC1 via the EGO complex, Mol. Cell 46 (2012) 105–110.

[140] S. Cen, A. Khorchid, H. Javanbakht, J. Gabor, T. Stello, K. Shiba, K. Musier-Forsyth, L. Kleiman, Incorporation of lysyl-tRNA synthetase into human immunodeficiency virus type 1, J. Virol. 75 (2001) 5043–5048.

[141] J. Gabor, S. Cen, H. Javanbakht, M. Niu, L. Kleiman, Effect of altering the tRNA(Lys)(3) concentration in human immunodeficiency virus type 1 upon its annealing to viral RNA, GagPol incorporation, and viral infectivity, J. Virol. 76 (2002) 9096–9102.

[142] F. Guo, S. Cen, M. Niu, H. Javanbakht, L. Kleiman, Specific inhibition of the synthesis of human lysyl-tRNA synthetase results in decreases in tRNA(Lys) incorporation, tRNA(3)(Lys) annealing to viral RNA, and viral infectivity in human immunodeficiency virus type 1, J. Virol. 77 (2003) 9817–9822.

[143] S. Cen, H. Javanbakht, M. Niu, L. Kleiman, Ability of wild-type and mutant lysyl-tRNA synthetase to facilitate tRNA(Lys) incorporation into human immunodeficiency virus type 1, J. Virol. 78 (2004) 1595–1601.

[144] V. Dewan, M. Wei, L. Kleiman, K. Musier-Forsyth, Dual role for motif 1 residues of human lysyl-tRNA synthetase in dimerization and packaging into HIV-1, J. Biol. Chem. 287 (2012) 41955–41962.

[145] A.A. Duchon, C. St Gelais, N. Titkemeier, J. Hatterschide, L. Wu, K. Musier-Forsyth, HIV-1 exploits a dynamic multi-aminoacyl-tRNA synthetase complex to enhance viral replication, J. Virol. 91 (2017) e01240–17.

[146] S. Cen, H. Javanbakht, S. Kim, K. Shiba, R. Craven, A. Rein, K. Ewalt, P. Schimmel, K. Musier-Forsyth, L. Kleiman, Retrovirus-specific packaging of aminoacyl-tRNA synthetases with cognate primer tRNAs, J. Virol. 76 (2002) 13111–13115.

[147] S.G. Park, H.J. Kim, Y.H. Min, E.-C. Choi, Y.K. Shin, B.-J. Park, S.W. Lee, S. Kim, Human lysyl-tRNA synthetase is secreted to trigger proinflammatory response, Proc. Natl. Acad. Sci. U. S. A. 102 (2005) 6356–6361.

[148] S.B. Kim, H.R. Kim, M.C. Park, S. Cho, P.C. Goughnour, D. Han, I. Yoon, Y. Kim, T. Kang, E. Song, P. Kim, H. Choi, J.Y. Mun, C. Song, S. Lee, H.S. Jung, S. Kim, Caspase-8 controls the secretion of inflammatory lysyl-tRNA synthetase in exosomes from cancer cells, J. Cell Biol. 216 (2017) 2201–2216.

[149] K. Meerschaert, E. Remue, A. De Ganck, A. Staes, C. Boucherie, K. Gevaert, J. Vandekerckhove, L. Kleiman, J. Gettemans, The tandem PDZ protein syntenin interacts with the aminoacyl tRNA synthetase complex in a lysyl-tRNA synthetase-dependent manner, J. Proteome Res. 7 (2008) 4962–4973.

[150] M.F. Baietti, Z. Zhang, E. Mortier, A. Melchior, G. Degeest, A. Geeraerts, Y. Ivarsson, F. Depoortere, C. Coomans, E. Vermeiren, P. Zimmermann, G. David, Syndecan-syntenin-ALIX regulates the biogenesis of exosomes, Nat. Cell Biol. 14 (2012) 677–685.

[151] K. Wakasugi, P. Schimmel, Two distinct cytokines released from a human aminoacyl-tRNA synthetase, Science 284 (1999) 147–151.

[152] R. Zeng, Y. Chen, Z. Zeng, W. Liu, X. Jiang, R. Liu, O. Qiang, X. Li, Effect of mini-tyrosyl-tRNA synthetase/mini-tryptophanyl-tRNA synthetase on ischemic angiogenesis in rats: proliferation and migration of endothelial cells, Heart Vessel. 26 (2011) 69–80.

[153] K. Wakasugi, B.M. Slike, J. Hood, A. Otani, K.L. Ewalt, M. Friedlander, D.A. Cheresh, P. Schimmel, A human aminoacyl-tRNA synthetase as a regulator of angiogenesis, Proc. Natl. Acad. Sci. U. S. A. 99 (2002) 173–177.

[154] R. Zeng, Y. Chen, Z. Zeng, X. Liu, R. Liu, O. Qiang, X. Li, Inhibition of mini-TyrRS-induced angiogenesis response in endothelial cells by VE-cadherin-dependent mini-TrpRS, Heart Vessel. 27 (2012) 193–201.

[155] Y. Greenberg, M. King, W.B. Kiosses, K. Ewalt, X. Yang, P. Schimmel, J.S. Reader, E. Tzima, The novel fragment of tyrosyl tRNA synthetase, mini-TyrRS, is secreted to induce an angiogenic response in endothelial cells, FASEB J. 22 (2008) 1597–1605.

[156] P.M. Biselli, A.R. Guerzoni, M.F. de Godoy, É.C. Pavarino-Bertelli, E.M. Goloni-Bertollo, Vascular endothelial growth factor genetic variability and coronary artery disease in Brazilian population, Heart Vessel. 23 (2008) 371–375.

[157] M.-N. Vo, X.-L. Yang, P. Schimmel, Dissociating quaternary structure regulates cell-signaling functions of a secreted human tRNA synthetase, J. Biol. Chem. 286 (2011) 11563–11568.

[158] Q. Zhou, M. Kapoor, M. Guo, R. Belani, X. Xu, W.B. Kiosses, M. Hanan, C. Park, E. Armour, M.-H. Do, L.A. Nangle, P. Schimmel, X.-L. Yang, Orthogonal use of a human tRNA synthetase active site to achieve multifunctionality, Nat. Struct. Mol. Biol. 17 (2010) 57–61.

[159] T. Nakamoto, M. Miyanokoshi, T. Tanaka, K. Wakasugi, Identification of a residue crucial for the angiostatic activity of human mini tryptophanyl-tRNA synthetase by focusing on its molecular evolution, Sci. Rep. 6 (2016) 24750.

[160] E. Tzima, J.S. Reader, M. Irani-Tehrani, K.L. Ewalt, M.A. Schwartz, P. Schimmel, VE-cadherin links tRNA synthetase cytokine to anti-angiogenic function, J. Biol. Chem. 280 (2005) 2405–2408.

[161] E. Tzima, P. Schimmel, Inhibition of tumor angiogenesis by a natural fragment of a tRNA synthetase, Science 80 (309) (2006) 1534–1539.

[162] R. Zeng, X.-F. Jiang, Y.-C. Chen, Y.-N. Xu, S.-H. Ma, Z. Zeng, R. Liu, O. Qiang, X. Li, VEGF, not VEGFR2, is associated with the angiogenesis effect of mini-TyrRS/mini-TrpRS in human umbilical vein endothelial cells in hypoxia, Cytotechnology 66 (2014) 655–665.

[163] K. Wakasugi, P. Schimmel, Highly differentiated motifs responsible for two cytokine activities of a split human tRNA synthetase, J. Biol. Chem. 274 (1999) 23155–23159.

[164] Y.H. Ahn, S. Park, J.J. Choi, B.-K. Park, K.H. Rhee, E. Kang, S. Ahn, C.-H. Lee, J.S. Lee, K.-S. Inn, M.-L. Cho, S.-H. Park, K. Park, H.J. Park, J.H. Lee, J.W. Park, N.H. Kwon, H. Shim, B.W. Han, P. Kim, J.-Y. Lee, Y. Jeon, J.W. Huh, M. Jin, S. Kim, Secreted tryptophanyl-tRNA synthetase as a primary defence system against infection, Nat. Microbiol. 2 (2016) 16191.

[165] T.F. Williams, A.C. Mirando, B. Wilkinson, C.S. Francklyn, K.M. Lounsbury, Secreted threonyl-tRNA synthetase stimulates endothelial cell migration and angiogenesis, Sci. Rep. 3 (2013) 1317.

[166] T.L. Wellman, M. Eckenstein, C. Wong, M. Rincon, T. Ashikaga, S.L. Mount, C.S. Francklyn, K.M. Lounsbury, Threonyl-tRNA synthetase overexpression correlates with angiogenic markers and progression of human ovarian cancer, BMC Cancer 14 (2014) 620.

[167] M. Kron, K. Marquard, M. Härtlein, S. Price, R. Leberman, An immunodominant antigen of Brugia malayi is an asparaginyl-tRNA synthetase, FEBS Lett. 374 (1995) 122–124.

[168] M. Kron, M. Petridis, Y. Milev, J. Leykam, M. Härtlein, Expression, localization and alternative function of cytoplasmic asparaginyl-tRNA synthetase in Brugia malayi, Mol. Biochem. Parasitol. 129 (2003) 33–39.

[169] B.L. Ramirez, O.M.Z. Howard, H.F. Dong, T. Edamatsu, P. Gao, M. Hartlein, M. Kron, *Brugia malayi* asparaginyl–transfer RNA synthetase induces chemotaxis of human leukocytes and activates G-protein–coupled receptors CXCR1 and CXCR2, J. Infect. Dis. 193 (2006) 1164–1171.

[170] M. Kron, J. Leykam, J. Kopaczewski, I. Matus, Identification of diadenosine triphosphate in Brugia malayi by reverse phase high performance liquid chromatography and MALDI mass spectrometry, J. Chromatogr. B Anal. Technol. Biomed. Life Sci. 856 (2007) 234–238.

[171] M.A. Kron, C. Wang, S. Vodanovic-Jankovic, O. Zack Howard, L.A. Kuhn, Interleukin-8-like activity in a filarial asparaginyl-tRNA synthetase, Mol. Biochem. Parasitol. 185 (2012) 66–69.

[172] J. Jothi D., M. Dhanraj, S. Shanmugam, S. Sanjana, M. Kron, A. Dhanasekaran, *Brugia malayi* asparaginyl-tRNA synthetase stimulates endothelial cell proliferation, vasodilation and angiogenesis, PLoS One 11 (2016) e0146132.

[173] M.C. Park, T. Kang, D. Jin, J.M. Han, S.B. Kim, Y.J. Park, K. Cho, Y.W. Park, M. Guo, W. He, X.-L. Yang, P. Schimmel, S. Kim, Secreted human glycyl-tRNA synthetase implicated in defense against ERK-activated tumorigenesis, Proc. Natl. Acad. Sci. U. S. A. 109 (2012) E640–7.

[174] W. He, G. Bai, H. Zhou, N. Wei, N.M. White, J. Lauer, H. Liu, Y. Shi, C.D. Dumitru, K. Lettieri, V. Shubayev, A. Jordanova, V. Guergueltcheva, P.R. Griffin, R.W. Burgess, S.L. Pfaff, X.-L. Yang, CMT2D neuropathy is linked to the neomorphic binding activity of glycyl-tRNA synthetase, Nature 526 (2015) 710–714.

[175] W.-S. Lo, E. Gardiner, Z. Xu, C.-F. Lau, F. Wang, J.J. Zhou, J.D. Mendlein, L.A. Nangle, K.P. Chiang, X.-L. Yang, K.-F. Au, W.H. Wong, M. Guo, M. Zhang, P. Schimmel, Human tRNA synthetase catalytic nulls with diverse functions, Science 345 (2014) 328–332.

[176] K.L. Seburn, L.A. Nangle, G.A. Cox, P. Schimmel, R.W. Burgess, An active dominant mutation of glycyl-tRNA synthetase causes neuropathy in a Charcot-Marie-

Tooth 2D mouse model, Neuron 51 (2006) 715–726.

[177] A. Jordanova, J. Irobi, F.P. Thomas, P. Van Dijck, K. Meerschaert, M. Dewil, I. Dierick, A. Jacobs, E. De Vriendt, V. Guergueltcheva, C.V. Rao, I. Tournev, F.A.A. Gondim, M. D'Hooghe, V. Van Gerwen, P. Callaerts, L. Van Den Bosch, J.-P. Timmermans, W. Robberecht, J. Gettemans, J.M. Thevelein, P. De Jonghe, I. Kremensky, V. Timmerman, Disrupted function and axonal distribution of mutant tyrosyl-tRNA synthetase in dominant intermediate Charcot-Marie-Tooth neuropathy, Nat. Genet. 38 (2006) 197–202.

[178] L.A. Nangle, W. Zhang, W. Xie, X.-L. Yang, P. Schimmel, Charcot-Marie-Tooth disease-associated mutant tRNA synthetases linked to altered dimer interface and neurite distribution defect, Proc. Natl. Acad. Sci. U. S. A. 104 (2007) 11239–11244.

[179] C.B. Kunst, E. Mezey, M.J. Brownstein, D. Patterson, Mutations in SOD1 associated with amyotrophic lateral sclerosis cause novel protein interactions, Nat. Genet. 15 (1997) 91–94.

[180] W.L. Sang, S.K. Young, K. Sunghoon, Multifunctional proteins in tumorigenesis: aminoacyl-tRNA synthet…: ingenta connect, Curr. Proteomics 3 (2006) 233–247.

[181] J.P. Kushner, D. Boll, J. Quagliana, S. Dickman, Elevated methionine-tRNA synthetase activity in human colon cancer, Proc. Soc. Exp. Biol. Med. 153 (1976) 273–276.

[182] E.Y. Kim, J.Y. Jung, A. Kim, K. Kim, Y.S. Chang, Methionyl-tRNA synthetase overexpression is associated with poor clinical outcomes in non-small cell lung cancer, BMC Cancer 17 (2017) 467.

[183] L.M. 't Hart, T. Hansen, I. Rietveld, J.M. Dekker, G. Nijpels, G.M.C. Janssen, P.A. Arp, A.G. Uitterlinden, T. Jørgensen, K. Borch-Johnsen, H.A.P. Pols, O. Pedersen, C.M. van Duijn, R.J. Heine, J.A. Maassen, Evidence that the mitochondrial leucyl tRNA synthetase (LARS2) gene represents a novel type 2 diabetes susceptibility gene, Diabetes 54 (2005) 1892–1895.

[184] E. Reiling, B. Jafar-Mohammadi, E. van 't Riet, M.N. Weedon, J.V. van Vliet-Ostaptchouk, T. Hansen, R. Saxena, T.W. van Haeften, P.A. Arp, S. Das, G. Nijpels, M.J. Groenewoud, E.C. van Hove, A.G. Uitterlinden, J.W.A. Smit, A.D. Morris, A.S.F. Doney, C.N.A. Palmer, C. Guiducci, A.T. Hattersley, T.M. Frayling, O. Pedersen, P.E. Slagboom, D.M. Altshuler, L. Groop, J.A. Romijn, J.A. Maassen, M.H. Hofker, J.M. Dekker, M.I. McCarthy, L.M. 't Hart, Genetic association analysis of LARS2 with type 2 diabetes, Diabetologia 53 (2010) 103–110.

[185] J.J. Zhou, F. Wang, Z. Xu, W.-S. Lo, C.-F. Lau, K.P. Chiang, L.A. Nangle, M.A. Ashlock, J.D. Mendlein, X.-L. Yang, M. Zhang, P. Schimmel, Secreted histidyl-tRNA synthetase splice variants elaborate major epitopes for autoantibodies in inflammatory myositis, J. Biol. Chem. 289 (2014) 19269–19275.

[186] O.M.Z. Howard, H.F. Dong, D. Yang, N. Raben, K. Nagaraju, A. Rosen, L. Casciola-Rosen, M. Härtlein, M. Kron, D. Yang, K. Yiadom, S. Dwivedi, P.H. Plotz, J.J. Oppenheim, Histidyl-tRNA synthetase and asparaginyl-tRNA synthetase, autoantigens in myositis, activate chemokine receptors on T lymphocytes and immature dendritic cells, J. Exp. Med. 196 (2002) 781–791.

[187] M.B. Mathews, R.M. Bernstein, Myositis autoantibody inhibits histidyl-tRNA synthetase: a model for autoimmunity, Nature 304 (1983) 177–179.

[188] M.B. Mathews, M. Reichlin, G.R. Hughes, R.M. Bernstein, Anti-threonyl-tRNA synthetase, a second myositis-related autoantibody, J. Exp. Med. 160 (1984) 420–434.

[189] L. Stojanov, M. Satoh, M. Hirakata, W.H. Reeves, Correlation of antisynthetase antibody levels with disease course in a patient with interstitial lung disease and elevated muscle enzymes, J. Clin. Rheumatol. 2 (1996) 89–95.

[190] M. Mahler, F.W. Miller, M.J. Fritzler, Idiopathic inflammatory myopathies and the anti-synthetase syndrome: a comprehensive review, Autoimmun. Rev. 13 (2014) 367–371.

[191] M. Cojocaru, I.M. Cojocaru, B. Chicos, New insights into antisynthetase syndrome, Maedica (Buchar) 11 (2016) 130–135.

Book chapter

Hemmerle *et al.*, 2020

Noncanonical inputs and outputs of
tRNA aminoacylation 2020

Noncanonical inputs and outputs of tRNA aminoacylation

Marine Hemmerle, Marion Wendenbaum, Guillaume Grob, Nathaniel Yakobov, Nassira Mahmoudi, Bruno Senger, Sylvain Debard, Frédéric Fischer, Hubert Dominique Becker[*]

Génétique Moléculaire, Génomique, Microbiologie, UMR 7156, CNRS, Université de Strasbourg, Strasbourg, France
[*]Corresponding author: e-mail address: h.becker@unistra.fr

Contents

Abstract

The aminoacylation reaction is one of most extensively studied cellular processes. The so-called "*canonical*" reaction is carried out by direct charging of an amino acid (aa) onto its corresponding transfer RNA (tRNA) by the cognate aminoacyl-tRNA synthetase (aaRS), and the *canonical* usage of the aminoacylated tRNA (aa-tRNA) is to translate a messenger RNA codon in a translating ribosome. However, four out of the 22 genetically-encoded aa are made "*noncanonically*" through a two-step or indirect route that usually compensate for a missing aaRS. Additionally, from the 22 proteinogenic aa, 13 are *noncanonically* used, by serving as substrates for the tRNA- or aa-tRNA-dependent synthesis of other cellular components. These nontranslational processes range from lipid aminoacylation, and heme, aa, antibiotic and peptidoglycan synthesis

to protein degradation. This chapter focuses on these noncanonical usages of aa-tRNAs and the ways of generating them, and also highlights the strategies that cells have evolved to balance the use of aa-tRNAs between protein synthesis and synthesis of other cellular components.
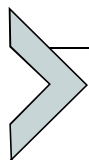
1. Introduction

Translation relies on the constant synthesis and delivery to the decoding ribosomes of a complete set of accurately aminoacylated transfer RNAs (aa–tRNAs). aa–tRNAs are the products of an enzymatic reaction termed tRNA aminoacylation, that is catalyzed by a family of ubiquitous enzymes called aminoacyl–tRNA synthetases (aaRSs) [1]. Elucidation of the aminoacylation reaction was concomitant with the characterization of tRNA and aaRSs [2–7]. In the "*canonical*" aminoacylation reaction, using a specific amino acid (aa), aaRSs catalyze the ATP-dependent formation of an aminoacyl–adenylate (aa~AMP), which enables this activated aa to be transferred directly onto the accepting $3'$- or $2'$OH of the terminal adenosine of the cognate tRNA (Fig. 1A). "*Canonical*" tRNA aminoacylation is often also termed "*direct*" tRNA aminoacylation and signifies that the aa and tRNA that are linked are cognate pairs and that, upon release, the aa-tRNA can be used directly in protein synthesis. Contrarily, the "*non-canonical*" tRNA aminoacylation, also termed "*alternate*" or "*indirect pathway,*" starts with an aa that is first charged onto a non–cognate tRNA by an aaRS, followed by its conversion into the cognate aa by a second enzymatic activity. The first description of a non–canonical pathway for tRNA aminoacylation occurred as early as 1968 by M. Wilcox and M. Nirenberg, who demonstrated that direct formation of glutaminyl–tRNA$^{\text{Glutamine}}$ (Gln-tRNA$^{\text{Gln}}$) by a glutaminyl–tRNA synthetase (GlnRS) was absent in three *Bacilli* species; the evidence indicated that they all required first the aminoacylation of tRNA$^{\text{Gln}}$ with glutamate (Glu), followed by the tRNA-dependent conversion of Glu into Gln, thereby demonstrating that tRNA can be a cofactor in aa biosynthesis [8]. The description of the first non–canonical aminoacylation reaction almost coincided with the first report of the non–canonical utilization of an aa-tRNA, *e.g.,* not for protein synthesis, and was that of lysyl–tRNA$^{\text{Lysine}}$ in the synthesis of *O*-lysyl phosphatidylglycerol in *Staphylococcus aureus* [9].

From the 22 genetically-encoded aa that have been identified to date, 18 are exclusively aminoacylated onto their cognate tRNAs through the
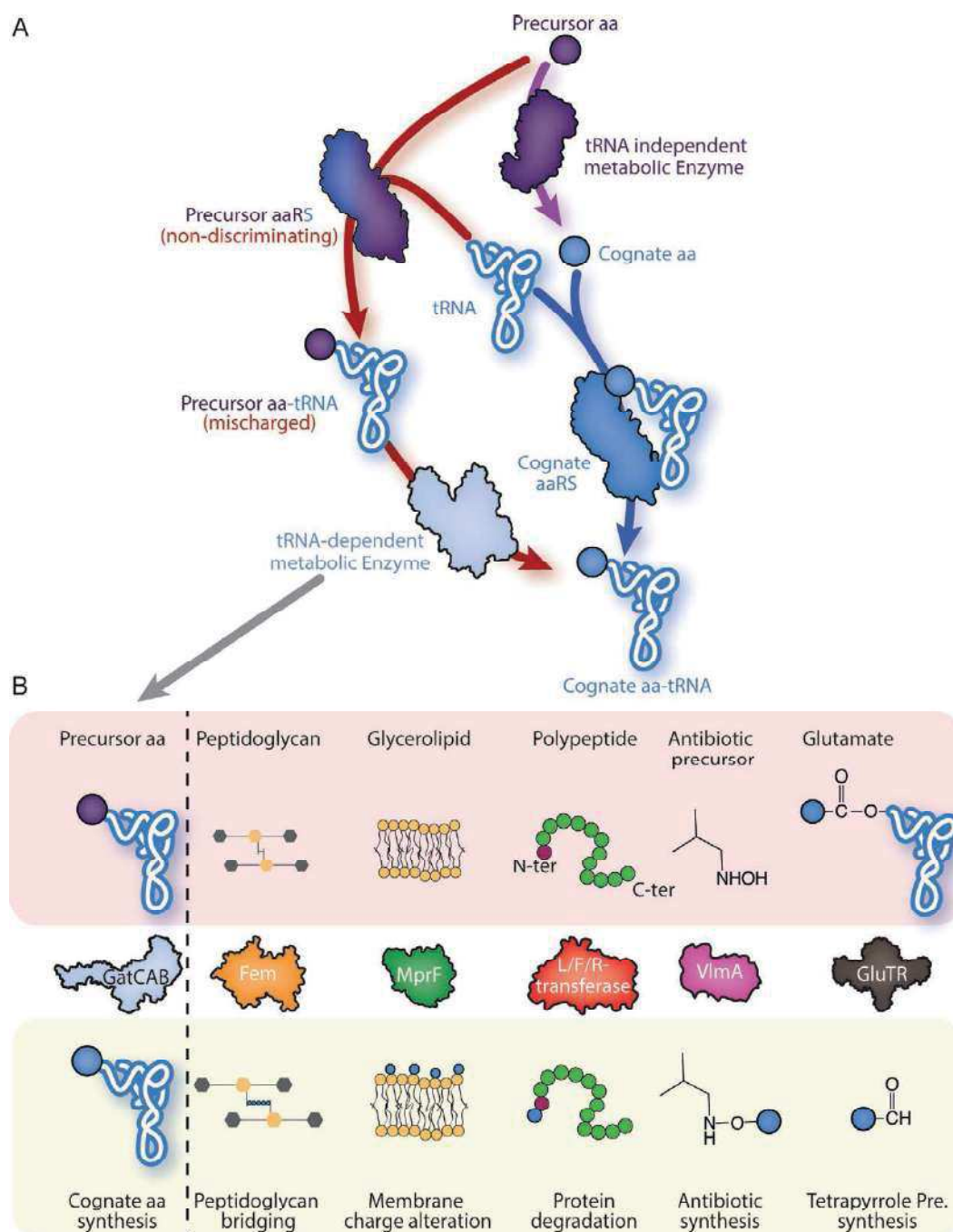
Fig. 1 Canonical and noncanonical tRNA aminoacylation reaction and nontranslational aa-tRNA usages. (A) Overview of the canonical tRNA aminoacylation (right side, blue arrows) and of the noncanonical 2-step reaction (left side, red arrows). For details see Fig. 2. (B) Schematic representations of the nontranslational usages of aa-tRNAs described in this chapter. The molecule that will be tRNA-dependently or aa-tRNA-dependently modified is indicated in the top row, the enzyme responsible for the tRNA-dependent modification in the middle and the product of the reaction or the fate of the compound tRNA-dependently modified is indicated in the bottom row.

canonical reaction (Ala, Arg, Asp, Glu, Gly, His, Ile, Leu, Lys, Met, Phe, Pro, Pyrrolysine (Pyl), Ser, Thr, Trp, Tyr and Val), one is strictly aminoacylated *via* a non-canonical aminoacylation reaction (Selenocysteine, Sec) and three are charged onto their corresponding tRNA either canonically or non-canonically (Asn, Cys and Gln). All four indirect pathways of tRNA aminoacylation have three main common features. They proceed *via* two consecutive steps (an exception is Sec-tRNA^{Sec} formation in archaea and eukaryotes that requires three reactions; see Fig. 2). The first step is the mis-charging of a tRNA with a non-cognate aa by a so-called non-discriminating aaRS (ND-aaRS) [10,11]. The second step is the conversion of the misacylated aa into the cognate one, while it is attached to the tRNA by a tRNA-dependent modifying enzyme [12]. Sometimes the ND-aaRS and the tRNA-dependent modifying enzyme form a complex that catalyzes both reactions without the release of the mischarged aa-tRNA intermediate [13]. The last common feature is that the noncognate aa of the misacylated aa-tRNA intermediate is always a metabolic precursor of the cognate final aa, in the tRNA-independent and regular metabolic pathway (*e.g.,* Asp for Asn, Glu for Gln, O-phosphoserine (Sep) for Sec; Fig. 1A). Among the 22 proteinogenic aa, 13 (Ala, Arg, Asp, Glu, Gly, Leu, Lys, Met, Phe, Thr, Trp, Val and Ser) can serve as substrates for the tRNA-dependent synthesis of other cellular components. Noteworthy, when the aa of an aa-tRNA is used for a non-canonical pathway, the tRNA carrier is generally not specific to the non-canonical usage but diverted from protein synthesis. This often requires adaptation of other components of the translation machinery that limit the negative impact that rerouting of aa-tRNAs could have on the efficiency or accuracy of protein synthesis [14]. The purpose of this chapter is to present the fascinating diversity of the non-canonical usages made by organisms of aa-tRNAs (Fig. 1B).
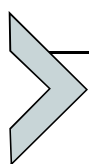
2. Non canonical aminoacylation of tRNAs and tRNA-dependent synthesis of amino acids

2.1 The two non-standard amino acids

In addition to the common set of 20 proteinogenic aa, two additional and non-standard aa are used for protein synthesis in some organisms: selenocysteine (Sec) and pyrrolysine (Pyl), respectively, known as the 21st and 22st genetically-encoded aa.
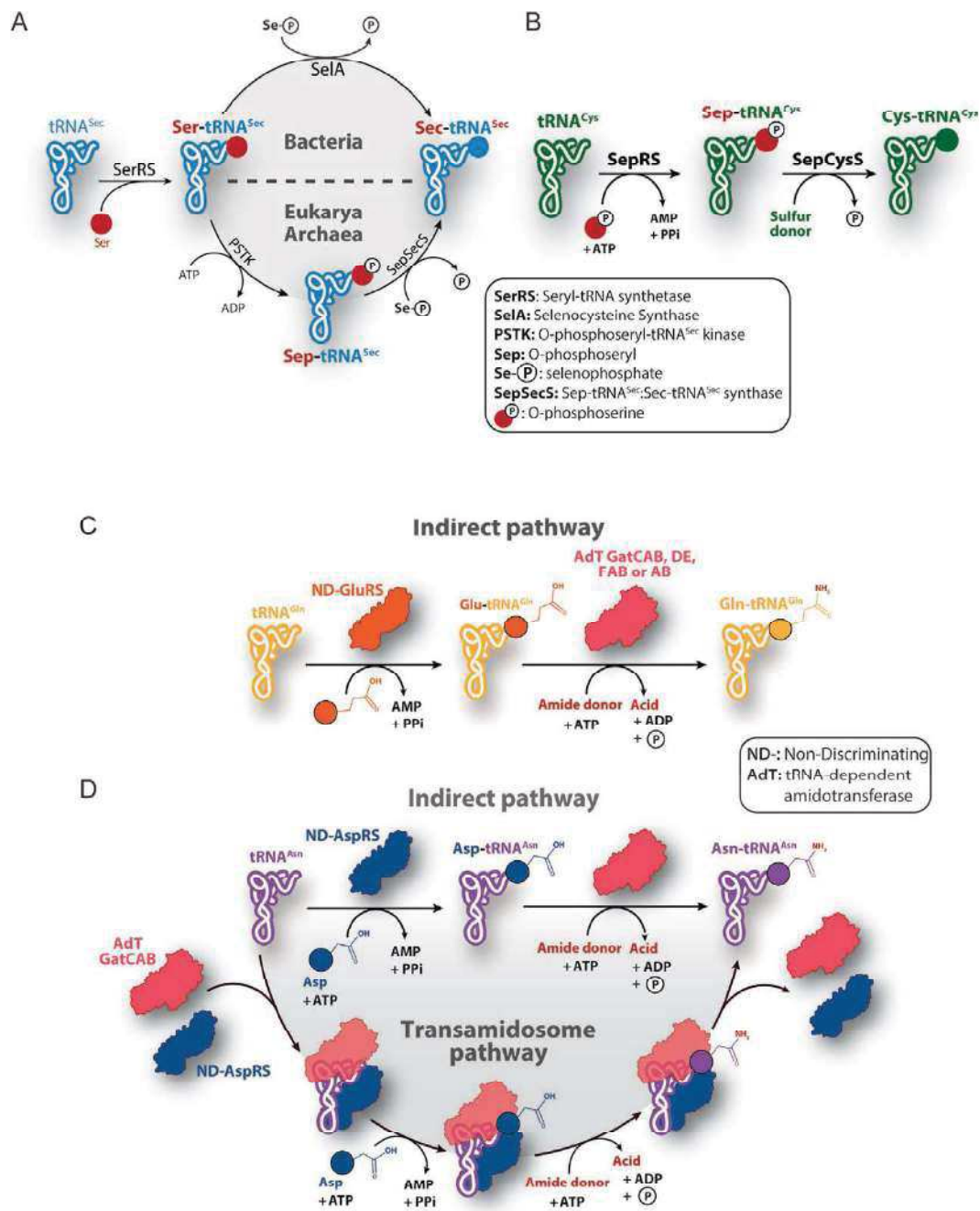
Fig. 2 Non-canonical pathways of aa-tRNA biosynthesis. (A): Biosynthesis of Sec-tRNA^{Sec} using a post-charging conversion of Sec by a two-step pathway in bacteria (upper panel) and a three-step pathway in eukaryotes and archaea (lower panel); (B) Two-step biosynthesis of Cys-tRNA^{Cys} in archaea lacking CysRS. (C) Two-step transamidation pathway of Gln-tRNA^{Gln} synthesis used by bacteria, archaea, mitochondria and chloroplasts. GatCAB AdT: Glutamyl-tRNA^{Gln} amidotransferase used by bacteria, most eukaryotic organelles; GatDE: Glutamyl-tRNA^{Gln} amidotransferase used by archaea; GatFAB AdT: Glutamyl-tRNA^{Gln} amidotransferase of yeast mitochondria; GatAB: Glutamyl-tRNA^{Gln} amidotransferase used by apicoplast. (D) Two-step transamidation pathway or transamidosome-mediated route of Asn-tRNA^{Asn} synthesis used by bacteria, archaea deprived of AsnRS or of asparagine synthetase. The amide donor is either Gln or Asn and is deaminated to form Glu or Asp (acid) during transamidation, respectively. *Panel B: adapted from J. Yuan, S. Palioura, J.C. Salazar, D. Su, P. O'Donoghue, M.J. Hohn, A.M. Cardoso, W.B. Whitman, D. Söll, RNA-dependent conversion of phosphoserine forms selenocysteine in eukaryotes and archaea, Proc. Natl. Acad. Sci. U. S. A. 103 (2006) 18923–18927.*

2.1.1 The 21st proteinogenic aa: Selenocysteine (Sec)

Selenocysteine incorporation has been discovered in 1986 both in mammals and bacteria [15,16]. Its incorporation into proteins depends on an in-frame UGA "opal" STOP codon, which is read through by ribosomes. Sec residues are found in the active sites of selenoproteins (25 genes in mammals, but none in fungi and higher plants). This non-ubiquitous proteinogenic aa has a higher nucleophilic reactivity than cysteine (Cys), thus facilitating selenoproteins in performing enhanced redox reactions and maintain redox homeostasis [17]. Sec is generated *via* two consecutive steps [18] (Fig. 2A) by tRNA-dependent modification of a Ser precursor attached to the opal suppressor tRNA^{Sec} [19]. Indeed, because tRNA^{Sec} and tRNA^{Ser} share the same tRNA identity elements, tRNA^{Sec} can be recognized by the seryl-tRNA synthetase (SerRS) and charged with Ser to form Ser-tRNA^{Sec} [20]. However, an additional base pair in the acceptor stem of tRNA^{Sec}—in comparison to all known tRNAs—prevents the recognition of the misacylated Ser-tRNA^{Sec} by the elongation factor thermo-unstable (EF-Tu), thus precluding misincorporation of Ser into proteins [21–23]. After serylation of tRNA^{Sec} by SerRS, the Ser residue is either (i) directly selenylated by SelA to form Sec-tRNA^{Sec} in bacteria [19], or (ii) phosphorylated by *O*-phosphoseryl-tRNA-kinase (PSTK) to form *O*-phosphoseryl-tRNA^{Sec} (Sep-tRNA^{Sec}), the latter activated aa being subsequently selenylated in a tRNA-dependent manner by the SepSecS enzyme in eukaryotes and archaea [24]. Both SelA and SepSecS are pyridoxal-5′–phosphate (PLP)-dependent enzymes and use selenophosphate as a selenium donor (Fig. 2A). Selenocysteinyl-tRNA^{Sec} is then transported to translating ribosomes by specific elongation factors: SelB in bacteria [25] and the eEFSec•SBP2 complex in eukaryotes [26,27]. Finally, incorporation of Sec requires pausing of the ribosomes at UGA "Sec" codons, which requires a *cis*-acting stem loop structure, called SElenoCysteine Insertion Sequence or SECIS, located downstream of the "Sec" UGA codons of selenoprotein mRNAs. Note that SECIS elements differ in length and structure between bacteria, archaea and eukaryotes [28–32].

2.1.2 The 22nd proteinogenic aa: Pyrrolysine (Pyl)

Pyrrolysine is a modified lysine with a 4-methylpyrroline-5-carboxylate group linked by an amide to the ε-amino group (ε-N). It was first discovered in 2002 in methanogenic archaea and later in several bacteria [33,34]. In methanogenic archaea, all genes encoding methylamine methyltransferases

(methane-generating enzymes) contain an in-frame UAG "amber" STOP codon that is translated into a pyrrolysyl residue. As for Sec, Pyl active site residues appear to be crucial for the activity of enzymes involved in methanogenesis [35]. Pyrrolysyl-tRNA^{Pyl} is synthesized by direct pyrrolysylation of an amber-suppressor tRNA^{Pyl} by the class IIc PylRS [36]. Pyl incorporation has become the first known example to date of direct aminoacylation of a tRNA with a non-standard proteinogenic aa. The structure of tRNA^{Pyl} differs from the classical tRNA structure because it displays for example a D- and TΨC-loop without their conserved representative residues [37]. Contrary to Sec-tRNA^{Sec} and its *trans*-specific factors, Pyl-tRNA^{Pyl} is transported to the A-site of the ribosome by the standard elongation factor EF-Tu [38]. In addition, in some cases the mRNA sequence context seems important for Pyl insertion, and a specific stem loop called PYrroLysyl Insertion Sequence or PYLIS has sometimes, but not always, been found directly next to the "amber" codon on mRNAs encoding for methylamine methyltransferases [39].

2.2 tRNA-dependent pathways of amino acid biosynthesis

Selenocysteine is not the only aa that requires multiple steps to be incorporated into proteins. In numerous organisms, analogous indirect pathways are also needed for the incorporation of standard aa into proteins. In those cases, the biosynthesis of the proteinogenic aa is tRNA-dependent and linked to the production of the corresponding cognate aa-tRNA.

For the majority of eukaryotes and very few bacteria, the 20 different types of standard aa-tRNAs are produced by a full and unique set of 20 different aaRSs. But in the majority of bacteria and all archaea, one or more aaRS genes is missing, suggesting that the aminoacylation of corresponding orphan tRNAs is performed by a non-canonical route. The organism that best illustrates missing aaRSs is the hyperthermophilic methanogenic archaea *Methanocaldococcus jannaschii*, whose genome was sequenced in 1996 and that lacks four expected aaRS genes: LysRS, CysRS, AsnRS and GlnRS [40]. It was shown in this archaeon that the lack of CysRS is compensated by a tRNA^{Cys}-dependent two-step pathway (Fig. 2B) similar to that of Sec-tRNA^{Sec} formation in bacteria. In this pathway, tRNA^{Cys} is first mischarged by a dedicated *O*-phosphoseryl-tRNA synthetase (SepRS) with Sep, before tRNA-dependent conversion of the Sep moiety into Cys by the PLP-dependent SepCysS enzyme that ressembles SepSecS [41].

AsnRS and especially GlnRS are also often missing in prokaryotes and in organelles [42]. All archaea and the majority of bacteria lack GlnRS, whereas AsnRS can be found in most bacteria and half of archaea. While all organelles do possess a dedicated AsnRS, an organellar GlnRS is never found, except in some protozoans [43]. When AsnRS and/or GlnRS is/are absent, direct tRNA charging with the two respective cognate aa—Asn and Gln—is compensated for by an indirect route called the transamidation pathway. It is a two-step pathway in which the metabolic precursors of Gln and Asn, respectively, Glu and Asp, are first attached onto the non-cognate tRNA^{Gln} and tRNA^{Asn} by ND-GluRS or ND-AspRS [10,44] (Fig. 2C). Once released from ND-aaRSs, the mischarged Glu- or Asp-tRNAs are transferred to tRNA-dependent amidotransferases (AdTs). AdTs first ATP-dependently activate the γ- or β-carboxyl group of the misacyled Glu- and Asp-tRNAs by phosphorylation, the activated side chains then being amidated, using an amido group donor, to form Gln-tRNA^{Gln} or Asn-tRNA^{Asn} [45]. All AdTs, regardless of their origins or types, usually use the γ-amide of a free Gln, with the release of Glu, to produce this amido group [46–48]. AdTs are complexes that always possess an amidase subunit to generate the amido group necessary for the amidation reaction, and a subunit that binds the misacylated aa-tRNA substrates and catalyzes the activation of the carboxyl group of the mischarged aa before amidation. The amido donor travels from one subunit to the other, enabling amidation of the misacylated tRNA, a reaction termed "transamidation." Accessory proteins also participate in the formation of the complex.

To date, four types of tRNA-dependent AdTs are known: the hetero-trimeric GatCAB and GatFAB and the heterodimeric GatDE and GatAB ("Gat" for glutamyl-tRNA^{Gln} amidotransferase). The GatCAB AdT (A: amidase, B: aa-tRNA binding, COOH activation and transamidation subunit, C: accessory chaperone) usually is a bispecific Glu/Asp-AdT that can generate Gln-tRNA^{Gln} and Asn-tRNA^{Asn}, such as in bacteria. In archaea GatCAB is a specific Asp-AdT [49]. The heterodimeric GatDE (E: amidase subunit, D: aa-tRNA binding, COOH activation and trans-amidation subunit) is an archaea-specific Glu-AdT [48] that only produces Gln-tRNA^{Gln}. In most eukaryotic organelles, such as mitochondria and chloroplasts, an organellar AdT is also required, and it is of the GatCAB-type. It functions as a Glu-AdT that synthesizes organellar Gln-tRNA^{Gln} in vivo [50,51]. Note that in plants, there is only a single organellar GatCAB AdT that is dually-targeted to mitochondria and chloroplasts. Of note, in mitochondria of the yeast *Saccharomyces cerevisiae*, formation of

the mitochondrial Gln-tRNA^{Gln} pool relies on a heterotrimeric GatFAB that differs from the homologous bacterial GatCAB by the presence of a fungi-specific GatF subunit that replaces structurally GatC. Recently, a heterodimeric GatAB AdT lacking a "C" subunit was found in the apicoplast of the human parasite *Plasmodium falciparum* to function as a Glu-AdT [52].

All organisms using an AdT to generate Gln-tRNA^{Gln} or Asn-tRNA^{Asn} or both also possess ND-GluRS and/or ND-AspRS that, in addition to regular Glu-tRNA^{Glu} and Asp-tRNA^{Asp}, respectively, provide the misacylated Glu-tRNA^{Gln} and Asp-tRNA^{Asn} [10,44]. Some organisms such as *Helicobacter pylori*, possess in addition to regular "discriminating" GluRS, a dedicated supernumerary tRNA^{Gln}-mischarging GluRS2 [11,53]. In organelles, the mitochondrial GluRS usually is the ND-GluRS that participates in the organellar transamidation pathway [51]. In plants, there is a dual-targeted ND-GluRS that participates in the chloroplast and mitochondrial transamidation pathways [50]. The yeast *S. cerevisiae* is however an exception, because it is the cytosolic GluRS that canonically produces the cytoplasmic Glu-tRNA^{Glu} pool which is imported into mitochondria, to specifically mischarge the mitochondrial tRNA^{Gln}. The *bona fide* mitochondrial GluRS only aminoacylates the mitochondrial tRNA^{Glu} [43,54].

Organisms that use the transamidation pathway to generate amidated aa-tRNAs have an adapted EF-Tu that has been shown to lack significant binding capacity for the misacylated Glu-tRNA^{Gln} and Asp-tRNA^{Asn} intermediates, thereby preventing misincorporation of Glu and Asp at Gln and Asn codons [13,54,55]. Another way to generate amidated aa-tRNAs without challenging the genetic code with the mischarged intermediates is the formation of so-called transamidosomes. These complexes are formed by binding of the ND-aaRS to the AdT in a tRNA-dependent manner. In the transamidosomes that have been described to date, the misacylated Asp-tRNA^{Asn} or Glu-tRNA^{Gln} generated by the complexed ND-AspRS or -GluRS are channeled to the AdT active site, without being released, and transamidated to release only the final amidated forms from the particle [56]. Bacterial (ND-AspRS•tRNA^{Asn}•GatCAB, Fig. 2D) and archaeal (ND-GluRS•tRNA^{Gln}•GatDE; [55]) transamidosomes have been characterized. The stoichiometry of their components (tRNA, ND-aaRS and AdT) varies as well as their stability and catalytic mechanism. The transamidosome of *Thermus thermophilus* is composed of 2 dimeric ND-AspRSs (four enzymes), four tRNA^{Asn} and 2 GatCAB AdTs (two enzymes); 2 tRNA^{Asn} molecules are substrates and two others are scaffolding

components that ensure the stability of the ribonucleoprotein particle throughout catalysis [14]. In *H. pylori*, only transient Glu- or Asp-transamidosomes have been identified [57,58].

While these four indirect pathways are compensatory routes for the synthesis of a given aa-tRNA when the cognate aaRS is absent, for two of them, Sec and Asn, they are (Sec) or can sometimes be (Asn) the sole metabolic pathway for the synthesis of the aa, which is therefore strictly tRNA-dependent [44].

3. aa-tRNA-dependent aminoacylation of lipids and cell-wall synthesis

3.1 Multiple peptide resistance factor (MprF)

In the early 60s, Macfarlane reported the presence of *O*-L-lysyl and *O*-L-alanyl esters of phosphatidylglycerol (PG) in *Clostridium welchii* and in *Staphylococcus aureus* [59]. However, that the enzymatic synthesis of lysyl-PG in *S. aureus* involves the transfer of the lysyl moiety from Lys-tRNA^{Lys} onto PG was not demonstrated until 1966 [9]. Over the last decades, a large number of studies detected aminoacylated lipids in several bacterial species, and showed that Lys-tRNA^{Lys} and Ala-tRNA^{Ala} are usually the aa donors for lipid aminoacylation and that PG, diacylglycerol or cardiolipin are the aa acceptors. Arg-PG and could also be detected but to a lesser extent [60]. In 2001, Peschel et al. demonstrated in *S. aureus* that the *mprF* gene encodes the lysyl-phosphatydyl glycerol synthase (LysPGS) responsible for LysPG synthesis [61]. They also showed that the cytoplasmic domain of LysPGS is responsible for the transfer of L-Lys from Lys-tRNA^{Lys} onto PG at the inner leaflet of the plasma membrane, whereas the N-terminal integral membrane domain flips the newly synthesized LysPG to the outer membrane leaflet [62]. The addition of positively- charged or neutral aa to PG by aminoacyl-phosphatidyl glycerol synthases (aaPGSs) reverses or neutralizes the net negative charge of the cell envelope [63], thereby decreasing the susceptibility of bacteria to positively-charged antimicrobial agents. Furthermore, aaPGS-dependent membrane remodeling participates in the adaptation of bacteria to environmental changes (pH, osmolarity, temperature), increases immune escape [64,65] and enhances virulence of *S. aureus* and *Listeria monocytogenes* upon infection of epithelial cells and macrophages in mice [66,67].

Some aaPGSs are specific for a single aa-tRNA (*e.g.,* Lys- or Ala-tRNA), and others exhibit broader substrate specificity and can utilize up to three

different aa-tRNAs as aa donors (*e.g.,* Lys-, Ala- or Arg-tRNA) [68,69]. It has been shown that the acceptor-stem of the tRNA and in particular its fifth base pair and the Cα of the corresponding aa are essential elements for the recognition of Ala-tRNA^{Ala} by the AlaPGS [70,71]. Structural analysis showed that the catalytic domain of AlaPGS from *Pseudomonas aeruginosa* and LysPGS from *Bacillus licheniformis* harbor a so-called dupli-GNAT (GCN5 *N*-acetyltransferase) domain, where the two GNATs are separated by a positively-charged alpha helix [72]. Such similar structures have also been described for other aminoacyl-tRNA transferases (AAT), including the Fem and L/F transferases described below. Site-directed mutagenesis based on the structures of aaPGSs, demonstrated that this positively- charged helix is essential for aa-tRNA recruitment. However, it is still not understood how bacteria regulate the balance between the usage of the aa-tRNA for protein synthesis *versus* lipid aminoacylation. Interestingly, *Mycobacterium* spp. encode a LysPGS (LysX) that is fused directly to a C-terminal lysyl-tRNA synthetase (LysRS) that is essential for the LysPG synthesis activity. This suggests that, in *Mycobacterium* spp., a dedicated pool of Lys-tRNA^{Lys} is synthesized and used by LysPGS, to produce LysPGs and that this pool escapes protein synthesis [73].
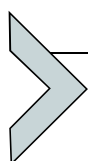
4. FemXAB

The peptidoglycan sacculus (murein) is a unique and essential structural element of bacterial cell walls found outside of the plasma membrane. It contributes to the maintenance of cell shape to preserve the cell integrity, and serves as a scaffold for the anchoring of other cell envelope components such as proteins and teichoic acids in Gram-positive bacteria.

Peptidoglycan synthesis is achieved by a succession of enzymatic events, that start with the formation of the well-known lipid II. This lipid harbors a so-called stem-peptide composed of the L-Ala$_1$-D-Glu$_2$-X$_3$-D-Ala$_4$-D-Ala$_5$ pentapeptide where X$_3$ is variable among species (L-Lys, δ-L-ornithine or ω-L, L-diaminopimelic acid) (Fig. 3A). At this stage, Fem transferases, which are non-ribosomal peptidyl transferases, use aa-tRNA as aa donors to form an "interpeptide bridge" that, in a later step, serves to cross-link the X$_3$ of the newly-synthesized peptidoglycan subunit (Lipid II released from its undecaprenyl-diphosphate) to the D-Ala$_4$ of an adjacent peptidoglycan stem-peptide [74,75]. The formation of the stem-peptide is tRNA-independent, whereas Fem ligase-mediated formation of the interpeptide bridge was shown to be tRNA-dependent.
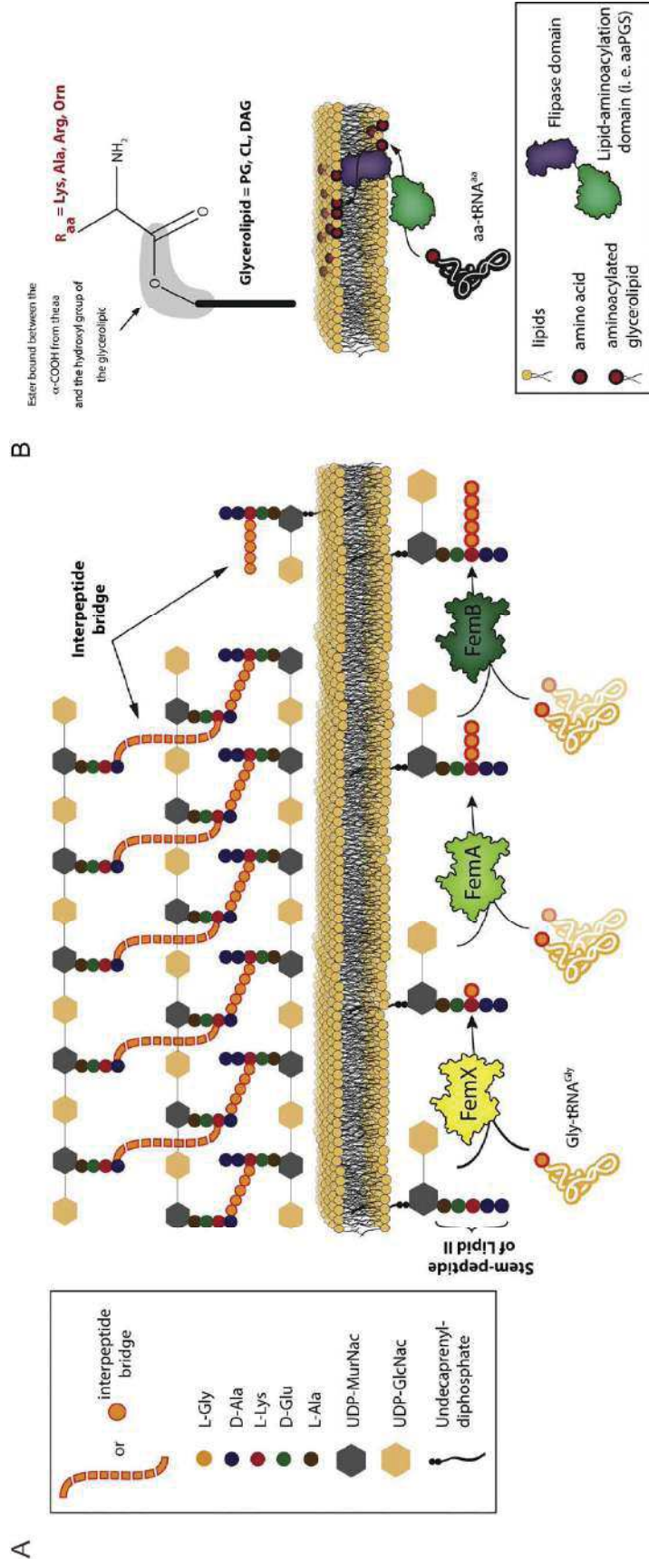
Fig. 3 Aminoacyl-tRNA-dependent cell wall remodeling in prokaryotes. (A) In *S. aureus*, the stem peptide composed of L-Ala$_1$-D-Glu$_2$-Lys$_3$-D-Ala$_4$-D-Ala$_5$ is added onto Lipid I to form the well-characterized Lipid II. Aminoacyl-tRNA transferases (ATT) belonging to the Fem ligases family then successively add a variable number of aa to form the interpeptide bridge. For example, in *S. aureus* FemX adds a single glycine, FemA adds Gly2 and Gly3 and finally, FemB adds Gly4 and Gly5 onto the L-Lys of the stem-peptide. The resulting peptidoglycan subunit is then flipped out to the outer cytoplasmic-membrane leaflet, and the link to the growing peptidoglycan saccule is made by PBP transpeptidases. MurNac: N-Acetylmuramic acid, GlcNac: N-Acetylglucosamine. (B) MprF and MprF-like proteins contain a C-terminal ATT domain (green) that reroutes aa-tRNA^{aa} from the translational machinery and transfers the aa moiety onto glycerolipids, and a N-terminal flipase domain (purple) that exposes the aminoacylated glycerolipid to the outer membrane leaflet. As schematized in the upper panel, different aa/lipid combinations were documented in prokaryotes as reviewed by Slavetinsky et al. [60]. PG: phosphatidylglycerol, DAG: diacylglycerol, CL: cardiolipin, R$_{aa}$: lateral chain of the indicated aa.

In *S. aureus*, 3 Fem ligases are required. FemX adds the first glycine residue (Gly_1) onto the stem-peptide at the ε–NH_2 group of L–Lys_3 [76,77], while FemA and FemB are essential for the addition of $Gly_{2,3}$ and $Gly_{4,5}$, respectively. These proteins are highly specific with respect to the position of the Gly residues that they attach [78]. Among the five $tRNA^{Gly}$ isoacceptors encoded by *S. aureus*, three of them have a weak binding capacity to EF–Tu, due to the replacement of G_{49}–U_{65} and G_{51}–C_{63} by A_{49}–U_{65} and A_{51}–U_{63} base pairs in the T–loop [79,80]. Furthermore, Rohrer et al. showed that the three $tRNA^{Gly}$ capable of escaping the translational machinery have G_{18} and G_{19} replaced by UU or CU [81]. The Fem factors are known to be essential for methicillin resistance, and are found in both resistant and susceptible *S. aureus* strains. The phenotypes of the FemAB null mutants of *S. aureus* showed a reduction of cell wall Gly content and strong morphological aberrations during cell division and separation [76]. The inactivation of the *femAB* operon reduces the interpeptide to a monoglycine, inducing a poorly crosslinked peptidoglycan. Decreased growth rate and hypersusceptibility to antibiotics such as methicillin were observed in *femAB* deleted strains, making FemAB a potential target to restore β–lactam susceptibility in methicillin-resistant *S. aureus* (MRSA) [82].

Staphylococcus simulans, *S. epidermidis* and *S. capitis* incorporate a variable ratio of L–Ser/Gly residues (but also L–Ala for *S. epidermidis*) into the interpeptide bridges to escape pentaglycine endopeptidase-mediated degradation. To our knowledge, $tRNA^{Ser}$ modifications are not involved in the distribution of Ser–$tRNA^{Ser}$ between peptidoglycan cross-linking and translation. Thus, bacteria may adapt the ratio of Ser–$tRNA^{Ser}$ used for each mechanism according to environmental conditions. *S. epidermis* encodes at least two $tRNA^{Gly}$ isoacceptors employed exclusively for interpeptide-chain formation [83]. Both contain CC or UU instead of the universal G_{18} and G_{19} di-nucleotide. Furthermore, the supplementary C_{32}–G_{38} base pair in the anticodon loop and, to a lesser extent, the impaired U_{10}–U_{25} base pairs as well as the weak post-transcriptional modification ratio in the D-loop are also considered as crucial to determine the fate of Gly–$tRNA^{Gly}$ isoacceptors.

In *S. pneumoniae*, MurM (homologue of the *S. aureus* FemA) adds L–Ser or L–Ala as the first residue to the L–Lys of the stem peptide [78,84], and MurN then adds L–Ala to form an interpeptide chain composed only of two residues [84].

Finally, *Weissella viridescens* harbors either a L–Ala–L–Ser or a L–Ala–L–Ser–L–Ala interpeptide chain [85]. Villet et al. showed that the C_{71} and C_{72}

from the tRNA^{Ala} are critical nucleotides for recognition by FemX, whereas the G$_3$-U$_{70}$, base pair considered as a strong identity determinant for recognition by AlaRS is dispensable [86]. Because MurM and FemX of *W. viridescens* recognize only two aa-tRNAs [87,88], it has been suggested that these two proteins may be involved in the complex discrimination between protein and peptidoglycan synthesis [89].

In summary, Gly-tRNA^{Gly}, Ala-tRNA^{Ala}, Ser-tRNA^{Ser} but also Thr-tRNA^{Thr} participate in peptidoglycan interpeptide chain formation. For a more detailed review of the interpeptide composition across bacterial species, refer to reports of Dare & Ibba or Schleifer & Kandler [83,90].
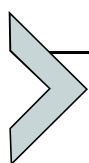
5. aa-tRNA-dependent synthesis of hemes

Only a small subset of the aa produced by the cell are used in protein synthesis, and we have seen that from this small pool some can be deviated to build molecules other than proteins. There are also several other pathways that require non-proteogenic aa and among them, the synthesis of heme necessitates δ-aminolevulinic acid (ALA), a pathway that is tRNA-dependent. ALA can be synthesized either from free glycine and succinyl-CoA (eukaryotes) or glutamate (bacteria and green plants), when the latter is bound to its cognate tRNA^{Glu} (reviewed in [91], Fig. 4).

ALA is the first molecule in the tetrapyrrole synthesis pathway that leads to heme biosynthesis in mammals and chlorophyll in plants. ALA biogenesis in plants and bacteria has been studied for more than four decades, and employs a simple three-step pathway. First, Glu is charged onto tRNA^{Glu} by GluRS [92–94]. Second, tRNA^{Glu}-bound Glu is reduced to glutamate
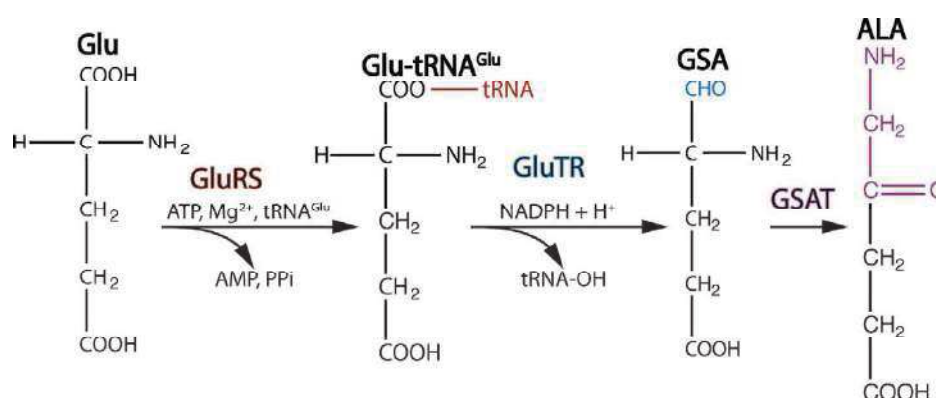
Fig. 4 C5 pathway of ALA formation. Glutamate (Glu) is attached directly onto tRNA^{Glu} by GluRS. Glu is then reduced to glutamate-1 semi-aldehyde (GSA) by glutamyl-tRNA reductase (GluTR) and further converted by glutamate aminomutase (GSAT) to δ-aminolevulinic acid (ALA).

semi-aldehyde (GSA) and detached from tRNA^{Glu} by glutamyl–tRNA reductase (GluTR) [95,96]. Finally, GSA is converted to the final product ALA by GSA aminomutase (GSAT) [97].

The finding that Glu is used to produce ALA in green plants [98,99] preceded the discovery that tRNA^{Glu} is required for ALA production [92–94]. Thus, Glu-tRNA^{Glu} formation is an absolute intermediate in the GSA formation by GluTR, an enzyme that has been shown to form a complex with GluRS [100] and together, both proteins have strict requirements for tRNA^{Glu} [101,102].

In bacteria, GluTR is encoded by the *hemA* gene that is part of the *hemAXCDBL* operon in which *hemX* codes for an integral membrane protein capable of negatively affecting the cellular concentration of *hemA* [103]. GluTR activity is rate-limiting in ALA formation [104] and in plants, it represents an ideal target for designing herbicides [105]. Its activity has been shown to be regulated by acting on the protein stability that is increased in heme limiting conditions in *S. typhimurium* [106]. Later, FLU, another negative regulator of GluTR was identified. Flu is a membrane-bound protein involved in chlorophyll biosynthesis that interacts directly with GluTR but not with GSAT [107,108]. It must be noted that although the levels of GluTR and GSAT control ALA production, they do not control directly chlorophyll synthesis in *Chlamydomonas reinhardtii*. A complex between GSAT and GluTR has been identified and proposed to protect the highly- reactive GSA intermediate [109].

ALA is the universal precursor of tetrapyrroles like hemes, and the latter have been shown to downregulate not only the activity of GluTR but also of GluRS, which is more surprising [110]. In addition, hemes are also capable of inhibiting aminoacylation activity of a Zn^{2+}-deprived form of human tryptophanyl–tRNA synthetase [111]. Moreover, holocytochrome *c* (*e.g.,* heme bound) can interact with tRNA, and this interaction was shown to mediate caspase-mediated apoptosis [112].

An essential GluTR–interacting protein named GluTRB that is localized in the thylakoid membrane, participates in the sub-compartmentalization of GluTR, to separate ALA pools in order to balance production of heme and chlorophyll [113]. The interaction of GluTRBP with GluTR stimulates its activity, but the latter is still inhibited in a heme-dependent concentration [114]. Binding of GluTRBP to GluTR also prevents FLU from inhibiting GluTR, but a ternary complex consisting of GluTR, GluTRBP and FLU can be formed, suggesting a biological role for the ternary complex in the regulation of the plant GluTR [115]. The complexity of this regulation

of GluTR expression/activity is reinforced by the finding that GluTR can be degraded from its N-terminus by the Clp protease, but not when protected by GluTRBP [116].

ALA utilization by bacteria leads to heme, an essential cofactor for *S. aureus* growth and colonization that becomes toxic at high concentrations, thereby underlining the necessity for these organisms to control tightly heme homeostasis [117]. In plants, subplastidial allocation of GluTR in the stroma and in membrane fractions reveals that when membrane-bound, GluTR is less active, and this is the result of the concerted actions of GluTR interacting proteins (FLU, GluTRBP, Clp protease and cpSRP43) [118,119]. Finally, in higher plants there are two isoforms for GluTR: GluTR1 that is expressed predominantly in green tissue, and GluTR2 that is expressed constitutively in all organs. It was recently shown that heme binding to GluTRBP inhibits its interaction with GluTR, thereby making it accessible to Clp protease, which participates in GluTR regulation [120].

Overall, the utilization of Glu-tRNA^{Glu} outside translation represents an intriguing example of how various metabolic pathways are interconnected. Glu-tRNA^{Glu} utilization for ALA production controls heme and chlorophyll biosynthesis, two molecules that are crucial for other cellular events that contribute to the life cycle of various organisms, and whose production seems to be subjected to tight and complex control.
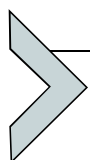
6. aa-tRNA-dependent formation of antibiotics

Peptide-based antibiotics can, at least in part, be synthesized tRNA-dependently, and are an important class of molecules because they provide organisms with defenses to fight against invading microbes, or to help them survive in a given ecological niche [89,121]. There is a group of antibiotics whose composition is based on peptides. There are two ways of synthesizing peptide-based antibiotics that both require tRNA: ribosomally- or non-ribosomally-synthesized peptidic antibiotics [122]. Those that are ribosomally-synthesized include defensins (30–40 aa in length; disrupt membrane integrity) that are a large class of Cys-rich peptide antibiotics whose Cys residues are regionally-specifically oxidized to stabilize the molecule and provide protease resistance. Similarly, lantibiotics are low molecular weight lanthionine-containing cyclic peptides that, like defensins, perturb membrane integrity. This class of molecules belongs to the superfamily of RiPP (ribosomally synthesized peptides that undergo extensive post-translational modifications). They are synthesized as precursors that

consist of an N-terminal leader peptide fused to a C-terminal core peptide containing modifications. Interestingly for some of them, a Glu-tRNA^{Glu} is used by a dehydratase to modify aa residues of the ribosomally-made peptide parts (reviewed in [123]). Aromatic heterocyclic peptide scaffolds derived from Cys, Ser and Thr residues [124] are another large family of ribosomally-derived antibiotics like microcin B17, patellamides and streptolysin S. It is noteworthy that microcins have a broad diversity of chemical structures and modifications, and are widely used as antitumoral and/or antimicrobial drugs [125]. The synthesis of these antibiotic compounds is rather complex and there are tens of genes that are required, and tRNAs are either involved as regulators of this process [122] or as carrier molecules for additional modifications with aa. tRNA-based regulation of antibiotic production is, for example, used by *Streptomyces coelicolor*. In this filamentous bacterium there is a single gene (*bldA*) that encodes the only tRNA^{Leu} capable of decoding the UUA rare Leu codon. The expression of this specific tRNA^{Leu} is very low in fresh cultures, but increases to reach its maximum as cultures get older. The tRNA^{Leu} expression pattern correlates with morphological differentiation and changes in antibiotic production [126]. This suggests a means of limiting ribosomal-mediated antibiotic synthesis in the host to physiologically appropriate circumstances by modulating tRNA availability. A similar mode of regulation has also been proposed for biofilm production, in which Hha proteins decrease biofilm production by repressing transcription of tRNAs decoding rare codons (argU and proL) normally involved in fimbriae production [127].

The second tRNA-dependent mode of synthesizing peptide-based antibiotics are the non-ribosomal antibiotic pathways. These rely on a series of enzymatic reactions that involve at one step an aa-tRNA. For example, valanimycin production involves a gene cluster containing 14 genes in *Streptomyces viridifaciens*, in which the VlmA protein catalyzes the transfer of a seryl residue from Ser-tRNA^{Ser} to the hydroxyl group of isobutylhydroxylamine to produce the O-seryl-isobutylhydroxylamine ester [128]. An intriguing fact concerning valanimycin production is that the Ser-tRNA^{Ser} used in the reaction is produced by a dedicated SerRS, named VlmL, encoded by the *vlmL* gene [129]. Similarly, production of a streptothricin-related antibiotic requires an intermediate, in which an amino sugar is aminoacylated with Gly by a Fem-like enzyme in a tRNA-dependent manner [130]. Overall, the enzymes involved in these types of modifications belong to the class of the aa-tRNA-dependent transferases that were identified over 50 years ago [131–133].

Although aa-tRNAs can be used to remodel several compounds, they can also be substrates for the synthesis of cyclic dipeptide-based antibiotics. They were long thought to be products released prematurely from the ribosome until the discovery of cyclodipeptides synthases [134]. Cyclodipeptides are further subjected to various modifications until the final product is obtained [135]. A strategy employing various enzymes to modify a core scaffold to produce differential tailoring is often used in nature to generate structural diversity. Such small molecule diversity enables easy evolution of new biological functions, and allows fine-tuning of existing ones [135,136]. Cyclodipeptide synthases genes, are often clustered with tailoring enzyme genes, most likely to facilitate the overall regulation of the cyclodipeptide-based compound production (for a review see [123]). Cyclic dipeptides are an interesting class of molecules because they constitute a rather convincing alternative over conventional antibiotics, as exemplified in their role in preventing quorum sensing pathogenesis of uropathogens [137].
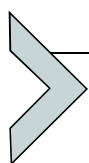
7. aa-tRNA-dependent degradation of proteins

In 1963, the participation of aa–tRNAs in protein degradation was first reported in prokaryotes, in which it was shown that ribosome-deprived extracts were still able to catalyze tRNA-dependent aminoacylation of proteins [138]. In eukaryotes, it was noted 23 years later that specific aa residues found in the N-terminus (N-t) of proteins could decrease dramatically the half-life of the corresponding protein in *S. cerevisiae* [139]. An enzymatic activity able to transfer the aa moiety of an aa-tRNA to the N-t of proteins leading to protein degradation was also identified in eukaryotes [140], and is presently termed the N-end rule pathway [141].

In bacteria, the N-end rule pathway includes three components: an aa-tRNA transferase responsible for the transfer of the aa moiety onto the protein that will be degraded, a N-recognin that binds the aminoacylated protein signaling it to the degradation machinery, the Clp protease complex. In eukaryotes, an additional preliminary step involving deamination of amide aa residues in N-t of the protein is catalyzed by a deamination enzyme. This enables the subsequent recognition by the aa-tRNA transferase, followed by signaling of the protein for degradation by the proteasome [142].

7.1 N-end rule pathway in prokaryotes

In 1963, Kaji et al. identified a protein fraction in *E. coli* that was able to transfer radioactively-labeled Leu onto proteins in the absence of ribosomes [138], thereby describing for the first time the activity of a leucyl-tRNA protein transferase. In 1973, Soffer demonstrated that Leu, Phe, and to a lower extent Met and Trp, can also be transferred onto the N-t residue of α-casein [143]. Later, it was discovered that the nature of the N-t residue of the targeted protein modulates the aa conjugation efficiency [139]. The residues onto which aa are efficiently transferred efficiently include the basic residues Arg, Gln, Lys and Pro, which were thereafter termed destabilizing residues. However, the mechanism linking addition of aa to the N-t of a protein to its degradation was not identified until Tobias et al. showed in 1991 that a bacterial strain lacking the Clp ATP-dependent protease degraded much less efficiently a protein carrying destabilizing residues [144]. This proved that Leu (or Phe) conjugation mediates degradation by recruiting the Clp protease [144]. The gene coding the leucyl−/phenylalanyl-tRNA transferase (L/F transferase) was identified 2 years later [145]. Notably, this gene is located near the gene encoding ClpA, a component of the Clp protease complex, which participates in the N-end rule pathway. In 1995, the gene encoding the protein was cloned, overexpressed and purified, allowing the development of an *in vitro* assay that lead to the characterization of its catalytic mechanism [146]. Since then, the structure of the aa-tRNA transferase was determined in complex with an aa-tRNA analog [147], and the mechanism of the peptide bond formation between the N-t residue and the aa transferred by the aa-tRNA transferase has been elucidated [148].

In sum, protein aminoacylation in prokaryotes is mediated by L/F transferases that modify a residue in N-t (preferentially recognizing a basic residue), which enables the recognition of the protein by ClpS, which in turn signals delivery of the proteins to the Clp protease complex for degradation. Note that ClpS belongs to the family of N-recognins, which are proteins that bind to aminoacylated proteins and enable their delivery to the degradation machinery (Fig. 5C).

7.2 N-end rule pathway in eukaryotes

In *S. cerevisiae* and higher eukaryotes, proteins are not aminoacylated directly to induce their degradation (Fig. 5B). Instead, a first step of deamidation converts the amide aa Asn and Gln to Asp and Glu. These deamination
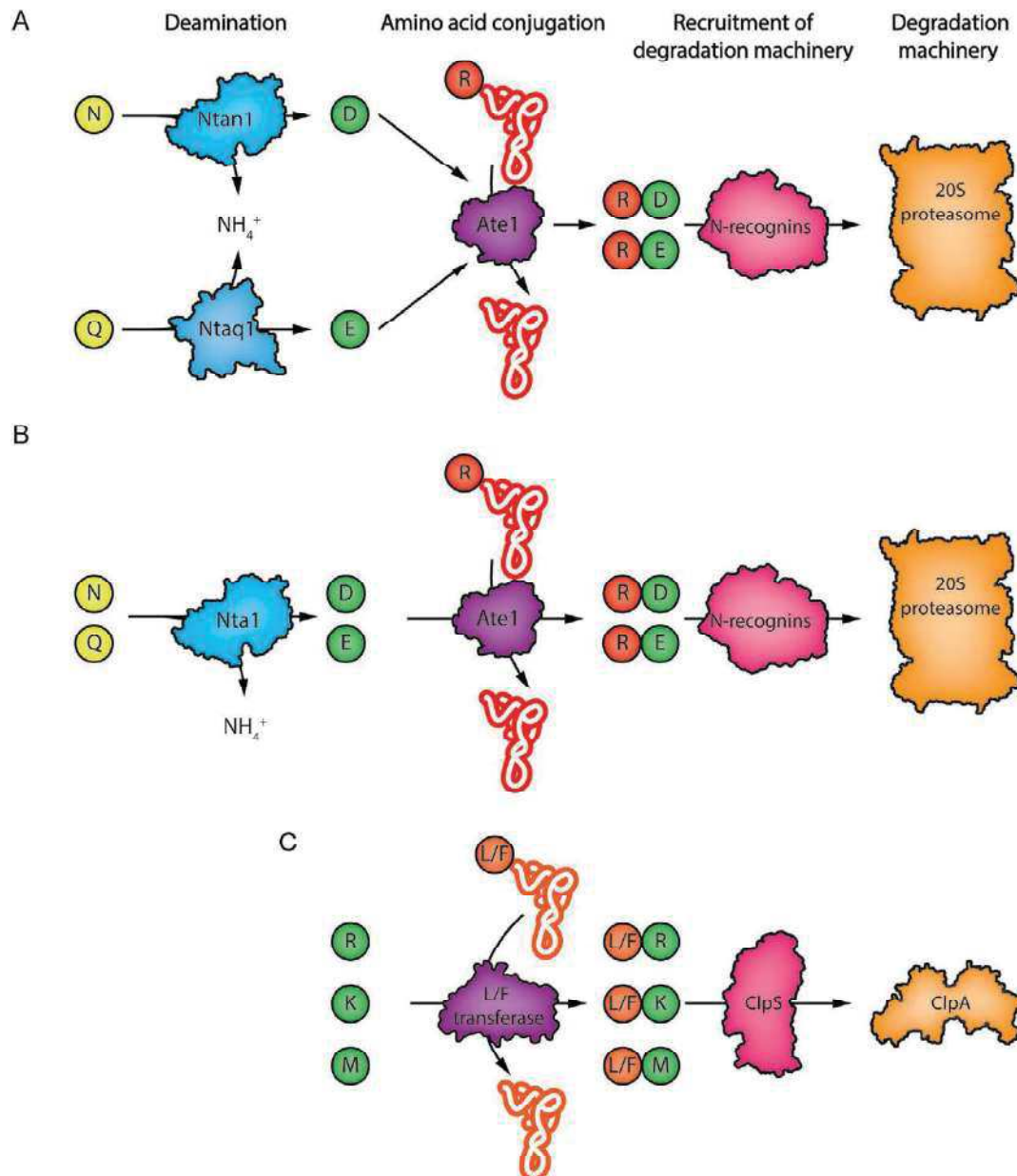
Fig. 5 Overview of the N-end rule pathway leading to protein degradation. (A) In mammals, protein degradation starts by the deamination of Gln (Q) or Asn (N) in first position at the N-ter of the protein. This leads to the arginylation of the N-ter of by Ate1, and subsequently to the binding of the protein by a N-recognin, which delivers it to the proteasome. (B) In fungi, the pathway is very similar, the sole difference being that the deamination step is performed by one enzyme both for Gln and Asn. (C) In prokaryotes there is no deamination step: Arg (R), Lys (K) and Met (M) are recognized by a leucyl-phenylalanine-tRNA transferase (L/F transferase) which transfers either Leu (L) or Phe (P) on the first amino acid in the N-ter of the protein. This so-called destabilizing residue is recognized by ClpS, which delivers the protein to the ClpA protease for degradation. *Panel C: adapted from T. Tasaki, S.M. Sriram, K.S. Park, Y.T. Kwon, The N-end rule pathway, Annu. Rev. Biochem. 81 (2012) 261–289.*

reactions are performed by Nta1 in fungi [149]. In mammals, deamination of Gln and Asn is performed by Ntaq1 and Ntan1, respectively [141,150] (Fig. 5A). After deamination, these residues can be aminoacylated by a unique arginyl-tRNA transferase, Ate1, both in *S. cerevisiae* and mammals [151,152]. Upon arginylation, the protein can be ubiquitinylated, a step mediated by a N–recognin. This leads finally to the degradation of the protein by the 26S proteasome.

This N–end rule mechanism is the only noncanonical pathway in which proteinogenic aa–tRNAs are used for protein degradation rather than for their synthesis. In this case, aa–tRNAs are diverted not only from their anabolic use, but become essential components of the protein catabolic pathway.
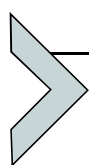
8. Concluding remarks

This chapter has been dedicated. Mainly to the fascinating diversity of the nontranslational mechanisms and processes that employ the aa moiety of an aa-tRNA. The first descriptions of these noncanonical usages of aa-tRNAs (Leu-tRNA^{Leu} to modify proteins and of Lys-tRNA^{Lys} in *O*-lysyl-phosphatidylglycerol synthesis) coincided with the characterization of the conventional aminoacylation reaction for protein synthesis [5–7,9]. Yet, these nontranslational usages are generally less well known than the primary historical role of aa–tRNA in protein synthesis, despite being equally essential for the cell. There is no doubt that new processes and functions will be unraveled in the future, and will enrich the existing functional repertoire of aa–tRNAs. As an example, the arginyltransferase Ate1, which transfers the arginyl moiety from Arg-tRNA^{Arg} to the N-terminus of proteins targeted for degradation by the N–end rule pathway, has recently also been shown in mammalian cells and in *Dictyostelium discoideum* to be implicated in the aminoacylation of internal residues of β–actin [153,154]. Interestingly the steady-state level of arginylated β–actin is relatively low but tends to increase in migratory cells, demonstrating that this post-translational aminoacylation is actively regulated in cells [153]. Arginylation of protein is not restricted to β–actin, because an increasing number of eukaryotic proteins appear to undergo Ate1–mediated arginylation of internal Asp and Glu residues; these arginylated proteins participate in myriad cellular processes ranging from embryogenesis, to cell migration and protein homeostasis [155].

There are however many unanswered issues when considering the non-translational processes that rely on the use of aa-tRNAs. One of the most important is how aa-tRNAs escape the translational machinery, and how cells achieve a balance between the use of the same aa-tRNA species for protein synthesis and/or for other cellular processes? In fact, though the various non-canonical usages of aa-tRNAs we describe in this chapter have been studied actively, it remains largely unknown how aa-tRNAs are diverted from their primary and canonical usage. In some cases, organisms have found a strategy that eliminates the competition between translation and nontranslational usages of an aa-tRNA by producing a dedicated pool of aa-tRNAs for a given non-canonical process. For example, *S. epidermis* encodes two tRNA^{Gly} isoacceptors dedicated exclusively to interpeptide-chain formation. Moreover, sometimes organisms have even acquired or evolved a supernumerary aaRS dedicated to the synthesis of specific aa-tRNAs (*e.g.,* LysRS fused to LysPGS in *Mycobacterium* for LysPG synthesis). Dedicating a given pool of tRNAs to nontranslational processes could also be accomplished by post-transcriptionally modifying tRNA nucleotides. Indeed, tRNAs undergo a series of post-transcriptional modifications, and some of them could potentially also serve to assign a given tRNA pool to a given nontranslational function. Finally, it was recently shown that, in eukaryotes, a single aaRSs can be localized in two or more subcellular compartments, and that these spatially-distinguished isoforms (called echoforms) can serve different roles, including the noncanonical roles that rely on the synthesis of a compartment-specific aa-tRNA [156].

Acknowledgments

References

[1] M. Ibba, D. Söll, Aminoacyl-tRNA synthesis, Annu. Rev. Biochem. 69 (2000) 617–650.
[2] N. Kresge, R.D. Simoni, R.L. Hill, The discovery of tRNA by Paul C .Zamecnik a soluble ribonucleic acid intermediate in protein synthesis, J. Biol. Chem. 280 (2005) 37–40.

[3] M.B. Hoagland, E.B. Keller, P.C. Zamecnik, Enzymatic carboxyl activation of amino acids, J. Biol. Chem. 218 (1956) 345–358.

[4] J.A. DeMoss, S.M. Genuth, G.D. Novelli, The enzymatic activation of amino acids via their acyl–adenylate derivatives, Proc. Natl. Acad. Sci. 42 (1956) 325–332.

[5] P. Berg, Acyl adenylates; an enzymatic mechanism of acetate activation, J. Biol. Chem. 222 (1956) 991–1013.

[6] P. Berg, Acyl adenylates; the interaction of adenosine triphosphate and L-methionine, J. Biol. Chem. 222 (1956) 1025–1034.

[7] M.B. Hoagland, M.L. Stephenson, J.F. Scott, L.I. Hecht, P.C. Zamecnik, A soluble ribonucleic acid intermediate in protein synthesis, J. Biol. Chem. 231 (1958) 241–257.

[8] M. Wilcox, M. Nirenberg, Transfer RNA as a cofactor coupling amino acid synthesis with that of protein, Proc. Natl. Acad. Sci. U. S. A. 61 (1968) 229–236.

[9] W.J. Lennarz, J.A. Nesbitt, J. Reiss, The participation of sRNA in the enzymatic synthesis of O-L-lysyl phosphatidylgylcerol in *Staphylococcus aureus*, Proc. Natl. Acad. Sci. U. S. A. 55 (1966) 934–941.

[10] J. Lapointe, L. Duplain, M. Proulx, A single glutamyl-tRNA synthetase aminoacylates tRNA(Glu) and tRNA(Gln) in Bacillus subtilis and efficiently misacylates *Escherichia coli* tRNA1(Gln) in vitro, J. Bacteriol. 165 (1986) 88–93.

[11] H.D. Becker, H. Roy, L. Moulinier, M.H. Mazauric, G. Keith, D. Kern, Thermus thermophilus contains an eubacterial and an archaebacterial aspartyl-tRNA synthetase, Biochemistry 39 (2000) 3216–3230.

[12] J. Yuan, K. Sheppard, D. Söll, Amino acid modifications on tRNA, Acta Biochim. Biophys. Sin. Shanghai 40 (2008) 539–553.

[13] H. Roy, H.D. Becker, M.H. Mazauric, D. Kern, Structural elements defining elongation factor Tu mediated suppression of codon ambiguity, Nucleic Acids Res. 35 (2007) 3420–3430.

[14] M. Blaise, M. Bailly, M. Frechin, M.A. Behrens, F. Fischer, C.L.P. Oliveira, H.D. Becker, J.S. Pedersen, S. Thirup, D. Kern, Crystal structure of a transfer-ribonucleoprotein particle that promotes asparagine formation, EMBO J. 29 (2010) 3118–3129.

[15] I. Chambers, J. Frampton, P. Goldfarb, N. Affara, W. McBain, P.R. Harrison, The structure of the mouse glutathione peroxidase gene: the selenocysteine in the active site is encoded by the 'termination' codon, TGA, EMBO J. 5 (1986) 1221–1227.

[16] F. Zinoni, A. Birkmann, T.C. Stadtman, A. Bock, Nucleotide sequence and expression of the selenocysteine-containing polypeptide of formate dehydrogenase (formate-hydrogen-lyase-linked) from *Escherichia coli*, Proc. Natl. Acad. Sci. U. S. A. 83 (1986) 4650–4654.

[17] E.S.J. Arnér, Selenoproteins-what unique properties can arise with selenocysteine in place of cysteine? Exp. Cell Res. 316 (2010) 1296–1303.

[18] B.J. Lee, P.J. Worland, J.N. Davis, T.C. Stadtman, D.L. Hatfield, Identification of a selenocysteyl-tRNA(Ser) in mammalian cells that recognizes the nonsense codon, UGA, J. Biol. Chem. 264 (1989) 9724–9727.

[19] W. Leinfelder, E. Zehelein, M.A. Mandrand-Berthelot, A. Böck, Gene for a novel tRNA species that accepts L-serine and cotranslationally inserts selenocysteine, Nature 331 (1988) 723–725.

[20] K.M. Holman, A.K. Puppala, J.W. Lee, L.E.E. Hyun, M. Simonović, Insights into substrate promiscuity of human seryl-tRNA synthetase, RNA 23 (2017) 1685–1699.

[21] Y. Itoh, S. Chiba, S.I. Sekine, S. Yokoyama, Crystal structure of human selenocysteine tRNA, Nucleic Acids Res. 37 (2009) 6259–6268.

[22] C. Baron, E. Westhof, A. Böck, R. Giegé, Solution structure of selenocysteine-inserting tRNA(Sec) from *Escherichia coli*. Comparison with canonical tRNA(Ser), J. Mol. Biol. 231 (1993) 274–292.

[23] C. Sturchler, E. Westhof, P. Carbon, A. Krol, Unique secondary and tertiary structural features of the eucaryotic selenocysteine tRNA(Sec), Nucleic Acids Res. 21 (1993) 1073–1079.

[24] J. Yuan, S. Palioura, J.C. Salazar, D. Su, P. O'Donoghue, M.J. Hohn, A.M. Cardoso, W.B. Whitman, D. Söll, RNA-dependent conversion of phosphoserine forms selenocysteine in eukaryotes and archaea, Proc. Natl. Acad. Sci. U. S. A. 103 (2006) 18923–18927.

[25] K. Forchhammer, W. Leinfelder, A. Böck, Identification of a novel translation factor necessary for the incorporation of selenocysteine into protein, Nature 342 (1989) 453–456.

[26] P.R. Copeland, J.E. Fletcher, B.A. Carlson, D.L. Hatfield, D.M. Driscoll, A novel RNA binding protein, SBP2, is required for the translation of mammalian selenoprotein mRNAs, EMBO J. 19 (2000) 306–314.

[27] D. Fagegaltier, N. Hubert, K. Yamada, T. Mizutani, P. Carbon, A. Krol, Characterization of mSelB, a novel mammalian elongation factor for selenoprotein translation, EMBO J. 19 (2000) 4796–4805.

[28] F. Zinoni, J. Heider, A. Böck, Features of the formate dehydrogenase mRNA necessary for decoding of the UGA codon as selenocysteine, Proc. Natl. Acad. Sci. U. S. A. 87 (1990) 4660–4664.

[29] S. Halboth, A. Klein, Methanococcus voltae harbors four gene clusters potentially encoding two [NiFe] and two [NiFeSe] hydrogenases, each of the cofactor F420-reducing or F420-non-reducing types, Mol. Gen. Genet. 233 (1992) 217–224.

[30] M.J. Berry, L. Banu, Y. Chen, S.J. Mandel, J.D. Kieffer, J.W. Harney, P.R. Larsen, Recognition of UGA as a selenocysteine codon in type I deiodinase requires sequences in the 3′ untranslated region, Nature 353 (1991) 273–276.

[31] S.C. Low, M.J. Berry, Knowing when not to stop: selenocysteine incorporation in eukaryotes, Trends Biochem. Sci. 21 (1996) 203–208.

[32] P. Cravedi, G. Mori, F. Fischer, R. Percudani, Evolution of the selenoproteome in helicobacter pylori and epsilonproteobacteria, Genome Biol. Evol. 7 (2015) 2692–2704.

[33] B. Hao, W. Gong, T.K. Ferguson, C.M. James, J.A. Krzycki, M.K. Chan, A new UAG-encoded residue in the structure of a methanogen methyltransferase, Science 296 (2002) 1462–1466 (80-..

[34] Y. Zhang, V.N. Gladyshev, High content of proteins containing 21st and 22nd amino acids, selenocysteine and pyrrolysine, in a symbiotic deltaproteobacterium of gutless worm Olavius algarvensis, Nucleic Acids Res. 35 (2007) 4952–4963.

[35] J.A. Krzycki, Function of genetically encoded pyrrolysine in corrinoid-dependent methylamine methyltransferases, Curr. Opin. Chem. Biol. 8 (2004) 484–491.

[36] S.K. Blight, R.C. Larue, A. Mahapatra, D.G. Longstaff, E. Chang, G. Zhao, P.T. Kang, K.B. Green-Church, M.K. Chan, J.A. Krzycki, Direct charging of tRNACUA with pyrrolysine in vitro and in vivo, Chem 17 (2004) 503–507.

[37] G. Srinivasan, C.M. James, J.A. Krzycki, Pyrrolysine encoded by UAG in archaea: charging of a UAG-decoding specialized tRNA, Science 296 (2002) 1459–1462. 80.

[38] A. Théobald-Dietrich, M. Frugier, R. Giegé, J. Rudinger-Thirion, Atypical archaeal tRNA pyrrolysine transcript behaves towards EF-Tu as a typical elongator tRNA, Nucleic Acids Res. 32 (2004) 1091–1096.

[39] A. Théobald-Dietrich, R. Giegé, J. Rudinger-Thirion, Evidence for the existence in mRNAs of a hairpin element responsible for ribosome dependent pyrrolysine insertion into proteins, Biochimie 87 (2005) 813–817.

[40] C.J. Bult, O. White, G.J. Olsen, L. Zhou, R.D. Fleischmann, G.G. Sutton, J.A. Blake, L.M. Fitzgerald, R.A. Clayton, D. Jeannine, A.R. Kerlavage, J.C. Venter, et al., Complete genome sequence of the methanogenic archaeon, Methanococcus jannaschii, Science 273 (1996) 1058–1073. 80.

[41] A. Sauerwald, W. Zhu, T.A. Major, H. Roy, S. Palioura, D. Jahn, W.B. Whitman, J.R. Yates, M. Ibba, D. Söll, RNA-dependent cysteine biosynthesis in archaea, Science 307 (2005) 1969–1972. 80.

[42] A. Chaliotis, P. Vlastaridis, D. Mossialos, M. Ibba, H.D. Becker, C. Stathopoulos, G.D. Amoutzias, The complex evolutionary history of aminoacyl-tRNA synthetases, Nucleic Acids Res. 45 (2017) 1059–1068.

[43] M. Frechin, B. Senger, M. Braye, D. Kern, R.P. Martin, H.D. Becker, Yeast mitochondrial Gln-tRNAGln is generated by a GatFAB-mediated transamidation pathway involving Arc1p-controlled subcellular sorting of cytosolic GluRS, Genes Dev. 23 (2009) 1119–1130.

[44] H.D. Becker, D. Kern, Thermus thermophilus: a link in evolution of the tRNA-dependent amino acid amidation pathways, Proc. Natl. Acad. Sci. U. S. A. 95 (1998) 12832–12837.

[45] A.W. Curnow, K.W. Hong, R. Yuan, S. Il Kim, O. Martins, W. Winkler, T.M. Henkin, D. Söll, Glu-tRNAGln amidotransferase: a novel heterotrimeric enzyme required for correct decoding of glutamine codons during translation, Proc. Natl. Acad. Sci. U. S. A. 94 (1997) 11819–11826.

[46] D. Jahn, Y.C. Kim, Y. Ishino, M.W. Chen, D. Söll, Purification and functional characterization of the Glu-tRNA(Gln) amidotransferase from Chlamydomonas reinhardtii, J. Biol. Chem. 265 (1990) 8059–8064.

[47] A.W. Curnow, M. Ibba, D. Soll, tRNA-dependent asparagine formation, Nature 382 (1996) 589–590.

[48] D.L. Tumbula, H.D. Becker, W. Chang, D. Söll, Domain-specific recruitment of amide amino acids for protein synthesis, Nature 407 (2000) 106–110.

[49] K. Sheppard, J. Yuan, M.J. Hohn, B. Jester, K.M. Devine, D. Söll, From one amino acid to another: tRNA-dependent amino acid biosynthesis, Nucleic Acids Res. 36 (2008) 1813–1825.

[50] C. Pujol, M. Bailly, D. Kern, L. Maréchal-Drouard, H. Becker, A.-M. Duchêne, Dual-targeted tRNA-dependent amidotransferase ensures both mitochondrial and chloroplastic Gln-tRNAGln synthesis in plants, Proc. Natl. Acad. Sci. U. S. A. 105 (2008) 6481–6485.

[51] A. Nagao, T. Suzuki, T. Katoh, Y. Sakaguchi, T. Suzuki, Biogenesis of glutaminyl-mt tRNAGln in human mitochondria, Proc. Natl. Acad. Sci. U. S. A. 106 (2009) 16209–16214.

[52] B.M. Mailu, L. Li, J. Arthur, T.M. Nelson, G. Ramasamy, K. Fritz-Wolf, K. Becker, M.J. Gardner, Plasmodium apicoplast Gln-tRNAGln biosynthesis utilizes a unique GatAB amidotransferase essential for erythrocytic stage parasites, J. Biol. Chem. 290 (2015) 29629–29641.

[53] S. Skouloubris, L.R. De Pouplana, H. De Reuse, T.L. Hendrickson, A noncognate aminoacyl-tRNA synthetase that may resolve a missing link in protein evolution, Proc. Natl. Acad. Sci. U. S. A. 100 (2003) 11297–11302.

[54] J. Rinehart, B. Krett, M.A.T. Rubio, J.D. Alfonzo, D. Söll, Saccharomyces cerevisiae imports the cytosolic pathway for Gln-tRNA synthesis into the mitochondrion, Genes Dev. 19 (2005) 583–592.

[55] T. Rampias, K. Sheppard, D. Söll, The archaeal transamidosome for RNA-dependent glutamine biosynthesis, Nucleic Acids Res. 38 (2010) 5774–5783.

[56] M. Bailly, M. Blaise, B. Lorber, H.D. Becker, D. Kern, The transamidosome: a dynamic ribonucleoprotein particle dedicated to prokaryotic tRNA-dependent asparagine biosynthesis, Mol. Cell 28 (2007) 228–239.

[57] J.L. Huot, F. Fischer, J. Corbeil, É. Madore, B. Lorber, G. Diss, T.L. Hendrickson, D. Kern, J. Lapointe, Gln-tRNAGln synthesis in a dynamic transamidosome from Helicobacter pylori, where GluRS2 hydrolyzes excess Glu-tRNAGln, Nucleic Acids Res. 39 (2011) 9306–9315.

[58] F. Fischer, J.L. Huot, B. Lorber, G. Diss, T.L. Hendrickson, H.D. Becker, J. Lapointe, D. Kern, The asparagine-transamidosome from Helicobacter pylori: a dual-kinetic mode in non-discriminating aspartyl-tRNA synthetase safeguards the genetic code, Nucleic Acids Res. 40 (2012) 4965–4976.

[59] M.G. Macfarlane, Characterization of lipoamino-acids as O-amino-acid esters of phosphatidyl-glycerol, Nature 196 (1962) 136–138.

[60] C. Slavetinsky, S. Kuhn, A. Peschel, Bacterial aminoacyl phospholipids—biosynthesis and role in basic cellular processes and pathogenicity, Biochim. Biophys. Acta Mol. Cell Biol. Lipids 1862 (2017) 1310–1318.

[61] A. Peschel, R.W. Jack, M. Otto, L.V. Collins, P. Staubitz, G. Nicholson, H. Kalbacher, W.F. Nieuwenhuizen, G. Jung, A. Tarkowski, K.P.M. Van Kessel, J.A.G. Van Strijp, Staphylococcus aureus resistance to human defensins and evasion of neutrophil killing via the novel virulence factor MprF is based on modification of membrane lipids with L-lysine, J. Exp. Med. 193 (2001) 1067–1076.

[62] C.M. Ernst, P. Staubitz, N.N. Mishra, S.J. Yang, G. Hornig, H. Kalbacher, A.S. Bayer, D. Kraus, A. Peschel, The bacterial defensin resistance protein MprF consists of separable domains for lipid lysinylation and antimicrobial peptide repulsion, PLoS Pathog. 5 (2009) 1–9.

[63] H. Roy, M. Ibba, Broad range amino acid specificity of RNA-dependent lipid remodeling by multiple peptide resistance factors, J. Biol. Chem. 284 (2009) 29677–29683.

[64] C. Weidenmaier, A. Peschel, V.A.J. Kempf, N. Lucindo, M.R. Yeaman, A.S. Bayer, DltABCD- and MprF-mediated cell envelope modifications of Staphylococcus aureus confer resistance to platelet microbicidal proteins and contribute to virulence in a rabbit endocarditis model, Infect. Immun. 73 (2005) 8033–8038.

[65] L. Friedman, J.D. Alder, J.A. Silverman, Genetic changes that correlate with reduced susceptibility to daptomycin in Staphylococcus aureus, Antimicrob. Agents Chemother. 50 (2006) 2137–2145.

[66] K. Thedieck, T. Hain, W. Mohamed, B.J. Tindall, M. Nimtz, T. Chakraborty, J. Wehland, L. Jänsch, The MprF protein is required for lysinylation of phospholipids in listerial membranes and confers resistance to cationic antimicrobial peptides (CAMPs) on Listeria monocytogenes, Mol. Microbiol. 62 (2006) 1325–1339.

[67] J. Zemansky, B.C. Kline, J.J. Woodward, J.H. Leber, H. Marquis, D.A. Portnoy, Development of a mariner-based transposon and identification of Listeria monocytogenes determinants, including the peptidyl-prolyl isomerase PrsA2, that contribute to its hemolytic phenotype, J. Bacteriol. 191 (2009) 3950–3964.

[68] R.N. Fields, H. Roy, Deciphering the tRNA-dependent lipid aminoacylation systems in bacteria: novel components and structural advances, RNA Biol. 15 (2018) 480–491.

[69] W. Arendt, S. Hebecker, S. Jäger, M. Nimtz, J. Moser, Resistance phenotypes mediated by aminoacyl-phosphatidylglycerol synthases, J. Bacteriol. 194 (2012) 1401–1416.

[70] H. Roy, M. Ibba, RNA-dependent lipid remodeling by bacterial multiple peptide resistance factors, Proc. Natl. Acad. Sci. U. S. A. 105 (2008) 4667–4672.

[71] S. Hebecker, W. Arendt, I.U. Heinemann, J.H.J. Tiefenau, M. Nimtz, M. Rohde, D. Söll, J. Moser, Alanyl-phosphatidylglycerol synthase: mechanism of substrate recognition during tRNA-dependent lipid modification in Pseudomonas aeruginosa, Mol. Microbiol. 80 (2011) 935–950.

[72] S. Hebecker, J. Krausze, T. Hasenkampf, J. Schneider, M. Groenewold, J. Reichelt, D. Jahn, D.W. Heinz, J. Moser, Structures of two bacterial resistance factors mediating tRNA-dependent aminoacylation of phosphatidylglycerol with lysine or alanine, Proc. Natl. Acad. Sci. U. S. A. 112 (2015) 10691–10696.

[73] E. Maloney, D. Stankowska, J. Zhang, M. Fol, Q.J. Cheng, S. Lun, W.R. Bishai, M. Rajagopalan, D. Chatterjee, M.V. Madiraju, The two-domain LysX protein of *Mycobacterium tuberculosis* is required for production of lysinylated phosphatidylglycerol and resistance to cationic antimicrobial peptides, PLoS Pathog. 5 (2009) 1–14.

[74] A. Bouhss, A.E. Trunkfield, T.D.H. Bugg, D. Mengin-Lecreulx, The biosynthesis of peptidoglycan lipid-linked intermediates, FEMS Microbiol. Rev. 32 (2008) 208–233.

[75] M. Jarick, U. Bertsche, M. Stahl, D. Schultz, K. Methling, M. Lalk, C. Stigloher, M. Steger, A. Schlosser, K. Ohlsen, The serine/threonine kinase Stk and the phosphatase Stp regulate cell wall synthesis in *Staphylococcus aureus*, Sci. Rep. 8 (2018) 1–13.

[76] U. Kopp, M. Roos, J. Wecke, H. Labischinski, Staphylococcal peptidoglycan interpeptide bridge biosynthesis: a novel antistaphylococcal target? Microb. Drug Resist. 2 (1996) 29–41.

[77] H. Labischinski, Consequences of the interaction of β-lactam antibiotics with penicillin binding proteins from sensitive and resistant *Staphylococcus aureus* strains, Med. Microbiol. Immunol. 181 (1992) 241–265.

[78] T. Schneider, M.M. Senn, B. Berger-Bächi, A. Tossi, H.G. Sahl, I. Wiedemann, In vitro assembly of a complete, pentaglycine interpeptide bridge containing cell wall precursor (lipid II-Gly5) of *Staphylococcus aureus*, Mol. Microbiol. 53 (2004) 675–685.

[79] S. Giannouli, A. Kyritsis, N. Malissovas, H.D. Becker, C. Stathopoulos, On the role of an unusual tRNAGly isoacceptor in *Staphylococcus aureus*, Biochimie 91 (2009) 344–351.

[80] L.E. Sanderson, O.C. Uhlenbeck, The 51-63 base pair of tRNA confers specificity for binding by EF-Tu, RNA 13 (2007) 835–840.

[81] S. Rohrer, K. Ehlert, M. Tschierske, H. Labischinski, B. Berger-Bachi, The essential *Staphylococcus aureus* gene fmhB is involved in the first step of peptidoglycan pentaglycine interpeptide formation, Proc. Natl. Acad. Sci. U. S. A. 96 (1999) 9351–9356.

[82] J. Hübscher, A. Jansen, O. Kotte, J. Schäfer, P.A. Majcherczyk, L.G. Harris, G. Bierbaum, M. Heinemann, B. Berger-Bächi, Living with an imperfect cell wall: compensation of femAB inactivation in *Staphylococcus aureus*, BMC Genomics 8 (2007) 1–14.

[83] K. Dare, M. Ibba, Roles of tRNA in cell wall biosynthesis, Wiley Interdiscip. Rev. RNA 3 (2012) 247–264.

[84] S.R. Filipe, A. Tomasz, Inhibition of the expression of penicillin resistance in *Streptococcus pneumoniae* by inactivation of cell wall muropeptide branching genes, Proc. Natl. Acad. Sci. U. S. A. 97 (2000) 4891–4896.

[85] S. Biarrotte-Sorin, A.P. Maillard, J. Delettré, W. Sougakoff, M. Arthur, C. Mayer, Crystal structures of Weissella viridescens FemX and its complex with UDP-MurNAc-pentapeptide: insights into FemABX family substrates recognition, Structure 12 (2004) 257–267.

[86] R. Villet, M. Fonvielle, P. Busca, M. Chemama, A.P. Maillard, J.E. Hugonnet, L. Dubost, A. Marie, N. Josseaume, S. Mesnage, C. Mayer, J.M. Valéry, M. Ethève-Quelquejeu, M. Arthur, Idiosyncratic features in tRNAs participating in bacterial cell wall synthesis, Nucleic Acids Res. 35 (2007) 6870–6883.

[87] M. Fonvielle, M. Chemama, M. Lecerf, R. Villet, P. Busca, A. Bouhss, M. Ethève-Quelquejeu, M. Arthur, Decoding the logic of the tRNA regiospecificity of nonribosomal FemX(Wv) aminoacyl transferase, Angew. Chem. Int. Ed. Engl. 49 (2010) 5115–5119.

[88] J. Shepherd, Characterisation of Pneumococcal Peptidoglycan Cross-linking Enzymology, 2011, pp. 1–330. https://www.semanticscholar.org/paper/Characterisation-of-pneumococcal-peptidoglycan-Shepherd/c432b7bb6343829e651d635c9f4b1251378cb54b.

[89] J. Shepherd, M. Ibba, Direction of aminoacylated transfer RNAs into antibiotic synthesis and peptidoglycan-mediated antibiotic resistance, FEBS Lett. 587 (2013) 2895–2904.

[90] K.H. Schleifer, O. Kandler, Peptidoglycan types of bacterial cell walls and their taxonomic implications, Bacteriol. Rev. 36 (1972) 407–477.

[91] P.A. Castelfranco, S.I. Beale, Chlorophyll biosynthesis: recent advances and areas of current interest, Annu. Rev. Plant Physiol. 34 (1983) 241–276.

[92] D.D. Huang, W.Y. Wang, S.P. Gough, C.G. Kannangara, δ-aminolevulinic acid-synthesizing enzymes need an RNA moiety for activity, Science 225 (1984) 1482–1484. 80.

[93] D.D. Huang, W.Y. Wang, Chlorophyll biosynthesis in Chlamydomonas starts with the formation of glutamyl-tRNA, J. Biol. Chem. 261 (1986) 13451–13455.

[94] A. Schön, G. Krupp, S. Gough, S. Berry-Lowe, C.G. Kannangara, D. Söll, The RNA required in the first step of chlorophyll biosynthesis is a chloroplast glutamate tRNA, Nature 322 (1986) 281–284.

[95] C. Gamini Kannangara, S.P. Gough, P. Bruyant, J. Kenneth Hoober, A. Kahn, D. von Wettstein, tRNAGlu as a cofactor in δ-aminolevulinate biosynthesis: steps that regulate chlorophyll synthesis, Trends Biochem. Sci. 13 (1988) 139–143.

[96] D. Peterson, A. Schön, D. Söll, The nucleotide sequences of barley cytoplasmic glutamate transfer RNAs and structural features essential for formation of δ-aminolevulinic acid, Plant Mol. Biol. 11 (1988) 293–299.

[97] B. Grimm, A. Bull, K.G. Welinder, S.P. Gough, C.G. Kannangara, Purification and partial amino acid sequence of the glutamate 1-semialdehyde aminotransferase of barley and Synechococcus, Carlsberg Res. Commun. 54 (1989) 67–79.

[98] S.I. Beale, P.A. Castelfranco, 14C incorporation from exogenous compounds into δ-aminolevulinic acid by greening cucumber cotyledons, Biochem. Biophys. Res. Commun. 52 (1973) 143–149.

[99] S.I. Beale, S.P. Gough, S. Granick, Biosynthesis of δ aminolevulinic acid from the intact carbon skeleton of glutamic acid in greening barley, Proc. Natl. Acad. Sci. U. S. A. 72 (1975) 2719–2723.

[100] D. Jahn, Complex formation between glutamyl-tRNA synthetase and glutamyl-tRNA reductase during the tRNA-dependent synthesis of 5-aminolevulinic acid in Chlamydomonas reinhardtii, FEBS Lett. 314 (1992) 77–80.

[101] R.D. Willows, C.G. Kannangara, B. Pontoppidan, Nucleotides of tRNA (Glu) involved in recognition by barley chloroplast glutamyl-tRNA synthetase and glutamyl-tRNA reductase, Biochim. Biophys. Acta Gene Struct. Expr. 1263 (1995) 228–234.

[102] L. Randau, S. Schauer, A. Ambrogelly, J.C. Salazar, J. Moser, S.I. Sekine, S. Yokoyama, D. Söll, D. Jahn, tRNA recognition by glutamyl-tRNA reductase, J. Biol. Chem. 279 (2004) 34931–34937.

[103] I. Schroder, P. Johansson, L. Rutberg, L. Hederstedt, The hemX gene of the Bacillus subtilis hemAXCDBL operon encodes a membrane protein, negatively affecting the steady-state cellular concentration of HemA (glutamyl-tRNA reductase), Microbiology 140 (1994) 731–740.

[104] L.Y. Wang, L. Brown, M. Elliott, T. Elliott, Regulation of heme biosynthesis in Salmonella typhimurium: activity of glutamyl-tRNA reductase (HemA) is greatly elevated during heme limitation by a mechanism which increases abundance of the protein, J. Bacteriol. 179 (1997) 2907–2914.

[105] P.J. Loida, R.L. Thompson, D.M. Walker, C.A. Cajacob, Novel inhibitors of glutamyl-tRNA(Glu) reductase identified through cell-based screening of the heme/chlorophyll biosynthetic pathway, Arch. Biochem. Biophys. 372 (1999) 230–237.

[106] L. Wang, M. Elliott, T. Elliott, Conditional stability of the HemA protein (Glutamyl-tRNA reductase) regulates heme biosynthesis in Salmonella typhimurium, J. Bacteriol. 181 (1999) 1211–1219.

[107] R. Meskauskiene, K. Apel, Interaction of FLU, a negative regulator of tetrapyrrole biosynthesis, with the glutamyl-tRNA reductase requires the tetratricopeptide repeat domain of FLU, FEBS Lett. 532 (2002) 27–30.

[108] D. Goslings, R. Meskauskiene, C. Kim, K.P. Lee, M. Nater, K. Apel, Concurrent interactions of heme and FLU with Glu tRNA reductase (HEMA1), the target of metabolic feedback inhibition of tetrapyrrole biosynthesis, in dark- and light-grown Arabidopsis plants, Plant J. 40 (2004) 957–967.

[109] C. Lüer, S. Schauer, K. Möbius, J. Schulze, W.D. Schubert, D.W. Heinz, D. Jahn, J. Moser, Complex formation between glutamyl-tRNA reductase and glutamate-1-semialdehyde 2,1-aminomutase in Escherichia coli during the initial reactions of porphyrin biosynthesis, J. Biol. Chem. 280 (2005) 18568–18572.

[110] G. Levicán, A. Katz, M. De Armas, H. Núñez, O. Orellana, Regulation of a glutamyl-tRNA synthetase by the heme status, Proc. Natl. Acad. Sci. U. S. A. 104 (2007) 3135–3140.

[111] K. Wakasugi, Human tryptophanyl-tRNA synthetase binds with heme to enhance its aminoacylation activity, Biochemistry 46 (2007) 11291–11298.

[112] M. Gorla, N.B.V. Sepuri, Perturbation of apoptosis upon binding of tRNA to the heme domain of cytochrome c, Apoptosis 19 (2014) 259–268.

[113] O. Czarnecki, B. Hedtke, M. Melzer, M. Rothbart, A. Richter, Y. Schröter, T. Pfannschmidt, B. Grimm, An Arabidopsis GluTR binding protein mediates spatial separation of 5-Aminolevulinic acid synthesis in chloroplasts, Plant Cell 23 (2011) 4476–4491.

[114] A. Zhao, Y. Fang, X. Chen, S. Zhao, W. Dong, Y. Lin, W. Gong, L. Liu, Crystal structure of Arabidopsis glutamyl-tRNA reductase in complex with its stimulator protein, Proc. Natl. Acad. Sci. U. S. A. 111 (2014) 6630–6635.

[115] Y. Fang, S. Zhao, F. Zhang, A. Zhao, W. Zhang, M. Zhang, L. Liu, The Arabidopsis glutamyl-tRNA reductase (GluTR) forms a ternary complex with FLU and GluTR-binding protein, Sci. Rep. 6 (2016) 4–10.

[116] J. Apitz, K. Nishimura, J. Schmied, A. Wolf, B. Hedtke, K.J. van Wijk, B. Grimm, Posttranslational control of ALA synthesis includes GluTR degradation by clp protease and stabilization by GluTR-binding protein, Plant Physiol. 170 (2016) 2040–2051.

[117] J.E. Choby, C.M. Grunenwald, A.I. Celis, S.Y. Gerdes, J.L. Dubois, P. Skaar, Staphylococcus aureus HemX modulates glutamyl-tRNA reductase abundance to regulate heme biosynthesis, MBio 9 (2018) 1–19.

[118] J. Schmied, Z. Hou, B. Hedtke, B. Grimm, Controlled partitioning of Glutamyl-tRNA reductase in stroma- and membrane-associated fractions affects the synthesis of 5-Aminolevulinic acid, Plant Cell Physiol. 59 (2018) 2204–2213.

[119] P. Wang, F.C. Liang, D. Wittmann, A. Siegel, S.O. Shan, B. Grimm, Chloroplast SRP43 acts as a chaperone for glutamyl-tRNA reductase, the rate-limiting enzyme in tetrapyrrole biosynthesis, Proc. Natl. Acad. Sci. U. S. A. 115 (2018) E3588–E3596.

[120] A.S. Richter, C. Banse, B. Grimm, The GluTR-binding protein is the heme-binding factor for feedback control of glutamyl-tRNA reductase, Elife 8 (2019) 1–18.

[121] E.C. Ulrich, W.A. van der Donk, Cameo appearances of aminoacyl-tRNA in natural product biosynthesis, Curr. Opin. Chem. Biol. 35 (2016) 29–36.

[122] E.M. Nolan, C.T. Walsh, How nature morphs peptide scaffolds into antibiotics, Chembiochem 10 (2009) 34–53.

[123] M. Moutiez, P. Belin, M. Gondry, Aminoacyl-tRNA-utilizing enzymes in natural product biosynthesis, Chem. Rev. 117 (2017) 5578–5618.

[124] R.S. Roy, A.M. Gehring, J.C. Milne, P.J. Belshaw, C.T. Walsh, Thiazole and oxazole peptides: biosynthesis and molecular machinery, Nat. Prod. Rep. 16 (1999) 249–263.

[125] S. Rebuffat, Microcins, Elsevier Inc., second ed., 2013.

[126] B.K. Leskiw, R. Mah, E.J. Lawlor, K.F. Chater, Accumulation of bldA-specified tRNA is temporally regulated in Streptomyces coelicolor A3(2), J. Bacteriol. 175 (1993) 1995–2005.

[127] R. García-Contreras, X.S. Zhang, Y. Kim, T.K. Wood, Protein translation and cell death: the role of rare tRNAs in biofilm formation and in activating dormant phage killer genes, PLoS One 3 (2008) 1–15.

[128] R.P. Garg, X.L. Qian, L.B. Alemany, S. Moran, R.J. Parry, Investigations of valanimycin biosynthesis: elucidation of the role of seryl-tRNA, Proc. Natl. Acad. Sci. U. S. A. 105 (2008) 6543–6547.

[129] R.P. Garg, J.M. Gonzalez, R.J. Parry, Biochemical characterization of VlmL, a seryl-tRNA synthetase encoded by the valanimycin biosynthetic gene cluster, J. Biol. Chem. 281 (2006) 26785–26791.

[130] C. Maruyama, H. Niikura, M. Izumikawa, J. Hashimoto, K. Shin-ya, M. Komatsu, H. Ikeda, M. Kuroda, T. Sekizuka, J. Ishikawa, Y. Hamano, tRNA-dependent aminoacylation of an amino sugar intermediate in the biosynthesis of a streptothricin-related antibiotic, Appl. Environ. Microbiol. 82 (2016) 3640–3648.

[131] A. Kaji, H. Kaji, G.D. Novelli, Soluble amino acid-incorporating system. I. Preparation of the system and nature of the reaction, J. Biol. Chem. 240 (1965) 1185–1191.

[132] A. Kaji, H. Kaji, G.D. Novelli, Soluble amino acid-incorporating system. II. Soluble nature of the system and the characterization of the radioactive product, J. Biol. Chem. 240 (1965) 1192–1197.

[133] M. Matsuhashi, C.P. Dietrich, J.L. Strominger, Biosynthesis of the peptidoglycan of bacterial cell walls iii. the role of soluble ribonucleic acid and of lipid intermediates in glycine incorporation in *staphylococcus aureus*, J. Biol. Chem. 242 (1967) 3191–3206.

[134] M. Gondry, L. Sauguet, P. Belin, R. Thai, R. Amouroux, C. Tellier, K. Tuphile, M. Jacquet, S. Braud, M. Courçon, C. Masson, S. Dubois, S. Lautru, A. Lecoq, S.I. Hashimoto, R. Genet, J.L. Pernodet, Cyclodipeptide synthases are a family of tRNA-dependent peptide bond-forming enzymes, Nat. Chem. Biol. 5 (2009) 414–420.

[135] T.W. Giessen, M.A. Marahiel, Ribosome-independent biosynthesis of biologically active peptides: application of synthetic biology to generate structural diversity, FEBS Lett. 586 (2012) 2065–2075.

[136] M.A. Fischbach, C.T. Walsh, J. Clardy, The evolution of gene collectives: how natural selection drives chemical innovation, Proc. Natl. Acad. Sci. U. S. A. 105 (2008) 4601–4608.

[137] S. Gowrishankar, S.K. Pandian, B. Balasubramaniam, K. Balamurugan, Quorum quelling efficacy of marine cyclic dipeptide –cyclo(L-leucyl-L-prolyl) against the uropathogen Serratia marcescens, Food Chem. Toxicol. 123 (2019) 326–336.

[138] H. Kaji, G.D. Novelli, A. Kaji, A soluble amino acid-incorporating system from rat liver, Biochim. Biophys. Acta 76 (1963) 474–477.

[139] A. Bachmair, D. Finley, A. Varshavsky, In vivo half-life of a protein is a function of its amino-terminal residue, Science 234 (1986) 179–186. 80.

[140] B. Bartel, I. Wünning, A. Varshavsky, The recognition component of the N-end rule pathway, EMBO J. 9 (1990) 3179–3189.

[141] S. Grigoryeve, A.E. Stewart, Y.T. Kwon, S.M. Arfin, R.A. Bradshaw, N.A. Jenkins, N.G. Copeland, A. Varshavsky, A mouse amidase specific for N-terminal asparagine: the gene, the enzyme, and their function in the N-end rule pathway, J. Biol. Chem. 271 (1996) 28521–28532.

[142] T. Tasaki, S.M. Sriram, K.S. Park, Y.T. Kwon, The N-end rule pathway, Annu. Rev. Biochem. 81 (2012) 261–289.

[143] R.L. Soffer, Peptide acceptors in the arginine transfer reaction, J. Biol. Chem. 248 (1973) 2918–2921.

[144] J.W. Tobias, T.E. Shrader, G. Rocap, A. Varshavsky, The N-end rule in bacteria, Science 254 (1991) 1374–1377. 80.

[145] T.E. Shrader, J.W. Tobias, A. Varshavsky, The N-end rule in *Escherichia coli*: cloning and analysis of the leucyl, phenylalanyl-tRNA-protein transferase gene aat, J. Bacteriol. 175 (1993) 4364–4374.

[146] G. Abramochkin, T.E. Shrader, The leucyl/phenylalanyl-tRNA-protein transferase. Overexpression and characterization of substrate recognition, domain structure, and secondary structure, J. Biol. Chem. 270 (1995) 20621–20628.

[147] K. Suto, Y. Shimizu, K. Watanabe, T. Ueda, S. Fukai, O. Nureki, K. Tomita, Crystal structures of leucyl/phenylalanyl-tRNA-protein transferase and its complex with an aminoacyl-tRNA analog, EMBO J. 25 (2006) 5942–5950.

[148] K. Watanabe, Y. Toh, K. Suto, Y. Shimizu, N. Oka, T. Wada, K. Tomita, Protein-based peptide-bond formation by aminoacyl-tRNA protein transferase, Nature 449 (2007) 867–871.

[149] R.T. Baker, A. Varshavsky, Yeast N-terminal Amidase, J. Biol. Chem. 270 (1995) 12065–12074.

[150] H. Wang, K.I. Piatkov, C.S. Brower, A. Varshavsky, Glutamine-specific N-terminal amidase, a component of the N-end rule pathway, Mol. Cell 34 (2009) 686–695.

[151] E. Balzi, M. Choder, W. Chen, A. Varshavsky, A. Goffeau, Cloning and functional analysis of the arginyl-tRNA-protein transferase gene ATE1 of *Saccharomyces cerevisiae*, J. Biol. Chem. 265 (1990) 7464–7471.

[152] A. Ciechanovers, S. Ferber, D. Ganoth, S. Elias, A. Hershko, S. Arfin, Purification and characterization of Arginyl-tRNA-protein transferase from rabbit reticulocytes, J. Biol. Chem. 263 (1988) 11155–11167.

[153] L. Chen, A. Kashina, Quantification of intracellular N-terminal β-actin arginylation, Sci. Rep. 9 (2019) 1–9.

[154] P. Batsios, H.C. Ishikawa-Ankerhold, H. Roth, M. Schleicher, C.C.L. Wong, A. Müller-Taubenberger, Ate1-mediated posttranslational arginylation affects substrate adhesion and cell migration in Dictyostelium discoideum, Mol. Biol. Cell 30 (2019) 453–466.

[155] J. Wang, I. Pavlyk, P. Vedula, S. Sterling, N.A. Leu, D.W. Dong, A. Kashina, Arginyltransferase ATE1 is targeted to the neuronal growth cones and regulates neurite outgrowth during brain development, Dev. Biol. 430 (2017) 41–51.

[156] N. Yakobov, S. Debard, F. Fischer, B. Senger, H.D. Becker, Cytosolic aminoacyl-tRNA synthetases: unanticipated relocations for unexpected functions, Biochim. Biophys. Acta, Gene Regul. Mech. 1861 (2018) 387–400.

Poster 1

Yakobov *et al.*, 2017a

tRNA-dependent membrane remodeling and resistance to antifungal drugs

Doctoral School Days 2017. March 22nd & 23rd, 2017,

Collège Doctoral Européen, Strasbourg, France

tRNA-dependent membrane remodeling and resistance to antifungal drugs

Nathaniel Yakobov, Frédéric Fischer, Bruno Senger & Hubert D. Becker

GMGM UMR 7156, Université de Strasbourg, CNRS IPCB, 4 Allée Konrad Roentgen, F-67081 Strasbourg

INTRODUCTION

Aminoacyl-tRNA-synthetases (aaRSs) are enzymes known to attach an amino acid onto its cognate tRNA[aa], leading to the formation of aa-tRNA[aa]s required for protein synthesis[1]. However, it was shown that these aa-tRNA[aa]s can be rerouted for other patways[2]. For example, in many bacterial species, the DUF2156 domain was shown to perform lipid modification by transferring the amino acid moiety from Lys-tRNA[Lys] to Phosphatidylglycerol which is one of the main membrane lipids found in gram positive bacteria[3]. Such membrane remodeling induces modification of membrane characteristics leading to higher virulence and resistance against CAMP (cationic Antimicrobial Peptides). Therefore, these proteins were qualified "Multiple peptide resistance Factors" (MprF).

Such cell wall remodeling strategies were not described in eukaryotes so far. However, we discovered a large number of fungal species, including human pathogens (i.e A. fumigatus) that contain proteins with a putative DUF2156 domain, making them promising MprF-like proteins. Since DUF2156 are not found in humans, they represent an attractive target for the development of novel antifungal drugs.

In order to investigate the similarities and differences between fungal "MprF like" (DUF2156 proteins) and bacterial MprF we established an in vivo model (S. cerevisiae, see below) and different in vitro assays. On the other hand the characterization of fungal DUF2156 proteins in Afu and other fungi species will allow us to establish an infection model to understand the physiological function of DUF2156 proteins.
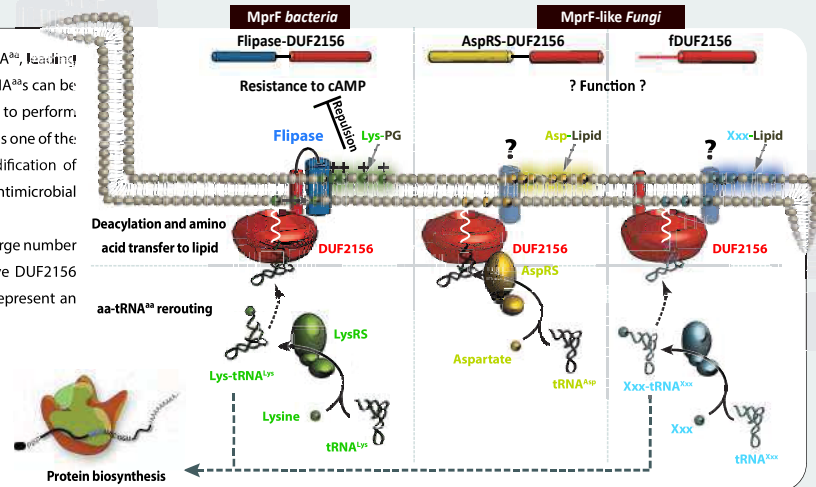
in vivo RESULTS

1. Fungal DUF2156 occurence

In silico analyses show that two types of DUF2156-containing proteins exist in fungi (**Fig. 1**).
- A freestanding DUF2156 (fDUF2156)
- An AspRS-DUF2156 fusion protein Preliminary phylogenetic studies suggest that they were acquired by Dikarya (green arrow) but not by other eukaryotes. Saccharomycotina species (red), among which the yeast Saccharomyces cerevisiae (Sce), subsequently lost all DUF2156 proteins. Sce is a well-established fungal model. We thus first used this heterologous model to characterize **AspRS-DUF2156** and **fDUF2156** in vivo.
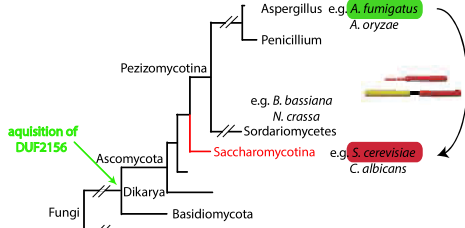
2. AspRS-DUF complements loss of AspRS from Sce

Growth phenotypes confirmed that AspRS-DUF2156 synthetizes sufficient Asp-tRNAsp to sustain protein synthesis, that the aminoacylation activity depends on the AspRS domain and that the DUF2156 domain is dispensable for aminoacylation of tRNA.

4. DUF2156 proteins associate with membranes

	P13 K	P100 K	S100 K
AspRS-DUF			
fDUF2156			

P13 K : ER, plasma membrane, nucleus, mitochondria, vacuole
P100 K : Endosomes, Golgi
S100 K : Cytosol, vesicles

Sub-fractionation shows that, as expected, both AspRS-DUF and fDUF2156 are found in membrane fractions (P13 : P100). Microscopy experiments are in progress.

fungi DUF2156 domain (phyre 2)
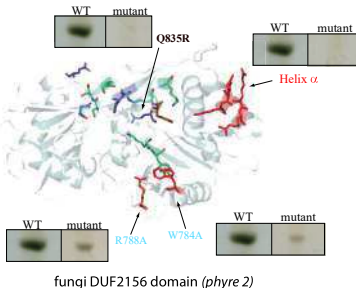
5. Fungi DUF2156 proteins monitor lipid modifications

Results confirm **two different DUF2156-dependent lipid modifications** in Sce membranes (heterologous expression). Identical modified lipids were observed in fungi naturally expressing DUF2156 proteins (Penicillium sp. B. bassiana and Y. lipolytica).

Expression in S. cerevisiae
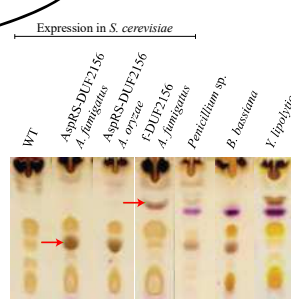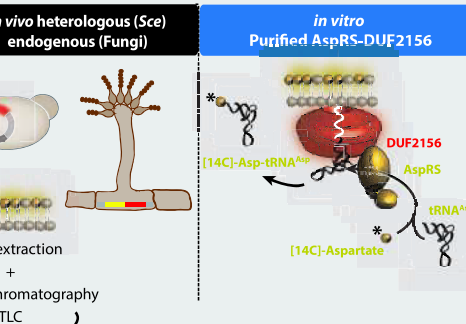
7. Fonctionnal probing of DUF2156 proteins

Mutations in tRNA-binding site (red) abolish lipid modification, whereas mutations within the active site (blue) decrease lipid aminoacylation activity. Similar analyses predicted **Q835** to be crucial for lipid modification (data not shown).

in vitro RESULTS

3. In vitro amino acid transfer assay

Consistant with in vivo experiments, **DUF2156 domain of AspRS-DUF2156 transfers Asp from Asp-tRNAAsp onto a yet- unknown lipid**, which is not PG. Ongoing work aims to identify this lipid. Similar experiments are in progress for fDUF2156.

	Total lipids from S. cerevisiae					PG
Enzyme from	Afu	Afu	Aor	Afu	Afu	Afu
Front						
[14C]-Asp-LX1						
[14C]-Asp-LX2						
Spots						
AspRS-DUF2156	+	−	+	+	+	+
AspRS ΔDUF2156	−	+	−	−	−	−
RNase	−	−	−	−	+	−

6. In vitro aminoacylation assay

Assays with radiolabeled Asp proved that the AspRS-DUF2156 is active for tRNAAsp aminoacylation in vitro.

▲ AspRS-DUF2156 A. fumigatus
□ AspRS-DUF2156 A. oryzae

in vivo heterologous (Sce) endogenous (Fungi)

in vitro Purified AspRS-DUF2156

Lipid extraction + thin layer chromatography TLC

PERSPECTIVES

- Modified lipid identification (H. Roy)
- Virulence / Resistance tests (JP. Latgé)

Deletion
fDUF2156 KO or AspRS-DUF KO or double KO

A. fumigatus
B. bassiana

Infection

G. mellonella
mouse
rice

- 3D structure C. Sauter
- 3D St w/wo ligands - in silico compound screening
- Localization
- Interactome (flippase, membrane binding….)
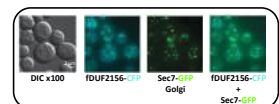
BIBLIOGRAPHY

1. Crick, F.H. (1958) Symposia of the SEB (12), 138163
2. Smirnova, E.V., (2012) (77), 15-25.
3. Roy, H. (2009) IUBMB Life , (61)10 : 940-953

Poster 2

Yakobov *et al.*, 2017b

Characterization of MprF-like lipid aminoacylation factors in fungi

11th aaRS meeting, Oct. 29th-Nov. 2nd, 2017,

Clearwater beach, Florida, USA

&

Doctoral School Days 2018. March 8th & 9th, 2018,

Strasbourg, Alsace, France

Characterization of MprF-like lipid aminoacylation factors in fungi

Nathaniel YAKOBOV[1], Frédéric FISCHER[1], Bruno SENGER[1], Hervé ROY[2], Tetsuo KUSHIRO[3], Isabelle MOUYNA[4], Thierry FONTAINE[4],

Jean-Paul LATGE[4] & Hubert D. BECKER[1]

[1]Génetique Moléculaire, Génomique, Microbiologie, UMR7156, CNRS, Université de Strasbourg, 67084 Strasbourg, Cedex, FRANCE
[2]Burnett School of Biomedical Sciences, College of Medicine, University of Central Florida, Orlando, FL 32826, USA
[3]Graduate School of Agriculture Meiji University, 1-1-1 Higashimita, Tama-ku, Kawasaki Kanagawa 214-8571, JAPAN
[4]Unité des Aspergillus, Institut Pasteur, 25 rue du Docteur Roux, 75724, Paris, Cedex 15, FRANCE
 email: h.becker@unistra.fr, frfischer@unistra.fr

INTRODUCTION

Aminoacyl-tRNA-synthetases (aaRSs) are enzymes that attach amino acids onto their cognate tRNA^{aa}, leading to the formation of the aa-tRNA^{aa}s required for protein synthesis[1]. However, it has been shown that aa-tRNA^{aa}s can be rerouted and serve in other pathways[2]. For example, in many bacterial species, the **DUF2156** domain was shown to perform lipid aminoacylation by transferring the amino acid moiety of Lys-tRNA^{Lys} onto phosphatidylglycerol, which is one of the main membrane lipids found in bacteria[3]. Such membrane remodeling induces modification of membrane characteristics leading to resistance against cAMPs (cationic Antimicrobial Peptides). Therefore, these proteins were qualified as "Multiple peptide resistance Factors" (MprF). Similar cell wall remodeling strategies have not been described in eukaryotes so far. However, we discovered a large number of fungal species, including human pathogens (see also poster "Novel lipid membrane aminoacylation factors in fungi") that contain proteins with a putative DUF2156 domain, making them promising MprF-like proteins. One of them is composed of an aspartyl-tRNA synthetase (AspRS) fused at its C-terminus to a DUF2156 domain (**AspRS-DUF2156**). We used different strategies, either *in vivo* or *in vitro*, to explore biochemically and functionally AspRS-DUF2156 from several fungal species (*Aspergillus fumigatus Afm*, *Aspergillus oryzae Aor* and *Neurospora crassa*). We constructed a heterologous expression model with the yeast *Saccharomyces cerevisiae* (*Sce*), that possesses no DUF2156 proteins, to study fungal MprF-like proteins. Here, we present our main results obtained with heterologous expression of fungal DUF2156 proteins in the *Sce* model and through *in vitro* assays with recombinant purified proteins.
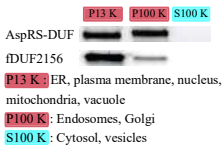
In vivo RESULTS

1 AspRS-DUF complements loss of AspRS from *Sce*

Growth phenotypes confirmed that **AspRS-DUF2156** synthetizes sufficient Asp-tRNA^{Asp} to sustain protein synthesis. Aminoacylation activity depends on the AspRS domain. As suspected, DUF2156 domain is dispensable for tRNA aspartylation.

QSPQ mutant : catalytic null

2 Fungal AspRS- DUF2156 heterologously modify lipids in *Sce*

Total lipids from *Sce* expressing either *Aor* or *Afm* AspRS-DUF2156 were extracted by the Bligh & Dyer **(A)** method and analyzed by TLC **(C)** on silica gel plates (Chloroform : Methanol 65 : 25 : 4). Results revealed the **DUF2156- dependent synthesis of an unknown lipid** in *Sce* membranes (Lipid X; red asterisks) in comparison to the WT *Sce*. Identical modified lipids were observed in fungi naturally expressing DUF2156 proteins (*not shown*).

Expression in *Sce*

3 Lipid X isolation : Separating Lipid classes on silica column

In order to isolate the unknown lipid X, lipid classes extracted from *Sce* expressing AspRS-DUF2156 were separated by flash chromatography **(B)** and analyzed by TLC. Differential elutions were performed with solvents containing different ratios of Chloroform : Methanol (indicated below)

i : *S. cerevisiae* WT - total lipids extract
ii : *S. cerevisiae* expressing AspRS-DUF2156 - total lipids extract

red asterisks: Lipid X

i *ii*   9 : 1   8 : 2   7 : 3   6 : 4

4 LC-MS/MS : Lipid X corresponds to Ergosteryl-Aspartate

Lipid X-enriched fractions were analyzed by LC-MS/MS (in collaboration with Dr. Herve Roy, Florida, USA). Lipid X was finally identified as **Ergosteryl 3β-O-aspartate (Erg-Asp)**.

Ergosterol

AspRS-DUF2156

Asp-tRNA^{Asp}

Ergosteryl-3β-O-aspartate
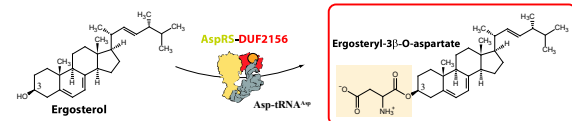
5 Functional probing of DUF2156 proteins

Mutations in tRNA-binding site (**red**), putative lipid binding site (**brown**) or active site (**blue**) decreased or abolished ergosterol modification activity.

DUF2156 domain Phyre2 model

GNAT domain I
lipid-binding site

GNAT domain II
aa-tRNA-binding site

Protein expressed in *S. cerevisiae*

Wild-type *Sce*
AspRS (ΔDUF2156)
AspRS-DUF2156 wild-type
AspRS-DUF2156 **N676A**
AspRS-DUF2156 **E711R**
AspRS-DUF2156 **E730R**
AspRS-DUF2156 **Q835R**
AspRS-DUF2156 **K837E**
AspRS-DUF2156 **Q835R K837E**

Protein expressed in *S. cerevisiae*

AspRS ΔDUF2156
AspRS-DUF2156 wild-type
AspRS-DUF2156 α5 (Ala)
AspRS-DUF2156 α5 (Glu)
AspRS-DUF2156 **W784A**
AspRS-DUF2156 **W784H**
AspRS-DUF2156 **R788A**

Helix α$_5$

In vivo
Heterologous Yeast model

In vitro
Purified AspRS-DUF2156

In vitro RESULTS

1 Recombinant AspRS-DUF2156 purification
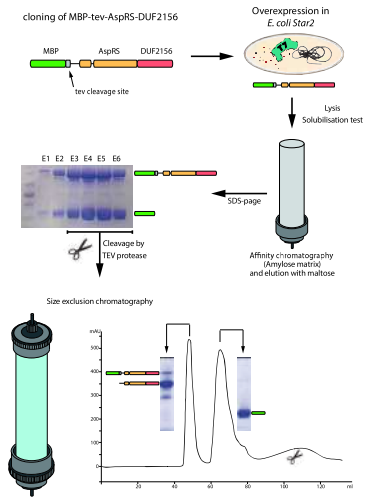
cloning of MBP-tev-AspRS-DUF2156

Overexpression in *E. coli Star2*

tev cleavage site

Lysis
Solubilisation test

SDS-page

Cleavage by TEV protease

Affinity chromatography (Amylose matrix) and elution with maltose

Size exclusion chromatography

2 *In vitro* tRNA aminoacylation assay

Assays with radiolabeled Asp proved that the **AspRS-DUF2156** is active for tRNA^{Asp} aminoacylation *in vitro*.

▲ AspRS-DUF2156 *A. fumigatus*
□ AspRS-DUF2156 *A. oryzae*
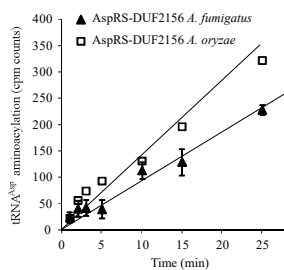
3 *In vitro* amino acid transfer assay

Consistant with *in vivo* experiments, **DUF2156 domain of AspRS-DUF2156 transfers Asp from Asp-tRNA^{Asp} onto Ergosterol**.

red asterisks: Lipid X

	Total lipids from *S. cerevisiae*					PG
Enzyme from	*Afm*	*Afm*	*Aor*	*Afm*	*Afm*	*Afm*
Front						
[14C]-Asp-LX1						
[14C]-Asp-LX2						
Spots						
AspRS-DUF2156	+	−	+	+	+	+
AspRS ΔDUF2156	−	+	−	−	−	−
RNase	−	−	−	+	−	−

PERSPECTIVES

- Similar investigations in progress for fDUF2156
- 3D structure (Dr. C. Sauter ; IBMC)
- Antibody synthesis
- Cinetic parameters
- 3D structure w/wo ligands - *in silico* compound screening
- Interactome (GST-Pull-down, immunoprecipitation)
- Localization

- Physiological function (Virulence / Resistance tests)

AspRS-DUF2156 KO

Antifungal drugs
-Amphothericine B
-Fluconazole
-Voriconazole

A. fumigatus
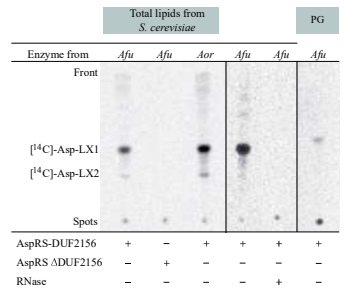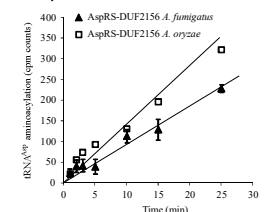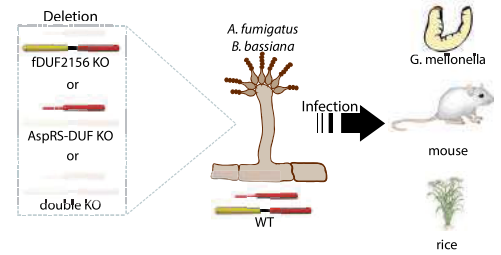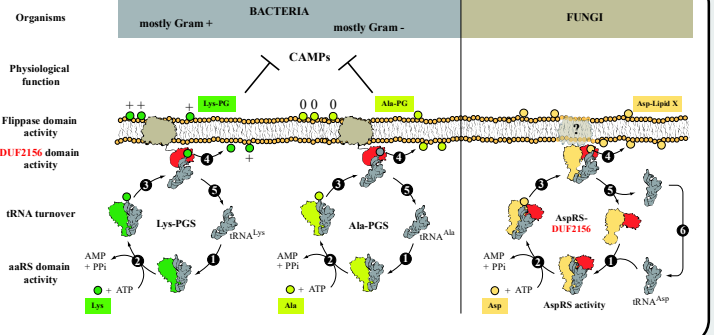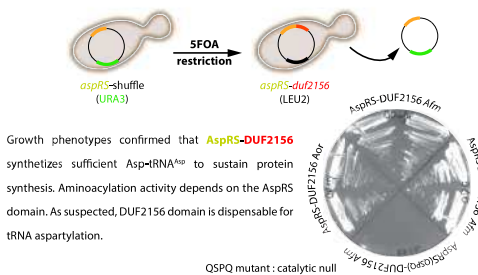*B. bassiana*
A. oryzae

Mouse

G. mellonella

Rice

1. Crick, F.H. (*1958*) Symposia of the SEB (**12**), 138163
2. Smirnova, E.V., (*2012*) (**77**), 15-25.
3. Roy, H. (*2009*) IUBMB Life , (**61**)10 : 940-953

Oral presentation

Yakobov *et al.*, 2018

Characterization of MprF-like lipid aminoacylation factors in fungi

27th tRNA conference, Sep. 23rd-27th, 2018, Strasbourg, Alsace, France

O6.8
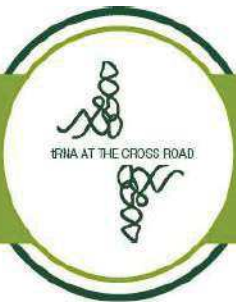
Characterizaton of MprF-like lipid aminoacylation factors in fungi

Yakobov, N [1], Fischer, F. [1,*] Senger, B. [1], Roy, H. [2], Kushiro, T. [3], Mouyna, I. [4], Fontaine, T. [4], Latgé, J.- P. [4], Becker, H. D[1,*]

[1] Génétique Moléculaire, Génomique, Microbiologie, UMR 7156, CNRS, Université de Strasbourg, 28 Rue Goethe, 67084 Strasbourg, Cedex, France [2] Burnett School of Biomedical Sciences, College of Medicine, University of Central Florida, Orlando, FL 32826, USA
[3] Graduate School of Agriculture Meiji University, 1-1-1 Higashimita,Tama-ku, Kawasaki Kanagawa 214-8571, Japan [4] Unité des Aspergillus, Institut Pasteur, 25 rue du Docteur Roux, 75724, Paris Cedex 15, France
*
  email: h.becker@unistra.fr, frfischer@unistra.fr

Appart from protein synthesis, aminoacyl-tRNAs (aa-tRNA) can be substrates of aminoacyl- tRNA transferases (ATT). In bacteria, DUF2156 domain-containing proteins catalyze the transfer of aa from aa-tRNA to an acceptor substrate. For example, MprF (Multiple Peptides Resistance Factors) are ATT that transfer lysine onto membrane lipids, which changes the charge properties of membranes and favor cationic antimicrobial peptides (cAMPs) resistance. MprF proteins were thought to be restricted to prokaryotes.

However, we discovered two types of DUF2156 proteins in fungi, including human pathogens such as Aspergillus fumigatus. We characterized both protein types from Aspergillus species both in vitro and in vivo and confirmed their capacity to modify lipids in a tRNA dependent manner. They appear to be structurally and functionally homologous to bacterial MprF. Further analyses confirmed that fungal DUF2156 enzymes, and the corresponding lipid modifications that they catalyze, are conserved in most of fungi.

BIBLIOGRAPHY

A

Adams, J. M., and M. R. Capecchi. 1966. 'N-formylmethionyl-sRNA as the initiator of protein synthesis', *Proc Natl Acad Sci U S A*, 55: 147-55.

Ador, L., A. Camasses, P. Erbs, J. Cavarelli, D. Moras, J. Gangloff, and G. Eriani. 1999. 'Active site mapping of yeast aspartyl-tRNA synthetase by in vivo selection of enzyme mutations lethal for cell growth', *J Mol Biol*, 288: 231-42.

Alcazar-Fuoli, L., and E. Mellado. 2012. 'Ergosterol biosynthesis in Aspergillus fumigatus: its relevance as an antifungal target and role in antifungal drug resistance', *Front Microbiol*, 3: 439.

Alvarez, F. J., L. M. Douglas, and J. B. Konopka. 2007. 'Sterol-rich plasma membrane domains in fungi', *Eukaryot Cell*, 6: 755-63.

Alvarez, H. M., and A. Steinbuchel. 2002. 'Triacylglycerols in prokaryotic microorganisms', *Appl Microbiol Biotechnol*, 60: 367-76.

Arendt, W., M. K. Groenewold, S. Hebecker, J. S. Dickschat, and J. Moser. 2013. 'Identification and characterization of a periplasmic aminoacyl-phosphatidylglycerol hydrolase responsible for Pseudomonas aeruginosa lipid homeostasis', *J Biol Chem*, 288: 24717-30.

Arendt, W., S. Hebecker, S. Jager, M. Nimtz, and J. Moser. 2012. 'Resistance phenotypes mediated by aminoacyl-phosphatidylglycerol synthases', *J Bacteriol*, 194: 1401-16.

Asahara, H., H. Himeno, K. Tamura, T. Hasegawa, K. Watanabe, and M. Shimizu. 1993. 'Recognition nucleotides of Escherichia coli tRNA(Leu) and its elements facilitating discrimination from tRNASer and tRNA(Tyr)', *J Mol Biol*, 231: 219-29.

Atila, M., G. Katselis, P. Chumala, and Y. Luo. 2016. 'Characterization of N-Succinylation of L-Lysylphosphatidylglycerol in Bacillus subtilis Using Tandem Mass Spectrometry', *J Am Soc Mass Spectrom*, 27: 1606-13.

Atila, M., and Y. Luo. 2016. 'Profiling and tandem mass spectrometry analysis of aminoacylated phospholipids in Bacillus subtilis', *F1000Res*, 5: 121.

B

Bagley, M. C., J. W. Dale, E. A. Merritt, and X. Xiong. 2005. 'Thiopeptide antibiotics', *Chem Rev*, 105: 685-714.

Bailly, M., M. Blaise, B. Lorber, H. D. Becker, and D. Kern. 2007. 'The transamidosome: a dynamic ribonucleoprotein particle dedicated to prokaryotic tRNA-dependent asparagine biosynthesis', *Mol Cell*, 28: 228-39.

Bain, J. M., A. Tavanti, A. D. Davidson, M. D. Jacobsen, D. Shaw, N. A. Gow, and F. C. Odds. 2007. 'Multilocus sequence typing of the pathogenic fungus Aspergillus fumigatus', *J Clin Microbiol*, 45: 1469-77.

Bao, Y., T. Sakinc, D. Laverde, D. Wobser, A. Benachour, C. Theilacker, A. Hartke, and J. Huebner. 2012. 'Role of mprF1 and mprF2 in the pathogenicity of Enterococcus faecalis', *PLoS One*, 7: e38458.

Bayer, A. S., T. Schneider, and H. G. Sahl. 2013. 'Mechanisms of daptomycin resistance in Staphylococcus aureus: role of the cell membrane and cell wall', *Ann N Y Acad Sci*, 1277: 139-58.

Bayram, O., O. S. Bayram, O. Valerius, B. Johnk, and G. H. Braus. 2012. 'Identification of protein complexes from filamentous fungi with tandem affinity purification', *Methods Mol Biol*, 944: 191-205.

Becker, H. D., and D. Kern. 1998. 'Thermus thermophilus: a link in evolution of the tRNA-dependent amino acid amidation pathways', *Proc Natl Acad Sci U S A*, 95: 12832-7.

Becker, H. D., J. Reinbolt, R. Kreutzer, R. Giege, and D. Kern. 1997. 'Existence of two distinct aspartyl-tRNA synthetases in Thermus thermophilus. Structural and biochemical properties of the two enzymes', *Biochemistry*, 36: 8785-97.

Beikirch, H., F. von der Haar, and F. Cramer. 1972. 'Tyrosyl-tRNA synthetase from baker's yeast. Isolation and some properties', *Eur J Biochem*, 26: 182-90.

Beining, P. R., E. Huff, B. Prescott, and T. S. Theodore. 1975. 'Characterization of the lipids of mesosomal vesicles and plasma membranes from Staphylococcus aureus', *J Bacteriol*, 121: 137-43.

Belrhali, H., A. Yaremchuk, M. Tukalo, K. Larsen, C. Berthet-Colominas, R. Leberman, B. Beijer, *et al.* 1994. 'Crystal structures at 2.5 angstrom resolution of seryl-tRNA synthetase complexed with two analogs of seryl adenylate', *Science*, 263: 1432-6.

Benson, T. E., D. B. Prince, V. T. Mutchler, K. A. Curry, A. M. Ho, R. W. Sarver, J. C. Hagadorn, G. H. Choi, and R. L. Garlick. 2002. 'X-ray crystal structure of Staphylococcus aureus FemA', *Structure*, 10: 1107-15.

Berry, M. J., L. Banu, J. W. Harney, and P. R. Larsen. 1993. 'Functional characterization of the eukaryotic SECIS elements which direct selenocysteine insertion at UGA codons', *EMBO J*, 12: 3315-22.

Beuning, P. J., and K. Musier-Forsyth. 1999. 'Transfer RNA recognition by aminoacyl-tRNA synthetases', *Biopolymers*, 52: 1-28.

Bhattacharya, S., B. D. Esquivel, and T. C. White. 2018. 'Overexpression or Deletion of Ergosterol Biosynthesis Genes Alters Doubling Time, Response to Stress Agents, and Drug Susceptibility in Saccharomyces cerevisiae', *mBio*, 9.

Bilokapic, S., J. Rokov Plavec, N. Ban, and I. Weygand-Durasevic. 2008. 'Structural flexibility of the methanogenic-type seryl-tRNA synthetase active site and its implication for specific substrate recognition', *FEBS J*, 275: 2831-44.

Birch, M., D. B. Drucker, I. Riba, S. J. Gaskell, and D. W. Denning. 1998. 'Polar lipids of Aspergillus fumigatus, A. niger, A. nidulans, A. flavus and A. terreus', *Med Mycol*, 36: 127-34.

Bittman, R., and S. A. Fischkoff. 1972. 'Fluorescence studies of the binding of the polyene antibiotics filipin 3, amphotericin B, nystatin, and lagosin to cholesterol', *Proc Natl Acad Sci U S A*, 69: 3795-9.

Blass, J. 1956. '[Nitrogen constituents of Vibrio comma phosphatides]', *Bull Soc Chim Biol (Paris)*, 38: 1305-14.

Bligh, E. G., and W. J. Dyer. 1959. 'A rapid method of total lipid extraction and purification', *Can J Biochem Physiol*, 37: 911-7.

Blight, S. K., R. C. Larue, A. Mahapatra, D. G. Longstaff, E. Chang, G. Zhao, P. T. Kang, *et al.* 2004. 'Direct charging of tRNA(CUA) with pyrrolysine in vitro and in vivo', *Nature*, 431: 333-5.

Blum, G., C. Hortnagl, E. Jukic, T. Erbeznik, T. Pumpel, H. Dietrich, M. Nagl, *et al.* 2013. 'New insight into amphotericin B resistance in Aspergillus terreus', *Antimicrob Agents Chemother*, 57: 1583-8.

Bouic, P. J. 2001. 'The role of phytosterols and phytosterolins in immune modulation: a review of the past 10 years', *Curr Opin Clin Nutr Metab Care*, 4: 471-5.

Brownell, J. E., J. Zhou, T. Ranalli, R. Kobayashi, D. G. Edmondson, S. Y. Roth, and C. D. Allis. 1996. 'Tetrahymena histone acetyltransferase A: a homolog to yeast Gcn5p linking histone acetylation to gene activation', *Cell*, 84: 843-51.

Bult, C. J., O. White, G. J. Olsen, L. Zhou, R. D. Fleischmann, G. G. Sutton, J. A. Blake, *et al.* 1996. 'Complete genome sequence of the methanogenic archaeon, Methanococcus jannaschii', *Science*, 273: 1058-73.

Busso, D., B. Delagoutte-Busso, and D. Moras. 2005. 'Construction of a set Gateway-based destination vectors for high-throughput cloning and expression screening in Escherichia coli', *Anal Biochem*, 343: 313-21.

C

Canny, M. D., F. M. Jucker, E. Kellogg, A. Khvorova, S. D. Jayasena, and A. Pardi. 2004. 'Fast cleavage kinetics of a natural hammerhead ribozyme', *J Am Chem Soc*, 126: 10848-9.

Carter, C. W., and W. L. Duax. 2002. 'Did tRNA synthetase classes arise on opposite strands of the same gene?', *Mol Cell*, 10: 705-8.

Cavarelli, J., G. Eriani, B. Rees, M. Ruff, M. Boeglin, A. Mitschler, F. Martin, *et al.* 1994. 'The active site of yeast aspartyl-tRNA synthetase: structural and functional aspects of the aminoacylation reaction', *EMBO J*, 13: 327-37.

Chabrol, EC.; Charonnat, R. . 1937. 'Une nouvelle reaction pour l'études des lipides: l'oleidemie. ', *La Presse Medicale*, 45: 1713–14.

Chambers, I., J. Frampton, P. Goldfarb, N. Affara, W. McBain, and P. R. Harrison. 1986. 'The structure of the mouse glutathione peroxidase gene: the selenocysteine in the active site is encoded by the 'termination' codon, TGA', *EMBO J*, 5: 1221-7.

Chan, P. P., and T. M. Lowe. 2009. 'GtRNAdb: a database of transfer RNA genes detected in genomic sequence', *Nucleic Acids Res*, 37: D93-7.

Chan, P. P., and T. M. Lowe. 2016. 'GtRNAdb 2.0: an expanded database of transfer RNA genes identified in complete and draft genomes', *Nucleic Acids Res*, 44: D184-9.

Chatterjee, C., M. Paul, L. Xie, and W. A. van der Donk. 2005. 'Biosynthesis and mode of action of lantibiotics', *Chem Rev*, 105: 633-84.

Chauhan, N., Y. Y. Sere, A. M. Sokol, J. Graumann, and A. K. Menon. 2020. 'A PhotoClick cholesterol-based quantitative proteomics screen for cytoplasmic sterol-binding proteins in Saccharomyces cerevisiae', *Yeast*, 37: 15-25.

Choudhary, V., R. Darwiche, D. Gfeller, V. Zoete, O. Michielin, and R. Schneiter. 2014. 'The caveolin-binding motif of the pathogen-related yeast protein Pry1, a member of the CAP protein superfamily, is required for in vivo export of cholesteryl acetate', *J Lipid Res*, 55: 883-94.

Choudhary, V., and R. Schneiter. 2012. 'Pathogen-Related Yeast (PRY) proteins and members of the CAP superfamily are secreted sterol-binding proteins', *Proc Natl Acad Sci U S A*, 109: 16882-7.

Cirigliano, A., A. Macone, M. M. Bianchi, S. Oliaro-Bosso, G. Balliano, R. Negri, and T. Rinaldi. 2019. 'Ergosterol reduction impairs mitochondrial DNA maintenance in S. cerevisiae', *Biochim Biophys Acta Mol Cell Biol Lipids*, 1864: 290-303.

Clejan, S., T. A. Krulwich, K. R. Mondrus, and D. Seto-Young. 1986. 'Membrane lipid composition of obligately and facultatively alkalophilic strains of Bacillus spp', *J Bacteriol*, 168: 334-40.

Cone, J. E., R. M. Del Rio, J. N. Davis, and T. C. Stadtman. 1976. 'Chemical characterization of the selenoprotein component of clostridial glycine reductase: identification of selenocysteine as the organoselenium moiety', *Proc Natl Acad Sci U S A*, 73: 2659-63.

Contreras, I., L. Shapiro, and S. Henry. 1978. 'Membrane phospholipid composition of Caulobacter crescentus', *J Bacteriol*, 135: 1130-6.

Crick, F. 1970. 'Central dogma of molecular biology', *Nature*, 227: 561-3.

Crick, F. H. 1966. 'Codon--anticodon pairing: the wobble hypothesis', *J Mol Biol*, 19: 548-55.

Crick, F. H. C. 1956. 'On degenerate templates and the adaptator hypothesis. A note for the RNA Tie Club.

'.

Curnow, A. W., Kw Hong, R. Yuan, Si Kim, O. Martins, W. Winkler, T. M. Henkin, and D. Soll. 1997. 'Glu-tRNAGln amidotransferase: a novel heterotrimeric enzyme required for correct decoding of glutamine codons during translation', *Proc Natl Acad Sci U S A*, 94: 11819-26.

Cusack, S. 1995. 'Eleven down and nine to go', *Nat Struct Biol*, 2: 824-31.

Custer, J. E., B. D. Goddard, S. F. Matter, and E. S. Kaneshiro. 2014. 'The relative proportions of different lipid classes and their fatty acid compositions change with culture age in the cariogenic dental pathogen Streptococcus mutans UA159', *Lipids*, 49: 543-54.

D

da Silva Ferreira, M. E., I. Malavazi, M. Savoldi, A. A. Brakhage, M. H. Goldman, H. S. Kim, W. C. Nierman, and G. H. Goldman. 2006. 'Transcriptome analysis of Aspergillus fumigatus exposed to voriconazole', *Curr Genet*, 50: 32-44.

Dare, K., and M. Ibba. 2012. 'Roles of tRNA in cell wall biosynthesis', *Wiley Interdiscip Rev RNA*, 3: 247-64.

Dare, K., J. Shepherd, H. Roy, S. Seveau, and M. Ibba. 2014. 'LysPGS formation in Listeria monocytogenes has broad roles in maintaining membrane integrity beyond antimicrobial peptide resistance', *Virulence*, 5: 534-46.

Darwiche, R., and R. Schneiter. 2017. 'A Ligand-Binding Assay to Measure the Affinity and Specificity of Sterol-Binding Proteins In Vitro', *Methods Mol Biol*, 1645: 361-68.

Datt, M., and A. Sharma. 2014. 'Novel and unique domains in aminoacyl-tRNA synthetases from human fungal pathogens Aspergillus niger, Candida albicans and Cryptococcus neoformans', *BMC Genomics*, 15: 1069.

Daum, G., N. D. Lees, M. Bard, and R. Dickson. 1998. 'Biochemistry, cell biology and molecular biology of lipids of Saccharomyces cerevisiae', *Yeast*, 14: 1471-510.

De Siervo, A. J., and A. D. Homola. 1980. 'Analysis of caulobacter crescentus lipids', *J Bacteriol*, 143: 1215-22.

Debard, S. 2019. 'Molecular dynamic of the methionyl-tRNA synthetase and its novel non-canonical functions in the yeast S. cerevisiae. PhD Thesis. ', University Of Strasbourg.

Debeaupuis, J. P., J. Sarfati, V. Chazalet, and J. P. Latge. 1997. 'Genetic diversity among clinical and environmental isolates of Aspergillus fumigatus', *Infect Immun*, 65: 3080-5.

den Kamp, J. A., I. Redai, and L. L. van Deenen. 1969. 'Phospholipid composition of Bacillus subtilis', *J Bacteriol*, 99: 298-303.

den Kamp, Ja Op, U. M. Houtsmuller, and L. L. van Deenen. 1965. 'On the phospholipids of Bacillus megaterium', *Biochim Biophys Acta*, 106: 438-41.

Dever, T. E., T. G. Kinzy, and G. D. Pavitt. 2016. 'Mechanism and Regulation of Protein Synthesis in Saccharomyces cerevisiae', *Genetics*, 203: 65-107.

Dey, A., and D. Wall. 2014. 'A genetic screen in Myxococcus xanthus identifies mutants that uncouple outer membrane exchange from a downstream cellular response', *J Bacteriol*, 196: 4324-32.

Dhingra, S., and R. A. Cramer. 2017. 'Regulation of Sterol Biosynthesis in the Human Fungal Pathogen Aspergillus fumigatus: Opportunities for Therapeutic Development', *Front Microbiol*, 8: 92.

Dock-Bregeon, A. C., A. Garcia, R. Giege, and D. Moras. 1990. 'The contacts of yeast tRNA(Ser) with seryl-tRNA synthetase studied by footprinting experiments', *Eur J Biochem*, 188: 283-90.

Doherty, E. A., and J. A. Doudna. 2000. 'Ribozyme structures and mechanisms', *Annu Rev Biochem*, 69: 597-615.

Donald, P. R., J. H. Lamprecht, M. Freestone, C. F. Albrecht, P. J. Bouic, D. Kotze, and P. P. van Jaarsveld. 1997. 'A randomised placebo-controlled trial of the efficacy of beta-sitosterol and its glucoside as adjuvants in the treatment of pulmonary tuberculosis', *Int J Tuberc Lung Dis*, 1: 518-22.

dos Santos Mota, J. M., J. A. den Kamp, H. M. Verheij, and L. L. van Deenen. 1970. 'Phospholipids of Streptococcus faecalis', *J Bacteriol*, 104: 611-9.

Douglas, L. M., and J. B. Konopka. 2014. 'Fungal membrane organization: the eisosome concept', *Annu Rev Microbiol*, 68: 377-93.

Dyer, P. S., and C. M. O'Gorman. 2012. 'Sexual development and cryptic sexuality in fungi: insights from Aspergillus species', *FEMS Microbiol Rev*, 36: 165-92.

E

Ejsing, C. S., J. L. Sampaio, V. Surendranath, E. Duchoslav, K. Ekroos, R. W. Klemm, K. Simons, and A. Shevchenko. 2009. 'Global analysis of the yeast lipidome by quantitative shotgun mass spectrometry', *Proc Natl Acad Sci U S A*, 106: 2136-41.

El-Gebali, S., J. Mistry, A. Bateman, S. R. Eddy, A. Luciani, S. C. Potter, M. Qureshi, *et al.* 2019. 'The Pfam protein families database in 2019', *Nucleic Acids Res*, 47: D427-D32.

Epand, R. F., P. B. Savage, and R. M. Epand. 2007. 'Bacterial lipid composition and the antimicrobial efficacy of cationic steroid compounds (Ceragenins)', *Biochim Biophys Acta*, 1768: 2500-9.

Epand, R. F., M. A. Schmitt, S. H. Gellman, and R. M. Epand. 2006. 'Role of membrane lipids in the mechanism of bacterial species selective toxicity by two alpha/beta-antimicrobial peptides', *Biochim Biophys Acta*, 1758: 1343-50.

Eriani, G., J. Cavarelli, F. Martin, G. Dirheimer, D. Moras, and J. Gangloff. 1993. 'Role of dimerization in yeast aspartyl-tRNA synthetase and importance of the class II invariant proline', *Proc Natl Acad Sci U S A*, 90: 10816-20.

Eriani, G., M. Delarue, O. Poch, J. Gangloff, and D. Moras. 1990. 'Partition of tRNA synthetases into two classes based on mutually exclusive sets of sequence motifs', *Nature*, 347: 203-6.

Ernst, C. M., S. Kuhn, C. J. Slavetinsky, B. Krismer, S. Heilbronner, C. Gekeler, D. Kraus, S. Wagner, and A. Peschel. 2015. 'The lipid-modifying multiple peptide resistance factor is an oligomer consisting of distinct interacting synthase and flippase subunits', *mBio*, 6.

Ernst, C. M., and A. Peschel. 2011. 'Broad-spectrum antimicrobial peptide resistance by MprF-mediated aminoacylation and flipping of phospholipids', *Mol Microbiol*, 80: 290-9.

Ernst, C. M., and A. Peschel. 2019. 'MprF-mediated daptomycin resistance', *Int J Med Microbiol*, 309: 359-63.

Ernst, C. M., C. J. Slavetinsky, S. Kuhn, J. N. Hauser, M. Nega, N. N. Mishra, C. Gekeler, A. S. Bayer, and A. Peschel. 2018. 'Gain-of-Function Mutations in the Phospholipid Flippase MprF Confer Specific Daptomycin Resistance', *mBio*, 9.

Ernst, C. M., P. Staubitz, N. N. Mishra, S. J. Yang, G. Hornig, H. Kalbacher, A. S. Bayer, D. Kraus, and A. Peschel. 2009. 'The bacterial defensin resistance protein MprF consists of separable domains for lipid lysinylation and antimicrobial peptide repulsion', *PLoS Pathog*, 5: e1000660.

F

Fantini, J., C. Di Scala, C. J. Baier, and F. J. Barrantes. 2016. 'Molecular mechanisms of protein-cholesterol interactions in plasma membranes: Functional distinction between topological (tilted) and consensus (CARC/CRAC) domains', *Chem Phys Lipids*, 199: 52-60.

Favrot, L., J. S. Blanchard, and O. Vergnolle. 2016. 'Bacterial GCN5-Related N-Acetyltransferases: From Resistance to Regulation', *Biochemistry*, 55: 989-1002.

Fechter, P., J. Rudinger, R. Giege, and A. Theobald-Dietrich. 1998. 'Ribozyme processed tRNA transcripts with unfriendly internal promoter for T7 RNA polymerase: production and activity', *FEBS Lett*, 436: 99-103.

Feofilova, E. P., Y. E. Sergeeva, I. S. Mysyakina, and D. A. Bokareva. 2015. '[Lipid Composition in Cell Walls and in Mycelial and Spore Cells of Mycelial Fungi]', *Mikrobiologiia*, 84: 204-11.

Fields, R. N., and H. Roy. 2018. 'Deciphering the tRNA-dependent lipid aminoacylation systems in bacteria: Novel components and structural advances', *RNA Biol*, 15: 480-91.

Fischer, R., N. Zekert, and N. Takeshita. 2008. 'Polarized growth in fungi--interplay between the cytoskeleton, positional markers and membrane domains', *Mol Microbiol*, 68: 813-26.

Fischer, W., and D. Arneth-Seifert. 1998. 'D-Alanylcardiolipin, a major component of the unique lipid pattern of Vagococcus fluvialis', *J Bacteriol*, 180: 2950-7.

Fischer, W., and K. Leopold. 1999. 'Polar lipids of four Listeria species containing L-lysylcardiolipin, a novel lipid structure, and other unique phospholipids', *Int J Syst Bacteriol*, 49 Pt 2: 653-62.

Fol, M., A. Globinska, P. Staczek, M. Kowalewicz-Kulbat, M. Druszczynska, M. V. Madiraju, and W. Rudnicka. 2013. 'The lack of L-PG production and the repercussions of it in regards to M. Tuberculosis interactions with mononuclear phagocytes', *Acta Microbiol Immunol Hung*, 60: 127-44.

Folch, J., M. Lees, and G. H. Sloane Stanley. 1957. 'A simple method for the isolation and purification of total lipides from animal tissues', *J Biol Chem*, 226: 497-509.

Fonvielle, M., I. Li de La Sierra-Gallay, A. H. El-Sagheer, M. Lecerf, D. Patin, D. Mellal, C. Mayer, *et al.* 2013. 'The structure of FemX(Wv) in complex with a peptidyl-RNA conjugate: mechanism of aminoacyl transfer from Ala-tRNA(Ala) to peptidoglycan precursors', *Angew Chem Int Ed Engl*, 52: 7278-81.

Francklyn, C., and P. Schimmel. 1989. 'Aminoacylation of RNA minihelices with alanine', *Nature*, 337: 478-81.

Frechin, M., D. Kern, R. P. Martin, H. D. Becker, and B. Senger. 2010. 'Arc1p: anchoring, routing, coordinating', *FEBS Lett*, 584: 427-33.

Frechin, M., B. Senger, M. Braye, D. Kern, R. P. Martin, and H. D. Becker. 2009. 'Yeast mitochondrial Gln-tRNA(Gln) is generated by a GatFAB-mediated transamidation pathway involving Arc1p-controlled subcellular sorting of cytosolic GluRS', *Genes Dev*, 23: 1119-30.

Fuchs, B., R. Suss, K. Teuber, M. Eibisch, and J. Schiller. 2011. 'Lipid analysis by thin-layer chromatography--a review of the current state', *J Chromatogr A*, 1218: 2754-74.

Fujino, T., Y. Goto, H. Suga, and H. Murakami. 2013. 'Reevaluation of the D-amino acid compatibility with the elongation event in translation', *J Am Chem Soc*, 135: 1830-7.

G

Gaby, W. L., R. N. Naughten, and C. Logan. 1959. 'The role of phospholipides in the metabolism of amino acids by the mold Penicillium chrysogenum', *Arch Biochem Biophys*, 82: 34-41.

Gaby, W. L., and R. Silberman. 1960. 'The role of phospholipides in the metabolism of amino acids. II. The incorporation of leucine and tyrosine in liver phospholipides', *Arch Biochem Biophys*, 87: 188-92.

Gale, E. F., and J. P. Folkes. 1965. 'The Incorporation of Glycerol and Lysine into the Lipid Fraction of Staphylococcus Aureus', *Biochem J*, 94: 390-400.

Garg, R. P., X. L. Qian, L. B. Alemany, S. Moran, and R. J. Parry. 2008. 'Investigations of valanimycin biosynthesis: elucidation of the role of seryl-tRNA', *Proc Natl Acad Sci U S A*, 105: 6543-7.

Gautam, P., J. Shankar, T. Madan, R. Sirdeshmukh, C. S. Sundaram, W. N. Gade, S. F. Basir, and P. U. Sarma. 2008. 'Proteomic and transcriptomic analysis of Aspergillus fumigatus on exposure to amphotericin B', *Antimicrob Agents Chemother*, 52: 4220-7.

Geiger, O., N. Gonzalez-Silva, I. M. Lopez-Lara, and C. Sohlenkamp. 2010. 'Amino acid-containing membrane lipids in bacteria', *Prog Lipid Res*, 49: 46-60.

Gibson, D. G. 2011. 'Enzymatic assembly of overlapping DNA fragments', *Methods Enzymol*, 498: 349-61.

Gibson, D. G., L. Young, R. Y. Chuang, J. C. Venter, C. A. Hutchison, 3rd, and H. O. Smith. 2009. 'Enzymatic assembly of DNA molecules up to several hundred kilobases', *Nat Methods*, 6: 343-5.

Gidden, J., J. Denson, R. Liyanage, D. M. Ivey, and J. O. Lay. 2009. 'Lipid Compositions in Escherichia coli and Bacillus subtilis During Growth as Determined by MALDI-TOF and TOF/TOF Mass Spectrometry', *Int J Mass Spectrom*, 283: 178-84.

Giege, R., M. Sissler, and C. Florentz. 1998. 'Universal rules and idiosyncratic features in tRNA identity', *Nucleic Acids Res*, 26: 5017-35.

Giessen, T. W., and M. A. Marahiel. 2012. 'Ribosome-independent biosynthesis of biologically active peptides: Application of synthetic biology to generate structural diversity', *FEBS Lett*, 586: 2065-75.

Gietz, R. D., and R. A. Woods. 2002. 'Transformation of yeast by lithium acetate/single-stranded carrier DNA/polyethylene glycol method', *Methods Enzymol*, 350: 87-96.

Goldgur, Y., L. Mosyak, L. Reshetnikova, V. Ankilova, O. Lavrik, S. Khodyreva, and M. Safro. 1997. 'The crystal structure of phenylalanyl-tRNA synthetase from thermus thermophilus complexed with cognate tRNAPhe', *Structure*, 5: 59-68.

Gondry, M., L. Sauguet, P. Belin, R. Thai, R. Amouroux, C. Tellier, K. Tuphile, *et al.* 2009. 'Cyclodipeptide synthases are a family of tRNA-dependent peptide bond-forming enzymes', *Nat Chem Biol*, 5: 414-20.

Goswami, S. K., and C. F. Frey. 1970. 'Manganous chloride spray reagent for cholesterol and bile acids on thin-layer chromatograms', *J Chromatogr*, 53: 389-90.

Gould, R. M., and W. J. Lennarz. 1967. 'Biosynthesis of aminoacyl derivatives of phosphatidylglycerol', *Biochem Biophys Res Commun*, 26: 512-5.

Gould, R. M., and W. J. Lennarz. 1970. 'Metabolism of Phosphatidylglycerol and Lysyl Phosphatidylglycerol in Staphylococcus aureus', *J Bacteriol*, 104: 1135-44.

Gould, R. M., M. P. Thornton, V. Liepkalns, and W. J. Lennarz. 1968. 'Participation of aminoacyl transfer ribonucleic acid in aminoacyl phosphatidylglycerol synthesis. II. Specificity of alanyl phosphatidylglycerol synthetase', *J Biol Chem*, 243: 3096-104.

Gray, K. C., D. S. Palacios, I. Dailey, M. M. Endo, B. E. Uno, B. C. Wilcock, and M. D. Burke. 2012. 'Amphotericin primarily kills yeast by simply binding ergosterol', *Proc Natl Acad Sci U S A*, 109: 2234-9.

Greenfield, E. A., J. DeCaprio, and M. Brahmandam. 2019. 'Preparing Protein Antigens from Sodium Dodecyl Sulfate-Polyacrylamide Gels for Immunization', *Cold Spring Harb Protoc*, 2019.

Griffiths, K. K., and P. Setlow. 2009. 'Effects of modification of membrane lipid composition on Bacillus subtilis sporulation and spore properties', *J Appl Microbiol*, 106: 2064-78.

Grille, S., A. Zaslawski, S. Thiele, J. Plat, and D. Warnecke. 2010. 'The functions of steryl glycosides come to those who wait: Recent advances in plants, fungi, bacteria and animals', *Prog Lipid Res*, 49: 262-88.

Groenewold, M. K., S. Hebecker, C. Fritz, S. Czolkoss, M. Wiesselmann, D. W. Heinz, D. Jahn, *et al.* 2019. 'Virulence of Agrobacterium tumefaciens requires lipid homeostasis mediated by the lysyl-phosphatidylglycerol hydrolase AcvB', *Mol Microbiol*, 111: 269-86.

Gsaller, F., P. Hortschansky, T. Furukawa, P. D. Carr, B. Rash, J. Capilla, C. Muller, *et al.* 2016. 'Sterol Biosynthesis and Azole Tolerance Is Governed by the Opposing Actions of SrbA and the CCAAT Binding Complex', *PLoS Pathog*, 12: e1005775.

Guo, M., and P. Schimmel. 2013. 'Essential nontranslational functions of tRNA synthetases', *Nat Chem Biol*, 9: 145-53.

Guo, M., and X. L. Yang. 2014. 'Architecture and metamorphosis', *Top Curr Chem*, 344: 89-118.

H

Haardt, M., and E. Bremer. 1996. 'Use of phoA and lacZ fusions to study the membrane topology of ProW, a component of the osmoregulated ProU transport system of Escherichia coli', *J Bacteriol*, 178: 5370-81.

Hachmann, A. B., E. R. Angert, and J. D. Helmann. 2009. 'Genetic analysis of factors affecting susceptibility of Bacillus subtilis to daptomycin', *Antimicrob Agents Chemother*, 53: 1598-609.

Haest, C. W., J. de Gier, Ja Op den Kamp, P. Bartels, and L. L. van Deenen. 1972. 'Chages in permeability of Staphylococcus aureus and derived liposomes with varying lipid composition', *Biochim Biophys Acta*, 255: 720-33.

Han, X., Y. Yang, F. Zhao, T. Zhang, and X. Yu. 2020. 'An improved protein lipid overlay assay for studying lipid-protein interactions', *Plant Methods*, 16: 33.

Hanus, L., E. Shohami, I. Bab, and R. Mechoulam. 2014. 'N-Acyl amino acids and their impact on biological processes', *Biofactors*, 40: 381-8.

Hartmann, T., M. Dumig, B. M. Jaber, E. Szewczyk, P. Olbermann, J. Morschhauser, and S. Krappmann. 2010. 'Validation of a self-excising marker in the human pathogen Aspergillus

fumigatus by employing the beta-rec/six site-specific recombination system', *Appl Environ Microbiol*, 76: 6313-7.

Hayes, B. M., M. A. Anderson, A. Traven, N. L. van der Weerden, and M. R. Bleackley. 2014. 'Activation of stress signalling pathways enhances tolerance of fungi to chemical fungicides and antifungal proteins', *Cell Mol Life Sci*, 71: 2651-66.

Hebecker, S., W. Arendt, I. U. Heinemann, J. H. Tiefenau, M. Nimtz, M. Rohde, D. Soll, and J. Moser. 2011. 'Alanyl-phosphatidylglycerol synthase: mechanism of substrate recognition during tRNA-dependent lipid modification in Pseudomonas aeruginosa', *Mol Microbiol*, 80: 935-50.

Hebecker, S., J. Krausze, T. Hasenkampf, J. Schneider, M. Groenewold, J. Reichelt, D. Jahn, D. W. Heinz, and J. Moser. 2015. 'Structures of two bacterial resistance factors mediating tRNA-dependent aminoacylation of phosphatidylglycerol with lysine or alanine', *Proc Natl Acad Sci U S A*, 112: 10691-6.

Hebeler, B. H., A. N. Chatterjee, and F. E. Young. 1973. 'Regulation of the bacterial cell wall: effect of antibiotics on lipid biosynthesis', *Antimicrob Agents Chemother*, 4: 346-53.

Heese-Peck, A., H. Pichler, B. Zanolari, R. Watanabe, G. Daum, and H. Riezman. 2002. 'Multiple functions of sterols in yeast endocytosis', *Mol Biol Cell*, 13: 2664-80.

Hemmerle, M., M. Wendenbaum, G. Grob, N. Yakobov, N. Mahmoudi, B. Senger, S. Debard, F. Fischer, and H. Becker. 2020. 'Noncanonical inputs and outputs of tRNA aminoacylation.' in, *The Enzymes*.

Hendler, R. W. 1959. 'Passage of radioactive amino acids through nonprotein fractions of hen oviduct during incorporation into protein', *J Biol Chem*, 234: 1466-73.

Henry, S. A., S. D. Kohlwein, and G. M. Carman. 2012. 'Metabolism and regulation of glycerolipids in the yeast Saccharomyces cerevisiae', *Genetics*, 190: 317-49.

Heuck, A. P., C. G. Savva, A. Holzenburg, and A. E. Johnson. 2007. 'Conformational changes that effect oligomerization and initiate pore formation are triggered throughout perfringolysin O upon binding to cholesterol', *J Biol Chem*, 282: 22629-37.

Hjelmstad, R. H., and R. M. Bell. 1990. 'The sn-1,2-diacylglycerol cholinephosphotransferase of Saccharomyces cerevisiae. Nucleotide sequence, transcriptional mapping, and gene product analysis of the CPT1 gene', *J Biol Chem*, 265: 1755-64.

Hoagland, M. B. 1955. 'An enzymic mechanism for amino acid activation in animal tissues', *Biochim Biophys Acta*, 16: 288-9.

Hoagland, M. B., M. L. Stephenson, J. F. Scott, L. I. Hecht, and P. C. Zamecnik. 1958. 'A soluble ribonucleic acid intermediate in protein synthesis', *J Biol Chem*, 231: 241-57.

Holley, R. W., J. Apgar, G. A. Everett, J. T. Madison, M. Marquisee, S. H. Merrill, J. R. Penswick, and A. Zamir. 1965. 'Structure of a Ribonucleic Acid', *Science*, 147: 1462-5.

Holm, L., and P. Rosenstrom. 2010. 'Dali server: conservation mapping in 3D', *Nucleic Acids Res*, 38: W545-9.

Holtta-Vuori, M., R. L. Uronen, J. Repakova, E. Salonen, I. Vattulainen, P. Panula, Z. Li, R. Bittman, and E. Ikonen. 2008. 'BODIPY-cholesterol: a new tool to visualize sterol trafficking in living cells and organisms', *Traffic*, 9: 1839-49.

Hopper, A. K. 2013. 'Transfer RNA post-transcriptional processing, turnover, and subcellular dynamics in the yeast Saccharomyces cerevisiae', *Genetics*, 194: 43-67.

Hopper, A. K., and R. T. Nostramo. 2019. 'tRNA Processing and Subcellular Trafficking Proteins Multitask in Pathways for Other RNAs', *Front Genet*, 10: 96.

Horn, F., T. Heinekamp, O. Kniemeyer, J. Pollmacher, V. Valiante, and A. A. Brakhage. 2012. 'Systems biology of fungal infection', *Front Microbiol*, 3: 108.

Hossain, A., and N. R. Kallenbach. 1974. 'Purification and subunit structure of tryptophanyl tRNA synthetase (TRS) from baker's yeast', *FEBS Lett*, 45: 202-5.

Hou, Y. M., and J. J Perona. 2005. 'Cysteinyl-tRNA synthetases', *Aminoacyl-tRNA synthetases (Ibba, M. Francklyn, C. and Cusack, S., Landes Biosciences Eds.)*: 12-23.

Houtsmuller, U. M., and Deenen L. van. 1963. 'Identification of a bacterial phospholipid as an O-ornithine ester of phosphatidyl glycerol', *Biochim Biophys Acta*, 70: 211-3.

Houtsmuller, U. M., and Deenen L. Van. 1964. 'On the Accumulation of Amino Acid Derivatives of Phosphatidylglycerol in Bacteria', *Biochim Biophys Acta*, 84: 96-8.

Houtsmuller, U. M., and L. L. van Deenen. 1965. 'On the amino acid esters of phosphatidyl glycerol from bacteria', *Biochim Biophys Acta*, 106: 564-76.

Hu, Z., B. He, L. Ma, Y. Sun, Y. Niu, and B. Zeng. 2017. 'Recent Advances in Ergosterol Biosynthesis and Regulation Mechanisms in Saccharomyces cerevisiae', *Indian J Microbiol*, 57: 270-77.

Hubert, N., C. Sturchler, E. Westhof, P. Carbon, and A. Krol. 1998. 'The 9/4 secondary structure of eukaryotic selenocysteine tRNA: more pieces of evidence', *RNA*, 4: 1029-33.

Hunter, G. D., and R. A. Goodsall. 1961. 'Lipo-amino acid complexes from Bacillus megaterium and their possible role in protein synthesis', *Biochem J*, 78: 564-70.

I

Ibba, M., A. W. Curnow, and D. Soll. 1997. 'Aminoacyl-tRNA synthesis: divergent routes to a common goal', *Trends Biochem Sci*, 22: 39-42.

Ibba, M., H. C. Losey, Y. Kawarabayasi, H. Kikuchi, S. Bunjun, and D. Soll. 1999. 'Substrate recognition by class I lysyl-tRNA synthetases: a molecular basis for gene displacement', *Proc Natl Acad Sci U S A*, 96: 418-23.

J

Jacques, I. B., M. Moutiez, J. Witwinowski, E. Darbon, C. Martel, J. Seguin, E. Favry, *et al.* 2015. 'Analysis of 51 cyclodipeptide synthases reveals the basis for substrate specificity', *Nat Chem Biol*, 11: 721-7.

Jacquier, N., and R. Schneiter. 2012. 'Mechanisms of sterol uptake and transport in yeast', *J Steroid Biochem Mol Biol*, 129: 70-8.

Jakubowski, H. 2011. 'Quality control in tRNA charging -- editing of homocysteine', *Acta Biochim Pol*, 58: 149-63.

Jakubowski, H., and E. Goldman. 1992. 'Editing of errors in selection of amino acids for protein synthesis', *Microbiol Rev*, 56: 412-29.

Jayaprakasha, G. K., Y. Jadegoud, G. A. Nagana Gowda, and B. S. Patil. 2010. 'Bioactive compounds from sour orange inhibit colon cancer cell proliferation and induce cell cycle arrest', *J Agric Food Chem*, 58: 180-6.

Jin, H., J. M. McCaffery, and E. Grote. 2008. 'Ergosterol promotes pheromone signaling and plasma membrane fusion in mating yeast', *J Cell Biol*, 180: 813-26.

Johansson, L., C. Chen, J. O. Thorell, A. Fredriksson, S. Stone-Elander, G. Gafvelin, and E. S. Arner. 2004. 'Exploiting the 21st amino acid-purifying and labeling proteins by selenolate targeting', *Nat Methods*, 1: 61-6.

Johnson, C. M., and A. D. Grossman. 2016. 'The Composition of the Cell Envelope Affects Conjugation in Bacillus subtilis', *J Bacteriol*, 198: 1241-9.

Jones, D. E., and J. D. Smith. 1979. 'Phospholipids of the differentiating bacterium Caulobacter crescentus', *Can J Biochem*, 57: 424-8.

Jorda, T., and S. Puig. 2020. 'Regulation of Ergosterol Biosynthesis in Saccharomyces cerevisiae', *Genes (Basel)*, 11.

K

Kaminski, D. M. 2014. 'Recent progress in the study of the interactions of amphotericin B with cholesterol and ergosterol in lipid environments', *Eur Biophys J*, 43: 453-67.

Kandaswamy, K., T. H. Liew, C. Y. Wang, E. Huston-Warren, U. Meyer-Hoffert, K. Hultenby, J. M. Schroder, *et al.* 2013. 'Focal targeting by human beta-defensin 2 disrupts localized virulence factor assembly sites in Enterococcus faecalis', *Proc Natl Acad Sci U S A*, 110: 20230-5.

Kapust, R. B., J. Tozser, J. D. Fox, D. E. Anderson, S. Cherry, T. D. Copeland, and D. S. Waugh. 2001. 'Tobacco etch virus protease: mechanism of autolysis and rational design of stable mutants with wild-type catalytic proficiency', *Protein Eng*, 14: 993-1000.

Kapust, R. B., and D. S. Waugh. 1999. 'Escherichia coli maltose-binding protein is uncommonly effective at promoting the solubility of polypeptides to which it is fused', *Protein Sci*, 8: 1668-74.

Katz, A., S. Elgamal, A. Rajkovic, and M. Ibba. 2016. 'Non-canonical roles of tRNAs and tRNA mimics in bacterial cell biology', *Mol Microbiol*, 101: 545-58.

Kelley, L. A., S. Mezulis, C. M. Yates, M. N. Wass, and M. J. Sternberg. 2015. 'The Phyre2 web portal for protein modeling, prediction and analysis', *Nat Protoc*, 10: 845-58.

Kelly, S. L., D. C. Lamb, D. E. Kelly, N. J. Manning, J. Loeffler, H. Hebart, U. Schumacher, and H. Einsele. 1997. 'Resistance to fluconazole and cross-resistance to amphotericin B in Candida albicans from AIDS patients caused by defective sterol delta5,6-desaturation', *FEBS Lett*, 400: 80-2.

Kenward, M. A., M. R. Brown, and J. J. Fryer. 1979. 'The influence of calcium or manganese on the resistance to EDTA, polymyxin B or cold shock, and the composition of Pseudomonas aeruginosa grown in glucose- or magnesium-depleted batch cultures', *J Appl Bacteriol*, 47: 489-503.

Khuller, G. K., and D. Subrahmanyam. 1970. 'On the ornithinyl ester of phosphatidylglycerol of Mycobacterium 607', *J Bacteriol*, 101: 654-6.

Kikuma, T., T. Tadokoro, J. I. Maruyama, and K. Kitamoto. 2017. 'AoAtg26, a putative sterol glucosyltransferase, is required for autophagic degradation of peroxisomes, mitochondria, and nuclei in the filamentous fungus Aspergillus oryzae', *Biosci Biotechnol Biochem*, 81: 384-95.

Kim, S. H. 1978. 'Three-dimensional structure of transfer RNA and its functional implications', *Adv Enzymol Relat Areas Mol Biol*, 46: 279-315.

Kim, S. H., G. J. Quigley, F. L. Suddath, A. McPherson, D. Sneden, J. J. Kim, J. Weinzierl, and A. Rich. 1973. 'Three-dimensional structure of yeast phenylalanine transfer RNA: folding of the polynucleotide chain', *Science*, 179: 285-8.

Kim, S. H., F. L. Suddath, G. J. Quigley, A. McPherson, J. L. Sussman, A. H. Wang, N. C. Seeman, and A. Rich. 1974. 'Three-dimensional tertiary structure of yeast phenylalanine transfer RNA', *Science*, 185: 435-40.

Kirschner, D. L., and T. K. Green. 2009. 'Separation and sensitive detection of D-amino acids in biological matrices', *J Sep Sci*, 32: 2305-18.

Klein, S., C. Lorenzo, S. Hoffmann, J. M. Walther, S. Storbeck, T. Piekarski, B. J. Tindall, *et al.* 2009. 'Adaptation of Pseudomonas aeruginosa to various conditions includes tRNA-dependent formation of alanyl-phosphatidylglycerol', *Mol Microbiol*, 71: 551-65.

Klionsky, D. J., K. Abdelmohsen, A. Abe, M. J. Abedin, H. Abeliovich, A. Acevedo Arozena, H. Adachi, *et al.* 2016. 'Guidelines for the use and interpretation of assays for monitoring autophagy (3rd edition)', *Autophagy*, 12: 1-222.

Knight, J. A., S. Anderson, and J. M. Rawle. 1972. 'Chemical basis of the sulfo-phospho-vanillin reaction for estimating total serum lipids', *Clin Chem*, 18: 199-202.

Kodaki, T., and S. Yamashita. 1989. 'Characterization of the methyltransferases in the yeast phosphatidylethanolamine methylation pathway by selective gene disruption', *Eur J Biochem*, 185: 243-51.

Kodedova, M., and H. Sychrova. 2015. 'Changes in the Sterol Composition of the Plasma Membrane Affect Membrane Potential, Salt Tolerance and the Activity of Multidrug Resistance Pumps in Saccharomyces cerevisiae', *PLoS One*, 10: e0139306.

Koffel, R., R. Tiwari, L. Falquet, and R. Schneiter. 2005. 'The Saccharomyces cerevisiae YLL012/YEH1, YLR020/YEH2, and TGL1 genes encode a novel family of membrane-anchored lipases that are required for steryl ester hydrolysis', *Mol Cell Biol*, 25: 1655-68.

Koh, C. S., and L. P. Sarin. 2018. 'Transfer RNA modification and infection - Implications for pathogenicity and host responses', *Biochim Biophys Acta Gene Regul Mech*, 1861: 419-32.

Koledin, T., G. L. Newton, and R. C. Fahey. 2002. 'Identification of the mycothiol synthase gene (mshD) encoding the acetyltransferase producing mycothiol in actinomycetes', *Arch Microbiol*, 178: 331-7.

Komatsuzawa, H., K. Ohta, T. Fujiwara, G. H. Choi, H. Labischinski, and M. Sugai. 2001. 'Cloning and sequencing of the gene, fmtC, which affects oxacillin resistance in methicillin-resistant Staphylococcus aureus', *FEMS Microbiol Lett*, 203: 49-54.

Koostra, W. L., and P. F. Smith. 1969. 'D- and L-Alanylphosphatidylglycerols from Mycoplasma laidlawii, strain B', *Biochemistry*, 8: 4794-806.

Koprivnjak, T., A. Peschel, M. H. Gelb, N. S. Liang, and J. P. Weiss. 2002. 'Role of charge properties of bacterial envelope in bactericidal action of human group IIA phospholipase A2 against Staphylococcus aureus', *J Biol Chem*, 277: 47636-44.

Korber, M., I. Klein, and G. Daum. 2017. 'Steryl ester synthesis, storage and hydrolysis: A contribution to sterol homeostasis', *Biochim Biophys Acta Mol Cell Biol Lipids*, 1862: 1534-45.

Koselny, K., N. Mutlu, A. Y. Minard, A. Kumar, D. J. Krysan, and M. Wellington. 2018. 'A Genome-Wide Screen of Deletion Mutants in the Filamentous Saccharomyces cerevisiae Background Identifies Ergosterol as a Direct Trigger of Macrophage Pyroptosis', *mBio*, 9.

Krappmann, S. 2015. 'Lightning up the worm: How to probe fungal virulence in an alternative mini-host by bioluminescence', *Virulence*, 6: 727-9.

Krishnan-Natesan, S. 2009. 'Terbinafine: a pharmacological and clinical review', *Expert Opin Pharmacother*, 10: 2723-33.

Kristan, K., and T. L. Rizner. 2012. 'Steroid-transforming enzymes in fungi', *J Steroid Biochem Mol Biol*, 129: 79-91.

Kristian, S. A., M. Durr, J. A. Van Strijp, B. Neumeister, and A. Peschel. 2003. 'MprF-mediated lysinylation of phospholipids in Staphylococcus aureus leads to protection against oxygen-independent neutrophil killing', *Infect Immun*, 71: 546-9.

Krzycki, J. A. 2004. 'Function of genetically encoded pyrrolysine in corrinoid-dependent methylamine methyltransferases', *Curr Opin Chem Biol*, 8: 484-91.

Kuhn, S., C. J. Slavetinsky, and A. Peschel. 2015. 'Synthesis and function of phospholipids in Staphylococcus aureus', *Int J Med Microbiol*, 305: 196-202.

Kuhnlein, R. P. 2012. 'Thematic review series: Lipid droplet synthesis and metabolism: from yeast to man. Lipid droplet-based storage fat metabolism in Drosophila', *J Lipid Res*, 53: 1430-6.

Kuncha, S. K., S. P. Kruparani, and R. Sankaranarayanan. 2019. 'Chiral checkpoints during protein biosynthesis', *J Biol Chem*, 294: 16535-48.

Kunimoto, S., W. Murofushi, I. Yamatsu, Y. Hasegawa, N. Sasaki, S. Kobayashi, T. Kobayashi, H. Murofushi, and K. Murakami-Murofushi. 2003. 'Cholesteryl glucoside-induced protection against gastric ulcer', *Cell Struct Funct*, 28: 179-86.

Kunkel, T. A., and K. Bebenek. 2000. 'DNA replication fidelity', *Annu Rev Biochem*, 69: 497-529.

L

Lamour, V., S. Quevillon, S. Diriong, V. C. N'Guyen, M. Lipinski, and M. Mirande. 1994. 'Evolution of the Glx-tRNA synthetase family: the glutaminyl enzyme as a case of horizontal gene transfer', *Proc Natl Acad Sci U S A*, 91: 8670-4.

Langley, K. E., M. P. Yaffe, and E. P. Kennedy. 1979. 'Biosynthesis of phospholipids in Bacillus megaterium', *J Bacteriol*, 140: 996-1007.

Lapointe, J., L. Duplain, and M. Proulx. 1986. 'A single glutamyl-tRNA synthetase aminoacylates tRNAGlu and tRNAGln in Bacillus subtilis and efficiently misacylates Escherichia coli tRNAGln1 in vitro', *J Bacteriol*, 165: 88-93.

Laporte, D., J. L. Huot, G. Bader, L. Enkler, B. Senger, and H. D. Becker. 2014. 'Exploring the evolutionary diversity and assembly modes of multi-aminoacyl-tRNA synthetase complexes: lessons from unicellular organisms', *FEBS Lett*, 588: 4268-78.

LaRiviere, F. J., A. D. Wolfson, and O. C. Uhlenbeck. 2001. 'Uniform binding of aminoacyl-tRNAs to elongation factor Tu by thermodynamic compensation', *Science*, 294: 165-8.

Latge, J. P. 1999. 'Aspergillus fumigatus and aspergillosis', *Clin Microbiol Rev*, 12: 310-50.

Latge, J. P., and G. Chamilos. 2019. 'Aspergillus fumigatus and Aspergillosis in 2019', *Clin Microbiol Rev*, 33.

Lautru, S., M. Gondry, R. Genet, and J. L. Pernodet. 2002. 'The albonoursin gene Cluster of S noursei biosynthesis of diketopiperazine metabolites independent of nonribosomal peptide synthetases', *Chem Biol*, 9: 1355-64.

Leinfelder, W., E. Zehelein, M. A. Mandrand-Berthelot, and A. Bock. 1988. 'Gene for a novel tRNA species that accepts L-serine and cotranslationally inserts selenocysteine', *Nature*, 331: 723-5.

Lennarz, W. J., P. P. Bonsen, and L. L. van Deenen. 1967. 'Substrate specificity of O-L-lysylphosphatidylglycerol synthetase. Enzymatic studies on the structure of O-L-lysylphosphatidylglycerol', *Biochemistry*, 6: 2307-12.

Lennarz, W. J., J. A. Nesbitt, 3rd, and J. Reiss. 1966. 'The participation of sRNA in the enzymatic synthesis of O-L-lysyl phosphatidylgylcerol in Staphylococcus aureus', *Proc Natl Acad Sci U S A*, 55: 934-41.

Lerouge, P., M. H. Lebas, C. Agapakis-Causse, and J. C. Prome. 1988. 'Isolation and structural characterization of a new non-phosphorylated lipoamino acid from Mycobacterium phlei', *Chem Phys Lipids*, 49: 161-6.

Levin, D. E. 2011. 'Regulation of cell wall biogenesis in Saccharomyces cerevisiae: the cell wall integrity signaling pathway', *Genetics*, 189: 1145-75.

Li, Y., and W. A. Prinz. 2004. 'ATP-binding cassette (ABC) transporters mediate nonvesicular, raft-modulated sterol movement from the plasma membrane to the endoplasmic reticulum', *J Biol Chem*, 279: 45226-34.

Ling, J., N. Reynolds, and M. Ibba. 2009. 'Aminoacyl-tRNA synthesis and translational quality control', *Annu Rev Microbiol*, 63: 61-78.

Liu, J. F., J. J. Xia, K. L. Nie, F. Wang, and L. Deng. 2019. 'Outline of the biosynthesis and regulation of ergosterol in yeast', *World J Microbiol Biotechnol*, 35: 98.

Liu, Z., M. Reches, I. Groisman, and H. Engelberg-Kulka. 1998. 'The nature of the minimal 'selenocysteine insertion sequence' (SECIS) in Escherichia coli', *Nucleic Acids Res*, 26: 896-902.

M

Macfarlane, M. G. 1962. '<macfarlane1962_Lipoaminoacids in particular AlaPG inC. welchii.pdf>', *Nature*, 196: 136-38.

Macfarlane, M. G. 1964. 'Phosphatidylglycerols and lipoamino acids', *Adv Lipid Res*, 2: 91-125.

Macheleidt, J., D. J. Mattern, J. Fischer, T. Netzker, J. Weber, V. Schroeckh, V. Valiante, and A. A. Brakhage. 2016. 'Regulation and Role of Fungal Secondary Metabolites', *Annu Rev Genet*, 50: 371-92.

Maekawa, M. 2017. 'Domain 4 (D4) of Perfringolysin O to Visualize Cholesterol in Cellular Membranes-The Update', *Sensors (Basel)*, 17.

Maekawa, M., Y. Yang, and G. D. Fairn. 2016. 'Perfringolysin O Theta Toxin as a Tool to Monitor the Distribution and Inhomogeneity of Cholesterol in Cellular Membranes', *Toxins (Basel)*, 8.

Mahida, J. 2019. *Dyeing Reagents for Thin-Layer and Paper Chromatography*.

Mailu, B. M., L. Li, J. Arthur, T. M. Nelson, G. Ramasamy, K. Fritz-Wolf, K. Becker, and M. J. Gardner. 2015. 'Plasmodium Apicoplast Gln-tRNAGln Biosynthesis Utilizes a Unique GatAB Amidotransferase Essential for Erythrocytic Stage Parasites', *J Biol Chem*, 290: 29629-41.

Maloney, E., S. Lun, D. Stankowska, H. Guo, M. Rajagoapalan, W. R. Bishai, and M. V. Madiraju. 2011. 'Alterations in phospholipid catabolism in Mycobacterium tuberculosis lysX mutant', *Front Microbiol*, 2: 19.

Maloney, E., D. Stankowska, J. Zhang, M. Fol, Q. J. Cheng, S. Lun, W. R. Bishai, *et al.* 2009. 'The two-domain LysX protein of Mycobacterium tuberculosis is required for production of lysinylated phosphatidylglycerol and resistance to cationic antimicrobial peptides', *PLoS Pathog*, 5: e1000534.

Man, S. M., R. Karki, and T. D. Kanneganti. 2017. 'Molecular mechanisms and functions of pyroptosis, inflammatory caspases and inflammasomes in infectious diseases', *Immunol Rev*, 277: 61-75.

Marck, C., and H. Grosjean. 2002. 'tRNomics: analysis of tRNA genes from 50 genomes of Eukarya, Archaea, and Bacteria reveals anticodon-sparing strategies and domain-specific features', *RNA*, 8: 1189-232.

Martick, M., and W. G. Scott. 2006. 'Tertiary contacts distant from the active site prime a ribozyme for catalysis', *Cell*, 126: 309-20.

Martzoukou, O., S. Amillis, A. Zervakou, S. Christoforidis, and G. Diallinas. 2017. 'The AP-2 complex has a specialized clathrin-independent role in apical endocytosis and polar growth in fungi', *Elife*, 6.

Matsuhashi, M., C. P. Dietrich, and J. L. Strominger. 1965. 'Incorporation of glycine into the cell wall glycopeptide in Staphylococcus aureus: role of sRNA and lipid intermediates', *Proc Natl Acad Sci U S A*, 54: 587-94.

Maxfield, F. R., and I. Tabas. 2005. 'Role of cholesterol and lipid organization in disease', *Nature*, 438: 612-21.

Mayadas, T. N., X. Cullere, and C. A. Lowell. 2014. 'The multifaceted functions of neutrophils', *Annu Rev Pathol*, 9: 181-218.

McEvoy, K., T. G. Normile, and M. D. Poeta. 2020. 'Antifungal Drug Development: Targeting the Fungal Sphingolipid Pathway', *J Fungi (Basel)*, 6.

McGraw, P., and S. A. Henry. 1989. 'Mutations in the Saccharomyces cerevisiae opi3 gene: effects on phospholipid methylation, growth and cross-pathway regulation of inositol synthesis', *Genetics*, 122: 317-30.

McMahon, A., H. Lu, and I. A. Butovich. 2013. 'The spectrophotometric sulfo-phospho-vanillin assessment of total lipids in human meibomian gland secretions', *Lipids*, 48: 513-25.

Mesa-Arango, A. C., N. Trevijano-Contador, E. Roman, R. Sanchez-Fresneda, C. Casas, E. Herrero, J. C. Arguelles, *et al.* 2014. 'The production of reactive oxygen species is a universal action mechanism of Amphotericin B against pathogenic yeasts and contributes to the fungicidal effect of this drug', *Antimicrob Agents Chemother*, 58: 6627-38.

Meyer, M., and B. Masquida. 2014. 'cis-Acting 5' hammerhead ribozyme optimization for in vitro transcription of highly structured RNAs', *Methods Mol Biol*, 1086: 21-40.

Mirande, M. 2017. 'The Aminoacyl-tRNA Synthetase Complex', *Subcell Biochem*, 83: 505-22.

Mitchell, L. A., Y. Cai, M. Taylor, A. M. Noronha, J. Chuang, L. Dai, and J. D. Boeke. 2013. 'Multichange isothermal mutagenesis: a new strategy for multiple site-directed mutations in plasmid DNA', *ACS Synth Biol*, 2: 473-7.

Mitra, S. K., and A. H. Mehler. 1967. 'The arginyl transfer ribonucleic acid synthetase of Escherichia coli', *J Biol Chem*, 242: 5490-4.

Montanes, F. M., A. Pascual-Ahuir, and M. Proft. 2011. 'Repression of ergosterol biosynthesis is essential for stress resistance and is mediated by the Hog1 MAP kinase and the Mot3 and Rox1 transcription factors', *Mol Microbiol*, 79: 1008-23.

Monteiro, M. C., M. de la Cruz, J. Cantizani, C. Moreno, J. R. Tormo, E. Mellado, J. R. De Lucas, *et al.* 2012. 'A new approach to drug discovery: high-throughput screening of microbial natural extracts against Aspergillus fumigatus using resazurin', *J Biomol Screen*, 17: 542-9.

Morioka, S., T. Shigemori, K. Hara, H. Morisaka, K. Kuroda, and M. Ueda. 2013. 'Effect of sterol composition on the activity of the yeast G-protein-coupled receptor Ste2', *Appl Microbiol Biotechnol*, 97: 4013-20.

Moser, R., M. Aktas, C. Fritz, and F. Narberhaus. 2014. 'Discovery of a bifunctional cardiolipin/phosphatidylethanolamine synthase in bacteria', *Mol Microbiol*, 92: 959-72.

Moulinier, L., S. Eiler, G. Eriani, J. Gangloff, J. C. Thierry, K. Gabriel, W. H. McClain, and D. Moras. 2001. 'The structure of an AspRS-tRNA(Asp) complex reveals a tRNA-dependent control mechanism', *EMBO J*, 20: 5290-301.

Moutiez, M., P. Belin, and M. Gondry. 2017. 'Aminoacyl-tRNA-Utilizing Enzymes in Natural Product Biosynthesis', *Chem Rev*, 117: 5578-618.

Mukai, T., A. Crnkovic, T. Umehara, N. N. Ivanova, N. C. Kyrpides, and D. Soll. 2017. 'RNA-Dependent Cysteine Biosynthesis in Bacteria and Archaea', *mBio*, 8.

Muller, A., M. Wenzel, H. Strahl, F. Grein, T. N. V. Saaki, B. Kohl, T. Siersma, *et al.* 2016. 'Daptomycin inhibits cell envelope synthesis by interfering with fluid membrane microdomains', *Proc Natl Acad Sci U S A*, 113: E7077-E86.

Mullner, H., D. Zweytick, R. Leber, F. Turnowsky, and G. Daum. 2004. 'Targeting of proteins involved in sterol biosynthesis to lipid particles of the yeast Saccharomyces cerevisiae', *Biochim Biophys Acta*, 1663: 9-13.

Myasnikov, A. G., A. Simonetti, S. Marzi, and B. P. Klaholz. 2009. 'Structure-function insights into prokaryotic and eukaryotic translation initiation', *Curr Opin Struct Biol*, 19: 300-9.

N

Nedelcu, D., J. Liu, Y. Xu, C. Jao, and A. Salic. 2013. 'Oxysterol binding to the extracellular domain of Smoothened in Hedgehog signaling', *Nat Chem Biol*, 9: 557-64.

Nesbitt, J. A., 3rd, and W. J. Lennarz. 1968. 'Participation of aminoacyl transfer ribonucleic acid in aminoacyl phosphatidylglycerol synthesis. I. Specificity of lysyl phosphatidylglycerol synthetase', *J Biol Chem*, 243: 3088-95.

Nikawa, J., Y. Tsukagoshi, and S. Yamashita. 1986. 'Cloning of a gene encoding choline transport in Saccharomyces cerevisiae', *J Bacteriol*, 166: 328-30.

Nirenberg, M., T. Caskey, R. Marshall, R. Brimacombe, D. Kellogg, B. Doctor, D. Hatfield, *et al.* 1966. 'The RNA code and protein synthesis', *Cold Spring Harb Symp Quant Biol*, 31: 11-24.

Nishi, H., H. Komatsuzawa, T. Fujiwara, N. McCallum, and M. Sugai. 2004. 'Reduced content of lysyl-phosphatidylglycerol in the cytoplasmic membrane affects susceptibility to moenomycin, as well as vancomycin, gentamicin, and antimicrobial peptides, in Staphylococcus aureus', *Antimicrob Agents Chemother*, 48: 4800-7.

Nishibori, A., J. Kusaka, H. Hara, M. Umeda, and K. Matsumoto. 2005. 'Phosphatidylethanolamine domains and localization of phospholipid synthases in Bacillus subtilis membranes', *J Bacteriol*, 187: 2163-74.

Nutzmann, H. W., C. Scazzocchio, and A. Osbourn. 2018. 'Metabolic Gene Clusters in Eukaryotes', *Annu Rev Genet*, 52: 159-83.

O

O'Donoghue, P., and Z. Luthey-Schulten. 2003. 'On the evolution of structure in aminoacyl-tRNA synthetases', *Microbiol Mol Biol Rev*, 67: 550-73.

O'Gorman, C. M., H. Fuller, and P. S. Dyer. 2009. 'Discovery of a sexual cycle in the opportunistic fungal pathogen Aspergillus fumigatus', *Nature*, 457: 471-4.

Oku, Y., K. Kurokawa, N. Ichihashi, and K. Sekimizu. 2004. 'Characterization of the Staphylococcus aureus mprF gene, involved in lysinylation of phosphatidylglycerol', *Microbiology*, 150: 45-51.

Onishi, J., M. Meinz, J. Thompson, J. Curotto, S. Dreikorn, M. Rosenbach, C. Douglas, *et al.* 2000. 'Discovery of novel antifungal (1,3)-beta-D-glucan synthase inhibitors', *Antimicrob Agents Chemother*, 44: 368-77.

Ordovas-Montanes, J. M., and J. M. Ordovas. 2012. 'Cholesterol, Inflammasomes, and Atherogenesis', *Curr Cardiovasc Risk Rep*, 6: 45-52.

Osman, C., M. Haag, F. T. Wieland, B. Brugger, and T. Langer. 2010. 'A mitochondrial phosphatase required for cardiolipin biosynthesis: the PGP phosphatase Gep4', *EMBO J*, 29: 1976-87.

p

Pan, T. 2013. 'Adaptive translation as a mechanism of stress response and adaptation', *Annu Rev Genet*, 47: 121-37.

Paoletti, M., C. Rydholm, E. U. Schwier, M. J. Anderson, G. Szakacs, F. Lutzoni, J. P. Debeaupuis, *et al.* 2005. 'Evidence for sexuality in the opportunistic fungal pathogen Aspergillus fumigatus', *Curr Biol*, 15: 1242-8.

Park, H. S., and J. H. Yu. 2016. 'Developmental regulators in Aspergillus fumigatus', *J Microbiol*, 54: 223-31.

Park, S. G., P. Schimmel, and S. Kim. 2008. 'Aminoacyl tRNA synthetases and their connections to disease', *Proc Natl Acad Sci U S A*, 105: 11043-9.

Park, S. J., and P. Schimmel. 1988. 'Evidence for interaction of an aminoacyl transfer RNA synthetase with a region important for the identity of its cognate transfer RNA', *J Biol Chem*, 263: 16527-30.

Parker, J. E., A. G. Warrilow, C. L. Price, J. G. Mullins, D. E. Kelly, and S. L. Kelly. 2014. 'Resistance to antifungals that target CYP51', *J Chem Biol*, 7: 143-61.

Paul, S., D. Diekema, and W. S. Moye-Rowley. 2013. 'Contributions of Aspergillus fumigatus ATP-binding cassette transporter proteins to drug resistance and virulence', *Eukaryot Cell*, 12: 1619-28.

Pearson, H. 2006. 'Genetics: what is a gene?', *Nature*, 441: 398-401.

Pennisi, E. 2007. 'Genomics. DNA study forces rethink of what it means to be a gene', *Science*, 316: 1556-7.

Perfect, J. R. 2017. 'The antifungal pipeline: a reality check', *Nat Rev Drug Discov*, 16: 603-16.

Perona, J. J., and A. Hadd. 2012. 'Structural diversity and protein engineering of the aminoacyl-tRNA synthetases', *Biochemistry*, 51: 8705-29.

Perona, J. J., and Y. M. Hou. 2007. 'Indirect readout of tRNA for aminoacylation', *Biochemistry*, 46: 10419-32.

Peschel, A. 2002. 'How do bacteria resist human antimicrobial peptides?', *Trends Microbiol*, 10: 179-86.

Peschel, A., R. W. Jack, M. Otto, L. V. Collins, P. Staubitz, G. Nicholson, H. Kalbacher, *et al.* 2001. 'Staphylococcus aureus resistance to human defensins and evasion of neutrophil killing via the novel virulence factor MprF is based on modification of membrane lipids with l-lysine', *J Exp Med*, 193: 1067-76.

Peter-Katalinic, J., and W. Fischer. 1998. 'alpha-d-glucopyranosyl-, d-alanyl- and l-lysylcardiolipin from gram-positive bacteria: analysis by fast atom bombardment mass spectrometry', *J Lipid Res*, 39: 2286-92.

Pham, Y., B. Kuhlman, G. L. Butterfoss, H. Hu, V. Weinreb, and C. W. Carter, Jr. 2010. 'Tryptophanyl-tRNA synthetase Urzyme: a model to recapitulate molecular evolution and investigate intramolecular complementation', *J Biol Chem*, 285: 38590-601.

Poggeler, S. 2002. 'Genomic evidence for mating abilities in the asexual pathogen Aspergillus fumigatus', *Curr Genet*, 42: 153-60.

Polycarpo, C., A. Ambrogelly, B. Ruan, D. Tumbula-Hansen, S. F. Ataide, R. Ishitani, S. Yokoyama, *et al.* 2003. 'Activation of the pyrrolysine suppressor tRNA requires formation of a ternary complex with class I and class II lysyl-tRNA synthetases', *Mol Cell*, 12: 287-94.

Portin, P., and A. Wilkins. 2017. 'The Evolving Definition of the Term "Gene"', *Genetics*, 205: 1353-64.

Putz, J., C. Florentz, F. Benseler, and R. Giege. 1994. 'A single methyl group prevents the mischarging of a tRNA', *Nat Struct Biol*, 1: 580-2.

Putz, J., J. D. Puglisi, C. Florentz, and R. Giege. 1991. 'Identity elements for specific aminoacylation of yeast tRNA(Asp) by cognate aspartyl-tRNA synthetase', *Science*, 252: 1696-9.

R

Raczniak, G., H. D. Becker, B. Min, and D. Soll. 2001. 'A single amidotransferase forms asparaginyl-tRNA and glutaminyl-tRNA in Chlamydia trachomatis', *J Biol Chem*, 276: 45862-7.

Radkov, A. D., and L. A. Moe. 2014. 'Bacterial synthesis of D-amino acids', *Appl Microbiol Biotechnol*, 98: 5363-74.

RajBhandary, U. L., and S. H. Chang. 1968. 'Studies on polynucleotides. LXXXII. Yeast phenylalanine transfer ribonucleic acid: partial digestion with ribonuclease T-1 and derivation of the total primary structure', *J Biol Chem*, 243: 598-608.

Ramakrishnan, V. 2002. 'Ribosome structure and the mechanism of translation', *Cell*, 108: 557-72.

Raran-Kurussi, S., and D. S. Waugh. 2012. 'The ability to enhance the solubility of its fusion partners is an intrinsic property of maltose-binding protein but their folding is either spontaneous or chaperone-mediated', *PLoS One*, 7: e49589.

Rasubala, L., D. Fourmy, T. Ose, D. Kohda, K. Maenaka, and S. Yoshizawa. 2005. 'Crystallization and preliminary X-ray analysis of the mRNA-binding domain of elongation factor SelB in complex with RNA', *Acta Crystallogr Sect F Struct Biol Cryst Commun*, 61: 296-8.

Rathnayake, U. M., W. N. Wood, and T. L. Hendrickson. 2017. 'Indirect tRNA aminoacylation during accurate translation and phenotypic mistranslation', *Curr Opin Chem Biol*, 41: 114-22.

Ravel, J. M., S. F. Wang, C. Heinemeyer, and W. Shive. 1965. 'Glutamyl and Glutaminyl Ribonucleic Acid Synthetases of Escherichia Coli W. Separation, Properties, and Stimulation of Adenosine Triphosphate-Pyrophosphate Exchange by Acceptor Ribonucleic Acid', *J Biol Chem*, 240: 432-8.

Reich, H. J., and R. J. Hondal. 2016. 'Why Nature Chose Selenium', *ACS Chem Biol*, 11: 821-41.

Rella, A., A. M. Farnoud, and M. Del Poeta. 2016. 'Plasma membrane lipids and their role in fungal virulence', *Prog Lipid Res*, 61: 63-72.

Rella, A., V. Mor, A. M. Farnoud, A. Singh, A. A. Shamseddine, E. Ivanova, N. Carpino, *et al.* 2015. 'Role of Sterylglucosidase 1 (Sgl1) on the pathogenicity of Cryptococcus neoformans: potential applications for vaccine development', *Front Microbiol*, 6: 836.

Rezanka, T., M. Kambourova, A. Derekova, I. Kolouchova, and K. Sigler. 2012. 'LC-ESI-MS/MS identification of polar lipids of two thermophilic Anoxybacillus bacteria containing a unique lipid pattern', *Lipids*, 47: 729-39.

Ribas de Pouplana, L., M. A. Santos, J. H. Zhu, P. J. Farabaugh, and B. Javid. 2014. 'Protein mistranslation: friend or foe?', *Trends Biochem Sci*, 39: 355-62.

Ribas de Pouplana, L., and P. Schimmel. 2001. 'Two classes of tRNA synthetases suggested by sterically compatible dockings on tRNA acceptor stem', *Cell*, 104: 191-3.

Rodin, A. S., E. Szathmary, and S. N. Rodin. 2009. 'One ancestor for two codes viewed from the perspective of two complementary modes of tRNA aminoacylation', *Biol Direct*, 4: 4.

Rodin, S. N., and S. Ohno. 1995. 'Two types of aminoacyl-tRNA synthetases could be originally encoded by complementary strands of the same nucleic acid', *Orig Life Evol Biosph*, 25: 565-89.

Rodrigues, M. L. 2018. 'The Multifunctional Fungal Ergosterol', *mBio*, 9.

Rosenberger, R. F., and J. Hilton. 1983. 'The frequency of transcriptional and translational errors at nonsense codons in the lacZ gene of Escherichia coli', *Mol Gen Genet*, 191: 207-12.

Rossmann, M. G., D. Moras, and K. W. Olsen. 1974. 'Chemical and biological evolution of nucleotide-binding protein', *Nature*, 250: 194-9.

Rowe, N. J., J. Tunstall, L. Galbraith, and S. G. Wilkinson. 2000. 'Lipid composition and taxonomy of [Pseudomonas] echinoides: transfer to the genus Sphingomonas', *Microbiology*, 146 (Pt 11): 3007-12.

Roy, H. 2009. 'Tuning the properties of the bacterial membrane with aminoacylated phosphatidylglycerol', *IUBMB Life*, 61: 940-53.

Roy, H., H. D. Becker, M. H. Mazauric, and D. Kern. 2007. 'Structural elements defining elongation factor Tu mediated suppression of codon ambiguity', *Nucleic Acids Res*, 35: 3420-30.

Roy, H., H. D. Becker, J. Reinbolt, and D. Kern. 2003. 'When contemporary aminoacyl-tRNA synthetases invent their cognate amino acid metabolism', *Proc Natl Acad Sci U S A*, 100: 9837-42.

Roy, H., and M. Ibba. 2008a. 'Monitoring Lys-tRNA(Lys) phosphatidylglycerol transferase activity', *Methods*, 44: 164-9.

Roy, H., and M. Ibba. 2008b. 'RNA-dependent lipid remodeling by bacterial multiple peptide resistance factors', *Proc Natl Acad Sci U S A*, 105: 4667-72.

Roy, H., and M. Ibba. 2009. 'Broad range amino acid specificity of RNA-dependent lipid remodeling by multiple peptide resistance factors', *J Biol Chem*, 284: 29677-83.

Rozgonyi, F., P. Biacs, K. Szitha, and J. Kiss. 1981. 'Effect of methicillin on the fatty acid composition of phospholipids in methicillin sensitive Staphylococcus aureus', *Acta Microbiol Acad Sci Hung*, 28: 97-110.

Rozgonyi, F., J. Kiss, P. Jekel, and L. Vaczi. 1980. 'Effect of methicillin on the phospholipid content of methicillin sensitive Staphylococcus aureus', *Acta Microbiol Acad Sci Hung*, 27: 31-40.

Rubin, H. E., T. Nerad, and F. Vaughan. 1982. 'Lactate acid inhibition of Salmonella typhimurium in yogurt', *J Dairy Sci*, 65: 197-203.

Rubio Gomez, M. A., and M. Ibba. 2020. 'Aminoacyl-tRNA Synthetases', *RNA*.

Rybak, M. Y., A. V. Rayevsky, O. I. Gudzera, and M. A. Tukalo. 2019. 'Stereospecificity control in aminoacyl-tRNA-synthetases: new evidence of d-amino acids activation and editing', *Nucleic Acids Res*, 47: 9777-88.

S

Saad, N. Y., V. Stamatopoulou, M. Braye, D. Drainas, C. Stathopoulos, and H. D. Becker. 2013. 'Two-codon T-box riboswitch binding two tRNAs', *Proc Natl Acad Sci U S A*, 110: 12756-61.

Sakaki, T., U. Zahringer, D. C. Warnecke, A. Fahl, W. Knogge, and E. Heinz. 2001. 'Sterol glycosides and cerebrosides accumulate in Pichia pastoris, Rhynchosporium secalis and other fungi under normal conditions or under heat shock and ethanol stress', *Yeast*, 18: 679-95.

Saliba, A. E., I. Vonkova, and A. C. Gavin. 2015. 'The systematic analysis of protein-lipid interactions comes of age', *Nat Rev Mol Cell Biol*, 16: 753-61.

Salzberg, L. I., and J. D. Helmann. 2008. 'Phenotypic and transcriptomic characterization of Bacillus subtilis mutants with grossly altered membrane composition', *J Bacteriol*, 190: 7797-807.

Sanglard, D., F. Ischer, T. Parkinson, D. Falconer, and J. Bille. 2003. 'Candida albicans mutations in the ergosterol biosynthetic pathway and resistance to several antifungal agents', *Antimicrob Agents Chemother*, 47: 2404-12.

Sankaranarayanan, R., A. C. Dock-Bregeon, B. Rees, M. Bovee, J. Caillet, P. Romby, C. S. Francklyn, and D. Moras. 2000. 'Zinc ion mediated amino acid discrimination by threonyl-tRNA synthetase', *Nat Struct Biol*, 7: 461-5.

Santos, A. X., and H. Riezman. 2012. 'Yeast as a model system for studying lipid homeostasis and function', *FEBS Lett*, 586: 2858-67.

Sato, T. K., R. K. Tweten, and A. E. Johnson. 2013. 'Disulfide-bond scanning reveals assembly state and beta-strand tilt angle of the PFO beta-barrel', *Nat Chem Biol*, 9: 383-9.

Satsangi, R. K., and G. E. Mott. 1992. 'Cholesterol immobilization via ether-linked sepharose gels', *Analyst*, 117: 953-7.

Sauerwald, A., W. Zhu, T. A. Major, H. Roy, S. Palioura, D. Jahn, W. B. Whitman, *et al.* 2005. 'RNA-dependent cysteine biosynthesis in archaea', *Science*, 307: 1969-72.

Sauguet, L., M. Moutiez, Y. Li, P. Belin, J. Seguin, M. H. Le Du, R. Thai, *et al.* 2011. 'Cyclodipeptide synthases, a family of class-I aminoacyl-tRNA synthetase-like enzymes involved in non-ribosomal peptide synthesis', *Nucleic Acids Res*, 39: 4475-89.

Schieber, A., H. Bruckner, and J. R. Ling. 1999. 'GC-MS analysis of diaminopimelic acid stereoisomers and amino acid enantiomers in rumen bacteria', *Biomed Chromatogr*, 13: 46-50.

Schimmel, P. 2018. 'The emerging complexity of the tRNA world: mammalian tRNAs beyond protein synthesis', *Nat Rev Mol Cell Biol*, 19: 45-58.

Schneiter, R., B. Brugger, R. Sandhoff, G. Zellnig, A. Leber, M. Lampl, K. Athenstaedt, *et al.* 1999. 'Electrospray ionization tandem mass spectrometry (ESI-MS/MS) analysis of the lipid molecular species composition of yeast subcellular membranes reveals acyl chain-based sorting/remodeling of distinct molecular species en route to the plasma membrane', *J Cell Biol*, 146: 741-54.

Serganov, A., and E. Nudler. 2013. 'A decade of riboswitches', *Cell*, 152: 17-24.

Shakoury-Elizeh, M., O. Protchenko, A. Berger, J. Cox, K. Gable, T. M. Dunn, W. A. Prinz, M. Bard, and C. C. Philpott. 2010. 'Metabolic response to iron deficiency in Saccharomyces cerevisiae', *J Biol Chem*, 285: 14823-33.

Sheehan, G., G. Clarke, and K. Kavanagh. 2018. 'Characterisation of the cellular and proteomic response of Galleria mellonella larvae to the development of invasive aspergillosis', *BMC Microbiol*, 18: 63.

Shen, N., L. Guo, B. Yang, Y. Jin, and J. Ding. 2006. 'Structure of human tryptophanyl-tRNA synthetase in complex with tRNATrp reveals the molecular basis of tRNA recognition and specificity', *Nucleic Acids Res*, 34: 3246-58.

Sheppard, K., J. Yuan, M. J. Hohn, B. Jester, K. M. Devine, and D. Soll. 2008. 'From one amino acid to another: tRNA-dependent amino acid biosynthesis', *Nucleic Acids Res*, 36: 1813-25.

Shirey, C. M., J. L. Scott, and R. V. Stahelin. 2017. 'Notes and tips for improving quality of lipid-protein overlay assays', *Anal Biochem*, 516: 9-12.

Short, S. A., and D. C. White. 1971. 'Metabolism of phosphatidylglycerol, lysylphosphatidylglycerol, and cardiolipin of Staphylococcus aureus', *J Bacteriol*, 108: 219-26.

Sievers, S., C. M. Ernst, T. Geiger, M. Hecker, C. Wolz, D. Becher, and A. Peschel. 2010. 'Changing the phospholipid composition of Staphylococcus aureus causes distinct changes in membrane proteome and membrane-sensory regulators', *Proteomics*, 10: 1685-93.

Slavetinsky, C. J., A. Peschel, and C. M. Ernst. 2012. 'Alanyl-phosphatidylglycerol and lysyl-phosphatidylglycerol are translocated by the same MprF flippases and have similar capacities to protect against the antibiotic daptomycin in Staphylococcus aureus', *Antimicrob Agents Chemother*, 56: 3492-7.

Slavetinsky, C., S. Kuhn, and A. Peschel. 2017. 'Bacterial aminoacyl phospholipids - Biosynthesis and role in basic cellular processes and pathogenicity', *Biochim Biophys Acta Mol Cell Biol Lipids*, 1862: 1310-18.

Smejkal, G. B., G. Hoppe, and H. F. Hoff. 1996. 'Filipin as a fluorescent probe of lipoprotein-derived sterols on thin-layer chromatograms', *Anal Biochem*, 239: 115-7.

Smith, A. M., J. S. Harrison, C. D. Grube, A. E. Sheppe, N. Sahara, R. Ishii, O. Nureki, and H. Roy. 2015. 'tRNA-dependent alanylation of diacylglycerol and phosphatidylglycerol in Corynebacterium glutamicum', *Mol Microbiol*, 98: 681-93.

Smith, A. M., J. S. Harrison, K. M. Sprague, and H. Roy. 2013. 'A conserved hydrolase responsible for the cleavage of aminoacylphosphatidylglycerol in the membrane of Enterococcus faecium', *J Biol Chem*, 288: 22768-76.

Sohlenkamp, C., K. E. de Rudder, and O. Geiger. 2004. 'Phosphatidylethanolamine is not essential for growth of Sinorhizobium meliloti on complex culture media', *J Bacteriol*, 186: 1667-77.

Sohlenkamp, C., K. A. Galindo-Lagunas, Z. Guan, P. Vinuesa, S. Robinson, J. Thomas-Oates, C. R. Raetz, and O. Geiger. 2007. 'The lipid lysyl-phosphatidylglycerol is present in membranes of Rhizobium tropici CIAT899 and confers increased resistance to polymyxin B under acidic growth conditions', *Mol Plant Microbe Interact*, 20: 1421-30.

Sohlenkamp, C., and O. Geiger. 2016. 'Bacterial membrane lipids: diversity in structures and pathways', *FEMS Microbiol Rev*, 40: 133-59.

Sokolov, S. S., N. I. Trushina, F. F. Severin, and D. A. Knorre. 2019. 'Ergosterol Turnover in Yeast: An Interplay between Biosynthesis and Transport', *Biochemistry (Mosc)*, 84: 346-57.

Sokolowski, M., R. Klassen, A. Bruch, R. Schaffrath, and S. Glatt. 2018. 'Cooperativity between different tRNA modifications and their modification pathways', *Biochim Biophys Acta Gene Regul Mech*, 1861: 409-18.

Solanko, L. M., A. Honigmann, H. S. Midtiby, F. W. Lund, J. R. Brewer, V. Dekaris, R. Bittman, C. Eggeling, and D. Wustner. 2013. 'Membrane orientation and lateral diffusion of BODIPY-cholesterol as a function of probe structure', *Biophys J*, 105: 2082-92.

Solanko, L. M., D. P. Sullivan, Y. Y. Sere, M. Szomek, A. Lunding, K. A. Solanko, A. Pizovic, *et al.* 2018. 'Ergosterol is mainly located in the cytoplasmic leaflet of the yeast plasma membrane', *Traffic*, 19: 198-214.

Soriani, F. M., I. Malavazi, M. E. da Silva Ferreira, M. Savoldi, M. R. Von Zeska Kress, M. H. de Souza Goldman, O. Loss, E. Bignell, and G. H. Goldman. 2008. 'Functional characterization of the Aspergillus fumigatus CRZ1 homologue, CrzA', *Mol Microbiol*, 67: 1274-91.

Speers, A. E., and C. C. Wu. 2007. 'Proteomics of integral membrane proteins--theory and application', *Chem Rev*, 107: 3687-714.

Sprinzl, M., and F. Cramer. 1975. 'Site of aminoacylation of tRNAs from Escherichia coli with respect to the 2'- or 3'-hydroxyl group of the terminal adenosine', *Proc Natl Acad Sci U S A*, 72: 3049-53.

Sprinzl, M., C. Horn, M. Brown, A. Ioudovitch, and S. Steinberg. 1998. 'Compilation of tRNA sequences and sequences of tRNA genes', *Nucleic Acids Res*, 26: 148-53.

Sprinzl, M., and K. S. Vassilenko. 2005. 'Compilation of tRNA sequences and sequences of tRNA genes', *Nucleic Acids Res*, 33: D139-40.

Srinivasan, G., C. M. James, and J. A. Krzycki. 2002. 'Pyrrolysine encoded by UAG in Archaea: charging of a UAG-decoding specialized tRNA', *Science*, 296: 1459-62.

Stanzel, M., A. Schon, and M. Sprinzl. 1994. 'Discrimination against misacylated tRNA by chloroplast elongation factor Tu', *Eur J Biochem*, 219: 435-9.

Starzyk, R. M., T. A. Webster, and P. Schimmel. 1987. 'Evidence for dispensable sequences inserted into a nucleotide fold', *Science*, 237: 1614-8.

Staubitz, P., and A. Peschel. 2002. 'MprF-mediated lysinylation of phospholipids in Bacillus subtilis--protection against bacteriocins in terrestrial habitats?', *Microbiology*, 148: 3331-32.

Staubitz, Petra, Heinz Neumann, Tanja Schneider, Imke Wiedemann, and Andreas Peschel. 2004. 'MprF-mediated biosynthesis of lysylphosphatidylglycerol, an important determinant in staphylococcal defensin resistance', *FEMS Microbiology Letters*, 231: 67-71.

Stern, R., and A. H. Mehler. 1965. 'Lysyl-sRNA synthetase from Escherichia coli', *Biochem Z*, 342: 400-9.

T

Tekaia, F., and J. P. Latge. 2005. 'Aspergillus fumigatus: saprophyte or pathogen?', *Curr Opin Microbiol*, 8: 385-92.

Thach, R. E., K. F. Dewey, J. C. Brown, and P. Doty. 1966. 'Formylmethionine codon AUG as an initiator of polypeptide synthesis', *Science*, 153: 416-8.

Thedieck, K., T. Hain, W. Mohamed, B. J. Tindall, M. Nimtz, T. Chakraborty, J. Wehland, and L. Jansch. 2006. 'The MprF protein is required for lysinylation of phospholipids in listerial membranes and confers resistance to cationic antimicrobial peptides (CAMPs) on Listeria monocytogenes', *Mol Microbiol*, 62: 1325-39.

Theobald-Dietrich, A., R. Giege, and J. Rudinger-Thirion. 2005. 'Evidence for the existence in mRNAs of a hairpin element responsible for ribosome dependent pyrrolysine insertion into proteins', *Biochimie*, 87: 813-7.

Tiwari, R., R. Koffel, and R. Schneiter. 2007. 'An acetylation/deacetylation cycle controls the export of sterols and steroids from S. cerevisiae', *EMBO J*, 26: 5109-19.

Trombe, M. C., M. A. Laneelle, and G. Laneelle. 1979. 'Lipid composition of aminopterin-resistant and sensitive strains of Streptococcus pneumoniae. Effect of aminopterin inhibition', *Biochim Biophys Acta*, 574: 290-300.

Trotter, P. J., and D. R. Voelker. 1995. 'Identification of a non-mitochondrial phosphatidylserine decarboxylase activity (PSD2) in the yeast Saccharomyces cerevisiae', *J Biol Chem*, 270: 6062-70.

Tujebajeva, R. M., P. R. Copeland, X. M. Xu, B. A. Carlson, J. W. Harney, D. M. Driscoll, D. L. Hatfield, and M. J. Berry. 2000. 'Decoding apparatus for eukaryotic selenocysteine insertion', *EMBO Rep*, 1: 158-63.

Tumbula, D. L., H. D. Becker, W. Z. Chang, and D. Soll. 2000. 'Domain-specific recruitment of amide amino acids for protein synthesis', *Nature*, 407: 106-10.

Tworowski, D., A. V. Feldman, and M. G. Safro. 2005. 'Electrostatic potential of aminoacyl-tRNA synthetase navigates tRNA on its pathway to the binding site', *J Mol Biol*, 350: 866-82.

V

Valencia-Sanchez, M. I., A. Rodriguez-Hernandez, R. Ferreira, H. A. Santamaria-Suarez, M. Arciniega, A. C. Dock-Bregeon, D. Moras, *et al*. 2016. 'Structural Insights into the Polyphyletic Origins of Glycyl tRNA Synthetases', *J Biol Chem*, 291: 14430-46.

Valiante, V., J. Macheleidt, M. Foge, and A. A. Brakhage. 2015. 'The Aspergillus fumigatus cell wall integrity signaling pathway: drug target, compensatory pathways, and virulence', *Front Microbiol*, 6: 325.

van Iterson, W., and J. A. den Kamp. 1969. 'Bacteria-shaped gymnoplasts (protoplasts) of Bacillus subtilis', *J Bacteriol*, 99: 304-15.

Van Leeuwen, M. R., W. Smant, W. de Boer, and J. Dijksterhuis. 2008. 'Filipin is a reliable in situ marker of ergosterol in the plasma membrane of germinating conidia (spores) of Penicillium discolor and stains intensively at the site of germ tube formation', *J Microbiol Methods*, 74: 64-73.

Vance, J. E. 2018. 'Historical perspective: phosphatidylserine and phosphatidylethanolamine from the 1800s to the present', *J Lipid Res*, 59: 923-44.

Vandeputte, P., G. Tronchin, G. Larcher, E. Ernoult, T. Berges, D. Chabasse, and J. P. Bouchara. 2008. 'A nonsense mutation in the ERG6 gene leads to reduced susceptibility to polyenes in a clinical isolate of Candida glabrata', *Antimicrob Agents Chemother*, 52: 3701-9.

Vare, V. Y., E. R. Eruysal, A. Narendran, K. L. Sarachan, and P. F. Agris. 2017. 'Chemical and Conformational Diversity of Modified Nucleosides Affects tRNA Structure and Function', *Biomolecules*, 7.

Vasil'eva, I. A., and N. A. Moor. 2007. 'Interaction of aminoacyl-tRNA synthetases with tRNA: general principles and distinguishing characteristics of the high-molecular-weight substrate recognition', *Biochemistry (Mosc)*, 72: 247-63.

Vasta, J.D.; Sherma, J. 2008. 'Analysis of lycopene in nutritional supplements by silica gel high-performance thin-layer chromatography with visible-mode densitometry', *Acta Chromatographica*, 20: 673–83.

Vences-Guzman, M. A., O. Geiger, and C. Sohlenkamp. 2012. 'Ornithine lipids and their structural modifications: from A to E and beyond', *FEMS Microbiol Lett*, 335: 1-10.

Verweij, P. E., A. Chowdhary, W. J. Melchers, and J. F. Meis. 2016. 'Azole Resistance in Aspergillus fumigatus: Can We Retain the Clinical Use of Mold-Active Antifungal Azoles?', *Clin Infect Dis*, 62: 362-8.

Vetting, M. W., S. L. Roderick, M. Yu, and J. S. Blanchard. 2003. 'Crystal structure of mycothiol synthase (Rv0819) from Mycobacterium tuberculosis shows structural homology to the GNAT family of N-acetyltransferases', *Protein Sci*, 12: 1954-9.

Vetting, M. W., M. Yu, P. M. Rendle, and J. S. Blanchard. 2006. 'The substrate-induced conformational change of Mycobacterium tuberculosis mycothiol synthase', *J Biol Chem*, 281: 2795-802.

W

Warnecke, D. C., M. Baltrusch, F. Buck, F. P. Wolter, and E. Heinz. 1997. 'UDP-glucose:sterol glucosyltransferase: cloning and functional expression in Escherichia coli', *Plant Mol Biol*, 35: 597-603.

Warnecke, D. C., and E. Heinz. 1994. 'Purification of a Membrane-Bound UDP-Glucose:Sterol [beta]-D-Glucosyltransferase Based on Its Solubility in Diethyl Ether', *Plant Physiol*, 105: 1067-73.

Warnecke, D., R. Erdmann, A. Fahl, B. Hube, F. Muller, T. Zank, U. Zahringer, and E. Heinz. 1999. 'Cloning and functional expression of UGT genes encoding sterol glucosyltransferases from Saccharomyces cerevisiae, Candida albicans, Pichia pastoris, and Dictyostelium discoideum', *J Biol Chem*, 274: 13048-59.

Watanabe, T., T. Ito, H. M. Goda, Y. Ishibashi, T. Miyamoto, K. Ikeda, R. Taguchi, N. Okino, and M. Ito. 2015. 'Sterylglucoside catabolism in Cryptococcus neoformans with endoglycoceramidase-related protein 2 (EGCrP2), the first steryl-beta-glucosidase identified in fungi', *J Biol Chem*, 290: 1005-19.

Weidenmaier, C., S. A. Kristian, and A. Peschel. 2003. 'Bacterial resistance to antimicrobial host defenses--an emerging target for novel antiinfective strategies?', *Curr Drug Targets*, 4: 643-9.

Weidenmaier, C., A. Peschel, V. A. Kempf, N. Lucindo, M. R. Yeaman, and A. S. Bayer. 2005. 'DltABCD- and MprF-mediated cell envelope modifications of Staphylococcus aureus confer resistance to platelet microbicidal proteins and contribute to virulence in a rabbit endocarditis model', *Infect Immun*, 73: 8033-8.

Westley, J., J. J. Wren, and H. K. Mitchell. 1957. 'Phospholipides containing amino acids other than serine. I. Detection', *J Biol Chem*, 229: 131-8.

White, T. C., K. A. Marr, and R. A. Bowden. 1998. 'Clinical, cellular, and molecular factors that contribute to antifungal drug resistance', *Clin Microbiol Rev*, 11: 382-402.

Wiltrout, E., J. M. Goodenbour, M. Frechin, and T. Pan. 2012. 'Misacylation of tRNA with methionine in Saccharomyces cerevisiae', *Nucleic Acids Res*, 40: 10494-506.

Woese, C. R., G. J. Olsen, M. Ibba, and D. Soll. 2000. 'Aminoacyl-tRNA synthetases, the genetic code, and the evolutionary process', *Microbiol Mol Biol Rev*, 64: 202-36.

Wolf, Y. I., L. Aravind, N. V. Grishin, and E. V. Koonin. 1999. 'Evolution of aminoacyl-tRNA synthetases--analysis of unique domain architectures and phylogenetic trees reveals a complex history of horizontal gene transfer events', *Genome Res*, 9: 689-710.

Wustner, D., F. W. Lund, C. Rohrl, and H. Stangl. 2016. 'Potential of BODIPY-cholesterol for analysis of cholesterol transport and diffusion in living cells', *Chem Phys Lipids*, 194: 12-28.

Y

Yabuuchi, E., Y. Kosako, I. Yano, H. Hotta, and Y. Nishiuchi. 1995. 'Transfer of two Burkholderia and an Alcaligenes species to Ralstonia gen. Nov.: Proposal of Ralstonia pickettii (Ralston, Palleroni and Doudoroff 1973) comb. Nov., Ralstonia solanacearum (Smith 1896) comb. Nov. and Ralstonia eutropha (Davis 1969) comb. Nov', *Microbiol Immunol*, 39: 897-904.

Yakobov, N., S. Debard, F. Fischer, B. Senger, and H. D. Becker. 2018. 'Cytosolic aminoacyl-tRNA synthetases: Unanticipated relocations for unexpected functions', *Biochim Biophys Acta Gene Regul Mech*, 1861: 387-400.

Yakobov, N., F. Fischer, N. Mahmoudi, Y. Saga, C. D. Grube, H. Roy, B. Senger, *et al.* 2020. 'RNA-dependent sterol aspartylation in fungi', *Proc Natl Acad Sci U S A.*

Yamashita, S., M. Oku, Y. Wasada, Y. Ano, and Y. Sakai. 2006. 'PI4P-signaling pathway for the synthesis of a nascent membrane structure in selective autophagy', *J Cell Biol*, 173: 709-17.

Yang, H., M. Bard, D. A. Bruner, A. Gleeson, R. J. Deckelbaum, G. Aljinovic, T. M. Pohl, R. Rothstein, and S. L. Sturley. 1996. 'Sterol esterification in yeast: a two-gene process', *Science*, 272: 1353-6.

Yao, P., and P. L. Fox. 2013. 'Aminoacyl-tRNA synthetases in medicine and disease', *EMBO Mol Med*, 5: 332-43.

Yaremchuk, A., I. Kriklivyi, M. Tukalo, and S. Cusack. 2002. 'Class I tyrosyl-tRNA synthetase has a class II mode of cognate tRNA recognition', *EMBO J*, 21: 3829-40.

Young, L. Y., C. M. Hull, and J. Heitman. 2003. 'Disruption of ergosterol biosynthesis confers resistance to amphotericin B in Candida lusitaniae', *Antimicrob Agents Chemother*, 47: 2717-24.

Yu, C., N. J. Kennedy, C. C. Chang, and J. A. Rothblatt. 1996. 'Molecular cloning and characterization of two isoforms of Saccharomyces cerevisiae acyl-CoA:sterol acyltransferase', *J Biol Chem*, 271: 24157-63.

Yuan, J., S. Palioura, J. C. Salazar, D. Su, P. O'Donoghue, M. J. Hohn, A. M. Cardoso, W. B. Whitman, and D. Soll. 2006. 'RNA-dependent conversion of phosphoserine forms selenocysteine in eukaryotes and archaea', *Proc Natl Acad Sci U S A*, 103: 18923-7.

Z

Zamecnik, P. C., M. L. Stephenson, and L. I. Hecht. 1958. 'Intermediate Reactions in Amino Acid Incorporation', *Proc Natl Acad Sci U S A*, 44: 73-8.

Zhang, C. M., T. Christian, K. J. Newberry, J. J. Perona, and Y. M. Hou. 2003. 'Zinc-mediated amino acid discrimination in cysteinyl-tRNA synthetase', *J Mol Biol*, 327: 911-7.

Zhang, P., W. Wu, Q. Chen, and M. Chen. 2019. 'Non-Coding RNAs and their Integrated Networks', *J Integr Bioinform*, 16.

Zhang, Y., and V. N. Gladyshev. 2007. 'High content of proteins containing 21st and 22nd amino acids, selenocysteine and pyrrolysine, in a symbiotic deltaproteobacterium of gutless worm Olavius algarvensis', *Nucleic Acids Res*, 35: 4952-63.

Zhang, Y. Q., Y. G. Chen, W. J. Li, X. P. Tian, L. H. Xu, and C. L. Jiang. 2005. 'Sphingomonas yunnanensis sp. nov., a novel gram-negative bacterium from a contaminated plate', *Int J Syst Evol Microbiol*, 55: 2361-4.

Zhang, Y. Q., S. Gamarra, G. Garcia-Effron, S. Park, D. S. Perlin, and R. Rao. 2010. 'Requirement for ergosterol in V-ATPase function underlies antifungal activity of azole drugs', *PLoS Pathog*, 6: e1000939.

Zinoni, F., A. Birkmann, T. C. Stadtman, and A. Bock. 1986. 'Nucleotide sequence and expression of the selenocysteine-containing polypeptide of formate dehydrogenase (formate-hydrogen-lyase-linked) from Escherichia coli', *Proc Natl Acad Sci U S A*, 83: 4650-4.

Zinoni, F., J. Heider, and A. Bock. 1990. 'Features of the formate dehydrogenase mRNA necessary for decoding of the UGA codon as selenocysteine', *Proc Natl Acad Sci U S A*, 87: 4660-4.

Zuker, M. 2003. 'Mfold web server for nucleic acid folding and hybridization prediction', *Nucleic Acids Res*, 31: 3406-15.

Zweytick, D., E. Leitner, S. D. Kohlwein, C. Yu, J. Rothblatt, and G. Daum. 2000. 'Contribution of Are1p and Are2p to steryl ester synthesis in the yeast Saccharomyces cerevisiae', *Eur J Biochem*, 267: 1075-82.

Nathaniel Yakobov

Découverte de l'aminoacylation ARNt dépendante de l'ergostérol chez les champignons

Résumé

Les aminoacyl-ARNt synthétases (aaRSs) sont des enzymes essentiels en charge de la production d'aminoacyl-ARNts (aa-ARNts) qui seront utilisés par le ribosome lors de la synthèse protéique. Néanmoins, les aa-tRNAs peuvent également servir de substrats dans d'autres voies métaboliques comme l'aminoacylation de glycérolipides chez les bactéries. Ainsi, les bactéries modifient leurs propriétés de surface afin d'augmenter leur résistance aux antimicrobiens, pathogénie ou virulence. Aucun mécanisme similaire n'a été mis en évidence chez les eucaryotes avant ma thèse car il était admis que la modification de lipides ARNt dépendante était réservée aux procaryotes. Pendant ma thèse, j'ai identifié une nouvelle classe de lipides modifiés chez les champignons, les stérols aminoacylés (AS). J'ai identifié l'ergosteryl-3β-O-L-aspartate (Erg-Asp) et l'ergosteryl-3β-O-glycine qui sont synthétisés par deux enzymes distinctes qui contiennent un domaine de fonction inconnu appelé DUF2156 qui est responsable de l'activité aminoacyl-tRNA transférase (*i.e.* du transfert de l'aa de l'aa-tRNA sur l'ergostérol). De manière intéressante, ces enzymes peuvent être classées en deux classes selon qu'elles sont fusionnées ou non à l'aaRS correspondante. Nous avons découvert que la déacylation de l'Asp de l'Erg-Asp est catalysé par une Erg-Asp hydrolase qui participe ainsi à l'homéostasie du stérol conjugué *in vivo*. Des études phylogénétiques suggèrent que la synthèse / dégradation d'AS est conservée chez les champignons « supérieurs » et aux vues du rôle central des stérols et de leurs formes conjuguées, nous proposons que la voie que nous venons d'identifier peut avoir des implications plus larges dans le remodelage membranaire, la signalisation, la résistance au antimicrobiens ou la pathogénie.

Mots-clés : aa-tRNA, aminoacyl-tRNA synthétase, ergostérol, champignons, aminoacylation de lipide

Summary

Aminoacyl-tRNA synthetases (aaRSs) are essential enzymes that produce aminoacyl-tRNAs (aa-tRNAs) that will be used for ribosome catalyzed protein synthesis. However, aa-tRNAs can also serve as substrates in other pathways like glycerolipid aminoacylation in bacteria. By doing so, bacteria modify their cell surface properties to improve drug resistance, pathogenicity, or virulence. No homologous lipid aminoacylation pathway has been uncovered in eukaryotes before my thesis and tRNA-dependent lipid remodeling was believed to be restricted to prokaryotes. During my thesis I identified a new class of fungal lipids, aminoacylated sterols (AS). I identified ergosteryl-3β-O-L-aspartate (Erg-Asp) and ergosteryl-3β-O-glycine that are synthesized by two distinct enzymes that contain a Domain of unknown function named DUF2156 which is responsible for the aminoacyl-tRNA transferase activity (*i. e.* the transfer of the aa-moiety from the aa-tRNA to ergosterol). Interestingly, those enzymes can be classified in two classes depending on their fusion to the cognate aaRS or not. We also uncovered that removal of the Asp modifier from Erg-Asp is catalyzed by a genuine Erg-Asp hydrolase participating in the turnover of the conjugated sterol in vivo. Phylogenomics suggest that AS synthesis/degradation pathways are conserved across "higher" fungi and given the central roles of sterols and conjugated sterols in these species, we propose that the herein uncovered pathway might have broader implications in membrane remodeling, trafficking, antimicrobial resistance, or pathogenicity.

Keywords: aa-tRNA, aminoacyl-tRNA synthetases, ergosterol, fungi, DUF2156, lipid aminoacylation